

Energy Efficient Mobility Systems

2019 Annual Progress Report

Vehicle Technologies Office

(This page intentionally left blank)

Disclaimer

This report was prepared as an account of work sponsored by an agency of the United States government. Neither the United States government nor any agency thereof, nor any of their employees, makes any warranty, express or implied, or assumes any legal liability or responsibility for the accuracy, completeness, or usefulness of any information, apparatus, product, or process disclosed or represents that its use would not infringe privately owned rights. Reference herein to any specific commercial product, process, or service by trade name, trademark, manufacturer, or otherwise does not necessarily constitute or imply its endorsement, recommendation, or favoring by the United States government or any agency thereof. The views and opinions of authors expressed herein do not necessarily state or reflect those of the United States government or any agency thereof.

Acknowledgements

We would like to acknowledge and thank the Pillar Leads of the SMART Mobility National Lab Consortium for their hard work and leadership during the last three years: Eric Rask (ANL), for leading research in Connected and Automated Vehicles; John Smart (INL), for guiding efforts in Advanced Fueling Infrastructure; David Smith (ORNL), for directing activities in Multi-Modal Freight; Anna Spurlock (LBNL), for guiding research on Mobility Decision Science; and Stan Young (NREL) for leading efforts in Urban Science. Additionally, we would like to thank Aymeric Rousseau (ANL) for his leadership of the cross-cutting SMART Mobility Modeling Workflow. SMART Mobility represents a cornerstone of the EEMS Program, and its success is due to the dedication of these individuals, as well as contributions from over 40 additional principle.

Acronyms

A

AADT	Average Annual Daily Traffic
AC	Alternating Current
ACC	Adaptive Cruise Control
accel	Acceleration
ACES	Automated, Connected, Efficient Shared Mobility
ACS	Advanced Combustion Systems
AEO	Annual Energy Outlook
AER	All-electric range
AFI	Advanced Fueling Infrastructure
AFV	Alternative Fuel Vehicle
AMD	Automated Mobility District
AMT	Automated Mechanical Transmission
ANL	Argonne National Laboratory
ANN	Artificial Neural Network
AOI	Areas of Interest
APEC	Asia Pacific Economic Council
APRF	Advanced Powertrain Research Facility
APT	Pressure Sensor
ASD	Aftermarket Safety Device
AT	Autonomous Taxi
ATDM	Active Transportation Demand Management
ATW	Active Transmission Warm up
AVTE	Advanced Vehicle Testing and Evaluation

B

BaSce	Baseline and Scenario
Batt	Battery
BEAM	Framework for Behavior, Energy, Autonomy, and Mobility
BEB	Battery Next-Generation Electric Transit Bus
BET	Battery Electric Truck
BEV	Battery Electric Vehicle
BMW	Bayerische Motoren Werke AG
BSFC	Brake Specific Fuel Consumption
BSM	Basic Safety Message
BTE	Brake Thermal Efficiency

C

CAC	Charge Air Cooler
CACC	Cooperative Adaptive Cruise Control
CAE	Computer-Aided Engineering
CAEV	Connected and automated electric vehicles

CAFE	Corporate Average Fuel Economy
CAN	Controller Area Network
CAV	Connected and automated vehicles
CARB	California Air Resources Board
CBD	Central Business District
CCS	Combined Charging System
CW, CCW	Clockwise, Counter Clockwise
CD	Charge-Depleting
CERV	Conference on Electric Roads and Vehicles
CFD	Computational Fluid Dynamics
CFDC	Commercial Fleet Data Center
CFL	Combined Fluid Loop
CH ₄	Methane
CHTS	California Household Travel Survey
CRHTI	Chicago Regional Household Travel Inventory
CIP	Common Integration Platform
CMAP	Chicago Metropolitan Agency for Planning
Cm ³	Cubic
CNG	Compressed Natural Gas
CO	Carbon monoxide
CO ₂	Carbon Dioxide
COMM	Commuter
Conv	Conventional Vehicle
COP	Coefficient of Performance
CPT	Cumulative prospect theory
CRADA	Cooperative Research and Development Agreement
CS	Charge Sustaining
Cs	Cold start
CV	Conventional vehicle

D

D3	Downloadable Dynamometer Database
DC	Direct current
DCFC	Direct Current Fast Charge
DCT	Dual-clutch transmission
decel	Deceleration
DER	Distributed energy resource
DFGM	Digital Flux Gate Magnetometer
DFMEA	Design of Failure Modes Analysis
DOE	U.S. Department of Energy
DOHC	Dual overhead cam
DS	Down speeding
DSM	Distributed Security Module
DSM	Diagnostic Security Module
DSP	Digital Signal Processor

DSRC	Dedicated Short Range Communications
DTA	Dynamic traffic assignment
DWPT	Dynamic Wireless Power Transfer
dt	Change in time
dv	Change in velocity
Dyno	Dynamometer

E

EAD	Signal eco-approach and departure
EAVS	Electrically Assisted Variable Speed Supercharger
EC	European Commission
EDV	Electric Drive Vehicle
EDX	Energy dispersive x-ray spectroscopy
EERE	Energy Efficiency and Renewable Energy
EGR	Exhaust Gas Recirculation
EG/W	Ethylene glycol/water
EIA	Energy Information Agency
EOL	End of life
EPA	Environmental Protection Agency
ePATHS	Electrical PCM Assisted Thermal Heating System
EREV	Extended-Range Electric Vehicles
ESIF	Energy Systems Integration Facility
ESS	Energy Storage System
ETT	Electric Transportation Technologies
E-TREE	Electric Truck with Range Extending Engine
EUMD	End-Use Measurement Device
EV	Electric Vehicle
EVI-Pro	Electric Vehicle Infrastructure Projection Tool
EV2G	Electric Vehicle-to-Grid
eVMT	Electric Vehicle Miles Traveled
EVSE	Electric Vehicle Service Equipment
EXV	Electronic Expansion Valve

F

FAF	Freight Analysis Framework
FASTSim	Future Automotive Systems Technology Simulator
FC	Fuel cell
FC	Fast charge
FCons	Fuel consumption
FCTO	Fuel Cell Technologies Office
FCV	Fuel Cell Vehicle
FCR	Fuel consumption rate
FE	Fuel Economy
FEA	Finite Element Analysis
FEX	Front-end Heat Exchanger

FFLEET	Freight Fleet Level Energy Estimation Tool
FG	Fixed gear ratio
FGLD	Fine-grained location data
FHWA	Federal Highway Administration
FLNA	Frito-Lay North America
FM	Friction Modifier
FMEP	Friction Mean Effective Pressure
FOA	Funding Opportunity Announcement
FTIR	Fourier transform infrared spectroscopy
FTP	Federal Test Procedure
FWD	Four wheel drive
FY	Fiscal year
G	
G	gram
GB	Gigabyte
GCEDV	Grid Connected Electrical Drive Vehicles
GEM	Gas Emissions Model
GGE	Gasoline gallon equivalent
GHG	Greenhouse Gas
GITT	Grid Interaction Tech Team
GM	General Motors
GMLC	Grid Modernization Lab Consortium
GnPs	Graphene nanoplatelets
GO	Graphene Oxide
GPRA	Government Performance and Results Act
GPS	Global Positioning System
GREET	Greenhouse gases, Regulated Emissions, and Energy use in Transportation
GSF1	Generic Speed Form 1
GSU	Grid side unit
GUI	Graphic User Interface
GVW	Gross Vehicle Weight
H	
h-APU	hybrid Auxiliary Power Unit
HC	Unburned hydrocarbons
HD	Heavy Duty
HEV	Hybrid-Electric Vehicle
HHDDT	Heavy Heavy-Duty Diesel Truck
HHV	Hydraulic Hybrid Vehicle
HIL	Hardware-In-the-Loop
HP	Heat Pump
Hp	Horsepower
HTML	HyperText Markup Language
HV	High Voltage

HVAC	Heating Ventilating and Air Conditioning
HWFET	Highway Fuel Economy Test
HPMS	Highway Performance Monitoring System
HVTB	High Voltage Traction Battery
HWY	Highway Program or Highway Fuel Economy Test Cycle
HPC	High Performance Computing
HTR	Heater
Hz	Hertz

I

I	Inertia
IC	Internal Combustion
ICDV	Internal Combustion Drive Vehicles
ICE	Internal Combustion Engine
ICTF	Intermodal Container Transfer Facility
ICU	Inverter-Charger Unit
IEB	Information Exchange Bus
IEC	International Electrotechnical Commission
IGBT	Insulated Gate Bipolar Transistors
IHX	Internal Heat Exchanger
INL	Idaho National Laboratory
IOT	Internet of Things
IR	Infrared Radiation
ISO	International Organization for Standardization
ITS	Intelligent Transportation Systems

J

JIT	Just-in-Time
-----	--------------

K

kg	Kilogram
km	Kilometer
kW	Kilowatt
kWh	Kilowatt hour

L

L	litre
L1	Level 1 benchmark
L2	Level 2 benchmark
Lbf	Pounds force
LCC	Liquid-Cooled Condenser
LCV	Long combination vehicle
LD	Light-duty
LH	line haul
Li	Lithium

LIB	Lithium ion battery
LLNL	Lawrence Livermore National Laboratory
LTC	Lockport Technical Center
LV	Leading Vehicle

M

M	Mass
MaaS	Mobility as a Service
MBSE	Model Based System Engineering
MEP	Mobility energy productivity (MEP)
MD	Medium Duty
MDCEV	Multiple Discrete-Continuous Extreme Value
MDS	Mobility Decision Science
mpg	Miles per gallon
MMTCE	Million Metric Tons of Carbon Equivalent
MIIT	Ministry of Industry and Information Technology
mi	Mile
MJ	Megajoules
MONLP	Multi-Objective Non-Linear Program
MORPC	Mid-Ohio Regional Planning Commission
MOSFET	Metal-Oxide Semiconductor Field-Effect Transistor
MNL	Multinomial Logit
mph	Miles per hour
MPGe	Miles per gallon equivalent, Miles per gallon gasoline equivalent
MTC	Metropolitan Transportation Commission
MTDC	Medium Truck Duty Cycle
MOVES	Motor Vehicle Emission Simulator
MPR	Market Penetration Rates
MRF	Moving Reference Frame
MURECP	Medium-Duty Urban Range Extended Connected Powertrain
MY	Model year
M2	Meters squared

N

NACFE	North American Council for Freight Efficiency
NDA	Non-Disclosure Agreement
NETL	National Energy Technology Laboratory
NHTS	National Household Travel Survey
NHTSA	National Highway Transportation Safety Administration
NM	Newton meters
NOx	Nitrogen oxides
NR	Natural Rubber
NRE	Non Recurring Engineering
NREL	National Renewable Energy Laboratory
NRT	National Retail Trucking

NVH	Noise, vibration, and harshness
NVUSD	Napa Valley Unified School District
NYSERDA	New York State Energy Research Development Authority

O

OBC	On-board charger
OCBC	Orange County Bus Cycle
OEM	Original Equipment Manufacturer
OneSAF	One Semi-Automated Forces
ORNL	Oak Ridge National Laboratories

P

P	Active Power
PC	Polycarbonate
PCM	Phase-Change Material
PCU	Power Control Unit
PCU	Powertrain Control Unit
PEEM	Power Electronics and Electric Motor
PEV	Plug-In Electric Vehicle
PFC	Power factor correction
PFI	Port fuel injection
PGW	Pittsburgh Glass Works
PHEV	Plug-in Hybrid Electric Vehicle
PHEV##	Plug-in hybrid electric vehicle with ## miles of all-electric range
PI	Principal Investigator
PID	Proportional+Integral+Derivative
PM	Permanent Magnet
PM	Particulate Matter
PMP	Pontryagin Minimum Principle
PMT	Passenger Miles Traveled
ppm	Parts per Million
PTC	Positive Temperature Coefficient (Electric Heater)
PTO	Power Take-Off
PVP	Polyvinylpyrrolidone
PWWMD	Public Works and Waste Management Department
λ	Power Factor
ϕ	Power Angle

Q

Q	Reactive power
QA	Quality assurance
QC	Quality control

R

R2	Coefficient of Determination
----	------------------------------

R/D	Receiver / Dryer
REV	New York State's Reforming the Energy Vision Initiative
REx	Range Extending Engine
rGO	reduced graphene oxide
RH	Relative Humidity
RMS	Root Mean Square
ROL	Ring-On-Liner
rpm	Revolutions Per Minute
RSU	Road Side Unit
RTRP-	Random-Thresholds, Random-Parameters Hierarchical Ordered Probit
RWDC	Real-World Drive-Cycle

S

S	Apparent power
SAE	Society of Automotive Engineers
SAV	Shared Automated Vehicles
SCAG	Southern California Association of Governments
SCAQMD	South Coast Air Quality Management District
SCIG	Southern California International Gateway
SDO	Standards Definition Organizations
SI	Système International d'Unités
SI	Gasoline Spark Ignition
SMART	Systems and Modeling for Accelerated Research in Transportation
SNR	Sensor
SOC	State of Charge
SPaT	Signal phase and timing
SPRINGS	Statistical Planning for Resilience in Next Generation Systems
SPL	Sound Pressure Level
SR	Speed Ratio
SS	Steady State
S/S	Start/Stop
SPaT	Signal Phase and Timing
STELLA	Strongly-TypEd, Lisp-like LAnguage
StAR	Storage-Assisted Recharging
SVET	Smart vehicle energy technology
SVTrip	Stochastic Vehicle Trip Creator

T

T	Torque
TA	Technical Area
TA	Torque Assist
TC	Thermocouple
TAZ	Traffic Analysis Zone
TCO	Total cost of ownership
TE	Thermoelectric

TE	Transmission Error
TES	Thermal Energy Storage
TGA	thermogravimetric analysis
THC	Total hydrocarbon emissions
TIM	Thermal Interface Materials
TLRP	Thermal Load Reduction Package
TN	Testing Network
TNC	Transportation Network Companies
TOU	Time-Of-Use
TRB	Transportation Research Board
TSDC	Transportation Secure Data Center
TSI	Turbocharged stratified injection
TUSD	Torrance Unified School District
TV	Trailing Vehicle
TXVs	Thermal Expansion Valves

U

U.S.	U.S. Driving Research and Innovation for Vehicle Efficiency and Energy Sustainability
UA	Transfer Coefficient
UC	Ultra-capacitor
UCR	University of California, Riverside
UDDS	Urban Dynamometer Driving Schedule
UM	University of Michigan
UN ECE	United Nations Economic Council for Europe
UNSW	University of New South Wales
UPS	United Parcel Service
URL	Uniform Resource Locator
US06	Environmental Protection Agency US06 or Supplemental Federal Test Procedure
USABC	United States Advanced Battery Consortium
USCAR	U.S. Council for Automotive Research
Util	Battery capacity utilization

V

V	Voltage
V2G	Vehicle-to-Grid
V2I	Vehicle-to-Infrastructure
V2V	Vehicle to Vehicle
VAr	Volt-Amp-reactive
VCC	Volvo Car Corp
VGI	Vehicle-Grid Integration
VGT	Variable Geometry Turbocharger
VHT	Vehicle hours traveled
VIP	Vacuum insulated panels
VKT	Vehicle kilometers traveled
VMT	Vehicle miles traveled

VOTT	Value-of-travel-time
VS	Vehicle Systems
VSATT	Vehicle Systems Analysis Technical Team
VSI	Vehicle Systems Integration
VSST	Vehicle Systems Simulation and Testing
VTCab	Vehicle Thermal Cab Simulator
VTIF	Vehicle Testing and Integration Facility
VTO	Vehicle Technologies Office

W

Dw	Change in Angle W
WCC	Water Cooled Condenser
WEC	World Endurance Championship
WEG	Water/Ethylene Glycol
Wh	Watt hour
WHR	Waste Heat Recovery
WPT	Wireless Power Transfer
WTP	Willingness to pay
WTW	Well-to-Wheels

X

XPS	X-ray photoelectron spectroscopy
-----	----------------------------------

Y

Z

ZI-HOPIT	Zero-Inflated Hierarchical Ordered Probit
ZOV	Zero-occupancy vehicle

Executive Summary

Our transportation system is changing. New, disruptive technologies such as connected and automated vehicles are being developed and will soon be introduced to the market. Innovative business models that provide car-sharing and ride-hailing services give new mobility options to consumers. Freight transport is evolving to meet the demands of a retail sector that is increasingly based on e-commerce. This shifting mobility landscape may offer opportunities to improve the economic and energy productivity of the U.S. transportation sector, while advancing the safety, affordability, and accessibility of transportation for all Americans.

During fiscal year 2017 (FY 2017), the U.S. Department of Energy (DOE) Vehicle Technologies Office (VTO) created the Energy Efficient Mobility Systems (EEMS) Program to understand the range of mobility futures that could result from these disruptive technologies and services, and to create solutions that improve mobility energy productivity, or the value derived from the transportation system per unit of energy consumed. Increases in mobility energy productivity result from improvements in the quality or output of the transportation system, and/or reductions in the energy used for transportation.

EEMS Program activities during FY 2019 focused on analytical research to understand the impacts that new mobility technologies and services will have at the vehicle, traveler, and overall transportation system-level. This research included the development of vehicle and transportation system simulation models and tools to evaluate the complex interactions among the various actors within the mobility landscape, analysis of empirical data to characterize which solutions may provide the largest benefits, and development of new control systems and algorithms that use vehicle connectivity and automation to improve the performance and efficiency of individual vehicles as well as the overall traffic system.

This document presents a brief overview of the EEMS Program and documents progress and results for projects within four of the five EEMS activity areas: (1) the SMART (Systems and Modeling for Accelerated Research in Transportation) Mobility Lab Consortium, (2) High Performance Computing and Big Data Solutions for Mobility Data, (3) Advanced R&D Projects conducted by industry and academia, and (4) Core Modeling, Simulation, and Evaluation. Similarly, the remaining EEMS activity area – (5) Living Labs (managed under VTO's Technology Integration Program). Each of the individual progress reports provide a project overview and highlights of the technical results.

Table of Contents

Acknowledgements.....	ii
Acronyms	iii
Executive Summary	xiii
Vehicle Technologies Office Overview	1
Energy Efficient Mobility Systems Program Overview.....	3
I SMART Mobility.....	15
I.1 Advanced Fueling Infrastructure.....	15
I.1.1 Quantify National Energy Impact of Electrified Shared Mobility with Infrastructure Support (ANL).....	15
I.1.2 Fueling Infrastructure for Future Shared and Shared-Automated Vehicles (INL).....	23
I.1.3 Dynamic Wireless Power Transfer Feasibility (ORNL).....	38
I.1.4 Charging Infrastructure Needs for Electrification of Freight Delivery Vehicles (INL, ORNL, NREL).....	45
I.2 Connected and Automated Vehicles.....	60
I.2.1 Traffic Microsimulation of Energy Impacts of CAV Concepts at Various Market Penetrations (LBNL) [Task 1.2].....	60
I.2.2 Impact of CAVs on Energy, Green House Gas, and Mobility in a Metropolitan Area (ANL) [Task 1.3].....	79
I.2.3 Energy-Efficient Connected and Automated Vehicles (ANL).....	85
I.2.4 Multi-Scale, multi-scenario assessment of system optimization opportunities due to vehicle connectivity and automation (ORNL) [Task 2.1.2].....	93
I.2.5 Aggregation Methods to Estimate National-Level Impacts of CAVs Scenarios (ANL, NREL, ORNL).....	102
I.2.6 Truck Cooperative Adaptive Cruise Control (CACC)/Platooning Testing: Measuring Energy Savings, Interaction with Aerodynamics Changes and Impacts of Control Enhancements: A Hardware-in-the-Loop Testbed for Evaluating Impacts of Connected Automated Vehicle on Arterials (LBNL) [Task 1.3.1].....	108
I.2.7 Experimental Evaluation of Cooperative ACC for Passenger Cars: Development of CACC Capability for Passenger Cars with Different Powertrains (LBNL, ANL) [Task 1.3.2].....	117
I.2.8 Experimental Evaluation of Eco-Driving Strategies (LBNL).....	132
I.2.9 Focused Validation and Data Collection to Support - Automated Vehicle Electrical Load Investigation (ANL).....	146
I.3 Mobility Decision Science.....	151
I.3.1 Whole Traveler Study (LBNL, INL, NREL)].....	151

I.3.2	Analyze the Spatial Distribution and Impacts of One-way Car-Sharing Programs on Transit Ridership and Energy Use (LBNL)	173
I.3.3	Mobility Behavior Responses to TNC Services (LBNL, NREL).....	181
I.3.4	Travel Time Use and Value with Mobility Services (ANL).....	192
I.3.5	Travel Behavior Simulation Modeling in POLARIS :Enhance Existing Models to Estimate Impact of Modal Shifts Intra-City Passenger Travel - Transit Focused (ANL)	198
I.4	Multi-Modal Freight.....	205
I.4.1	Multi-Modal Energy Analysis for Inter-City Freight Movement (NREL, ANL).....	205
I.4.2	Optimization of Intra-City Freight Movement with New Delivery Methods (ORNL, INL) [Task 3.1].....	219
I.4.3	Energy and Mobility Impact of Inter/Intracity Freight Movement Using Data-Driven Agent-Based System Simulation (ANL)	226
I.5	Urban Science	233
I.5.1	Data and Models Informing Smart Cities (NREL) [Task 2.1.1].....	233
I.5.2	Mobility Energy Productivity Metric (NREL) [task 2.1.2]	242
I.5.3	SMART Urban Typology (NREL, LBNL) [Task 2.1.5]	248
I.5.4	Long-Term Land Use and Infrastructure: Coupling Land Use Models and Network Flow Models (LBNL) [Task 2.2.2].....	255
I.5.5	Long SMART Cities Topology – Curbs and Parking (NREL) [Task 2.2.5]	262
I.5.6	Assessing Urban Impact: Automated Mobility Districts (NREL) [Task 2.4.1].....	268
I.5.7	UrbanSim to ABM Workflow Integration (LBNL) [Task 2.5]	276
I.5.8	The Signal Control Network as the Urban Mobility Nerve Center (NREL, ORNL, KSU) [Task 4.1].....	280
I.6	Workflow	289
I.6.1	General Microsimulation to Meso-simulation (LBNL, ANL).....	289
I.6.2	SMART Mobility Tools and Process Development (ANL)	305
I.6.3	Workflow to simulate connected and automated vehicle control under realistic traffic conditions (ANL, LBNL)	312
I.6.4	Demonstrate MEP Benefit of Intelligent EV Infrastructure Design Using ABMs (NREL, LBNL, ANL)	319
I.6.5	Transportation System Control for Taxi/TNC Simulations (ANL, LBNL).....	326
I.6.6	BEAM (LBNL)	332
II	High Performance Computing and Big Data	338
II.1.1	HPC-Enabled Deep-Learning and Simulation for AV Development (ORNL, NREL).....	338
II.1.2	Real-Time Data and Simulation for Optimizing Regional Mobility in the United States	344

II.1.3	Reinforcement Learning-based Traffic Control to Optimize Energy Usage and Throughput (ORNL)	357
II.1.4	Ubiquitous Traffic Volume Estimation through Machine Learning Procedures (NREL)	363
II.1.5	Transportation Data Analytics (Big Data Systems for Mobility (BDSM)) (LBNL)	370
III	Advanced Technology R&D	382
III.1.1	Energy Impact of Connected and Automated Vehicle Technologies (University of Michigan, ANL)	382
III.1.2	Boosting Energy Efficiency of Heterogeneous Connected and Automated Vehicle (CAV) Fleets via Anticipative and Cooperative Vehicle Guidance (Clemson University).....	387
III.1.3	Evaluating Energy Efficiency Opportunities from Connected and Automated Vehicle Deployments Coupled with Shared Mobility in California (UCR/NREL).....	396
III.1.4	Developing an Eco-Cooperative Automated Control System (Virginia Tech)	403
IV	Core Modeling, Simulation, and Evaluation.....	410
IV.1.1	Livewire Data Platform (NREL, INL, PNNL)	410
IV.1.2	Virtual and Physical Proving Ground for Development and Validation of Future Mobility Technologies (ORNL)	415
IV.1.3	Core Modeling, Simulation and Evaluation (ANL).....	421

List of Figures

Figure 1 Operation State of Automated Ride-Hail BEVs with Sparse (left) and Rich (right) Charging Infrastructure.....	8
Figure 2 Time Series of Fuel Consumption Impacts of ACC and CACC Vehicles (Upper graph is for CACC cases, Lower graph is for ACC Cases.....	9
Figure 3 Energy Consumption Savings Relative to Baseline for Lead Vehicle	9
Figure 4 Degree of Substitution and Supplementation of Delivery for Household Shopping Trips	10
Figure 5 POLARIS Simulation: Mode Share by Scenario.....	11
Figure 6 Effect of Parcel Lockers on Total Energy Consumption (Chicago).....	11
Figure 7 VMT & Energy Use with Retail Purchasing and Powertrain Efficiency Improvements	12
Figure 8 MEP Maps for Denver, CO (Left: All Modes; Center: Car; Right: Transit/Walk/Bike).....	12
Figure 9 Percent Reduction in Fuel Consumption by Flow Rate and Penetration.....	13
Figure 10 The Livewire Data Platform Concept.....	13
Figure 11 Road-Load Data from Second Vehicle in Two-Vehicle Platoon.....	14
Figure I.1.1.1 Analytical framework of national energy impacts of ride hailing and personal EVs.....	17
Figure I.1.1.2 National energy consumption reduction (shown as percentages) as a function of ride-hailing demand, BEV market penetration, and charging infrastructure. Green means a reduction, yellow means relatively no change, and red means an increase. (Energy refers to energy consumption for pump-to-wheel)..	19
Figure I.1.1.3 Energy consumption (quads) in 2030 for the case with charging infrastructure growth: (a) gasoline consumption (quads); and (b) electricity consumption (quads).....	19
Figure I.1.1.4 National carbon emission reduction (shown as percentages, original unit is Million Metric Tons of Carbon Equivalent or MMTc) as a function of ride-hailing demand, BEV market penetration, and charging infrastructure. Green means a reduction, yellow means relatively no change, and red means an increase. (Carbon emissions include emissions from upstream and vehicle use).....	20
Figure I.1.1.5 National carbon emissions at different electric grid mix.....	20
Figure I.1.2.1 Integration of FCSPlan with BEAM and network simulations	25
Figure I.1.2.2 FCSPlan and BEAM integration	25
Figure I.1.2.3 Hosting venues of EVGo's DCFCs	26
Figure I.1.2.4 Populus survey results for TNC driver share by motivation and income.....	27
Figure I.1.2.5 Populus survey results for TNC driver share by driving frequency and income.....	28
Figure I.1.2.6 Populus survey results for TNC driver share by residence type, tenure, and income	28
Figure I.1.2.7 Spatial distribution of chargers in San Francisco Bay Area by network type. “Depot” chargers are exclusively available to fully automated, driverless ride-hailing vehicles while “public” chargers are shared between ride-hailing and personal-use EV drivers.	30
Figure I.1.2.8 Number of vehicles (left) in all scenarios discussed in this section and number of fast chargers (right) in each infrastructure scenario	31
Figure I.1.2.9 Number of charging sessions by infrastructure scenario (x-axis), vehicle range scenario (panel), and charger power scenario (point color)	32

Figure I.1.2.10 Passenger miles served by EVs in ride-hailing fleet by infrastructure scenario (x-axis), vehicle range scenario (panel), and charger power scenario (trend color)	32
Figure I.1.2.11 Distribution of the ride-hailing fleet into operating states over the 24-hour simulation period for scenario with 100-mile range EVs and sparse, 50-kW charging infrastructure. Horizontal panels separate vehicle types and vertical panels separate time spent by each vehicle (top) and distance traveled by all vehicles (bottom).	33
Figure I.1.2.12 Distribution of the ride-hailing fleet into operating states over the 24-hour simulation period for scenario with 100 mile range EVs and Rich, 50kW charging infrastructure. Horizontal panels separate vehicle types and vertical panels separate time spent by each vehicle (top) and distance traveled by all vehicles (bottom).	34
Figure I.1.2.13 Cost per passenger mile for the EVs in the ride-hailing fleet (both human-driven and AEVs), for both networks of fast charging infrastructure (both public and depot), and for the electricity and demand chargers necessary to supply the fleet with energy. The passenger miles traveled are only those that occur in EVs. The range scenarios vary with the columns of the panels, the power capacity scenarios vary with the rows, and the infrastructure scenarios vary across the x-axis.	35
Figure I.1.3.1 Block diagram of a typical track-based dynamic wireless power transfer system.	39
Figure I.1.3.2 Efficiency analysis of track-based DWPT system with respect to the track length.	41
Figure I.1.3.3 Variation of the track-to-vehicle mutual inductance with respect to vehicle position.	41
Figure I.1.4.1 Distribution of Trucks and Annual Miles within Weight Class by Primary Trip Distance.....	49
Figure I.1.4.2 Average Annual Miles Traveled per Vehicle by Primary Trip Distance and Vehicle Weight Class.....	49
Figure I.1.4.5 Circuits driven by a single truck over several days. There is wide variety of circuits.	53
Figure I.1.4.6 Range remaining at each stop for depot only charging	55
Figure I.1.4.7 Range remaining at each stop if charging is available at each stop	56
Figure I.1.4.8 Number of Trips with Given Available Range at Arrival (300-mile range/150 and 350 kwh)...	57
Figure I.1.4.9 Number of Trips with Given Available Range at Arrival (500-mile range/150 and 350 kwh)...	58
Figure I.2.1.1 Comparison of the proposed algorithm and actuated control.....	63
Figure I.2.1.2 Multilane freeway merge section	64
Figure I.2.1.3 Land configuration and road geometry	65
Figure I.2.1.4 Time series of fuel consumption rate under various CACC and ACC market.....	67
Figure I.2.1.5 Temporal and spatial patterns of the vehicle fuel consumption rate for the 40% CACC case....	68
Figure I.2.1.6 Simulated intersection and signal control parameters	69
Figure I.2.1.7 Intersection capacity per direction with CACC market penetration.....	70
Figure I.2.1.8 Average vehicle speed under various CACC market penetrations.....	71
Figure I.2.1.9 Average vehicle fuel economy (MPG) under various CACC market penetrations.....	71
Figure I.2.1.10 Emission and fuel consumption estimates at varying levels of on-ramp demand.....	73
Figure I.2.2.1 Flowchart for SAV fleet operation in POLARIS	80
Figure I.2.2.2 Spatial extent of geofencing (overlapped) in the Chicago Metropolitan Area.....	81
Figure I.2.2.3 Calibrated fundamental diagrams for the four models with varying penetration rates	82
Figure I.2.2.4 Temporal distribution of VHT by auto-based mode for (a) SAV and (b) private-AV scenarios	83

Figure I.2.3.1 Comparison of the adaptive cruise control model in RoadRunner with test data 86

Figure I.2.3.2 Schematic diagram of the human driver model: P&D model [left] and action model [right]..... 87

Figure I.2.3.3 Normalized cross correlation power (NCCP) between experimental and simulation data for 27 segments [top] and for one sample [bottom]. 88

Figure I.2.3.4 Speed traces for a BEV with different control strategies 89

Figure I.2.3.5: Energy consumption savings relative to baseline control for a vehicle in lead position, with current powertrain technology, for various powertrains 89

Figure I.2.3.6 Energy consumption savings for lead vehicle, conventional, current versus future technologies 90

Figure I.2.3.7 Energy consumption of following vehicle (control versus baseline) with current technology and various powertrains 91

Figure I.2.3.8 Energy consumption of following baseline vehicle (lead: control versus baseline) with current technology and various powertrains 91

Figure I.2.4.1 On-ramp model used for analysis..... 94

Figure I.2.4.2 Average fuel economy changes with respect to baseline for three traffic demand scenarios and different market penetration rates of CAVs. The legends at the right of each figure indicate the percentage of LDCAVs and HDCAVs respectively 94

Figure I.2.4.3. Corridor modeled in VISSIM and histogram of observed vs simulated vehicle speeds in the 20.5 N mile marker 95

Figure I.2.4.4 Percentage of electrified vehicles considered for each fleet distribution scenario. 96

Figure I.2.4.5 Fuel and energy consumption results for the current time fleet distribution scenario..... 97

Figure I.2.4.6 Average fuel and energy consumption results for the short-term scenario 97

Figure I.2.4.7 Average fuel and energy consumption results for the long-term scenario 98

Figure I.2.4.8 University of Delaware Scaled SMART City testbed..... 98

Figure I.2.4.9 Traffic Simulation network in VISSIM based on the W I 94/N US 23 On-Ramp in the Washtenaw county in Ann Arbor, Michigan. 99

Figure I.2.4.10 Speed and acceleration volatilities in the main road, and ramp 100

Figure I.2.5.1 Highlighted PMT, and Energy changes with ride pooling for ideal and suboptimal sharing scenarios..... 105

Figure I.2.5.2 Histogram showing changes in total light-duty vehicle energy consumption..... 106

Figure I.2.6.1 Components and Data Flow of the Presented HIL Testbed 109

Figure I.2.6.2 Comparison of the proposed algorithm and actuated control..... 110

Figure I.2.6.3 Traffic Signal Control Phase Definition..... 111

Figure I.2.6.4 Snapshot of the Server Program..... 113

Figure I.2.6.5 Layout of the test track..... 114

Figure I.2.7.1 Overall CACC System Structure for vehicles with all types of powertrains 119

Figure I.2.7.2 ACC override acceleration envelope for 2017 Prius Prime 123

Figure I.2.7.3 Powertrain response to ACC acceleration override for 2017 Prius Prime 123

Figure I.2.7.4 Accelerator pedal map for 2017 Toyota Prius Prime 124

Figure I.2.7.5 Powertrain response to accelerator pedal override on 2017 Toyota Prius Prime	124
Figure I.2.7.6 ACC override acceleration envelope for 2013 Ford Taurus	125
Figure I.2.7.7 Powertrain response to ACC acceleration override for 2013 Ford Taurus	125
Figure I.2.7.8 Accelerator pedal map for 2013 Ford Taurus	126
Figure I.2.7.9 Powertrain response to accelerator pedal override on 2013 Ford Taurus	126
Figure I.2.7.10 Accelerator pedal map for 2014 Honda Accord.....	127
Figure I.2.7.11 Powertrain response to accelerator pedal override on 2014 Honda Accord.....	127
Figure I.2.7.12 Brake pedal map for 2014 Honda Accord.....	127
Figure I.2.7.13 Brake system response to brake pedal override on 2014 Honda Accord.....	127
Figure I.2.7.14 ACC acceleration command override MiM diagram	128
Figure I.2.7.15 Pedal override DC voltage injection diagram	128
Figure I.2.7.16 Speed tracking using the torque mapping developed from the dynamometer test: upper – reference speed (blue) and measured speed (red); lower: speed tracking error, acceleration control command, and drive mode (0-manual; 2-automatic control)	129
Figure I.2.7.17 Speed tracking directly using the ACC command from the upper level control: upper – reference speed (blue) and measured speed (red); lower: speed tracking error, acceleration control command, and drive mode (0-manual; 2-automatic control)	129
Figure I.2.8.1 Vehicle detections at Santa Clara St./4 th St. in San Jose, California.....	134
Figure I.2.8.2 Vehicle detections at a stop sign controlled intersection in Pleasant Hill, California.....	135
Figure I.2.8.3 Vehicle detection from image and projection on map, and speed profile of the vehicles.....	138
Figure I.2.8.4 Case of scenario 1: EAD Case I: EAD vehicle slows down but does not make full stop. Non-EAD vehicle nearby makes nearly a full stop (from left to right speed, speed vs distance to intersection, deceleration).....	140
Figure I.2.8.5 EAD Case I: a no-EAD vehicle follows the EAD vehicle	141
Figure I.2.8.6 EAD Case II: EAD and no-EAD vehicles travel in adjacent lanes and arrives at intersection as similar time	142
Figure I.2.8.7 EAD Case III: EAD and no-EAD vehicles travel in adjacent lanes and arrives at intersection as similar time.....	142
Figure I.2.8.8 EAD Case IV: EAD trailed behind from no-EAD vehicles travel in the adjacent lane	143
Figure I.2.9.1 Cadillac CT6 Instrumentation Overview	147
Figure I.2.9.2 Ford Fusion HEV (FEV AV Demonstrator) Instrumentation Overview.....	148
Figure I.3.1.1 Overall degree of substitution and supplementation of delivery for household shopping trips	155
Figure I.3.1.2 Likes and Dislikes of Online Shopping Differentiated by Subpopulations.....	156
Figure I.3.1.3 Percent of households that choose mass transit, segmented by distance from residence to the nearest.....	158
Figure I.3.1.4 Life course patterns of family, career status, and mode use in five life course cohorts	160
Figure I.3.1.5 Marginal effects of life events (indicated by row facet) on mode use by cohorts (indicated by column facet). Solid bars indicate values are statistically different from zero at the 10% level.....	161

Figure I.3.1.6 Difference in the marginal effects of life events (indicated by row facets) on (a) women relative to men, and (b) on GenX (born in and after 1965) relative to older generation (born before 1965). Solid bars indicate values statistically different from zero at 10% level. 162

Figure I.3.2.1 Spatial Distribution of Vehicle Shedding..... 175

Figure I.3.2.2 Spatial Distribution of Personal Vehicle Suppression..... 176

Figure I.3.2.3 Spatial Distribution of Impact on Rail Use 177

Figure I.3.3.1 Low and high energy estimates of net energy impact of ridesourcing service in Austin..... 183

Figure I.3.3.2 Range in estimated change in per capita vehicle registrations after TNC entry, by city (only cities with statistically significant effects shown)..... 184

Figure I.3.3.3 Comparison of Texas DMV light-duty vehicle registrations with Polk, US DOT, and Ward’s registrations, by year..... 185

Figure I.3.3.4 Texas DMV and Polk light-duty vehicle registrations for 5 popular models, by year 186

Figure I.3.3.5 Texas DMV and Polk light-duty vehicle registrations in 3 zip codes, by year 187

Figure I.3.3.6 Willingness to share and the sharing success rate of authorized trips over time..... 189

Figure I.3.4.1 A typical example of discrete choice experiment task presented to the respondents 194

Figure I.3.4.2 The impact of activity engagement on travel utility..... 195

Figure I.3.4.3 Elasticity of VMT with respect to travel time 195

Figure I.3.4.4 Statistically significant VMT and VHT sensitivity to changes in key behavioral parameters .. 196

Figure I.3.5.1 Improvements to POLARIS behavioral models under MDS 199

Figure I.3.5.2 Changes in (a) PMT and VMT and (b) PHT and VHT per capita by AV ownership for scenario C..... 202

Figure I.3.5.3 Household vehicle retirement rates by traffic analysis zone for (a) A-high, (b) B-high, and (c) C-high scenarios 202

Figure I.4.1.1 Total F-MEP score, illustrative implementation in Columbus, OH..... 208

Figure I.4.1.2 National scale inter-city F-MEP map using FAF zonal structure 209

Figure I.4.1.3 Illustration of commodity-mode-specific inter-city F-MEP..... 209

Figure I.4.1.4 Change (%) in total F-MEP for hypothetical truck electrification scenario 210

Figure I.4.1.5 Results of truck network assignment and temporal disaggregation 211

Figure I.4.1.6 Impact of platoon size on fuel cost savings..... 212

Figure I.4.1.7 Impact of inter-truck gap on fuel cost savings 212

Figure I.4.1.8 Impact of platoon size on rural interstate highway capacity 212

Figure I.4.1.9 Electrified powertrain sales share projection 213

Figure I.4.1.10 Projected petroleum savings potential due to class 7&8 truck electrification..... 213

Figure I.4.1.11 Powertrain Adoption within Trip Distance Bins, 2050..... 214

Figure I.4.1.12 Change in 2045 freight flow due to cost reductions from truck load-pooling..... 215

Figure I.4.1.13 Total 2045 freight energy consumption for truck load-pooling scenarios 215

Figure I.4.1.14 Truck energy consumption for payload and empty truck factor scenarios..... 216

Figure I.4.1.15 Change in freight flows for multimodal load-pooling scenarios in 2045..... 217

Figure I.4.1.16 Energy consumption in 2045 for multimodal load-pooling scenarios	217
Figure I.4.2.1 Energy Estimates from one-mile delivery tests (INL)	221
Figure I.4.2.2 Energy estimates from internal logs versus external instruments (INL).....	221
Figure I.4.2.3 Total average daily energy usage by scenario for UPS and FedEx Chicago Fleets	222
Figure I.4.2.4 Effect of alternative technologies on fleet-wide average daily energy usage for Chicago.....	223
Figure I.4.2.5 Effect of parcel lockers on total energy usage: Chicago	224
Figure I.4.3.1 Left: Top-Down Model Implementation and Process for Workflow Scenario Analysis; Right: Routing for E-commerce Analysis.....	228
Figure I.4.3.2 Supply Chain Formation in Ground-Up (Fully Agent-Based) Model.....	228
Figure I.4.3.3 Base and Projected MDT/HDT VMT and Energy Consumption across Scenarios	229
Figure I.4.3.4 VMT and Energy Use with Retail Purchasing and Powertrain Efficiency Improvements	230
Figure I.5.1.1 Parking Revenue per Passenger	236
Figure I.5.1.2 Distributions of Transactions per Mode at SFO.....	236
Figure I.5.1.3.....	237
Figure I.5.1.4 Survey Question response statistics	237
Figure I.5.1.5 EEMS Program Mission Statement.....	238
Figure I.5.1.6 Definition of Mobility	238
Figure I.5.1.7 Factors that affect the MEP Metric	239
Figure I.5.1.8 MEP Score overlay of SAN Francisco Area	239
Figure I.5.2.1 Thirty minute isochrone for biking	243
Figure I.5.2.2 MEP maps by mode for Denver, CO: A) All modes; B) Car; C) Transit, walk, and bike combined.....	244
Figure I.5.2.3 MEP Scenario Analysis Results for Chicago, IL.	246
Figure I.5.3.1 Map of New York state clustering results.....	251
Figure I.5.3.2 Spider plots showing indicators of independent variables, in scaled relation to each other, for each of the four cluster settlement types.....	251
Figure I.5.3.3 Mobility and energy outcomes by typology.....	252
Figure I.5.3.4 Overview of Interactions in Transportation Systems	252
Figure I.5.4.1 Diagram of integrated workflow for Scenarios B and C.....	257
Figure I.5.4.2 A: Sharing is Caring, B: Tech Takeover, C: All About Me, BAU: Business as Usual (vehicle tech.), VTO: VTO Goals Achieved (vehicle tech.).....	259
Figure I.5.4.3 Rent vs. Jobs Nearby.....	259
Figure I.5.4.4 Job Density vs Jobs Nearby	260
Figure I.5.4.5 Population Density vs. Jobs Nearby.....	260
Figure I.5.4.6 A: Sharing is Caring, B: Tech Takeover, C: All About Me, BAU: Business as Usual (vehicle tech.), VTO: VTO Goals Achieved (vehicle tech.).....	261
Figure I.5.5.1 Diagram of schematic curbside allocation in a dense urban area.....	262

Figure I.5.5.2 Schematic spatial layout of case study.....	265
Figure I.5.6.1 Workflow of the AMD Modeling and Simulation Toolkit	269
Figure I.5.6.2 Satellite Photo and Simulation Route Configuration. The modeling and simul -Taxi Test Field Phase 0 (CU-ICAR) and Phase 1 (Verdae District) at Greenville, SC: (a) satellite image (b) AMD Simulation Network And Fixed-Route Configuration	270
Figure I.5.6.3 Travel costs with Tabu-search based optimization and RSRH	271
Figure I.5.7.1 POLARIS-UrbanSim Workflow	277
Figure I.5.7.2 POLARIS accessibility measures for (a) base2015 and (b) difference between base2025 and base2015	278
Figure I.5.7.3 Population density from UrbanSim runs for (a) base 2015, (b) base 2025 and (c) base 2040 ..	278
Figure I.5.8.1 Vissim simulation model for the studied comparisons traffic network.....	283
Figure I.5.8.2 Comparison of average vehicle delay during the simulation test period for three types of control: pre-time (base case), linear control and linear optimal control. Initial green = 60s,.....	284
Figure I.5.8.3 Distribution of the delays over the simulation test period for pre-timed (base case), linear control and linear optimal control. Initial green = 60s,.....	284
Figure I.5.8.4 Algorithm performance as a function of sensing range.....	285
Figure I.5.8.5 Safety comparison between signal performance and crashes at an intersection.....	287
Figure I.6.1.1 The Framework for the Model of TNC Parking Maneuver with PATH Model.....	292
Figure I.6.1.2 Parking Maneuver Algorithm.....	293
Figure I.6.1.3 San Pablo Avenue Network for simulation	294
Figure I.6.1.4 Microscopic traffic simulation in Aimsun. Left: the scope of the freeway corridor with location of detector stations from PeMS; Right: the Aimsun network model	296
Figure I.6.1.5 Time-dependent network density	301
Figure I.6.1.6 Average speed in the network	301
Figure I.6.2.1 BEBOP Super Computer Resource at Argonne	306
Figure I.6.2.2 RoadRunner workflow to simulate a CAV scenario	308
Figure I.6.2.3 Large-scale RoadRunner simulation workflow.....	309
Figure I.6.2.4 RoadRunner vehicles can now be run in IPG CarMaker (left) and CARLA (right)	309
Figure I.6.2.5 RoadRunner user interface based on AMBER framework	310
Figure I.6.2.6 SVTRIP user interface based on AMBER framework.....	311
Figure I.6.3.1 Adding realistic traffic to RoadRunner simulations through linkages with SVTRIP and Aimsun.....	313
Figure I.6.3.2 Simulink diagram of a RoadRunner scenario with dummy lead SVTRIP vehicle.....	314
Figure I.6.3.3 Structure using Aimsun microAPI to link RoadRunner to Aimsun	315
Figure I.6.3.4 Structure using Aimsun microSDK to link RoadRunner to Aimsun.....	315
Figure I.6.3.5 Speed of dummy SVTRIP vehicle called within RoadRunner.....	316
Figure I.6.3.6 Vehicle speed for 2 vehicles with or without traffic (left), and fuel consumed by the first vehicle (right).....	316

Figure I.6.3.7 Speed and acceleration trajectory of five RoadRunner vehicles [solid red lines], which are either human-driven vehicles [left] or eco-driving CAVs [right], and default Aimsun human-driven vehicles [dotted blue lines]	317
Figure I.6.4.1 POLARIS-simulated PEV public charging demand from unconstrained network (background) and EVI-Pro synthesized charging station locations (foreground).	321
Figure I.6.4.2 Modeling workflow between BEAM, EVI-Pro, and FCSPlan (Fast Charging Station Plan) to site charging infrastructure for BEAM simulations.	322
Figure I.6.4.3 BEAM-simulated PEV public charging demand from unconstrained network (background) and EVI-Pro synthesized charging station locations (foreground).	322
Figure I.6.4.4 Simulated charging demand across Chicago in the six workflow scenarios.	323
Figure I.6.5.1 Modules associated with TNC Operation in POLARIS.....	327
Figure I.6.5.2 TNC Results (a) Change in key TNC metrics from baseline (b) share of empty miles and travel hours.....	328
Figure I.6.5.3 Share of vehicles performing pickup, dropoff, repositioning trips or idle by time of day for scenarios (a) A1 and A4, (b) B1 and B4.....	329
Figure I.6.5.4 Vehicle miles traveled by TNC’s for the San Francisco Bay Area across the workflow scenarios, differentiating between miles without a passenger (hatched) and miles with multiple passengers (blue).....	330
Figure I.6.5.5 Average wait times for TNC trips across the workflow scenarios.	331
Figure I.6.6.1 High Level Scenario Description	334
Figure I.6.6.2 Modal Market Shares for the San Francisco Bay Area across Scenarios.....	335
Figure I.6.6.3 Context-specific value of travel time (VOTT) weighting factors averaged over all trips for each mode, across the workflow scenarios. Because travel time is undesirable, lower VOTT factors make a mode more attractive, leading to higher modal shares as well as higher MEP which is based on generalized travel time	336
Figure I.6.6.4 Aggregate MEP values for the workflow scenarios disaggregated by mode	337
Figure II.1.1.1 Example RGB Image from CARLA (https://carla.readthedocs.io/en/latest/cameras_and_sensors/).....	341
Figure II.1.1.2 Example Semantic Segmented Image from CARLA (https://carla.readthedocs.io/en/latest/cameras_and_sensors/).....	341
Figure II.1.1.3 Example Depth Images from CARLA (https://carla.readthedocs.io/en/latest/cameras_and_sensors/).....	341
Figure II.1.1.4 Scalable learning architecture for multi-client learning. AI-gym RL framework for CARLA capable of running on large GPU-based HPC systems.....	342
Figure II.1.1.5 Combining imitation learning and reinforcement learning to accelerate vehicle controller training (from [1]).....	342
Figure II.1.1.6 2D AI-gym driving simulator. Learning to drive in 2D (with “distance to obstacles” and/or “location of obstacles” as observation) is much faster than learning directly in CARLA.....	342
Figure II.1.1.7 SUMO gym environment allows for RL using realistic driving (continuous control) within existing microscopic traffic simulator.	342
Figure II.1.1.8 Combining simulated driving in 2D and 3D. (top left) Camera view in CARLA, (top right) corresponding view in 2D simulator showing pseudo-LIDAR beams, (bottom) the “observation” in 2D providing distance-to-lane-boundary as a function of angle (green=forward “view”, blue=side and back “view”).....	343

Figure II.1.2.1 345

Figure II.1.2.2 Fuel consumption for Shallowford Rd. Region for the original signal timing and for an improved signal timing plan. 350

Figure II.1.2.3 Time lost (left) and average speeds (right) for passenger (orange) and truck (blue) traffic. Solid lines denote results with elevation data whereas dashed lines are without elevation. 350

Figure II.1.2.4 Chattanooga-Hamilton road network color coded according to maximum altitude in feet of each link in the network (left), and normalized energy consumption (gge per meter) for each link in the AB (middle) and BA (right) directions, predicted by a generalized model for a conventional vehicle running on gasoline. 352

Figure II.1.2.5 The estimated energy consumption of vehicles running in the SUMO. Passenger cars consumed less energy despite having traveled the longest distance (about 2000 miles). Trailers consumed the most significant amount of fuel. Trailers and trucks only traveled about one-third of the distance of passenger cars. 353

Figure II.1.2.6 Screenshots of different parts of the situational awareness tool. Top: Landing page (left), corridors page (middle), and metrics page (right). Bottom: Region view with some of the sensors (left) and MEP (right). 354

Figure II.1.2.7 Traffic crashes from the TITAN database for December 3–9, 2018 (left), and Hamilton County 911 vehicle and non-vehicle incidents by time of day (middle) and day of the week (right). 355

Figure II.1.3.1 Data collection to estimate fuel consumption using GRIDSMART cameras. GRIDSMART installations at ORNL will be used in conjunction with a ground imaging system. The simultaneous captures will be used to produce a library of images suitable for training a machine learning algorithm to estimate fuel consumption. 358

Figure II.1.3.2 SUMO simulation with Deep Q-Learning with visual information from adjacent intersections. “Regular” fuel consumers are on the left and heavy fuel consumers are on the right. These results show a flattening of the right distribution indicating the learned control policy using GRIDSMART-like visual information stops heavy fuel consumers for minimal times. 361

Figure II.1.4.1 Volume estimation modeling framework 364

Figure II.1.4.2 A web application prototype for the volume estimation 365

Figure II.1.4.3 Geospatial distribution of CCSs on Denver roadway network 366

Figure II.1.4.4 Performance of XGBoost Algorithm in Predicting Traffic Volumes 368

Figure II.1.5.1 Distribution of MAE for different number of partitions. 372

Figure II.1.5.2 Training time for DCRNNs with different number of partitions 373

Figure II.1.5.3 Distribution of MAE of all nodes 373

Figure II.1.5.4 Box plot distribution of MAE for speed and flow forecasting. From left to right the box plots show the results of: speed forecasting from speed only model, speed forecasting from multi-output model, flow forecasting from flow only model, and flow forecasting from multi-output model. 373

Figure II.1.5.5 Closeness of the predicted flow and speed with observed flow and speed plotted in the form of a fundamental traffic flow diagram. 374

Figure II.1.5.6 Data ingestion framework 374

Figure II.1.5.7 Hypothetical incident location in red 375

Figure II.1.5.8 Traffic flow without rerouting 375

Figure II.1.5.9 Traffic flow with rerouting 375

Figure II.1.5.10 Simulation parallel scaling with 100% active vehicle rerouting penetration on Cori.....	376
Figure II.1.5.11 Preliminary vehicles assessed for data-driven estimation technique	376
Figure II.1.5.12 Example Speed vs Time and corresponding tractive force versus speed plots for two example drive cycles.....	376
Figure II.1.5.13 Chevrolet Bolt predicted versus actual energy consumption.....	377
Figure II.1.5.14 Instant energy consumption prediction for Nissan Leaf using LSTM. Note negative values denote discharging energy from the battery, i.e., driving, and the positive values mean the charging energy into the battery, i.e., braking mode.....	378
Figure II.1.5.15 Instant fuel consumption prediction for Nissan Altima using LSTM.....	378
Figure II.1.5.16 Average fuel consumption rate calculations using the GPS probe data for Nissan Altima, Ford Focus and Ford F-150.....	378
Figure II.1.5.17 Scaling Performance and the need for HPC.....	379
Figure II.1.5.18 Comparing the prediction of the classical BPR function with that of the data-driven counterpart. Classical BPR underestimates the travel time (in other words paints a more optimistic picture)	379
Figure III.1.2.1 Inverse probability density function of position with comparison of constant and linearly decaying probability.	388
Figure III.1.2.2 Block diagram of the optimal lane selection NLP distributed MPC framework.	389
Figure III.1.2.3 The chassis dynamometer VIL setup.....	389
Figure III.1.2.4 Mean fleet fuel efficiency improvements over the 0% CAV case at each input vehicle volume/hour	390
Figure III.1.2.5 Cell density plots showing dense groups of vehicles in the network at 0%, 30% CAV penetration. With the introduction of CAVs, shockwave effects were dissipated.....	390
Figure III.1.2.6 Energy improvement relative to the reactive baseline algorithm of [3] at varied CAV market penetration rate.	390
Figure III.1.2.7 VISSIM traffic network.....	391
Figure III.1.2.8 Percent reduction in fuel consumption (bottom) and travel time (top) compared to NLC vehicles at 1924 (left), 2478 (center), and 3927 (right) vehicles per hour and desired speeds distributed about 80 kph.	391
Figure III.1.2.9 Low-level speed controller performance comparison at low speed range.....	392
Figure III.1.3.1 Model framework	397
Figure III.1.3.2 System architecture for the activity generation and simulation model.....	399
Figure III.1.3.4 Mode shares before and after introducing AVs.....	401
Figure III.1.3.5 Activities in northern City of Riverside area.....	401
Figure III.1.3.6 The impact of CAV penetration rate on (a) traffic throughput capacity and (b) travel time ..	402
Figure III.1.4.1 Proposed Eco-CAC system	404
Figure III.1.4.2 LA network - speed harmonization logic test network (LA network).....	406
Figure III.1.4.3 Eco-CACC-I controller test results.....	407
Figure IV.1.1.1 Livewire Data Platform Concept.....	411
Figure IV.1.1.2 FY19 TSDC Data Additions	412

Figure IV.1.1.3 Fleet DNA Data Additions 413

Figure IV.1.2.1 Electric drive in-the-loop installation utilizing IPG Carmaker Real-Time environment. 418

Figure IV.1.2.2 PTV Vissim micro-traffic and IPG Carmaker co-simulating in a single environment..... 419

Figure IV.1.2.3 ORNL truck following algorithm in practice utilizing the High Definition phenological radar model. 419

Figure IV.1.2.4 ORNL modular communications stack. 420

Figure IV.1.2.5 HIL testing of the V2V test in the IPG Carmaker environment. 420

Figure IV.1.3.1 Energy for transportation workflow 423

Figure IV.1.3.2 Overview of the sizing and performance evaluation process in AMBER..... 424

Figure IV.1.3.3 Vehicle-in-the-loop concepts 425

Figure IV.1.3.4 Comparison of test vehicle operation on a US06 cycle with varying longitudinal models 426

Figure IV.1.3.5 Overview of the vehicle-in-the-loop environment 426

Figure IV.1.3.6 Road load reduction data from second vehicle in two-vehicle platoon at 70 MPH along with a fit of a phenomenological model from the literature 428

Figure IV.1.3.7 Three-vehicle platoon direct axle torque results for various gaps at 70 MPH 428

List of Tables

Table 1. Alignment of EEMS Activities with Strategic Goals	6
Table I.1.1.1 Grid Mix Assumed for Each Scenario	20
Table I.1.2.1 Primary Independent Variable Parameters and Key Assumptions	29
Table I.1.4.1. Factors by which to Segment the Freight Trucking Industry	46
Table I.1.4.2 Approximate charge times in hours for different types of chargers based on a 2 kWh/mile usage	47
Table I.1.4.3 Distribution of fleets and trucks by fleet size	47
Table I.1.4.4 Summary of Suitability for Full Vehicle Sample	57
Table I.2.1.1 Screenshot of Autonomie Output Results.....	64
Table I.2.1.2 Average Vehicle MPG under Traffic Inputs of 10% and 100% Intersection Capacity	72
Table I.2.1.3 Comparison of Stop Time and Number of Stops on Mainline vs On-Ramp	74
Table I.2.1.4 Summary of Emission and Fuel Consumption Estimates (No metering vs. local responsive ramp metering).....	75
Table I.2.2.1 Fleet Metrics by Geofence Scenario and Vehicle Ownership Reduction.....	81
Table I.2.3.1 Summary of the Main Variables in the Case Study.....	88
Table I.2.4.1 Market Penetration Rates Considered for Assessment.....	96
Table I.2.4.2 Summary of Statistics for the Entry Time Error.....	99
Table I.2.6.1 Data Mapping Rule Linking Traffic Simulation and Test CAVs.....	111
Table I.2.6.2 Signal Time Messages from the Simulation.....	111
Table I.2.6.3 Procedure for Test System Synchronization.....	112
Table I.2.8.1 Unproductive Fuel Consumption by Scenarios	133
Table I.2.8.2 Vehicle Stopping and Fuel Consumption at Signalized Intersection.....	136
Table I.2.8.3 Vehicle Stopping and Fuel Consumption at Unsignalized Intersection	138
Table I.2.8.4 Fuel Saving Results Reported by various Studies on Eco Approach and Departure.....	139
Table I.2.8.5 Eco-Driving Vehicle Fuel Consumption	144
Table I.2.9.1 Key Contributors to Observed Super Cruise On-Road Accessory Loads	148
Table I.2.9.2 Key Contributors to Observed AV Demonstrator On-Road Accessory Loads	149
Table I.3.1.1 Summary of Analysis and Deliverables Plan	153
Table I.3.1.2 Means Comparisons: Hypotheses 1 and 4.....	164
Table I.3.1.3 Means Comparisons: Hypotheses 2 and 3	165
Table I.3.1.4 Logit Results (odd ratios) by Hypothesis	166
Table I.3.4.1 Impact on Mobility and Energy as VOTT Changes	196
Table I.3.5.1 Household E-Commerce Demand Model: Parameter Estimates.....	201
Table I.4.1.1 Criteria for Road Link Platooning Eligibility	211
Table I.4.1.2 2050 Sales Fleet Lifetime Cost (\$/mile).....	214

Table I.4.1.3 Scenarios Exploring the Impact of Truck Payload and Empty Truck Factor 216

Table I.4.3.1 Results: MDT and HDT Impacts across Workflow Scenarios 229

Table I.5.2.1 MEP Inputs from Various Models across the Workflow 245

Table I.5.5.1: Summary of Selected Findings, Organized by City ID 264

Table I.5.5.2: Results from case study sensitivity analyses 266

Table I.5.6.1 Performance Metrics of Mode Choice Results 273

Table I.5.8.1 Energy Equivalence of Safety at All Roads and Intersections 286

Table I.6.1.1 $v - \rho$ PFD Coefficients Determined with Baseline Traffic Demand for All Market Penetration Levels 298

Table I.6.1.2 $v - \rho$ PFD Coefficients Calibrated with Simulation Data with 20% Higher Demand over the Baseline T 299

Table I.6.1.3 $q - \rho$ PFD Coefficients for the Right Limb Calibrated with Simulation Data with 20% Higher Demand over the Baseline Traffic 300

Table I.6.1.4 Simulation Results Varying the Market Share of TNC Vehicles 302

Table I.6.3.1 Summary of Two Possible Ways to Link RoadRunner to Aimsun 314

Table I.6.4.1 Summary of EVI-Pro public charging networks simulated for BEAM workflow. 324

Table I.6.5.1 – TNC Fleet Impacts by Size and Demand 329

Table I.6.6.1 Differences in various aggregate metrics from baseline across the Workflow Scenarios. 334

Table II.1.3.1 Confusion Matrix for Near Lane 360

Table II.1.4.1 Performance Assessment of Various Machine Learning Models to Predict Hourly Traffic Volumes 367

Table III.1.2.1 Relative performance results in homogeneous CAV traffic. 390

Table III.1.2.2 Dynamic Speed Tracking Performance. 392

Table III.1.2.3 The Errors in Flow Meter Measurements and OBD Estimations Compared to the Initial Fuel in the Tank. 393

Table III.1.3.1 Fundamental Influencing Factors 399

Table III.1.4.1 System-Wide Impacts of Eco-routing on Large Networks 405

Table III.1.4.2 Network-Wide Benefits of Speed Harmonization Logic 407

Table IV.1.3.1 Gear-Skipping Impact on Pickup Truck Drive-Cycle Fuel Economy 423

Table IV.1.3.2 Gear-skipping impact on pickup truck acceleration performance 423

Table IV.1.3.3 Sizing Requirement Summary for Components Used in Heavy Vehicles 424

(This page intentionally left blank)

Vehicle Technologies Office Overview

Vehicles move our national economy. Annually, vehicles transport 11 billion tons of freight—about \$35 billion worth of goods each day¹—and move people more than 3 trillion vehicle-miles.² Growing our economy requires transportation and transportation requires energy. The transportation sector accounts for approximately 30% of total U.S. energy needs³ and 70% of U.S. petroleum consumption.⁴ The average U.S. household spends over 15% of its total family expenditures on transportation, making it the most expensive spending category after housing.⁵

The Vehicle Technologies Office (VTO) has a comprehensive portfolio of early-stage research to enable industry to accelerate the development and widespread use of a variety of promising sustainable transportation technologies. The research pathways focus on fuel diversification, vehicle efficiency, energy storage, and mobility energy productivity that can improve the overall energy efficiency and efficacy of the transportation or mobility system. VTO leverages the unique capabilities and world-class expertise of the National Laboratory system to develop innovations in electrification, including advanced battery technologies; advanced combustion engines and fuels, including co-optimized systems; advanced materials for lighter-weight vehicle structures; and energy efficient mobility systems.

VTO is uniquely positioned to address early-stage challenges due to strategic public-private research partnerships with industry (e.g., U.S. DRIVE, 21st Century Truck Partnership) that leverage relevant expertise. These partnerships prevent duplication of effort, focus DOE research on critical R&D barriers, and accelerate progress. VTO focuses on research that industry does not have the technical capability to undertake on its own, usually due to a high degree of scientific or technical uncertainty, or that is too far from market realization to merit industry resources.

Annual Progress Report

As shown in the organization chart (below), VTO is organized by technology area: Batteries & Electrification R&D, Materials Technologies, Advanced Engine & Fuel R&D, Energy Efficient Mobility Systems, Technology Integration, and Analysis. Each year, VTO's technology areas prepare an Annual Progress Report (APR) that details progress and accomplishments during the fiscal year. VTO is pleased to submit this APR for Fiscal Year (FY) 2019. In this APR, each project active during FY 2019 describes work conducted in support of VTO's mission. Individual project descriptions in this APR detail funding, objectives, approach, results, and conclusions during FY 2019.

¹ Bureau of Transportation Statistics, Department of Transportation, Transportation Statistics Annual Report 2018, Table 4-1. <https://www.bts.gov/tsar>.

² Transportation Energy Data Book 37th Edition, Oak Ridge National Laboratory (ORNL), 2019. Table 3.8 Shares of Highway Vehicle-Miles Traveled by Vehicle Type, 1970-2017.

³ Ibid. Table 2.1. U.S. Consumption of Total Energy by End-use Sector, 1950-2018.

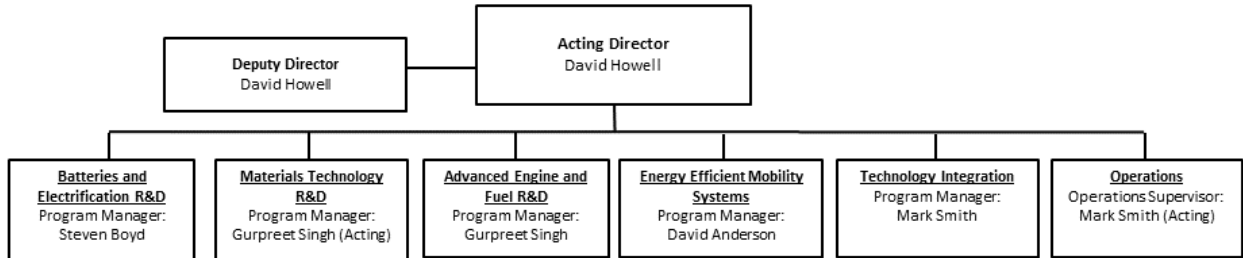
⁴ Ibid. Table 1.12. U.S. Transportation Petroleum Use as a Percent of U.S. Petroleum Production, 2018.

⁵ Ibid. Table 10.1. Average Annual Expenditures of Households by Income, 2016.

Organization Chart

Vehicle Technologies Office

February 2020



Energy Efficient Mobility Systems Program Overview

Introduction

On behalf of the Energy Efficient Mobility Systems (EEMS) Program of the U.S. DOE's EERE VTO, we are pleased to submit this Annual Progress Report (APR) for Fiscal Year (FY) 2019.

The introduction of disruptive transportation technologies and services, such as connected and automated vehicles, car-sharing, and ride-hailing services, provides new, low-cost mobility options for consumers. Additionally, the evolving retail sector, shaped by the convenience of online shopping, has resulted in not only a shift in how we transport and deliver goods, but it has also had ripple effects in personal transportation. This transforming mobility landscape presents a significant opportunity to improve economic and energy productivity and advance safety, affordability, and accessibility in the transportation sector.

While these changes in the transportation system can provide benefits to the American public, they also present risks, challenges, and questions that must be addressed. DOE conducts research to understand how this transformation will affect transportation energy consumption and identifies opportunities to create more efficient, affordable, reliable, accessible, and secure transportation options that enhance mobility for individuals and businesses. Within DOE's Office of Energy Efficiency and Renewable Energy (EERE), the EEMS Program is responsible for this research portfolio.

This APR describes work that the EEMS Program conducted during FY 2019 in support of the EEMS Program goals as described in the following section.

Mission and Goals

The EEMS Program supports VTO's mission to improve transportation energy efficiency through low-cost, secure, and clean energy technologies. EEMS conducts early-stage research and development (R&D) at the vehicle, traveler, and system levels, creating knowledge, insights, tools, and technology solutions that increase *mobility energy productivity* for individuals and businesses. This multi-level approach is critical to understanding the opportunities that exist for optimizing the overall transportation system. The EEMS Program uses this approach to develop tools and capabilities to evaluate the energy impacts of new mobility solutions, and to create new technologies that provide economic benefits to all Americans through enhanced mobility.

During FY 2019, the EEMS Program developed an accessibility metric framework known as *mobility energy productivity*. Because EEMS aims not only to reduce the energy consumed in the transportation system, but also to reduce the time and cost associated with moving people and goods while improving access to mobility, a comprehensive metric that incorporates all three factors (energy, time, and cost) is required. Mobility energy productivity (MEP) is used as a lens through which the EEMS program can evaluate the mobility impacts that potential technologies and services may have, and by which program success can be measured as it develops new mobility solutions.

The EEMS Program works towards achieving three strategic goals in order to reach the program's overall goal of *identifying critical pathways and developing innovative technology solutions to enable significant improvements in mobility energy productivity when adopted at scale*. Each strategic goal is discrete, but all three goals are interrelated such that the success in any one goal furthers the achievement of the other two.

STRATEGIC GOAL #1: Develop new tools, techniques, and core capabilities to understand and identify the most important levers to improve the energy productivity of future integrated mobility systems.

STRATEGIC GOAL #2: Identify and support early stage R&D to develop innovative technologies that enable energy efficient future mobility systems

STRATEGIC GOAL #3: Share research insights, and coordinate and collaborate with stakeholders to support energy efficient local and regional transportation systems.

Program Organization

To achieve its programmatic goals, the EEMS Program implements five coordinated areas of focus, each with its own set of projects. As indicated in Table 1, each of these five activity areas directly supports at least one of the three EEMS strategic goals, and indirectly supports the others. The five activity areas are:

- Systems & Modeling for Accelerated Research in Transportation (SMART) Mobility Laboratory Consortium
- High-Performance Computing & Big Data
- Advanced R&D Projects
- Core Modeling, Simulation, and Evaluation
- Living Laboratories

SMART Mobility Lab Consortium

The SMART Mobility Lab Consortium is a multi-year, multi-laboratory collaborative dedicated to further understanding the energy implications and opportunities of advanced mobility solutions. The effort consists of five pillars of research:

1. Connected and Automated Vehicles (CAVs): Understanding the energy, technology, and usage implications of connectivity and automation and identifying efficient CAV solutions.
2. Mobility Decision Science (MDS): Understanding the human role in the mobility system, including travel decision-making and technology adoption in the context of future mobility.
3. Multi-Modal Freight (MMF): Evaluating the evolution of freight movement and understanding the impacts of new modes for long-distance freight transport and last-mile goods delivery.
4. Urban Science (US): Understanding the linkages between transportation networks and the built environment, and identifying the potential to enhance access to economic opportunity.
5. Advanced Fueling Infrastructure (AFI): Understanding the costs, benefits, and requirements for fueling and charging infrastructure to support energy efficient future mobility systems.

The SMART Mobility Lab Consortium supports EEMS Strategic Goal #1 as the program's primary effort to create tools and generate knowledge about how future mobility systems may evolve and identify ways to reduce their energy intensity. The consortium also directly supports Strategic Goal #2 by identifying R&D gaps that the EEMS Program may address through its advanced research portfolio. The SMART Lab Mobility Consortium will also generate insights that will be shared with mobility stakeholders, indirectly supporting Strategic Goal #3.

High Performance Computing and Big Data

The EEMS Program uses the national laboratories' capabilities in high performance computing (HPC) and big data analytics to research the application of artificial intelligence (AI) techniques such as machine/deep learning and data science tools. These efforts assist in the design, planning, and operation of future mobility systems. HPC helps manage, store, analyze, and visualize conclusions from big data. AI serves to recognize patterns and extract actionable information to answer transportation-related questions through predictive data analytics applied to both vehicle/infrastructure (physical) data and human decision-making (behavioral) data.

The EEMS Program develops and applies the national laboratories' HPC expertise, machine learning, and big data science to find solutions to real-world transportation energy challenges. The program's efforts in this area include:

The HPC4Mobility initiative establishes projects that partner national lab capabilities with third parties who have access to data. The initiative is aimed at accelerating the discovery, design, and development of energy efficient mobility systems by enabling access to computational capabilities and data science expertise in the DOE laboratories. Projects selected under HPC4Mobility will reduce the time and cost required for mobility infrastructure planning, decision-making, and enable optimized control of intelligent transportation systems in real-time.

Additional projects within the Big Data portfolio support the national laboratories to develop the scalable data science and HPC-supported computational framework needed to build next-generation transportation/mobility system models and operational analytics. These projects include multi-lab efforts focused on developing city/regional-scale "digital twins" of the transportation system and applying deep-learning techniques to support the development of resilient automated vehicle control systems.

HPC4Mobility and Big Data initiatives merge exploratory findings of the SMART Mobility Lab Consortium, specific data sets from public and private entities, and unparalleled computational and analytical resources. These resources will solve specific transportation energy challenges faced by cities, states, and regions across the United States, such as how to plan and operate their transportation systems in a way that improves energy efficiency, as their populations grow and new mobility options become available. In doing so, it directly supports Strategic Goals #1 and #2. This activity indirectly supports Strategic Goal #3, as it involves collaboration with stakeholders in the mobility ecosystem to be successful.

Advanced R&D Projects

The EEMS Program's Advanced R&D activities focus on innovative, early-stage, and scalable mobility projects and target system-level opportunities to reduce the energy intensity of the movement of people and goods. The program partners with industry and academia to research and develop technology solutions that lead to mobility improvements through advancements in hardware, software, control systems, advanced sensing and computing, and powertrain components. Competitive funding opportunity announcements (FOAs) solicit project proposals to develop technology solutions that progress the state of the art towards the EEMS Program's targets. Through cost-shared cooperative agreements, FOAs provide technology companies the opportunity to develop innovative and disruptive solutions that the private sector would not otherwise consider due to their risk or uncertainty of return-on-investment, but which could result in enormous public benefits if successful. These solicitations may be broad in scope, calling for a wide variety of proposals for technology development efforts across a range of potential concepts, or may specifically target an explicitly defined research concept. Additionally, the EEMS Program solicits R&D proposals from the national laboratories through periodic lab calls and directly initiate targeted projects with individual labs or lab consortia to leverage specific lab capabilities.

The R&D project portfolio directly supports Strategic Goal #2 by developing innovative technology solutions for mobility. This activity indirectly supports Strategic Goals #1 and #3 since the results from these R&D efforts feed into the analytical work to understand the impacts of these new technologies, and are disseminated to the stakeholder community.

Core Modeling, Simulation, and Evaluation

VTO has successfully conducted hardware evaluations of component and vehicle technologies, developed vehicle systems models based on the results of these evaluations, and performed simulation and analysis of potential vehicle powertrain solutions built upon these models. The EEMS Program develops and maintains these critical capabilities within the national lab system in order to test, evaluate, model, and simulate advanced components, powertrains, vehicles, and transportation systems. These capabilities include vehicle

and component test procedure development, highly instrumented hardware evaluation, controls algorithm validation, high-fidelity physical simulation, and transportation data management and analysis. These capabilities are critical to the EEMS Program in evaluating the energy and mobility outcomes of future transportation systems, and other VTO R&D programs in quantifying the performance and efficiency benefits of specific powertrain technologies under development.

The suite of core VTO evaluation and simulation tools is critical to the EEMS Program’s ability to understand the impacts of future mobility and directly supports Strategic Goal #1. The tool set is also important in identifying research opportunities and producing insights to share with mobility stakeholders and indirectly supports Strategic Goals #2 and #3.

Living Laboratories

EEMS Living Laboratories, led by VTO’s Technology Integration Program, works with cities and stakeholders to demonstrate and evaluate new mobility technologies in the field and collect data. These projects are an important feedback mechanism to R&D and provide a source of real-world data to test, validate, and improve models, simulations, software, and hardware. The EEMS Program coordinates and collaborates with stakeholders to support city and regional efforts to develop energy efficient transportation systems through key elements of an implementation strategy: stakeholder engagement, Living Laboratory projects, and technical assistance.

As the primary insight sharing and stakeholder collaboration element of the EEMS Program, Living Laboratories directly supports Strategic Goal #3. Additionally, the data collected through the Living Labs activity is important to the analytical and R&D efforts and indirectly supports Strategic Goals #1 and #2.

The table below shows how the EEMS activities align with the EEMS strategic goals.

Table 1. Alignment of EEMS Activities with Strategic Goals

EEMS STRATEGIC ALIGNMENT			
LEGEND ● = Activity Directly Supports Goal ▲ = Activity Indirectly Supports Goal	Goal 1: Tools, Techniques, & Capabilities to Understand & Improve Mobility Energy Productivity	Goal 2: Early Stage R&D to Develop Innovative Technology Solutions for Efficient Future Mobility Systems	Goal 3: Insight Sharing, Stakeholder Coordination and Collaboration on Local & Regional Transportation Systems
SMART Mobility	●	●	▲
HPC/Big Data Analytics	●	●	▲
Advanced R&D	▲	●	▲
Core VTO Tools	●	▲	▲
Living Laboratories	▲	▲	●

Coordination

The EEMS program coordinates its activities with other federal agencies, industry stakeholders, and other members of the mobility research community.

Coordination between EEMS and other federal programs focused on connected, automated, and efficient transportation systems is critically important. DOE was a key contributor to *Ensuring American Leadership in Automated Vehicle Technologies – Automated Vehicles 4.0*, a multi-agency report published by the National Science and Technology Council and the U.S. Department of Transportation in January 2020.⁶ EEMS also participates in planning discussions with various modal administrations within USDOT, including the Federal Highway Administration (FHWA), Federal Transit Administration (FTA), and the National Highway Traffic Safety Administration (NHTSA). Coordination with USDOT is critically important due to the linkage between VTO’s research and development activities to create efficient, secure, and sustainable transportation technologies, and USDOT’s mission to ensure our nation has the safest, most efficient and modern transportation system in the world.⁷

In addition to intergovernmental collaboration with DOT, the EEMS Program coordinates with industry partners. For example, U.S. DRIVE (“Driving Research and Innovation for Vehicle efficiency and Energy sustainability”) is a non-binding and voluntary government-industry partnership focused on advanced automotive and related energy infrastructure technology research and development.⁸ In 2019, U.S. DRIVE convened a new Vehicle and Mobility Systems Analysis Technical Team (VMSATT), to identify the most promising areas of pre-competitive mobility research of interest to the government, automotive industry, energy sector, and utility company partners. Additionally, the EEMS Program coordinates with the medium- and heavy-duty trucking and freight industry through the 21st Century Truck Partnership (21CTP)⁹, by pursuing collaborative research and development to realize its vision for our nation’s trucks and buses to safely and cost-effectively move larger volumes of freight and greater numbers of passengers while emitting little or no pollution. The EEMS Program is directly involved with the Operational Efficiency Technical Team within the truck partnership.

The EEMS Program continually seeks additional high-value opportunities to engage with relevant stakeholders in order to share EEMS-funded research results and learn from other mobility-related efforts. For example, the EEMS Program is a governmental sponsor and member of the National Academies/Transportation Research Board Forum on Preparing for Automated Vehicles and Shared Mobility¹⁰, which brings together public, private and other research organizational partners to share perspectives about how the deployment of automated vehicles and shared mobility services may dramatically increase safety, reduce congestion, improve access, enhance sustainability, and spur economic development. The SMART Mobility Lab Consortium has also convened an Executive Advisory Board, comprised of experts and decision-makers representing the automotive industry, technology companies, academia, non-governmental organizations, non-profits, and other transportation-related associations. This board provides input and review to the research conducted by the Consortium, and helps ensure the work performed is aligned with a variety of mobility stakeholders.

⁶ <https://www.transportation.gov/sites/dot.gov/files/docs/policy-initiatives/automated-vehicles/360956/ensuringamericanleadershipav4.pdf>

⁷ <https://www.transportation.gov/about>

⁸ <https://www.energy.gov/eere/vehicles/us-drive>

⁹ <https://www.energy.gov/eere/vehicles/21st-century-truck-partnership>

¹⁰ <http://www.trb.org/TRBAVSMForum/AVSMForum.aspx>

Project Funding

VTO selects and funds critical research through a combination of competitive funding opportunity announcement (FOA) selections, and direct funding to its national laboratories. Competitive FOA projects are fully funded through the duration of the project in the year that the funding is awarded. Funding for direct funded and competitive award projects are contingent on annual Congressional budget appropriations.

The VTO Technology Integration Program funded and has primary management responsibility for Living Laboratories projects during FY 2019. Living Laboratories projects are not included in the FY2019 EEMS APR.

Research Highlights

FY2019 was the third year for Energy Efficient Mobility Systems Program activities, and many of the Program's initial research efforts concluded and delivered results this year. The SMART Mobility Lab Consortium focused on completing individual research projects, and on linking together multiple simulation models to create a multi-fidelity, end-to-end modeling workflow to capture the complex interactions among mobility decision-making, technology implementation, mobility service models and modes, land use, and EV charging infrastructure. This activity produced many research findings and insights about the energy and mobility impacts of new transportation technologies and services. Two new projects were awarded within EEMS' Advanced R&D portfolio in FY2019, and research in the High Performance Computing and Big Data research area made significant progress. Meanwhile, advancements were made in the modeling, simulation, evaluation, and data management tools that support the EEMS Program and VTO more broadly. Results, insights, and progress from these four areas are described in detail through the remainder of this Annual Progress Report. Selected highlights and accomplishments from these activities are summarized here.

- Through the SMART Mobility Advanced Fueling Infrastructure pillar, LBNL and INL used multiple modeling tools and analytical methods to design charging networks and simulate their use by EVs in specific case studies, in order to examine the cost/benefit trade-offs inherent with different approaches to charging infrastructure to serve human-driven and automated electric ride-hailing vehicles. In these studies, parameters defining charging infrastructure were varied, such as the number, location, and power level of charging stations, to determine the effect on EV use and overall system cost. The team found that, without sufficient charging infrastructure, an automated electric vehicle (AEV) ride-hail fleet will be impaired by long queues for charging. In a hybrid ride-hailing fleet with both AEVs and human-driven EVs, charging infrastructure can make a substantial difference in the ability of the overall fleet to serve customer demand, though there is a point of diminished returns when increasing the availability of DC fast charging infrastructure. (I.1.2 – Fueling Infrastructure for Future Shared and Shared-Automated Vehicles)

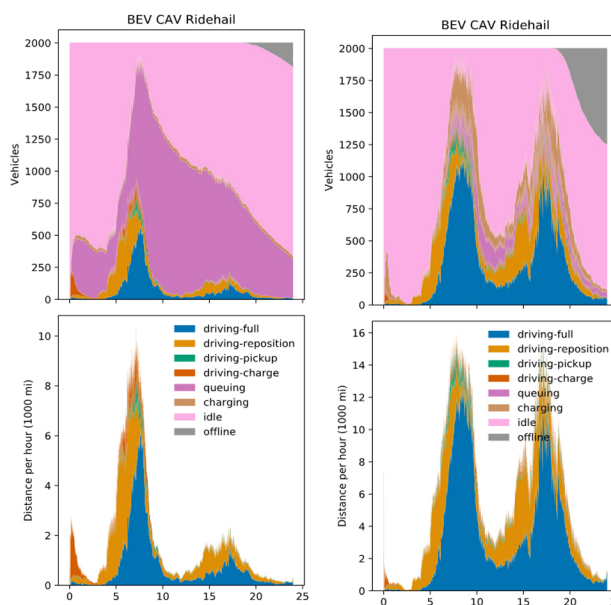


Figure 1 Operation State of Automated Ride-Hail BEVs with Sparse (left) and Rich (right) Charging Infrastructure

- A CAVs Pillar task performed by LBNL developed and applied traffic microsimulation tools to predict the impacts that connected and automated vehicle systems will have on traffic and energy consumption. The team developed a modeling framework that includes microscopic traffic models that depict the interactions among vehicles with adaptive cruise control (ACC), cooperative adaptive cruise control (CACC) and manually driven vehicles, providing a solid foundation for modeling the car following and lane changing behavior in mixed traffic with the CACC operation strategies. The team found significant benefits of CACC over ACC in terms of both highway capacity and fuel consumption – benefits which vary greatly depending upon market penetration of the technology. (I.2.1 – Traffic Microsimulation of Energy Impacts of CAV Concepts at Various Market Penetrations)
- Another task within the CAVs pillar, led by ANL, developed and implemented advanced eco-driving control algorithms for connected and automated vehicles using RoadRunner, a multi-vehicle simulation tool also developed by the team. The large-scale study showed that automation and connectivity combined with energy-focused control strategies may result in significant energy savings – up to 20% – although results are highly dependent on the type of road and driving scenario (highway, suburban, urban, mixed) and powertrain type (conventional, hybrid, or battery-electric). (I.2.3 – Energy Efficient Connected and Automated Vehicles)

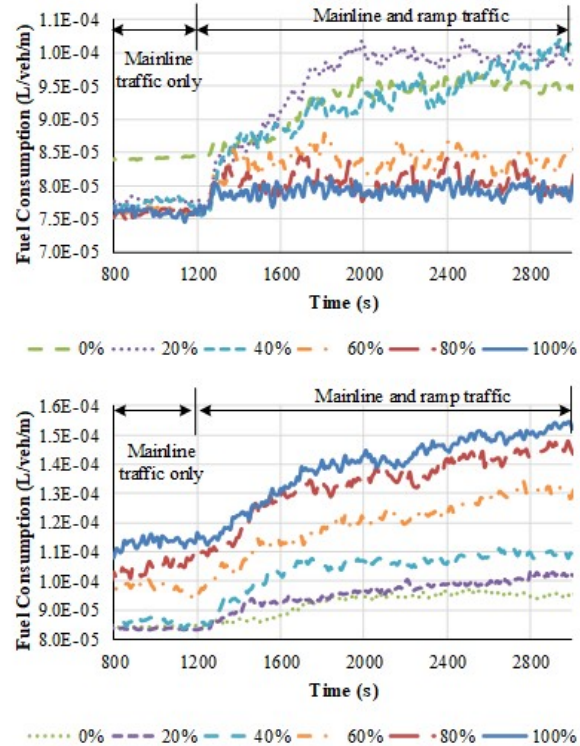


Figure 2 Time Series of Fuel Consumption Impacts of ACC and CACC Vehicles (Upper graph is for CACC cases, Lower graph is for ACC Cases)

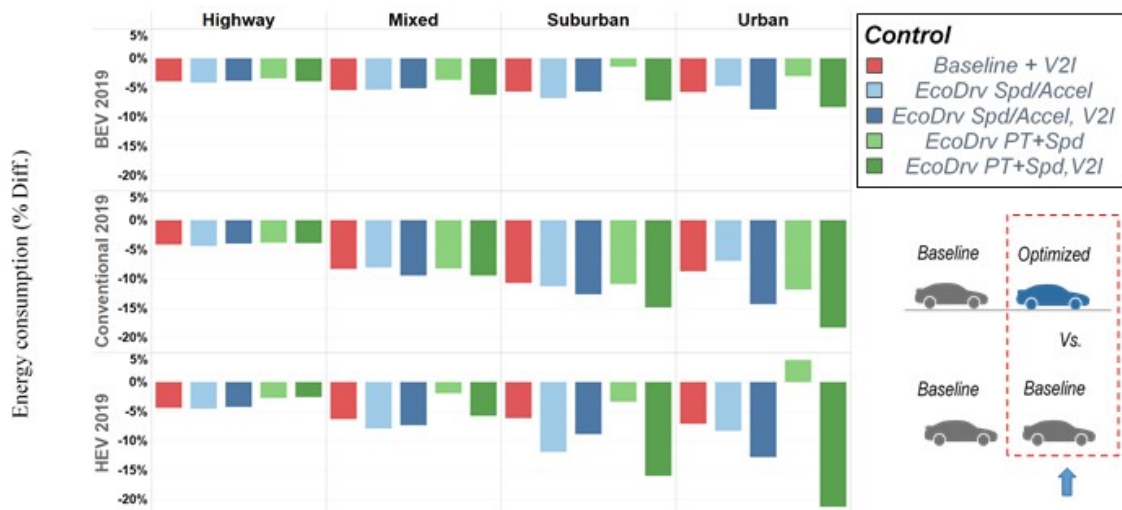


Figure 3 Energy Consumption Savings Relative to Baseline for Lead Vehicle

- Within the Mobility Decision Science pillar, a team led by LBNL, INL, and NREL completed the WholeTraveler Behavioral Study, a regional survey that aimed to descriptively understand the relationships between key life decisions and its corresponding impact on transportation. The findings reveal multiple nuanced relationships among transportation choices and their costs and benefits at the individual and system levels. An example is e-commerce, which has grown in popularity because of the time-saving and convenience benefits of ordering with delivery compared to taking a shopping trip. The team found that, although e-commerce generally replaces more trips than it adds in delivery activity, there is significant variation across the population in this behavior. Additionally, the team elucidated the complexities of the interactions between ride-hailing vehicles and other modes such as transit, with ride-hailing either enabling transit ridership or stealing from it based on factors such as distance of the traveler from a transit station. (I.3.1 – Whole Traveler Study)

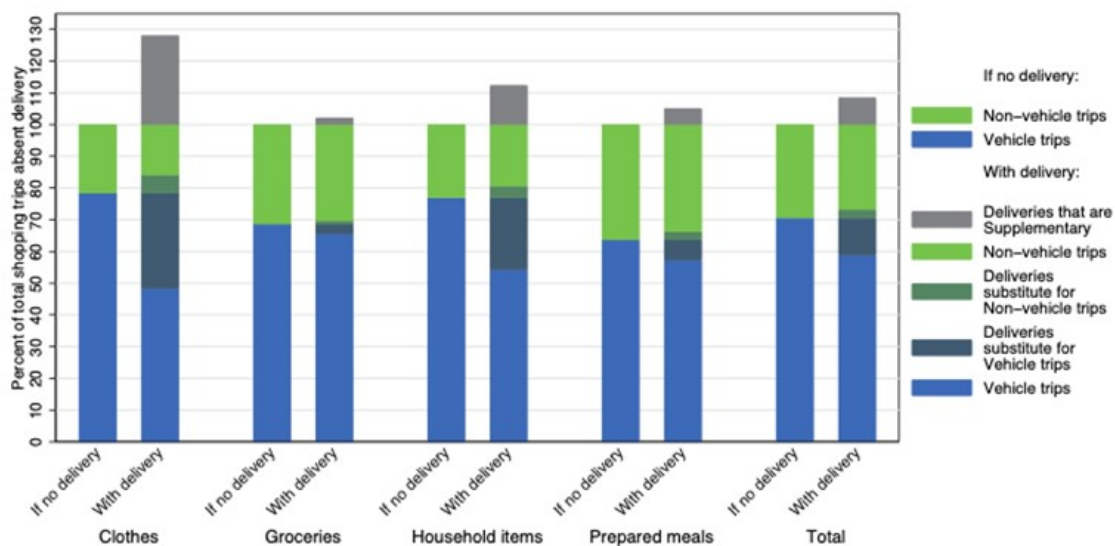


Figure 4 Degree of Substitution and Supplementation of Delivery for Household Shopping Trips

- Mobility Decision Science work led by ANL focused on developing behavioral models as part of agent-based transportation system simulation tools to better characterize individual traveler and mobility decisions. This work included the development of a detailed parking structure (e.g., locations, rates, and type) into the POLARIS model, enhanced activity generation relevant to the value of travel time (VOTT) and multitasking opportunities, simulation of transit buses in mixed traffic, creation of a household-level e-commerce participation model, and incorporation of a vehicle disposal model for future mobility scenarios. Simulation results for a variety of scenarios (a near-term, high-sharing, partial-automation Scenario A; a long-term, high-sharing, high-automation Scenario B, and a long-term, low-sharing, high-automation Scenario C) show the likely modal splits for travelers in the Chicago metropolitan area. (I.3.5 – Travel Behavior Simulation Modeling in POLARIS)

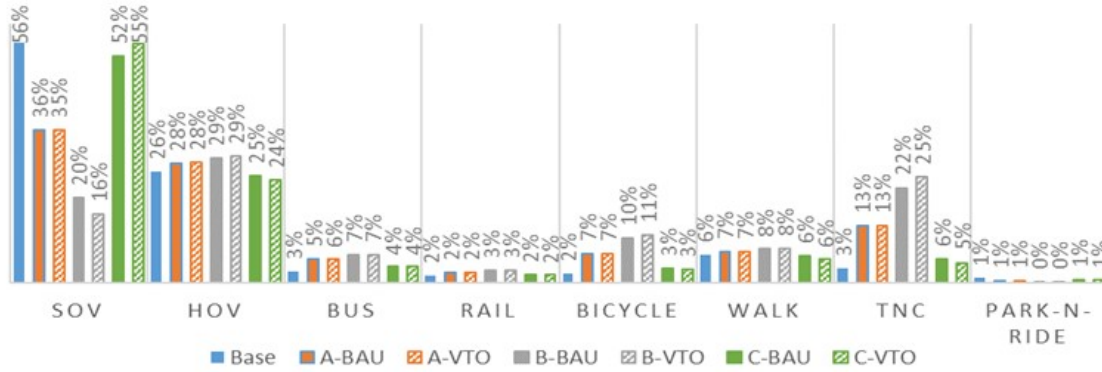


Figure 5 POLARIS Simulation: Mode Share by Scenario

- ORNL and INL led research within the Multi-Modal Freight pillar of SMART Mobility to understand the future of freight transport by evaluating the energy impacts of changes in freight delivery in urban environments due to changes in consumer behavior and new delivery technologies and methods. Research. The team’s research included an investigation of energy profiles of drones through field and laboratory testing, and the development of a model to estimate a synthetic fleet population and service area for two major carriers in Chicago. Results indicate that substantial energy savings are available from changes in delivery methods, though the overall savings depends heavily on the behavior of consumers and composition of the light-duty vehicle fleet (e.g., what passenger vehicles are used to retrieve packages from parcel lockers). (I.4.2 – Optimization of Intra-City Freight Movement with New Delivery Methods)

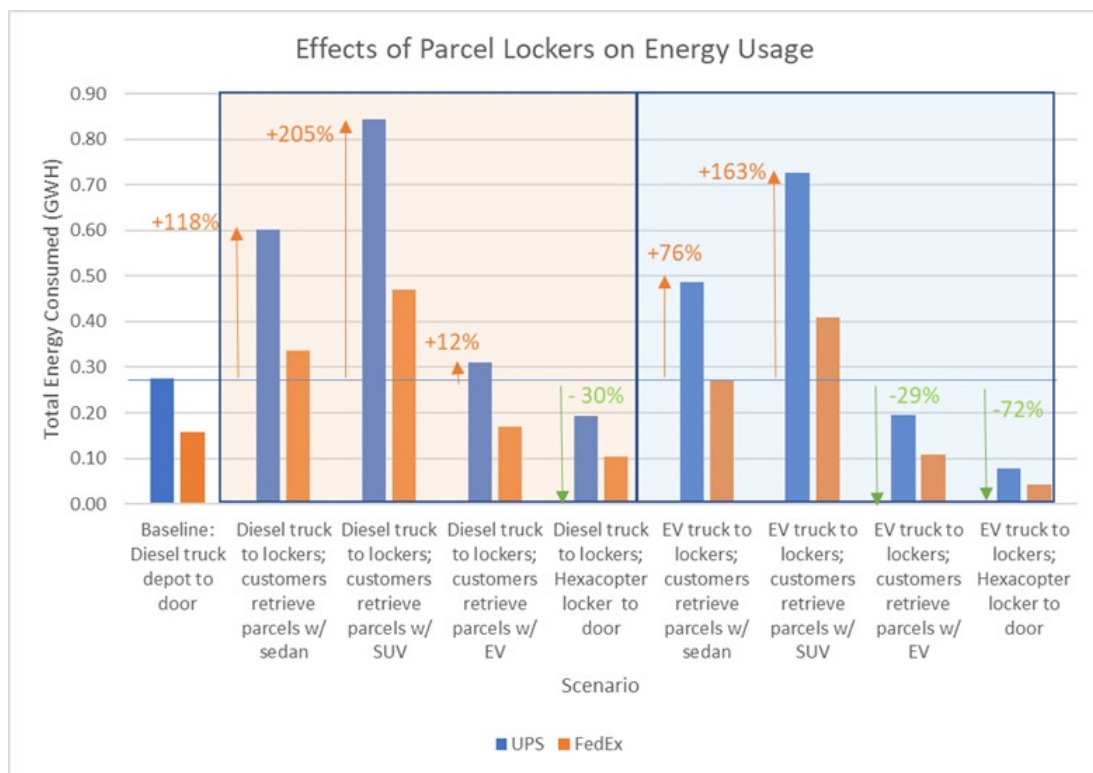


Figure 6 Effect of Parcel Lockers on Total Energy Consumption (Chicago)

- Multi-Modal Freight research led by ANL developed and applied a freight model to evaluate the impacts of freight transportation on vehicle miles traveled (VMT) and energy consumption. The results establish the baseline energy and VMT impacts of freight, demonstrating that freight vehicles have a disproportionately high energy impact (30% of fuel) relative to their VMT (10% of VMT). The team found that, with projected increases of 24% in truck traffic in the next two decades, increased market penetration of efficient powertrain technologies can have sizeable impacts on freight energy consumption, reducing long-term energy use by up to 23–37% compared to the base year in spite of increased freight demand.

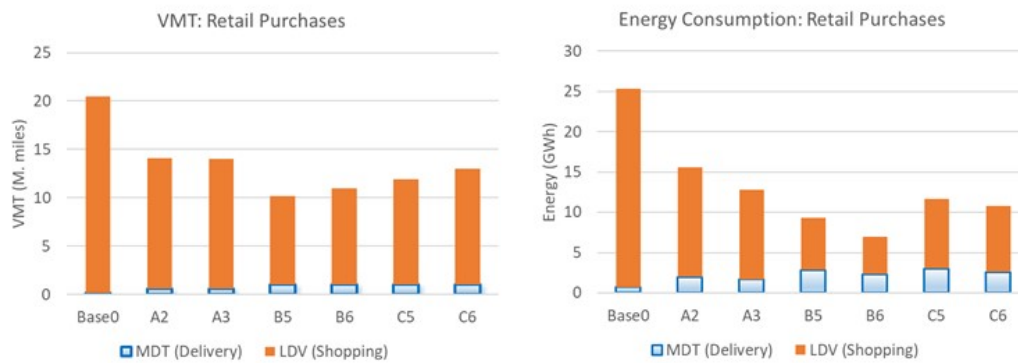


Figure 7 VMT & Energy Use with Retail Purchasing and Powertrain Efficiency Improvements

- Additionally, although e-commerce delivery vehicles create additional truck VMT, e-commerce is shown to reduce overall retail VMT by up to 56% because each delivery adds just a small amount of additional distance to an efficient delivery tour, creating net savings by replacing relatively long-distance shopping trips. Researchers estimated that e-commerce will also reduce net retail transportation energy use between 16% and 33% in the long term, enhancing the benefits of improved powertrain technologies (which alone account for 34–46% of long-term energy reduction). (I.4.3 – Energy and Mobility Impact of Inter/Intra-city Freight Movement using Data-Driven Agent-Based System Simulation)
- Within SMART Mobility’s Urban Science pillar, researchers at NREL completed development of the Mobility Energy Productivity (MEP) metric, a comprehensive metric that reflects energy productivity, affordability and accessibility of current and future mobility services. As part of this activity, the team also developed a calculation module that can be integrated into travel demand models to accurately capture the primary and secondary impacts of new technologies and services on mobility within a region. (I.5.2 – Mobility Energy Productivity Metric)

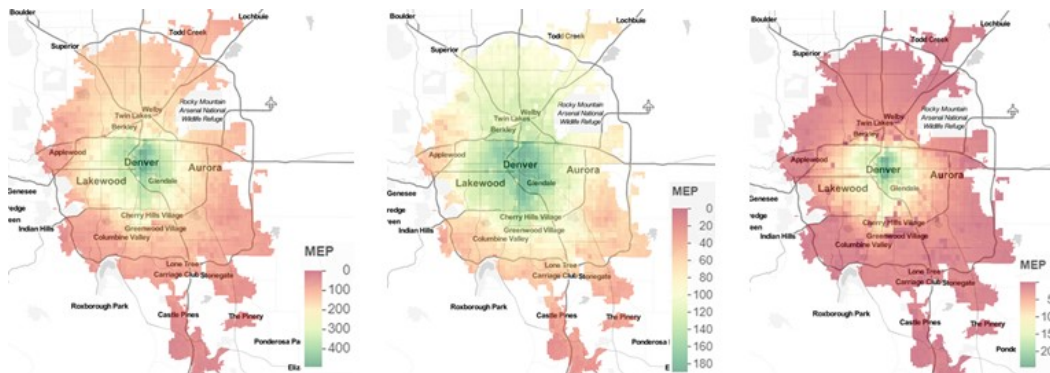


Figure 8 MEP Maps for Denver, CO (Left: All Modes; Center: Car; Right: Transit/Walk/Bike)

- Within EEMS' Advanced R&D Portfolio, Clemson University developed a novel anticipative car following and lane selection algorithm for connected and automated vehicles. The control algorithms, which use information exchange between CAVs to save energy, reduce braking, and harmonize traffic, were implemented in traffic microsimulations at different levels of CAV penetration to analyze energy saving potential, and validated using a Vehicle-in-the-Loop (VIL) testbed to demonstrate the benefits to real CAVs driven on a test-track. Results show that CAVs using the car-following algorithm use 8-33% less energy than human-driven vehicles. The team also demonstrated that vehicles using an optimal lane-selection model could save up to 13.4% of fuel compared to human-driven vehicles, and up to 20.2% relative to vehicle that do not change lanes, dependent upon technology penetration and traffic flow. (III.1.2 – Boosting Energy Efficiency of Heterogeneous Connected and Automated Vehicle (CAV) Fleets via Anticipative and Cooperative Vehicle Guidance)

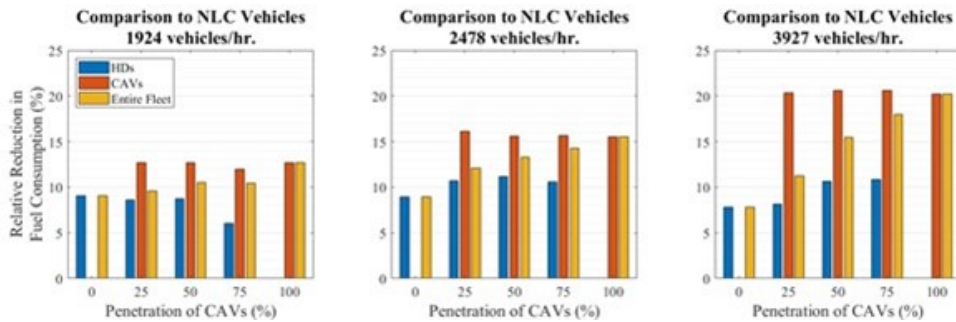


Figure 9 Percent Reduction in Fuel Consumption by Flow Rate and Penetration

- Under the Core Modeling, Simulation, and Evaluation activity area, a team led by NREL, PNNL, and INL completed the first phase of building the Livewire Data Platform, with three objectives: to provide a platform allowing easy and secure data sharing and discovery making it easy to search and share transportation and mobility-related data; to create a community that builds partnerships and collaboration around data rather than competition; and to create a system that allows shared data to grow in size and complexity as EEMS evolves. The goal for this year was to launch an initial version of a data sharing website. This was accomplished, and the platform successfully made available 38 datasets from nine projects. The platform allows for three methods of data sharing: as a data hub, by API, and direct links. (IV.1.1 – Livewire Data Platform)

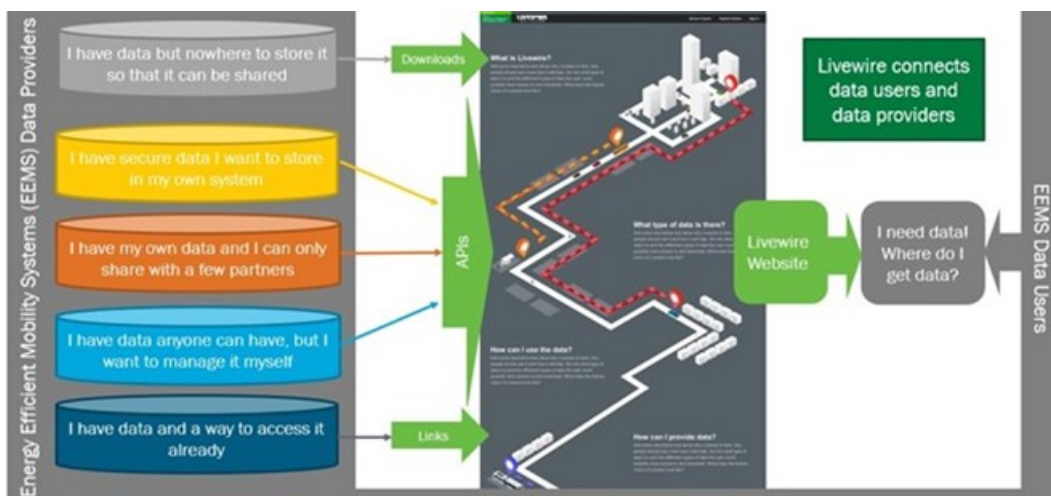


Figure 10 The Livewire Data Platform Concept

- ANL led work under the Core Modeling, Simulation, and Evaluation activity area focused improving simulation tools such as Autonomie and AMBER (Advanced Model-Based Engineering Repository), and conducting experiments to generate empirical data to validate simulation models. The team developed new vehicle-in-the-loop (VIL) capabilities to evaluate real vehicle operation within an emulated traffic environment, and conducted direct aerodynamic road-load measurements on-track for platooning vehicles. Precise, repeatable experiments such as this are critical to ensuring robust results from simulation studies of new mobility technologies. (IV.1.3 – Core Modeling, Simulation, and Evaluation)

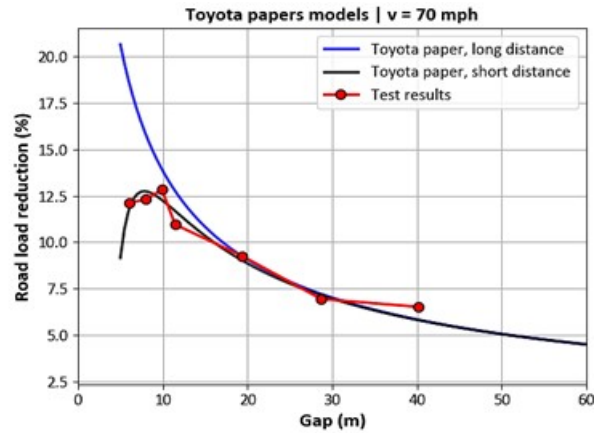


Figure 11 Road-Load Data from Second Vehicle in Two-Vehicle Platoon

We are pleased to submit the Annual Progress Report for the Energy Efficient Mobility Systems Program for FY 2019. Inquiries regarding the EEMS Program and its research activities may be directed to the undersigned.

David L. Anderson
Program Manager

Erin E. Boyd
Technology Manager

Heather Croteau
Technology Manager

Prasad Gupte
Technology Manager

I SMART Mobility

I.1 Advanced Fueling Infrastructure

I.1.1 Quantify National Energy Impact of Electrified Shared Mobility with Infrastructure Support (ANL)

Yan (Joann) Zhou, Principal Investigator

Argonne National Laboratory
9700 S Cass Ave
Lemont, IL 60439
E-mail: yzhou@anl.gov

Eric Wood, Principal Investigator

National Renewable Energy Laboratory
15013 Denver West Parkway
Golden, CO 80401
E-mail: Eric.Wood@nrel.gov

Fei Xie, Principal Investigator

Oak Ridge National Laboratory
2360 Cherahala Boulevard
Knoxville, TN 37932
E-mail: xief@ornl.gov

Erin Boyd, DOE Technology Manager

U.S. Department of Energy
E-mail: Erin.Boyd@ee.doe.gov

Start Date: October 1, 2018

End Date: September 30, 2019

Project Funding (FY19): \$500,000

DOE share: \$500,000

Non-DOE share: \$0

Project Introduction

Infrastructure has long been a major barrier to battery electric vehicles (BEVs) adoption. Cost-effective charging infrastructure is crucial to support the future energy efficient transportation systems. The rapid development and deployment of advanced public charging technologies (e.g., direct current fast charging (DCFC)), coupled with other smart mobility solutions such as vehicle connectivity and shared mobility, will affect future vehicle ownership and use, electricity generation, and alternative fuel energy market. This will further result in major changes in the utilization of alternative transportation modes, energy consumption, and economic activity. Understanding the magnitude and sensitivity of these impacts is key to identifying barriers and achieving mainstream adoption of BEVs.

Objectives

Within this scope, our objective is to quantify the national energy impact of ride-hailing PEVs as compared with privately owned PEVs and ride-hailing ICEVs with varying infrastructure support (e.g., Level 2, DCFC, high power FC). This task helps DOE to understand changes in petroleum and electricity consumption while providing mobility of service (e.g., ride-hailing) using infrastructure supported electrification. This task aims to quantify impact of ride-hailing on national energy and carbon emissions of light-duty vehicles at various ride-hailing demand, infrastructure support, and market penetration of electrified vehicles.

Approach

Energy consumption and emissions of the national light-duty vehicle fleet is a function of the amount of vehicle miles traveled (VMT), vehicle efficiency miles per gallon gasoline equivalent (MPGGE), vehicles market shares (sales), and vehicle survival rates by segment and powertrain technologies. This study separates LDV to three segments; urban ride-hailing, urban personal vehicles, and non-urban personal vehicles. Vehicle market shares and survival rates together determines fleet composition. The following sections explains the assumptions and methodologies used in estimating fleet VMT and fleet composition in more details.

National fleet VMT from 2017 to 2030

National fleet VMT of personal vehicles and ride-hailing vehicles' service VMT (excluding deadheading) is assumed to follow Energy Information Administration (EIA) Annual Energy Outlook (AEO) projections [1]. This study focuses on urban areas because ride-hailing vehicles are mainly located and operating in urban areas in the short-to-middle term [2]. According to the U.S. Census, urban stands for any area with population more than 50,000 [3]. Using national household travel survey (NHTS) [4], highway statistics [5], and census data [3], the urban areas were estimated to cover 72% of the total population and 65% of total LDV stock.

Ride-hailing VMT consists of (1) VMT with passengers; (2) VMT without passengers (deadheading or empty miles); and (3) VMT while out of service (i.e., personal-use miles [not considered in this study because only full-time ride-hailing drivers were modeled]). (1) VMT with passengers is defined by ride-hailing demand, which is the percentage of total VMT in urban area that needs to be served by ride-hailing vehicles. (2) Ride-hailing would affect the total VMT due to induced travel (not considered in this study) and deadheading travel (considered in the sensitivity analysis) (i.e., when no passenger is present). When ride-hailing demand and the number of ride-hailing vehicles are low at the 2017 level (e.g., national average, 0.29% of total vehicle miles traveled), the deadheading miles account for 49% of total travel distance for ride-hailing vehicles according to RideAustin [6]. In the modeling of national energy and emissions as a function of ride-hailing demand, deadheading miles were assumed to drop significantly when ride-hailing demand and the number of ride-hailing vehicles are both high (e.g., 100% of total passenger miles traveled). Literature on this issue is still very limited. The relationship between ride-hailing demand and deadheading miles, which is affected by driver behavior, urban layout and traffic conditions, is not well established in the literature. Therefore, for the purpose of showcasing the spectrum of the potential national energy impact from ride-hailing, when ride-hailing demand grows from 0.29% to 100%, it was assumed that the deadheading miles percentage of total travel drops linearly from 49% to 5%.

Composition of the fleet

Fleet composition depends on vehicles market (sales) penetration by powertrain technologies and vehicle survival rates. The ride-hailing and personal-use vehicle fleets were estimated separately from 2017 to 2030 because they have different survival rates and market composition. BEV share, percentage of ride-hailing BEVs in ride-hailing fleet is an input. It is estimated based on given ride-hailing demand and average VMT per ride-hailing vehicle. With the estimated number of ride hailing BEVs, regional simulation provides future charging coverage optimized to support their travel. Then we quantified charging opportunity for any given charging coverage, and projected resulting market penetration of personal EVs due to increased charging opportunity and other factors. Market penetration of vehicle powertrain technologies (except BEVs and PHEVs) and vehicle fuel efficiencies were assumed to follow the projections made by EIA AEO [1]. Vehicle survival rate stands for percentage of vehicle remained on road by vehicle age. Fast vehicle turn-over, shorter survival rate, would lead to more newer vehicles on the road and higher fleet average fuel efficiency. Assuming the ride-hailing vehicle has similar lifetime VMT as personal vehicle (about 200,000 miles) a full-time ride-hailing vehicle is assumed to have an average life of seven years. We estimated the survival function of ride-hailing vehicles using the assumptions of lifetime VMT, annual VMT, and average vehicle age mentioned above. These estimates are factored into VISION model [7] to estimate the fleet composition.

National energy consumption and emissions

We estimated the nation’s energy consumption and emission using Argonne’s VISION model. VISION model [7] is a scenario tool that estimates the energy and emission impacts of advanced fuel and vehicle technologies in the transportation sector by fuel type, vehicle powertrain type, and vehicle class.

Bottom-up approach

With given number of BEVs and travel demand, the EVI-Pro model [8] was used to estimate the number of chargers and charging level (e.g., Level 2, DCFC, 150-kW) by location for a given year of the chosen study area. In EVI-Pro, future charging stations are optimized to serve ride-hailing charging demand based on their travel pattern and pre-assumed electric range. Using Austin as a case study, EVI-Pro simulated the charging infrastructure requirements in 2030, which was converted to charging coverage in 2030. By dividing the 2030 coverage by 2017 coverage (i.e., the starting condition), the growth rate in charging coverage needed for Austin was estimated to support the given electrified ride-hailing fleet size and their charging demand in 2030. And the growth rate needed in charging coverage for each state was estimated, urban areas only, to support the same level of electrified ride-hailing fleet size and charging demand. The growth rates were weighted by state considering their current ride-hailing demand and charging coverage in urban areas. Following charging opportunity curves developed earlier, we quantified the charging opportunities for personal vehicle by state with the estimated charging coverage in 2030. Then, the ORNL’s MA3T model was used to project the personal EV market penetration by state from 2017 to 2030 with the estimated charging opportunity and simulated average charging level [9]. Other factors affecting EV market penetration are considered in MA3T model. Finally, using the project market penetration, estimated fleet VMT and fleet composition, the reduction in petroleum and increase in electricity was quantified due to electrified ride-hailing vehicles using ANL’s VISION model [7]. Figure I.1.1.1 shows the overall bottom-up approach.

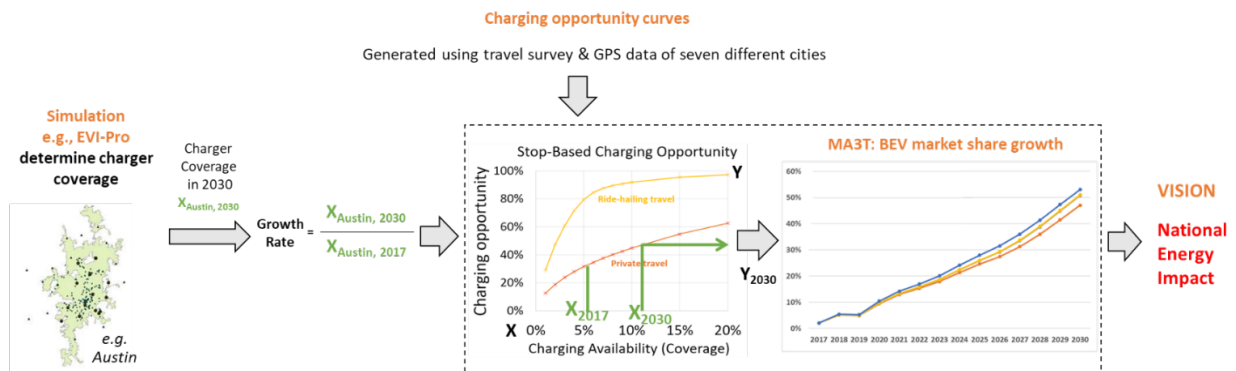


Figure I.1.1.1 Analytical framework of national energy impacts of ride hailing and personal EVs.

Top-down Approach

It is noted that the bottom-up simulation approach is highly region-specific, and dependent on the unique travel patterns of a given region. It also subject to availability of trip data with origins and destination information. Therefore, we also developed a top-down approach, based on probability of charging, to mathematically identify the number of chargers needed with a given ride-hailing BEV fleet size and charging demand using data such as NHTS. In this approach, the number of daily trip stops in urban areas was first determined and categorized by population density groups. Then, the charging probability was determined at each population density group based on distribution of battery SOC and average trip distance. An M/M/c queuing model [10] was used (the first M: the arrival process is Poisson, the second M: the service times are exponential, and c: the number of servers), a multi-server queuing model where arrivals form a single queue and are governed by a Poisson process and service times are exponentially distributed, to estimate the required number of chargers for each 0.25 × 0.25 mile grid cell. Finally, the charging coverage was quantified as a function of percentage of total vehicle trips served by ride hailing BEVs and critical battery SOC. Critical battery SOC means that

vehicles need to be recharged at this level, which could vary by driver, vehicle model, charger level, and mobility type. After estimating the charging coverage, the charging opportunity curve was used to estimate the charging opportunities and then project the personal BEV market penetration. Finally, we quantified the national energy and carbon emissions as a function of ride-hailing demand and the share of BEVs in ride-hailing fleets.

Results

This year's annual report highlights the results from top-down approach, as last year's report showed results from bottom-up approach. We conducted an analysis using top-down approach by varying ride-hailing demand and share of BEVs in the ride-hailing fleet and quantified the range of resulting energy consumption and carbon emissions. Figure I.1.1.2 shows the percentage of energy reduction in 2030 compared to the baseline in 2030, as a function of ride-hailing demand and BEV market penetration. The baseline means ride-hailing demand equals to 0.29%, %BEV sales in 2030 is 32.4%, with infrastructure coverage fixed from 2017 to 2030. Red represents an increase in energy while green indicates a reduction. Ride-hailing vehicle life was assumed to be seven years.

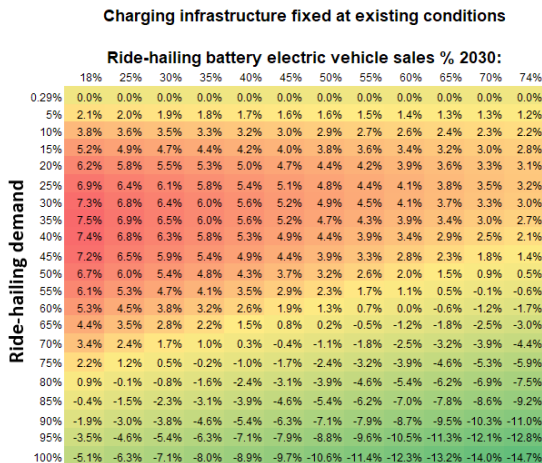
The impact of charging infrastructure. The right-hand-side chart is the scenario where the charging infrastructure grows in response to the growing number of ride-hailing EVs, and the left-hand-side chart has charging infrastructure fixed at 2017 level (in order to be comparable with our high ride-hailing demand case, charging infrastructure coverage is fixed at 5.3% as Columbus). By comparing both sides, the effect of charging infrastructure alone was shown, and the resulting reduction in national energy consumption was about 2%.

The impact of ride-hailing and BEV penetration. High annual VMT of ride-hailing leads to faster turnover rate of vehicles, resulting in newer and more fuel-efficient vehicles in the fleet. As shown in both charts, in a scenario where ride-hailing demand is high (e.g., 100% of vehicle miles traveled) and BEV market penetration reaches 74% in 2030, the national energy consumption of LDVs is expected to reduce by 18.1% compared to the baseline “-RH/-Infrastructure” in 2030.

The impact of deadheading is shown in the red zone. When ride-hailing demand grows from 0.29% to 100%, total vehicle miles traveled first increases due to deadheading miles but drops later due to improved fleet operation efficiency and less deadheading at high ride-hailing demand. The red zone in the chart shows the increase in energy consumption where ride-hailing demand is around 40-50% and BEV market penetration is at low levels around 18-40%. Note this result is based on the following assumptions. The total VMT demand excluding deadheading follows AEO projection, and deadheading trip miles were added to the total VMT demand. When ride-hailing demand is growing from 0.29% to 100%, the deadheading miles percentage of total travel drops linearly from 49% to 5%.

Therefore, improved charging infrastructure, faster fleet turnover rate due to ride-hailing, and high BEV market penetration can significantly reduce national energy consumption of LDVs, with the caveat that deadheading may compromise the benefits of ride-hailing vehicles when transitioning from a low ride-hailing-demand market to a high ride-hailing-demand market. Additional information, including sales, total VMT and ride-hailing VMT (RH VMT) at different ride-hailing demand levels.

Carbon:



Carbon:

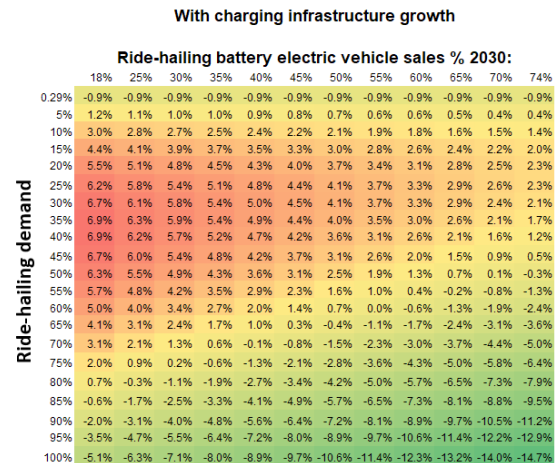


Figure I.1.1.4 National carbon emission reduction (shown as percentages, original unit is Million Metric Tons of Carbon Equivalent or MMTc) as a function of ride-hailing demand, BEV market penetration, and charging infrastructure. Green means a reduction, yellow means relatively no change, and red means an increase. (Carbon emissions include emissions from upstream and vehicle use)

Figure I.1.1.5 shows carbon emissions at different scenarios of electric grid mix. The scenario “+RH/+ Infrastructure with Renewable Electricity” has the lowest carbon emissions (282.66 MMTc). In the chart “-RH” means ride-hailing demand is 0.29%, “+RH” means ride-hailing demand is 100%, “-Infrastructure” means holding infrastructure coverage at 2017 level, “+ Infrastructure” means infrastructure coverage grows. The grid mix scenarios are defined as below, according to VISION 2017 model, as shown in Table I.1.1.1.

Table I.1.1.1 Grid Mix Assumed for Each Scenario.

	Coal	Petroleum	Natural Gas	Nuclear	Renewables
Reference	23.1%	0.2%	33.7%	17.3%	25.7%
Renewable	26.7%	0.2%	24.6%	17.1%	31.4%
Natural Gas	27.1%	0.2%	36.9%	17.4%	18.4%
Nuclear	26.7%	0.2%	24.6%	30.4%	18.1%

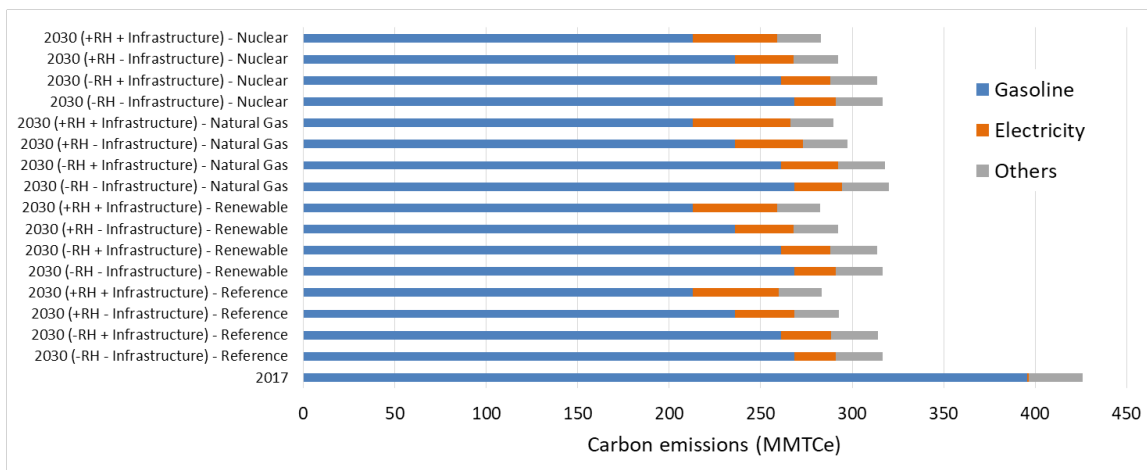


Figure I.1.1.5 National carbon emissions at different electric grid mix.

Conclusions

We quantified national energy impacts of ride-hailing EVs as a function of different levels of charging infrastructure support and ride-hailing demand. Results show that improved charging infrastructure, faster fleet turnover rate due to ride-hailing, and high BEV market penetration can significantly reduce national energy consumption of light-duty vehicles. However, deadheading may compromise the benefits of ride-hailing vehicles when transitioning from a low ride-hailing-demand market to a high ride-hailing-demand market. To reduce gasoline consumption, results indicate that it is desirable to have ride-hailing demand of 80% and above if BEV market penetration is lower than 50% in 2030, or a ride-hailing demand of 50% and above if BEV market penetration is higher than 50% in 2030.

Key Publications

1. Bi, Zicheng, Yan Zhou, Fei Xie, Zhenhong Lin, Eric Wood, Dong-Yeon Lee. “National Energy Impact Analysis of Electrified Ride-Hailing Mobility”. Transportation Research Board Annual Meeting, 2020.
2. Moniot, Matthew, Clement Rames, and Erin Burrell. “Feasibility Analysis of Taxi Fleet Electrification using 4.9 Million Miles of Real-World Driving Data”. No. 2019-01-0392. SAE Technical Paper, 2019.

References

1. EIA. “Annual Energy Outlook.” U.S. Energy Information Administration (EIA). 2017. <https://www.eia.gov/outlooks/aeo>
2. Wenzel, Tom, Clement Rames, Eleftheria Kontou, and Alejandro Henao. “Travel and Energy Implications of Ridesourcing Service in Austin, Texas.” *Transportation Research Part D: Transport and Environment* 70 (2019): 18-34.
3. US Census Bureau. “U.S. Census Database.” United States Census Bureau. 2019. <https://census.gov>
4. USDOT. “2017 National Household Travel Survey.” United States Department of Transportation. 2018. <https://nhts.ornl.gov/assets/2017UsersGuide.pdf>
5. USDOT. “Highway Statistics.” United States Department of Transportation. 2017. <https://www.fhwa.dot.gov/policyinformation/statistics.cfm>
6. Moniot, Matthew, Clement Rames, and Erin Burrell. “Feasibility Analysis of Taxi Fleet Electrification using 4.9 Million Miles of Real-World Driving Data”. No. 2019-01-0392. *SAE Technical Paper*, 2019.
7. Zhou, Yan. “VISION Model.” Argonne National Laboratory. 2018. <https://www.anl.gov/es/vision-model>
8. Wood, Eric. “EVI-Pro.” National Renewable Energy Laboratory. 2018. <https://www.nrel.gov/news/program/2018/nrels-evi-pro-lite-tool-paves-the-way-for-future-electric-vehicle-infrastructure-planning.html>
9. Lin, Zhenhong, and Fei Xie. “MA3T Model.” Oak Ridge National Laboratory. 2019. <https://www.ornl.gov/content/ma3t-model>
10. Xie, Fei, Changzheng Liu, Shengyin Li, Zhenhong Lin, and Yongxi Huang. “Long-term strategic planning of inter-city fast charging infrastructure for battery electric vehicles.” *Transportation Research Part E: Logistics and Transportation Review* 109 (2018): 261-276.

Acknowledgements

This work is supported by the U.S. Department of Energy, Office of Energy Efficiency and Renewable Energy (EERE), Vehicle Technologies Office (VTO). We first thank David Anderson, Program Manager of Energy Efficient Mobility Systems (EEMS), Erin Boyd, technology manager of EEMS, for their generous support and guidance. We also thank John Smart, the pillar lead of Advanced Fueling Infrastructure for his support and guidance on this task. Lastly, we thank Zicheng Bi, Zhenhong Lin and Dong-Yeon Lee for their contribution to this work and publications.

I.1.2 Fueling Infrastructure for Future Shared and Shared-Automated Vehicles (INL)

John Smart, Principal Investigator

Idaho National Laboratory
775 MK Simpson Boulevard
Idaho Falls, ID 83415
E-mail: John.Smart@inl.gov

Erin Boyd, DOE Technology Manager

U.S. Department of Energy
E-mail: Erin.Boyd@ee.doe.gov

Start Date: October 1, 2016

End Date: September 30, 2019

Project Funding (FY19): \$930,000

DOE share: \$930,000

Non-DOE share: \$0

Project Introduction

Electrification of Diverse Transportation Modes Prompts New Questions about Charging Infrastructure

Since the introduction of modern electric vehicles (EVs) in 2010, the amount of charging infrastructure installed in the United States has been steadily growing to meet the changing needs of a small but growing EV market. [1] By Spring 2019, an estimated 28,122 public charging stations were installed nationwide, according to the U.S. Department of Energy's (DOE's) Alternative Fuels Data Center. [2] In conjunction with the build-out of charging infrastructure, researchers and policy makers have conducted numerous studies to understand the charging needs of EV drivers and develop new methods for efficiently planning charging infrastructure. [3]-[6] The vast majority of this work has been focused on developing charging infrastructure to serve privately owned, light-duty EVs operated for personal use.

During this same time period, the concept of ride-hailing has risen in popularity. Enabled by information technology, mobility service companies were created that offer inexpensive, flexible, convenient personal transportation alternatives to conventional taxi and livery services. Transportation network companies (TNCs) such as Uber and Lyft have popularized the practice of private vehicle owners providing ride-hailing services using their own cars. The number of rides offered by TNCs has increased dramatically; the ride-hailing company Uber took 5 years to deliver its first billion rides but delivered its second billion in the first half of 2016 alone. [7]

In parallel with the rise of ride hailing, the technology (tech) and automotive industries have made significant investments to develop fully automated, self-driving vehicles. A plethora of established and start-up companies such as Waymo, Cruise, Zoox, Tesla Motors, Uber, Lyft, and Ford Motor Company are actively developing and demonstrating self-driving vehicle technology. Automakers, shared mobility service companies, tech companies, and market analysts are all predicting that automated ride-hailing vehicles will bring about disruptive market changes. [8],[9]

With the electrification of increasingly diverse transportation modes and vehicles types, there are many questions about how charging infrastructure should evolve to meet the needs of human-driven and automated EVs providing ride-hailing. What is the right kind of charging infrastructure for these vehicles? How much is needed? Where should it be located? After all, benefits of transportation electrification can only be realized if adequate, cost-effective charging infrastructure is in place to support it.

Between 2016 and 2019, researchers in the AFI Pillar used sophisticated modeling, simulation, and data analysis tools to address these questions and investigate trade-offs in different charging infrastructure network designs for human-driven and fully automated ride-hailing EVs. This report documents the findings in the final year of this research.

Objectives

Through agent-based simulation, this project quantified trade-offs inherent with different approaches to charging infrastructure for human-driven and fully automated ride-hailing vehicles.

Approach

Understanding New Market Segments for Transportation Electrification

To understand the charging infrastructure needed to support future mobility, scenarios for analysis and simulation must be developed that describe what that future market might look like. Although it is not possible to accurately predict the future, factors that motivate consumer behavior can be examined to develop reasonable, potential future scenarios. The three SMART Mobility Workflow Common Scenarios discussed in SMART Mobility Modeling Workflow Report were created in this way to provide common scenarios for all researchers across the SMART Mobility Laboratory Consortium. To define these scenarios, the consortium set assumptions for a broad range of behavioral factors, such as traveler preference for personal vehicle use versus other modes like ride hailing or transit, consumer adoption of different vehicle technologies like automation, and propensity of consumers to shop online. System-level assumptions consistent with behavioral assumptions were also defined, such as freight demand and land use, to provide necessary inputs for simulation.

Because the AFI Pillar is focused on EVs and charging infrastructure to a greater degree than other pillars, it needed to establish additional assumptions. The AFI Pillar performed analysis to add detailed assumptions to the three Common Scenarios to reflect how ride-hailing vehicles are used. To do this, the Pillar characterized ride hailing EV owner/operator interests and vehicle use by analyzing survey data from Populus and real-world driving data shared by RideAustin and Columbus Yellow Cab.

Charging Network Design Trade-offs

After characterizing ride-hailing EV driver interests and motivations, the AFI Pillar developed an approach to address the question: what are the cost/benefit trade-offs inherent with different approaches to designing charging infrastructure to serve light-duty human-driven and automated ride-hailing vehicles? To do this, the AFI Pillar used multiple modeling tools and analytical methods to design charging networks and simulate their use by EVs in specific case studies. In these studies, parameters defining charging infrastructure were varied, such as the number, location, and power level of charging stations, to determine the effect on EV use and cost.

Any public or private entity motivated to install public charging infrastructure enters the planning process with a finite budget for the number of charging stations, chargers, and plugs that can be supported. To design an optimized network and achieve the greatest return on investment, it is important to estimate the locations, number of plugs, and charging speeds that an EV fleet may demand of the future network. This type of forecasting problem is one that lends itself well to a simulation-oriented approach informed by high-resolution spatial-temporal data.

The AFI Pillar used two simulation tools, EVI-Pro and FCSPlan to study public charging infrastructure for ride-hailing vehicles. These tools use a similar approach of simulating charging demand using an unconstrained network and then clustering the resulting demand for charging in time and space to design a public network. EVI-Pro relies on real-world travel data to simulate charging behavior for various fleet electrification scenarios. It uses travel data to identify locations where EVs will need to be charged to have enough range to complete their daily driving. All possible charging locations are then spatially aggregated using a hierarchical clustering algorithm in EVI-Pro to generate a set of discrete charging locations, each with a limited number of plugs and charging capacity. The AFI Pillar used EVI-Pro to simulate charging infrastructure to serve human-driven ride-hailing vehicles in case studies in the San Francisco Bay Area in California.

Similar to the hierarchical clustering approach used in EVI-Pro, FCSPlan uses K-means clustering to site charging station locations and numbers of individual charge plugs in simulated networks. The AFI Pillar used this tool to simulate charging networks for automated electric ride-hailing fleets in the San Francisco Bay Area in California. Concepts for charger system planning and design were combined with large-scale transportation system network modeling using BEAM. Figure I.1.2.1 below shows the general scheme for integrating FCSPlan with BEAM.

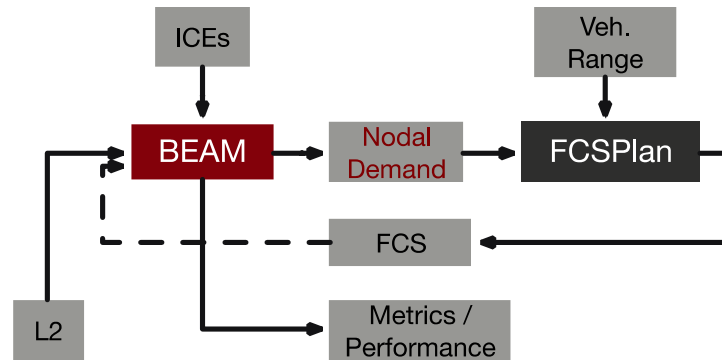


Figure I.1.2.1 Integration of FCSPlan with BEAM and network simulations

FCSPlan uses a two-stage computational geometry-based heuristic approach. In the first stage, BEAM outputs are used to identify charging demand from an AEV fleet serving elastic demand. In the second stage, a hybrid algorithm based on K-means clustering is used to site and size charging stations based on the charging demands identified by BEAM. K-means clustering is a widely used and understood method for solving this type of problem. The FCSPlan approach is summarized graphically in Figure I.1.2.2.

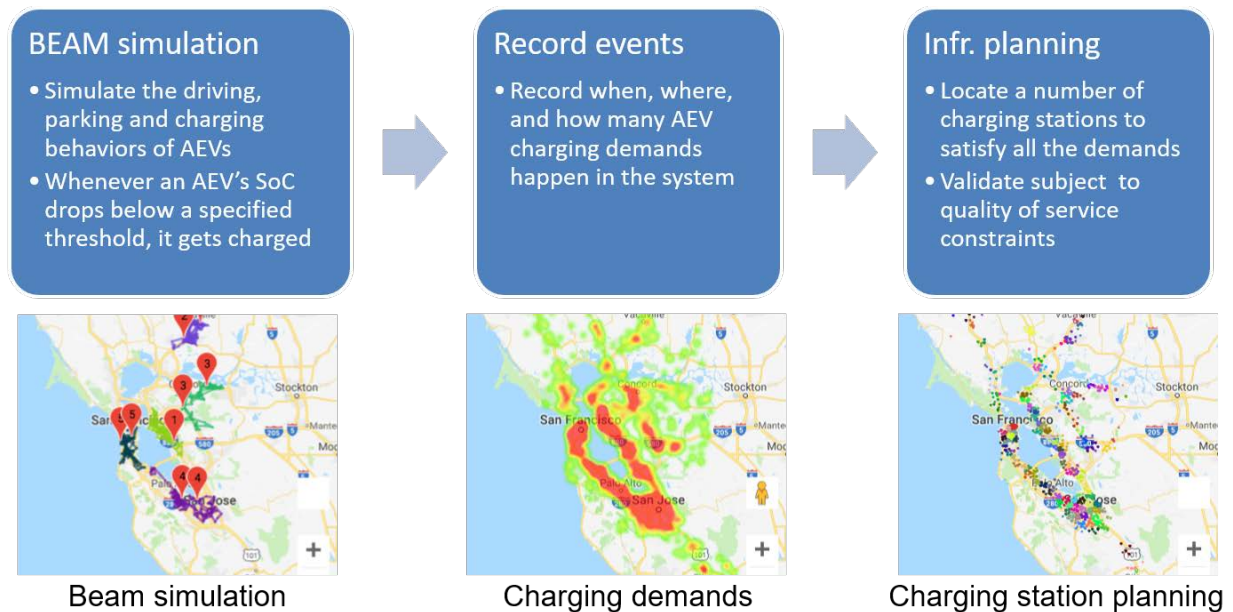


Figure I.1.2.2 FCSPlan and BEAM integration

EVI-Pro and FCSPlan are designed to optimize charging networks to satisfy all charging demand. These tools provide useful insights about ideal charging infrastructure design, but they do not take into account practical constraints on charging station installation, such as real estate scarcity, unwillingness of local land owners to install charging stations, and adequacy of facilities at desired locations to support charging stations and their

users. [10] Therefore, the AFI Pillar developed an alternative to the simulation-centric approaches of EVI-Pro and FCSPlan to envision future charging infrastructure that mimics today's networks.

A trend-based approach was developed using existing data on real-world public charging networks. Location data for DC fast chargers (DCFCs) were obtained from the U.S. Department of Energy's Alternative Fuels Data Center and manually classified based on location type. Analysis of the two largest DCFC networks indicated that a majority of present-day DCFCs are hosted in retail spaces. 96% of Electrify America's DCFCs are hosted by retail businesses, of which 65% are big box stores (such as Walmart). Figure I.1.2.3 reveals a similar finding, in that 87% of EVgo's DCFCs are hosted by retail stores. DCFC installation in these large retail spaces is potentially convenient due to the large parking areas and availability of high electric power.

The AFI Pillar used these trends to create a future, hypothetical charging infrastructure network that mimics today's network. To do so, the AFI Pillar increased the number of DC fast charger station locations in a metropolitan area by 50%, siting stations at locations representative of today's location types. The number of charging plugs at each location was selected so that the distribution of the number of plugs at new stations matched the distribution of the number of plugs at today's stations. This approach was developed to create a "sparse" charging network, relative to the demand-based, "rich" charging networks generated by EVI-Pro and FCSPlan.

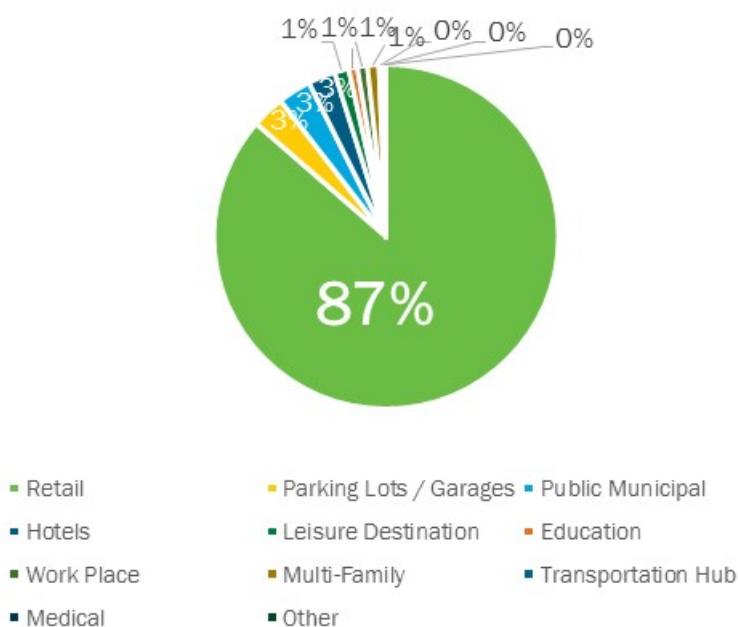


Figure I.1.2.3 Hosting venues of EVGo's DCFCs

Results

The AFI Pillar analyzed data provided by Populus, RideAustin, and Columbus Yellow Cab to shed light on TNC and taxi drivers' circumstances, motivations, and interests. Insights from data collection and analysis efforts include the following:

- Deadheading represents a significant percentage of present-day TNC operations, accounting for approximately 50% of vehicle miles traveled (VMT) in both RideAustin and Columbus Yellow Cab datasets.
- Populus data suggests that vehicles used within TNC fleets are likely more fuel efficient than the average United States light-duty vehicles, with TNC drivers reporting high shares of sedan body types and relatively recent model years.

- The majority of TNC drivers in RideAustin and Populus data were found to drive part-time with relatively low VMT. A minority of TNC drivers operate full time (~10%), with high annual VMT (~30,000, excluding VMT accumulation for personal travel).
- A significant number of drivers appear to be buying new vehicles for TNC use (approximately 50% in the Populus data).

Most full-time TNC driving days in RideAustin and Columbus Yellow Cab data could be accommodated with battery electric vehicle with 250 miles of range (BEV250) and overnight charging. Drivers likely become significantly more reliant on fast charging when residential charging is not an option (approximately 40% of Populus TNC drivers report living in an apartment).

Real-world Ride-hailing Data Analysis: Populus Transportation Networking Company Driver Survey

The Populus TNC Driver Survey represents a subset of responses from a general population survey, filtered to only individuals reporting to have recently driven for a TNC. Given a lack of driver demographic data to describe the present-day population of TNC drivers, it was unclear how to statistically stratify this sample without target distributions. As such, summaries of raw response data were calculated by household income levels, without assumed weights for the share of drivers residing in each income bracket.

Figure I.1.2.4 shows the distribution of TNC driver responses when asked to list the primary reason they are currently (or have recently) driven for a TNC. Drivers report a plethora of motivations for why they drive for a TNC, such as being in between jobs or preferring flexible hours. Interestingly, nearly a quarter of drivers report non-financial reasons as their primary motivation (e.g., keep busy, meet new people). The share of drivers reporting discretionary motivations generally decreases with decreasing household income.

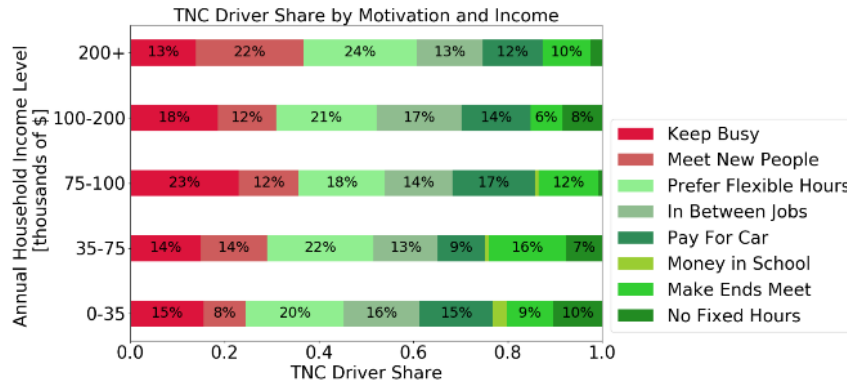


Figure I.1.2.4 Populus survey results for TNC driver share by motivation and income

Figure I.1.2.5 shows the distribution of TNC drivers by frequency of driving (e.g., a few days a month, a few days a week, several days a week, daily or almost daily). Consistent with findings from RideAustin data, a minority of drivers (~10%) report driving for a TNC daily. No meaningful differences by income bin were observed.

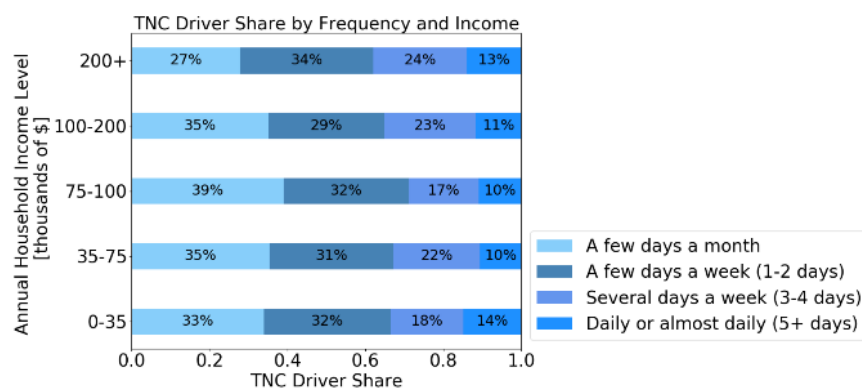


Figure I.1.2.5 Populus survey results for TNC driver share by driving frequency and income

Figure I.1.2.6 shows the distribution of TNC drivers by residency type (single versus multi-family home and whether they rent or own their home). Residence type was found to correlate strongly with household income with the share of drivers renting their home or living in a multi-family unit increasing dramatically as household income decreases. Given the residential charging challenges typically associated with multi-family housing, this data suggests the potential for poor access to residential charging for many TNC drivers, especially those with low income.

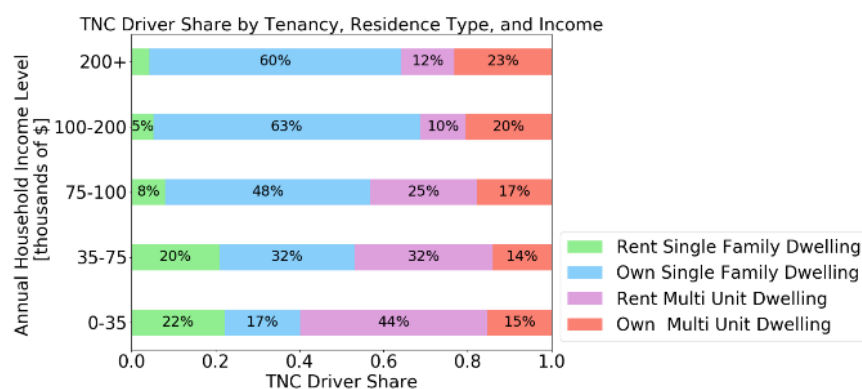


Figure I.1.2.6 Populus survey results for TNC driver share by residence type, tenure, and income

Charging Network Design Trade-offs: Charging Infrastructure Planning for Electric Ride-hailing Vehicles in the San Francisco Bay Area

For future ride hailing EV fleets, the development of a significant amount of DC fast charging is expected to be needed to supplement overnight charging of the vehicles, be they human driven or automated. These vehicles in the future may be fully battery powered, some type of plug-in hybrid vehicle with significant electric range, or hydrogen fuel cell powered. In the relative near term, battery electric vehicles (BEVs) are a leading candidate due to more competitive “total costs of ownership” and zero-tailpipe emission operation.

There is a complex set of trade-offs to consider regarding the provision of charging infrastructure for these vehicles, especially in relation to:

- Geographic layout and design (charge plugs per location) and relative density of the charging network

- Power level of the DC fast charging network (e.g., 50 kW, 150 kW, etc.)
- Battery size and driving range
- Relative size of the ride-hailing fleet in each region.

There also are questions to consider about the degree to which these DC fast charge networks will be dedicated to the operation of ride-hailing fleets, or potentially shared with privately-owned vehicles. Hence, this project examines questions around the balancing of vehicle range, fleet size, charge power, and number of stations, as well as the impact of different charging infrastructure network designs on mobility metrics (e.g., VMT, energy consumed, downtime, overall fleet economics).

In this effort, the concepts for charger system planning and design are combined with large-scale transportation system network modeling using BEAM, an agent-based simulation model of the San Francisco Bay area. The research framework and matrix of analysis scenarios are described below, followed by example results and interpretation of the scenario simulations.

Framework of Charging System Planning Based on BEAM

The BEAM modeling framework was extended to simulate detailed charging operations for both ride-hailing and personal-use EVs. Ride-hailing charging behavior is modeled separately for human-driven versus fully automated vehicles. This analysis is based on the SMART Workflow Scenario “B – Technology Takeover” where the ride-hailing fleet is a mixture of human-operated and driverless vehicles and traveler preferences are weighted toward shared modes, including pooled ride hailing.

Three parameters (vehicle range, charger power, and charging network size) were varied across the 24 simulated scenarios. Table I.1.2.1 lists these primary independent variables and other key assumptions used in this analysis.

Table I.1.2.1 Primary Independent Variable Parameters and Key Assumptions

Topic	Assumptions	Value	Notes
Vehicle Properties	Vehicle range	100/200/300 miles	All BEVs in each scenario have uniform range
	Market share of EVs in fleet	24%	Consistent with SMART Mobility Common Scenario “B-BAU”
Ride-hailing Fleet Size	Total # Vehicles	13,800	
Personal Fleet Size	# EVs	14,600	
Charging Infrastructure	Power capacity of fast chargers	50/100kW	All chargers in each scenario have uniform power capacity
Public Fast Charging Network Size	Sparse	50 chargers	Public network is used by human-driven ride-hailing and personal EV drivers
	Rich 10%	230 chargers	
	Rich 20%	440 chargers	
	Rich 100%	2,180 chargers	
Depot Fast Charging Network Size	Sparse	20 chargers	Depot network is used only by fully-automated ride-hailing EVs
	Rich 10%	220 chargers	
	Rich 20%	430 chargers	
	Rich 100%	2,170 chargers	

The AFI pillar team developed 24 variations around Scenario B, changing the range of the EVs, the power capacity of the chargers, and the quantity and distribution of the fast charging infrastructure. The fast charging infrastructure is separated into two distinct networks; the “Public” network is shared between personal-use EV drivers and ride-hailing EV drivers, while the “Depot” network is used exclusively by the automated electric vehicles (AEVs) in the ride-hailing fleet.

Table I.1.2.1 lists the parameters varied across the 24 model runs of BEAM along with other key assumptions used in this analysis. While it is expected that future real-world ride-hailing fleets will feature a mix of EVs with different driving ranges, modeling distributed ranges is reserved for future work due to the complex interactions between the charging network and driving range. Similarly, within each scenario, the power level of each charging plug in the fast charge network is uniform; all chargers are either 50 kW or 100 kW. These scenarios thus allow for direct comparisons related to EV driving range and charge network power level but are not argued to be entirely realistic in terms of expected future configurations.

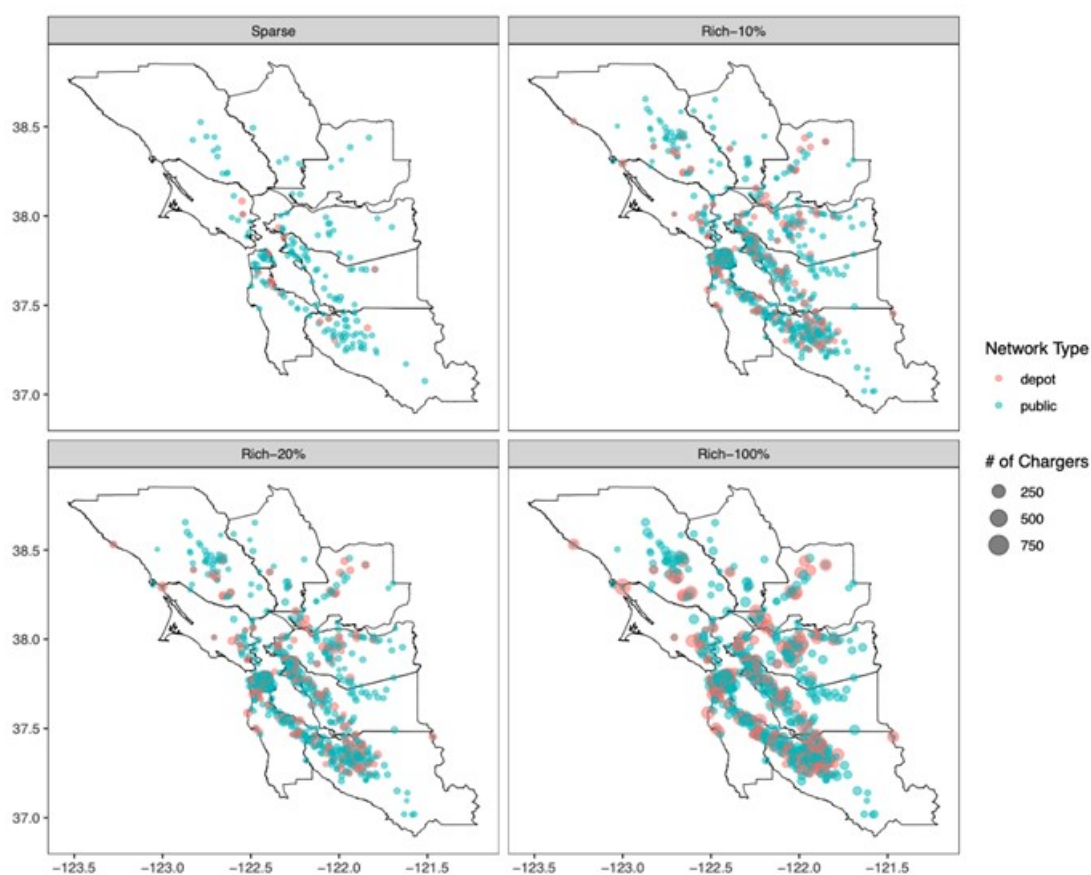


Figure I.1.2.7 Spatial distribution of chargers in San Francisco Bay Area by network type. “Depot” chargers are exclusively available to fully automated, driverless ride-hailing vehicles while “public” chargers are shared between ride-hailing and personal-use EV drivers.

Two charging infrastructure networks were developed to put reasonable bounds on the investment that might be required to support a fleet of ride-hailing vehicles. A “Sparse” network was designed using a data-driven approach based on existing public charging infrastructure in the San Francisco Bay Area. The Sparse scenario is intended to be an incremental addition of charging infrastructure, adding 50% more fast chargers than are available today. A “Rich” charging network was designed using two tools for charging infrastructure siting: the EVI-Pro tool was used to design the public charging infrastructure and the Fast Charging Station Plan

(FCSPlan) was used to design the depot charging infrastructure. [11] Because the Rich scenario ended up with substantially more chargers than Sparse, two intermediate infrastructure scenarios were developed that interpolate between Sparse and Rich. The Rich-10%, and Rich-20% scenarios are the result of adding 10% and 20% (respectively) of the difference in the number of chargers between Rich-100% and Sparse. The spatial distribution of Rich-10% and Rich-20% were equivalent to Rich-100% (Figure I.1.2.7). In other words, the intermediate scenarios have the same number of charging sites, just a proportional number of charging plugs at each site.

In Figure I.1.2.8, the numbers of vehicles are shown (left) relevant to operations of the ride-hailing fleet. Personal-use EVs are included in this figure because these vehicles compete for charging with human-driven ride-hailing vehicles and their presence therefore impacts fleet operations. Also shown (right) are the number of DC fast chargers simulated across the four scenarios.

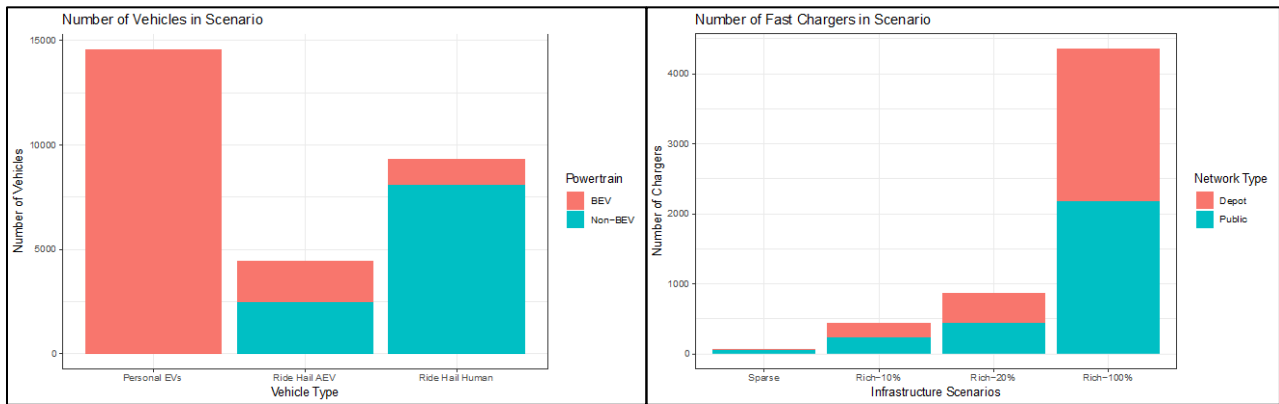


Figure I.1.2.8 Number of vehicles (left) in all scenarios discussed in this section and number of fast chargers (right) in each infrastructure scenario

Figure I.1.2.9 presents the number of individual EV charging sessions that occur in each charging infrastructure scenario and for each combination of range and charger capacity varied. The y-axis is the number of charging sessions in the network, including both depot and public chargers. The size of the symbol represents the relative amount of energy delivered or the intensity of charger utilization, the type of symbol represents the type of vehicle (personal or ride-hailing EV and human driven or automated), and the color of the symbol relates to the charge plug power level. The figure shows that 100-mile AEVs must make much heavier use of the depot charge network, as expected, and that there is much less difference between the 200-mile EV and 300-mile EV cases. This is because 200-mile EVs are capable of completing much of their daily travel with charge in their battery at the start the day [12], making the charging demand only modestly higher than the 300-mile range scenarios. Across all combinations of range and charging power, the Sparse infrastructure scenario doesn't enable all charging that would otherwise happen by the AEV fleet. There is a dramatic jump in the number of charging sessions between Sparse and Rich-10%. From Rich-10% to Rich-100% there is additional use of the infrastructure, but this growth diminishes with increases in vehicle range.

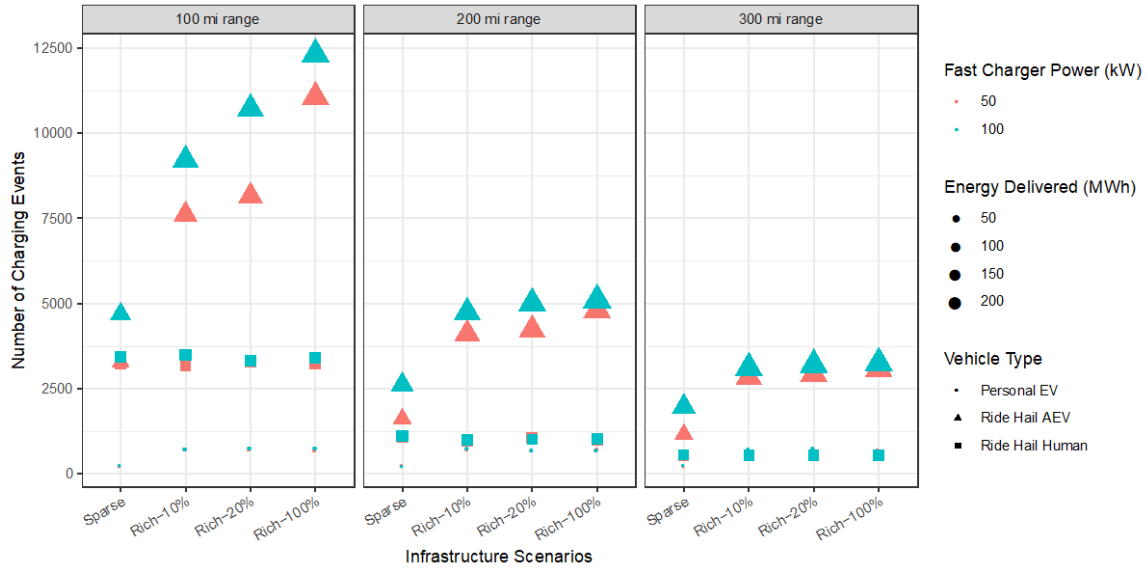


Figure I.1.2.9 Number of charging sessions by infrastructure scenario (x-axis), vehicle range scenario (panel), and charger power scenario (point color)

Figure I.1.2.10 presents the passenger miles traveled (PMT) by the EVs in the ride-hail fleet for each combination of infrastructure, range, and charging power. The 100-kW power level combined with 300-mile range EVs yields the highest levels of PMT across all infrastructure scenarios. However, when vehicle range is 300 miles and charger power is 100 kW, the benefit of infrastructure on PMT is saturated after the Rich-10% scenario. Similarly, with 50-kW chargers and 300 miles of range, the benefit is saturated after the Rich-20% scenario. Across the other scenarios, there is a monotonically increasing relationship between more charging infrastructure and the passenger miles than can be served by the fleet.

Charging infrastructure provides the greatest relative benefit to fleets with the lowest range, where PMT served by 100-mile vehicles roughly doubles between the Sparse and the Rich-10% scenarios.

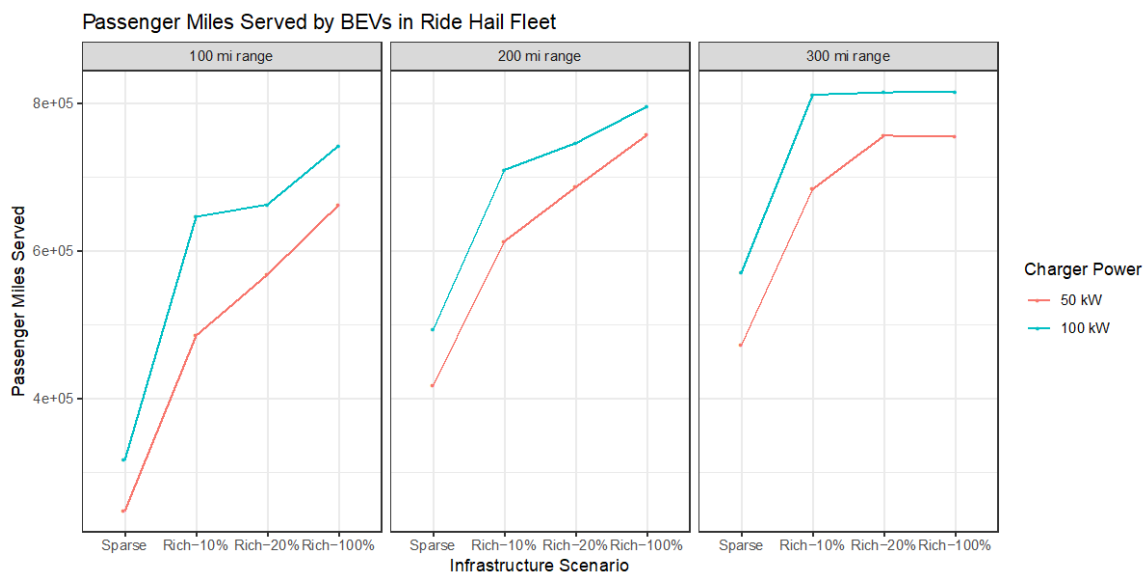


Figure I.1.2.10 Passenger miles served by EVs in ride-hailing fleet by infrastructure scenario (x-axis), vehicle range scenario (panel), and charger power scenario (trend color)

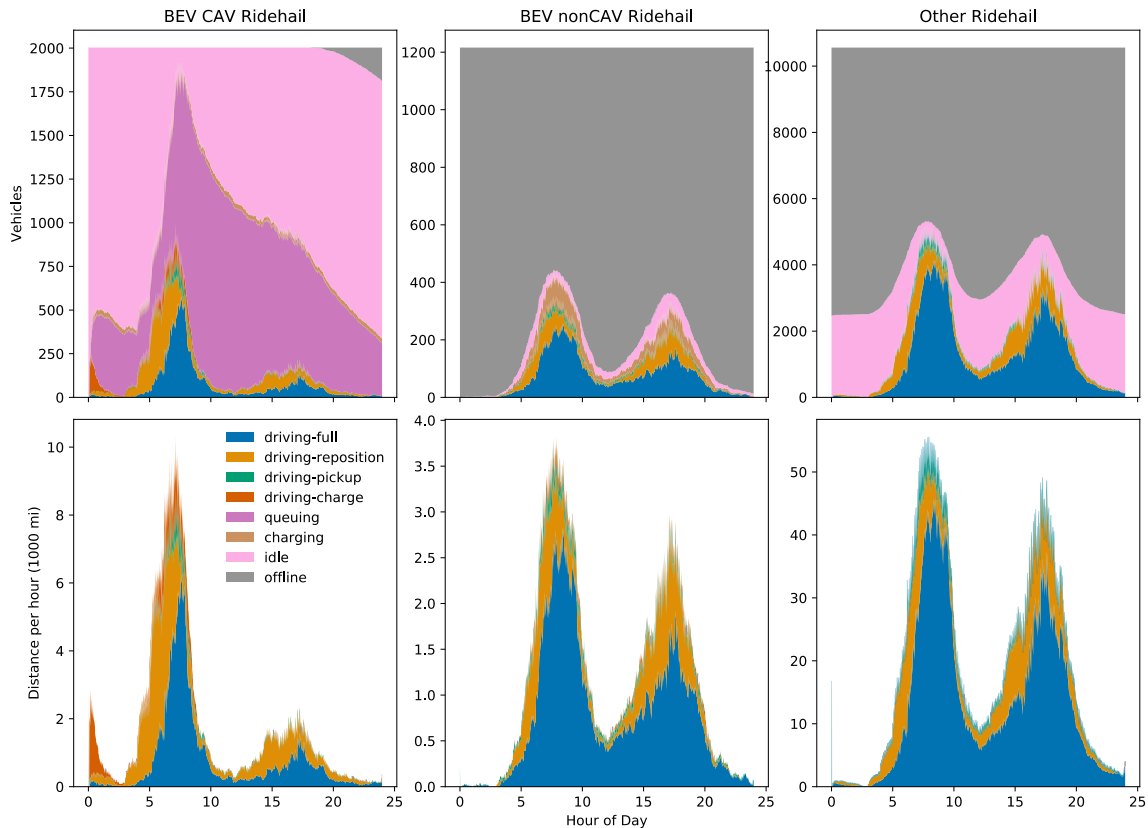


Figure I.1.2.11 Distribution of the ride-hailing fleet into operating states over the 24-hour simulation period for scenario with 100-mile range EVs and sparse, 50-kW charging infrastructure. Horizontal panels separate vehicle types and vertical panels separate time spent by each vehicle (top) and distance traveled by all vehicles (bottom).

The overall operational states of the vehicles in the ride-hailing fleet are shown in Figure I.1.2.11 and Figure I.1.2.12 for the sparse and rich infrastructure cases respectively with 100-mile range EVs and 50kW chargers. For the purpose of this report, the term “connected and automated vehicle (CAV)” refers to a fully automated, driverless vehicle.

A few features are particularly noteworthy in these plots. First, the time spent and miles driven by vehicles with passengers (blue region in the plots) are much greater for the automated electric ride-hail vehicles in the rich infrastructure scenario than in the sparse infrastructure cases. In the sparse infrastructure scenario, there is a large amount of queuing for the AEVs (purple is in the plots), especially in the middle of the day, representing pent-up demand for charging to provide more mobility services.

Second, the ride hailing EV fleet with human drivers is much less impacted by the difference between the sparse and rich infrastructure cases. Because humans drive during a shift (3.5 hours on average), the distance driven each day allows them to limit charging to 1–2 sessions per day. There is enough capacity in the Sparse infrastructure scenario to supply this amount of demand without adversely impacting the ability of human drivers to continue serving customer demand. As can be seen in Figure I.1.2.9, the number of charging sessions for human ride-hailing drivers does not increase significantly from Sparse to any Rich scenario, though the use of fast chargers by personal EV drivers does increase with more infrastructure availability.

Finally, the improved efficacy of the AEV fleet in the rich infrastructure scenario comes at some expense of driving intensity of the non-EV, “other” ride-hailing fleet. The impact is noticeable but not dramatic because

the scenarios include mostly (about 75%) conventional vehicles that are only somewhat perturbed by this effect.

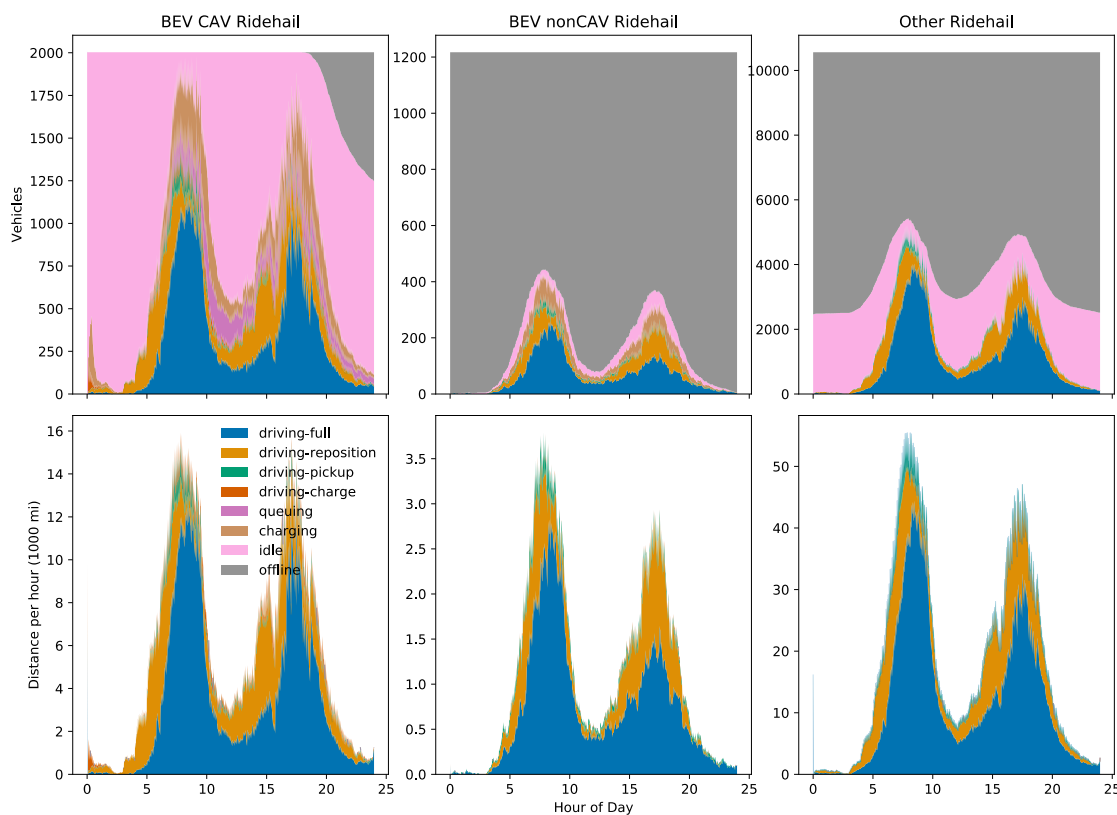


Figure I.1.2.12 Distribution of the ride-hailing fleet into operating states over the 24-hour simulation period for scenario with 100 mile range EVs and Rich, 50kW charging infrastructure. Horizontal panels separate vehicle types and vertical panels separate time spent by each vehicle (top) and distance traveled by all vehicles (bottom).

Finally, in Figure I.1.2.13 the cost results of each scenario are summarized. Included in the cost is the vehicle capital cost for both human-driven and automated EVs, the infrastructure cost for all fast charging (both depot and public networks) and the electricity required to charge all vehicles in the ride-hailing fleet. All costs are normalized by the number of passenger-miles served by the EVs in the fleet.

In the Sparse scenarios, the majority of costs are in the vehicles, but in the three Rich scenarios, increases in total vehicle miles traveled lead to more energy required per passenger mile served (due to extra miles driven both to charge and associated with deadheading and repositioning). In the Rich-100% scenario, infrastructure becomes a major component (roughly 1/3) of the total cost.

Overall, the cost results argue that investment in charging infrastructure to go past the Sparse level could be warranted given the dramatic increases in level of service they enable with modest increases in cost. There are diminishing returns to passenger-miles served by going from Rich-10% out to Rich-100% (Figure I.1.2.8) and the per-mile cost increase in a roughly linear trend. At what point an entity might stop investing in infrastructure would depend on the priorities and competing opportunities to enhance fleet performance, as well as the specific combination of vehicle range and charger power that is of interest.

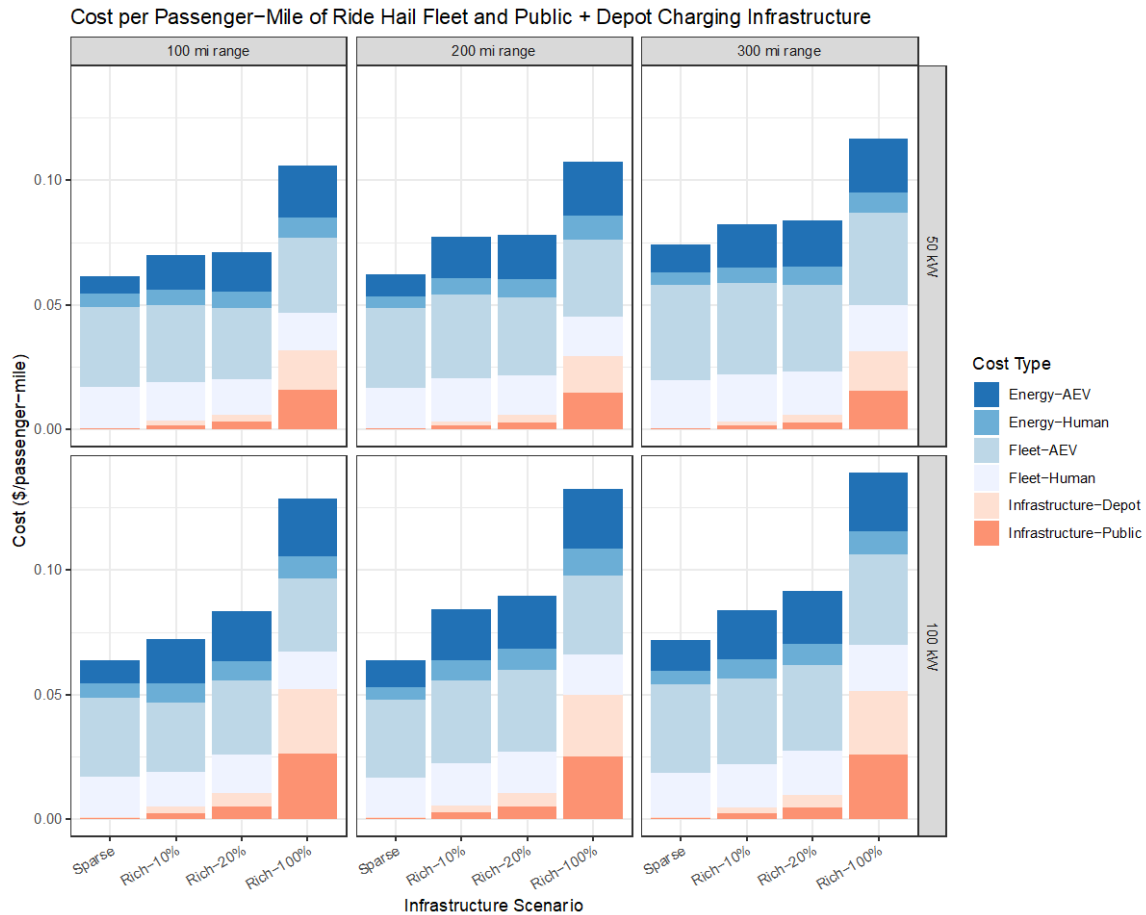


Figure I.1.2.13 Cost per passenger mile for the EVs in the ride-hailing fleet (both human-driven and AEVs), for both networks of fast charging infrastructure (both public and depot), and for the electricity and demand chargers necessary to supply the fleet with energy. The passenger miles traveled are only those that occur in EVs. The range scenarios vary with the columns of the panels, the power capacity scenarios vary with the rows, and the infrastructure scenarios vary across the x-axis.

Conclusions

The AFI Pillar used multiple modeling tools and analytical methods to design charging networks and simulate their use by EVs in specific case studies, in order to examine the cost/benefit trade-offs inherent with different approaches to charging infrastructure to serve human-driven and automated electric ride-hailing vehicles. In these studies, parameters defining charging infrastructure were varied, such as the number, location, and power level of charging stations, to determine the effect on EV use and overall system cost. The simulation results for the San Francisco Bay Area illustrate the need to include many interdependent factors in order to sufficiently capture the dynamics of electrified ride-hailing operations. The following are key findings from this research:

- An AEV fleet operated without enough charging infrastructure will be severely impaired. Queuing lengths can become dramatically long, leading to stranded investment in the form of idle AEVs and lost revenue in the form of missed ride requests.
- In a hybrid ride-hailing fleet with both AEVs and human-driven EVs, charging infrastructure can make a substantial difference in the ability of the overall fleet to serve customer demand, especially for low-range EVs. For an infrastructure investment of less than \$0.01/passenger-mile, 100-mile EVs can double the number of passenger-miles served.

- To increase the ability of human-driven and AEV ride-hailing fleets to serve more passengers, more DC fast charging is generally better, but there is a point of diminished returns where additional chargers do not yield additional PMT. For ride-hailing fleets with 300-mile range vehicles, charger saturation, or the point where additional public DC fast chargers do not yield additional PMT, can be achieved with relatively low infrastructure investment. For 300-mile vehicles, saturation occurred at a ratio of one 50-kW charger for every 3 vehicles and at a rate of one 100-kW charger for every 7 vehicles. Adding more chargers than these levels does not enhance fleet performance. Lower-range vehicles would require more infrastructure to achieve saturation.
- Caution should be used when considering aggregate charger saturation metrics for human-driven ride-hailing fleets. Because of variation in human drivers' shift length, driving behavior, and battery state of charge at the beginning of each shift, some drivers will need to charge more than others throughout the day. Even if the amount of available charging infrastructure allows the fleet to satisfy passenger demand, fares will not be evenly distributed across all drivers. Some drivers may be "stuck" at charging stations more than others. Therefore, careful attention should be paid to the tail of the distribution of negative experiences borne by drivers. Conversely, charging infrastructure can be optimized for an AEV ride-hailing fleet using only aggregate metrics, because individual AEVs can be dispatched (or not) for the benefit of the fleet.

Key Publications

1. Motoaki, Yutaka. "Location-Allocation of Electric Vehicle Fast Chargers—Research and Practice." *World Electric Vehicle Journal* 10, no. 1 (June 2019): 12. doi.org/10.3390/wevj10010012.
2. Zhang, Hongcai, Colin J.R. Sheppard, Timothy E. Lipman, and Scott J. Moura (2018), "Joint Fleet Sizing and Charging System Planning for Autonomous Electric Vehicles," *IEEE Intelligent Transportation Systems Transactions*, T-ITS-18-11-1073.R2.
3. Zhang, Hongcai, Colin J.R. Sheppard, Timothy E. Lipman, Teng Zeng, and Scott J. Moura (2019, submitted), "Charging Infrastructure Demands of Shared-Use Autonomous Electric Vehicles in Urban Areas," *Transportation Research – D*.

References

1. Morrissey, Patrick, Peter Weldon, and Margaret O'Mahony. "Future standard and fast charging infrastructure planning: An analysis of electric vehicle charging behavior." *Energy Policy* 89 (2016): 257-270.
2. DOE. AFDC. (2019). Electric Vehicle Charging Station Locations. Retrieved from afdc.energy.gov/fuels/electricity_locations.html#/analyze?fuel=ELEC&country=US&access=private
3. Davidov, Sreten, and Miloš Pantoš. "Planning of electric vehicle infrastructure based on charging reliability and quality of service." *Energy* 118 (2017): 1156-1167.
4. Micari, Salvatore, et al. "Electric vehicle charging infrastructure planning in a road network." *Renewable and Sustainable Energy Reviews* 80 (2017): 98-108.
5. Wood, Eric W., et al. "Charging Electric Vehicles in Smart Cities: An EVI-Pro Analysis of Columbus, Ohio." No. NREL/TP-5400-70367. National Renewable Energy Lab. (NREL), Golden, CO (United States), 2018.
6. He, Fang, Yafeng Yin, and Jing Zhou. "Deploying public charging stations for electric vehicles on urban road networks." *Transportation Research Part C: Emerging Technologies* 60 (2015): 227-240.
7. Solomon, B. (2016). Uber just completed its two billionth ride. *Forbes*. July 18, 2016.
8. "Electric, shared and autonomous vehicles will revolutionize transport in the world's cities over the next 15 years," *Bloomberg New Energy Finance and McKinsey & Company*, Oct 11, 2016.

9. Bliss, L., “The Future of Autonomous Vehicles Is Shared,” CityLab, Jan 6, 2017
10. Motoaki, Yutaka. “Location-Allocation of Electric Vehicle Fast Chargers—Research and Practice.” *World Electric Vehicle Journal* 10, no. 1 (June 2019): 12. doi.org/10.3390/wevj10010012
11. H. Zhang, C. Sheppard, T Lipman, S Moura (2018), “Joint Fleet Sizing and Charging System Planning for Autonomous Electric Vehicles.” Under peer review. arxiv.org/abs/1811.00234
12. All BEV vehicles are initialized to begin the day with a random battery state of charge distributed uniformly between 20% and 100%.

I.1.3 Dynamic Wireless Power Transfer Feasibility (ORNL)

Omer C. Onar, Principal Investigator

Oak Ridge National Laboratory, Power Electronics and Electric Machinery Group
National Transportation Research Center, 2360 Cherahala Boulevard
Knoxville, TN 37932
E-mail: onaroc@ornl.gov

David E. Smith, Principal Investigator

National Transportation Research Center, 2360 Cherahala Boulevard
Knoxville, TN 37932
E-mail: smithde@ornl.gov

Erin Boyd, DOE Technology Manager

Energy Efficient Mobility Systems Program
Vehicle Technologies Office
Office of Energy Efficiency and Renewable Energy
U.S. Department of Energy
E-mail: erin.boyd@ee.doe.gov

Start Date: October 1, 2017

End Date: September 30, 2019

Project Funding (FY19): \$235,000

DOE share: \$235,000

Non-DOE share: \$0

Project Introduction

Connected and automated systems are on path to dominate the future of vehicles, buildings, and the power grid due to the potential for significant improvements in energy efficiency, sustainability, security, congestion mitigation, and convenience. This transition will include the emergence of connected and automated vehicles (CAVs) for the transportation of people and goods.

Although some of the areas are partially worked on in the field of CAVs, such as sensors, connectivity, and communications. However, refueling (charging) methods and the charging infrastructure requirements remain unaddressed. While having the self-driving and self-parking functionalities, not having self-charging capability would be a failure for the CAVs. Moreover, a fleet of a CAVs for ride-shared vehicle applications would be a high cost-intensive investment which requires very high-utilization; therefore, it would not be practical to stop and charge these vehicles in the middle of the day for several hours. With dynamic wireless charging systems, these vehicles can be recharged while they are in operation which eliminates the down time for these vehicles.

Not only for the CAVs but in general for all the EVs, range anxiety and the cost of battery packs are among the most important barriers against future adoption. As one means of increasing the adoption rate of automated electric vehicles (AEVs), wireless charging can be a one of the fueling methods of charging AEVs due to ease of charging with no wired connection. Wireless charging is a safe, convenient, flexible, and efficient method for charging the electric vehicles [1]. Substantial reductions in petroleum consumption and greenhouse gas emissions are possible with electrified vehicles and roadways. With dynamic wireless charging, AEVs can self-charge and have ideally unlimited all-electric range and their battery packs can be reduced which would result in overall weight and cost reduction while improving the fuel economy. According to a study [2], the market share of plug-in EVs could increase up to 65% among the total light duty vehicle sales if 1% of the roadways were electrified with 60kW dynamic wireless charging systems.

Furthermore, dynamic wireless charging is a key enabling technology for the connected and automated vehicles by automating their charging process, increasing their range, wirelessly connecting them to the power grid, and reducing their battery pack size and weight with improved fuel economy (reduced energy consumption). The dynamic wireless charging technology is based on the electromagnetic coupling between a

roadway electrified with coils or long wire loops under the road surface and a receiver coupler mounted underneath the electric vehicle. Power ratings, track (electrified roadway section) length, electric and electromagnetic field emissions and confinement, efficiency, lateral misalignment tolerance, power transfer continuity, geometric layout and design of the tracks, and resonant tuning configurations are the areas with research needs for the field of dynamic wireless charging systems.

Objectives

This project aims at analyzing vehicle energy consumption levels and accordingly determine the needs of an optimally designed dynamic wireless charging system to be deployed for refueling the connected and automated vehicles. The overall project objectives can be summarized as follows:

- Identify vehicle energy consumption levels (including auxiliary energy consumption) for given vehicle specifications, drive cycles, constant speed operations, and traffic conditions (speed variations).
- Based on the vehicle energy consumption levels, identify the dynamic wireless power transfer (DWPT) requirements and size and design of the DWPT system specifications for a given route conditions for AEVs.
- Develop an optimization framework for optimal design of the power rating, track length, and placement of DWPT systems by minimizing the power rating, and track length while maximizing the range extension or energy delivery to the vehicles for providing charge sustaining operation.
- Analyze the grid requirements and system impact on the grid.

Approach

DWPT technology is based on the electromagnetic coupling between a roadway electrified with coils or long wire loops under the road surface and a receiver coupler mounted underneath the EV. Although simple in concept, DWPT systems are highly complex and are still in the research stage. There is a myriad of design parameters that must be carefully optimized to achieve a functional, cost-effective design. These parameters include power rating, the length of electrified roadway sections, referred to as track length, and the distance between tracks, design of the electromagnetic coils within each track and resonant tuning configurations. The selection of these and other parameters influence electric and electromagnetic field emissions, charging efficiency, power transfer continuity, and system cost. The project team explored DWPT designs for EVs and AEVs to determine the techno-economic feasibility of DWPT for future mobility.

System Description

In a DWPT system, the system components include electrical infrastructure (grid), grid-side power electronics including the front-end rectifier and the high-frequency power inverter, electromagnetic couplers and the resonant tuning components, and the vehicle-side power electronics including the rectifier and filter stage, as shown in Figure I.1.3.1.

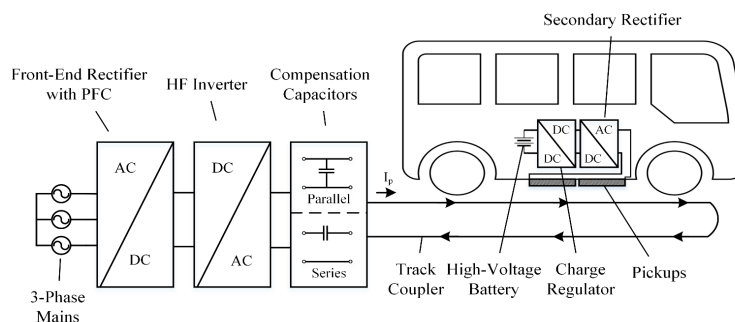


Figure I.1.3.1 Block diagram of a typical track-based dynamic wireless power transfer system.

In this subsection, vehicle energy consumption, finite element analysis (FEA) based modeling for power transfer characteristics, grid impact and requirements analysis, and the DWPT system optimization are presented.

Modeling of Vehicle Energy Consumption

Power rating and sizing of DWPT systems depend on the vehicle energy consumption levels because the DWPT systems must be sized and designed in order to accomplish charge sustaining mode of operation or considerable range extension. Energy consumptions of vehicles should be evaluated on known duty cycles and constant speed operations. For the vehicle energy consumption levels, models and databases created by other national laboratories have been utilized. Point A-to-B constant speed modeling for light-, medium-, and heavy-duty vehicle classes are analyzed considering the cases with and without auxiliary power. Constant speed modeling energy consumption models can be especially useful where the automated driving infrastructure can potentially eliminate the stops. Using the vehicle average power consumption levels and the route distance, the DWPT system can be sized in terms of the power level of the electrified roadway track and the section length of it under the assumption of rectangular and continuous power transfer profile to the vehicle. Average power consumption at constant speeds is based on Eq. (1) with the rolling coefficient $\mu_r=0.0065$, equivalent powertrain efficiency $\eta_{eq}=85\%$, and air density $\rho=1.225 \text{ kg/m}^3$.

$$P(v) = \frac{\mu_r M g}{\eta_{eq}} v + \frac{C_d A v^3}{2 \eta_{eq}} + P_{aux} \quad (1)$$

Modeling of Dynamic Wireless Power Transfer Systems

Inductive power transfer is used to transmit power from DWPT transmitters to receivers mounted on the underside of the AEVs. Due to the airgap between the transmitters and receivers, the inductive links are loosely coupled and the coupling coefficient, $k_i = M_i / \sqrt{L_0 L_i}$ is significantly less than 1, where the couplers in the inductive link are designated by number i where $i = 0$ designates the roadside DWPT transmitter and $i = 1, 2$, are the receivers. Multiple AEVs can be powered from the same DWPT transmitter. The equivalent receiver loads R can be varied to regulate the power flow between the roadside DWPT transmitter and the vehicle receivers, which can be accomplished by onboard dc/dc converters. Conduction losses are calculated for the DWPT transmitter and receivers from the parasitic resistances $R_i = (2l_i + 2z_i)$ where ρ is the equivalent DC resistance of the Litz cable per length. For the DWPT transmitter and receivers, 4/0 Litz wire cable is assumed with $\rho 0.056 \Omega/1000$. Skin effect losses and bundling effects can be neglected as the cable is made from braided 38-AWG wire. With an operating frequency of 85 kHz, the strand diameter of 38-AWG wire will be less than one-half the skin depth, virtually eliminating that component of the alternating current (AC) resistance [4]. Through the mutual coupling of the inductors M_i , each load resistance R is reflected to the DWPT transmitter. Due to the following distance between the vehicles, the cross coupling between the receivers $_{1,i}$ is assumed to be zero. At resonance, this provides the following relationship for the input voltage V_o and current I_o .

$$V_o = I_o (R_o + \sum_{i=1}^N \frac{(\omega M_i)^2}{R_i + R_{Li}}) \quad (2)$$

From this relationship, the transmitter input power P_o and the receiver output powers P_i are written as a function of the input voltage V_o , the input current I_o , parasitic resistances R_i , and loads of the system.

$$P_o = V_o I_o = I_o^2 (R_o + \sum_{i=1}^N \frac{(\omega M_i)^2}{R_i + R_{Li}}) \quad (3) \quad P_i = I_o^2 \frac{(\omega M_i)^2 R_{Li}}{(R_i + R_{Li})^2} \quad (4)$$

Finite Element Analysis-based Modeling of Mutual Inductance and Power Transfer Characteristics

To analyze and validate the power transfer characteristics of long-track based DWPT deployments, the finite element analysis (FEA) model of a DWPT road section was completed. This FEA model validates the assumptions in the power transfer profile and continuity along the track. While the smaller lumped coils

approach has very high peak-efficiency because of the limited coil length, there are power pulsations as the vehicle passes over one coil to another. Moreover, the energy delivered to the vehicle is limited in this approach because the energy delivery is a function of the time integration of the power transfer curve. With the long track approach, the power starts from zero and gradually increases to the peak value as the vehicle starts getting aligned with the transmit track; then, power transfer stays almost constant along the track, and it gradually falls as the vehicle clears the track. Because the track is relatively longer, the power transfer stays almost constant along the track. The FEA model developed validates these power transfer characteristics while identifying the DWPT track parameters, track to vehicle power transfer efficiency as a function of the track length, and the mutual inductance variation with respect to the vehicle position. The DWPT track-to-vehicle mutual inductance has also been modeled, which is an indication of the power transfer profile to the vehicle. The key findings on the power transfer efficiency with respect to the track length and ferrite thickness and the parameters for the FEA model are provided in Figure I.1.3.2 and Figure I.1.3.3. In addition to the trapezoidal-shaped mutual inductance and power transfer characteristics, the other important key takeaway is that the track-to-vehicle efficiency can be 95% for tracks shorter than 100 m with a ferrite thickness of 1/16 in. Longer tracks require thicker ferrites to maintain similar levels of efficiency.

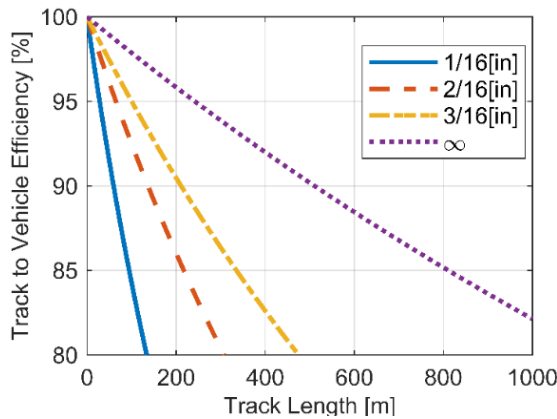


Figure I.1.3.2 Efficiency analysis of track-based DWPT system with respect to the track length.

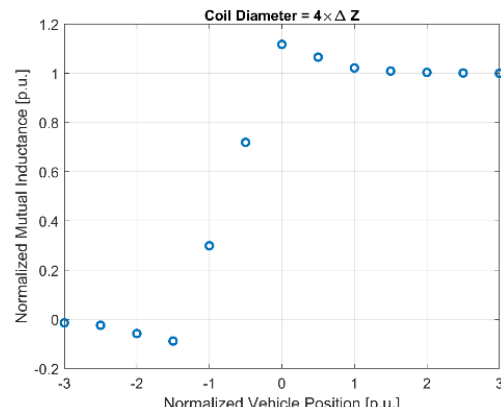


Figure I.1.3.3 Variation of the track-to-vehicle mutual inductance with respect to vehicle position.

Grid Impact and Requirements Analysis of DWPT Systems

Project team also evaluated the impact of the DWPT systems on the power system/grid to assess the grid infrastructure requirements that provides power to the DWPT systems. Additionally, electromagnetic transient (EMT) studies were performed to quantify the impact of DWPT systems on the grid. These studies are used to understand the grid infrastructure requirements to reduce the voltage variations in the grid. The reduced voltage variations can improve the stability of grids and avoid inadvertent protection triggers. For the DWPT models, the DWPT system requirements were quantified based on the charge-sustaining mode of operation for the vehicles. The grid impact and grid infrastructure requirements analyses are detailed in [3]. According to the findings, a DWPT system with conventional grid interface converters would have considerable voltage fluctuations on the grid side due to the power pulsations. Smart inverters with Volt/VAr supply capability or integration with energy storage systems and/or renewable energies can be a viable solution to improve the grid stability and resiliency.

Results

It is thought that the first deployment of the DWPT technology will occur in primary roadways, which corresponds to the interstates and other freeways and expressways. This is because 10% of all the roadways correspond to the 60% of all the distances travelled. Because there are more vehicle miles travelled on primary roadways, it is more likely to see the first deployments on primary roadways. Similar to the HOV lanes, there will be only one lane electrified with DWPT technology at the beginning. If the transmitter lengths are designed accordingly, for a given average speed and following distances, it can be assumed that only one

vehicle can be coupled with one transmitter at a time. Under traffic congestion where more vehicles can exist on transmitter couplers, the total power from the transmitter should be regulated to the maximum power (i.e., vehicles would share the total available power) which would change the findings. Or the DWPT systems could be designed for the worst-case scenarios with maximum number of vehicles on a transmitter is considered; however, this option would require significant overdesigning which would not be an optimal solution. Once the power transfer characteristics are analyzed, the optimal sizing of a dynamic wireless power transfer (DWPT) system can be analyzed for highway applications. The system parameters must be selected carefully to reduce the overall cost per mile of DWPT. Among these parameters, system length is important due to its impact on the system coupling coefficient, overall efficiency, and the cost of construction and installation. The impact of this effect will increase if the quality factor of the system is low. Because high-efficiency operation is paramount for DWPT to be practical from both a capital and operational cost standpoint and the quality factors of systems may be limited, transmitter sizes will be constrained by the dimensions of smaller vehicles. In this case, it is advantageous to consider utilizing the longer lengths of heavier vehicles to have multiple paralleled receivers. This will both decrease the initial capital cost and ensure the maximum utilization of the DWPT system which will drive down the cost of using the system for all. If these costs are low enough, DWPT could revolutionize future transportation by eliminating range-anxiety and enabling long distance, charge-sustaining trips in CAVs. This would increase the mobility of both freight and passengers and ultimately help remove the barrier of long-distance travel from transportation electrification. The analysis included an interoperable DWPT system that can be used to charge all classes of CAVs including light-duty vehicles (LDV) and heavy-duty vehicles (HDV). For example, a DWPT system may be designed to have transmitter lengths shorter than the length of a HDV to maximize efficiency for a LDV. Due to this, it may rely on having multiple receivers on a HDV to scale the power transfer relative to a LDV. With 42% roadway coverage, the system could enable charge-sustaining operation for both LDVs and HDVs at 70 mph. For the system covered here, a multi-objective optimization problem was formulated with an objective function. Finally, with the inclusion of efficiency and length constraints, Pareto fronts of the solutions were generated by using a weighing sum method.

As seen from the results in Figure I.1.3.4, it is important to limit the coverage of DWPT systems due to the large expense of roadway construction. However, there are practical tradeoffs between the power rating and coverage of the system. With low coverages, the onboard energy storage and electronics of EVs must facilitate high-charge rates. However, the power ratings in this case may still be lower than what would be required with high-power static charging because the DWPT system can transfer energy over a longer period than static charging systems while the EV is on the move. An upper limit to the area-related power density can also be achieved by wireless-charging systems.

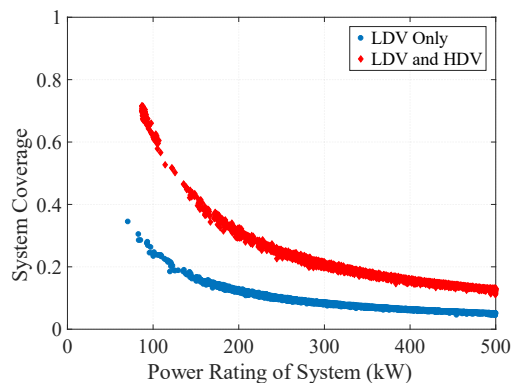


Figure I.1.3.4 Pareto solutions from the optimization model for two different cases (LDV only and LDV and HDV together).

Figure I.1.3.4 also recommends that around 200–250-kW power rating of the transmitters, 8–12% of the roadways should be electrified for LDVs only and this is a very reasonable solution that requires not too high of a power rating and not too high of coverage rates because the power rating would increase the cost of the power electronics and magnetics and high-coverage rate would increase the construction and installation costs.

As a more long-term but realistic deployment scenario, multiple vehicles on electrified highway lanes can be considered. This part of the findings involves analyzing the impact of connected and automated vehicles (CAV) on the dynamic wireless power transfer (DWPT) system design for future deployment scenarios. In this case, AEVs can travel in coordinated groups, with each AEV in the group is powered by the same DWPT section. As the distribution of smaller light-duty vehicles (LDVs) and larger heavy-duty vehicles (HDVs) in

each group is varied, the DWPT system power level, transmitter length, and the equivalent receiver loads should be adjusted to minimize the infrastructure requirements and energy losses of the DWPT system. The outputs from this analysis are used to determine the optimal groupings of vehicles for a given DWPT system. The analysis suggests that AEV coordination could aid the deployment of DWPT systems and reduce the overall infrastructure and energy losses of DWPT systems. The methodology involves using the vehicle energy consumption information, inductive power transfer model, and the optimization formulation. The optimization formulation uses the variables including the system power level P_{sys} , the DWPT transmitter length l_{sys} , the system coverage β_{road} , and the value of the equivalent receiver loads, $R_{L,\text{LDV}}$ and $R_{L,\text{HDV}}$. The optimization is then performed for many possible numbers of light-duty vehicles (LDVs) n_{LDV} and heavy-duty vehicles (HDVs) n_{HDV} . This formulation seeks to minimize the infrastructure and energy requirements of the DWPT system on a per-mile basis. More details on this formulation and optimization results are given in [5].

Conclusions

DWPT can automate the charging process of AEVs and enable them to charge while driving. Analysis of DWPT to support highway driving found that a DWPT system capable of providing up to 250 kW of charging power, installed in 8-10% of the primary roadways in the United States, is sufficient to enable continuous, charge-sustaining operation for light-duty vehicles averaging 65 mph. When including heavy-duty trucks, DWPT system coverage must increase to 40–45% of primary roadways to support driving at 65 mph. Like in the transit application, DWPT technology allows EVs to have smaller batteries and use narrower state-of-charge windows, which reduces cost and increases battery life. Preliminary analysis of DWPT with grid integration requirements found that DWPT systems will need voltage and reactive power control or will need to be integrated with energy storage and/or renewable energy systems to dampen transients in power flow from the grid and prevent grid stability problems.

Key Publications

1. Foote, Andrew, Omer C. Onar, Suman Debnath, Jason Pries, Veda Prakash Galigekere, and Burak Ozpineci. "System Design of Dynamic Wireless Power Transfer for Automated Highways." *2019 IEEE Transportation Electrification Conference and Expo (ITEC)*, June 2019, 1–5.
2. Debnath, Suman, Andrew Foote, Omer C. Onar, and Madhu Chinthavali. "Grid Impact Studies from Dynamic Wireless Charging in Smart Automated Highways." *2018 IEEE Transportation Electrification Conference and Expo (ITEC)*, June 2018, 950–55.
3. Foote, A., O. C. Onar, S. Debnath, M. Chinthavali, B. Ozpineci, and D. E. Smith. "Optimal Sizing of a Dynamic Wireless Power Transfer System for Highway Applications." *2018 IEEE Transportation Electrification Conference and Expo (ITEC)*, June 2018.
4. Foote, Andrew, and Omer C. Onar. "A Review of High-Power Wireless Power Transfer." *2017 IEEE Transportation Electrification Conference and Expo (ITEC)*, June 2017, 234–40.
5. Foote, Andrew, Burak Ozpineci, Madhu Chinthavali, and Jan-Mou Li. "Sizing Dynamic Wireless Charging for Light-Duty Electric Vehicles in Roadway Applications." *2016 IEEE PELS Workshop on Emerging Technologies: Wireless Power Transfer (WoW)*, October 2016, 224–30.

References

1. Onar, Omer C., Madhu Chinthavali, Steven L. Campbell, Larry E. Seiber, and Cliff P. White. "Vehicular Integration of Wireless Power Transfer Systems and Hardware Interoperability Case Studies." *IEEE Transactions on Industry Applications* 55, no. 5 (2019): 5223–34.
2. Lin, Zhenhong, Jan-Mou Li, and Jing Dong. "Dynamic Wireless Power Transfer: Potential Impact on Plug-in Electric Vehicle Adoption." *Dynamic Wireless Power Transfer: Potential Impact on Plug-in Electric Vehicle Adoption* 2014, no. 1 (April 1, 2014): 1–11.

3. Debnath, Suman, Andrew Foote, Omer C. Onar, and Madhu Chinthavali. “Grid Impact Studies from Dynamic Wireless Charging in Smart Automated Highways.” *2018 IEEE Transportation Electrification Conference and Expo (ITEC)*, June 2018, 950–55.
4. Muhlethaler, J., “Modeling and multi-objective optimization of inductive power components,” *Thesis, ETH / Power Electronic Systems Laboratory*, 2012.
5. Foote, Andrew, Omer C. Onar, Suman Debnath, Jason Pries, Veda Prakash Galigekere, and Burak Ozpineci. “System Design of Dynamic Wireless Power Transfer for Automated Highways.” *2019 IEEE Transportation Electrification Conference and Expo (ITEC)*, June 2019, 1–5.

Acknowledgements

Project team would like to thank AFI Pillar Lead Mr. John Smart of the Idaho National Laboratory (INL) for his continuous support and guidance on this project. SMART Mobility

I.1.4 Charging Infrastructure Needs for Electrification of Freight Delivery Vehicles (INL, ORNL, NREL)

Victor Walker, Principal Investigator

Idaho National Laboratory
775 MK Simpson Boulevard
Idaho Falls, ID 83415
E-mail: Victor.Walker@inl.gov

Amy Moore, Principal Investigator

Oak Ridge National Laboratory
P.O. Box 2008
Oak Ridge, TN 37831
E-mail: mooram@ornl.gov

Alicia Birky, Principal Investigator

National Renewable Energy Laboratory
15013 Denver West Parkway
Golden, CO 80401
E-mail: Alicia.birky@nrel.gov

Erin Boyd, DOE Technology Manager

U.S. Department of Energy
E-mail: Erin.Boyd@ee.doe.gov

Start Date: October 1, 2018

End Date: September 30, 2019

Project Funding (FY19): \$250,000

DOE share: \$250,000

Non-DOE share: \$0

Project Introduction

Widespread truck electrification has the potential to significantly reduce petroleum consumption and cost for the trucking industry. Trucks moving freight account for 25% of all fuel consumed by U.S. transportation, [1] and fuel accounts for 20% of operation costs for freight companies. [2] Electrification would create many benefits for reducing overall energy costs but would require a large investment in infrastructure to support electrification by either public or private parties. This project investigates the foundations of how to approach this problem and identifies several of the key elements which need to be studied to help support this issue.

The freight industry is complex and there are numerous business models that would require varying degrees of charging infrastructure and/or changes to their operations to enable electrification, especially with limited-range vehicles. Although it is true that about 75% of trucks are used primarily for trips of less than 200 miles, [3] drivers of Class 7/8 trucks often chain trips together, such that their overall distance traveled before returning to a central location is much longer than the expected range of electric trucks.

The variety and complexity of operations in the freight trucking industry make it challenging to discern where electric trucks are beneficial, what kind of charging infrastructure is needed for electrification to be feasible, and who bears the costs and benefits of charging infrastructure investment. Charging infrastructure costs must be weighed against the cost of operational changes, such as routing and dispatching changes. Electric truck operations also must be conducted within the confines of regulation, including the maximum allowable time driver can continuously operate their trucks. The relatively long length of charging time, even with high-power chargers, may be highly problematic for trucking companies who strive to maximize miles driven within regulated shift lengths. New tools are needed to help trucking companies manage complex decisions surrounding electrification and charging infrastructure, which is the focus of this effort.

Objectives

This project examined several key contributing factors associated with the adoption of electrification of trucks in the freight industry and how those will impact charging infrastructure design. The objective was to produce a framework for examining the problem of electric freight charging infrastructure and a report on what the next steps of research will entail. This will provide decision makers with a path forward to better enable charging infrastructure decisions.

This project sought to answer the research question: What is needed to understand trade-offs inherent with different approaches to designing charging infrastructure for Class 7/8 electric trucks for freight transport?

Approach

Truck manufacturers are bringing electric trucks to market based on the need to reduce energy consumption. Energy efficiency improvements in trucking has far lagged light-duty vehicles, and it is hoped that electrification can provide a valuable energy efficiency improvement. Electric trucks will need charging infrastructure to support them. Therefore, the researchers analyzed the freight trucking industry to understand the characteristics of potential future electric freight truck market segments that charging infrastructure will need to serve.

The freight trucking and shipping industry is complex and highly segmented, so researchers reviewed data and reports about the industry to divide it into segments. Data were obtained from publicly available sources, such as the U.S. Department of Transportation's Federal Motor Carrier Safety Administration, U.S. Department of Commerce, and private databases.

The trucking industry was segmented based on operations of different types of trucking companies, also known as motor carriers. Four factors were considered: cargo ownership, cargo type, shipment size, and typical operating range. [4] For each of these factors, motor carriers operations were placed within two or three categories, as shown in Table I.1.4.1.

Table I.1.4.1. Factors by which to Segment the Freight Trucking Industry

Cargo Ownership	Cargo Type	Operating Range	Shipment Size
For-hire Private	Freight Parcel Specialized	Local Regional Long-haul	Truckload Less-than-truckload

For each prevalent industry segment (defined by different combinations of these factors), the researchers characterized trucking operations, owner/operator interests, and regulations that govern operations. Results of this analysis were used to define modeling scenarios and assumptions.

A critical consideration for the trucking industry is charging time, because time spent charging directly impacts a fleet's financial bottom line and driver pay, which is usually based on miles driven rather than time.

On the vehicle side, truck batteries are expected to be large, in terms of storage capacity, volume, and weight, in order to provide heavy trucks with up to 500 miles of range. Some estimates put a 500-mile range battery weighing approximately 11,000 pounds. [5]

Several truck companies have estimated that the average energy use of electric heavy-duty trucks will be approximately 2 kWh per mile. This value in the analysis. [6],[7]

On the charging infrastructure side, multiple charging technologies are available to freight trucks. The primary technologies available today include conductive (plug-in) chargers with power levels up to 600 kilowatts (with faster capacity being studied); static, inductive wireless charging that provided up to 250 kW to the vehicle

while parked; and catenary technology that provides a direct feed of electricity to trucks along fixed routes, either while parked or during driving.

Using these figures, simple estimates were calculated for the time required to fully charge an electric Class 7/8 truck with a nearly empty battery. For comparative estimates, Table I.1.4.2 below shows charging times when using 150 kW, 250 kW, 350 kW, and 600 kW charging systems to replenish batteries sufficient to provide 150 miles and 500 miles of driving range.

Table I.1.4.2 Approximate charge times in hours for different types of chargers based on a 2 kWh/mile usage

Charge Power:	150 kW	250 kW	350 kW	600 kW
150 Mile Range	2.0	1.2	0.85	0.5
500 Mile Range	6.6	4.0	2.85	1.6

The team chose to model a fleet of electric Class 7/8 trucks with 300 and 500 miles of electric range that charge at 150 and 350 kilowatts as these options are the most developed and should be available in the near term. Real-world operational data describing the driving and parking behavior of 22 conventional diesel-powered trucks was obtained from FleetDNA, a database of real-world data that is managed by National Renewable Energy Laboratory (NREL). [8] Researchers analyzed data from a private, regional-haul motor carrier fleet based in Dallas, Texas to create spatial-temporal trip segments as inputs to the model. Two different charging stations location scenarios were then implemented in the model.

Results

Motor Carrier Business Overview

Analysis of 2013 IHS registration data shows that there were about 8.5 million medium- and heavy-duty vehicles registered to around 950,000 unique businesses. [9] The majority of fleets are small (Table I.1.4.3) and 86% of motor carriers own five or fewer trucks while 98% own 25 or fewer trucks. However, there are just more than 300 fleets that own more than 1,000 vehicles each and these fleets account for nearly half of all registered trucks

Table I.1.4.3 Distribution of fleets and trucks by fleet size

Number of vehicles	<5	5–25	26–100	101–250	251–1,000	>1,000
Percentage of fleets	86.1%	11.5%	1.96%	0.30%	0.13%	0.03%
Percentage of trucks	16.4%	13.7%	10.0%	5.15%	6.57%	48.2%

Source: Motor Carrier Census Information, Federal Motor Carrier Safety Administration, U.S. Department of Transportation (FHWA 2017).

The size of the fleet may have a significant impact on whether the operation will choose to invest in a capital-heavy electric charging infrastructure for their trucks or rely on public charging. And because many of the smaller operators' contract with others to haul freight, the investment in private infrastructure for many of the fleets may involve split incentives where those who would benefit most from electrification may not be the ones with the capital to perform an install. While those who may own facilities may not see a direct return on investment for purchased equipment.

Similarly, different segments of the motor carrier business will have different opportunities and challenges when considering an electric vehicle charging infrastructure. For the purposes of this study, motor carriers are

divided into business segments based on their cargo ownership, cargo type, shipper load size, and typical operating range. [10] Cargo ownership is divided into two classifications: for-hire and private. Cargo type has three major divisions: freight, parcel, and specialized. Operating range is divided into three classifications: local, regional, and long-haul. Shipment size has two classifications: truckload, and less-than-truckload. These service segments will have significantly different impacts on operations and are described in more detail below.

Cargo Ownership

Motor carriers can be classified into two groups based on the ownership of cargo:

- For-hire carriers: transport passengers, regulated property, or household goods owned by others for compensation.
- Private motor carriers: transport their own cargo, usually as a part of a business that produces, uses, sells, and/or buys the cargo that is being hauled. Cargo ownership can impact where private charging infrastructure should be installed. Typically, private motor carriers will be delivering materials to their own facilities which could be used for chargers, while for-hire carriers will make deliveries to facilities owned by others.

Cargo Type

Cargo type reflects the major type of goods that a motor carrier is moving.

- Freight: Bulk items typically in large containers or portions of containers, or items that can be placed in a specific trailer for movement. This is the vast majority of all goods movements.
- Parcel Delivery: Transportation of cargo owned by others as individual packages. These packages are normally smaller items less than 150 pounds and can be combined with many others in a distribution network.
- Specialized: Specialized cargo requires specific types of vehicles to move freight. This may include material such as cement or non-trailer supported vehicles. It can also provide movement as part of a shipping system, such as drayage and transloading. (These normally take place in localized environments such as ports, container yards, and rail yards.)

The cargo type can impact electrification and charging infrastructure as it influences the operations and types of vehicles needed to support the business. The movement of typical freight can normally be accomplished with a tractor pulling a trailer and can be applied to several types of operations. Parcel delivery; however, often requires a specialized approach to networked sorting and medium-duty vehicles for final distribution. And specialized cargo may require custom vehicles that operate in limited environments, but which may need a specialized charging infrastructure.

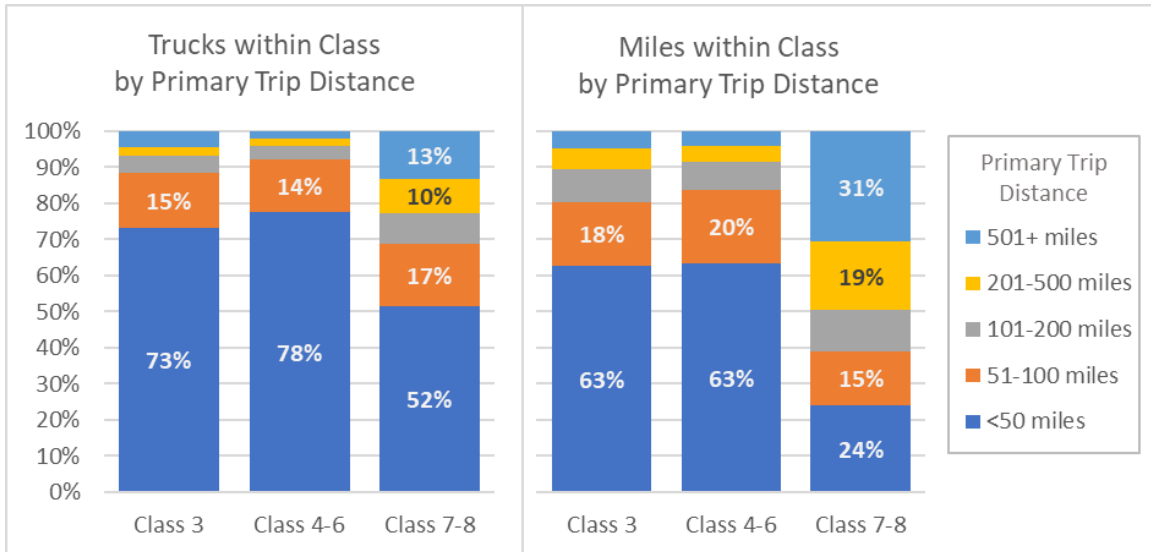
Operating Range

Motor carriers and vehicles can also be classified based on the primary range of operation. This analysis uses three classifications: long-haul, regional, and local carriers. Generally, long-haul is more than 500 miles, regional to be between 50 and 500 miles, and local to have a radius of less than 50 miles.

Figure I.1.4.1 shows the distribution of trucks and miles by primary trip distance for each truck weight class, and Figure I.1.4.2 shows the average annual miles traveled per vehicle. From these figures, several important insights about the usage of trucks carriers can be discerned, namely:

- Most Class 3-6 trucks are used primarily in local service with trip length of 50 miles or less.

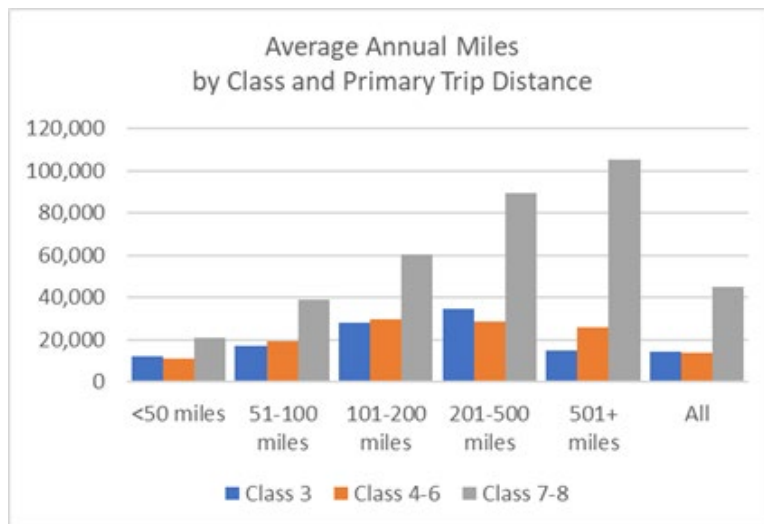
- About half of Class 7-8 trucks are used locally, while 23% are used primarily for trips more than 200 miles.
- Within each interval of range of operation, the miles traveled per heavy truck is considerably higher than miles traveled per lighter truck and the overall average miles traveled by a Class 7-8 truck (45,240) is more than three times that of a Class 4-6 truck (13,650).



Source: U.S. Department of Commerce, Bureau of the Census, 2002 Vehicle Inventory and Use Survey

Vehicle class is defined as follows:
 Class 3: gross vehicle weight rating is 10,001 to 19,500 pounds.
 Class 4-6: gross vehicle weight rating is 19,501 to 26,000 pounds.
 Class 7-8: gross vehicle weight rating is 26,001 pounds or more.

Figure I.1.4.1 Distribution of Trucks and Annual Miles within Weight Class by Primary Trip Distance



Source: U.S. Department of Commerce, Bureau of the Census, 2002 Vehicle Inventory and Use Survey

Figure I.1.4.2 Average Annual Miles Traveled per Vehicle by Primary Trip Distance and Vehicle Weight Class

The operating range has a significant impact on the way that a charging infrastructure may be deployed. Because the range is typically defined from a centralized depot environment, local and regional operations have a greater opportunity to utilize private charging infrastructure. These ranges are typically within the projected range operations of electric trucks that have been announced. Long-haul trucks and operations will be more heavily dependent on public charging infrastructure.

Shipment Size

For-hire carriers can further be classified into two groups based on the type of service:

- Truckload (TL) carriers contract an entire truck or trailer to move a load for a single shipper with one origin and destination, typically long-haul service.
- Less-than-truckload (LTL) carriers collect smaller shipments from multiple cargo owners at local pick-up points, consolidate them onto a truck, and distribute goods through a delivery network. These networks may consist of both regional distribution routes and long-haul segments.

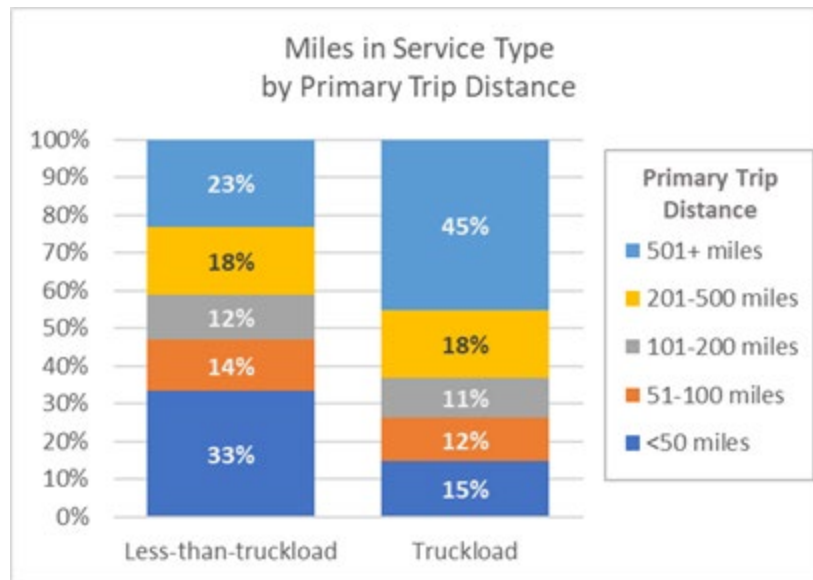
The operation patterns of TL and LTL carriers are often different from each other. In TL operations, the trucks often do not operate on fixed routes and schedules, but instead move between various client facilities as needed. On the other hand, a LTL firm usually operates on set routes between its hub terminals and between these terminals and client origins and destinations. Each LTL business may have a uniquely designed network operation for its specific purposes and these operations can be complicated. Some LTL firms are dedicated to regional service and drivers may depart from each terminal, deliver and pick up loads, and return to the terminal. Other firms may also provide a nation-wide long-haul service that involves long-distance transports that can be in excess of 1,000 miles. [11]

Figure I.1.4.3 shows the distribution of trucks used and miles traveled by truck weight class for TL and LTL carriers. Figure I.1.4.4 shows that TL carriers' operations are characterized by longer hauls and heavier vehicles, with 63% of miles accounted for by trucks whose primary trip distances are more than 200 miles and 96% of the miles traveled by Class 7-8 trucks. Meanwhile, LTL carriers use Class 4-6 vehicles as often as Class 7-8, though the smaller vehicles are used for shorter trips such that more than two-thirds of the miles are accounted for by Class 7-8.



Source: U.S. Department of Commerce, Bureau of the Census, 2002 Vehicle Inventory and Use Survey

Figure I.1.4.3 Distribution of Trucks and Miles by Truck Weight Class for Truckload and Less-than-truckload Service



Source: U.S. Department of Commerce, Bureau of the Census, 2002 Vehicle Inventory and Use Survey

Figure I.1.4.4 Distribution of Miles by Primary Trip Distance for Truckload and Less-than-truckload Service

The business models reflected in the shipment sizes of for-hire carriers will influence where a private charging infrastructure could be made available. A hub-and-spoke model with designated routes may have more opportunity for introducing chargers at key points. Where full-truck load point-to-point operations may depend more on public infrastructure.

Incentives and Motives

Trucking Regulations

Trucking carriers determine the operation patterns (route, trip length, and driving duration) as well as the type of trucks based on the business characteristics described above. However, both the operations and the vehicles are constrained by regulations set by the Federal Motor Carrier Safety Administration of the U.S. Department of Transportation. These regulations can have a significant impact on how operations are carried out and how these operations may impact the adoption of electric vehicles and the methods of utilizing a charging infrastructure.

For example, the type of pay affects the trucker's driving behavior and his/her needs, which in turn set the requirements for the vehicle performance and operations. Drivers of heavy trucks and tractor-trailers are usually paid by how many miles they drive. [12] The survey conducted by the National Institute for Occupational Safety and Health reported that 65.9% of the respondents were paid by the mile. [13] This means that many drivers, especially those who operate long-haul transports, have incentive to drive consecutive hours without stopping. However, drivers' hours of service are subject to the following regulations: [14]

- 11-Hour Driving Limit: Driver may drive a maximum of 11 hours after 10 consecutive hours off duty.
- 14-Hour Limit: Driver may not drive beyond the 14th consecutive hour after coming on duty, following 10 consecutive hours off duty.
- Rest Breaks: Driver must take a 30-minute break after 8 consecutive hours of driving.
- 60/70-Hour Limit: Driver may not drive after 60/70 hours on duty in 7/8 consecutive days.

Currently, time used in charging is considered duty hours. This is also true of time spent at a customer's loading docks. Adding large amounts of time during a drive cycle for charging would impact the ability of driver's ability to drive miles for which they would be paid. It would also impact how business need to meet their delivery demands and their ability to get to appropriate stopping locations after a drive cycle.

On the vehicle side, federal weight standards are perhaps the most limiting factor in the determination of payloads and vehicle specification. Federal weight standards apply to commercial vehicle operations on the Interstate Highway System; however, states may set their own commercial vehicle weight standards and have different exceptions to federal truck weight limits. In addition to the gross weight, per-axle weight and axle spacing is specified to reduce the risk of damage to highway bridges by requiring more axles, or a longer wheelbase to compensate for vehicle weight. Federal standards for commercial vehicle maximum weights on the interstate highway system are as follows: [\[15\]](#)

- **Single-Axle Weight:** The total weight on one or more axles whose centers are spaced not more than 40 inches apart. The federal single-axle weight limit on the interstate highway system is 20,000 pounds.
- **Tandem-Axle Weight:** The total weight on two or more consecutive axles whose centers are spaced more than 40 inches apart but not more than 96 inches apart. The federal tandem-axle weight limit on the interstate highway system is 34,000 pounds.
- **Gross Weight:** The maximum weight of a vehicle or vehicle combination and any load thereon on the interstate highway system is 80,000 pounds.

Batteries to provide a larger range would also require heavier weight that would need to be offset by less available payload. Some of the weight would be offset by lighter engines, but if the overall impacts lower the available weight for cargo then it would directly impact the amount of material that the trucking provider can move and will impact their profit margins.

These regulations and segmentations provide key implications for electrification of trucks and supporting charging infrastructure. For instance, the miles traveled by a heavy truck is considerably higher than the miles traveled by a lighter truck. In terms of performance requirements for electric truck and charger, the truckers' incentive to drive consecutive hours (up to 11 hours) indicates the need for long-range trucks. However, weight regulations would necessarily create a trade-off between a longer range (heavier battery pack) and a smaller payload. Each of these trade-offs needs to be considered to create a cost-benefit approach for freight operators.

Private Infrastructure Motivations

Fleet operators considering electric charging options have complicated choices associated with how to best integrate charging into their operations. The installation of a private charging infrastructure can allow them to take advantage of times when their operating profiles may have trucks available for charging versus being in active use. These infrastructure investment decisions are based heavily on the business segment and regulation constraints described above. The installation costs, rate costs, and use of private chargers is balanced against the availability, rates, and route integration capabilities of public charging infrastructure.

The business models for developing a charging infrastructure must consider the charging rate of installed chargers, the number of chargers to meet the demands of the fleet, and the placement of chargers to best complement the charging opportunities. The costs of installing charging stations goes up with higher-capacity chargers and electricity rates may go up if several chargers operating at once impacts peak-rate charges for facilities. Also, as most private charging chargers would be placed at existing facilities the grid capabilities, land use considerations, and management of the movement of vehicles through a charging infrastructure all become key elements of the decision models for a private charging infrastructure.

In interviews with industry participants, the difficulty to understand, prepare for, and manage the interplay of these installation choices was a key concern of those considering electrification.

Considering Charging Infrastructure for a Regional-haul Private Motor Carrier in Dallas, Texas

As discussed above, there are many trade-offs to be considered for electrification of heavy-duty trucks. Decisions around the use of electric trucks and the installation of charging infrastructure are significantly impacted by different business dynamics and the needs of a specific fleet.

To examine charging infrastructure options to support truck fleet electrification in more depth, researchers gathered real-world data from a private, freight, regional-haul motor carrier fleet based in Dallas, TX. This fleet ships freight and palletized goods from a regional distribution center in Dallas to stores and warehouses in several states in the southern United States, as well as connects to other regional distribution centers as needed. This fleet offers several types of real-world trips that offer a mix of scenarios – from short haul trips returning to the distribution center to long-haul trips. The fact that it is private offers several options for installing chargers at destination locations and a chance to examine the impacts of different solutions.

This data was gathered from 22 trucks operating out of the distribution center over the period of one month.

All the trucks were Class 7 and 8 heavy-duty diesel trucks carrying trailers of goods to be delivered to retail stores, outlets, and other distribution centers. The recorded data was analyzed, and each stop was identified. Trips were identified as drives between stops and circuits were identified as a chain of trips which started and returned to the central distribution center. During each circuit, data loggers recorded the driving duration between stops, the distance between them, and the time the truck dwelled at each destination. At most destinations, trucks were parked at the loading docks while goods were unloaded. Trucks were sometimes parked at other destinations overnight.

Figure I.1.4.5 shows the circuits for a single truck in the fleet. Each color represents a single circuit driven by the vehicle; with each dot representing a longer stop on that circuit.

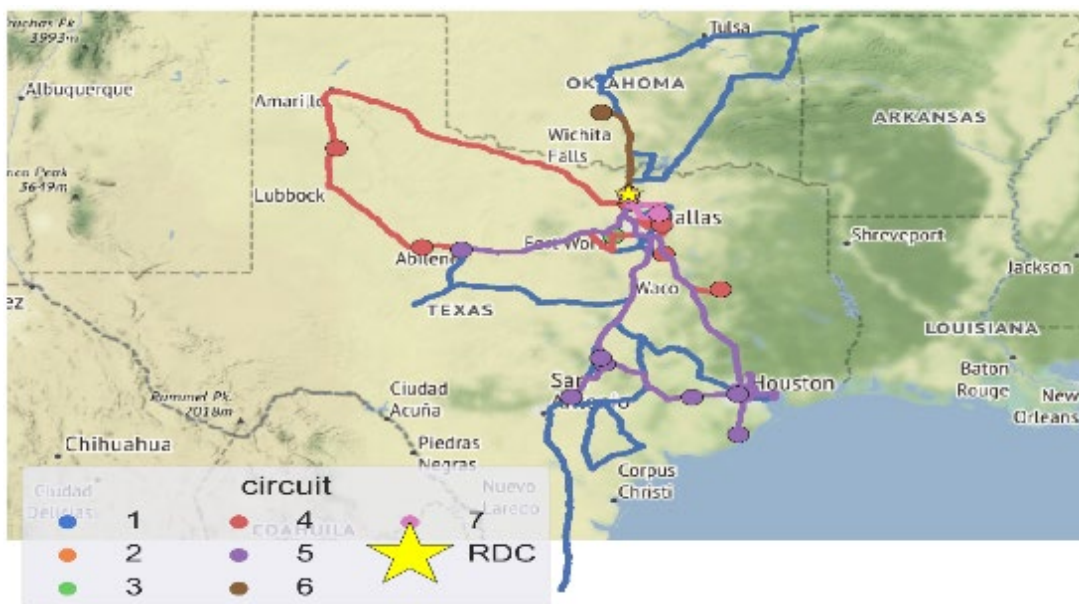


Figure I.1.4.5 Circuits driven by a single truck over several days. There is wide variety of circuits.

The data indicates a wide variety of circuit types over the month, with some circuits performing short trips to local stops and returning the same day, and others involving multi-day circuits covering hundreds of miles. A single truck tractor is often assigned to many different types of circuits throughout the month. These characteristics provide a useful examination of the issues that may face several types of fleet operators.

In this evaluation, the analysis examined several options of infrastructure and vehicle configurations for the distribution center to electrify its fleet. It looked at how to provide private charging to maximize utility, and how much public charging would then be needed to support the distribution network if it was used in the same manner as the diesel fleet based on the current data.

First, because the distribution center activity would be starting at the centralized distribution center depot it was assumed that the fleet could install chargers at the distribution center to provide power to the trucks while they were there either loading goods or waiting for their next circuit. This would include installations at any other distribution centers the trucks may visit. Secondly, because the company owned each of the delivery locations, it was assumed that it would be an option to install chargers at the loading and unloading docks of these retail stores so that the trucks could be charging during the unloading of goods.

For the purpose of this examination, it was assumed that the trucks would only stay to charge at each of the locations for the same amount of time that was recorded in the existing real-world data and not stay longer to complete a charge. It was further assumed that the chargers would be available during the entire stop at a location. Each of the charging options at either the distribution centers or stores was chosen to be either a 150-kW charger or a 350-kW charger, as these are publicly available. And two ranges of vehicles, a 300-mile range vehicle and a 500-mile vehicle, are considered.

Single Vehicle Impact

To help examine how vehicle availability would be influenced by these options, an individual schedule for one of the trucks in the dataset was chosen for a case study. For this schedule, the truck made 24 separate trips, defined by a driving segment between cargo activities. The circuits originated at the regional distribution center (RDC), performed a set of trips to stores and other distribution centers and terminated at the same RDC. The trips segments ranged from 50 miles to over 400 miles. Four of the trip segments exceeded the 300 miles of range, while none of the trips exceeded the 500 miles of range.

To examine how much charging would be needed to complete a given trip, the analysis looked at the amount of range that would be remaining when the truck arrived at a destination at the end of the trip. Assuming each truck started with either the 300- or 500-mile range available, the truck would use that range to reach a destination. If the remaining range available was negative that meant that the vehicle would have needed to use public charging to complete the trip. Then, if charging was available at that destination, the amount of charge they would have received at the given charge rate and truck dwell time (given by the time stopped either for unloading or at the end of the travel day) was converted to a range and added back to the available range amount used for the next trip.

The first case considered the scenario where there was only charging available at the RDC depots. This would mean that the vehicle would only be able to charge from the private infrastructure at the beginning and end of each circuit (there were 7 circuits in this example set but two of them had stops at other RDC's).

Figure I.1.4.6 shows the resulting analysis of available range at each stop. The greatest negative numbers represent the total amount of public charge that would be needed to complete that circuit.

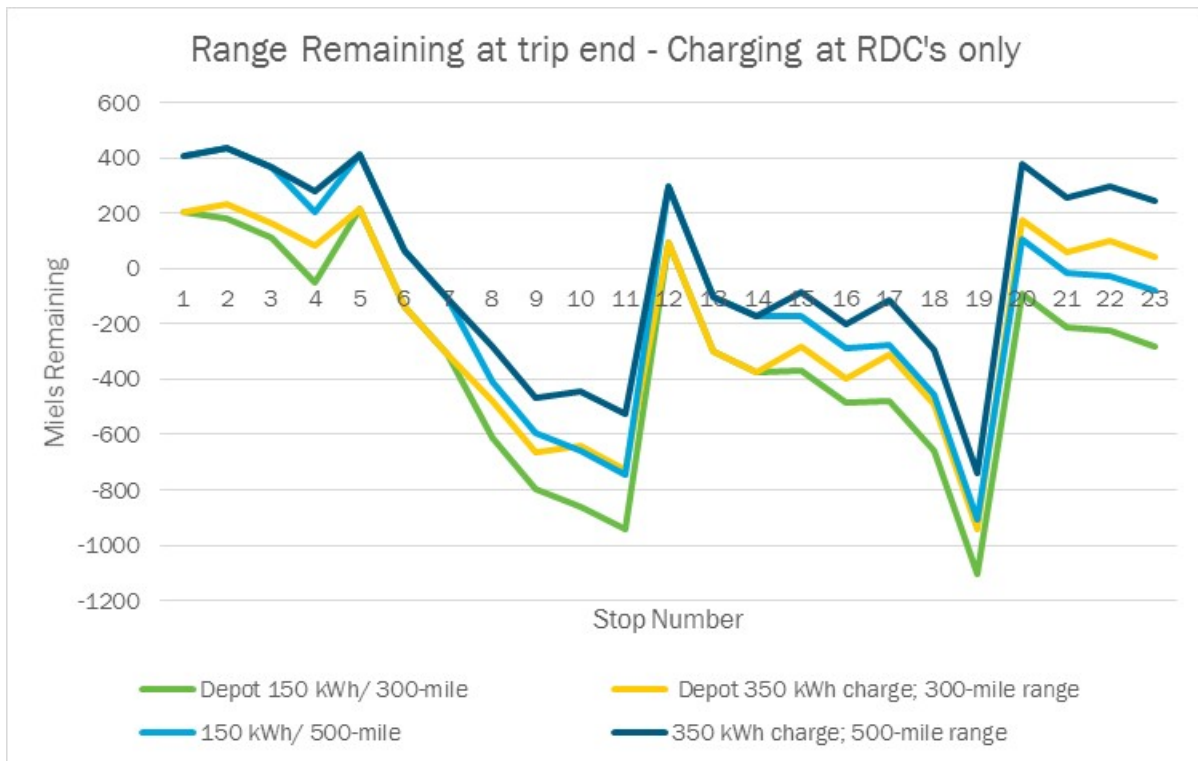


Figure I.1.4.6 Range remaining at each stop for depot only charging

For the shorter circuits, the 150-KW charger and either the 300- or 500-range vehicle was sufficient. But on the longer circuits, and where the return visit to the depot was relatively short, the need for public charging increased. At the end of stop 11, the 300-range vehicle with 150-kW chargers would have required 944 miles of public charging (equivalent to 12.5 hours of charge at the 150-kW rate). The 350 kW and 500-mile vehicles would have required 527 miles of charging (equivalent to 5.2 hours at the 350 rate). Similarly, at the end of stop 19, the 300-mile 150-kW scenario needed 1106 miles worth of public charging, while the 500-mile 350-kW scenario needed 741 miles worth of public charging.

Next, the scenario was considered where the company would install a charger at each of the docks, which would allow the vehicles to receive charge while they were unloading or loading. It was again assumed that the time at the dock would not be changed from the current data set (it would include the unloading times as they were with diesel trucks and included times that they would be parked over-night due to end of day restrictions). These chargers would increase the range of the truck at every stop they made but may not offset the range lost in reaching the delivery location. Once again, the remaining range at the end of each trip was recorded, and negative numbers reflect the need for public charging before reaching those locations. Figure I.1.4.7 shows the resulting range available or needed at the trip end for each scenario.

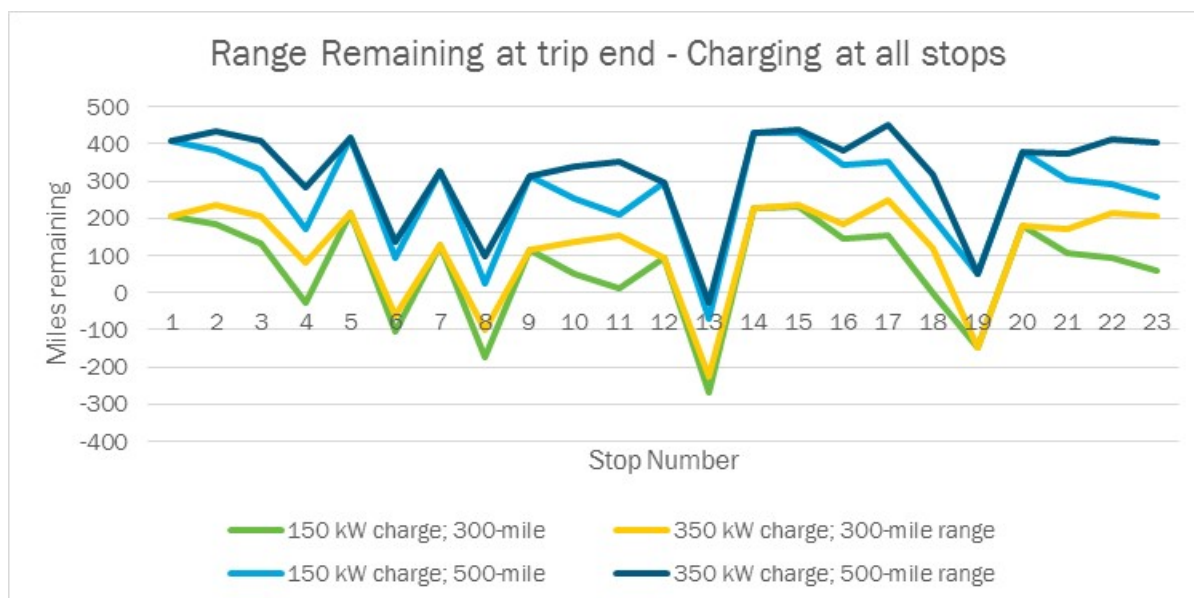


Figure I.1.4.7 Range remaining at each stop if charging is available at each stop

In this set of scenarios, only five trips would require public charging of 29, 105, 175, 268, and 149 miles for a total of 726 miles with the 150-kW chargers and the 300 range. Changing to 350-kW chargers would reduce the number of trips needing charging to four with a total 537 miles. If the range was increased to 500 miles, then only 1 trip would need public charging. For 68 miles using a 150-kW charger and 25 miles with a 350-kW solution.

The single vehicle example reflects that having charging stations at each location greatly improves the range and applicability of the EV fleet (even with slower charge rates). The solution of even slow charging stations at each location seems to meet most of the trips for this vehicle.

Full Dataset Vehicle Impact

After evaluating the outcomes of the single vehicle, researchers also examined the applicability of the solutions to the entire dataset. The dataset for the entire range of 22 trucks included 819 trips total. Only 135 of the trips were more than 300 miles and 30 of those were more than 500 miles and would be considered true long-haul trips. In total, 84% of the trips were less than 300 miles.

This analysis applies the same set of options for charging infrastructure and vehicle range to the entire dataset. Table I.1.4.4 below lists the number of trips where the charging and vehicle combination would be sufficient to complete the trip without the need for public charging. Charging only at the RDC resulted in only 23% and 33% of trips being sufficient for the 300-mile vehicles. While with a 500-mile vehicle this was sufficient for almost half (49% of trips). Adding charging at the delivery locations increased the ability of the charging infrastructure to support up to 94% of the trips recorded.

Table I.1.4.4 Summary of Suitability for Full Vehicle Sample

Vehicle / Charger type	# of Trips	% of Total
300 Mile / 150 kW RDC only	190	23%
300 Mile / 350 kW RDC only	271	33%
500 Mile / 150 kW RDC only	305	37%
500 Mile / 350 kW RDC only	398	49%
300 Mile / 150 kW all stops	577	70%
300 Mile / 350 kW all stops	650	79%
500 Mile / 150 kW all stops	732	89%
500 Mile / 350 kW all stops	772	94%

Figure I.1.4.8 and Figure I.1.4.9 show a breakdown of the number of trips with different amounts of range remaining at the end of the trip for scenarios with charging at each stop. Trips below bucket 7 would require public charging. The lower the bucket number, the more charge that would have been needed at public charging. This evaluation shows that a far majority of the number of trips would be met with the charging infrastructure, with a small number needing significantly more range than is available. And the difference between the 150- and 350-kW chargers is not as impactful as the range of the vehicle increases.

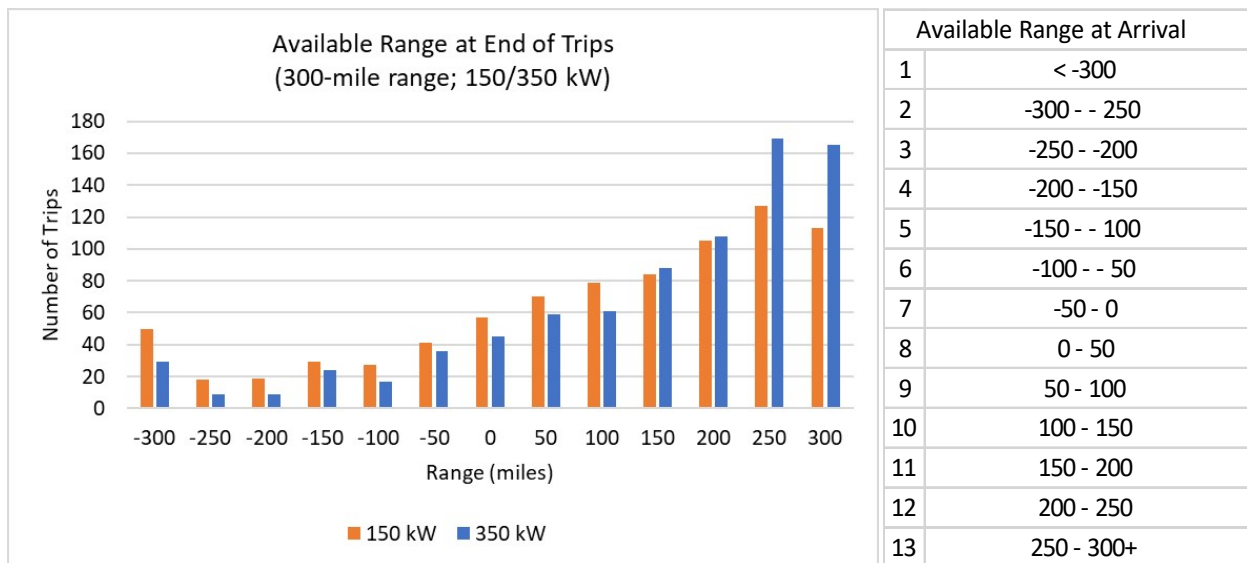


Figure I.1.4.8 Number of Trips with Given Available Range at Arrival (300-mile range/150 and 350 kwh)

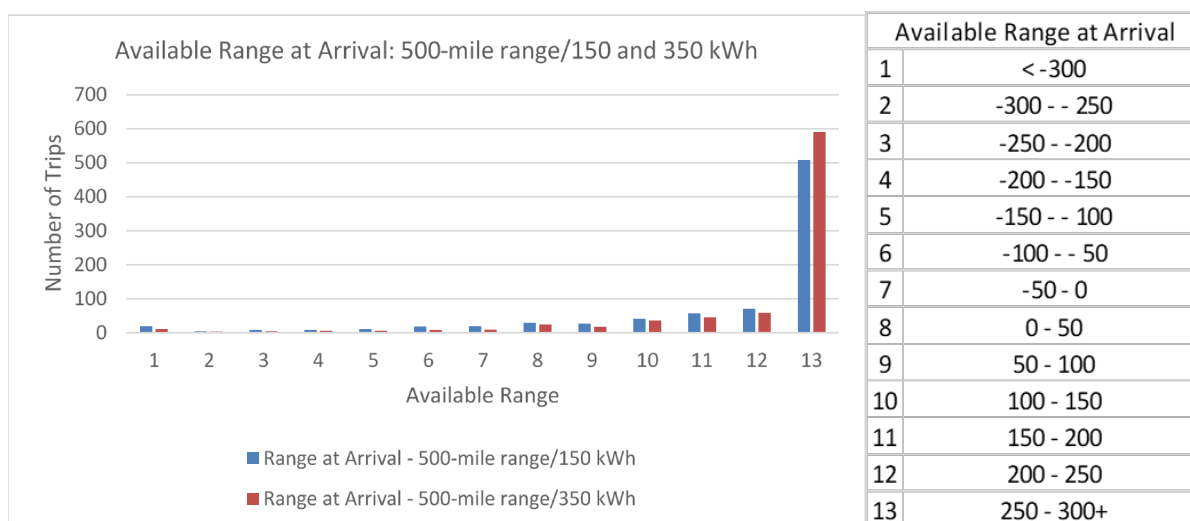


Figure I.1.4.9 Number of Trips with Given Available Range at Arrival (500-mile range/150 and 350 kWh)

Discussion of Results

The scenarios modeled in this analysis are a very small portion of the decisions needed and models which should be applied to assist fleets of vehicle operators. This analysis shows that strategically placing even lower-cost chargers at key places in the network could readily provide for a large majority of the charging needs for a regional distribution fleet. And would significantly reduce the dependence on public chargers as well as charge time during duty cycles.

However, these scenarios utilize some ideal assumptions which need more analysis, such as allowing a charger at every location and only look at the charger from the viewpoint of a single vehicle. There may be locations which would be more strategic for placement of chargers that may not require installations at every stop. Similarly, even though this analysis assumes that a vehicle could use a charger until charged completely, this may not be the most effective use of the charging infrastructure when considering an entire fleet.

Fleets would wish to consider costs of the installations and rates of electrical charges as well as the types and number of chargers needed. They would also benefit from the ability to analyze their operational network depending on their business characteristics to determine which portions of their fleet would be easiest and most cost-effective to electrify. They would then need tools to help them optimize their routing and operations to take advantage of these choices.

The results of this analysis indicate the need for further sets of tools and trade-off analysis to help fleet operators deal with the complex issues of both choosing EVs for their operations and for choosing how to implement charging infrastructure support for their freight vehicles.

Conclusions

Studying the freight industry revealed that widespread truck electrification has the potential to significantly reduce petroleum consumption and cost—trucks moving freight account for 25% of all fuel consumed by United States transportation, and fuel accounts for 20% of operation costs for freight companies. However, the freight industry is complex and there are numerous business models that would require varying degrees of charging infrastructure and/or changes to their operations, in order to adopt limited-range electric trucks. Although it is true that about 75% of trucks are used primarily for trips of less than 200 miles, drivers of Class 7/8 trucks often chain trips together, such that their overall distance traveled before returning home is much

longer than the expected range of electric trucks. This means that charging infrastructure is needed at intermediate destinations or along trucking routes, even for short- and regional-haul fleets.

The variety and complexity of operations in the freight trucking industry make it challenging to discern where electric trucks are beneficial, what kind of charging infrastructure is needed for electrification to be feasible, and who bears the costs and benefits of charging infrastructure investment. Charging infrastructure costs must be weighed against the cost of operational changes, such as routing and dispatching changes. Electric truck operations also must be conducted within the confines of regulation, including the maximum allowable time driver can continuously operate their trucks. The relatively long length of charging time, even with high-power chargers, may be highly problematic for trucking companies who strive to maximize miles driven within regulated shift lengths. New tools are needed to help trucking companies manage complex decisions surrounding electrification and charging infrastructure.

References

1. EIA. 2019. "Monthly Energy Review." DOE/EIA-0035(2019/2). U.S. Energy Information Administration. January 2019.
2. FHWA. 2017. "Evaluation of U.S. Commercial Motor Carrier Industry Challenges and Opportunities." U.S. Department of Transportation Federal Highway Administration. February 1, 2017.
3. US Department of Commerce, Bureau of the Census. "2002 Vehicle Inventory and Use Survey." <https://www.census.gov/library/publications/2002/econ/census/vehicle-inventory-and-use-survey.html>
4. FMCSA. 2019. Accessed March 2019. <http://ask.fmcsa.dot.gov/>
5. Turpen, Aaron. "Tesla Semi Truck's Battery Pack and Overall Weight Explored." TESLARATI, February 26, 2018. <https://www.teslarati.com/how-much-tesla-semi-truck-battery-pack-weigh/>.
6. Kevin Walkowicz, Jason Lustbader, Ken Kelly, and Alicia Birky, "Data and Data Analytics Workshop for Medium and Heavy-Duty Commercial Trucks," Green Truck Summit. Indianapolis Convention Center, 06-Mar-2019
7. "Tesla, Inc." Tesla Semi. Accessed September 1, 2019. <https://www.tesla.com/semi>.
8. "Fleet DNA: Commercial Fleet Vehicle Operating Data." NREL.gov. National Renewable Energy Laboratory (NREL). Accessed September 1, 2019. <https://www.nrel.gov/transportation/fleettest-fleet-dna.html>.
9. Includes vehicles with a Gross Vehicle Weight Rating (GVWR) over 10,000 lbs. Unique businesses were estimated from a unique combination of business name, vocation, and carrier type designation.
10. FMCSA. 2019. Accessed March 2019. <http://ask.fmcsa.dot.gov/>
11. FMCSA. 2018a. "Motor Carrier Census Information, Federal Motor Carrier Safety Administration." U.S. Department of Transportation. 2018. Accessed March 2019. ai.fmcsa.dot.gov/SMS/Tools/Downloads.aspx.
12. (Bureau of Labor Statistics 2019)
13. Chen, Guang, W. Karl Sieber, Jennifer E. Lincoln, Jan Birdsey, Edward M. Hitchcock, Akinori Nakata, Cynthia F. Robinson., James W. Collins, Marie H. Sweeney, NIOSH national survey of long-haul truck drivers: Injury and safety, Accident Analysis & Prevention, Volume 85, 2015, Pages 66-72.
14. FMCSA. 2018b. "Summary of Hours of Service Regulations, Motor Carrier Census Information." Federal Motor Carrier Safety Administration, U.S. Department of Transportation, fmcsa.dot.gov/regulations/hours-service/summary-hours-service-regulations.
15. FHWA. 2018. "Bridge Formula Weights." U.S. Department of Transportation Federal Highway Administration. ops.fhwa.dot.gov/Freight/publications/brdg_frm_wghts/index.htm. June 20, 2018.

I.2 Connected and Automated Vehicles

I.2.1 Traffic Microsimulation of Energy Impacts of CAV Concepts at Various Market Penetrations (LBNL) [Task 1.2]

Xiao-Yun Lu, Principal Investigator

Building 190
Lawrence Berkeley National Laboratory (LBNL)
1 Cyclotron Road, Berkeley, CA
E-mail: xiaoyunlu@lbl.gov

Erin Boyd, DOE Technology Manager

U.S. Department of Energy
E-mail: erin.boyd@ee.doe.gov

Start Date: October 1, 2018

End Date: September 30, 2019

Project Funding (FY19): \$250,000

DOE share: \$250,000

Non-DOE share: \$0

Project Introduction

This project is to develop and apply traffic microsimulation tools to predict the impacts that connected and automated vehicle (CAV) systems are likely to have on traffic and energy consumption. The CAV systems only exist today in very limited numbers of prototype vehicles with limited capabilities, which makes it impossible to do realistic field tests that can directly measure traffic or energy consumption impacts. Consequently, it is necessary to depend on large-scale use of simulations to predict what would happen when the CAV systems are deployed in large numbers. Producing realistic estimates of the impacts is challenging because it requires high-fidelity models that are sensitive to the changes in vehicle behaviors that will occur when they are equipped with CAV technology.

U.S. Environmental Protection Agency (EPA) has shown that transportation accounts for 29% of U.S. greenhouse gas emissions. As for the state-level emission statistics, the transportation sector accounts for almost 50 percent of California's total greenhouse gases, according to the data from the California Air Resources Board (CARB); while light-duty vehicles, make up 70 percent of the sector's Green House Gas (GHG) emissions. Additionally, approximately 80 percent of the smog in California comes from vehicle emissions. Vehicle fuel consumption and emissions play an important role in the environmental impact and vehicle manufactures have made significant progress in reducing fuel consumption and emissions by introducing new powertrain technologies and more efficient vehicle designs. Despite the effort in improving vehicles, fuel consumption and emissions due to traffic congestion and excessive delay have yet to be resolved. Nevertheless, we expect that traffic management and control strategies that improve capacity and reduce delay and travel time would also lead to lower fuel consumption and emissions because there would less stop and go waves and idling. The goal of this project is to investigate how the Autonomie model can capture the impact of macroscopic level traffic management and control on fuel consumption and emissions. In this project, we present a classic example of modern traffic management strategy: freeway ramp metering, which aims to prevent capacity drop and increase mainline throughput on freeway with merging on-ramps. Minnesota's previous study suggested that ramp metering could reduce emissions by 1,161 tons annually (1). The estimated benefits in this report may not be accurate and realistic because the emissions and fuel consumption calculations were made based only on average speeds of all vehicles in different time intervals; they did not consider speed fluctuations and stop-and-go waves of individual vehicles that are observed on real world freeway facilities. This can be done by analyzing detailed vehicle trajectories, which were not considered in the above study.

Objectives

The project objectives include:

- Refining traffic microsimulation models that were developed under previous research projects supported by the U.S. DOT so that they can represent a wider range of CAV alternatives
- Extending previous traffic microsimulation models from freeway applications to urban signalized arterial applications, including the vehicle interactions with the traffic signal control systems
- Integrating the traffic microsimulations with post-processing to produce estimates of the energy consumption derived from the vehicle motion trajectories
- Applying the traffic microsimulations to diverse transportation networks, including rural and urban freeway environments, high-density and low-density signalized arterial corridors, and environments with both high and low percentages of truck traffic, so that the differences in energy impacts can be better understood to support subsequent national impact projections
- Producing estimates of the energy that can be saved for different levels of market penetration of automation systems operating at different levels of automation, both with and without connectivity, in specific scenarios that can be extrapolated to represent national impacts.
- Examining how the Autonomie model can capture the impact of freeway traffic management and control on fuel consumption and vehicle emissions at merge bottlenecks using detailed vehicle trajectory data that precisely captures the speed fluctuations and stop-and-go waves that are associated with capacity drop at freeway merge bottlenecks. The study will choose ramp metering as a typical control measure, and will be conducted through microscopic simulation, as field experiments may be extremely costly and impractical.

Approach

Our modeling framework includes the microscopic traffic models that depict the interactions among ACC/CACC vehicles and manually driven vehicles, as well as the overall impacts of the CACC string operation on the traffic flow. The traffic models provided a solid foundation for modeling the car following and lane changing behavior in mixed traffic with the CACC operation strategies. The traffic models also depicted the effects of traffic control and management strategies including the CACC vehicle dedicated lane in freeways, vehicle-to-vehicle (V2V) communications between CACC vehicles and manually driven vehicles, and cooperative traffic signal control algorithm. The fuel consumption model computed the vehicle fuel consumption rates based on the second-by-second vehicle speed and acceleration data generated by the traffic models.

1. Human Driver Model

The human driver model is used to update the position and speed of the manually driven vehicles in the simulation. Particularly, the car following behavior is depicted by Newell's simplified car-following model [1] with constraints for safety and free-flow accelerations. The safety acceleration is derived from the safe distance term in Gipps' car-following model [2]. It specifies a subject vehicle's maximum allowable acceleration under the collision avoidance constraint. The free-flow acceleration is derived from the free-flow component of the Intelligent Driver Model [3], which provides the upper limit of the acceleration when a vehicle accelerates in light traffic. The acceleration of a subject vehicle at each simulation interval is determined as follows:

$$a = \min(a_N, a_{free}, a_{safe}) \quad (1)$$

Where a_F : free-flow acceleration; a_N : Newell acceleration; a_{safe} : safe acceleration.

The acceleration terms in Equation 1 are given as follows:

$$a_N(t) = ((d(t) - d_{jam}) / \tau_h - v(t)) / (\tau_h / 2) \quad (2)$$

$$a_{free}(t) = a_{max} [1 - (v(t) / v_{free})^\alpha] \quad (3)$$

$$a_{safe}(t) = (v_{safe}(t + \tau_r) - v(t)) / \tau_r \quad (4)$$

$$v_{safe}(t + \tau_r) = A(t) + \sqrt{A(t)^2 - C(t)} \quad (5)$$

$$A(t) = -b_f \tau_r \quad (6)$$

$$C(t) = b_f [2(d(t) - d_{jam}) - v(t) \tau_r - v_l(t)^2 / (-b)] \quad (7)$$

where τ_h : desired headway [s]; $v(t)$: speed of the subject vehicle [m/s]; d_{jam} : jam gap [m]; a_{max} : maximum acceleration [m/s²]; v_{free} : free flow speed [m/s]; α : acceleration exponent; τ_r : reaction time [s]; $v(t + \tau_r)$: speed of the subject vehicle after reaction time [m/s]; $v_l(t)$: speed of the preceding vehicle [m/s]; b_f : most severe braking that the subject driver wishes to undertake [m/s²]; b : the subject driver's estimate of preceding vehicle's most severe braking capabilities [m/s²]; $d(t)$: clearance gap with regard to the leader at time t [m].

When a subject driver is making a lane changing maneuver or just completes a lane changing maneuver, the driver will temporarily accept shorter desired time gap and jam gap and her/his reaction will be faster for achieving a safe lane changing operation. Similarly, if the subject driver actively creates a gap for a lane changer or receives a lane changer that just merges in front, the driver's car following behavior also temporarily changes. To depict the above car following states, the driver's desired headway, jam gap, and reaction time used in Equations 2 to 7 for the regular car following state will temporarily decrease when a subject driver adopts those modes. Afterwards, the parameters will linearly increase until they return to the normal values.

2. ACC and CACC Models

The CC, ACC and CACC vehicle following models were reported before, which were calibrated and validated with field test data of a few CACC vehicles driving in those modes in public traffic. Those data should capture the dynamic interaction between CC/ACC/CACC vehicles with manually drive vehicles.

3. Cooperative Traffic Signal Control Algorithm

The testbed, we have used a cooperative signal control algorithm that adopts the CACC datasets and the datasets collected by the traditional fixed traffic sensors to predict the future traffic conditions. The prediction allows the signal controller to assign signal priority to the intersection approach that accommodates the most CACC strings. Such a control strategy can significantly enhance the CACC string operation, which ultimately improves the overall intersection performance. The structure of the signal control algorithm is briefly introduced as follows. The detailed algorithm description can be found in [5].

The objective of the proposed cooperative signal control algorithm is to determine proper green times for the eight-phase signal controller such that the resulting signal phase and timing (SPaT) scheme maximizes the overall throughput of the intersection. This would indirectly improve the vehicle energy consumption performance. It improves the intersection operation by assigning green time more efficiently than the fixed or actuated signal control. Figure I.2.1.1 shows a conceptual comparison between the cooperative algorithm and a typical actuated control algorithm. With the actuated controller, vehicle A from the westbound approach would trigger green time extensions. The extended green time only allows a few vehicles in the dashed box to pass the intersection. On the other hand, our algorithm reallocates the green time such that the extended green time is given to a different approach where several CACC strings are coming. The resulting green time split allows vehicles in those CACC strings to pass the intersection without waiting for another green cycle, thus leading to improved intersection throughput.

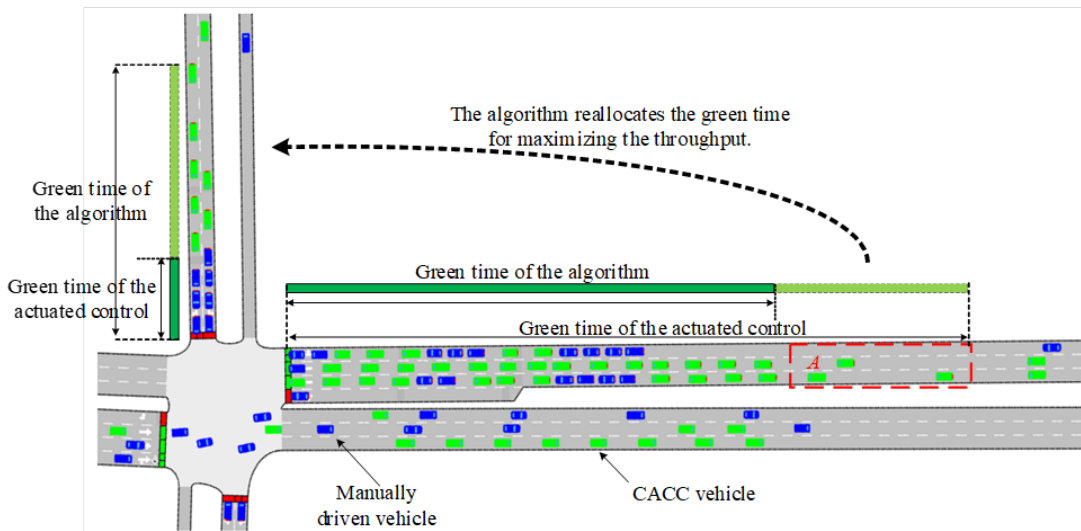


Figure I.2.1.1 Comparison of the proposed algorithm and actuated control

4. Fuel and Emission Evaluation Using Autonomie

Fuel Consumption and Emissions Modeling

Many researchers have studied fuel consumption and emission models [11],[12]. Typically, modal emissions models, such as MOVES model, use the concept of operating bins to calculate the emission rate [13]. They use the vehicle trajectory data generated from the simulation to calculate the fraction of time each vehicle spends in different operating bins, which are categorized by speed, acceleration, and scaled tractive power (STP). Then, the average emission rate for a vehicle could be calculated using its operation mode distribution with the emission rates table. However, we would prefer to use second-by-second detailed trajectory data to precisely model the effect of speed fluctuations and stop-and-go waves (all of which are associated with capacity drop) on fuel consumption and emissions. Unfortunately, many previous studies [12],[14],[15] raised the concern regarding the intense computation burden associated with analyzing second-by-second vehicle trajectory data. As a compromise, these models use operating bins to divide each vehicle's travel time into various groups based on its speed and acceleration data (or other attributes) at that time, where each group has its own emission rate. But no matter how precisely these modes are divided, we cannot precisely capture the effect of speed fluctuation and stop-and-go waves.

Autonomie for Energy Evaluation

Autonomie, developed by Argonne National Laboratory (Argonne) in collaboration with General Motors, is a MATLAB-based software environment and framework for automotive control system design, simulation, and analysis [11]. In Autonomie, it simulates each vehicle's fuel consumption and emissions based on details such as engine speed and gear position at every timestamp, using on second-by-second trajectory data generated by microscopic simulation. This allows the model to capture speed fluctuation (i.e., acceleration, deceleration, and idling) and stop-and-go waves. Contrary to our expectation, Autonomie uses parallel computing methods to achieve high computational efficiency. By building models automatically, Autonomie allows the quick simulation of a very large number of component technologies and powertrain configurations. The model has been validated for several powertrain configurations and vehicle classes using Argonne's Advanced Powertrain Research Facility (APRF) vehicle test data [17],[19]. This enables us to precisely model realistic fuel consumption and emissions. In this study, the simulation experiments only included conventional gasoline powered vehicles as alternative powertrains still represent a very small market penetration.

The steps of Autonomie's energy evaluation are shown below:

Step 1: Export the trajectory SQLite files generated in Aimsun to .csv files to run (using 10% trajectory data for energy evaluation can maintain reasonable accuracy while significantly reduce computation time);

Step 2: Setup parameters, which includes: AimSun trajectory filename, Scenario file: ANL provided xml file defining the scenarios and vehicle mapping, Vehicle class: ‘LD’ for light-duty and ‘HD’ for medium-duty/heavy-duty, and Output results filename: Energy results database filename (.csv);

Step 3: Obtain the results database: the results is in .csv format, each row corresponds to the results of a single trip in the trajectory database, and the information (columns) includes Vehicle ID / Vehicle filename, Fuel consumption (kg), Fuel consumption per mile (kg/mile), Electrical consumption (J), Driving distance (miles), Fuel economy (mpg), Emissions – GHGs, VOC, CO, PM10, PM2p5, NOx, SOx, BC, POC, CH4, N2O (kg/km), and Vehicle manufacturing cost (2015\$).

Table I.2.1.1 Screenshot of Autonomie Output Results

Vehicle ID	Fuel Consumption [kg]	Fuel Consumption Per Mile [kg/mile]	Electrical Consumption [J]	Driving Distance [miles]	Fuel Economy [mpg]	GHGS [kg/km]	VOC [kg/km]	CO [kg/km]	PM10 [kg/km]	PM2p5 [kg/km]	NOx [kg/km]	SOx [kg/km]	BC [kg/km]	POC [kg/km]	CH4 [kg/km]	N2O [kg/km]	Vehicle Name	Vehicle Manufacturing Cost [2015\$]
10016	0.246993741	0.082364134	-5368.358819	2.998801137	34.06	0.198411887	0.000176139	0.001332749	1.85E-05	9.38E-06	0.000122922	4.61E-05	1.55E-06	2.80E-06	0.000246345	9.46E-06	conv_Midsize_SUV_si_LV10_CT	23480.539
10041	0.278193426	0.09402952	-3717.843136	2.958250516	29.83	0.226537424	0.000201107	0.001521167	2.11E-05	1.07E-05	0.000151764	5.27E-05	1.77E-06	3.19E-06	0.000281265	1.08E-05	conv_Midsize_SUV_si_LV10_CT	23480.539
10070	0.234878667	0.092875832	-4556.514662	2.528953584	30.20	0.223734144	0.000198619	0.001502884	2.08E-05	1.06E-05	0.000149886	5.20E-05	1.75E-06	3.16E-06	0.000277785	1.07E-05	conv_Midsize_SUV_si_LV10_CT	23480.539
10075	0.080933345	0.064665257	-4834.482103	1.251573849	43.38	0.155776005	0.000138289	0.00104636	1.45E-05	7.37E-06	0.000104359	3.62E-05	1.22E-06	2.20E-06	0.000193409	7.43E-06	conv_Midsize_si_LV10_CT	23286.4274
10081	0.243364869	0.090259318	-4522.718766	2.528221429	29.14	0.231884826	0.000205854	0.001557589	2.16E-05	1.10E-05	0.000155347	5.39E-05	1.81E-06	3.27E-06	0.000287905	1.11E-05	conv_Small_SUV_si_LV10_CT	23507.1886
10088	0.327770135	0.080423291	-3371.351	4.07562326	34.88	0.193736475	0.000171988	0.001301343	1.80E-05	9.16E-06	0.00012979	4.50E-05	1.51E-06	2.73E-06	0.00024054	9.24E-06	conv_Compact_si_LV10_CT	22803.6184
10093	0.205288327	0.072515138	-2792.846472	2.83097204	38.68	0.174686051	0.000155076	0.00117338	1.63E-05	8.26E-06	0.000117027	4.06E-05	1.37E-06	2.46E-06	0.000216887	8.33E-06	conv_Compact_si_LV10_CT	22803.6184
10128	0.270847047	0.09412065	-8254.808193	2.877658058	29.80	0.226732862	0.000201281	0.001522983	2.11E-05	1.07E-05	0.000151895	5.27E-05	1.77E-06	3.20E-06	0.000281508	1.08E-05	conv_Compact_si_LV10_CT	22803.6184
10152	0.210311563	0.05420928	-4172.578948	1.994969754	26.61	0.253954777	0.000225447	0.001205835	2.36E-05	1.20E-05	0.000170132	5.90E-05	1.98E-06	3.58E-06	0.000315306	1.21E-05	conv_Midsize_SUV_si_LV10_CT	23480.539
10154	0.209517781	0.076142345	-4358.659226	2.751699157	36.84	0.183422848	0.000162833	0.00123073	1.71E-05	8.67E-06	0.000122881	4.26E-05	1.43E-06	2.59E-06	0.000277736	8.74E-06	conv_Small_SUV_si_LV10_CT	23507.1886
10169	0.209629128	0.079407912	-2410.234405	2.63990228	35.32	0.191290468	0.000169817	0.001284913	1.78E-05	9.04E-06	0.000128151	4.45E-05	1.49E-06	2.70E-06	0.000237503	9.12E-06	conv_Midsize_si_LV10_CT	23286.4274
1017	0.917548728	0.092910545	-5173.205217	9.875614493	30.19	0.223817768	0.000198693	0.001503402	2.08E-05	1.06E-05	0.000149942	5.20E-05	1.75E-06	3.16E-06	0.000277889	1.07E-05	conv_Small_SUV_si_LV10_CT	23507.1886
10179	0.233640651	0.07206974	-2584.028859	3.241868948	38.92	0.173613105	0.000154124	0.001166173	1.62E-05	8.21E-06	0.000116309	4.04E-05	1.36E-06	2.45E-06	0.000215555	8.28E-06	conv_Compact_si_LV10_CT	22803.6184
1018	0.139153025	0.129726018	4368.288004	1.072668587	21.62	0.312504763	0.000277424	0.002099912	2.91E-05	1.48E-05	0.000209356	7.26E-05	2.44E-06	4.41E-06	0.000388001	1.49E-05	conv_Compact_si_LV10_CT	22803.6184
10181	0.229682953	0.085675212	-4107.409881	2.680856553	32.74	0.206388141	0.00018322	0.001386326	1.92E-05	9.76E-06	0.000138266	4.80E-05	1.61E-06	2.91E-06	0.000256248	9.84E-06	conv_Midsize_si_LV10_CT	23480.539
10217	0.35497761	0.114860018	-9729.288679	3.090523714	24.42	0.276693166	0.000245633	0.00185857	2.58E-05	1.31E-05	0.000185365	6.43E-05	2.16E-06	3.90E-06	0.000343538	1.32E-05	conv_Small_SUV_si_LV10_CT	23507.1886
10247	0.280007015	0.162542473	-5394.839181	1.722699834	17.26	0.39158282	0.000347604	0.002630128	3.65E-05	1.85E-05	0.000262317	9.10E-05	3.06E-06	5.52E-06	0.000486153	1.87E-05	conv_Pickup_si_LV10_CT	25438.4248
10251	0.270073494	0.097116777	-3473.787941	2.873868855	28.88	0.233950411	0.000207888	0.001571464	2.18E-05	1.11E-05	0.00015673	5.44E-05	1.83E-06	3.30E-06	0.000290469	1.12E-05	conv_Midsize_SUV_si_LV10_CT	23480.539
10272	0.112528065	0.11405149	1333.564238	1.06554375	24.59	0.274745455	0.000243904	0.001845487	2.56E-05	1.30E-05	0.00018406	6.39E-05	2.15E-06	3.87E-06	0.00034112	1.31E-05	conv_Small_SUV_si_LV10_CT	23507.1886
10313	0.278088324	0.101206575	-3358.080875	2.747729824	27.72	0.24380257	0.000216434	0.001637641	2.27E-05	1.15E-05	0.000163331	5.67E-05	1.91E-06	3.44E-06	0.000302701	1.16E-05	conv_Midsize_SUV_si_LV10_CT	23480.539

Microscopic Simulation of Freeway Merge

This study used the PATH model [2] to simulate realistic car following and lane changing behavior that lead to capacity drop at freeway merge bottlenecks Figure I.2.1.2. The PATH model has been proven, calibrated and validated, and discussed in detail in several studies [20],[23]. The PATH model is also more effective than the proprietary driver behavior models in commercial microscopic simulation software packages, as the proprietary models cannot replicate capacity drop [24]. The PATH model was incorporated into a commercial microscopic simulation package AIMSUN [25] using micro software development kit (MicroSDK). As shown in Figure I.2.1.2, a simple freeway merge was first built in the AIMSUN microscopic simulation software [25]. The merge section consists of a freeway mainline with 4 lanes, an on-ramp, and a 155-meter acceleration lane.

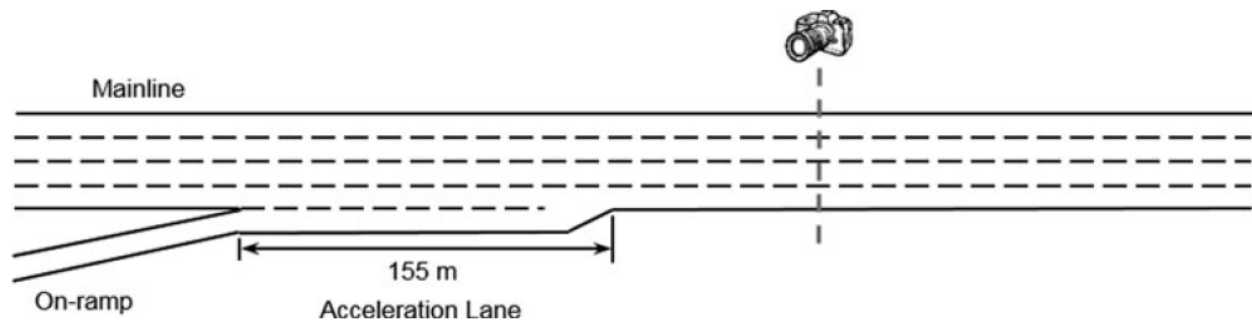


Figure I.2.1.2 Multilane freeway merge section

In the freeway merge simulation experiments, we first determined the capacity of the freeway mainline (zero on-ramp demand) by measuring the maximum 15-minute moving average flow downstream of the merging area (at the location indicated by the camera and the dotted line in Figure I.2.1.2). This was done according to

the definition specified in the Highway Capacity Manual [26]. This first experiment simulated a constant and relatively low traffic demand for one hour, and if the freeway remained free-flowing, then we conducted subsequent simulations using slightly higher demand input (e.g., plus 1000 veh/hr), until we can observe congested conditions and the capacity (defined as the highest observed 15-minute moving average flow) no longer increased as the input became larger. Afterwards, these procedures were repeated with identical freeway mainline demand and an additional on-ramp demand of 300 veh/hr, 600 veh/hr, 900 veh/hr, 1200 veh/hr, and 1500 veh/hr to determine whether the capacity previously observed would decrease following the introduction of merging traffic. We expect that the capacity of this merge section would decrease as on-ramp demand became sufficiently high (for example at 600 veh/hr). Finally, we activated the ramp metering at a metering rate equal to the maximum on-ramp demand at which the capacity of the freeway merge did not diminish. All the above simulations were conducted for 10 replications with different random seeds. Lastly, each simulation run would generate a SQLite database with detailed vehicle trajectory including vehicle speed, acceleration, timestamp, and position (x-y coordinates). The database will be used as input for the fuel consumption and emissions analysis using a model known as Autonomie.

After the simple freeway merge experiments, a microscopic simulation network of the SR99 northbound corridor (Figure I.2.1.3) was then built using the most up to date road geometry, lane configurations, speed limits, and 5-minute interval loop detector data from the Performance Measurement System (PeMS). PeMS is an integrated CA state-wide highway data system; all the highway data from 12 Districts are forwarded to the system every 30 s in real-time for traffic monitoring and management. The PeMS data were used as the inputs in demand at the most upstream location of the simulation network and the entry points of the on-ramps, and as the turning percentages at any applicable mainline off-ramp split. The simulation lasted for 6 hours from 5:00 AM to 11:00 AM in a typical day, and this 6-hour period encompasses periods prior to, during, and after the typical morning peak. Ramp metering rates were obtained from the look-up table provided by Caltrans District 3 and the local responsive algorithm was modeled in the microscopic simulation via the AIMSUN API (Application Programming Interface).

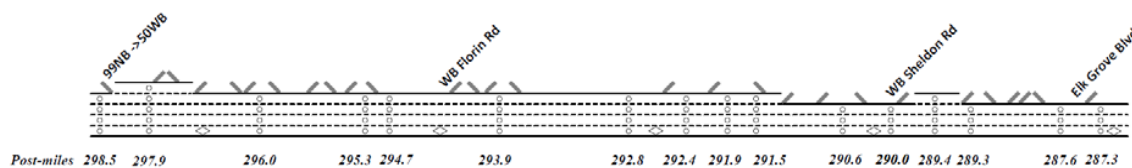


Figure I.2.1.3 Land configuration and road geometry

Results

1. Impacts of CACC on a Freeway On-Ramp Bottleneck

The case studies were performed in a typical freeway on-ramp merging area displayed in Figure I.2.1.3. The red boxes indicate the source links, through which the simulated vehicles are released into the network. There is a 2-kilometer ‘warm-up’ mainline segment immediately downstream from the mainline source link, followed by a 1-kilometer homogeneous freeway segment before the merging link. The simulated vehicles use the warm-up segment to reach a stable car-following state after entering the network. This segment also allows CACC vehicles to form stable CACC vehicle strings in the CACC analysis cases. The traffic data collected downstream from the warm-up section was used for the analysis. The vehicle fuel consumption was computed based on the vehicle speed and acceleration data by using the Virginia Tech Comprehensive Power-based Fuel Consumption Model [6].

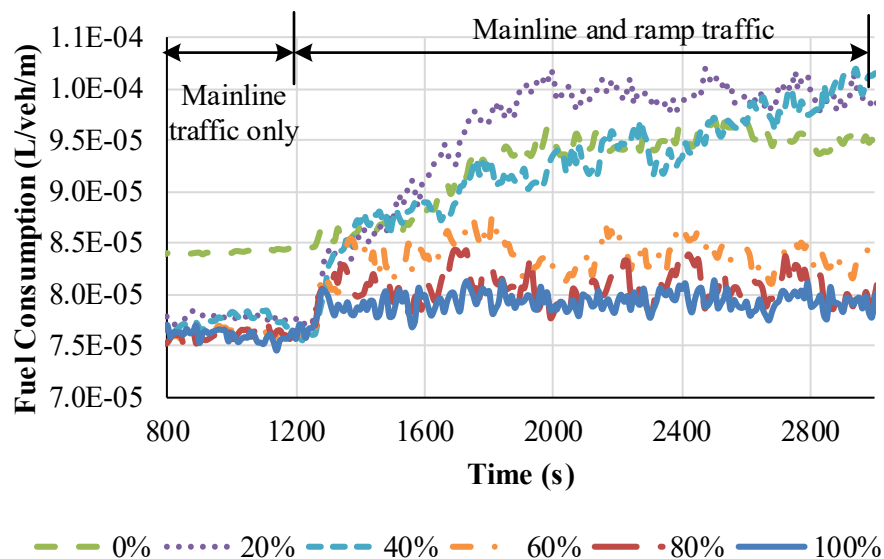
The freeway upstream mainline input was 1950 veh/hr/lane, which was the pipeline capacity when all vehicles were manually driven. The on-ramp input was 600 veh/hr. This on-ramp demand was sufficient to trigger traffic congestion when the mainline input approaches the capacity. The CACC and ACC market penetrations

considered in the analysis ranged from 20% to 100%, in 20% increments. When the ACC/CACC market penetration is less than 100%, the ACC and CACC vehicles were randomly generated at the beginning of the simulated network based on the ACC/CACC market penetration. The same ACC/CACC market penetration was used for both the freeway mainline input and the on-ramp input. Each scenario has simulated 5 replications with each for one hour. In addition to the effect of CACC market penetration, we also considered the impact of the CACC string operation strategies on the vehicle fuel efficiency under low or medium CACC market penetrations. The strategies tested in this study were the CACC vehicle with managed lane (ML) and the implementation of vehicle awareness devices (VAD) on the non-CACC vehicles. A VAD vehicle is a manually driven vehicle equipped with a wireless communication device that broadcasts the vehicle's real-time operation information (e.g., speed, acceleration, and yaw rate). Its car following and lane changing behavior is the same as the normal manually driven vehicles. When a CACC vehicle is following the VAD vehicle, the CACC controller can receive the preceding VAD vehicle's data and perform the automated speed control as if it is following a CACC vehicle string leader.

1.1 Fuel Consumption Rates of ACC and CACC Cases

Figure I.2.1.4 depicts the comparison of the fuel consumption rates among various CACC and ACC market penetrations. The fuel consumption decreases with the CACC market penetration. Such a trend is associated with the increase of CACC vehicle strings in the traffic stream. As more CACC vehicles operate in the strings, they adopt shorter time gaps, thereby occupying less freeway space. As a result, many long gaps are created between CACC strings. The on-ramp vehicles can easily merge into those gaps without forcing the mainline traffic to slow down. It therefore leads to a smoother traffic stream with more efficient vehicle fuel economy. In addition, the left part of Figure I.2.1.4a shows that all CACC cases perform substantially better than the human driver case when there is no on-ramp traffic. It implies that a small portion of CACC vehicles can already stabilize the traffic flow in the homogeneous freeway segment and bring about energy savings. However, when there are traffic disturbances from the on-ramp, the low CACC market penetration cases become worse than the human driver case. When the population of CACC vehicles is small, most of them must adopt the ACC controller because they cannot find a CACC vehicle leader. The ACC controller can intensify the disturbances caused by the on-ramp traffic, leading to more severe traffic oscillations and worse fuel economy.

(a) CACC cases



(b) ACC cases

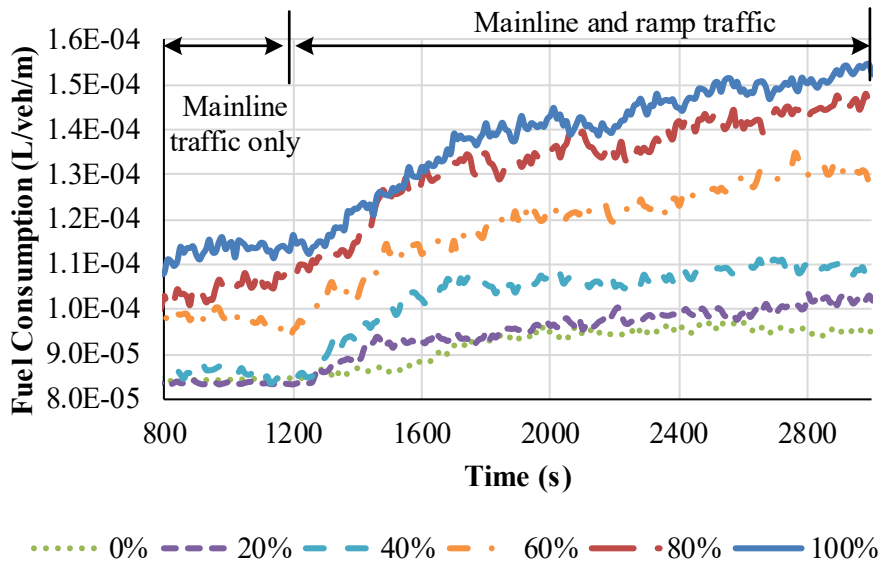


Figure I.2.1.4 Time series of fuel consumption rate under various CACC and ACC market

1.2 Fuel Consumption Rates under the Influence of CACC String Operation Strategies

The CACC operation cannot bring about substantial capacity improvement while maintaining the same vehicle fuel economy until the market penetration reaches a higher level. This might hinder the initial deployment of the vehicle automation system in the existing highway system. Previous studies showed that the implementation of specific CACC operation strategies can improve the effectiveness of CACC under the lower market penetration cases [7]. Those strategies might also improve the vehicle fuel efficiency. For this reason, we further analyzed the influence of the operation strategies (i.e., ML and VAD) on the vehicle fuel consumption rate under low and medium CACC market penetrations.

Figure I.2.1.5 shows the temporal and spatial patterns of the vehicle fuel consumption rate for the 40% CACC case when the upstream mainline input is fixed at 1950 veh/hr/lane (i.e., the capacity of the human driver only case) and the on-ramp traffic is 600 veh/hr (Similar observations are found for the 20% and 60% CACC cases). The results prove that the vehicle fuel efficiency can be significantly improved when the application of the ACC controller (without V2V cooperation) is reduced. The VAD strategy performs better than the ML strategy because the former can completely remove the impact of the ACC car following behavior, whereas the latter only eliminates the ACC usage in the managed lane.

Another interesting observation is that the vehicle fuel consumption rate of the 40%_ML case is higher than the 40% case when there is no on-ramp input. There are two contributing factors to this observation. One cause is that the ML strategy induces additional vehicle lane changes between the managed lane and general-purpose lane, which trigger local traffic disturbances. Another reason is that the managed lane only serves 25% of the total traffic or 62.5% of the total CACC traffic. The remaining 37.5% of the CACC vehicles are scattered in the general-purpose lanes. Since the CACC market penetration in the general-purpose lanes is low, there is a large probability that those CACC vehicles still use the ACC controller in the traffic stream.

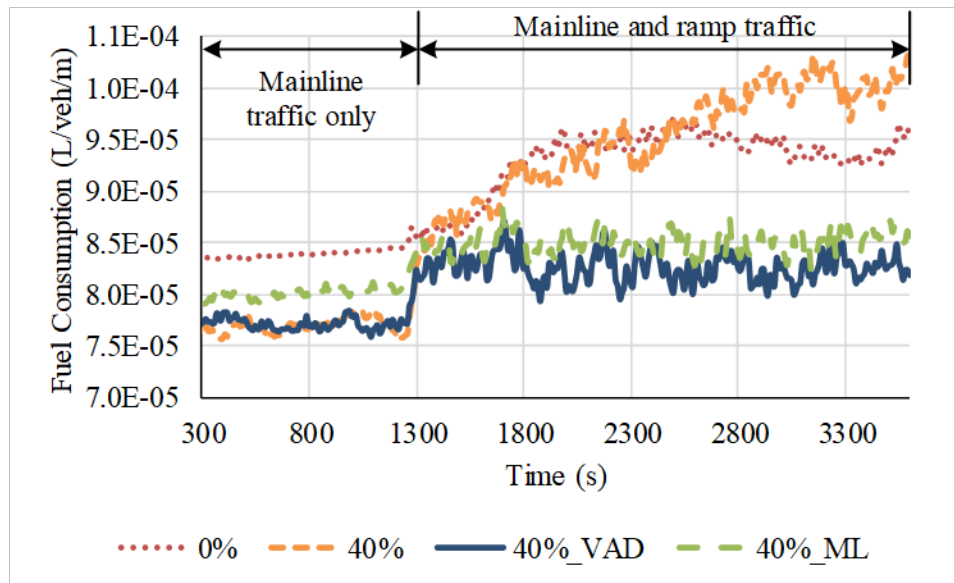


Figure I.2.1.5 Temporal and spatial patterns of the vehicle fuel consumption rate for the 40% CACC case

5. Signal Operation of Intersection with CAVs

We tested the performance of the cooperative signal control algorithm in a simulation environment. The simulation experiments offer a performance comparison for a four-way signalized intersection with and without the cooperative signal control algorithm. The test intersection is a four-way intersection as illustrated by Figure I.2.1.6. The southbound and northbound approaches are major approaches with two through lanes and a dedicated left turn lane. The westbound and eastbound approaches are minor approaches with one through and right turn lane and one left turn lane. The major approach has a traffic demand of 95% through movement and 5% left turn movement. The traffic volume of the minor approach contains 45% left turn demand, 45% right turn demand, and 10% through demand. The baseline simulation has been performed under 0% CACC case. The baseline signal adopts a typical actuated signal controller. The parameters of the controller, including the green, yellow and all red time, are shown in Figure I.2.1.6. Those parameters are determined based on the method described in the Highway Capacity Manual [8]. In addition to the baseline simulation, we also conducted analyses for scenarios of 20%, 40%, 60%, 80% and 100% CACC market penetrations. We had 5 simulation runs for each scenario. Each run covered 10 minutes warm-up period and 1-hour simulation time.

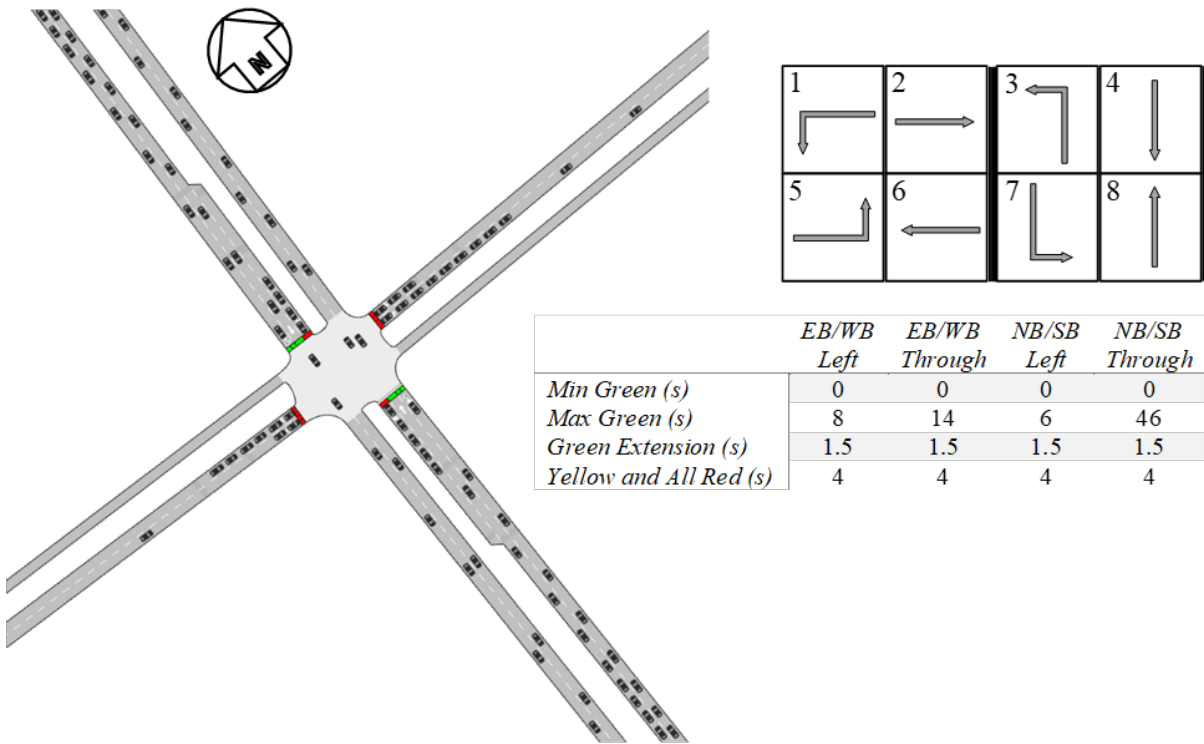


Figure I.2.1.6 Simulated intersection and signal control parameters

2.1 Impacts of CACC on Intersection Capacity

We first investigate the impacts of CACC on the intersection capacity when the default actuated signal controller is used. The intersection capacity with various CACC market penetrations is shown in Figure I.2.1.7. We observe a 67% capacity increase for the major approach (i.e., the northbound and southbound approach), and a 49% increase for the minor approach (i.e., the eastbound and westbound approach) when the CACC market penetration is 100%. The capacity of the major approach is substantially larger than the minor approach because the major approach has more lanes and it is assigned longer maximum green time (see Figure I.2.1.6). For the major approach, the capacity first increases quadratically as the market penetration changes from 0% to 40%. Afterwards, the increase follows a linear trend. The rate of increase becomes smaller because of the influence of the lane changing behaviors occurred near the intersection stop bar. When a subject vehicle needs to make a left turn at the intersection, it must make mandatory lane changes towards the left turn lane. In higher CACC market penetration cases where the CACC string operation may prevent the subject vehicle from finding a sufficient gap upstream from the intersection, the lane changing vehicle is often forced to make aggressive last-minute lane changes near the intersection. This would greatly interrupt the queue discharging flow of the CACC strings. As a result, the capacity benefit that could have been provided by the CACC string operation is substantially decreased.

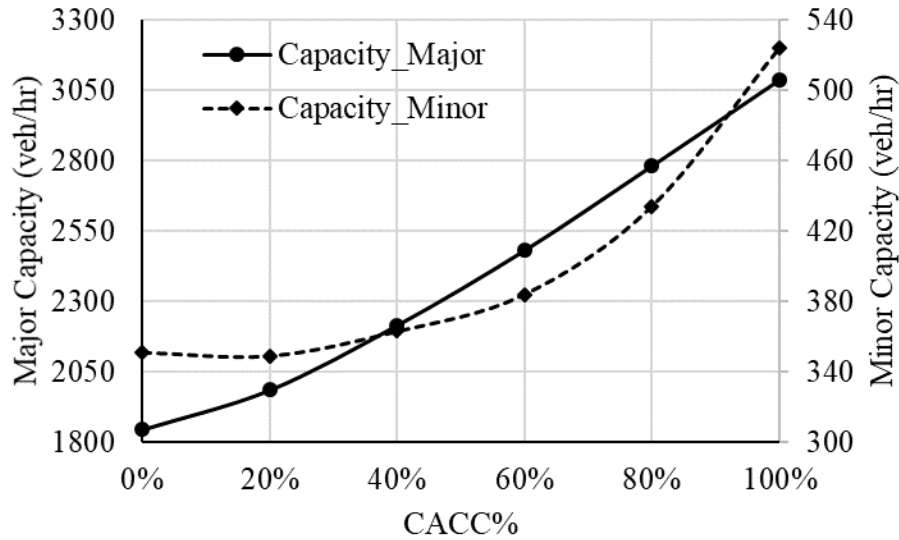


Figure I.2.1.7 Intersection capacity per direction with CACC market penetration

2.2 Impacts of the Signal Control Algorithm with CACC Market Penetration

We aim to determine the impacts of the proposed signal control algorithm under various CACC market penetrations. In the simulation runs, the traffic demand input for the major approach was 1800 vehicles per hour and the demand for the minor approach was 350 vehicles per hour. Those inputs were the intersection capacity measured in the 0% CACC case (see Figure I.2.1.8). The average vehicle speed and average vehicle miles travelled per gallon fuel consumed (MPG) were used to depict the effects of the algorithm on both the traffic flow and vehicle fuel consumption.

The vehicle speed and MPG variations with respect to CACC market penetration are shown in Figure I.2.1.8 and Figure I.2.1.9. The results show that the proposed cooperative signal control algorithm can assign the green time more efficiently than the default actuated controller. Consequently, the queued vehicles can be released from the intersection within a control cycle even in cases with 20% or lower CACC vehicles. For this reason, the algorithm brings about great performance improvement in the 0% and 20% CACC cases. Notably, the algorithm performs well in the 0% CACC case where the SPaT computation completely relies on the vehicle count and speed data obtained via the fixed traffic sensors. With such limited datasets, the algorithm can still generate green time distributions that substantially improve the speed and MPG. This demonstrates the robustness of the proposed algorithm.

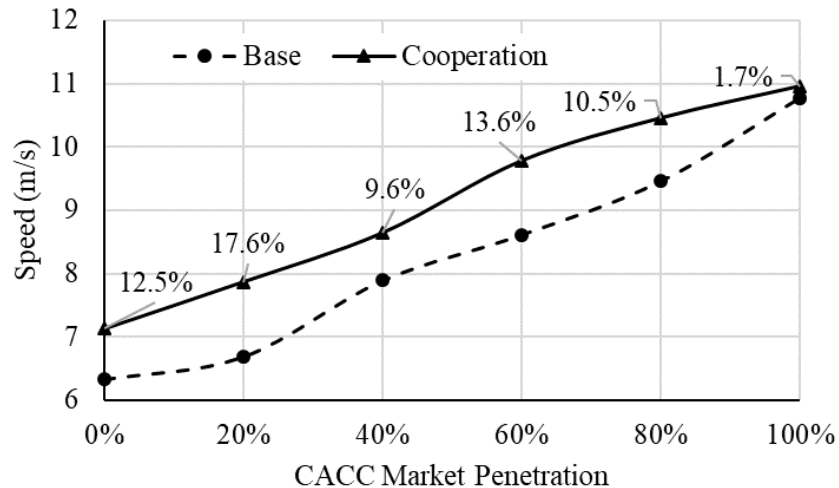


Figure I.2.1.8 Average vehicle speed under various CACC market penetrations

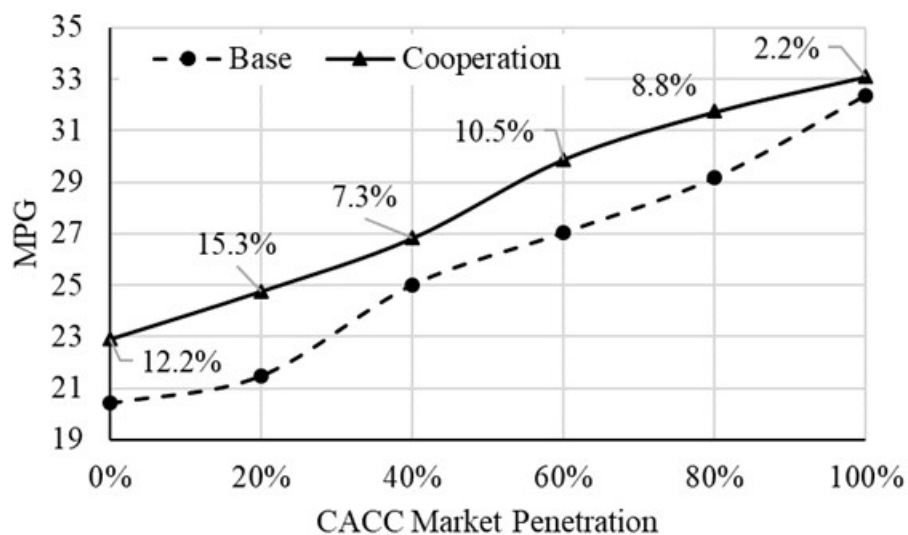


Figure I.2.1.9 Average vehicle fuel economy (MPG) under various CACC market penetrations

2.3 Implementation of the Signal Control Algorithm with Vehicle Trajectory Planning

We have implemented the proposed signal control algorithm with an optimal vehicle trajectory planning strategy presented in [9]. The energy saving due to the implementation of the trajectory planning becomes much less significant. Table I.2.1.2 shows the average vehicle MPG when the CACC market penetration is 100% and the traffic demand is 10% and 100% of the intersection capacity measured in the manual driver case. It shows that the vehicle fuel efficiency only has a minor increase when the demand is 10% of the intersection capacity. The fuel economy even becomes worse when the demand is 100% of capacity. As the trajectory planning algorithm asks the subject vehicle to start decelerating earlier than it does in the baseline case, it also causes the following vehicles to join the queue initiated by the leader at an earlier time. Because of the early start of the queue accumulation, more vehicles upstream from the subject vehicle will be affected by the queue. Many of the queued vehicles would have passed the intersection without slowing down if the trajectory planning is not implemented. In this case, the benefit of the trajectory planning for individual subject vehicles is largely offset by the energy loss of the extra queued vehicles. Such an energy loss trend becomes greater as

the traffic demand increases. This analysis indicates that we need to improve the trajectory planning algorithm such that it optimizes both the fuel consumption of the subject vehicle, and the overall traffic flow.

Table I.2.1.2 Average Vehicle MPG under Traffic Inputs of 10% and 100% Intersection Capacity

	10 % Capacity			100% capacity		
	Baseline	Trajectory Planning	Δ	Baseline	Trajectory Planning	Δ
Overall	31.4	31.5	0.1%	29.4	29.2	-0.8%
NB	32.1	32.1	0.0%	30.1	29.8	-0.9%
SB	32.0	32.1	0.3%	29.8	29.5	-0.8%
WB	20.6	20.5	-0.6%	19.9	19.7	-1.3%
EB	18.5	18.3	-1.3%	20.8	20.7	-0.4%

The analysis has shown that capacity drop at the freeway merge can be replicated in simulation, and metering the on-ramp can mitigate capacity drop and improve mobility at the freeway merge. Capacity drop at the freeway merge has a negative environmental impact while metering the on-ramp properly can mitigate the negative environmental impact, which can be all captured by Autonomie model. Finally, the effectiveness of traffic management can influence fuel consumption and emissions: effective strategies such as ramp metering that prevents capacity drop can reduce emissions but inefficient strategies such as the local responsive ramp metering (LRRM) implemented on SR-99 corridor can do the opposite to fuel consumption and emissions.

6. Fuel Consumption and Emissions on Simple Freeway Merge

Fuel consumption and various types of emissions were calculated via Autonomie. For emissions, empirical studies indicate that NO_x, CO, HC and CO₂ are four most important performance metrics for quantifying the environmental impacts in the transportation sector [10],[12],[19]. In addition, PM 2.5 was selected because it is closely linked to deaths from heart and lung diseases [27]. We measured the average fuel consumption and emissions metrics on a per-kilometer and per-vehicle basis in order to account for the fact that different scenarios have different number of vehicles simulated (due to varying on-ramp demand) and that vehicles travel varying distances.

As shown in Figure I.2.1.10, the solid lines represent the fuel consumption or emissions estimates of the freeway merge (mainline and on-ramp combined), while the dotted lines represent the fuel consumption and emissions estimates at on-ramp only. Prior to implementing ramp metering, the average fuel consumption and emissions increases at a constant rate as the on-ramp demand increases from 300 veh/hr to 900 veh/hr, afterwards, the average fuel consumption and emissions still increase but at a slightly lower rate. This indicates that there is a correlation between the previously observed capacity drop and average fuel consumption and emissions; capacity drop due to high on-ramp demand can lead to as much as a 57% additional fuel consumption and emissions per kilometer for each vehicle (compared with the case where the on-ramp demand is absent).

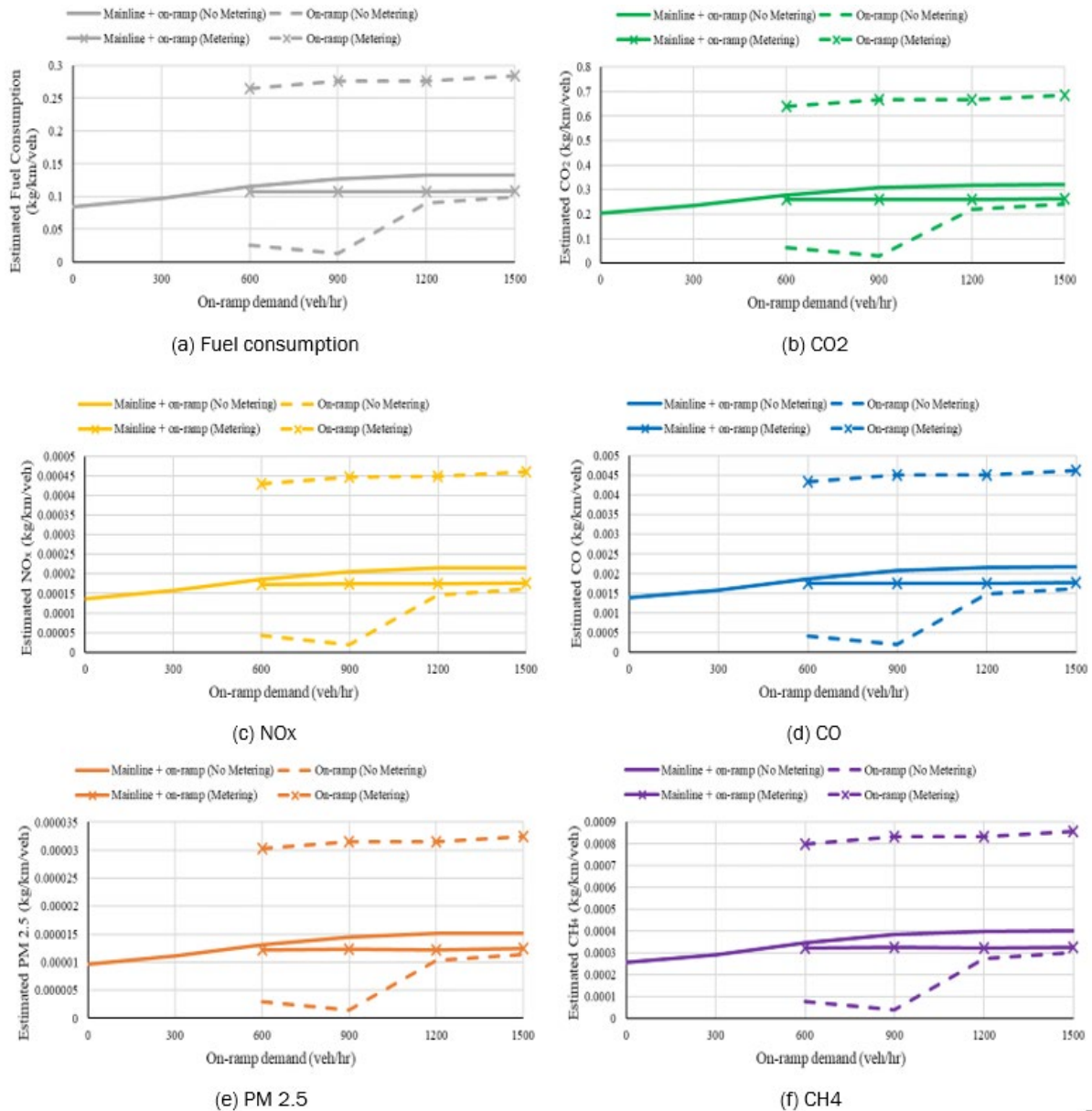


Figure I.2.1.10 Emission and fuel consumption estimates at varying levels of on-ramp demand

Also shown in Figure I.2.1.10, once the on-ramp had been metered at a fixed rate of 400 veh/hr for on-ramp demands of 600 veh/hr or higher, the average fuel consumption and emissions are no longer as high as those observed without ramp metering. This improvement in average fuel consumption and emissions can be as high as 20% at high on-ramp demands (1200 veh/hr to 1500 veh/hr). This can be attributed to the higher overall freeway merge capacity leading to lower delay and less travel time. In addition, careful inspection of Figure I.2.1.10 reveals an interesting finding: metering the on-ramp when the on-ramp demand is 600 veh/hr or higher restricted the on-ramp flow and caused the average fuel consumption and emissions to increase significantly, and this is also correlated to the significant increase in the stop time and total number of stops on the on-ramp shown in Table I.2.1.3. However, despite that ramp metering increased the number of stops and stop time on the on-ramp, it shows that the higher freeway merge capacity led to fewer stops and less stop time on the mainline, which contributed to overall reduction in average fuel consumption and emissions. This phenomenon

is very similar to the observation that ramp metering improves the overall capacity of the freeway merge at the expense of restricting the flow and increasing the delay of the on-ramp.

Table I.2.1.3 Comparison of Stop Time and Number of Stops on Mainline vs On-Ramp

On-ramp demand (veh/hr)	No Metering				Metering			
	600	900	1200	1500	600	900	1200	1500
Stop time (sec)								
Mainline	0.04	4.11	10.56	11.25	0	0	0	0
On-ramp	0	0.95	59.41	67.9	437.98	498.01	500.76	506.27
Number of stops (#/veh)								
Mainline	0	0.11	0.21	0.22	0	0	0	0
On-ramp	0	0.11	0.62	0.67	1	1	1	1

Fuel Consumption and Emissions on SR-99 network

The simulation of SR-99 network is trying to further examine the power of Autonomie to quantify the corresponding environmental impact, under a realistic and complicated circumstance when the on-ramp metering is implemented for the whole system. The local responsive algorithm helps mitigate the mainline traffic congestion via adding more restrictions to the on-ramp traffic summarizes the various types of emission and fuel consumption estimates for both no metering and local responsive ramp metering case. We can see that emissions for mainline without metering are all a little bit smaller than those with local responsive metering, while these estimates at on-ramps without metering are all much smaller than those with metering (except the fuel economy measurement). However, it's worth mentioning that fuel economy (unit: miles per gallon) for mainline traffic after activating the LRRM increases about 6.5%, indicating that mainline traffic gets some environmental benefits from the LRRM. As for the overall performance, all the measurements get worse, which are consistent with the previous findings that the mainline throughput get decreased due to the metering. All these findings correspond to the mobility performance. Therefore, although the LRRM can bring some benefits for the mainline traffic, the overall environmental performance cannot be improved. This is a good example to show that inefficient control strategies such as the SR-99 local responsive ramp metering can do the opposite to fuel consumption and emissions. Thus, in future studies, more efficient ramp metering control strategies need to be adopted such as fuzzy logic control or coordinated ramp metering (CRM) control.

Table I.2.1.4 Summary of Emission and Fuel Consumption Estimates (No metering vs. local responsive ramp metering)

Ramp metering strategy	No metering			Local responsive		
	Overall	Mainline	On-ramp	Overall	Mainline	On-ramp
Fuel economy (mpg)	29.06	27.88	61.69	27.95	29.68	50.71
NOx (kg/veh/mile)	0.00017	0.00018	9E-05	0.00018	0.00019	0.00013
CO (kg/veh/mile)	0.00171	0.00185	0.00091	0.00177	0.00191	0.00128
CO2 (kg/veh/mile)	0.253	0.273	0.134	0.262	0.283	0.190
HC (kg/veh/mile)	0.000316	0.000341	0.000168	0.000327	0.000353	0.000237
PM 2.5 (kg/veh/mile)	1.2E-05	1.29E-05	6.34E-06	1.24E-05	1.34E-05	8.96E-06

Conclusions

By using a state-of-the-art microscopic traffic model, this study explores the influence of ACC and CACC operations on vehicle fuel efficiency. The traffic models not only accurately reproduce the interactions among the manually driven vehicles, ACC vehicles, and CACC vehicles, but also explicitly depict the operation of CACC vehicle strings and the impacts of the advanced signal control algorithm. Such modeling capabilities are critical for quantifying the impact of the advanced technologies on vehicle fuel consumption and understanding the mechanisms behind the observations. Our study takes both traffic mobility and energy consumption impacts into consideration. The results should be able to provide comprehensive insights to help guide future ACC/CACC implementation decisions.

Our findings highlight the importance of incorporating vehicle connectivity into the ACC systems. While the ACC controller can make the traffic flow unstable, CACC can improve the traffic flow stability and efficiency by allowing CACC vehicle string operations. Comparing the 100% ACC case and the 100% CACC case, the fuel consumption rate of the former is almost twice that of the latter. The CACC string operation can also lead to substantial freeway capacity improvement without degrading the per vehicle fuel efficiency. At 100% CACC market penetration, the capacity can increase 49% while maintaining equivalent vehicle fuel efficiency. The benefit of CACC is very small at lower market penetrations. But such a condition can be significantly improved once the ML or VAD strategy is implemented. At 40% market penetration, these strategies can increase the capacity by 15% to 19%, which is significantly higher than the 1% increase in capacity achieved without ML or VAD.

The performance of the cooperative signal control algorithm has been tested against an actuated signal controller at a simulated four-way intersection. The test results show that the algorithm can improve the average intersection speed by 1.7% to 13.6% and the average vehicle MPG by 2.2% to 15.3% when the intersection demand equals the capacity measured in the manual vehicle only case. The most significant impact is observed in the lower CACC market penetration cases. Under those cases, the algorithm can substantially improve the traffic mobility and vehicle fuel economy by reducing or eliminating the need to wait for multiple cycles before passing the intersection. In the medium or high CACC market penetration case, the algorithm performs the best when the traffic demand is close to the intersection capacity measured under the actuated signal control. Particularly, the average speed is increased by 13% and average MPG by 11% in the 100% CACC case; and the average speed is raised by 36% and MPG by 34% in the 40% CACC case. The algorithm also performs well in the 0% CACC case where it completely relies on the traffic information monitored by the fixed traffic sensors. The speed and MPG can be raised by 12.5% and 12.2%, respectively. The improvement

in the manual vehicle only case demonstrates the robustness of the proposed algorithm. When the non-CACC vehicles are all connected, the performance of the algorithm can be further improved in the 0% CACC case (e.g., 37% speed increase and 29% MPG increase). Nonetheless, the benefit of the connected non-CACC vehicles decreases significantly as the CACC market penetration reaches 20%. It indicates that the information required by the algorithm can be sufficiently obtained from the CACC vehicles once the market penetration is 20% or higher.

We have also performed a preliminary analysis that quantifies the intersection performance when the proposed signal control algorithm is combined with a vehicle trajectory planning algorithm. This part of work is still ongoing.

This study also conducted microscopic simulations to examine whether the Autonomie model can capture the environmental impacts induced by the traffic management controls. Simulations of a freeway merge with four mainline lanes and an on-ramp were calibrated to real world conditions, and detailed vehicle trajectory data were collected from the simulations and used as inputs for determining the average fuel consumption and emissions using a model known as Autonomie. The results of the simulation experiments showed that the average fuel consumption and emissions per distance and per vehicle increases as the on-ramp demand increases, and can be significantly higher (as much as 57% higher) when the capacity drop is present. However, the simulations also revealed that metering the on-ramp at a fixed rate of 400 veh/hr prevented capacity drop when the on-ramp demand is high (600 veh/hr or above), and further reduce the average fuel consumption and emissions by up to 20%. Afterwards, the simulations of SR-99 corridor were chosen to further examine the impacts of ramp metering on emission and fuel consumptions, under realistic and complicated circumstance. The Autonomie model showed that the LRRM could only bring some environmental benefits for the mainline traffic (6.5% increase of fuel economy), while the overall emission and fuel consumption performance get worse.

This study provided a better understanding of how Autonomie model can capture the variation of vehicle fuel consumption and emissions at freeway merges due to the ramp metering. As the local responsive ramp metering control cannot work efficiently to benefit the whole SR-99 corridor, the next step is to look at another realistic freeway corridor that performs well with implemented traffic management and control methods and investigate their impacts on fuel consumption and emissions. This will further demonstrate that when traffic management is done properly and efficiently, it can have environmental benefits. Furthermore, other traffic management and control approaches such as variable speed limit and managed lanes can be explored, as the emissions and fuel consumption calculated by Autonomie model are reliable and accurate.

Key Publications

1. Liu, Hao, Xiao-Yun Lu, and Steven E. Shladover. "Traffic signal control by leveraging Cooperative Adaptive Cruise Control (CACC) vehicle platooning capabilities." *Transportation Research Part C: Emerging Technologies* 104 (2019): 390-407.
2. H. Liu, X. Y. Lu and S. Shladover, *Mobility and Energy Consumption Impacts of Cooperative Adaptive Cruise Control (CACC) Vehicle Strings on an Urban Freeway Corridor*, accepted to 99th Annual TRB Meeting Washington, D.C., Jan. 2020
3. M. Yang, D. Kan, and X. Y. Lu, *Improving fuel efficiency at freeway merge by metering its on-ramp*, accepted to 99th Annual TRB Meeting Washington, D.C., Jan. 2020

References

1. Newell, G. F. (2002). A simplified car-following theory: a lower order model. *Transportation Research Part B: Methodological*, 36(3), 195-205.
2. Ciuffo, B., Punzo, V., & Montanino, M., 2012. Thirty years of Gipps' car-following model: applications, developments, and new features. *Transportation Research Record* 2315, 89-99.

3. Kesting, A., Treiber, M., & Helbing, D. (2010). Enhanced intelligent driver model to access the impact of driving strategies on traffic capacity. *Philosophical Transactions of the Royal Society of London A: Mathematical, Physical and Engineering Sciences*, 368(1928), 4585-4605.
4. Nowakowski, C., O'Connell, J., Shladover, S., and Cody, D. (2010a). Cooperative Adaptive Cruise Control: Driver Acceptance of Following Gap Settings Less Than One Second. *Proceedings of the Human Factors and Ergonomics Society 54th Annual Meeting*. Santa Monica, CA: The Human Factors and Ergonomics Society.
5. Liu, Hao, Xiao-Yun Lu, and Steven E. Shladover. "Traffic signal control by leveraging Cooperative Adaptive Cruise Control (CACC) vehicle platooning capabilities." *Transportation Research Part C: Emerging Technologies* 104 (2019): 390-407.
6. Rakha, H. A., Ahn, K., Moran, K., Scaerens, B., & Van den Bulck, E. (2011). Virginia tech comprehensive power-based fuel consumption model: model development and testing. *Transportation Research Part D: Transport and Environment*, 16(7), 492-503.
7. Shladover, S. E., Nowakowski, C., Lu, X. Y., & Ferlis, R. (2015). Cooperative adaptive cruise control: definitions and operating concepts. *Transportation Research Record: Journal of the Transportation Research Board*, (2489), 145-152.
8. TRB. "Highway Capacity Manual." *Transportation Research Board, National Research Council*, Washington, DC, USA, 2010.
9. Altan, O.D., Wu, G., Barth, M.J., Boriboonsomsin, K., Stark, J.A., 2017. GlidePath: eco-friendly automated approach and departure at signalized intersections. *IEEE Trans. Intell. Veh.* 2 (4), 266–277.
10. Minnesota Department of Transportation (2001), Twin cities ramp meter evaluation, Cambridge Systematics, Inc., Cambridge, MA, 2001.
11. Islam, E., Moawad, A., Kim, N., & Rousseau, A., 2017. An Extensive Study on Sizing, Energy Consumption, and Cost of Advanced Vehicle Technologies (No. ANL/ESD-17/17). Argonne National Lab (ANL), Lemont, IL (United States).
12. Barth, M., Scora, G., & Younglove, T., 1999. Estimating emissions and fuel consumption for different levels of freeway congestion. *Transportation Research Record*, 1664 (1), 47-57.
13. Bibeka, A., Songchitruksa, P., & Zhang, Y., 2019. Assessing environmental impacts of ad-hoc truck platooning on multilane freeways. *Journal of Intelligent Transportation Systems*, 1-12.
14. Zhou, X., Liu, J., Qu, Y., & Scholar, P. D., 2016. Evaluating and calibrating emission impacts of traffic management strategies through simplified emission estimation model and mesoscopic dynamic traffic simulators (No. NTC2014-SU-R-08).
15. Ahn, K., Rakha, H., Trani, A., & Van Aerde, M., 2002. Estimating vehicle fuel consumption and emissions based on instantaneous speed and acceleration levels. *Journal of transportation engineering*, 128 (2), 182-190.
16. Rakha, H. A., Ahn, K., Moran, K., Scaerens, B., & Van den Bulck, E., 2011. Virginia tech comprehensive power-based fuel consumption model: model development and testing. *Transportation Research Part D* 16 (7), 492-503.
17. Kim, N., Carlson, R., Jehlik, F., & Rousseau, A., 2009. Tahoe HEV model development in PSAT (No. 2009-01-1307). SAE Technical Paper.

18. Kim N., A. Rousseau, E. Rask., 2012. Autonomie Model Validation with Test Data for 2010 Toyota Prius (No. 2012-01-1040). SAE Technical Paper.
19. Kim N., N. Kim, A. Rousseau, M. Duoba., 2013. Validating Volt PHEV Model with Dynamometer Test Data using Autonomie (No. SAE 2013-01-1458). SAE Technical Paper.
20. Lu, X., Kan, X., Shladover, S.E., Wei, D., Ferlis, R.A., 2017. An enhanced microscopic traffic simulation model for application to connected automated vehicles. Transportation Research Board 96th Annual Meeting, Washington, DC.
21. Liu, H., Kan, X. D., Shladover, S. E., Lu, X. Y., & Ferlis, R. E., 2018. Modeling impacts of Cooperative Adaptive Cruise Control on mixed traffic flow in multi-lane freeway facilities. Transportation Research Part C 95, 261-279.
22. Liu, H., Kan, X., Shladover, S. E., Lu, X. Y., & Ferlis, R. E., 2018. Impact of cooperative adaptive cruise control on multilane freeway merge capacity. Journal of Intelligent Transportation Systems, 22 (3), 263-275.
23. Liu, H., Kan, X. D., Shladover, S. E., Lu, X. Y., & Ferlis, R. A., 2018. Quantifying Influences of Cooperative Adaptive Cruise Control (CACC) Vehicle String Operation Strategies on Mixed Traffic Flow. Transportation Research Board 97th Annual Meeting, Washington, DC.
24. Kan, X. D., Xiao, L., Liu, H., Wang, M., Schakel, W. J., Lu, X. Y., ... & Ferlis, R. A., 2019. Cross-Comparison and Calibration of Two Microscopic Traffic Simulation Models for Complex Freeway Corridors with Dedicated Lanes. Journal of Advanced Transportation, 2019.
25. TSS Aimsun. <http://www.aimsun.com/>. Accessed on April 8, 2019.
26. Manual-HCM, H. C. (2010). National Transportation Research Board.
27. Wang, X. R., & Gao, H. O., 2011. Exposure to fine particle mass and number concentrations in urban transportation environments of New York City. Transportation Research Part D 16 (5), 384-391.

Acknowledgements

We acknowledge the contributions of Hao Liu (Partners for Advanced Transportation Technology (PATH), University of California Berkeley (UCB)), Xingan (David) Kan (Department of Civil and Environmental Engineering, UCB), and MingYuan Yang, (UCB)

I.2.2 Impact of CAVs on Energy, Green House Gas, and Mobility in a Metropolitan Area (ANL) [Task 1.3]

Joshua Auld, Principal Investigator

Argonne National Laboratory
9700 S Cass Avenue
Lemont, IL 60439
E-mail: jauld@anl.gov

Erin Boyd, DOE Technology Manager

U.S. Department of Energy
E-mail: erin.boyd@ee.doe.gov

Start Date: October 1, 2018

End Date: September 30, 2019

Project Funding (FY19): \$750,000

DOE Share: \$750,000

Non-DOE Share: \$0

Project Introduction

This task seeks to estimate the mobility, energy, and productivity (MEP) impacts of different connected and automated vehicle (CAV) technologies in a metropolitan region. Since there are no data on CAVs, we rely on rational assumptions and behavioral models. Communication technologies and increased levels of automation probably will reshape urban transportation in the coming decades. CAVs may have an impact in different ways. Vehicles with a higher degree of automation can drive at shorter gaps, and this could increase road capacity. In addition, transportation management strategies, such as traffic signals, can be greatly improved by the availability of more information due to vehicles' communication capabilities. Furthermore, the combination of these aspects opens possibilities for new applications and services. Therefore, it is necessary to understand the potential impacts of CAVs on future mobility.

Objectives

The main objective of this task is to quantify the mobility, energy, and MEP impacts of different CAV technologies. The following are the major components:

- Energy, mobility, and MEP impact of shared automated vehicle (SAV) fleets;
- Energy, mobility, and MEP impact of household CAV sharing; and
- Impact of CAV technology on traffic flow from microsimulation.

Approach

Energy, Mobility, and MEP Impacts of SAV Fleets

Dynamic ride-sharing services have become more common in recent years. When these services are executed correctly, they provide cheaper but more reliable service to travelers, and the total vehicle miles traveled (VMT) and energy use are minimized. A simple heuristic algorithm that is developed and implemented is based on vehicle proximity and total traveler delay. Another model improvement is "geofencing." Past studies point to the rise in VMT and empty miles traveled with the use of SAVs. Research has shown that dynamic ride-sharing can mitigate this issue, but the percentage of travelers willing to share their rides in the near future remains low (Krueger et al. 2016; Gurumurthy and Kockelman 2019). With the sprawling nature of urban regions in the United States, trips being made, for example, from a city's central business district (CBD) to a suburban or exurban home are, on average, longer than the average trip. SAVs are expected to provide cost savings and emission benefits, but at the same time, an in-depth analysis of policies that can curb rising VMT needs to be conducted. Fagnant et al. (2015) suggest that areas with higher trip densities have better fleet

performance metrics and add fewer VMT. Constraining an SAV fleet's service within such a carefully chosen "geofence" may be key to mitigating congestion. Figure I.2.2.1 shows a flowchart of SAV operations in POLARIS, our transportation system simulation tool.

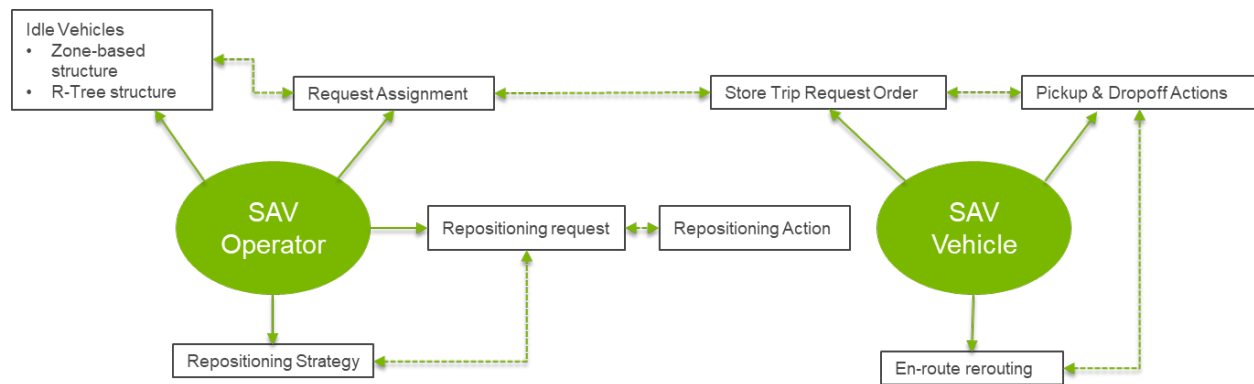


Figure I.2.2.1 Flowchart for SAV fleet operation in POLARIS

Energy, Mobility, and MEP Impact of Household CAV Sharing

There are more than 10 million households in the Chicago Metropolitan Area. In a scenario in which most of these households own one or more CAVs, it is a challenge to model how household members share their available fleet. First, we converted our existing intrahousehold vehicle-sharing (IHVS) optimization code from Gurobi to CPLEX and then modified it to run on a high-performance computer (HPC). Finally, we have a workflow in which POLARIS is run on a local workstation and communicates with the HPC for running the IHVS optimization code.

CAV Technology Impact on Traffic flow from Microsimulation

Since POLARIS uses a mesoscopic traffic model, car-following and lane-changing behaviors are not modeled directly, but their effects are captured using the fundamental diagrams. These models are critical for the modeling of platoons, as well as regular traffic. After developing car-following and lane-changing models under different market penetration rates of CAVs in a microscopic simulation framework, we have updated the fundamental diagrams used in the mesoscopic simulation framework of POLARIS.

Results

Geographically Constrained SAV Operation (Geofencing)

Six scenarios were investigated: five with distinct geofences and, for baseline comparison, one without a fence. Figure I.2.2.2 depicts the geofence scenarios. All the fences include the areas of the fences inscribed in the Chicago Metropolitan Area. For example, the exurban core area (depicted in blue in Figure I.2.2.2) includes all the zones of the suburban core, city of Chicago, urban core, and downtown Chicago. In addition, all scenarios assumed three different levels of vehicle ownership reduction: 10%, 50%, and 100%. A higher reduction in vehicle ownership tends to increase transportation network company (TNC) demand.

Table I.2.4.1 summarizes the results. Without a geofence, average wait times were consistently higher across all ownership scenarios than those for scenarios with fences. System VMT was reduced the least in the scenario without a fence largely owing to a higher empty VMT (eVMT) of the SAV fleet. A lower rate of SAV requests in the 10% reduction scenario translated to more of them being served, compared to the 50% scenario with the same fleet. The percentage of requests met rose significantly in these two scenarios with the use of geofences because of higher trip densities. When all trips were served by SAVs, the increase in percentage of requests met was not significant. This result may be due to the larger fleet required to serve the region without the fences to begin with.

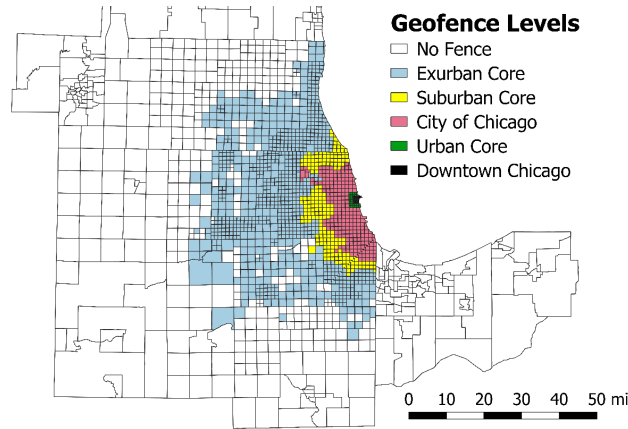


Figure I.2.2.2 Spatial extent of geofencing (overlapped) in the Chicago Metropolitan Area

Geofences chosen around the CBD or urban core did not prove to be useful, and lower vehicle ownership was not seen to be influential since the number of households in the CBD is likely low compared to that in the suburbs. Nearly half the fleet’s VMT was without a passenger, and average wait times were 5 minutes (in the 10% and 50% scenarios) to 15 minutes (in the 100% scenario) more depending on the percentage reduction in ownership. System VMT was still lower than the baseline scenario because the share of SAV VMT was very low in the 10% and 50% ownership reduction scenarios. The large reductions in VMT observed under the geofences in the 100% scenario were counterintuitive and may have been a result of undercounting the VMT of a trip unserved by an SAV outside of the geofence. In the initial stages of SAV adoption, many short trips within a well-developed CBD is most likely to be captured by transit or other nonmotorized modes.

Table I.2.2.1 Fleet Metrics by Geofence Scenario and Vehicle Ownership Reduction

Avg. # of HH Vehicles	Geofence Scenario	Avg. Wait Time (min)	Avg. Assignment Time (min)	% of Requests Met	Avg. # of Trips per Vehicle	% Avg. Idle Time	% Change in VMT
10% Ownership Reduction							
0.59	Downtown	15.9	0.6	64.8	11.3	74.8	-4.6
0.68	Urban core	14.1	0.6	49.2	7.8	83.7	-4.8
0.95	City of Chicago	6.5	0.5	63.3	13.0	73.7	-4.3
1.08	Suburban core	5.5	0.5	99.8	12.9	73.9	-4.4
1.35	Exurban core	7.0	0.6	99.1	14.7	67.5	-3.9
1.41	No fence	10.1	0.8	89.1	16.3	57.9	-3.0

Avg. # of HH Vehicles	Geofence Scenario	Avg. Wait Time (min)	Avg. Assignment Time (min)	% of Requests Met	Avg. # of Trips per Vehicle	% Avg. Idle Time	% Change in VMT
50% Vehicle Ownership Reduction							
0.33	Downtown	17.3	1.3	60.5	15.4	62.3	-19.1
0.38	Urban core	15.5	0.6	71.7	11.1	75.0	-18.9
0.55	City of Chicago	8.0	0.7	90.6	19.3	62.2	-18.6
0.63	Suburban Core	7.4	0.6	91.4	20.3	60.2	-18.4
0.81	Exurban core	11.8	1.2	79.6	25.2	42.6	-16.5
0.85	No fence	13.0	1.4	69.4	22.3	45.5	-15.2
100% Vehicle Ownership Reduction							
0	Downtown	24.1	0.7	47.8	5.6	81.1	-27.3
0	Urban core	20.5	0.7	58.9	4.1	87.8	-26.7
0	City of Chicago	5.3	0.5	92.4	7.6	87.0	-25.1
0	Suburban core	4.6	0.5	94.9	9.1	84.7	-24.5
0	Exurban Core	7.0	0.6	92.8	16.8	66.5	-20.0
0	No fence	9.4	0.7	92.3	18.1	56.8	-13.1

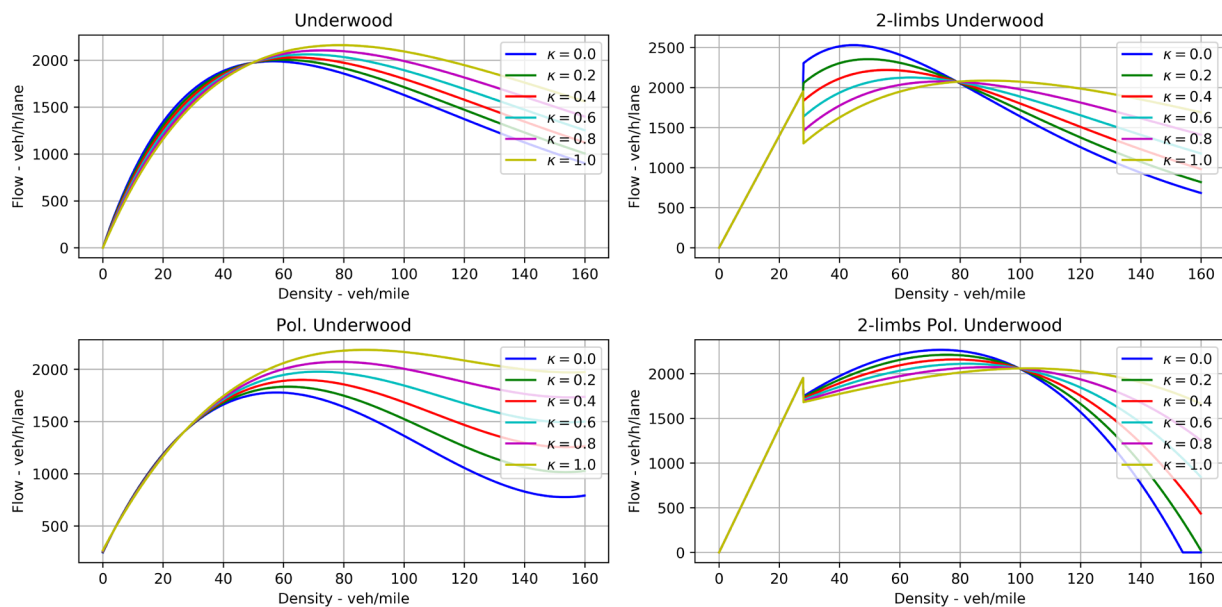


Figure I.2.2.3 Calibrated fundamental diagrams for the four models with varying penetration rates

CACC Impacts on Traffic Flow

Location-specific fundamental diagrams were calibrated for different locations based on microscopic simulation. Figure I.2.2.3 depicts the fundamental diagram for the four models with varying penetration rates.

The traffic flow simulation model in POLARIS was adapted in order to replicate the generated curves. Since the traffic flow model in POLARIS assumes a triangular fundamental diagram (density-flow relationship), the model and parameter were implemented in POLARIS with a triangular fundamental diagram. The relative impacts of the penetration rate of CACC on capacity remained the same.

Impacts of Privately-Owned Automated Vehicles

A main concern related to fully automated vehicles (AVs) is an increase in travel demand due to empty trips. For privately owned AVs, empty trips arise when an AV need to be repositioned to serve a household member at a different location than its last drop-off. Also, empty trips can occur when vehicles are sent home to avoid parking costs. In this study, we assessed the impacts of private AVs based on household AV trip schedules generated according to the household members’ activity plan. The use of private AVs leads to drastically increased VMT. With a 52% penetration of private AVs, there is an increase of 30% in VMT. This is driven by two primary phenomena: the increase in unloaded VMT due to inefficient repositioning in the private-AV scenario, and the increase in overall VMT driven by the assumed reduction in value of travel time (VOTT) in a private AV. Both findings are displayed in Figure I.2.2.4, which shows the distribution of vehicle hours traveled (VHT) by time of day. The temporal VHT is split by whether the vehicle is a private AV or SAV fleet, the automation level, and whether the vehicle is driving empty. There is substantially more travel with much of that taking place within the private-AV scenario (solid orange); this is driven largely by the VOTT reduction. However, there is also additional unloaded travel. Compared to a scenario in which AVs are shared, the unloaded travel occurs only in SAV (automated TNC) vehicles, with only 14% of total SAV travel hours being unloaded. However, in the C-high scenario, there is a much greater amount of travel in private AVs, and almost 22% of that travel is occurring in unloaded vehicles. This means that overall, fully 17% of all VHT in the system are driven unloaded in this scenario.

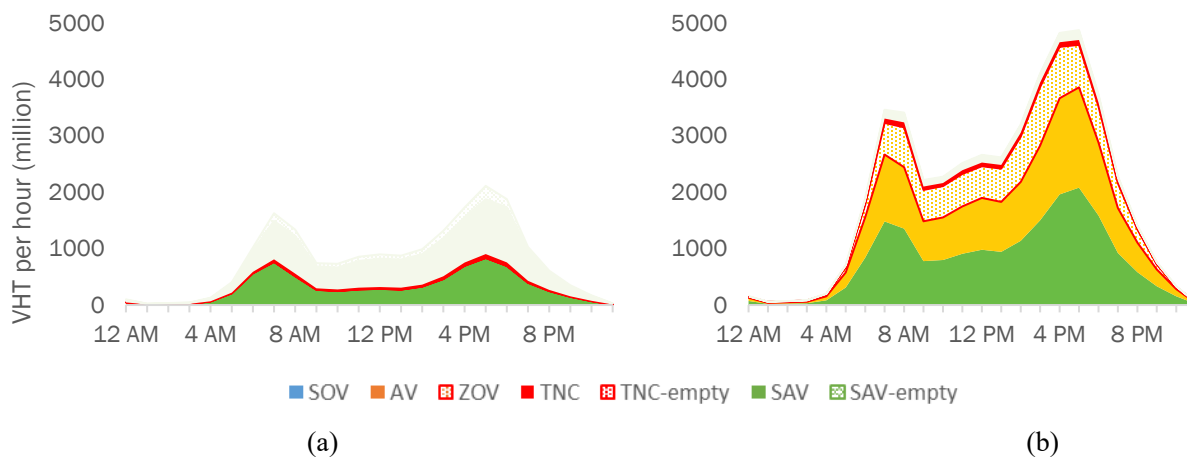


Figure I.2.2.4 Temporal distribution of VHT by auto-based mode for (a) SAV and (b) private-AV scenarios

The finding that private automation results in higher VMT is corroborated by previous studies conducted by Harb et al. (2018). However, the naturalistic experiment conducted by Harb et al. (2018) produced a higher percentage of zero-occupant vehicle (ZOV) trips than the current study, resulting in a somewhat higher VMT compared to the current study. This might be because in that study, ZOV trips (driven by chauffeurs) conducted household errands. In the current study ZOV trips were conducted exclusively to reposition the vehicle without any opportunity to address household needs. In addition, in the current study only 52% of households owned an AV, so if ownership was extended to 100%, the VMT increase of 30% could have doubled, which would match the experimental finding of an 85% increase quite closely.

The findings of the SAV and private-AV scenarios studied here broadly align with previous simulation observations regarding VMT and VHT increases as well. The 30% increase in VMT observed in this study is substantially higher than the 16% increase observed in the AV scenario by Simoni et al. (2019), although in that study AV repositioning was not simulated, and this accounted for a substantial portion of the increase in this study. This could also explain why that study found a greater VMT increase in the SAV scenario than in the AV scenario, which is the opposite finding here. Zhao and Kockelman (2018) also found a VMT increase of up to 41%, although that study mentions significant limitations due to the use of a four-step travel demand model, such as the lack of repositioning travel. Rodier et al. (2018) also found substantially lower increases in VMT, up to 11% in AV and 18% in SAV scenarios, again opposite the findings in this study. In that study, the lower VMT can be explained by the modest reduction in drive VOTT assumed (25%), along with the lack of vehicle repositioning trips.

Conclusions

Different aspects of the impact of CAVs were studied. On one hand, CAVs can improve traffic flow efficiency on freeways and SAV fleet efficiency can be improved by applying geofencing strategies. On the other hand, privately owned CAVs can lead to a substantial increase in VMT propelled by ZOV trips when AVs are being repositioned to serve another household member.

Key Publications

1. de Souza, F., O. Verbas, and J. Auld, 2019, “Mesoscopic Traffic Flow Model for Agent-Based Simulation.” *Procedia Computer Science* 151: 858–863.
2. Gurumurthy, K. M., J. Auld, and K. Kockelman, 2019, “A System of Shared Autonomous Vehicles for Chicago: Understanding the Effect of Geofencing the Service.” Paper presented at Automated Vehicle Symposium, Orlando, FL, July 15–18.
3. Gurumurthy, K.M., F. de Souza, A. Enam, and J. Auld, “A Large-Scale Simulation of Shared Autonomous Vehicles: Integrating the Supply and Demand Perspectives, accepted for Transportation Research Board Annual Meeting, 2020.

References

1. Harb, M., Y. Xiao, G. Circella, P. L. Mokhtarian, and J. L. Walker, 2018, “Projecting travelers into a world of self-driving vehicles: estimating travel behavior implications via a naturalistic experiment,” *Transportation* 45(6): 1671–1685.
2. Rodier, C., M. Jaller, E. Pourrahmani, J. Bischoff, J. Freedman, and A. Pahwa, 20018. “Automated vehicle scenarios: Simulation of system-level travel effects using agent-based demand and supply models in the San Francisco Bay area,” UC Davis Institute of Transport Studies.
3. Simoni, M. D., K. M. Kockelman, K. M. Gurumurthy, and J. Bischoff, 2019, “Congestion pricing in a world of self-driving vehicles: An analysis of different strategies in alternative future scenarios,” *Transportation Research Part C: Emerging Technologies* 98: 167–185.
4. Zhao, Y., and K. M. Kockelman, 2018, “Anticipating the regional impacts of connected and automated vehicle travel in Austin, Texas,” *Journal of Urban Planning and Development* 144(4): 04018032.

I.2.3 Energy-Efficient Connected and Automated Vehicles (ANL)

Dominik Karbowski, Principal Investigator

Argonne National Laboratory
 9700 S Cass Avenue, Building 362
 Lemont, IL 60439
 Phone: (630) 252-5362; Fax: (630) 252-3443
 E-mail: dkarbowski@anl.gov

Erin Boyd, DOE Technology Manager

U.S. Department of Energy
 E-mail: erin.boyd@ee.doe.gov

Start Date: October 1, 2016	End Date: September 30, 2019	
Project Funding (FY19): \$850,000	DOE Share: \$850,000	Non-DOE Share: \$0

Project Introduction

One significant way connected and automated vehicles (CAVs) can provide energy savings is through better vehicle speed and/or powertrain control. Perception sensors and connectivity provide increased awareness of the surrounding environment and enable control optimization, while automation provides the necessary level of controllability for the application of the optimization. In parallel, vehicles feature an ever-broader range of advanced powertrain technologies, from hybridization to transmissions with a high number of gears, designed to improve overall vehicle efficiency. In this project, we research eco-driving and energy management strategies for advanced powertrain-equipped CAVs, including conventional engine-powered vehicles, hybrid vehicles (HEVs), and electric-powered vehicles (BEVs). We also analyze how vehicles are driven and, as a result, develop models of existing CAV technologies and of human drivers, and integrate them into RoadRunner, the tool we have created to support eco-driving research.

Objectives

The objectives of this task are as follows:

- To estimate the energy-saving potential of advanced powertrain technologies in the context of vehicle automation and connectivity;
- To develop and evaluate eco-driving and energy management strategies relying on connectivity and/or automation to provide maximum energy savings, especially for vehicles with advanced powertrain technologies; and
- To facilitate the development of energy-saving automated driving algorithms by the industry and research community through model-based system engineering.

Approach

Eco-driving for CAV

Eco-driving consists of adjusting vehicle speed to minimize energy consumption. Eco-driving can be systematically applied to automated vehicles, because of the control of the speed by a machine. In a comprehensive picture, vehicle energy consumption takes place in three stages: well-to-tank, tank-to-vehicle, and vehicle-to-miles. The eco-driving problem relates to the last two stages—it concerns not only the vehicle kinetic and potential energy conversion but also the onboard energy efficiency. We have developed two eco-driving control strategies: *speed-only* eco-driving, which focuses mostly on the vehicle-to-miles stage, and *speed+powertrain* eco-driving, which considers the tank-to-vehicle and vehicle-to-miles stages as a compound problem.

In the *speed-only* eco-driving strategy, we formulated an optimal control problem to minimize acceleration energy subject to the state constraints imposed by speed limits and the preceding vehicle and solved it to derive analytical closed-form optimal solutions through optimal control theory. The closed-form solutions as a function of boundary conditions guarantee a high updating rate because of efficient computation without any numerical solvers; moreover, they can be applied to all types of vehicles (e.g., BEVs, conventional internal combustion engine vehicles).

In the *speed+powertrain* strategy, the objective of the optimal control is the explicit minimization of energy consumption, and it directly controls the powertrain components, such as engine torque and gear for a conventional vehicle, as well as motor torque in a parallel hybrid vehicle. In addition to incorporating the efficiency map of powertrain components, powertrain-aware eco-driving has a better understanding of the kinetic energy recuperation capability because of its detailed modeling of the powertrain.

We not only solved the optimization problems but also moved the eco-driving strategies closer to real-world implementation, in order to properly assess their potential impact in the real world. The eco-driving strategies were integrated into “online” controllers within RoadRunner; they can run in real-time systems, use inputs realistically available in a CAV, output commands necessary for the proper operation of the vehicle, and are robust enough to deal with perturbations, dynamic response, and uncertainty in the prediction of the future horizon. The resulting controllers are also designed to work in a broad range of operating conditions, including cruising, car-following, and intersection approach and departure. In order to be real-world implementable, the eco-driver controllers make use of the receding horizon concept. At each time step, the optimization algorithms solve the eco-driving problem over an entire finite horizon (e.g., 250 meters), but apply only the first step of the solution. In the following time step, the horizon window moves one step further and the optimization is performed again, thus creating a feedback loop critical to the stability of the system.

Adaptive Cruise-Control Model Development and Validation in RoadRunner

Many modern vehicles already feature partial driving automation, for example, longitudinal speed control for highway driving. With adaptive cruise control (ACC), the vehicle drives at a speed set by the driver if no preceding vehicle is detected (using radar or stereoscopic cameras), and otherwise modulates its speed to maintain a safe distance with the preceding vehicle. The ACC feature of the 2016 Toyota Prius Prime was tested on a chassis dynamometer. With no actual moving vehicle to detect, a method of overwriting the gap measurement from the sensor was designed and implemented. As a result, it is possible to test a situation in which the ACC controller commands the actual vehicle on the dynamometer to follow a virtual lead vehicle, itself following a set drive cycle. The data were then used to validate an ACC model in RoadRunner and applied to a validated Autonomie model of the Prius Prime. As shown in Figure I.2.3.1, the inter-vehicle gap is well matched.

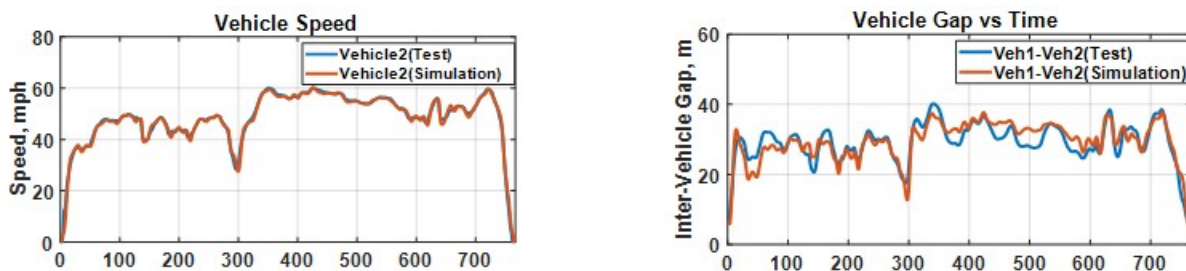


Figure I.2.3.1 Comparison of the adaptive cruise control model in RoadRunner with test data

Human Driver Model Development and Validation in RoadRunner

Modeling the human driver is critical for the development and evaluation of powertrain and/or driving controls relying on automation and connectivity. Thanks to high-fidelity human driver models, it is possible to surround *in simulation* an energy-optimized vehicle with vehicles realistically replicating human-driven vehicles. A good human driver model is also necessary as a baseline when the potential benefits of new control algorithms are being evaluated. As a result, we have developed a high-fidelity dynamic human driver model, combining data-driven and analytical approaches, and have integrated it into RoadRunner.

The human driver model consists of two parts: a Perception and Decision (P&D) model, and an action model, as shown in Figure I.2.3.2. The P&D model aims to capture the cognitive process occurring in the human brain. The P&D model determines the driving regimes (e.g., accelerating to increase speed, cruising to maintain speed, braking to stop) and its timing and duration based on the current situation. On the other hand, the action model aims to capture human driving behaviors that have an impact on the state of the vehicle (position, speed, and acceleration) based on Newtonian laws of motion. The action model is bounded by the regimes and conditions computed by the P&D model.

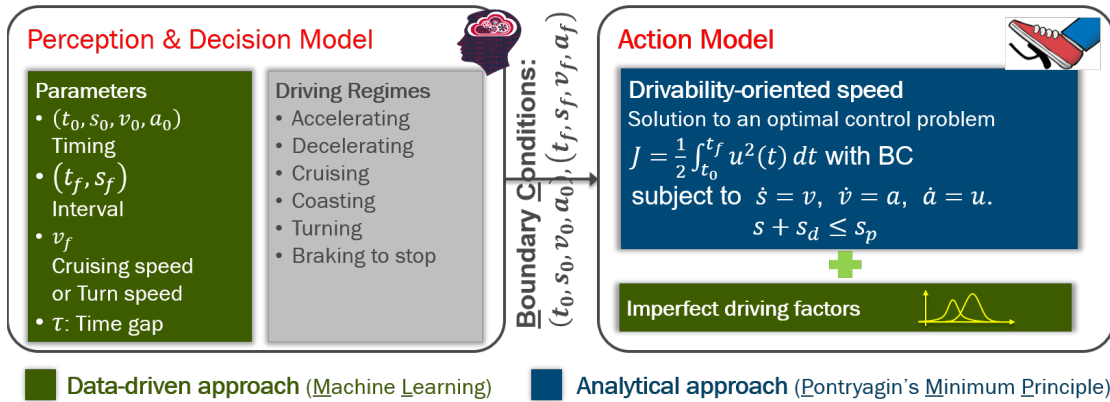


Figure I.2.3.2 Schematic diagram of the human driver model: P&D model [left] and action model [right]

To validate the model, we used data collected by a highly instrumented vehicle driving on real roads, equipped with a dash video camera, GPS tracker, and radar. Through filtering, map-matching, and machine-vision, we established a dataset that includes road attributes (e.g., speed limit, road type), state of traffic lights, and distance to preceding vehicle—all factors for driving decisions. We first focused on development and validation of the action model. We assumed that drivers prioritize driving comfort, while avoiding any collisions with the preceding vehicle and obeying traffic rules; this assumption leads to the formulation of human driving as an optimal control problem minimizing jerk (the derivative of acceleration) energy. Deriving analytical optimal solutions by employing optimal control theory can compute vehicle state trajectories with low computational burden. Adding the state constraint imposed by the vehicle in front can describe car-following features with anticipation of the vehicle in front. The trajectories of the vehicles in the post-processed data were clustered into four distinct driving regimes—accelerating, cruising, coasting, and braking. Based on the assumption of a perfect P&D model, the information required by the action model (i.e., boundary conditions) was extracted for each driving regime. Results for 27 segments between two intersections demonstrate that trajectories generated by the action model of the human driver using this information are well matched with those of experimental data, as shown in Figure I.2.3.3.

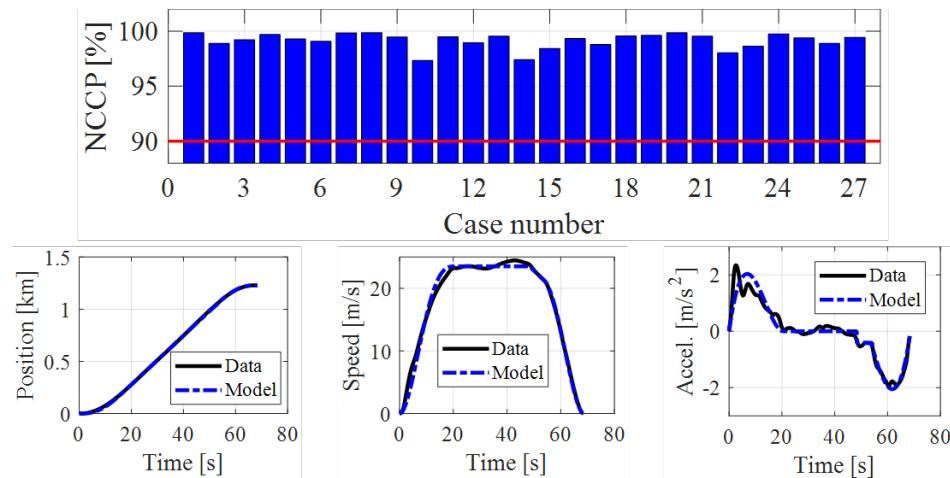


Figure I.2.3.3 Normalized cross correlation power (NCCP) between experimental and simulation data for 27 segments [top] and for one sample [bottom].

Results

Study Setup

We estimated the energy benefits of eco-driving strategies for a midsize car, and for a variety of driving scenarios and powertrain technologies, in a large-scale study summarized in Table I.2.3.1.

Table I.2.3.1 Summary of the Main Variables in the Case Study

Variable/Parameter	Description
Powertrain (PT)	<ul style="list-style-type: none"> Conventional: powered by an internal combustion engine HEV: parallel pre-transmission hybrid electric BEV: battery electric vehicle with 200-mile range
PT technology scenario	<ul style="list-style-type: none"> Current technology Short-term future technology: better engine/motor efficiency, lighter battery, etc.
Control	<ul style="list-style-type: none"> Baseline: no optimization Speed-only eco-driving [EcoDrv Spd/Accel] Speed+powertrain eco-driving [EcoDrv PT+Spd]
Connectivity	<ul style="list-style-type: none"> No vehicle-to-infrastructure (V2I) information: vehicle does not receive any information from the outside. V2I: vehicle receives information about signal phase and timing.
Scenario	Two vehicles following each other
Routes	Real-world routes extracted from HERE maps: 9 highway, 9 suburban, 6 urban, 6 mixed combining all types roads

One simulation includes two vehicles following each other; one or both vehicles feature an “advanced control,” while the others use the baseline control. The baseline control is the human driver model. Each control has an option of being connected to the infrastructure (V2I), in which case it uses an “eco-approach” algorithm to avoid idling at red lights. The baseline with V2I would correspond to a non-energy optimized automated vehicle. Each vehicle includes an Autonomie powertrain model, corresponding to a vehicle created

for the SMART workflow. We examine two powertrain technology scenarios: current technology and short-term future with US DOE VTO targets.

Study Results

Figure I.2.3.4 shows the speed profiles for various driving control strategies for the same example route for a BEV. All three controllers with V2I connectivity have information about the current and future state of the second traffic light (at 1,670 meters), and slow down before the light so as not to stop and idle, unlike the baseline case without V2I, which must stop. The two vehicles with eco-driving controllers have smoother speeds than the two baseline controllers.

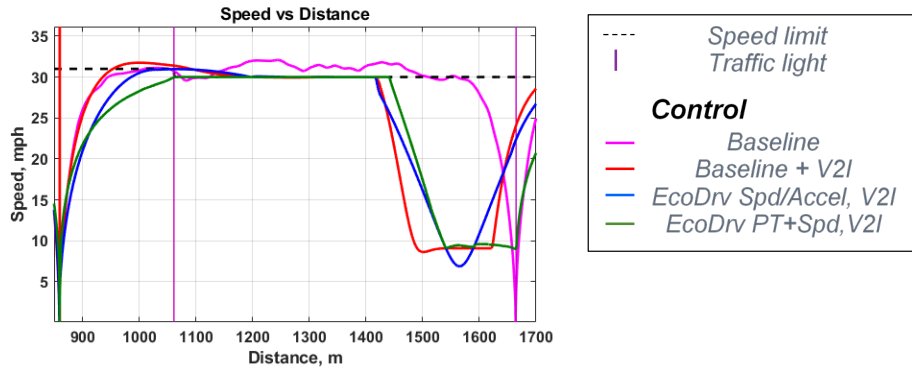


Figure I.2.3.4 Speed traces for a BEV with different control strategies

The speed+powertrain eco-driving with V2I strategy shows the highest energy savings, up to 20% fuel savings for the lead vehicle, as shown in Figure I.2.3.5.

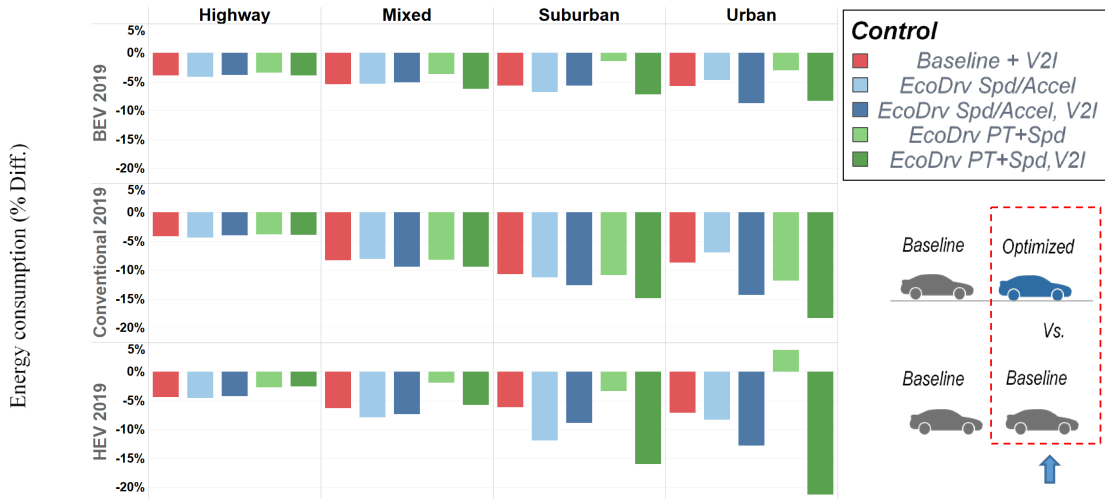


Figure I.2.3.5: Energy consumption savings relative to baseline control for a vehicle in lead position, with current powertrain technology, for various powertrains

That strategy is particularly beneficial for the HEV, for which there is greater potential for optimization because of the dual power sources. The speed-only eco-driving, however, also brings good results, especially for the BEV, and is more robust to the lack of V2I connectivity. This results from the formulation of the optimization, which is different in each strategy. The speed-only eco-driving tries to minimize the acceleration

energy ($\int a^2$), which may not always be energy-optimal but leads nonetheless to gentler accelerations and smoother driving. The speed+powertrain strategy, on the other hand, explicitly minimizes energy consumption. It often means stronger accelerations as high component efficiency occurs at higher loads, which may lead in some cases to more energy-wasting braking events when the future horizon is unknown, as is the case without V2I. For both strategies, energy savings are greater in urban situations than in highway situations, and V2I connectivity helps bring greater savings, at least an additional 5% in urban scenarios (compared to no V2I).

Eco-driving affects energy savings differently depending on the powertrain technology scenario; Figure I.2.3.6 shows the energy savings for a conventional vehicle in lead position in both current and future technology scenarios. For the conventional vehicle, there are significantly more energy savings in the future technology scenario, for all eco-driving strategies. One reason is that eco-driving tends to reduce overall tractive effort and thus the engine load, which often leads to lower engine efficiency. The future technology case, however, assumes strong improvements in efficiency in these low load areas. This is especially true for the speed-only control, in which lower engine loads are most prevalent.

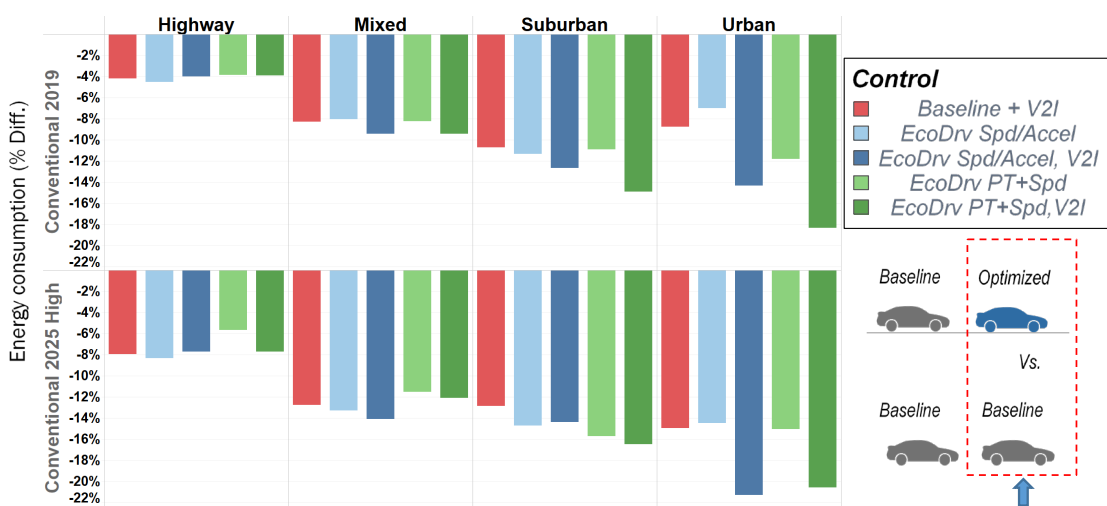


Figure I.2.3.6 Energy consumption savings for lead vehicle, conventional, current versus future technologies

All controllers evaluated in the study can deal with a preceding vehicle, that is, car-following. It is therefore also of interest to analyze the impact of eco-driving on the following vehicle. Here we examine two situations: in the first one (Figure I.2.3.7), a vehicle *equipped* in an optimized or eco-driving control strategy follows a baseline vehicle and is compared to a baseline following another baseline. In the second situation (Figure I.2.3.8), we compare the energy savings of two *non-equipped*, baseline vehicles, following another baseline or an equipped vehicle. When an equipped vehicle follows a non-equipped vehicle (first case, Figure I.2.3.7), eco-driving still leads to energy savings, but they are lower than those when the vehicle is in a lead position (Figure I.2.3.5). This is because the lead vehicle constrains the preceding vehicle at least occasionally, so the optimal unconstrained solution can no longer be applied. A good preceding vehicle speed prediction is also critical to achieving optimal results; optimizing for speed can then be more robust.

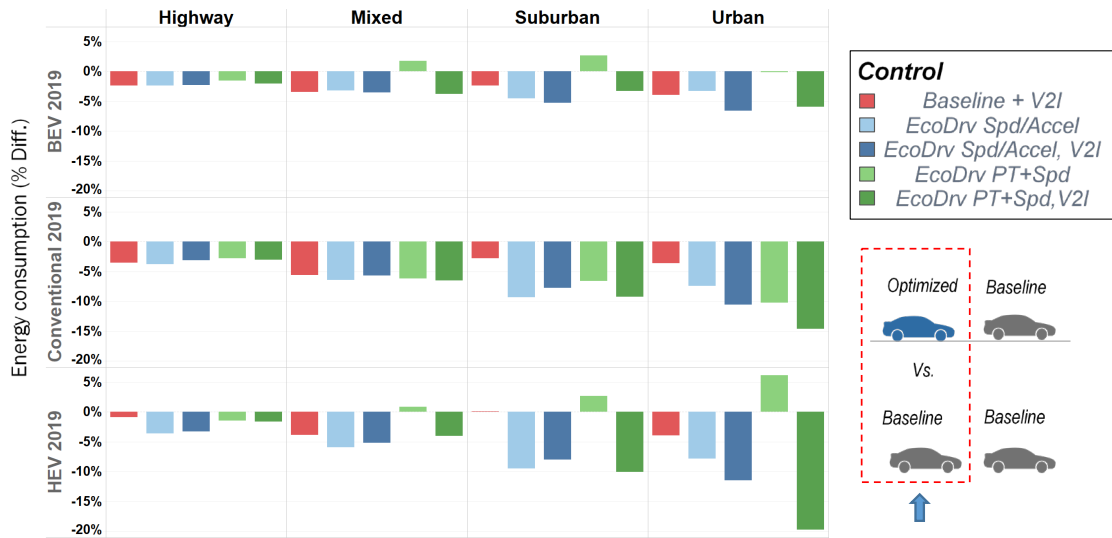


Figure I.2.3.7 Energy consumption of following vehicle (control versus baseline) with current technology and various powertrains

A non-equipped vehicle following an optimized one generally saves energy as well, as shown in Figure I.2.3.8. The following vehicle benefits from the anticipation (with V2I) or “smoother” driving of the lead vehicle. The savings are greater for the conventional vehicle, which always benefits from reduced braking. The speed-only eco-driving strategy is generally better for the following vehicle, as the speed+powertrain not only considers kinetic energy optimization but also onboard energy management. Without that energy management optimization aspect, the following vehicle may lose some of the benefits of the speed+powertrain strategy of the lead vehicle.

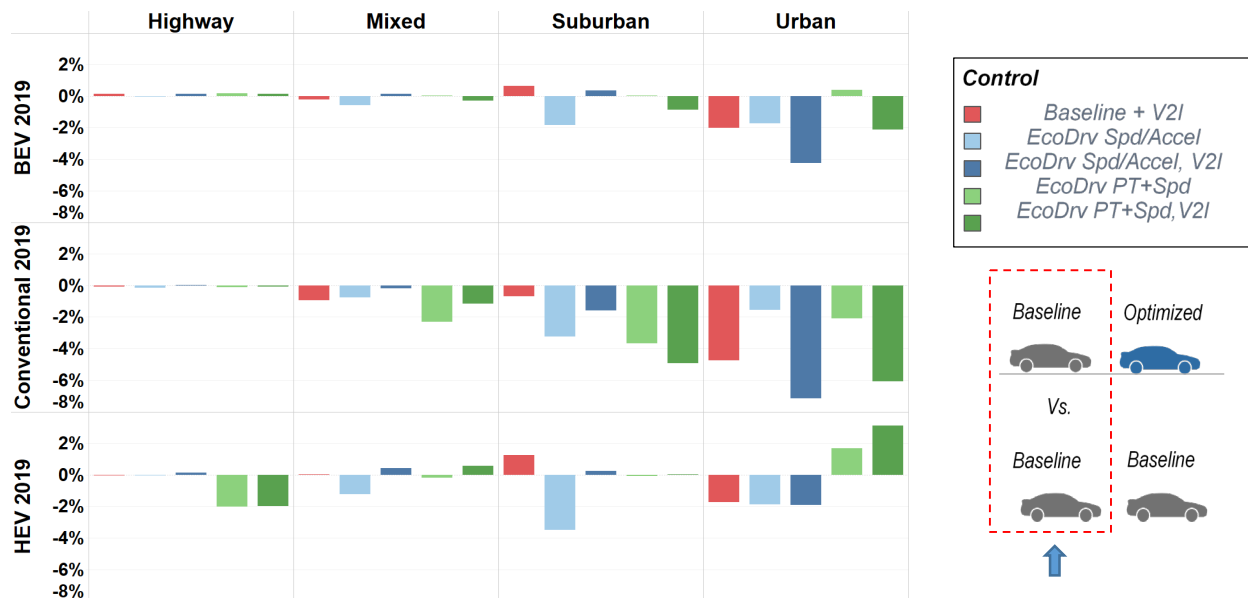


Figure I.2.3.8 Energy consumption of following baseline vehicle (lead: control versus baseline) with current technology and various powertrains

Conclusions

In the final year of this 3-year project, we added new models to RoadRunner, implemented advanced eco-driving algorithms for CAVs, and performed a large-scale study to evaluate their energy impacts. Our novel approach to human driver modeling shows promising results and will be developed further with larger datasets for training; it also provides a solid baseline scenario for the case study. We completed the development of the eco-driving control strategy, optimizing both speed and powertrain for three types of powertrains and demonstrated it provides the highest energy savings. We also developed a simpler and faster control that acts upon the speed only, is not powertrain-specific, and yet also leads to good energy savings. Both controllers were implemented in RoadRunner and can be implemented in real-time controllers. The large-scale study showed that automation and connectivity combined with energy-focused control results in significant savings, up to 20%, although results are highly dependent on the type of road and scenario. Vehicle-to-infrastructure (V2I) connectivity enables better knowledge of the future horizon and improves the performance of the optimization, especially for the speed+powertrain eco-driving strategy. Future research will focus on future horizon prediction, larger case studies involving traffic conditions, and in-vehicle validation.

Key Publications

1. Han, Jihun, Dominik Karbowski, Namdoo Kim, and Aymeric Rousseau. “Human Driver Modeling Based on Analytical Optimal Solutions: Stopping Behaviors at the Intersections.” In *ASME 2019 Dynamic Systems and Control Conference*. Park City, Utah, USA: ASME, 2019.
2. Jeong, Jongryeol, Namdoo Kim, Dominik Karbowski, and Aymeric Rousseau. “Implementation of Model Predictive Control into Closed-Loop Micro-Traffic Simulation for Connected Automated Vehicle.” In *9th IFAC International Symposium on Advances in Automotive Control*. Orleans, France, 2019.
3. Jeong, Jongryeol, Daliang Shen, Namdoo Kim, Dominik Karbowski, and Aymeric Rousseau. “Online Implementation of Optimal Control with Receding Horizon for Eco-Driving of an Electric Vehicle.” In *IEEE Vehicle Power and Propulsion Conference (VPPC)*. Hanoi, Vietnam, 2019.
4. Karbowski, Dominik, Jongryeol Jeong, Koen Elands, and Iulian Dobrovolschi. “Model-Predictive Eco-Driving for Electrified Connected and Automated Vehicles.” In *32th Electric Vehicle Symposium (EVS32)*. Lyon, France, 2019.

Acknowledgements

We thank Argonne researchers Eric Rask and Kevin Stutenberg for collecting and providing the test data used in validation. We also thank Argonne researchers Jongryeol Jeong, Daliang Shen, Jihun Han, and Namdoo Kim.

I.2.4 Multi-Scale, multi-scenario assessment of system optimization opportunities due to vehicle connectivity and automation (ORNL) [Task 2.1.2]

Jackeline Rios-Torres, Principal Investigator

Oak Ridge National Laboratory
2360 Cherahala Boulevard
Knoxville, TN 37921
Phone: (865) 946-1542
E-mail: riostorresj@ornl.gov

Erin Boyd, DOE Technology Manager

U.S. Department of Energy
E-mail: erin.boyd@ee.doe.gov

Start Date: October 1, 2018	End Date: September 30, 2019	
Project Funding (FY19): \$381,000	DOE share: \$381,000	Non-DOE share: \$0

Project Introduction

Connectivity and automation provide opportunities for implementation of innovative and effective system-level monitoring and control. Coordination control systems for connected and automated vehicles (CAVs) operating in different traffic scenarios can potentially improve traffic efficiency, safety, and energy consumption. However, most of the current research in connectivity and automation is focused mainly on safety leaving still many open questions and uncertainty regarding the energy impacts of these new technologies. The uncertainties become even higher when the interaction between human drivers and vehicles with connectivity and automation capabilities is considered. In this context, further exploration of mobility gains and energy savings potential is needed. This project aims to investigate opportunities to optimize traffic systems through connectivity and automation and assess their performance under different scenarios. It explores the potential energy savings and efficiency improvements that can be achieved through coordination control systems for CAVs, contributing to the SMART Mobility program goal of yielding meaningful insights on how SMART technologies can improve Mobility Energy Productivity. It will also provide new insights regarding efficient coordination/control strategies that could offer energy and mobility improvements. The objective of the optimal merging coordination is to enable smoother traffic flow by controlling the merging sequence and optimizing the vehicles' speed profile

Objectives

Develop optimal vehicle coordination strategies to increase mobility energy efficiency and a simulation framework to verify their effectiveness in partial and full CAVs market penetration scenarios

- Apply the developed coordination framework and assess its performance on traffic corridors considering heterogeneous traffic and different market penetration rates

Approach

The approach taken to accomplish the objectives of the project for this period of performance involved:

1. Simulation-based assessment of the CAVs optimal coordination framework applied to a single on-ramp, considering different traffic scenarios, market penetration rates (MPR) and heterogeneous traffic.
2. Selection, modeling and calibration of a real-world traffic corridor segment in VISSIM.

3. Implementation and simulation-based assessment of the CAVs coordination framework on the VISSIM corridor model.
4. Exploration of the challenges that communication related uncertainties can impose on the optimal coordination framework (collaboration with University of Delaware)
5. Safety-oriented analysis. Used the driving volatility as a surrogate measure of safety to study the safety impacts of optimal coordination in a highway on-ramp (unfunded collaboration with University of Tennessee Knoxville)

Results

1. Simulation-based assessment of the CAVs optimal coordination framework applied to a single on-ramp

The objective of the optimal lane merging coordination is to enable smoother traffic flow by controlling the merging sequence and optimizing the vehicles' speed profile. We performed analysis for a single on-ramp (Figure I.2.4.1) considering three traffic demands, i.e., 1800 veh/h, 2000 veh/h and 2200 veh/h, and a 60%-40% ratio between the main road and the on-ramp demand. For each scenario, we simulated a total of 12 CAVs market penetration rates. To assess the fuel, energy and emissions implications, we compared the results for each scenario against a baseline scenario where all the vehicles were human-driven. The estimates for the measures of effectiveness (fuel, electrical consumption, emissions, etc.) were obtained using the workflow baseline fleet scenario for current time (CT).

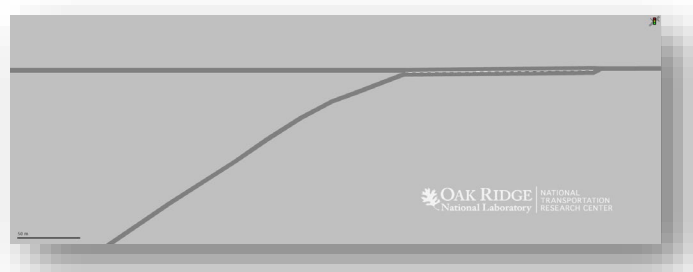


Figure I.2.4.1 On-ramp model used for analysis

The plots in Figure I.2.4.2 represent the average fuel economy change for the three traffic demands under the CT fleet scenario and show that benefits are sensitive to traffic demand. The higher benefits in terms of average fuel economy occur in scenarios with moderate congestion (e.g., 2000 veh/h) because the vehicles will still have some freedom to accelerate/decelerate in an optimal way. Under heavy traffic, the vehicles are more constrained in their responses due to the smaller headways and the idling condition starts dominating, reducing the potential to improve the average fuel economy and save fuel. Still, the average fuel economy in heavier traffic can increase between 2% to 20% depending on the MPR.

At lower traffic demands, the reduced traffic on the main road allows more human drivers to merge without conflicts in the baseline scenario, avoiding significant acceleration/deceleration changes. This results in already smoother travel patterns than in moderate traffic and thus reduced opportunities for improvement. Nevertheless, the fuel economy at full penetration can increase to about 12%.

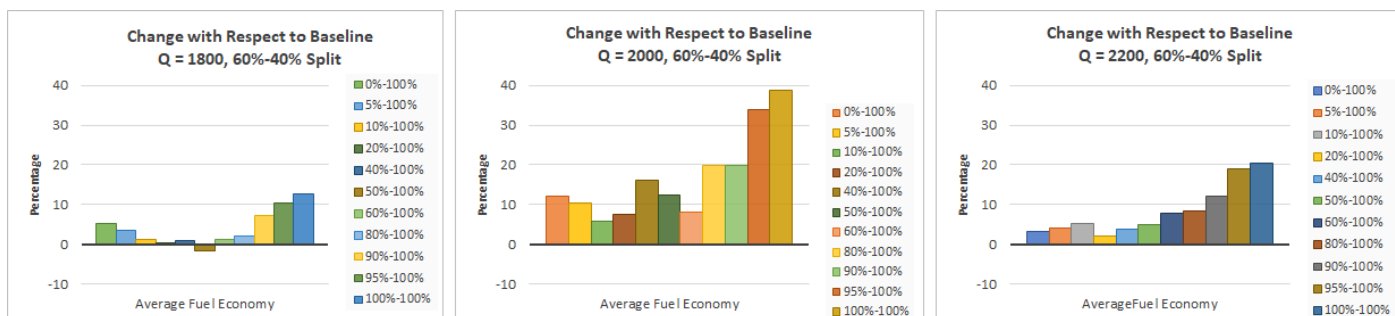


Figure I.2.4.2 Average fuel economy changes with respect to baseline for three traffic demand scenarios and different market penetration rates of CAVs. The legends at the right of each figure indicate the percentage of LCAVs and HCAVs respectively

Notably, at lower MPR for all the simulated traffic demands, there is increased uncertainty regarding the benefits in fuel economy due to CAVs being adversely affected by the non-smooth driving of the human-driven vehicles when attempting to merge.

2. Selection, modeling and calibration of a real-world traffic corridor segment in VISSIM. A 6-mile segment of the I75 corridor was selected based on traffic data availability

Based on traffic data availability, we modeled a 6-mile segment of the I75 corridor in VISSIM (Figure I.2.4.3) and calibrated it to resemble real traffic conditions. Traffic data, including volume, speed, and on/off ramp traffic, were obtained from Tennessee Department of Transportation's (TDOT) traffic sensors and cameras. These data were then used to calibrate vehicles' speed distributions as the measure of effectiveness (MOE). The VISSIM model was calibrated so that vehicles' speed distribution in the simulation model is comparable to the field observations.

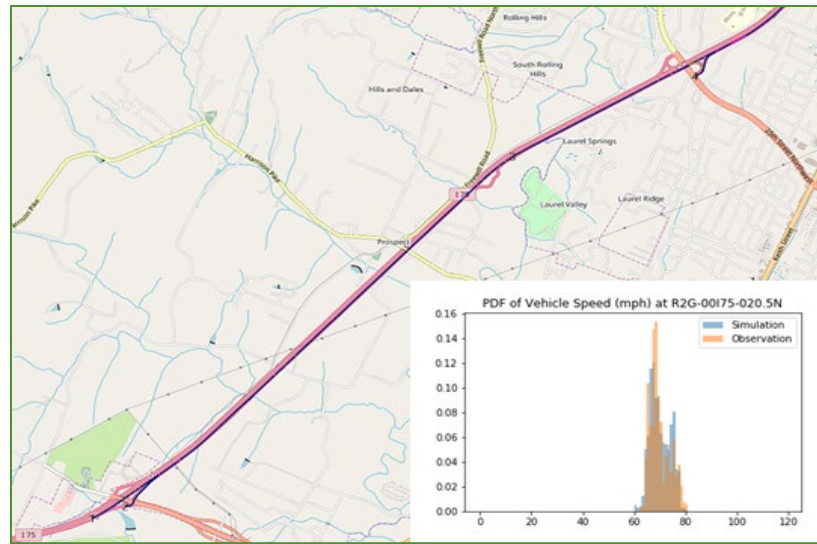


Figure I.2.4.3. Corridor modeled in VISSIM and histogram of observed vs simulated vehicle speeds in the 20.5 N mile marker

As part of the calibration process we used the Latin Hypercube Design, a design of experiment (DOE) sampling method, to select 100 comprehensive parameter sets for the initial calibration. Each parameter set was simulated in VISSIM, each with a different random seed. Results based on these simulation settings, in terms of vehicle traveling speeds, along with the observed speeds from RDS data, are shown in Figure I.2.4.3 (bottom right corner).

3. Implementation and simulation-based assessment of the CAVs coordination framework on the VISSIM corridor model

The impacts of optimal CAVs coordination were assessed considering the five workflow baseline fleet scenarios: current term (CT), short term low automation, short term high automation, long term low automation and long-term high automation. For each scenario we study eight MPR as defined in the percentage of the average number of electrified vehicles for each simulated fleet scenario are shown in Figure I.2.4.4.

Table I.2.4.1 Market Penetration Rates Considered for Assessment

Scenario:	Baseline	2	3	4	5	6	7	8
%MPR Light Duty CAVs	0	0	5	10	20	50	80	100
%MPR Heavy Duty CAVs	0	100	100	100	100	100	100	100

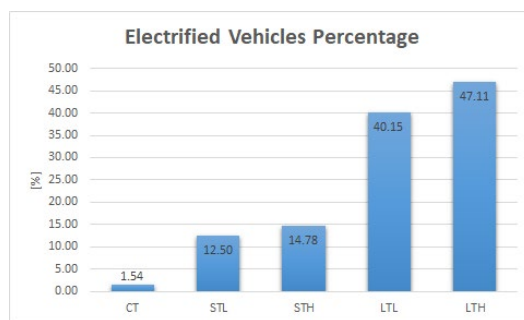


Figure I.2.4.4 Percentage of electrified vehicles considered for each fleet distribution scenario.

3.1 Current term fleet distribution

In the current time fleet scenario, the fuel savings tend to increase steadily with increased MPR when more than 10% of the vehicles on the road are CAVs and reach a maximum of about 7% at full CAVs MPR (Figure I.2.4.5). In contrast, the average electrical consumption can eventually increase under lower MPR but decreases steadily when the MPR exceeds 50%. It is important to note that, the electrified vehicles obtained when estimating the energy consumption account for only 1.54% of the fleet.

3.2 Results for short term fleet distribution

In the case of the short-term low automation scenario, the overall trend of the fuel savings is similar to that of the current term when more than 10% of the vehicles on the network are CAVs. When only 5% LDVs and 100% HDVs are CAVs the fuel consumption increases slightly. This result can be because the fleet is randomly distributed when estimating the performance indicator. For example, although the speed profiles are a constant across multiple simulation runs of a given scenario, the sequence of the vehicles following the speed patterns change each time that a new fuel estimation is done (random ordering results in non-repeatability). Regarding the electrical consumption, the savings increase when more than 20% of the vehicles are CAVs, however at full penetration there is a slight increase in the electrical energy consumed. This particular case requires further exploration, preliminary observations point to the fact that there is not always the same ratio between the electrified vehicles types that are represented for each MPR scenario. One reason for this to happen is that we only kept the fuel/energy consumption data for the vehicles that travelled at least a minimum distance of 2.5 miles (ensuring that they have at least been coordinated through the first on-ramp) thus, some electrified vehicles can be taken out among the discarded data.

In the short-term high automation scenario, there is not a steadily increasing pattern for the average fuel consumption savings, but the savings can still range between 3 to 7% with more than 20% CAVs. For lower market penetration rates, the level of savings is lower than for the CT and STL scenarios. This implies that at lower MPR the additional electrical consumption due to sensors reduces the potential to save energy of the coordination strategy.

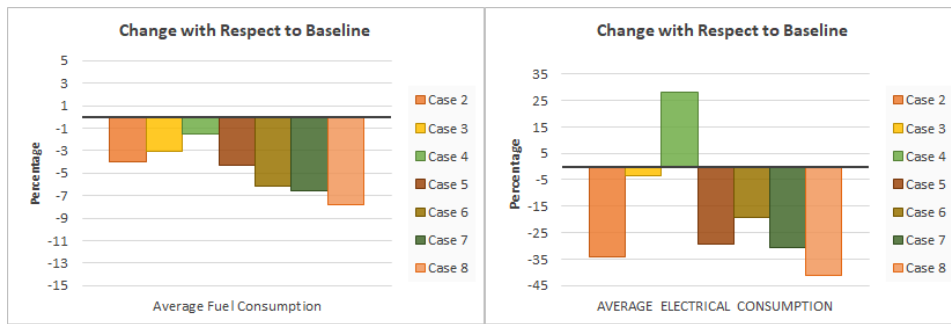


Figure I.2.4.5 Fuel and energy consumption results for the current time fleet distribution scenario

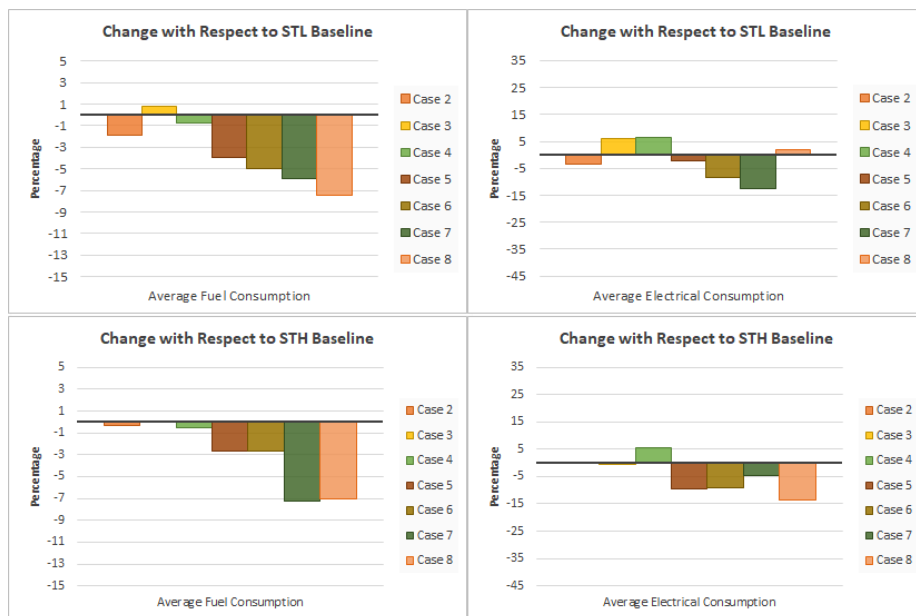


Figure I.2.4.6 Average fuel and energy consumption results for the short-term scenario

3.3 Long term fleet distribution

In the long-term scenario, the trends for the average fuel consumption and the electrical savings is similar for the low and high automation cases. Overall, the values for the fuel consumption case are slightly higher in the case of high automation, while the contrary is observed for the case of the average electrical consumption, i.e., the values are lower for the high automation scenario. In this case is also apparent that the additional electrical consumption due to the additional sensors of the highly automated vehicles reduces the potential of the optimal coordination framework to save energy.

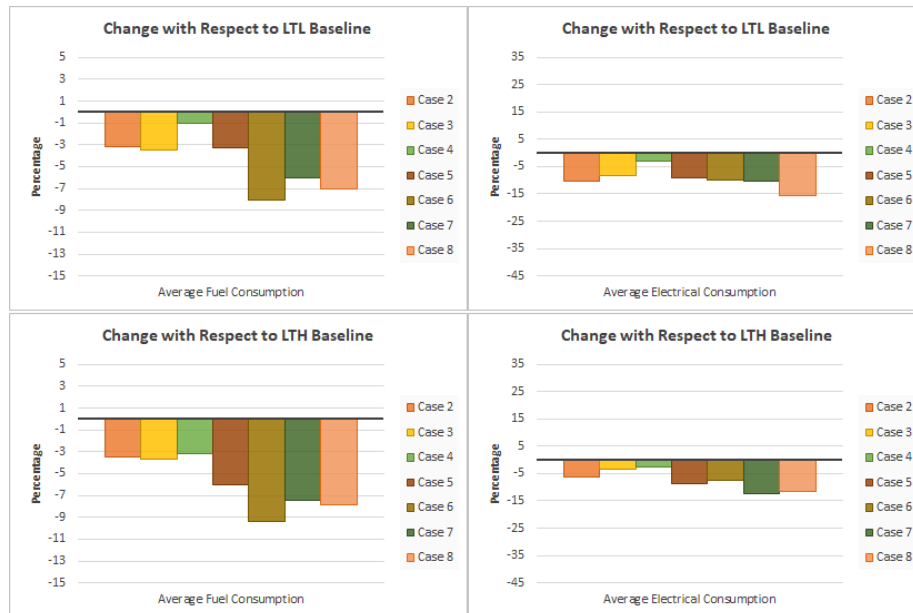


Figure I.2.4.7 Average fuel and energy consumption results for the long-term scenario

4. Exploration of the challenges that communication-related uncertainties can impose on the optimal coordination framework (collaboration with University of Delaware)

Experiments were carried out in the University of Delaware Scaled Smart City (UDSSC) (Figure I.2.4.8) a 1:25 scale testbed, designed to replicate real-world traffic scenarios and test cutting-edge control technologies in a safe and scaled environment. UDSSC is a fully integrated smart city, which can be used to validate the efficiency of control and learning algorithms and their applicability in hardware. It utilizes high-end computers, a VICON motion capture system, and scaled CAVs to simulate a variety of control strategies with up to 35 scaled CAVs. Each CAV has a Raspberry Pi 3B with a 1.2 GHz quad-core ARM processor and communicates with the mainframe computer (Processor: Intel Core i7 – 6950X CPU @ 3.00 GHz x 20, Memory: 125.8 Gb).

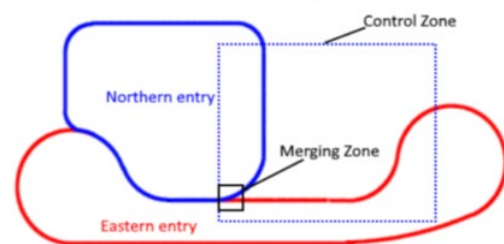


Figure I.2.4.8 University of Delaware Scaled SMART City testbed

We considered two loops of UDSSC (Figure I.2.4.8) for the path of CAVs, which includes a mainstream representing the highway and a merging roadway connecting to it. Each loop has a starting point which enables us to have enough CAVs ready to run an experiment. In each experiment, a random number of CAVs between 4 and 6 is assigned for each entry. CAVs in mainstream comes from East to West, and CAVs from north merges to the mainstream road.

In the baseline scenario CAV’s from the north should yield to the mainstream CAVs. In an optimal framework with upper level control, upon arriving the control zone, CAVs compute the time that they should enter the merging zone. A simple FIFO scheduling policy is chosen, i.e., the CAV which enters the control zone first, must enter the merging zone first as well, each CAV computes its schedule upon entering the control zone and find its energy optimal control input. Upon entering the control zone, we store the entry information of each

CAV, namely, their position and intended merging time (time to reach the merging zone). Similarly, when the CAV enters the merging zone, we store the actual merging time to quantify the error with respect to the initially planned merging time. We ran 44 experiments in the UDSSC for the merging roadway scenario and computed the scheduling error for all CAVs in all experiments. The summary of the error data statistics is included in Table I.2.4.2. The results show that, even though the errors are mainly distributed around 0, high error values in the initial estimation of the merging time can still occur, which may jeopardize the safety of the traffic network. Future work should aim to further study the causes of uncertainty, quantify and model the errors in a explore methods to account for the uncertainty for calculation of the low-level control (optimal speed).

Table I.2.4.2 Summary of Statistics for the Entry Time Error

Maximum	Mean	Median	Minimum	Standard Deviation	Variance
5.53	0.34	0.124	-5.46	0.73	0.53

5. Safety-Oriented Analysis

To investigate the efficiency and safety benefits of enabling cooperative driving by enabling automated vehicles to communicate with each other, we modeled a merging scenario in PTV VISSIM, based on the W I 94/N US 23 On-Ramp in the Washtenaw county in Ann Arbor, Michigan (Figure I.2.4.9). The longer blue segment represents the rightmost length of the highway with a total distance of 1,086 m and the on-ramp is represented by the shorter segment with a total distance of 560 m. we assume that all the vehicles share their state information which includes their speed and position and are able to communicate via V2X with other vehicle and infrastructure; similar to (Letter & Elefteriadou, 2017; Z. Wang, Wu, & Barth, 2018) we only model the rightmost lane of the highway for the onramp merging and consider a single lane on-ramp; the default lane change model in VISSIM is used to allow the vehicles to join the main road in the merging zone. A baseline scenario in which all the vehicles are assumed to be human driven without coordination is simulated and used to assess the effectiveness of the coordination system in terms of safety and fuel consumption. Then, the optimal coordination system was simulated using the same traffic conditions as in the baseline scenario.



Figure I.2.4.9 Traffic Simulation network in VISSIM based on the W I 94/N US 23 On-Ramp in the Washtenaw county in Ann Arbor, Michigan.

According to the results, waves of stop and go operation are seen on the ramp road for the baseline scenario. Meanwhile, the coordination control system can save fuel consumption by about 25% (the average fuel consumption is reduced by about 30%) as it resolves the stop-and-go waves. To evaluate the safety performance of the coordination system, two surrogate safety performance measures were utilized: number of longitudinal conflicts and driving volatility (X. Wang, Khattak, Liu, Masghati-Amoli, & Son, 2014). This safety analysis revealed that, compared to the baseline scenario, the coordination system enhances the safety performance of the merging area by eliminating the number of longitudinal conflicts. In addition, Figure I.2.4.10 shows driving volatility significantly dropped under the optimal coordination systems for the ramp segment, indicating improved safety performance. Although there was an increase in the main road speed volatility given that the vehicles should adjust their speed to provide appropriate gaps for the vehicles merging from the on-ramp, there is a slight reduction in the acceleration volatility which also contribute to a safer operation.



Figure I.2.4.10 Speed and acceleration volatilities in the main road, and ramp

Conclusions

Our focus on FY19 has been on microsimulation-based analysis of the implications that optimal coordination of CAVs can have when applied to merging on-ramps. We have considered efficiency and safety indicators under different traffic scenarios with varying CAVs market penetration rates and heterogeneous vehicle fleets. The analysis considering a single on-ramp showed that the benefits in terms of fuel economy/consumption are highly sensitive to the traffic demand and the CAVs market penetration rate. Notably, at higher MPRs, i.e., more than 50%, the fuel economy benefits seem to increase proportionally with the MPR, while at lower MPR values there is higher uncertainty on the benefits level.

The analysis considering a 6-mile segment of the I75 corridor revealed that, given a light traffic scenario, there is opportunity to improve the traffic efficiency by enabling coordinated merging control mostly when the CAVs MPR is higher than 20%. At lower penetration rates both the fuel and electricity consumption benefits are low or might even increase. Future work should combine results of additional simulation runs to ensure statistical significance.

It is important to highlight that the available traffic data was more representative of free flow conditions and light traffic and as such, the benefits of applying coordination are moderate. Future work should consider additional baseline traffic scenarios for an intracity corridor under different traffic conditions, i.e., from moderate to heavy congestion to get more insights on the full range of benefits that is attainable through coordination on real world corridors. Also, when computing the respective consumption indicators, we considered the full vehicle fleet that travelled the corridor, independently of whether the vehicle was controlled or not. While this way we might be accounting for the impact of coordination on the overall traffic network, future work should be devoted to find appropriate ways to quantify the direct benefits of coordination and explore how far upstream and downstream the merging point the traffic is affected/improved by the coordination itself. We anticipate that corridors with shorter segments between on-ramps would render higher percentages of improvement under similar traffic conditions. In addition, since the vehicles on the left-most

lane are not being controlled, their fuel consumption will reduce the impact on the overall system fuel consumption percentage improvement results.

Key Publications

1. Rios-Torres, J., Han, J., Arvin, R., Khattak, A., “Safety, traffic and energy impacts of optimal coordination control systems for connected vehicles at highway on-ramps,” 99th Annual Meeting Transportation Research Board, 2020 (forthcoming)
2. Zhao, L., Malikopoulos, A. A., Rios-Torres, J., “On the Traffic Impacts of Optimally Controlled Connected and Automated Vehicles”, Proceedings of the 2019 IEEE Conference on Control Technology and Applications (CCTA), 2019
3. J. Rios-Torres and A. Malikopoulos, "Impact of Partial Penetrations of Connected and Automated Vehicles on Fuel Consumption and Traffic Flow," in IEEE Transactions on Intelligent Vehicles. doi: 10.1109/TIV.2018.2873899
4. Han, J., Rios-Torres, J., Vahidi, A., Sciarretta, A., “Impact of model simplification on optimal control of combustion engine and electric vehicles considering control input constraints” 2018 IEEE Vehicle Power and Propulsion Conference

References

1. Letter, C., & Elefteriadou, L. (2017). Efficient control of fully automated connected vehicles at freeway merge segments. *Transportation Research Part C: Emerging Technologies*, 80, 190–205. <https://doi.org/10.1016/j.trc.2017.04.015>
2. Wang, X., Khattak, A. J., Liu, J., Masghati-Amoli, G., & Son, S. (2014). What is the level of volatility in instantaneous driving decisions? *Transportation Research Part C: Emerging Technologies*, 58, 413–427. <https://doi.org/10.1016/j.trc.2014.12.014>
3. Wang, Z., Wu, G., & Barth, M. (2018). Distributed Consensus-Based Cooperative Highway On-Ramp Merging Using V2X Communications. *SAE Technical Paper*. <https://doi.org/10.4271/2018-01-1177>

Acknowledgements

We acknowledge the valuable contributions of Ross Wang, Hyeonsup Lim, Zulqarnain Khattak, Andreas Malikopoulos, Jihun Han, Ramin Arvin and Asad Khattak, and the continued support of Eric Rask (CAVs Pillar lead).

We thank the Systems Modeling and Control Group from Argonne National Laboratory for providing vehicle fleet distribution models for fuel consumption estimation.

I.2.5 Aggregation Methods to Estimate National-Level Impacts of CAVs Scenarios (ANL, NREL, ORNL)

Thomas Stephens and David Gohlke Principal Investigators

Argonne National Laboratory
9700 S Cass Avenue, Lemont, IL 60439
Phone: (630) 252-2997
E-mail: tstephens@anl.gov, gohlke@anl.gov

Jeffrey Gonder, Principal Investigator

National Renewable Energy Laboratory
15013 Denver West Parkway, Golden, CO 80401
Phone: (303) 275-4462
E-mail: Jeff.Gonder@nrel.gov

Paul Leiby, Principal Investigator

Oak Ridge National Laboratory
1 Bethel Valley Road, Oak Ridge, TN 37830
Phone: (865) 574-2742
E-mail: LeibyPN@ornl.gov

Erin Boyd, DOE Technology Manager

U.S. Department of Energy
E-mail: erin.boyd@ee.doe.gov

Start Date: October 1, 2018	End Date: September 30, 2019
Project Funding (FY19): \$260,000	DOE share: \$260,000 Non-DOE share: \$0

Project Introduction

The purpose of this task is to synthesize SMART Mobility and related research on Connected and Automated Vehicles (CAVs) to a national level, to deliver estimated impacts of CAVs, and better understand the factors on which these impacts depend.

Objectives

Task objectives include:

- Quantify potential impacts of specific Connected and Automated Vehicle (CAV) technologies at a national level based on results of in-depth CAVs case studies and scenarios, in a bottom-up approach.
- Develop and apply an aggregate, medium-to-longer-term model of national/regional travel and energy demand implications of CAVs, in a top-down approach
- Expand the previous CAV Bounding Report (Stephens et al., 2016), providing greater detail regarding the factors, sensitivities, and interactions.

Approach

To quantify CAVs impacts nationally based on results of in-depth studies (bottom-up), methods were developed to 1) model the traffic flow results of POLARIS CAVs simulations in a way that can be used in a national-level rollout, 2) aggregate vehicle-level energy use from other SMART Mobility tasks with traffic flow changes estimates from the previous model.

To model the national/regional-level travel and energy demand using the top-down approach, a national-level modeling framework CAVESIM was developed to produce estimates of national or regional changes in vehicle-miles-traveled (VMT) and fuel use.

To expand the previous CAV Bounding Report, results from SMART Mobility tasks and recent literature were reviewed and synthesized to estimate the approximate distributions of CAVs impacts considering two dozen factors and their possible interactions to give overall distributions of changes in energy use and travel demand.

The bottom-up approach for expanding travel demand proved to be challenging, and the transferability methods developed in previous years, while successful for expanding some metrics from regional simulations were not adequate for expanding VMT results (Shabanpour et al., 2018). However, models for other travel demand metrics, specifically changes in traffic flows at a link level were successfully modeled using detailed results from POLARIS simulations of CAVs in the Chicago metropolitan area. The changes in average daily traffic (ADT) was the difference in traffic flow on each link from two scenarios modeled in POLARIS, one with full penetration of CAVs with CACC and smart intersections (requiring no stopping), and the other a baseline (no CAVs) scenario.

Traffic flow differences were modeled using two methods, K-nearest neighbors (KNN) and random forest (RF). In both modeling approaches, 70% of the data were used for training, and 30% were used for validation. Both models give the change in ADT using explanatory variables describing link properties, network properties, and land use and population demographics in census block groups through which links pass.

The other portion of the prior fiscal year bottom-up approach development involved formulating a methodology which estimated vehicle fuel efficiency in different driving conditions (separately for various combinations of powertrain and CAV versus non-CAV technologies) and subsequently weighted the condition-specific energy efficiency by the amount of driving that occurs in each condition. Full national-level application of this methodology under different scenarios was not supported in FY19, but wrap up activities that were supported, as summarized in the Results section below.

The top-down approach in CAVESIM is meant to quickly analyze changes in VMT and passenger-miles-traveled (PMT), and energy use for various CAVs scenarios at a national level. CAVESIM is an aggregate national impacts model that integrates market and economic drivers using established theory of consumer/traveler economic behavior. The approach utilized an economic equilibrium framework to account for interactions between full travel cost (fuel, vehicle, time, other) and other attributes and constraints important to consumers and producers, and to estimate market outcomes of travel demand, vehicle efficiency, congestion and speed, energy use, and emissions. CAVESIM includes some reduced form representations of results from other technology and travel simulation models (e.g., CAV technologies and energy intensity, and travel activity and congestion), and can integrate key technological and behavioral results from more detailed simulation models.

CAVESIM represents nine technological mechanisms by which automation can alter vehicle energy efficiency and costs, as well as accounting for the effects of electrification and shared mobility. Other “mechanisms” or impacts of technology have direct or indirect effects on demand, i.e., through altering travel time cost or inducing new demand from underserved demographic segments. Vehicle types are identified with demand segments, consistent with the SMART Mobility analysis workflow, are distinguished by level of automation (3 types), fuel-type/drivetrain (currently 3 types), and vehicle use case (private or shared). Each vehicle’s energy intensity is based on the assumed technology set and the vehicle type and demand segment categories, which alter the energy intensity of the base vehicle type (conventional gasoline, no automation). VMT responses are based on associated changes in total travel cost and consumer utility maximization.

The updated study of CAVs energy and travel impacts estimated distributions of reported CAVs impacts for 24 factors, accounting for their interactions. Estimated impacts on travel demand (VMT), fuel economy, and energy were collected from over 400 sources. Distributions of impacts of each factor were estimated as well as

the magnitude and sign of their interactions. Random draws of many samples from distributions of each factor were used to estimate distributions of overall impacts. Subsets of results relevant to specific scenarios were examined including the SMART Mobility common scenarios, partial automation, electrification, and others.

Results

Wrap-Up Activities on Bottom up Methodology Components

The two models developed to estimate changes in average daily traffic (ADT) flows due to CAVs have good accuracy. In the KNN model achieved an accuracy of 83.5 %, and the RF model achieved an accuracy of 87.1%. These models, if validated for other areas, could be used to estimate changes in traffic flows in such areas, and could possibly be extended to all links in the U.S. This would be useable in the energy aggregation framework described below.

Wrap up activities for the energy aggregation approach included transfer of the methodology to estimate regional-level energy consumption in the San Francisco Bay Area using Lawrence Berkeley National Laboratory's BEAM model (see forthcoming publication of Capstone Reports for the Workflow and for the CAVs activities under the SMART Mobility Laboratory Consortium). In addition, publication of a journal article featuring a variant of this methodology was completed in FY19 jointly with collaborators from Volvo Car Corporation based on real-world driving data for vehicles in both partially automated and in fully human-driven operation (Zhu et al).

Top-Down Modeling of Integrated Market and Economic Drivers for National-Level CAV Sensitivities

The CAVESIM model was extended to account for some aspects of shared mobility, in particular “empty” vehicle travel (deadheading) and sharing of rides (ride pooling). Ride pooling may be an important strategy for the improvement of Mobility Energy Productivity by limiting growth in unproductive VMT or energy use from vehicle repositioning and empty or low-occupancy vehicle travel. The purpose is to explore and represent key outcomes and tradeoffs from ride-pooling at the aggregate level.

National-level analysis of a range of CAVs scenarios of highly automated vehicles using the CAVESIM model showed that national VMT and fuel use by CAVs can be expected to differ from that of manual vehicles under a range of assumptions about future CAV technology and mileage-based costs. Scenarios modeled show net energy differences between -8% and +12% (Leiby and Rubin, 2018). The model accounts for major components of generalized costs and their interdependencies, showing how different components of generalized cost change under different economic, behavioral, or technological conditions.

Ride-pooling, i.e., ridesharing with increased vehicle occupancy, can help achieve the benefits of new mobility systems and thus the impacts of automation technologies, and pooled riding (multiple passengers in shared vehicles) on Vehicle Miles Traveled (VMT) and Passenger Miles Traveled (PMT) were also assessed. The response is based on the economic benefits (travel cost savings, including vehicle operation costs and travel time costs) and the potential disbenefits of ride pooling (disutility of sharing space, and incremental travel distance and delay). Impacts were explored over a range of values and are shown in Figure I.2.5.1 below.

Total cost per passenger mile in pooled travel is the sum of the passenger's share of vehicle operating costs and the passenger's time cost. Passenger time cost when pooling is affected by two factors: the increased trip travel time caused by any detours or delays in picking up or dropping off other passengers; and the disutility cost associated with sharing ride space. We capture these latter effects, which are still being studied, through elasticities with respect to pooling level. Increased occupancy from pooling can erode the travel-time-cost advantage of ride services. This entails some tradeoff with pooling between the passenger's declining share of the vehicle operating costs with potentially rising trip duration and time costs.

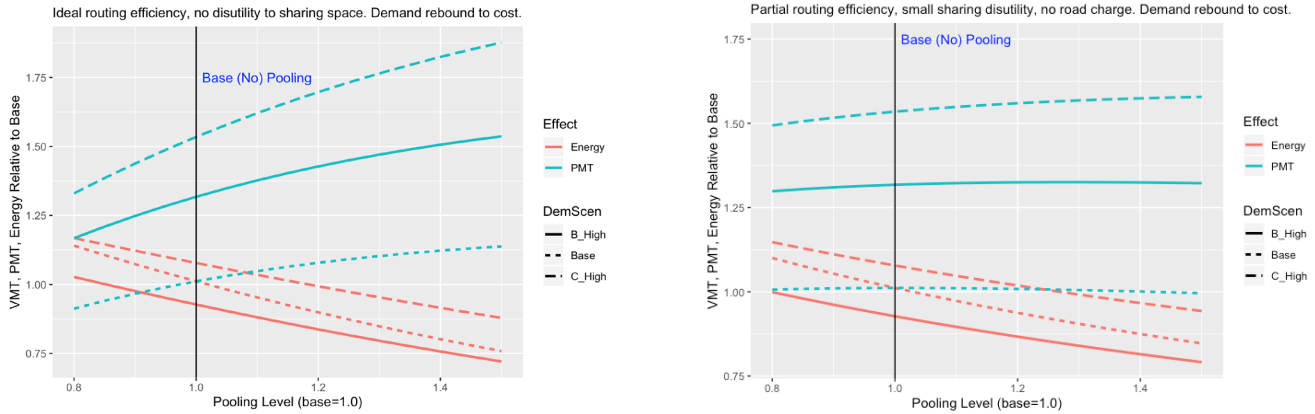


Figure I.2.5.1 Highlighted PMT, and Energy changes with ride pooling for ideal and suboptimal sharing scenarios

Bounding Study Update

While the updated impact estimates show similar ranges as the 2016 report, in this update we estimate the distributions of impacts considering interactions, and distributions show that the bounds are not likely outcomes, and CAVs impacts on energy and vehicle-miles traveled (VMT) will very probably be more modest than indicated by the bounds. Initial numbers show that 90% of cases are between a 25% reduction and a 160% increase in VMT, but that energy efficiency improvements lead to an average increase in 30% in energy consumption, with 90% of cases between -35% and +120% of a non-automated scenario. Distributions were generated for VMT, changes in fuel consumption rate, and changes in total energy consumption. Figure I.1.1.2 shows a histogram for changes in total energy consumption (relative to a no-CAVs baseline).

The top factors leading to increase in energy usage are induced travel from easier and cheaper travel (both additional travel by today’s travelers and new travel by the currently underserved), repositioning of empty vehicles, and on-vehicle electronics power draw, while the largest potential levers for reducing fuel consumption are vehicle rightsizing, ridesharing, and drive smoothing. No single factor changes energy consumption by more than a factor of two, though 9 of 24 factors change total energy consumption by more than 10%. Some factors have large variations due to scenarios with widely different futures, e.g., ridesharing, with most of the highest potential for VMT reductions coming from scenarios with fleet-owned vehicle. Other factors have a large range of potential outcomes within the same scenarios, e.g., electronics power draw, with large uncertainty in the magnitude of typical auxiliary electrical loads for CAVs hardware.

Finally, results of subsets of studies relevant to selected scenarios were analyzed, and distributions for several scenarios are narrower than for the entire set of results most factors for partial automation have smaller impacts on energy and VMT. Overall bounds of energy consumption are driven by outliers for each factor, and estimated distributions show that more modest impacts are much more likely than extreme cases.

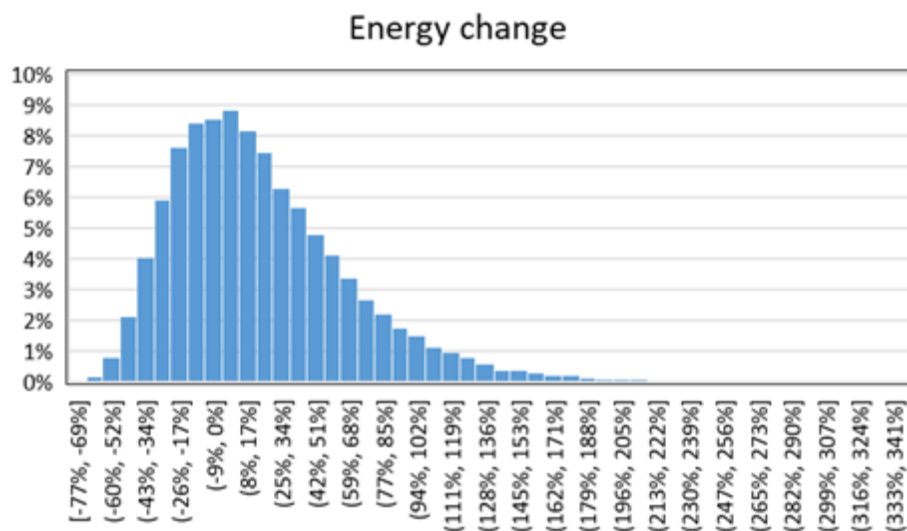


Figure I.2.5.2 Histogram showing changes in total light-duty vehicle energy consumption

Conclusions

Progress was made on modeling national CAVs energy and travel behavior impacts and in synthesizing results of CAVs research by SMART Mobility investigators and by related research.

In the bottom-up subtask to expand results of detailed CAVs simulations, models were developed to give changes in traffic flows due to CAVs deployment in the Chicago metropolitan area, taking results of POLARIS simulations and other data as input.

Wrap up of the bottom-up subtask to expand results of detailed CAVs simulations included evaluating modeling to estimate changes in traffic flows due to CAVs deployment in the Chicago metropolitan area based on results of POLARIS simulations and other data as inputs. Additional activities included applying the energy estimation roll-up methodology for metropolitan area modeling using BEAM in San Francisco, and jointly publishing a journal article with colleagues from Volvo Car Corporation on applying a variation of this methodology to estimate energy consumption impacts from a partial automation technology operating on-road.

Models developed for changes in traffic flow models reveal important dependencies on local link, network, demographic, transportation, and land use characteristics. Changes are sensitive to details of the links and the network and to some demographic variables, and are less sensitive to other variables; however, these other variables still have a significant influence. Further examination of how these factors influence CAVs-induced changes in traffic flows under different conditions may clarify system-level interactions between the factors, and better understanding how CAVs can change travel patterns and energy use.

In the Top-down approach, CAVESIM results confirm how cost-responsive travel demand is attentive to changes in different components of total road travel costs, of which energy is only a limited fraction. Thus, the private economic incentives for energy efficiency are considered in the context of features and objectives related to other travel costs, including those related to capital cost and convenience (value of travel time). Benchmarked aggregate scenarios confirm some outcomes similar to more disaggregated urban-area models, and highlight that net energy impacts still vary substantially across technological and behavioral (demand) assumptions

CAVESIM results to date also indicate that cost-based strategies such as road use charges or disincentives for zero-passenger travel can accompany the development of CAVs for their private mobility benefits while

balancing other transportation planning objectives. Simulations for various levels of pooling (see above) show that the effect of pooling on PMT (mobility) is likely to depend strongly on the efficiency of pooled tour routing (which affects operating costs for the operator and time costs for the rider), as well as whether riders have significant disutility from sharing space in the pooled vehicle.

The updated study of CAVs energy and travel impacts shows similar ranges as the 2016 report, but in this update the estimated distributions show that the bounds are not likely outcomes, and that CAVs impacts on energy and vehicle-miles traveled (VMT) will very probably be more modest than indicated by the bounds.

While the earlier study highlighted the uncertainty in energy consumption, interactions between factors were not considered, and the wide range reported earlier range was driven by unlikely outlier points and not representative of real-world scenarios. By examining distributions and considering interactions, the updated study shows that while outcomes are still widely distributed, that 90% of cases are between a 3% reduction and a 146% increase in VMT, but that energy efficiency improvements lead to an average increase of 20% for energy consumption, with 90% of cases between -39% and +106% of a non-automated scenario.

Key Publications

1. Zhu, L.; Gonder, J.; Bjarkvik, E.; Pourabdollah, M. and Lindenberg, B. "An Automated Vehicle Fuel Economy Benefits Evaluation Framework Using Real-World Travel and Traffic Data." *IEEE Intelligent Transportation Systems Magazine*, Volume 11, Issue 3, 2019, pp. 29-41. doi.org/10.1109/MITS.2019.2919537

References

1. Leiby, P. J. Rubin (2018) "Efficient Fuel and VMT Fiscal Incentives for Automated Vehicles," Paper 18-04530 presented at the 97th Annual Meeting of the Transportation Research Board, Jan 7-11, Washington, DC, <https://trid.trb.org/view/1496760>.
2. Shabanpour R., A. Mohammadian, J. Auld, T. Stephens (2018) "Developing a Spatial Transferability Platform to Analyze National-level Impacts of Connected and Automated Vehicles," In *The Practice of Spatial Analysis*, Springer.
3. Stephens T.S., J. Gonder, Y. Chen, Z. Lin, C., C. Liu, and D. Gohlke (2016) "Estimated Bounds and Important Factors for Fuel Use and Consumer Costs of Connected and Automated Vehicles," National Renewable Energy Laboratory Technical Report NREL/TP-5400-67216, <http://www.nrel.gov/docs/fy17osti/67216.pdf>.

Acknowledgements

We acknowledge the contributions of Prof. Kouros Mohammadian, Ramin Shabanpour, and Amir Parsa at the University of Illinois at Chicago.

I.2.6 Truck Cooperative Adaptive Cruise Control (CACC)/Platooning Testing: Measuring Energy Savings, Interaction with Aerodynamics Changes and Impacts of Control Enhancements: A Hardware-in-the-Loop Testbed for Evaluating Impacts of Connected Automated Vehicle on Arterials (LBNL) [Task 1.3.1]

Xiao-Yun Lu, Principal Investigator

Building 190
Lawrence Berkeley National Laboratory (LBNL)
1 Cyclotron Road, Berkeley, CA
E-mail: xiaoyunlu@lbl.gov

Erin Boyd, DOE Technology Manager

U.S. Department of Energy
E-mail: erin.boyd@ee.doe.gov

Start Date: October 1, 2018	End Date: September 30, 2019	
Project Funding (FY19): \$75,000	DOE share: \$75,000	Non-DOE share: \$0

Project Introduction

This task is intended to continue the task proposed for FY18 for CACC truck intersection operational test. It is a hardware and real-time simulation in the loop CACC truck operational test. It contains the following components to facilitate a reasonable test scenario: (a) the intersection traffic is generated by the real-time simulation with which the three CACC truck movements are imbedded; (b) Active Traffic Signal Control (ATSC) is based on the real-time simulation generated traffic for all the movements; the ATSC algorithm is intended to maximize the throughput and minimize the Total Delay directly, and to minimize the Total Energy Consumption indirectly; we may consider mixed traffic in the sense that some simulated vehicle may be assumed to be CAVs of certain types; (c) the intersection 2070 traffic controller; and (d) all components are linked and synchronized using DSRC (Dedicated Short Range Communication), WIFI and wireless modem. With such set-up, a similar traffic patten can be repeated many times to evaluate the energy consumption which has two parts: (i) the overall traffic energy consumption based on an energy model developed in Task 1.2; and (b) the actual fuel consumption of the three trucks measured by fuel rate from the J-1939 Bus (an SAE standard CAN Bus for trucks).

Objectives

To assess more sophisticated arterial operation effects on fuel consumption for mixed traffic with CAVs. Active Traffic Signal Control approaches will be developed to incorporate with CAV operation in real-time simulation and in real-world for overall traffic direct mobility and indirect fuel saving improvement.

Approach

Figure I.2.6.1 shows the Concept of Operation. It includes a test CAV fleet, a test track, a microscopic traffic simulation model, a real-world traffic signal control system, a communication layer, and a server program. Among those components, the test CAVs are the experiment subject. The test tack and traffic control system offer a physical test environment. The simulation model is responsible for generating virtual traffic flow. The server program is used to coordinate the operation of each test system via various communication medians. A typical experiment in the testbed contains the following steps:

Step 1: Develop a simulation road network based on the physical layout of the test track.

Step 2: Initiate the traffic simulation to create a virtual traffic stream.

Step 3: Synchronize the clocks of the simulation, traffic signal controller, and test CAVs.

Step 4: Build a connection between the traffic simulation and the traffic controller; start update traffic signals based on the virtual traffic.

Step 5: Build a connection between the traffic simulation and the test CAVs; start the data interchange between the real and virtual vehicles.

Step 6: Begin the test; start collecting test data.

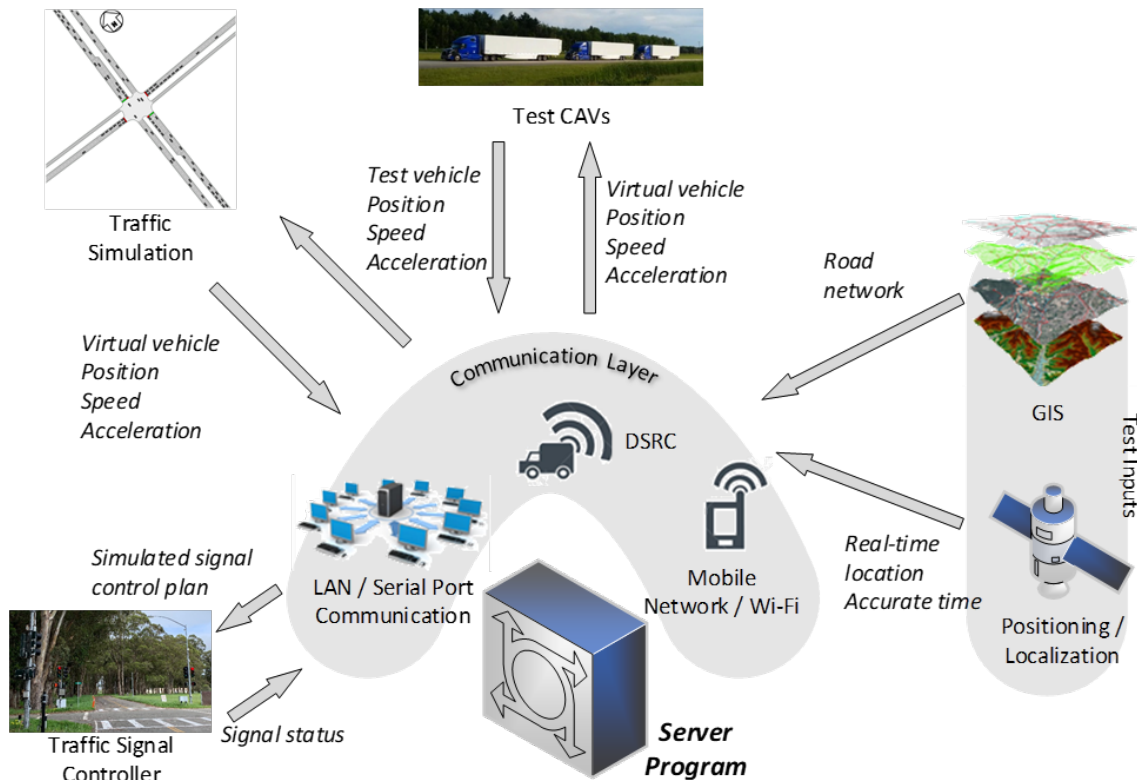


Figure I.2.6.1 Components and Data Flow of the Presented HIL Testbed

In this following, four subsections describe the research approach taken for this project. They describe the important algorithms of the system operation with CAVs, including the test connected automated vehicle fleet, microscopic traffic flow model, cooperative traffic signal control algorithm, and communication among test systems.

1. CACC Trucks

The test fleet consists of three Volvo trucks equipped with Cooperative Adaptive Cruise Control (CACC). The test vehicles have the capability to perform connected automated longitudinal control in a vehicle string with shorter than normal truck following gaps [1],[3],[4],[5].

2. Microscopic Traffic Simulation Model in Aimsun

The microscopic simulation of mixed traffic in Aimsun with CAVs and manually driven vehicles were developed in previous projects and reported in [6] – [14].

3. Cooperative Traffic Signal Control Algorithm

The objective of the proposed cooperative signal control algorithm is to determine proper green times for the eight-phase signal controller such that the resulting signal phase and timing (SPaT) scheme maximizes the overall throughput of the intersection. This would indirectly improve the vehicle energy consumption performance. It improves the intersection operation by assigning green time more efficiently than the fixed or actuated signal control. Figure I.2.6.2 shows a conceptual comparison between the cooperative algorithm and a typical actuated control algorithm. With the actuated controller, vehicle A from the westbound approach would trigger green time extensions. The extended green time only allows a few vehicles in the dashed box to pass the intersection. On the other hand, our algorithm reallocates the green time such that the extended green time is given to a different approach where several CACC strings are coming. The resulting green time split allows vehicles in those CACC strings to pass the intersection without waiting for another green cycle, thus leading to improved intersection throughput.

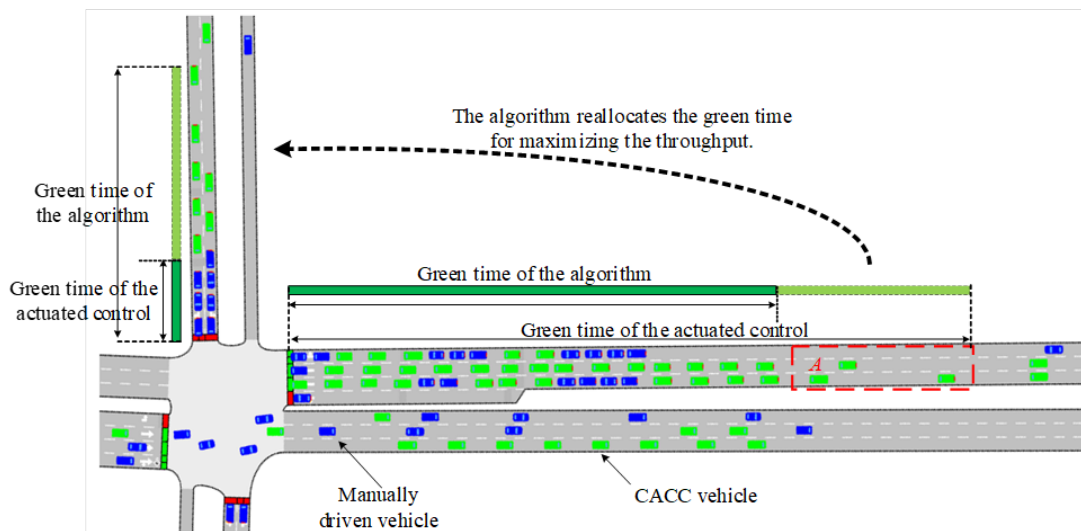


Figure I.2.6.2 Comparison of the proposed algorithm and actuated control

The effectiveness of the algorithm has been tested in a simulated 4-way signalized intersection. The algorithm substantially outperforms the traditional actuated controller as it perceives the traffic flow more comprehensively and assigns the green time resource more efficiently than the traditional controller. Particularly, the average vehicle speed and the average vehicle miles travelled per gallon fuel consumed (MPG) can be increased by more than 10% when the CACC market penetration is 100%. In mixed traffic where CACC fleets frequently interact with manually driven vehicles, the algorithm is found to be more beneficial. The speed and MPG improvement exceed 30% when the CACC market penetration is 40%. The signal control algorithm can bring about significant benefit even when the CACC market penetration is 0%.

4. Communication among Test Systems

The testbed adopts DSRC among the real-time simulation, the CAVs, and the traffic signal controller.

4.1. Communication between Test CAVs and Real-time Simulation

Since the communication occurs wirelessly via DSRC, the Basic Safety Message (BSM) defined by the J2735 standard is adopted to carry the location, speed, and acceleration information. The simulation, however, adopts an enteral vehicle structure to store the vehicle status information. In this case, we have developed a data map to match the data items used in different systems. Table I.2.6.1 shows the data map.

Table I.2.6.1 Data Mapping Rule Linking Traffic Simulation and Test CAVs

	Simulation	Test CAV
Data Structure	<pre>Vehicle Status Struct { int ID; long timestamp; (millisecond) double speed; (m/s) double acceleration; (m/s2) double latitude; (degree) double longitude; (degree) }</pre>	<pre>Basic Safety Message (BSM) { core_data { int id; long secMark; (millisecond) long speed; (0.02 m/s precision) long acceleration; (0.01 m/s2 precision) long latitude; (10-7 degree precision) long longitude; (10-7 degree precision) } }</pre>

4.2. Communication between Signal Controller and Simulation

The data interchange between the traffic signal controller and the simulation is achieved via the serial port communication. The communication is initiated by the simulation 400 milliseconds before the end of a simulated signal control cycle. At each update interval, the simulation sends the signal time plan of the next cycle to the traffic controller. The signal message from the simulation contains the following fields with Phase definition in Figure I.2.6.3:

Table I.2.6.2 Signal Time Messages from the Simulation

Byte Position	Name	Unit
0	Cycle Length	seconds, 0-254 seconds range, 255=error
1	Yellow time	seconds, 0-254 seconds range, 255=error
2	All red time	seconds, 0-254 seconds range, 255=error
3	Total time of phase 1 ^a	seconds, 0-254 seconds range, 255=error
4	Total time of phase 2	seconds, 0-254 seconds range, 255=error
5	Total time of phase 3	seconds, 0-254 seconds range, 255=error
6	Total time of phase 4	seconds, 0-254 seconds range, 255=error
7	Total time of phase 5	seconds, 0-254 seconds range, 255=error
8	Total time of phase 6	seconds, 0-254 seconds range, 255=error
9	Total time of phase 7	seconds, 0-254 seconds range, 255=error
10	Total time of phase 8	seconds, 0-254 seconds range, 255=error

^a: The total time of a phase is defined as (green + yellow + all red) in seconds. The phase ID is defined as the follows:

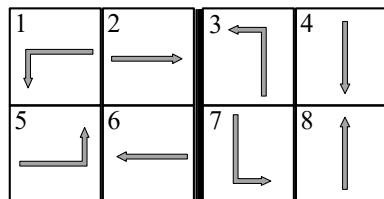


Figure I.2.6.3 Traffic Signal Control Phase Definition

4.3. Communication between Signal Controller and Test CAVs

The controller will send the BSM with the following messages:

- secMark = current time;

- speed = 0;
- acceleration = 0;
- latitude = latitude of the signal head;
- longitude = longitude of the signal head;

5. Server Program

The server program hosts the communication algorithms described in the previous section. In addition, it also coordinates the execution of the overall test systems. The server program adopts the following procedure to synchronize the test systems:

Table I.2.6.3 Procedure for Test System Synchronization

Line Number	Procedure
1	Pause the traffic simulation at the beginning of a simulated signal control cycle.
2	Send the simulated signal plan to the traffic controller for implementation in the next cycle.
3	Get the remaining time t_r of the current signal control cycle from the signal controller.
4	While $t_r > 0$
5	Continue pausing the traffic simulation.
6	Get updated t_r .
7	End while.
8	Resume the traffic simulation (signal controller and traffic simulation synchronized).
9	Create placeholder vehicles that represent the test CAVs in the simulated network.
10	Stop all simulated vehicles and the placeholder vehicles.
11	Start sending speeds and locations of the simulated vehicles to the test CAVs.
12	The test CAVs start updating their movements based on the virtual traffic information.
13	Receive locations and speeds of the test CAVs.
14	While CAV locations \neq placeholder vehicle locations
15	Continue stopping all simulated vehicles.
16	Get updated CAV locations.
17	End while
18	Let all simulated vehicles update their movements based on the traffic flow model.
19	Update the movements of the placeholder vehicles based on the received CAV data.
20	Synchronization complete.

A screen shot of the server program is shown in Figure I.2.6.4. The main window of the program contains three parts. The upper left part shows the real-time speed and location of the test CAVs and their virtual preceding vehicle. The server receives the operation status of those vehicles every 100 milliseconds and updates the plots every 1 second. The lower left part displays the information of the traffic signal controller. The left subplot depicts the green times of each signal phase graphically. The current second counter is also shown under the green time bars. The right subplot demonstrates the signal cycle length, cycle start time, and green times for all phases. This gives an overview of the current signal control plan. The server obtains the signal control information 400 milliseconds before the start of a signal cycle and updates the plots every 1 second. The right part of the server program is used to configure the HIL experiment. The user can specify the IP addresses and communication ports of individual test systems in the panel.

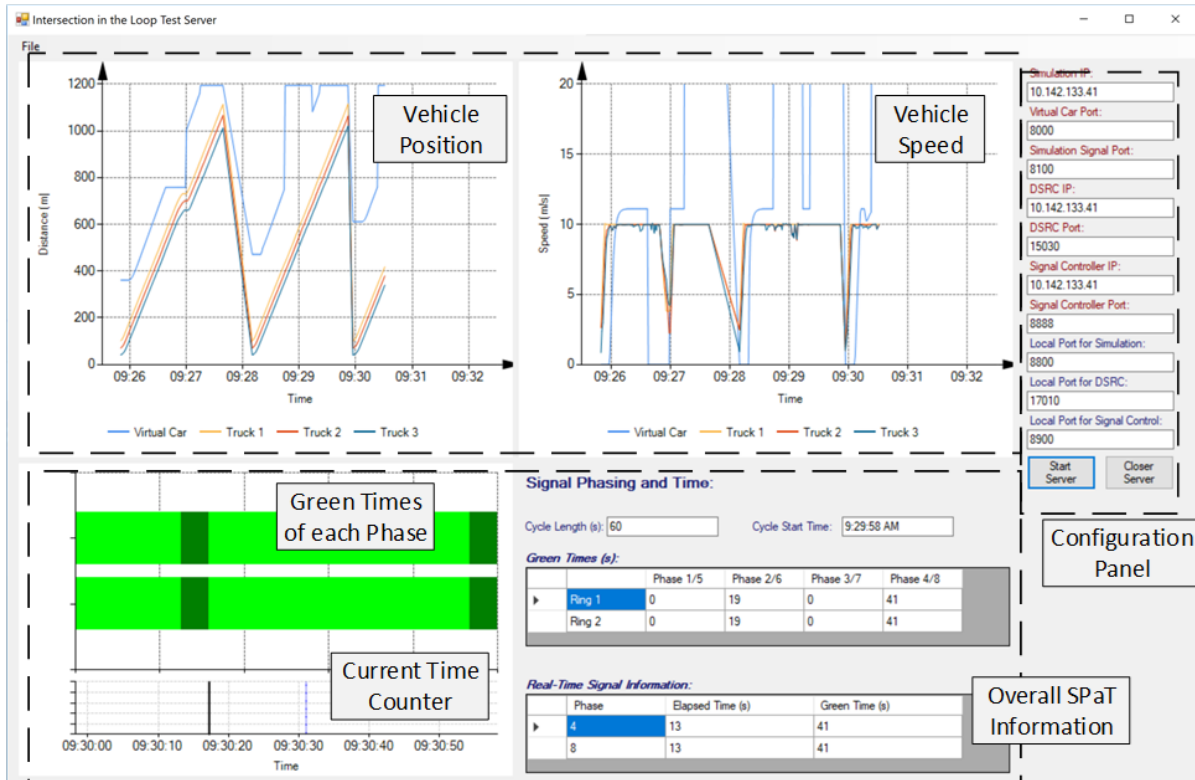


Figure I.2.6.4 Snapshot of the Server Program

Results

CAV Experiments with the Testbed

We plan to carry out the experiments with the HIL testbed in Richmond Field Station, a UC Berkeley campus that hosts an exclusive CAV test track, a test signalized intersection, and advanced traffic management and communication systems. In the test, the cooperative signal control algorithm will be implemented in the real-world controller and its impact on the CAV operation will be monitored. As Figure I.2.6.4 shows, a test run starts at the red bar and ends at the green bar of the test track. The test track has one lane each direction. No lane changing behaviors are permitted on the test track. This makes the test environment easy to control. To ensure safety of the test personals, there are no other traffic except the test CAVs in the test route during a test run. The signalized intersection is located about 750 meters downstream from the start location. The test vehicles would react to the traffic signals as they approach to the intersection. A roadside unit (RSU) installed at the intersection continuously broadcasts the SPaT and virtual preceding vehicle information via DSRC every 100 milliseconds. The information allows the automated controllers of test CAVs to update the vehicle acceleration and speed as if they are traveling in a real traffic stream. The drivers of the test CAVs are

responsible to perform lane tracking and keeping tasks during the tests. They are also instructed to abort the test should there is an emergency condition.

In the CAV experiments, we design test scenarios by considering parameters related to the traffic demand, the signal control algorithm, and the CACC string operation (Figure I.2.6.5). Particularly, the following variables are considered to define the test scenarios:

Volume capacity ratio (V/C ratio): 0.8, 1.0 and 1.2.

Cooperative traffic signal control algorithm: on and off.

CACC string operation: one vehicle ACC operation and three vehicles CACC fleet.

The combination of the above variables would result in 12 experiment scenarios. We plan to take 10 runs for each scenario for collecting enough data samples. The travel time, delay, average speed, vehicle fuel consumption, and intersection throughput are used to quantify the performance of the test scenarios.

We are still running the CAV tests. The test result analysis will be presented in the forthcoming reports.

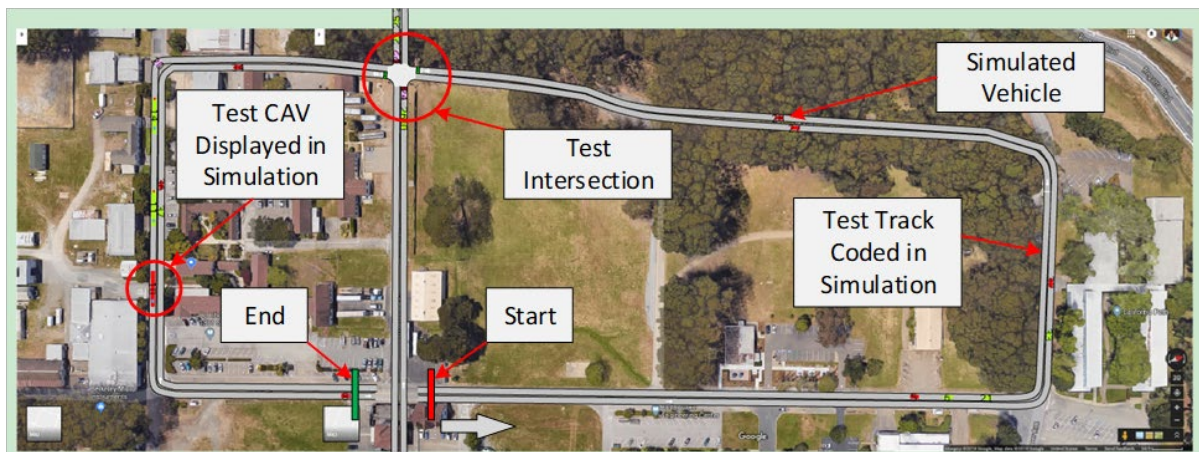


Figure I.2.6.5 Layout of the test track

Conclusions

We have developed a HIL testbed for evaluating the impacts of CAV on arterial traffic operations. The testbed contains SAE level 1 test CAVs that are equipped with CACC, a real-world intersection with advanced traffic signal controller and communication systems, and real-time microscopic traffic simulation that generate virtual traffic streams.

The testbed adopts a server program that allows researchers to execute functions of individual test systems without working on complicated system configurations and/or modifications. In addition, it will coordinate the operation of the test systems by establishing communication channels for real-time control message interchange. The tool will also offer a graphic user interface that depicts the real-time vehicle and traffic signal information during a test. The HIL testbed will help research teams carry out CAV system evaluation with the state-of-the-art test capabilities. It is particularly useful for the prototype CAV system examination because it greatly simplifies the CAV test process while maintaining a realistic test environment.

The project team is still working on the following tasks:

- Low speed control of CACC on three Volvo trucks for speed between 0-13 [mph]
- Localization of CACC truck to determine in real-time the distance to intersection

- System integration

Once those tasks have been accomplished, preliminary test will start. We will use the FY-2019 funding to accomplish all the proposed tasks.

Key Publications

1. Liu, Hao, Xiao-Yun Lu, and Steven E. Shladover. "Traffic signal control by leveraging Cooperative Adaptive Cruise Control (CACC) vehicle platooning capabilities." *Transportation Research Part C: Emerging Technologies* 104 (2019): 390-407.

References

1. Spring, J., Nelson, D., Lu, X. Y., 2018. CACC Truck Instrumentation and Software Development. PATH Research Report for FHWA Exploratory Advanced Research Program Cooperative Agreement DTFH61-13-H00012, Task 2.3 – Equip Trucks for Experiments.
2. Yang, S., Shladover, S., Lu, X. Y., Ramezani, H., Kailas, A., Altan, O., 2018. A First Investigation of Truck Drivers' Preferences and Behaviors Using a Prototype Cooperative Adaptive Cruise Control System. Accepted for Publication in *Transportation Research Record: Journal of the Transportation Research Board*, 2672(34): 39–48.
3. Lu, X. Y., Shladover, S. Truck CACC System Design and DSRC Messages, 2018. PATH Research Report for FHWA Exploratory Advanced Research Program Cooperative Agreement DTFH61-13-H00012, Task 2.1 – Design CACC Control System for the Trucks.
4. Nowakowski, C., Thompson, D., Shladover, S., Kailas, A., Lu, X. Y., 2016. Operational Concepts for Truck Cooperative Adaptive Cruise Control (CACC) Maneuvers. *Transportation Research Record: Journal of the Transportation Research Board*, 2559: 57–64.
5. Lu, X. Y., Shladover, S., Kailas, A., Altan, O., 2018. Messages for Cooperative Adaptive Cruise Control Using V2V Communication in Real Traffic (F., Wu, ed.), Taylor & Francis Group, CRC Press.
6. Yeo, H., Skabardonis, A., Halkias, J., Colyar, J., Alexiadis, V., 2008. Oversaturated freeway flow algorithm for use in next generation simulation. *Transport. Res. Record: J. Transport. Res. Board* 2088, 68–79.
7. Milanés, V., Shladover, S.E., 2014. Modeling cooperative and autonomous adaptive cruise control dynamic responses using experimental data. *Transport. Res. Part C: Emerg. Technol.* 48, 285–300.
8. Milanés, V., Shladover, S.E., 2015. Handling cut-in vehicles in strings of cooperative ACC vehicles. *J. Intell. Transport. Syst.* 1–14.
9. Milanés, V., Shladover, S.E., Spring, J., Nowakowski, C., Kawazoe, H., Nakamura, M., 2014. Cooperative adaptive cruise control in real traffic situations. *IEEE Trans. Intell. Transp. Syst.* 15 (1), 296–305.
10. Lu, X., Kan, X., Shladover, S.E., Wei, D., Ferlis, R.A., 2017. An enhanced microscopic traffic simulation model for application to connected automated vehicles. In: *Transportation Research Board 96th Annual Meeting*, Washington, DC.
11. Lu, X.Y., Lee, J., Chen, D., Bared, J., Dailey, D., Shladover, S.E., 2014, January. Freeway micro-simulation calibration: Case study using Aimsun and VISSIM with detailed field data. In: *93rd Annual Meeting of the Transportation Research Board*, Washington, DC.

12. Xiao, L., Wang, M., Schakel, W.J., Shladover, S.E., van Arem, B., 2017a. Modeling lane change behavior on a highway with a high occupancy vehicle lane with continuous access and egress. In: Transportation Research Board 96th Annual Meeting, Washington, DC.
13. Xiao, L., Wang, M., van Arem, B., 2017b. Realistic car-following models for microscopic simulation of adaptive and cooperative adaptive cruise control vehicles. In: Transportation Research Board 96th Annual Meeting, Washington, DC.
14. Liu, H., Kan, X.D., Shladover, S.E., Lu, X.Y. and Ferlis, R.E., 2018. Modeling impacts of Cooperative Adaptive Cruise Control on mixed traffic flow in multi-lane freeway facilities. *Transportation Research Part C: Emerging Technologies*, 95, pp.261-279.
15. Liu, Hao, Xiao-Yun Lu, and Steven E. Shladover. "Traffic signal control by leveraging Cooperative Adaptive Cruise Control (CACC) vehicle platooning capabilities." *Transportation Research Part C: Emerging Technologies* 104 (2019): 390-407.
16. TRB. "Highway Capacity Manual." Transportation Research Board, National Research Council, Washington, DC, USA, 2010.
17. Altan, Osman D., Guoyuan Wu, Matthew J. Barth, Kanok Boriboonsomsin, and John A. Stark. "GlidePath: Eco-friendly automated approach and departure at signalized intersections." *IEEE Transactions on Intelligent Vehicles* 2, no. 4 (2017): 266-277.

Acknowledgements

We acknowledge the contributions of University of California Berkeley (UCB) PATH staff Hao Liu and John Spring.

I.2.7 Experimental Evaluation of Cooperative ACC for Passenger Cars: Development of CACC Capability for Passenger Cars with Different Powertrains (LBNL, ANL) [Task 1.3.2]

Xiao-Yun Lu, Principal Investigator

Building 190
Lawrence Berkeley National Laboratory (LBNL)
1 Cyclotron Road, Berkeley, CA
E-mail: xiaoyunlu@lbl.gov

Erin Boyd, DOE Technology Manager

U.S. Department of Energy
E-mail: erin.boyd@ee.doe.gov

Start Date: October 1, 2018	End Date: September 30, 2019	
Funding for LBNL (FY19): \$400,000	DOE share: \$400,000	Non-DOE share: \$0

Project Introduction

Previous research and development on CACC (Cooperative Adaptive Cruise Control) at LBNL and PATH (also in the U.S. and internationally) were mainly concentrated on IC engine vehicles of the same type for transportation mobility purposes. *CACC for vehicles of different types and different powertrains have not been developed and implemented*, although the automatic control of vehicles with different power sources will be an important part of the energy savings for CACC. The work proposed here for DOE/VTO will develop the CACC string with at least three power types: IC engine (gasoline and/or diesel), hybrid electric, and fully electric, which offers many new possibilities. With this connected automated vehicle string platform, DOE/VTO can conduct extensive research, development and data collection for energy saving and emission reduction studies in the long run. The collected data in real-world traffic can be used for calibration of microscopic simulation models for more accurate meso- and macroscopic level energy consumption and emission change evaluation.

Objectives

This project will continue the work of FY18 on the development of CACC capabilities for 4 passenger cars with different powertrains. It will include: initial control tuning, and refinement at low speed; on-track testing of developed 4-vehicle CACC for fuel economy impacts of select CACC strategies at high speed; and resolving any implementation issues related to mixed vehicle performance envelopes and benefits (fast response) & challenges (SOC management and performance) due to electrification.

Approach

Proposed Scope of Work and Team Engagement

The following approaches are adopted in the development CACC capability on 4 passenger cars with different powertrain types including: IC engine, hybrid electric parallel, hybrid electric serial, and full electric. They are divided between LBNL and ANL teams.

The roles of LBNL team will include:

- Purchase and develop 4 Central Control Computer PC-104
- Install Real-time operating system QNX
- Develop lower level software including interfaces with commercially available remote sensors (such as radar, lidar and video camera, or their combination), DSRC units and CAN Bus

- Preliminarily implement CACC on the 4 vehicles in this phase
- Conduct initial test with ANL and INL on a test track; candidate test tracks include: (a) GoMomentum Station in California (<http://gomentumstation.net/>); (b) Navy Air Station in Alameda, in California; and (c) the previous Crows Landing NASA airport, now named Crows Landing Industrial Business Park (CLIBP), running by Stanislaus County. They are all in the proximity of Berkeley California.
- all the test sites are in the proximity of LBNL

Additional points:

- Each vehicle is to have a DSRC Unit (the cost will be added to the required budget)
- Accessible to CAN bus for data reading and control

1. The roles ANL team (Eric Rask's Group) will include:

- Purchase and provide 4 passenger cars with the above specified powertrains
- Provide interface protocol with CAN Bus for real-time data reading and control
- Provide interface protocol with (accelerator and brake, whichever applicable) pedal deflection for real-time lower level control activation
- Develop acceleration, accelerator/brake pedal mapping with Dynamometer at ANL
- Assist and coordinate with LBNL for CACC overall system development

Design of Control Structure

The overall control system structure is shown as in Figure I.2.7.1. The upper level control is to generate desired acceleration based on sensor measurement of the subject vehicle of the following information:

- Vehicle wheel speed information from CAN (Control Area Network) Bus
- Relative distance, speed and acceleration with respect to the immediate front vehicle based on remote sensor measurement
- Front vehicle information passed by vehicle onboard DSRC (Dedicated Short-Range Communication) unit. The information list has been described in detail in [CAV_DSRC].

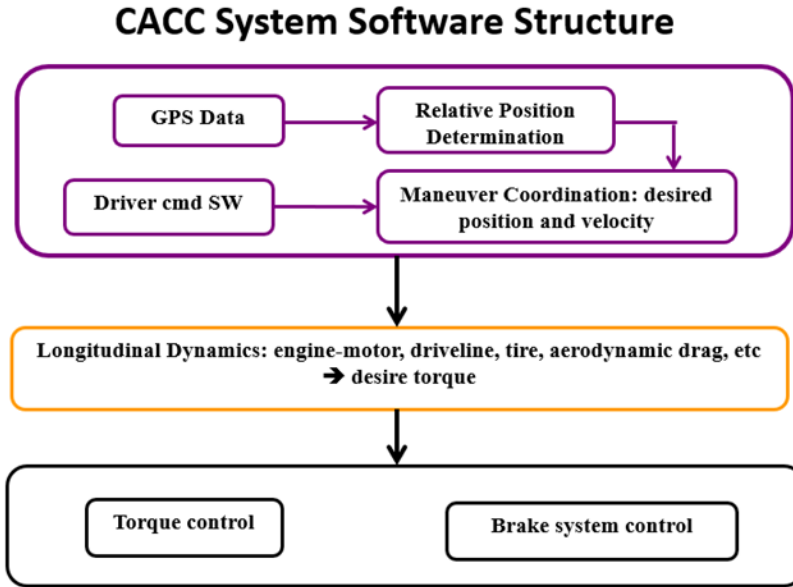


Figure I.2.7.1 Overall CACC System Structure for vehicles with all types of powertrains

CACC Upper Level Control Strategy

The model for upper level control is based on a simple linear second order kinematic model. The feedback control for upper level control is integrated in the following sense: CC, ACC and CACC share the same feedback control structure of (Eq. I-1). The feedforward parts for CC, ACC and CACC are designed according to the control objectives.

$$\begin{aligned}
 \ddot{\varepsilon}_i(t) + k_{i,1}\dot{\varepsilon}_i(t) + k_{i,2}\varepsilon_i(t) &= 0 \\
 \varepsilon_i(t) &= x_i(t) - x_{ref}(t) \\
 \dot{\varepsilon}_i(t) &= v_i(t) - v_{ref}(t) \\
 \ddot{\varepsilon}_i(t) &= a_{i,des}(t) - a_{ref}(t)
 \end{aligned} \tag{1}$$

$x(t)$ – distance w. r. t. an inertia coordinate system

$v(t)$ – speed w. r. t. the inertia coordinate system

$a(t)$ – acceleration w. r. t. the inertia coordinate system

$x_{pre}(t)$ – relative distance to the preceding vehicle

$v_{pre}(t)$ – preceding vehicle speed measure

$a_{pre}(t)$ – p receding vehicle acceleration measured

$(x_{ref}(t), v_{ref}(t), a_{ref}(t))$ – reference distance, speed and acceleration for control w. r. t. an inertia coordinate system

$(k_{i,1}, k_{i,2})$ – are coefficients to be determined in control design in the following characteristic polynomial (Eq. I-2).

The coefficients are chosen such that the following characteristic polynomials are Hurwitz for $i = 1, \dots, N$ where N is the number of vehicles in the platoon or string:

$$H(s) = s^2 + (k_{i,1} + (i-1)k_{i,2}T_g)s + k_{i,2} \quad (2)$$

Besides, the two eigenvalues are purposely chosen as real negative $(-\lambda_{i,1}, -\lambda_{i,2})$ such that

$$\begin{aligned} k_{i,2} &= \lambda_{i,1} \cdot \lambda_{i,2} \\ k_{i,1} &= -(\lambda_{i,1} + \lambda_{i,2}) \\ \lambda_{i,1} &> \lambda_{i,2} > 0 \end{aligned} \quad (3)$$

The main task for upper level control of CC, ACC and CACC is to design the feedforward part, i.e., the reference trajectories for the subject vehicle. With such control gain choice, the analysis in [ACC_CACC_2] (also see the Appendix) proved that: (a) the feedback control on each vehicle is robustly stable; and (b) the overall system is *ultimately bounded string stable*.

CACC System Development

ANL Team:

- Developed interface and lower level control of Hybrid vehicle Prius including acceleration and torque mapping for lower level control with Dynamometer
- Developed interface strategies for Honda Accord (Hybrid) and Ford Taurus (IC engine) for CAN accessing for data reading and for control actuation
- Developed mapping for acceleration pedal deflection, vehicle acceleration mapping for the whole speed profiles for all three vehicles: Toyota Prius, Honda Accord, and Ford Torus

LBNL Team:

- Preliminarily developed PC-104 control computer
- Longitudinal control design
- Preliminarily implemented longitudinal control
- Two control methods implementations
- Preliminary system integration
- Preliminary low test on test track at Berkeley

Joint activities of LBNL, ANL and INL (Matthew Shirk):

- Experimental test planning
- Coordination of system development
- Collaborative execution of testing.

Vehicle Mapping Development

For the purpose of developing CACC (Cooperative ACC) controllers for a mixed group of vehicles and powertrains, it is important to obtain a comprehensive map of the powertrain response to longitudinal acceleration commands. Not only does each vehicle have a different acceleration envelope, but the response to an acceleration command varies by vehicle and powertrain type as well. For the three vehicles used in this project, longitudinal acceleration commands, both positive and negative, were achieved through one of two ways: 1) direct pedal override through analog voltage injection, or 2) ACC (Adaptive Cruise Control) acceleration command override through a CAN (Control Area Network) bus in the middle. A more detailed explanation of these two approaches will be presented later, but they are mentioned here due to the important difference as it relates to the vehicle mapping requirements for these two methods.

The following Table I.2.7.1 shows the lower level control capabilities of the three vehicles which will be discussed in more details below:

Table I.2.7.1 Vehicle Lower Level Interface and Control Strategies

Vehicle Model	Powertrain Type	Acceleration control through ACC & CAN Bust	Acceleration control through accelerator pedal deflection	Deceleration control through ACC & CAN Bus	Deceleration control through brake pedal deflection	Comments
2017 Toyota Prius	Hybrid Parallel	Yes	Yes; through a direct analog voltage; for whole speed range; and acceleration the driver can achieve; the deceleration is limmited to $>-5.9[m/s^2]$	Yes	N.A.	acceleration control through pedal may have less delays
2014 Honda Accord PHEV	Hybrid Serial	N.A.	Yes; through a direct analog voltage; for whole speed and acceleration ranges the driver can achieve	N.A.	Yes; through CAN; for whole speed and deceleration range the driver can achieve	acceleration and deceleration controls through accelerator/brake pedals may have less delay
2013 Ford Taurus	IC Engine	Yes; for speed over 19 [mph]; max acceleration $< 2 [m/s^2]$	Yes; through a direct anaog voltage; for whole speed and acceleration ranges the driver can achieve	Yes ; for spped over 19 [mph] max deceleration $> -3.1 [m/s^2]$	N.A.	Acceleration control through pedal may have less delays

For the direct pedal override method, the powertrain response map for longitudinal acceleration consists of a surface plot of pedal position vs. vehicle acceleration vs. vehicle speed. This map is acquired from targeted dynamometer testing covering a wide range of vehicle speed and acceleration points and provides a lookup table for the required pedal position to achieve a desired acceleration from the vehicle. This method applies to either accelerator or brake pedal for positive or negative acceleration, respectively.

For the ACC acceleration command override, the powertrain response mapping consists of an entirely different plot. Since the ACC acceleration command is already in units of acceleration, the desired acceleration from the CACC controller can be directly requested from the vehicle. However, it is necessary to know the acceleration envelope of the vehicle with ACC acceleration control. More specifically, what is the minimum and maximum acceleration capability through ACC acceleration override at any given vehicle speed. This map is obtained through targeted dynamometer testing, aimed at covering the acceleration limits of the vehicle at a wide range of vehicle speeds, and may be less than or equal to the absolute acceleration limits of the vehicle with driver inputs to the pedals.

Finally, for both the direct pedal override and ACC acceleration command override, it is important to find the powertrain response to a desired acceleration request. The response characteristics of interest include the time to achieve a desired acceleration and the amount of overshoot and oscillation of the vehicle acceleration rate. In the case where acceleration override for one vehicle is achievable through both direct pedal override and ACC acceleration command override, the method with the more favorable powertrain response characteristics would be selected for the CACC control development. All the mapping data applicable to each of the vehicles selected for the CACC development is presented next.

Results

2017 Prius Prime

The 2017 Prius Prime selected for this project comes factory equipped with a full speed range capable ACC system. This gives the ability to control positive and negative acceleration of the vehicle through ACC acceleration command override for speeds between zero and maximum vehicle speed. Figure I.2.7.2 shows the acceleration envelope of the ACC acceleration override method compared to manual driving for the 2017 Prius Prime.

The maximum positive acceleration using the ACC override method is equal to the absolute positive acceleration limit of the vehicle. The maximum deceleration is limited to -5.9 m/s^2 , which is less than the maximum possible deceleration of the vehicle, but it is sufficient for CACC system development in this project.

The powertrain response using the ACC acceleration override method for positive and negative step changes in acceleration command is shown in. As shown in, the ACC acceleration override method has a significant time delay to achieve the desired acceleration as well as a large overshoot and prolonged oscillation. This response could be compared to the direct pedal override method for positive acceleration to determine which method would be more favorable for a CACC controller. Unfortunately, it is not possible to do a direct pedal override for the braking system on this vehicle, and the ACC deceleration override is the only method that could be used for brake control of this vehicle.

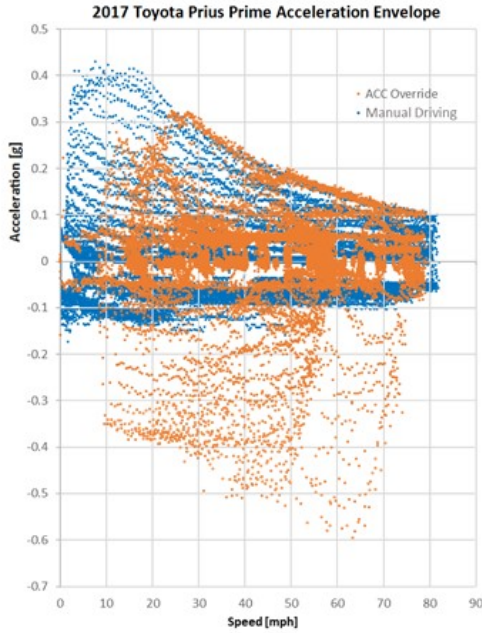


Figure I.2.7.2 ACC override acceleration envelope for 2017 Prius Prime

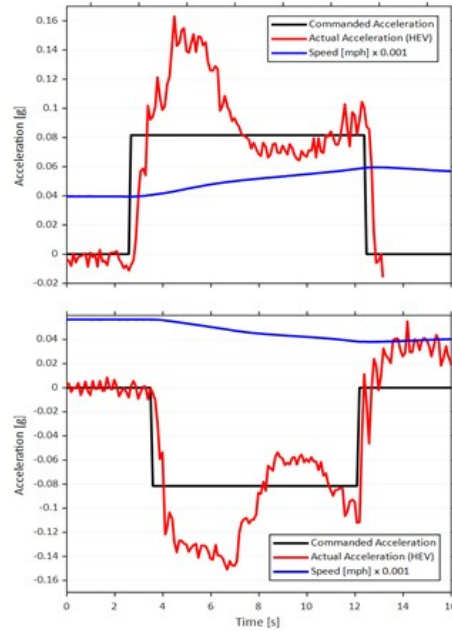


Figure I.2.7.3 Powertrain response to ACC acceleration override for 2017 Prius Prime

Since it is possible to use a direct pedal override for the accelerator pedal of the 2017 Prius Prime, dynamometer testing covering a wide range of vehicle speeds and acceleration rates was performed to create a map of accelerator pedal position as a function of acceleration and vehicle speed. Figure I.2.7.4 shows a 3D plot of the accelerator pedal map for the 2017 Prius Prime.

It should be noted that in addition to positive acceleration of the vehicle, some negative acceleration can also be controlled using the accelerator pedal override. At high vehicle speeds, the road-load of the vehicle is so high that a low accelerator pedal command results in vehicle deceleration. This is the braking effect of the power regeneration of the alternator.

Finally, the powertrain response to an acceleration request through a direct pedal override is shown in Figure I.2.7.5.

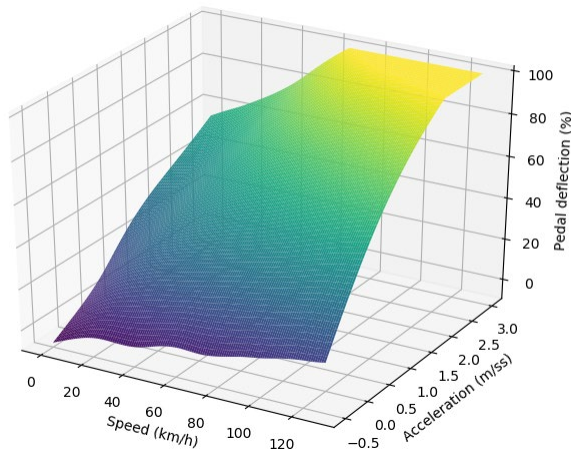


Figure I.2.7.4 Accelerator pedal map for 2017 Toyota Prius Prime

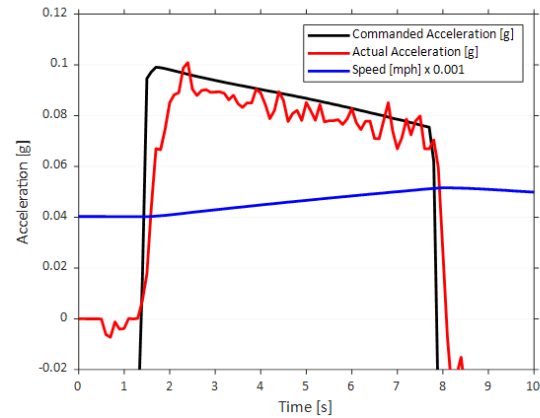


Figure I.2.7.5 Powertrain response to accelerator pedal override on 2017 Toyota Prius Prime

The direct pedal override response plot is slightly different from the ACC acceleration override plot because instead of step change in acceleration command, it is showing the powertrain response to a step change in pedal command. Since the direct pedal override method does not directly request a desired acceleration from the vehicle, the actual vehicle acceleration is compared to an estimate of the commanded vehicle acceleration based on the accelerator pedal map in Figure I.2.7.4. Based on the comparison of actual and estimated vehicle acceleration, the direct pedal override method appears to have a lower powertrain response time and almost no overshoot or oscillation as compared to the ACC acceleration override. Therefore, a direct pedal override is better suited for positive acceleration CACC control of the 2017 Prius Prime, but the ACC acceleration override is the only possible method for negative acceleration control instead of going through the brake pedal.

2013 Ford Taurus

The 2013 Ford Taurus selected for this project comes with a factory equipped ACC system for speed above 19 mph. This gives the ability to control positive and negative acceleration of the vehicle through ACC acceleration command override for speeds above 19 mph only. Figure I.2.7.6 shows the acceleration envelope of the ACC acceleration override method for the 2013 Ford Taurus.

The maximum positive acceleration of this method is 2 m/s^2 , which is less than the absolute positive acceleration limit of the vehicle. The maximum deceleration is limit -3.1 m/s^2 , which is also less than the maximum deceleration of the vehicle but is deemed sufficient for this project.

The powertrain response using the ACC acceleration override method is shown in Figure I.2.7.7 for positive and negative step changes in acceleration command.

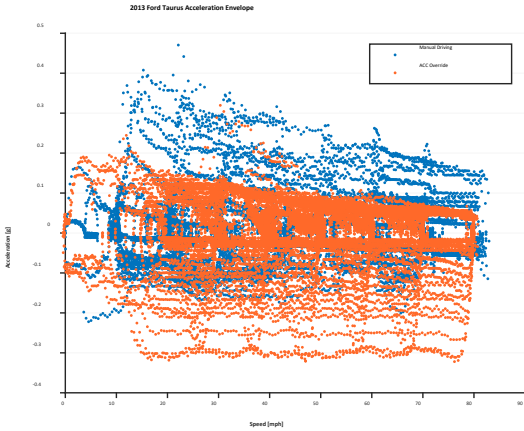


Figure I.2.7.6 ACC override acceleration envelope for 2013 Ford Taurus

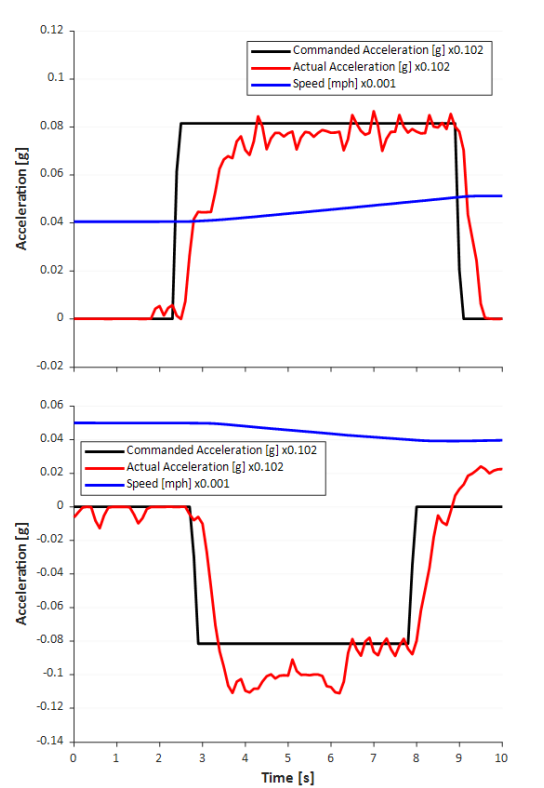


Figure I.2.7.7 Powertrain response to ACC acceleration override for 2013 Ford Taurus

The ACC acceleration override method for the 2013 Ford Taurus has a significant time delay to achieve the desired acceleration for both positive and negative acceleration commands. While there is no overshoot for positive acceleration commands, there is a significant overshoot for deceleration commands. Since a direct accelerator pedal override method is possible, the positive acceleration powertrain response could be compared to the direct pedal override method for the accelerator pedal. In addition to a possible difference in powertrain response, the direct pedal override would provide full vehicle acceleration capability. Unfortunately, as is the case with the Toyota Prius, it is not possible to do a direct pedal override for the braking system on the Ford Taurus.

As with the Toyota Prius, dynamometer tests covering a wide range of vehicle speeds and acceleration rates were performed to create a map of accelerator pedal position as a function of acceleration and vehicle speed for the 2013 Ford Taurus. Figure I.2.7.8 shows the accelerator pedal map for the 2013 Ford Taurus.

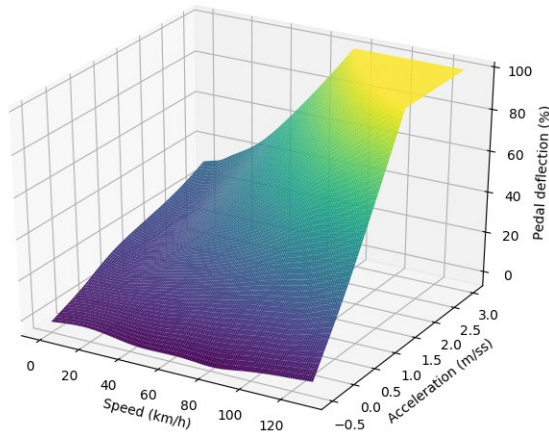


Figure I.2.7.8 Accelerator pedal map for 2013 Ford Taurus

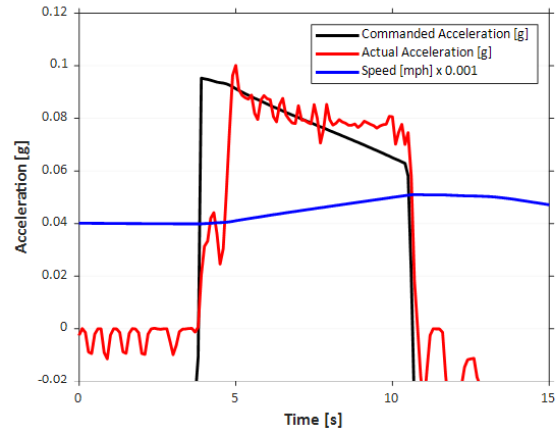


Figure I.2.7.9 Powertrain response to accelerator pedal override on 2013 Ford Taurus

Unlike that ACC acceleration override, the direct pedal override of the accelerator pedal can provide the absolute maximum acceleration at any vehicle speed.

Finally, the powertrain response of the direct accelerator pedal override for the 2013 Ford Taurus is shown in Figure I.2.7.9.

The direct pedal override response plot shows the powertrain response to a step change in accelerator pedal command. The actual vehicle acceleration is compared to an estimate of the commanded vehicle acceleration based on the accelerator pedal map in Figure I.2.7.8. Based on the comparison of actual and estimated vehicle acceleration, the direct pedal override method appears to have a lower powertrain response time as compared to the ACC acceleration override. Taking into consideration the limited positive acceleration of the ACC acceleration override method, the direct pedal override appears to be better suited for positive acceleration CACC control of the 2013 Ford Taurus. Unfortunately, a pedal override method is not possible for the braking system on the Ford Taurus and the ACC acceleration override is the only possible method for negative acceleration control.

2014 Honda Accord PHEV

The 2014 Honda Accord PHEV selected for this project comes factory equipped with an ACC system operable above 19 mph. However, unlike the Toyota Prius and Ford Taurus, the ACC system on the Honda Accord does not have an ACC acceleration command which can be overridden. Instead, the ACC system on the Honda Accord uses direct pedal overrides to control both positive and negative acceleration of the vehicle. As a result, the only method of acceleration control on the Honda Accord is through direct accelerator and brake pedal overrides. The accelerator pedal override is done through a direct analog voltage injection similar to that of the Toyota Prius and Ford Taurus, while the brake pedal override is done through a CAN bus man in the middle. This gives the ability to control positive and negative acceleration through the full vehicle speed range.

Targeted dynamometer tests covering a wide range of vehicle speeds and acceleration rates were performed to create a map of accelerator pedal position as a function of acceleration and vehicle speed for the 2014 Honda Accord. Figure I.2.7.10 shows the accelerator pedal map for the 2014 Honda Accord.

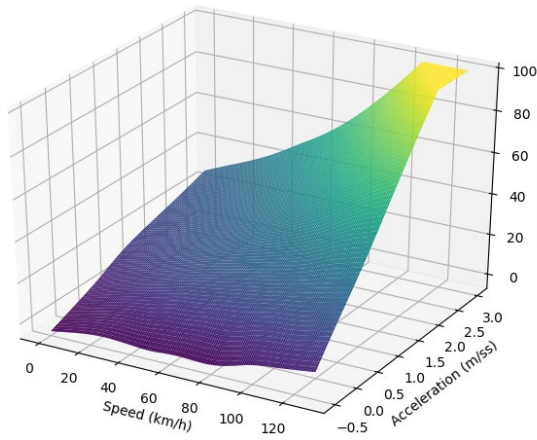


Figure I.2.7.10 Accelerator pedal map for 2014 Honda Accord

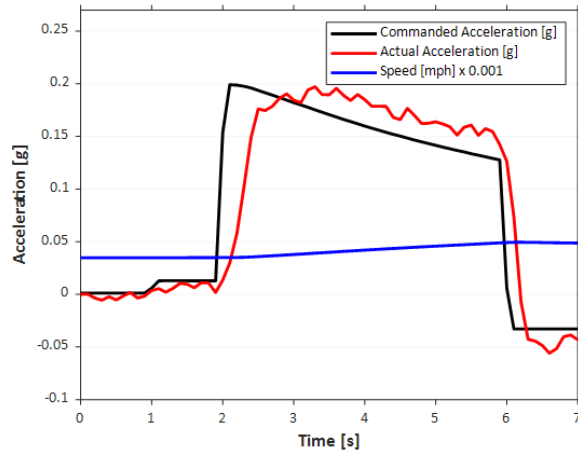


Figure I.2.7.11 Powertrain response to accelerator pedal override on 2014 Honda Accord

The direct pedal override of the accelerator pedal can provide absolute maximum vehicle acceleration at any vehicle speed. The powertrain response to the direct accelerator pedal override for the 2014 Honda Accord is shown in Figure I.2.7.11.

The actual vehicle acceleration for a step change in accelerator pedal command is compared to the estimated vehicle acceleration based on the accelerator pedal map in Figure I.2.7.10. The direct accelerator pedal override has a relatively low powertrain response time with some overshoot.

Unlike the Toyota Prius and Ford Taurus, a pedal override method for the braking system was possible on the Honda Accord. The brake pedal override was achieved through a man in the middle override of the CAN bus similar to the acceleration command override on the Toyota Prius and Ford Taurus. This enabled a brake pedal map similar to the accelerator pedal map to be created. Figure I.2.7.12 shows the brake pedal map for the 2014 Honda Accord.

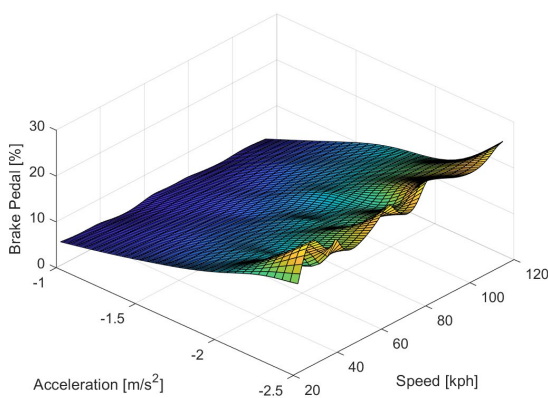


Figure I.2.7.12 Brake pedal map for 2014 Honda Accord

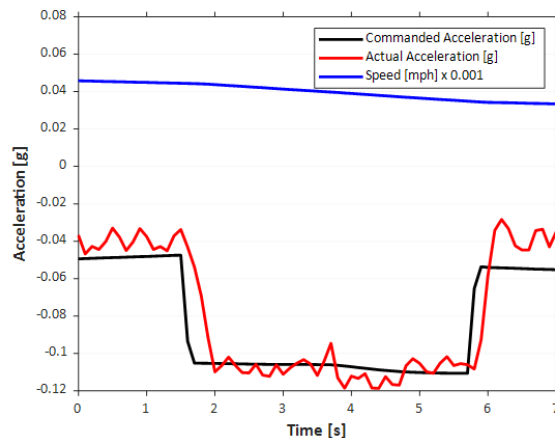


Figure I.2.7.13 Brake system response to brake pedal override on 2014 Honda Accord

The brake pedal override on the Honda Accord can provide a higher deceleration rate than both the Toyota Prius and Ford Taurus ACC acceleration override methods for braking, up to the absolute maximum vehicle deceleration.

Finally, the brake system response to the brake pedal override for the 2014 Honda Accord is shown in Figure I.2.7.13.

The estimated vehicle deceleration for a step change in brake pedal command is compared to the estimated vehicle deceleration based on the brake pedal map in Figure I.2.7.12. The brake system response with brake pedal override on the 2014 Honda Accords shows very fast response with no overshoot or oscillations.

ACC Acceleration Command Override

The ACC acceleration command override is accomplished through a CAN bus man in the middle (MiM) implemented between a vehicle's ACC electronic control unit (ECU), responsible for the stock ACC control, and the Central Gateway Module (CGM), which distributes the appropriate CAN messages to the rest of the vehicle dynamic controllers. The CAN message that contains the acceleration/deceleration command from the ACC ECU is intercepted by the MiM and overridden with the desired output from a custom longitudinal controller, as shown in Figure I.2.7.14

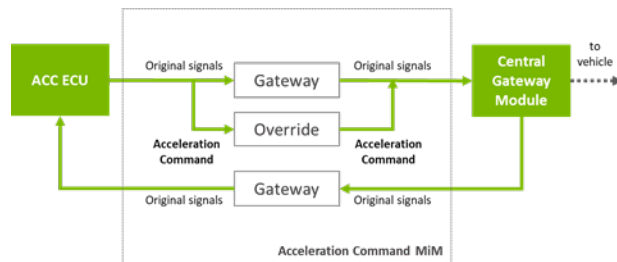


Figure I.2.7.14 ACC acceleration command override MiM diagram

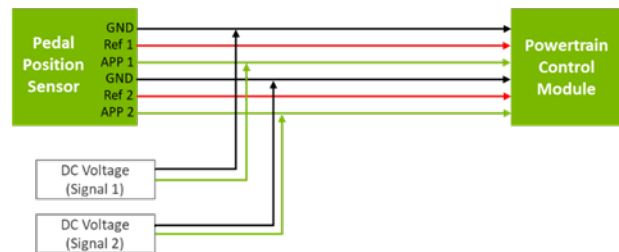


Figure I.2.7.15 Pedal override DC voltage injection diagram

The MiM approach shown in Figure I.2.7.14 applies to the ACC acceleration command override of both the 2017 Prius Prime and 2013 Ford Taurus. It is also very similar to the brake pedal override of the 2014 Honda Accord, with the only difference being that instead of an override of an acceleration command message, the MiM overrides a brake pedal command message.

Direct Pedal Override

The direct pedal override of the accelerator pedal on all three vehicles is accomplished with an analog voltage injection on the accelerator pedal position sensor. The accelerator pedal position sensor consists of either a pair of potentiometer or Hall Effect sensors connected directly to the vehicle's powertrain control module (PCM). A pair of DC analog voltages corresponding to a desired pedal position are injected directly onto the two signal wires going to the vehicle's PCM as shown in Figure I.2.7.15.

The DC voltage to pedal position follows a linear relationship for all three cars with a slightly different offset and slope value for each one. The accelerator pedal position signal (APP1 and APP2) are also related according to: $APP1 = 2 * (APP2)$.

Preliminary Test Results for Toyota Prius

The following plots shows the preliminary test results of the feedback control for speed tracking in two approaches:

- Speed tracking using the torque mapping developed from the dynamometer test
- Speed tracking directly using the ACC command from the upper level control

By comparing those two approaches, it can be observed that both approaches have obvious overshoot at the changes from acceleration to constant speed. This may be due to the induced delay of the ACC control actuation. Therefore, the project team is seeking another control approach by using acceleration pedal deflection for control actuation instead of using the internal ACC actuation.

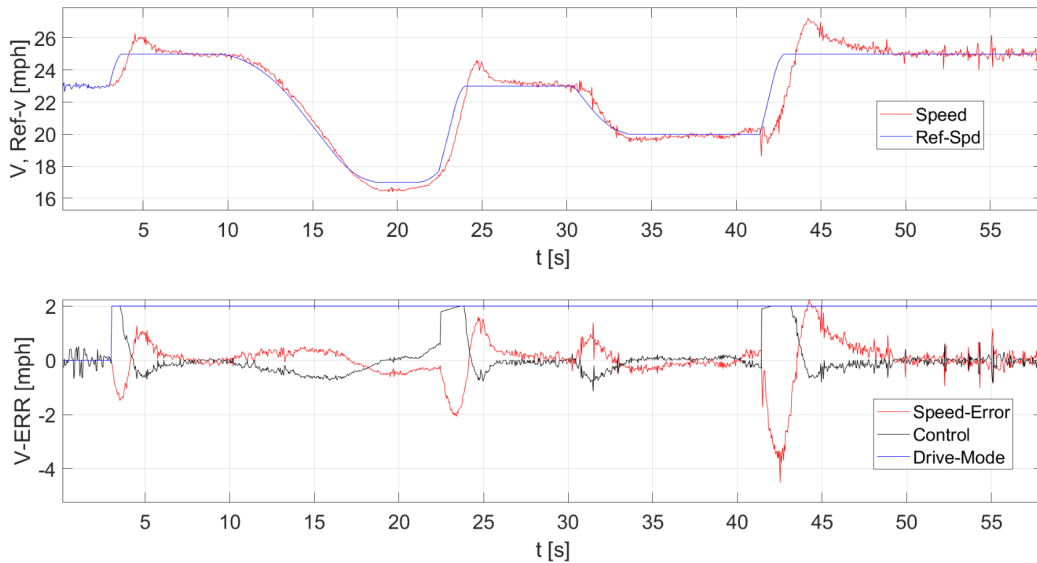


Figure I.2.7.16 Speed tracking using the torque mapping developed from the dynamometer test: upper – reference speed (blue) and measured speed (red); lower: speed tracking error, acceleration control command, and drive mode (0-manual; 2-automatic control)

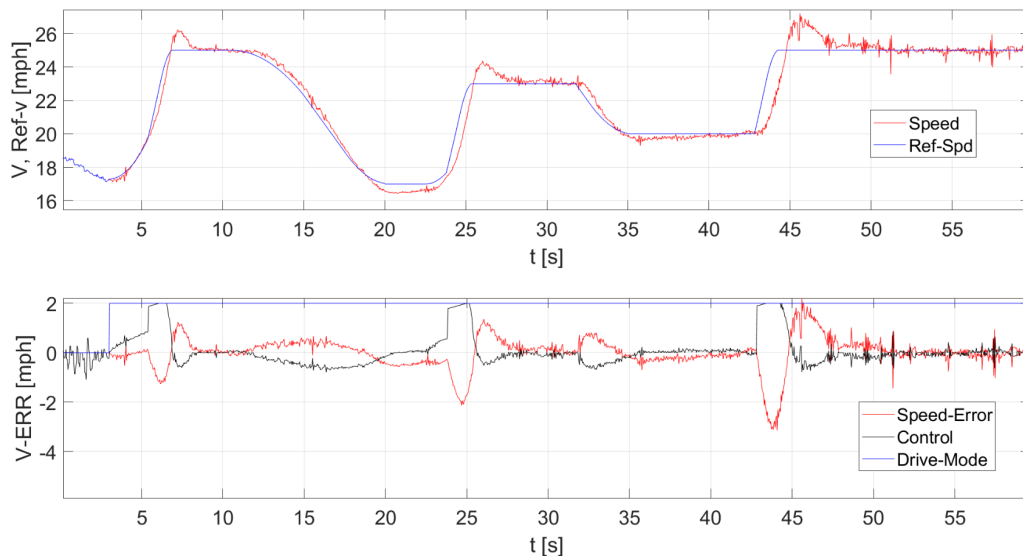


Figure I.2.7.17 Speed tracking directly using the ACC command from the upper level control: upper – reference speed (blue) and measured speed (red); lower: speed tracking error, acceleration control command, and drive mode (0-manual; 2-automatic control)

Conclusions

The project team has accomplished the following during FY19:

ANL:

- Developed lower level physical control interface actuations for 3 vehicles: Toyota Prius, Honda Accord and Ford Torus
- Developed look-up table (speed, acceleration and pedal deflection) for control actuation of all three vehicles
- Developed brake pedal deflection look-up table for Honda Accord
- Shipped all the vehicles to Berkeley around September 20th, 2019

LBNL:

- Built up PC-104 computer and installed real-time operating systems
- Purchased and developed DSRC and developing communication packet for V2V communications
- Developed a generic Cooperative Adaptive Cruise Control (CACC) strategy for all three vehicles
- Preliminarily implemented the CACC control on Toyota Prius and tested

Tasks to be Accomplished by ANL Team

- To purchase and develop the interface capability of the 4th vehicle (EV)
- To develop torque mapping for vehicle acceleration control
- To develop torque mapping for deceleration control
- To work with LBNL for PC-104 computer interface from QNX
- To accomplish the vehicle transfer to LBNL for insurance etc. the project

Tasks to be Accomplished by LBNL Team

- To accomplish the vehicle transfer to LBNL for the project from ANL for insurance etc.
- Install PC-104 control computers on vehicles
- Install DSRC and developing communication packet
- Developing 2nd and 3rd car by building interface of PC-104 with the 2nd and 3rd cars (Accord and Taurus) with the help from ANL
- Low speed of 3-car CACC
- Preliminary field tests and control tuning
- High speed test and control tuning for performance improvement of CACC.

The project team will use FY19 funding to accomplish the proposed work.

References

1. [ACC_CACC_1] X. Y. Lu, J. K. Hedrick and M. Drew, 2002, ACC/CACC - Control design, stability and robust performance, Proc. of American Control Conference - 2002, p4327-4332, May 8-10, Anchorage, Alaska
2. [ACC_CACC_2] X. Y. Lu, S.E. Shladover, 2017, Integrated ACC and CACC Development for Heavy-Duty Truck Partial Automation, American Control Conference, (ACC-17), May 24-26, Seattle, WA, USA
3. [CAV_DSRC] X. Y. Lu, Shladover, A. Kailas, and S. Shladover, O. Altan, Messages for Cooperative Adaptive Cruise Control Using V2V Communication in Real Traffic, Fei Wu Eds, Taylor & Francis Group, CRC Press, 20

Acknowledgements

We acknowledge the contributions of Eric Rask (ANL), Simeon M. Iliev (ANL), John Spring (UCB PATH), and David Nelson (UCB PATH) to this project.

I.2.8 Experimental Evaluation of Eco-Driving Strategies (LBNL)

Wei-Bin Zhang, Principal Investigator

Lawrence Berkeley National Lab
1 Cyclotron Road
Berkeley, CA 94720
E-mail: wbzhang@berkeley.edu

Erin Boyd, DOE Technology Manager

U.S. Department of Energy
E-mail: erin.boyd@ee.doe.gov

Start Date: October 1, 2018

End Date: September 30, 2019

Project Funding (FY19): \$300,000

DOE share: \$300,000

Non-DOE share: \$0

Project Introduction

The goal of this project is to analytically and experimentally evaluate the energy saving benefits (to both the subject vehicle and vehicles following behind) and impacts on efficiency and safety of surrounding traffic. We investigated a broad set of Eco-driving strategies in order to fully understand the potential energy-related benefits and impacts of each. Furthermore, we analytically and experimentally quantified the benefits and impacts of intersection Eco-Approach and Departure (EAD) assistant strategies.

Objectives

- Analysis of Eco-Driving strategies for a wide range of driving scenarios and applications to quantify the strategies with the largest energy savings.
- Collection of comprehensive vehicle trajectory level traffic data at the CA arterial test corridor to establish a baseline energy model for individual vehicles and the overall traffic for various traffic conditions.
- Use an instrumented vehicle (with Eco-approach and departure advisory and traffic detection capabilities) in the field to quantify realistic energy saving benefits of the subject vehicle and impacts on safety and efficiency to surrounding traffic (e.g., measures: accel, decel, headways, and Time to Collision).

Approach

Task 1. Assessment of Eco-Driving Strategies

Analysis of Eco-Driving strategies for a wide range of driving scenarios and applications will be evaluated to establish a foundational understanding of associated energy implications and assess where the biggest gains can be made.

Task 2. Field data collection at an urban arterial corridor

Portable video data collection devices are used to collect 360-degree video data at 10 signalized intersections and a number unsignalized intersections. Comprehensive vehicle trajectory level traffic data are abstracted from the video data collected to establish a baseline energy model for individual vehicles and the overall traffic for various traffic conditions.

Task 3. Data analyses

Data processing tools are developed for detection and tracking vehicles movements. Models are developed to process data to enable assessments of the fuel consumptions and emissions for vehicles traveling in traffic

under real-world conditions. Data analyses will be conducted to establish a baseline energy model for individual vehicles and the overall traffic for various traffic conditions (free flow to heavy congestions).

Task 4. Field testing involving ECO approach and departure

The ECO Approach and Departure will be experimentally evaluated using a commercially available EAD app Enlighten developed by Connected Signals. An instrumented vehicle (with Eco-approach and departure advisory and traffic detection capabilities) and a number of conventional vehicles are used in the field to quantify realistic energy saving benefits of the subject vehicle and impacts on safety and efficiency to surrounding traffic (e.g., measures: accel, decel, headways, and TTC).

Results

1. Assessment of Eco-Driving Strategies

1.1 Estimation of unproductive fuel consumption

The Urban Mobility Report (UMR) provides a widely accepted accounting of the magnitude of problems the nation faces on wasted fuel and excessive emission due to congestions [1]. However, the estimated 3.1 billion gallons of the wasted fuel reported in the UMS study did not consider the fuel-wasting driving practices or behaviors and inefficient traffic controls that are not congestion related. These missing elements in the UMR analyses are among the issues to be addressed for an in-depth understanding on where and how much the wasted fuel problem can be tackled by Eco-Driving strategies.

Our study identified five major scenarios where fuel is consumed unproductively. The unproductive fuel/energy consumption is defined as fuel/energy consumed, in addition to the baseline fuel consumption, due to driving at speeds lower or higher than the prescribed speed limit, with unnecessary decelerations, accelerations, and stops. Over ~10 billion gallons of unproductive fuel consumption, in addition to the 3.1 billion gallons of wasted fuel reported in the UMR, have been identified for 1) driving at speeds higher than 55 mph, 2) unnecessary stops at unsignalized intersections, and 3) idling [2]. We also identified additional wasted fuel that are unaccounted in the UMR due to stop-and-go driving in congested traffic on highways and during stops in front of traffic signals. Table I.2.8.1 provides a summary of the findings on unproductive fuel consumptions.

Table I.2.8.1 Unproductive Fuel Consumption by Scenarios

Gaps in Wasted Fuel Estimation in UMR	Estimated unproductive fuel consumptions (gallons)
Speed higher than 65 mph	1 to 3 billion
Unnecessary stops at stop signs	2 - 3 billion
Idling	6 billion
Approximate stop and go with lower average speed	10% of fuel wasted for stop and go traffic
Approximate intersection traffic with average speed	Up to 50% of fuel wasted at congested signalized intersections

1.2 Identify Fuel Saving Opportunities Through Eco Driving technologies

Studies were conducted to identified opportunities for saving energy from the perspective of energy dissipation for various types of vehicles. Eco-Driving control strategies focus on reducing ‘power to the wheel’ dissipated energy. Because substantial energy is consumed for tasks that do not physically move the vehicle (such as heat dissipation), the upper limit of the Eco-Driving addressable fraction of total vehicle energy consumption is approximately 30% for combustion engines, 40% for hybrid vehicles and 65% for electric vehicles.

The general Eco-Driving strategies include: (a) avoid harsh deceleration/acceleration, (b) drive at appropriate speeds, (c) reduce air drag, (d) minimize idling, and (e) select less congested routes. Research and development to-date have explored Eco-Driving technologies for all these areas. We have conducted an extensive review of the state-of-the-art technologies. A large set of work has been found in four application categories: Eco-Approach and Departure, platooning at intersections or on freeways, and Eco-Route. Results from simulation and field testing vary significantly, often with unrealistic high fuel saving benefits. It is difficult to make apple-to-apple comparisons among these studies, as we found substantial differences in the assumptions, baselines used, uncertainties involved for before-and-after comparison and the limited test runs involved in these studies. Furthermore, almost all studies under review only focus on fuel savings for subject vehicles, with little or no consideration of impacts to the surrounding vehicles and the overall traffic system. Various deployment issues are not adequately addressed in these studies. Therefore, there are urgent needs to thoroughly understand the realistic fuel benefits vs. costs of various Eco-Driving technologies and applications and the deployment issues of these technologies. To do so, effective Measure of Effectiveness (MOE) must be developed and scientifically sound field evaluation need to be conducted. In addition to fuel saving benefits, the implications on safety and efficiency at the system level for large scale deployment the deployment of Eco Driving technologies need to be assessed.

2. Data Needs and Data Collection for Supporting Objectively Evaluation of Unproductive Fuel Consumption

2.1 Comprehensive Data Collection at Signalized Intersections

Our study has identified that the average nature of the data used in the UMR may have large estimation errors. The UMR study uses average speeds at 15 minutes intervals to calculate the fuel consumption at signal controlled arterial corridors. However, in the real world, the cumulative fuel consumption at intersections are affected by the capacity of the intersections, the traffic volume, the traffic control strategies, and the driving behaviors of individual vehicles drivers. In order to estimate the fuel consumption at signalized intersection, video data were collected at ten intersections along San Clara St. between San Pedros St. and 5th St. in San Jose, California, as shown in Figure I.2.8.1 A cumulative 160 hours of videos were taken, with 16TB data saved.



Figure I.2.8.1 Vehicle detections at Santa Clara St./4th St. in San Jose, California

2.2 Comprehensive Data collection at Unsignalized Intersections

Stop signs have been a most common safety treatment for over six million intersections in the United States. At intersection controlled by stop signs, all the arriving vehicles are required to make a full stop, even when there are no conflicting vehicles at other approaches. While facilitating safety management at unsignalized intersections, stop signs also introduce travel delays, unproductive fuel consumption and resulting emissions and, in some cases, increased safety hazard levels. To evaluate the level of unproductive fuel consumptions at unsignalized intersections in comparison with the intersections have different traffic control treatment (i.e., roundabout and signal controlled), we collected comprehensive traffic data at five intersections in two California cities and additional sampled data at a few intersections in two other California cities. The data collection sites include stop signed controlled intersections, roundabout and signalized controlled intersections.

Cameras with 360° field of views were installed at intersections to capture panoramas of the intersections. The video data are processed using image processing techniques to abstract vehicle trajectories. In total, ~90 hours of video data were recorded at four unsignalized intersections with a data size of over 5TB. Figure I.2.8.2 illustrates the top view of the intersection where video data were collected in Pleasant Hill, California. The red lines mark the stop line. The green points mark the driving vehicles, the red points are stopping vehicles, and yellow points are conflicting vehicles.

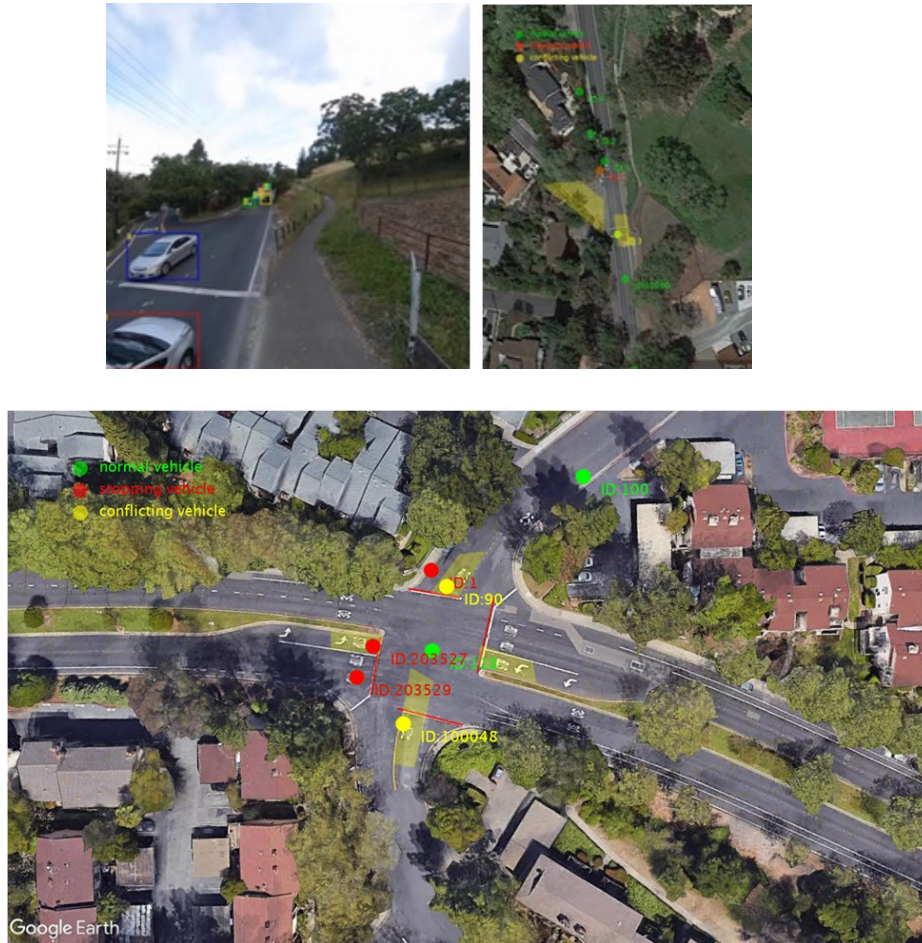


Figure I.2.8.2 Vehicle detections at a stop sign controlled intersection in Pleasant Hill, California

2.3 Video Processing to Derive Vehicle Trajectory and Fuel Consumption Data

The 360° video data provides a panorama of the intersections. Image processing algorithms aided by deep learning are used to detect vehicles within each of the image frames, then to track their movements and to project the vehicles on the Google map as shown in Figure I.2.8.1 and Figure I.2.8.2. The fuel consumption calculation is based on the VT- Micro Model [3]. For the baseline, we calculated the fuel consumption of the vehicles that keeps a steady speed passing the intersection.

3. Estimation of Unproductive fuel consumptions at signalized and stop sign Controlled Intersections Through Field Data

3.1 Unproductive Fuel Consumption at Signalized Intersections

Real-world vehicle trajectory data derived from the video data is used to estimate the total fuel consumptions at intersections as well as unproductive the fuel consumption. The unproductive fuel consumption for signalized

intersection is defined as the portion of fuel consumption for vehicles being stopped by traffic control when no vehicles nor pedestrian activities present at the conflicting approaches. At the time when this report is written, a thorough case analysis on the traffic behaviors and unproductive fuel consumption was conducted for the southbound traffic at the intersection located on Santa Clara St. and 4th St. Table 2 summarizes the data from the analysis. The vehicles arriving per hour and the estimated fuel consumption are given. For the stopping vehicles, we analyzed two scenarios, i.e., with and without arriving vehicles at the conflicting approach. Fuel consumption is evaluated within an 80-meter range centered at the test intersection. The following key findings are made through data analysis:

- The field data from the test intersection showed that for vehicles stopping at the intersection, over 80% of the time they do not encounter other vehicles at the conflicting approach. The unproductive fuel consumed by unnecessary stops is over 15% of total intersection fuel consumption.
- This analysis suggests that more intelligent signal operation supported by Connected Vehicle technologies could lead to additional fuel consumption benefits due reducing unnecessary stops.

Table I.2.8.2 Vehicle Stopping and Fuel Consumption at Signalized Intersection

Event		Average fuel consumption per arrival (gram)						Average fuel consumption		Unproductive Fuel Consumption per hour (gram/gallon)
		07:30-08:30	08:30-09:30	09:30-10:30	10:30-11:30	11:30-12:30	12:30-13:30	Per arrival (gram)	hourly average (gallon)	
Arrival at Red Phase	Conflicting vehicles present	25 (7.0%)	33 (7.2%)	61 (12.8%)	75 (14.5%)	103 (14.5%)	51 (19.2%)	28.7	0.51	0/0
	No conflicting vehicles present	172 (48.5%)	220 (48.0%)	150 (31.5%)	177 (34.2%)	224 (41.8%)	72 (24.7%)	25.1	1.31	2828/0.87
Arrival at Green Phase (passing through)		157 (44.4%)	205 (44.7%)	265 (55.6%)	265 (47.8%)	208 (38.9%)	168 (57.7%)	16.6	1.08	0/0
Total number of arrivals		354	458	476	517	535	291		2.9	2828/0.87

3.2 Unproductive Fuel Consumptions at Stop Sign Controlled Intersections

Analysis is conducted to assess the driving behaviors and unproductive fuel consumption at unsignalized intersections using data derived from the collected videos. The unproductive fuel consumption for unsignalized intersection is defined as the portion of fuel consumption by vehicles making deceleration and stops at the intersections when no vehicles nor pedestrian activities present at the conflicting approaches. Figure I.2.8.3 shows the vehicle speeds as a function of distance to the stop line. We classify the vehicle behaviors into complete stop (speed <1mph, blue), rolling stops (1 mph <speed<5mph, green) and running stop signs (speed>5mph, red). From Figure I.2.8.3, one can see that although all vehicles decreased their speeds when approaching the stop line (dashed line), only a portion of the vehicles made complete stops (blue lines) as required by the traffic laws. A significant portion of the vehicles did not come to full stop. Table I.2.8.3 summarizes 4 hours of data collected at a stop sign controlled intersection in Pleasant Hill, California. Analyses were conducted to classify the vehicle behaviors into complete stop, rolling stops and running stop signs. The following key findings are made through the data analysis:

- Large percentages of vehicles do not stop at stop sign controlled intersections: The data at this case study intersection shows that, although most of the vehicles decelerate while approaching the stop line, as high as 70% of the arriving vehicles fail to make a full stop.
- Of the 30% of vehicles that made a full stop for this case study, close to about 17% of the vehicles made full stops when there were vehicles at the conflicting approaches, whereas, roughly 13% of vehicles made full stops when no vehicles appeared at other approaches. The study suggests that most of the full stops made at stop lines at this test intersection are likely caused by the presence of conflicting vehicles rather than by the stop signs. Further analysis shows that the rate of rolling stops and stop sign running has an inverse relationship with the rate of conflicting vehicles. Specific to this intersection, vehicles arriving from the east and west approaches had higher rolling stop and stop sign running rate, where the rate of conflicting vehicles from South and North approaches are lower.
- The study concluded that the all-way stop signs at this intersection are ineffective and potentially induce safety hazards. The disobedience of stop signs can have negative consequences - when some drivers expect that other drivers follow the rules, stop sign running creates safety hazards that potentially result in crashes.
- The study further concluded that stops and slow-down-then-speed up movements without the presence of conflicting vehicle cause significant unproductive fuel consumption. For the case example in Table 3, 30% fuel can be saved if vehicles are allowed to pass the intersection at a steady speed at 35km/h when no vehicles appear at conflicting approaches. The unnecessary stops and slow-down-then-speed up movements account for 30% of the total fuel consumption at the intersection.

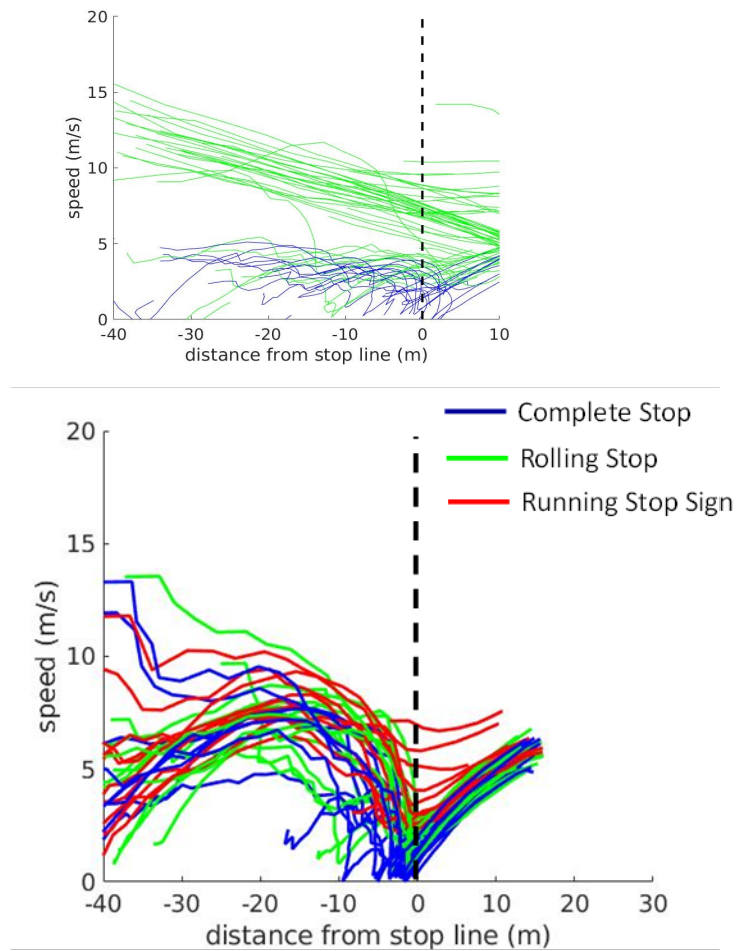


Figure I.2.8.3 Vehicle detection from image and projection on map, and speed profile of the vehicles

Table I.2.8.3 Vehicle Stopping and Fuel Consumption at Unsignalized Intersection

	Event	# of arrivals/hour					Average fuel consumption per arrival (Grams)	Average hourly fuel consumption (gallon)	Unproductive Fuel Consumption (gallon)
		East	West	South	North	Total			
Full stop	w/conflicting vehicles	68 (22.9 %)	49 (14.16%)	14 (15.0 %)	20 (16.1 %)	151 (17.56%)	20.4	0.96	0
	w/o conflicting vehicles	20 (8.8%)	29 (10.8%)	15 (16.1 %)	15 (12.1 %)	79 (9.1)	17.6	0.43	0.24
Rolling vehicles	w/conflicting vehicles	34 (11.4 %)	31 (8.9 %)	5 (5.3 %)	16 (12.9 %)	86 (10.0 %)	15.9	0.42	0
	w/o conflicting vehicles	97 (34.1%)	132 (38.1 %)	33 (35.4 %)	33 (26.6 %)	295 (34.3 %)	14.6	1.34	0.64
Running vehicles	w/conflicting vehicles	11 (3.7 %)	22 (6.3 %)	3 (3.2 %)	5 (4.0 %)	41 (4.7 %)	13.4	0.17	0
	w/o conflicting vehicles	67 (22.56%)	83 (23.99%)	23 (24.73%)	35 (28.23%)	208 (24.19%)	12.2	0.79	0.29

	Event	# of arrivals/hour					Average fuel consumption per arrival (Grams)	Average hourly fuel consumption (gallon)	Unproductive Fuel Consumption (gallon)
		East	West	South	North	Total			
	Reference steady speed vehicle @ 22mph						7.6		
	Total	297	346	93	124	860	15.4	4.12	1.17

4. Field Evaluation of Eco Approach and Departure Application

Significant research efforts on Eco Approach and Departure (EAD) have been reported. Table I.2.8.4 summarizes the studies involving experimental evaluation of EAD.

Table I.2.8.4 Fuel Saving Results Reported by various Studies on Eco Approach and Departure

Selected EAD References	Test site (w/ traffic [T] or w/o traffic [I])	#_signal/length/speed	Fuel saving
Koukoumidis et al. (2011)	Cambridge, MA [T]	3; 0.3mi, 30mph	20.3%
Barth et al. (2012)	Richmond Field Station, CA [I]	1, 0.2mi, 25mph	13.6%
Atlan et al. (2017)	Automated EAD @ TFHRC in VA [I]	1, 0.2mi, 20-25mph	2~46% Vs. driver -6~50% Vs. driver with EAD
Meng et al. (2015)	El Camino Real, CA [T]	10, 1.7mi, 35mph	3%~4%
Mintsis et al. (2017)	Thessaloniki, Greece ([T] 341 taxis tested for months)	12, 1.6mi, 37mph	6.0% -9.1%
Hao et al. (2019)	El Camino Real, CA [T]	10, 1.7mi, 35mph	2% All trips 6% (less vehicle following @<10m)

The large variation of the reported fuel saving benefits (2%-50%) raises *questions* about the underlying assumptions, test methods, the quality and the interpretation of data of these studies and presents a need for objective evaluation of the EAD to understand the true benefits under various conditions. Specifically, typical field evaluation of Intelligent Transportation Systems (ITS) technologies involves before-and-after field testing, which often encounters constraints such as change of testing conditions, limited number of runs for statistically sound assessment, etc. In order to overcome these shortcomings, Eco-Approach and Departure (EAD) application has been field-evaluated under this task to directly compare driving behaviors and fuel consumptions of the test vehicles instrumented with EAD function (with EAD) with their neighborhood vehicles in the same traffic steam (without EAD). Five test vehicles including a fully instrumented test vehicle with 360° sensing capability were used for the field testing. An EAD app Enlighten developed by Connected Signals were used to provide EAD information to the test drivers. The test vehicles with EAD are driving continuously for 6-8 hours per day for two days along the test corridor in San Jose where traffic data is collected. In average, ~10 EAD vehicles with EAD arrive at each test intersection every hour, totaling ~1500 arrivals at 10 testing intersections. The trajectories of all vehicles approaching at the intersections are analyzed. Data analysis is conducted to evaluate whether and how much differences are made by drivers with EAD and

by those without EAD information in the surrounding vehicles. This direct with/out comparison supports objective assessment of fuel savings of EAD at intersections.

The following EAD application scenarios are evaluated:

Scenario 1: The vehicles approach the intersection near the end of a red phase. An EAD instrumented vehicle slows down and accelerates to pass the intersection. By avoiding a full stop, the fuel consumption caused by braking is mitigated, and the vehicle requires less acceleration to achieve leaving speed, which also contribute to fuel saving.

Scenario 2: Vehicles approach the intersection near the end of green phase. Two actions may be taken as a result of the EAD recommendation, i.e., cruise and gentle stop.

Scenario 2-Cruise: EAD vehicle uses the green counting down information to estimate the time to arrive at the intersection. If the driver determines that crossing is a possibility before the red phase starts and situation allows, he/she may maintain the speed to cross the intersection. This scenario (2-Cruise) will lead to the best fuel consumption performance as the vehicle can avoid waiting for a full red phase. However, to achieve this maneuver, the driver may accelerate to catch the end of the green phase. This driving behavior introduces safety risks so therefore should not be encouraged.

Scenario 2-Gentle Stop: Advanced EAD warning of vehicle not being able to pass the intersection at the end of green phase can facilitate fuel saving by enabling a vehicle to start coasting sooner than the vehicles without EAD information.

Figure I.2.8.4 shows an example of Scenario 1, where vehicles approach an intersection when the signal switches from red to green, thus not requiring a full stop if provided with sufficient information. The red line represents the vehicle with EAD, and the blue line is the no-EAD vehicle. The vehicle with EAD guidance gently decelerated then accelerated to avoid a full stop, while the no-EAD vehicle nearly came to a full stop and then speed up to pass the intersection. The vehicle with EAD therefore consumed less fuel than the vehicle without EAD. The comparison of the trajectories of the two vehicles shows the strong correlation of the fuel-saving behavior of the EAD vehicle with the red light count down information. Among the 82 passes of EAD vehicles, two additional Scenario 1 cases are observed, but without adjacent no-EAD vehicles for comparison.

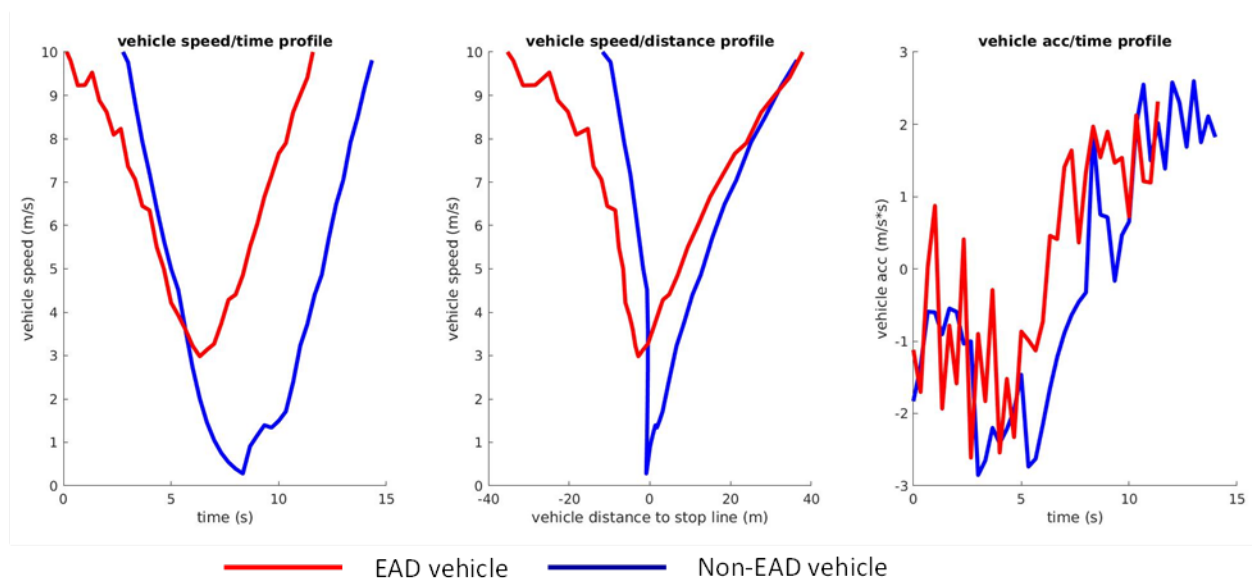


Figure I.2.8.4 Case of scenario 1: EAD Case I: EAD vehicle slows down but does not make full stop. Non-EAD vehicle nearby makes nearly a full stop (from left to right speed, speed vs distance to intersection, deceleration)

Figure I.2.8.5 –Figure I.2.8.7 show four example cases for a vehicle approaching an intersection when the signal switches from green to red and a full stop is necessary, but the approach distance allows for a smoother decelerating trajectory (similar to Scenario 2 above). Vehicle speed and deceleration of all approaching vehicles, particularly the frequency and magnitude of deceleration of the vehicles are used to evaluate the differences in driving behaviors of vehicles with and without EAD. The red line represents the vehicle with EAD, while the blue and green lines represent the no-EAD vehicles in following, ahead and parallel positions. Case I, as shown in Figure 4, presents a scenario under which a no-EAD vehicle follows the EAD vehicle. As the leader EAD vehicle performs gentle deceleration, the trailing no-EAD vehicle applies gentler deceleration. In this case, both vehicles have fuel savings while the no-EAD vehicle consumes even less fuel than the EAD vehicle.

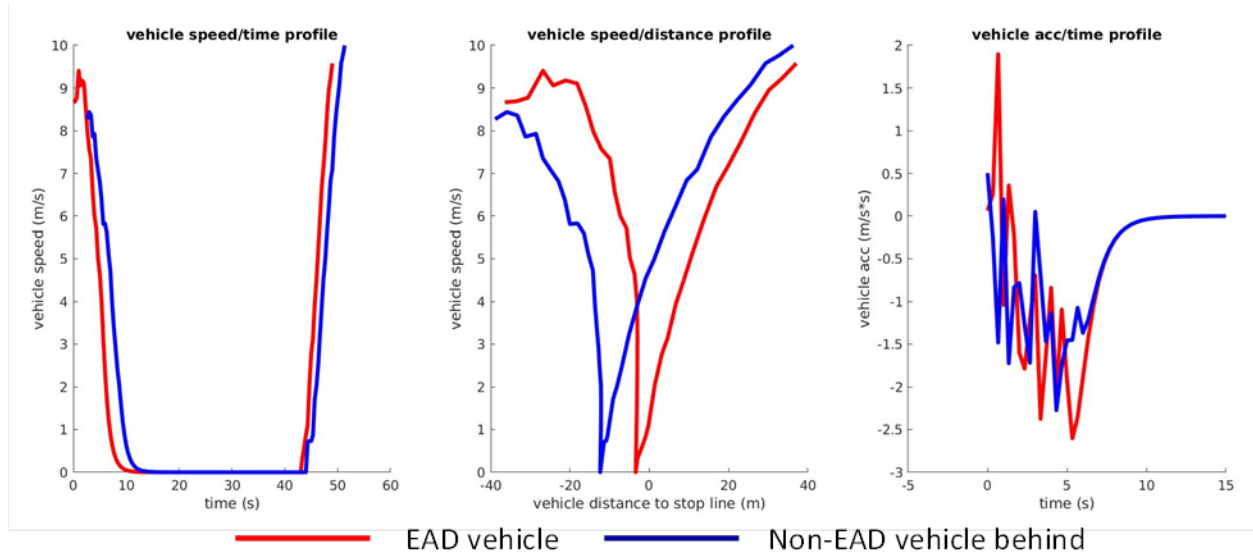


Figure I.2.8.5 EAD Case I: a no-EAD vehicle follows the EAD vehicle

In Cases II and III, shown in Figure I.2.8.6 and Figure I.2.8.7 the EAD vehicle travels in a lane adjacent to the lane where the no-EAD vehicles travel. In comparison with no-EAD vehicles, gentler deceleration is observed for the EAD vehicle, hence some fuel savings are expected.

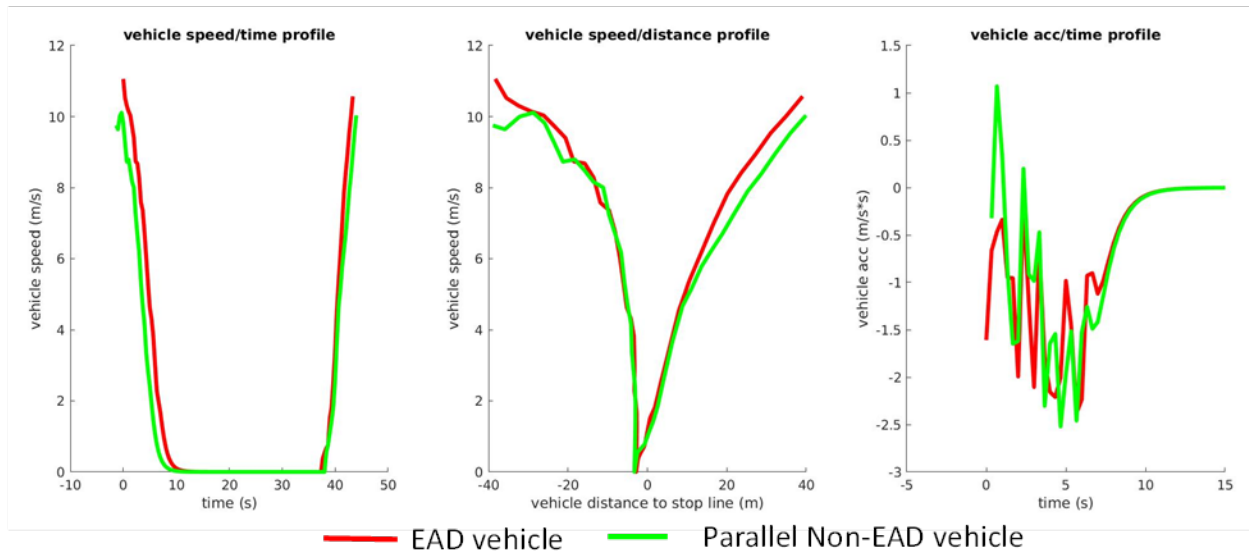


Figure I.2.8.6 EAD Case II: EAD and no-EAD vehicles travel in adjacent lanes and arrives at intersection as similar time

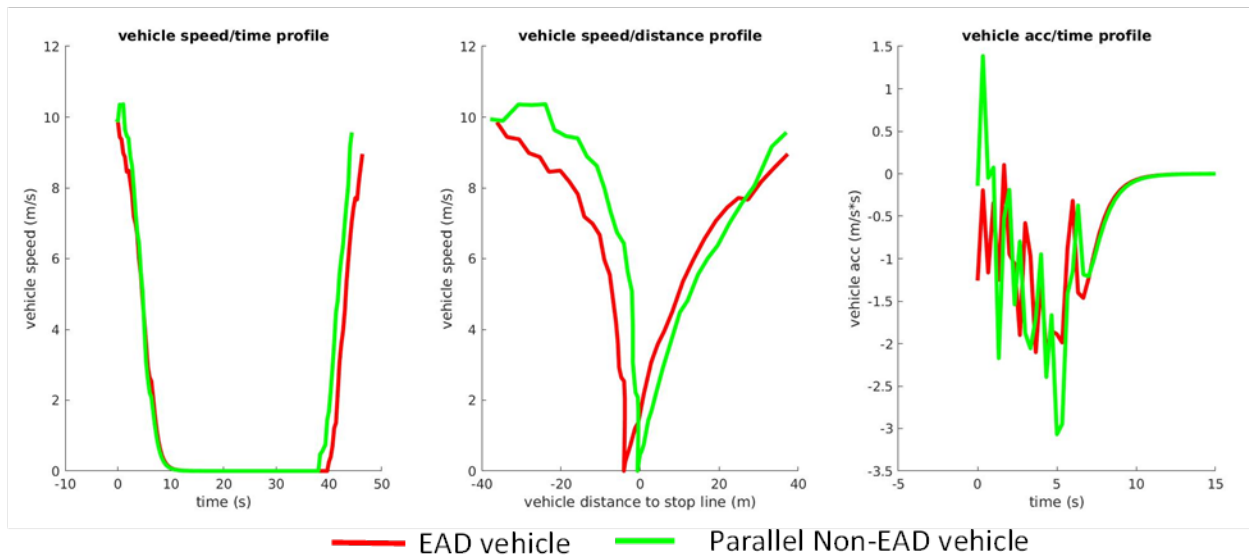


Figure I.2.8.7 EAD Case III: EAD and no-EAD vehicles travel in adjacent lanes and arrives at intersection as similar time

In the Case IV, shown in Figure I.2.8.8 the EAD vehicle was initially about 40-50 meters trailing behind the lead no-EAD vehicle in the adjacent lane. When the EAD vehicle is about 30 meters away from the intersection, the signal switched to red. The EAD vehicle uses similar pattern and magnitude of the deceleration as the no-EAD vehicles, resulting in a similar level of fuel consumption. In this case, the red signal display appeared to play a dominant role in influencing the driver's decisions.

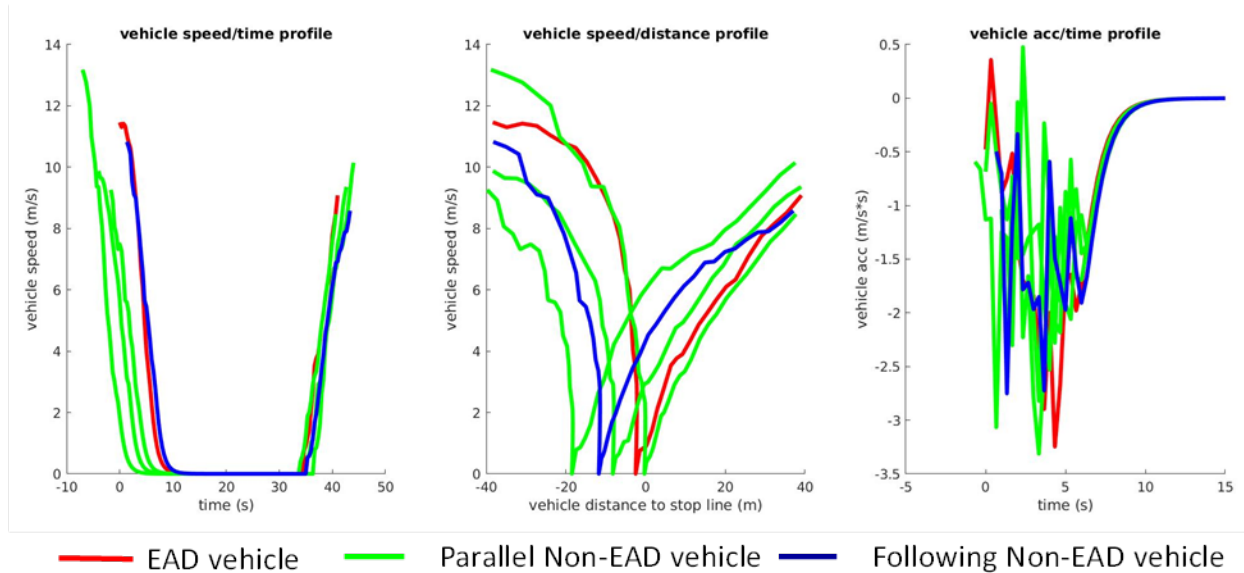


Figure I.2.8.8 EAD Case IV: EAD trailed behind from no-EAD vehicles travel in the adjacent lane

Table I.2.8.5 summarizes the fuel consumption of the vehicles with EAD and the vehicles without EAD based on the total data of 12 hours. The driving behaviors within the 80-meter range centered at the test intersection are analyzed and resulting fuel consumption is estimated. The following key findings are made through data analysis:

- The evaluation methods greatly affect the findings in the evaluation results. The evaluation uses directly comparison of with and without treatment offers an objective way for evaluating EAD and most Eco-Driving applications.
- The baseline distance to the intersection is one of the most critical variables that can strongly influence the magnitude of the fuel saving benefits.
- The largest benefits that EAD offer is during an instrumented vehicle approaches an intersection at the end of a green phase/transition into the red phase. Among the total of 82 arrivals by EAD vehicles, EAD is only applicable for about 15% of cases, and does not offer any benefits for the remaining cases. More specifically, EAD enabled 3.7% of arriving vehicles to pass through the intersection without stopping at the end of red phase (Scenario 1) and 12.2% of vehicles to arrive with gentle deceleration. This is a relatively infrequent event for most of the trip types.
- In the four case studies, through comparing the deceleration profiles of vehicles with and without EAD, only marginal average fuel saving benefits are observed. Note that these are small sample of the test cases. Further analyses need to be conducted on the larger set of vehicle arrival cases to derive conclusive assessment of EAD fuel saving benefits.

Table I.2.8.5 Eco-Driving Vehicle Fuel Consumption

		# of occurrence	% of Arrivals for EAD Vehicles	Average fuel consumption per occurrence(grams)	Cumulative Fuel Consumption (grams)
All Vehicles	Cruise	2549		16.6	42313
	Stopped	2747		26.3	72246
Vehicles w/EAD	Arrive during green phase	52	63.4%		
	Arrive during red phase	17	20.7%		
	Arrive at end of red phase (EAD Scenario 1)	3	3.7%	21.3	63.9
	Pass at end of green (EAD Scenario 2 Cruise)	0	0%		
	Arrive at end of green (EAD Scenario 2 general stop)	10	12.2%	22.8	228

Conclusions

The following accomplishments have been made under this task:

1. Identified ~10 billion gallons of annual unproductive fuel consumption (by scenarios), in addition to the 3.1 billion gallons of wasted fuel reported in the National Mobility Scorecard.
2. Identified opportunities for saving energy through Eco-Driving technologies.
3. Reviewed a large set of existing work on Eco-Driving technologies and formulated a field-wide perspective on the status, estimation gaps, and research & development needs.
4. Collection of vehicle trajectory level data at 10 signalized intersections along W/E Santa Clara St. in San Jose and at five unsignalized intersections (including roundabout and stop sign controlled intersections). Data for one signalized intersection and one stop sign controlled intersection has been analyzed.
5. Eco Approach and Departure has been evaluated in conjunction of the traffic data collection at signalized intersections in San Jose. Case studies have been conducted.

The key technical findings are summarized below:

- Estimated unproductive fuel consumption at the national level: At least ~10 Billion gallons of unproductive fuel is consumed annually, in addition to the National Mobility Scorecard estimated 3.1 billion gallons wasted fuel. The scenarios that contributed to large unproductive fuel consumption include: Driving speeds higher than 65 mph, unnecessary stops at unsignalized intersections, unnecessary stops at signalized intersections, idling, in addition to stop and go in congestions.
- Field evaluation of unproductive fuel consumptions at unsignalized intersections: Field evaluation of unproductive fuel consumptions at stop sign controlled intersection. Data shows that high percentage of vehicles arriving at intersections do not encounter conflicting traffic, and unnecessary stops produce unproductive fuel consumption. ‘Stop sign rollers’ frequently occur, presenting safety hazards. Among

the necessary stops, large percentage of vehicle stops appears to be triggered by the presence of conflicting vehicles, rather than the stop signs.

- Field evaluation of unproductive fuel consumptions at signalized intersections: Unproductive fuel consumptions are produced by vehicle stops when no conflicting vehicles.
- Field evaluation of Eco Approach and Departure: Case studies of field data shows that the opportunities to gain fuel savings is relatively infrequent. Change of behavior for vehicles with EAD may result in marginal benefits.
- Note that the analyses performed for signalized, unsignalized and EAD are case studies. Due to time constraint, only a fraction of the data and test cases can be processed and analyzed under the current phase of the project.
- The team plans to share the traffic data within the SMART Mobility project team and is working on resolving privacy and authorization issues.

Key Publications

1. Jiali Bao, Wei-Bin Zhang, Alex Wang, A Data-Driven Approach to a Comparative Study of Signalized and Stop Sign Controlled Intersections and Roundabouts, submitted for presentation at the 6th TRB International Roundabout Conference, Monterey, California, May 2020
2. Workshop plan submitted to the IEEE Intelligent Vehicles Symposium, Las Vegas, June 23-26, 2020 (conditionally approved).
3. Special Session Proposal submitted to IEEE International Conference on Intelligent Transportation Systems, Rhodes, Greece, September 20-23, 2020

References

1. The Urban Mobility Scorecard
2. <https://www.anl.gov/es/reducing-vehicle-idling>
3. Rakha, Hesham, Kyoung-ho Ahn, and Antonio Trani. "Development of VT-Micro model for estimating hot stabilized light duty vehicle and truck emissions." *Transportation Research Part D: Transport and Environment* 9.1 (2004): 49-74.

Acknowledgements

Jiali Bao, Lian Cui and Mike Miles of Lawrence Berkeley National Laboratory, Jacob Tsao of San Jose State University and I-Ming Chen, Ching-yao Chan and Pin Wang of University of California at Berkeley made substantial contributions to the research results reported herein. The research team would like to thank Erin Boyd and David Anderson of United States Department of Energy for their guidance, through review and technical and programmatic assistance. The research team would also like to express appreciation for ten UC Berkeley volunteers and San Jose building managers for their assistance and help for conducting the data collection and field testing.

I.2.9 Focused Validation and Data Collection to Support - Automated Vehicle Electrical Load Investigation (ANL)

Eric Rask, Principal Research Engineer

Argonne National Laboratory
9700 South Cass Avenue
Lemont, IL 60439
E-mail: erask@anl.gov

Erin Boyd, DOE Technology Manager

U.S. Department of Energy
E-mail: erin.boyd@ee.doe.gov

Start Date: October 1, 2018

End Date: September 30, 2019

Project Funding (FY19): \$243,000

DOE share: \$243,000

Non-DOE share: \$0

Project Introduction

In decades past, considerable effort has been put forth to improve vehicle range and fuel/energy consumption. Today's vehicles continue to improve upon these gains; however, a range of new assisted driving features is proving additional challenges to these improvements due to the sensing, actuation, and processing power required by these systems. This work investigates the power consumed by the sensors, controllers, and actuators of 1) a production hands-free automated driving system and 2) a snapshot regarding the expected power required from a more automated development vehicle, which can provide a range of higher-level automated driving features. Currently, there is significant uncertainty regarding the expected accessory loads associated with a range of automated driving functionality from basic hands-free operation to highly automated driving.

Objectives

The overall goal of this project is to quantify the additional sensing, processing, and actuation loads for a Highly Automated Vehicle (HAV) prototype (supplied by project partner FEV) and Level-3 Vehicle (GM Super-cruise) under a range of realistic operating conditions. This will help provide information about the real-world observed loads associated with a range of automation features as well as highlights some insights for future trends related to system-level solutions, loads for automation levels beyond the current production systems, and areas for additional research.

Approach

To support this assessment a production 2018 Cadillac CT6 with the "Super Cruise" advanced driver assist features was selected as well as a 2018 Ford Fusion which serves as a development platform for a range of L3/L4/L5 sensor development and autonomous controls research from project partner FEV. Each vehicle was instrumented with many voltage and current sense points. Sense points were focused around overall vehicle ADAS power consumption as well as at individual sensors, their controlling ECUs, and the actuators which they control. An array of additional sensors and cameras were used to facilitate and record the actual testing in order to better understand the surrounding operational conditions during testing. Aside from overall 12V and alternator power measurements, the power consumed by the "convention" accessory systems (HVAC, traditional accessories) was not included in the reported results and was not instrumented to the degree of detail as the ADAS and automation related systems.

Sensor types evaluated included dual band RADAR, LiDAR, visual optics and DGPS as examples. Where additional sensors might be applied, the results below can be expanded to reflect their use.

The results, though reflective of other systems are specific only to those measured and the specific suppliers of the sensors suites evaluated.

Both vehicles were public road tested in very similar environments of weather, road and traffic/sensor loading conditions. Voltage and Current was sensed in numerous locations on these systems and results aligned to the variables contained as part of the review. As there was limited access to raw data (direct sensor output, and data rendering) determinations of sensor/system loading were made through external sensors in an effort to determine power needs based upon specific sensor loading (power consumption due to the number of points being tracked. e.g., light and heavy traffic conditions). There were no means in which to alter point cloud information where sensor fusion techniques were used. Therefore, power consumption may reflect an aggregate of various sensors and only reflect that consumed in support of the autonomous feature.

Furthermore, energy consumption specific to the series production system and optimization in place for data handling, processing, or control was not determined. Real world energy consumption characteristics will be impacted by the strategies implemented by these subsystems

An overview of the instrumentation for each vehicle is provided below:

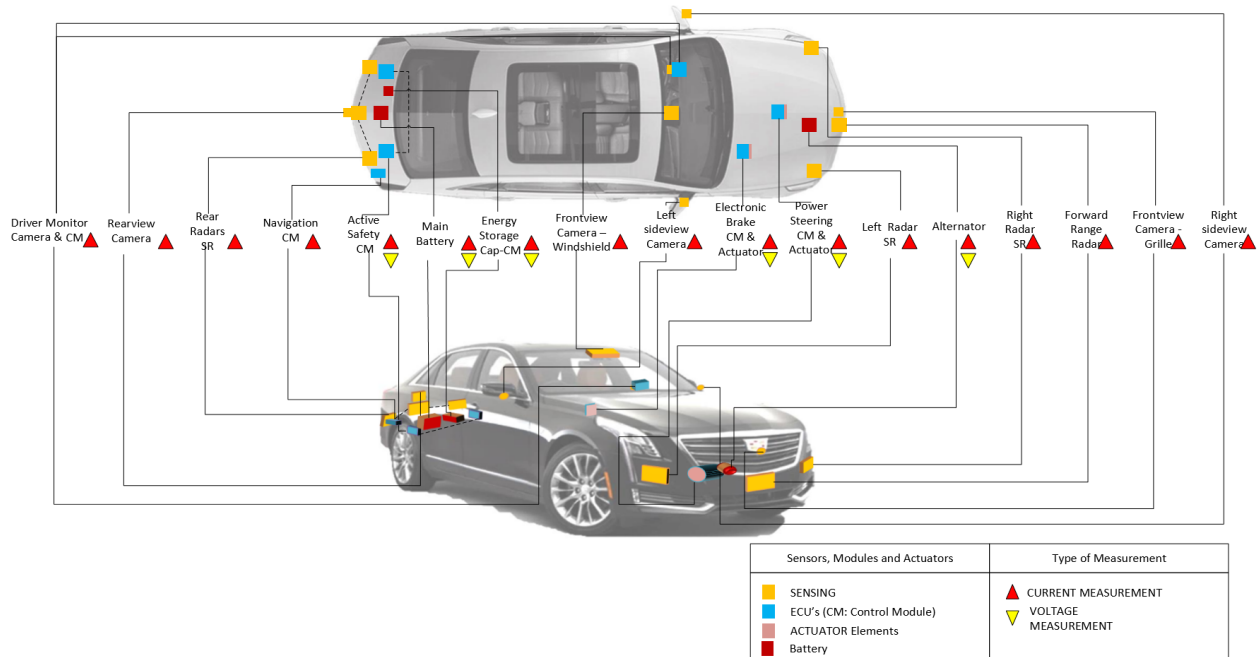


Figure I.2.9.1 Cadillac CT6 Instrumentation Overview

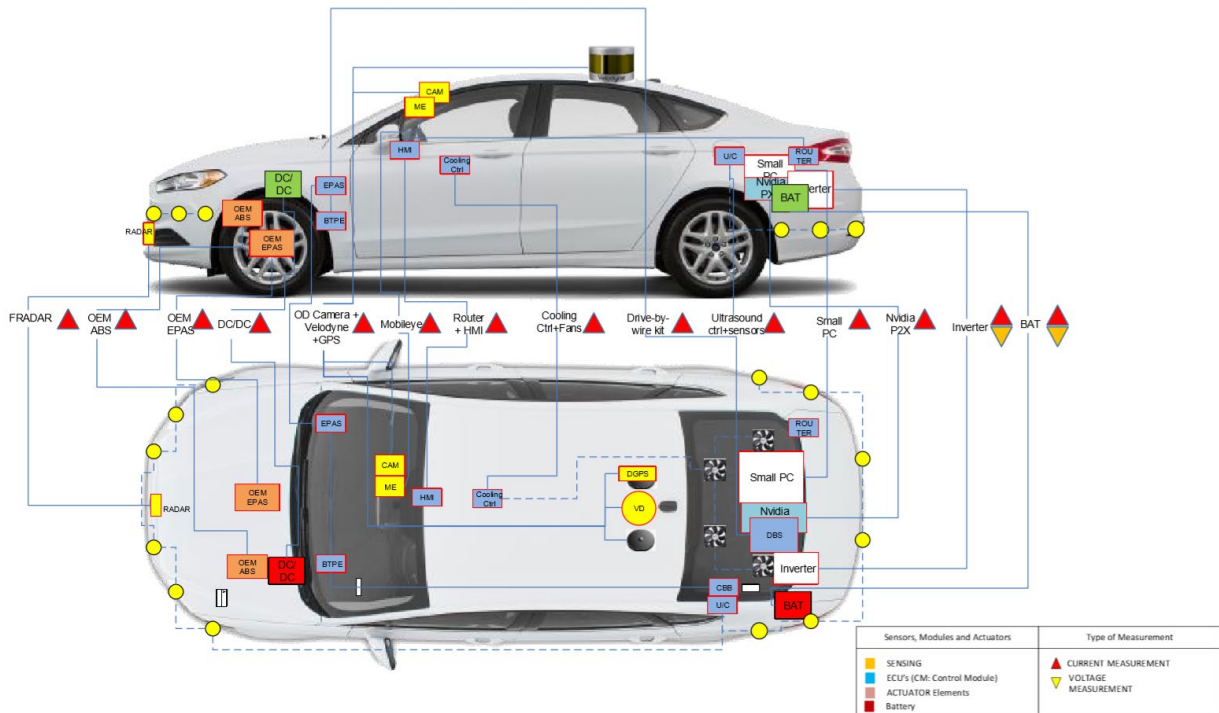


Figure I.2.9.2 Ford Fusion HEV (FEV AV Demonstrator) Instrumentation Overview

Results

CT6 with Super Cruise Highlighted Results

Freeway driving with Super Cruise enabled, resulted in an overall power consumption increase of 98W or ~12% to a total average accessory load of 917W. This 917W includes all other normal vehicle functions which accounted for ~818W as measured at the 12V battery/alternator. The sensors themselves consumed ~48W, roughly 50% of the overall increase. The ECU's supporting the specific ADAS feature under review consumed ~36W, roughly 37% of the overall increase. The actuators used to provide the appropriate vehicle response consumed ~15W or 16% the overall increase. The results were consistent regardless as to the environment or loading of the sensor/system. For example, there was no measurable difference in system loading even in no traffic situations.

Table I.2.9.1 Key Contributors to Observed Super Cruise On-Road Accessory Loads

Component	Average Observed Power Draw During SuperCruise Operation
RADAR [Aggregate, 6 total]	40W
Cameras [Aggregate, 5 total] (driver monitor not included)	9W
Active Safety Control Modules [ASCM] (Aggregate, 2 Modules)	24W
Driver Monitoring Control Module (DMCM)	7W
Video Processing Control Module [VPCM]	7W

The device which saw the greatest difference in power consumption due to activation of Super Cruise was the DMCM which varied by ~3W, likely due to the illumination of the driver's face during operation to ensure driver attentiveness. Surprisingly, the additional loads due to the other vehicle sensors and processing changed minimally when Super Cruise was either activated or deactivated. For instance, during freeway driving with Super Cruise system enabled, there was an almost identical increase observed for accessory loads as compared to freeway driving with normal cruise and ADAS enabled or even manual driving where these features were disabled but not unpowered. In all instances the increase due to the ADAS/Super Cruise related sensing, actuation, and processing was roughly 96W.

AV Demonstrator Highlighted Results

The development platform was tested utilizing an L3-esque Highway Pilot and L4-esque Urban Pilot in support of Traffic Jam Chauffer and Waypoint Navigation functions. Overall the autonomous system under review consumed ~390W with 260W in support of processing and required cooling. RADAR was similar to the CT6 at 8W.

Table I.2.9.2 Key Contributors to Observed AV Demonstrator On-Road Accessory Loads

Component	Average Observed Power Draw During SuperCruise Operation
NVIDIA PX2 Controller	127W
Small PC	80W
Cooling Fan	53W
Ethernet Router and HMI	45W
LIDAR, DGPS, OD Camera	34W
RADAR	8W
IMU and Synced-Camera System	1.7W

During operation, the system cooling fan utilizes a varying duty cycle and as such power consumption varied accordingly, between 35W (manual drive) and 55 W (Waypoint Navigation). All other sense points were reasonably similar regardless as to any influence in environment.

Conclusions

This initial assessment was to start the process of quantifying current power needs for current automated vehicle capabilities as well as to draw insight into where these needs might evolve for a range of automation capabilities ranging from hands-free driving to near or fully automated driving systems. The significant increase in processing power relative to the Super Cruise and Demonstrator vehicle highlights one of the primary issues facing highly automated vehicles, in that high processing loads are likely to negate some of the other efficiency gains enabled by the systems. Moreover, the cooling loads associated with these systems may also need to be assessed in greater detail due to the elevated loads required for cooling these systems.

While the AVs evaluated consumed additional power for the sensing, processing, and actuation functions, another useful conclusion from this work is that it is important to consider the entire spectrum of loads associated with different AV capabilities when estimating the impact of a system. While fully automated L4/L5 vehicles may require significantly increased loads on the order of 1-2kW, many automation features can be enabled, for certain driving scenarios, with a much lower overall penalty for accessory loads. Therefore, they do not suffer from the large decrease in expected benefits observed at the much more elevated accessory load levels.

Acknowledgements

The authors of this report gratefully acknowledge the significant project management and execution support provided by the project team at FEV. In addition to providing the Demonstrator vehicle for this testing, they also were contracted to perform most of the instrumentation, testing, and analysis discussed in this and related reports.

I.3 Mobility Decision Science

I.3.1 Whole Traveler Study (LBNL, INL, NREL)

Anna Spurlock, Principal Investigator

Lawrence Berkeley National Lab
1 Cyclotron Road
Berkeley, CA 94720
E-mail: caspurlock@lbl.gov

Victor Walker, Principal Investigator

Idaho National Lab
2525 Fremont Avenue
Idaho Falls, ID 83402
E-mail: victor.walker@inl.gov

Andrew Duvall, Principal Investigator

National Renewable Energy Lab
1617 Cole Boulevard
Lakewood, CO 80401
E-mail: andrew.duvall@nrel.gov

Prasad Gupte, DOE Technology Manager

U.S. Department of Energy
E-mail: prasad.gupte@ee.doe.gov

Start Date: October 1, 2018	End Date: September 30, 2019	
Project Funding (FY19): \$929,000	DOE share: \$929,000	Non-DOE share: \$0

Project Introduction

The Whole Traveler study is a regionally survey that aims to descriptively understand the relationships between key life decisions and its corresponding impact on transportation. It will focus on the dynamics of lifestyles in characterizing and classifying the population, predict “change-points” in lifestyle that can be used to understand the impact of emerging transportation options and how they may affect travel choices in the future. Finally, it will improve behavioral data in transportation system models and vehicle choice models.

Objectives

Explore the question: How does the US traveler (segmented by demographics) make decisions on or impacting transportation energy use in the:

- Very short-term: reroute, mode choice
- Short-term: Day-ahead travel planning
- Medium-term: Vehicle ownership & type
- Long-term: Housing location, etc.
- Identify historic patterns in lifecycle trajectories and map out relationships with transportation behaviors to be used to predict change-points and decision points when people would be most likely to respond to policy incentives.

- Connect definitions of heterogeneous traveler groups based on lifecycle trajectories with data on other dimensions of heterogeneity including personality/psychological traits, environmental preferences, metrics of risk aversion and intertemporal discounting, traditional demographic data, and other historic behavior patterns (such as technology adoption) to determine the most useful definition of heterogeneity that can best explain variation in behavioral outcomes of interest: openness to CAV and/or EV adoption/use, car ownership patterns, degree to which TNCs are compliments or substitutes to car ownership or public transportation use, and short term high resolution travel behavior patterns (locational GPS data).
- Use insights from all the above analyses to inform expansion and enrichment of agent-based modeling efforts within SMART Mobility.

Approach

The approach taken in this study involves a survey-based data collection, and subsequent analyses to answer a variety of research questions.

The survey was conducted in two phases: (1) Phase 1 is an online survey collecting information on respondents: transportation needs and preferences, psychological characteristics of interest, demographic characteristics, and the timing of key historic life events; and (2) the second phase of the survey is a GPS data collection phase, where participants provide a week's worth of their Google Location History GPS data collected on their smartphone, and answer a short series of questions about their transportation choices during that week.

The survey is focused in the nine core counties of the San Francisco Bay Area (Alameda, Contra Costa, Marin, Napa, San Francisco, San Mateo, Santa Clara, Solano, and Sonoma). The sampling method used is an address-Based random sample in this region.

The survey design and subsequent analyses are geared towards answering a series of pressing questions. The analysis approach used varies depending on the question being explored. For the most part, data analysis uses standard econometric and statistical techniques, such as linear regression and discrete choice modeling.

In some instances, the analyses approach itself is innovative and novel. In particular, machine learning clustering methods designed for clustering multivariate sequences (such as Optimal Matching) are used to identify archetypal lifecycle trajectory patterns. These clustered sequences, or archetypal patterns, can then be further analyzed to understand broad patterns in life phase transitions across the population, and the relationship between shifts in these patterns and critical transportation related decisions.

Results

Below summarizes the analysis and deliverable plan for Whole Traveler, including when products were delivered to DOE if applicable. The remainder of the Results section of this report provides a summary of the results from items 4–7 in this table:

Decision-Making:Table I.3.1.1 Summary of Analysis and Deliverables Plan

Description	Preliminary Analysis:				Delivered to DOE	Final revisions/ under review at publication	Published
	starting	underway	complete	Refining analysis and writing up			
1 Describing the users: Understanding adoption of and interest in shared, electrified, and automated transportation in the San Francisco Bay Area					Q3 2018 (Early)		Transportation Research Part D
2 Children at home: how transitions through family stages relate to mobility patterns in the San Francisco Bay Area					Q3 2018 (Early)	Being prepared for journal submission	
3 The WholeTraveler Transportation Behavior Survey: Decision-Making Data related to Transportation Energy Use in the San Francisco Bay Area					Q1 FY2019	Under review at the journal Transportation	
4 Children, Income, and the Impact of Home-Delivery on Household Shopping Trips					Q3 FY2019	Accepted for TRB and recommended for consideration for publication in TRR	
5 Tensions and complementarities in mass transit and ride-hailing decisions through a survey-based randomization					Q3 FY2019	Accepted for TRB	
6 Life course as a contextual system to investigate the effects of life events, gender and generation on travel mode usage					Q3 FY2019 (Early Q4 deliverable)	Accepted for TRB and recommended for consideration for publication in TRR	
7 Risk, Personality, Cost, or Household Tasks? Hypothesis Testing of Gender Differences in Plug-in Electric Vehicle Interest					Q4 FY2019	Accepted for TRB	
8 Modeling Multimodality in the San Francisco Bay Area: How Human and Environmental Considerations Affect Transportation Behavior					Draft complete, revising		
9 No title yet: Variability and flexibility in short-term mode choice, route choice, travel time					Delayed due to difficulty with GPS data		
10 No title yet: Estimation of value of travel time					Delayed due to difficulty with GPS data		
11 No title yet: Effect of uncertainty in ride-hailing prices on mode choice					Determined no publication-worthy results		

Children, Income, and the Impact of Home-Delivery on Household Shopping Trips

E-commerce and on-demand delivery are growing quickly in the United States and across the world. Online retail sales almost doubled as a percent of U.S. retail sales between 2012 and 2017 (U.S. Census Bureau, 2013; 2018). In addition, as of June 2018, more than 95 million people in the U.S. were paying for Amazon Prime (through which an annual fee gains the subscriber access to benefits such as free 2-day shipping) subscriptions (Statista, 2019). This is close to 40% of the U.S. adult population. This expanding home delivery is associated with societal benefits and costs. Benefits of home delivery include time savings; increased choice of products and prices; and convenience (Darian, 1987; Harris et al., 2017; Chu et al., 2008; Sabatini, 2011; Chintagunta et al., 2012; Lee et al., 2017).

However, e-commerce and delivery also impact vehicle miles traveled (VMT) in the transportation system and resulting energy consumption, air quality, and congestion. Determining the potential energy impact is complex (e.g., Salomon, 1985; 1986). If a delivery trip substitutes for a personal vehicle trip, the delivery truck may be less energy efficient than the vehicle replaced but may decrease the total energy use and VMT in the system if multiple items are delivered on a given route. However, home delivery may add to overall shopping related VMT if deliveries supplement (add to) the number of existing personal or household trips to the store. These supplemental home delivery trips may occur for various reasons: a household may order items for delivery that they could have purchased during an existing shopping trip; some home delivery purchases, such as meal delivery, may not have been purchased in the absence of a delivery option; and e-commerce may generate new demand for trips to a store. Delivery trips may also replace trips that otherwise would have been made by walking or biking. Empirical research to-date is mixed. Some results suggest that e-commerce supplements in-store shopping, leading to an overall increase in shopping travel (Cao et al., 2010; Zhou and Wang, 2014, Ding and Lu, 2017; Lee et al., 2017), while some suggest that it substitutes, leading to a decrease (Sim and Koi, 2002; Tonn and Hemrick, 2004; Weltevreden and van Rietbergen, 2007, Suel and Polak, 2017). Data from the National Household Travel Survey (NHTS) shows that from 2009 to 2018, the percentage of person-trips per household with the purpose of shopping decreased from 21% to 18%, and the per-person VMT associated with shopping decreased from 14% to 12% (McGuckin and Fucci, 2018). This decrease may be related to the concurrent increased prevalence of home delivery, or may be related to other factors.

Shopping behavior and the use of e-commerce varies based on household characteristics. For example, in both 2009 and 2017, households with children of any age averaged more deliveries than those without children (4 vs. 2 per month in 2009, and 7 vs. 4 per month in 2017). Households with both older teens and younger children averaged the largest increase in deliveries received per month (from 4 to 7) between 2009 and 2017 (McGuckin and Fucci, 2018).

Related to this observation, overall purchasing decisions have been found to be fundamentally related to family life cycle characteristics, including children in the home, and household income (e.g., Lansing and Morgan, 1955; Brown and Deaton, 1972; Wagner and Hanna, 1983; Kehily et al., 2014). Children in the home can be a major constraint on shopping time and flexibility (Kwan, 2000), while higher income means less constraint on expenditure, but a higher opportunity cost of time. All these factors likely influence choice of shopping mode. Empirical evidence relating time constraint or pressure to online shopping behavior is mixed. Ferrell (2005) finds a negative correlation between online shopping frequency and in-store shopping frequency, particularly for consumers with greater time constraints, suggesting that those with greater time constraints might replace shopping trips with online shopping. However, Lee et al. (2017) find that those who reported being very busy or having increased time pressure were no more or less likely to shop online. Such heterogeneity in e-commerce use and underlying motivations suggest that the resulting impacts of delivery on household shopping trips may differ based household characteristics that are largely defined by time and financial constraints, such as household income and the presence of children in the home. This motivates our focus on household income and the presence of children in the home in this paper.

In this paper, we examine the degree to which home delivery trips substitute for and/or supplement household shopping trips. We consider impacts across two separate modal categories for shopping trips: (1) vehicle

(personal vehicle, taxi, or ride-hailing); and (2) non-vehicle (walking, biking, or using public transit). We categorize purchases into the four product categories (groceries, clothing, household items, and prepared meals). We drill down on two key household characteristics: income and the presence of children in the home. We test four hypotheses focusing largely on the role time saving and convenience differentially motivate people to engage in delivery, and the resulting impact on shopping travel, based on their income and child status.

We find that the question of how increased online shopping and expanded goods delivery affect household shopping trips has a nuanced and complicated answer. We found in aggregate that the balance between substitution and supplementation tended to reinforce the subset of the literature (Sim and Koi, 2002; Tonn and Hemrick, 2004; Weltevreden and van Rietbergen, 2007; Suel and Polak, 2017) that has found more substitution for vehicle trips on net as opposed to supplementation (Figure I.3.1.1). However, there is significant heterogeneity in shopping mode choice and in the degree to which engagement in e-commerce supplements or substitutes for shopping trips. Interestingly, consistent with Weltevreden and van Rietbergen (2009), we found that for a large proportion of our sample deliveries either fully substitute for (55% to 70%) or fully supplement (20% to 35%) shopping trips. This contrasts with all households using deliveries to supplement a little and substitute for a little of their shopping trips.

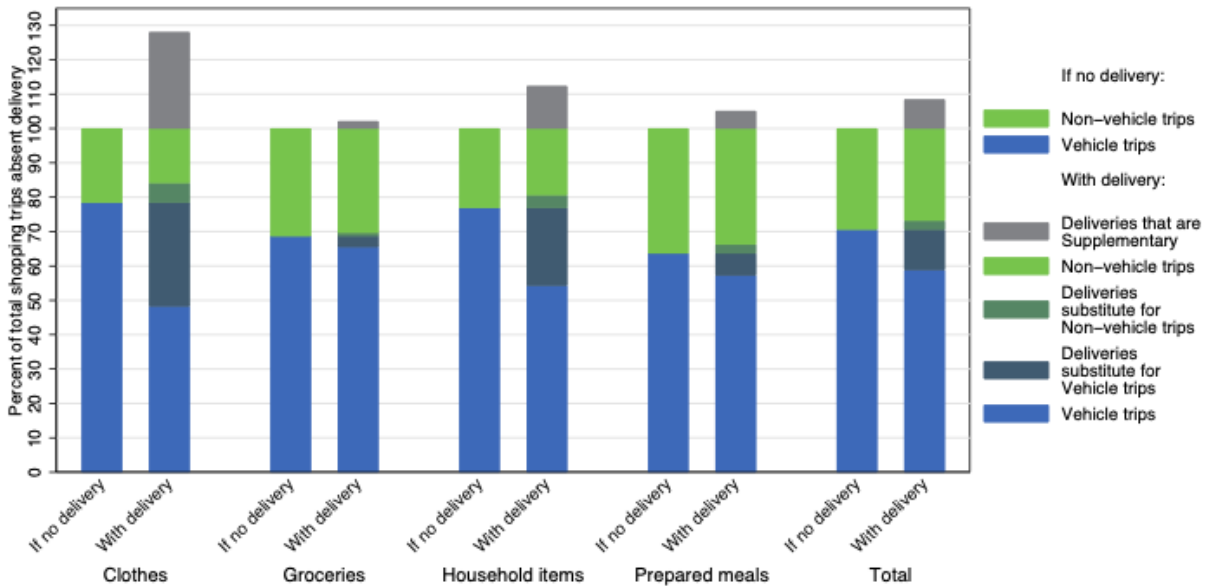


Figure I.3.1.1 Overall degree of substitution and supplementation of delivery for household shopping trips

We found evidence consistent with all our Hypotheses with one interesting exception. We did find, consistent with Hypothesis 1 and previous literature (Darian, 1987; Harris et al., 2017; Sabatini, 2011; Chintagunta et al., 2012), that time and convenience, among other factors, are important to consumers when considering whether or not to make a purchase online, and specifically time-saving is more of a motivating factor for higher income households and households with children relative to their counterparts (Figure I.3.1.2). In addition, consistent with Hypothesis 2, lower income people were more likely to be negatively influenced by delivery charges (Figure I.3.1.2).

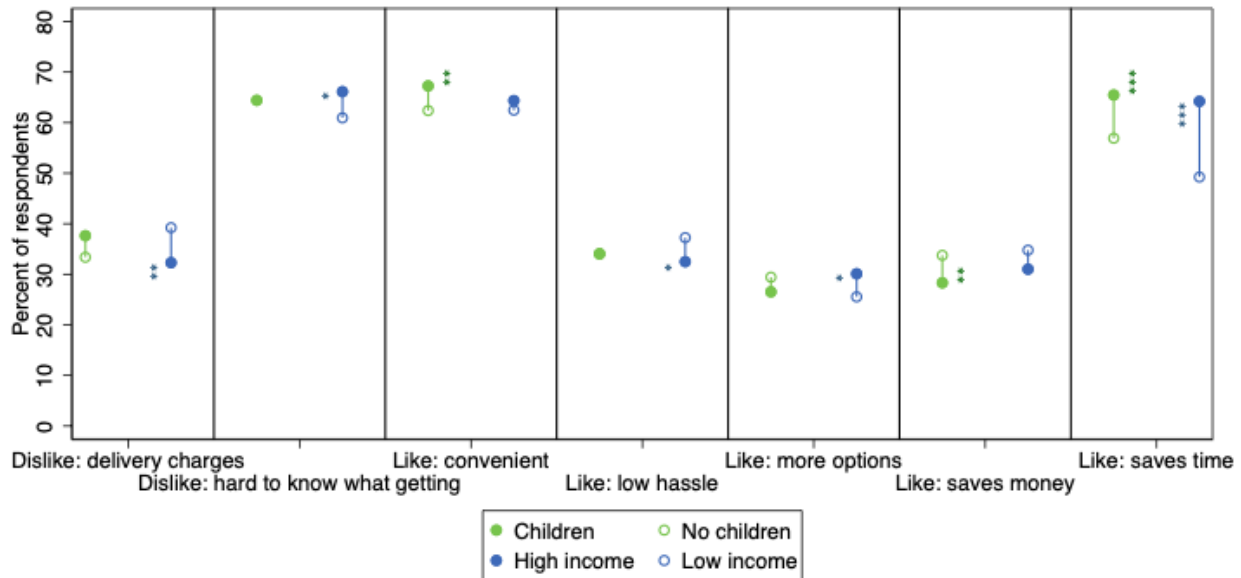


Figure I.3.1.2 Likes and Dislikes of Online Shopping Differentiated by Subpopulations.

*** $p < 0.01$, ** $p < 0.05$, * $p < 0.1$

However, this motivation for time-savings translated through to delivery utilization and the degree to which these deliveries substitute and supplement for shopping trips in a mixed way. Consistent with Hypothesis 3, higher-income households are more likely to receive deliveries overall, and across all item types and households with children were also relatively more likely to choose delivery, particularly for household items and clothing compared to households with no children. However, the time-saving motivation for these categories of households did not translate through to these deliveries being relatively more likely to substitute for shopping trips, as was posited in Hypothesis 4. Indeed, prepared meal purchase behavior is a particularly interesting case demonstrating significant distinctions between high- and low-income households and households with and without children. Households with children (by 15 percentage points) and higher-income households (by 12 percentage points) are significantly more likely to have prepared meal delivery supplement trips relative to their counterparts. This speaks to the fact that increased convenience and time-saving aspects of meal delivery may substitute more for cooking at home, rather than for a trip to a restaurant. Indeed, for higher income households prepared meal delivery, which they're more likely to order relative to lower income households, is actually significantly less likely (by 16 percentage points) to substitute for a vehicle trip relative to lower income households. These results suggest that the marginal activities for saving time for those that are either more time constrained or have a higher opportunity cost of their time isn't necessarily the time it takes to make a shopping trip, but appears more so to be the time involved in other activities, such as preparing meals.

Tensions and Complementarities between Mass Transit and Ride-hailing through a Survey-based Randomization

The rapid expansion of Transportation Network Companies (TNCs) such as Uber and Lyft, has brought into sharp focus the need for transportation policy and infrastructure planning to incorporate future trends in ride-hailing services and its energy impact. However, the current understanding of the impact of ride-hailing on congestion, shifts in mode choices, and overall energy efficiency of the transportation sector is incomplete, and hampered by a lack of data (Jin et al. 2018). Findings have been mixed, with some studies suggesting large modal shifts, increases in congestion and vehicle miles traveled, while others find inconclusive results, or scope for complementarity with mass transit, and even increases in energy efficiency (Erhardt et al. 2019). The importance of understanding the impact of ride-hailing is magnified by the expected significant future declines in its cost of use as TNCs roll out cheaper service options, as competition grows, and as operating costs decline

through more efficient cars or autonomous vehicle technology. A simulation of New York City showed Uber and Lyft fares could fall by 80%, “and become cheaper than a metro ticket,” over the next decade when taking into account the impact of automation in the ride-hailing market (i.e., “robo-taxis”) (Rapier 2019). It is therefore crucial to understand the interaction between a potential decrease in the cost of using ride-hailing and the resulting change in other mode choices in order to form predictions of and plan for future transit use, overall energy use of the transportation system, and changes in infrastructure needs. In this paper, we focus on the causal effect of decreases in the cost of using ride-hailing on mass transit use. We design our study to be able to capture potential non-linearities in the impact of price declines, and differences in substitution and complementarity at different radii from public transit terminals.

It is difficult to isolate the causal effect of ride-hailing services on public transit because of unobserved correlation between the introduction of these services and other changes in the economy, incomes, and other social factors. What our approach contributes is an experimental method, which, while hypothetical, isolates the causal effect of changes in per-mile prices of ride-hailing services on public transit systems. Additionally, we focus our lens on the future by using per-mile price variation that represents scenarios in which these services could become much more cost competitive relative to alternatives, and therefore likely to have bigger impacts.

Our main research question looks at how declines in the cost of using ride-hailing impacts mass transit use. How much ride-hailing prices will drop in the future is uncertain and depends on the level of automation, competition, regulation, etc. Therefore, we study three different price points, which allows us to separate our estimates based on the level of price decline. Each survey participant is randomly assigned one of three ride-hailing per-mile price points: \$0.20 per mile, \$0.70 per mile, and \$1.2 per mile. By studying the impact of price drops across the \$0.70/mile and \$0.20/mile groups (with \$1.20/mile group as the reference category) we are able to capture possible nonlinearities in the effect of declining ride-hailing prices, which has not been directly addressed in the research so far.

The literature demonstrates that ride-hailing has the potential to both substitute and complement mass transit depending on context. For example, the shorter travel times often associated with ride-hailing could result in substitution of mass transit, however, in other circumstances ride-hailing can provide important first/last mile linkage to mass transit ports. The strength of the latter effect is likely to vary by distance from mass transit terminals, therefore without rich data that observes participants’ origin and destination locations relative to mass transit station it will be difficult to observe it. To capture this effect, we assess the heterogeneity of our findings by studying effects across subjects that live at different distances from the nearest Bay Area Rapid Transit (BART) station, BART being the primary mass transit system in the Bay Area for commuter trips. This allows us to explore different conditions under which substitution and complementarity between ride-hailing and mass transit can emerge. For example, by looking separately at the effect of lower ride-hailing prices on people who live far from the nearest BART station relative to those that live very close, we can see if the hypothesized complementarity due to increased connectivity or first/last mile linkage emerges.

Our results suggest that the impact of predicted future declines in ride-hailing costs on mass transit use (and therefore its energy impact) will not be homogenous across the population, nor will it be monotonic. It will vary significantly by how much the cost of ride-hailing changes and by the relative benefits of ride-hailing as an ingress or egress method for accessing mass transit, here examined based on how far away individuals live from a mass transit station.

We show that when the cost of ride-hailing drops sharply, it serves as a substitute for mass transit, whereas when it drops only moderately, the results are more mixed. There is evidence of significant and robust complementarity for participants that live medium to long distances away from a BART station (between 6 and 16 miles; see Figure I.3.1.3). These results suggest that forecasts of the impact of future price declines on mass

transit use (and on energy efficiency of the transportation sector in general) should pay close attention to the level of the price decline as well as the potential for geographic variation in effects.

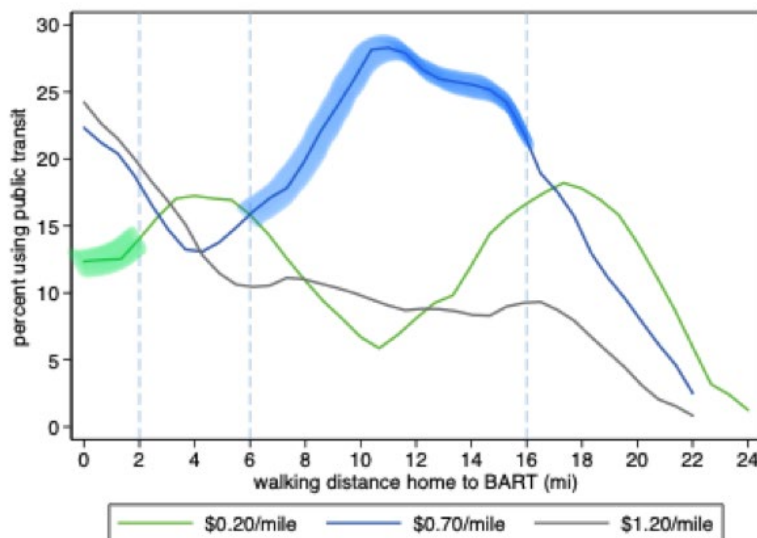


Figure I.3.1.3 Percent of households that choose mass transit, segmented by distance from residence to the nearest

Note: Highlighted portions represent sections of the graph for which the average effect within that distance range for that treatment group are statistically significantly different from the \$1.20/mile group in that same distance range. The portion highlighted in green suggests substitution between ride-hailing and mass transit, and the portion highlighted in blue suggests complementarity.

One explanation for our findings could be that at a moderate price drop, ride-hailing is not affordable enough to take regularly for the full commute, but rather it serves as a first/last mile link to a mass transit stop. Whereas at a very low price, ride-hailing is sufficiently inexpensive to completely replace mass transit for regular commutes.

The substitution effect at the \$0.20/mile appears to be driven entirely by those that live very close to BART. Figure I.3.1.3 helps demonstrate this. We see that for those living 0-2 miles from BART, those in the \$1.20/mile and \$0.70/mile report similar likelihood of using BART, however those in the \$0.20/mile group reported a significantly lower likelihood. This finding suggests that when there is substitution away from mass transit, it is likely to be concentrated among residents living close to mass transit.

Those that live very close to a BART station are, unsurprisingly, characterized by a higher underlying likelihood of using BART. Our data shows that those that live close to the BART are significantly more likely to use it than those that do not. Similarly, Figure I.3.1.3 shows that the reference category, the \$1.20/mile group, demonstrates the highest likelihood of selecting mass transit use when they are within 0-2 miles of the BART. Therefore, the significant substitution arises from the combination of high mass transit use by the reference category in the 0-2-mile range, and the distinct decline in the likelihood of selecting mass transit when participants are assigned to \$0.20/mile ride-hailing.

Our findings also show an uptick in mass transit use by those who live medium to longer distances away from the BART when price of ride-hailing is \$0.70/mile. At this price, which represents a moderate drop in prices relative to \$1.20/mile, the net effect results in ride-hailing being more of a complement to mass transit. It is possible that this effect is driven by participants who previously did not have a feasible, convenient, or affordable way of using the BART for their regular commute. Moderately priced ride-hailing can now help link participants to mass transit ports. Another way that ride-hailing can complement mass transit use is as a

failsafe to possible public transit outages, unpredictable or infrequent run times, or an unexpected need to quickly get home. With access to more affordable ride-hailing, people can now use mass transit with the assurance of having access to another convenient mode of travel when mass transit becomes unusable or doesn't fit an immediate need. This result is robust to accounting for actual mass transit use, suggesting that this complementarity is not just driven by non-users of mass transit who do not have experience using mass transit and are therefore, possibly making unrealistic projections of their behavior in a hypothetical setting where they have access to cheaper ride-hailing prices.

In sum, we find important heterogeneity and non-linearity in the price response of mass transit use to ride-hailing price variation: a steep drop in ride-hailing prices results in ride-hailing substituting for and crowding out mass transit, especially for those that live close to mass transit stations; however, ride-hailing can complement mass transit with moderate drops in ride-hailing prices, especially for those that live medium to longer distances from a mass transit station.

Life course as a contextual system to investigate the effects of life events, gender, and generation on travel mode use

It has been suggested that transportation mode choices are largely habitual (Clark et al. 2016). To effectively promote more energy-efficient modes, it is important to understand key factors associated with formation of and changes in travel behavior. Major life events—such as attending school, becoming employed, getting married, and having a child—can impact people's routine travel behavior and make them switch between available transportation modes (Clark et al. 2016; Oakil et al. 2016; Beige and Axhausen 2012). The dynamic changes and events within individual travelers' life contexts may cause these mode-use changes, but factors such as gender and generation may also have an influence. Consequently, many studies explore changes in travel choice associated with life events in relation to a rich set of internal and external contextual factors including socio-demographics (such as age, gender, employment type, household structure, and income) (Clark et al. 2016), travel attitudes towards flexibility and environment (Verplanken et al. 2008), and built environment and transportation infrastructure (Cervero 2002). However, most studies rely on short-term cross-sectional data and fail to capture time-varying factors at household or personal levels associated with the dynamics of travel choices over the longer term (Kitamura et al. 2009). Some studies investigating long-term trends use static life-cycle stages to contextualize travel decisions (Susilo et al. 2019), but these stages—as snapshots in time of a life course—are treated independently, without considering the dynamics present in the longer life history.

Recent studies propose to analyze the dynamics of travel choices over life courses from a longitudinal perspective, which requires more than cross-sectional data. Beige and Axhausen (2012; 2017), argue that the life course itself can be treated as a contextual system, because life events and their associated mobility-relevant choices are dynamically connected to individuals' past and future experiences and decisions. Research on mobility biography and life-oriented approaches (Zhang and Van Acker 2017; Oakil et al. 2014; Zhang and Chikaraishi 2014) and reviews by Rau and Manton (2016) and Beige and Axhausen (2017) recognize the interdependency of choices across various life domains and integrate the temporal dimensions into the analyses of long-term mobility in a comprehensive way. Although these emerging studies have begun to provide more of a life course perspective on the influence of life events on mobility choices, more is known about aggregated changes associated with life events and general trends over age, whereas less is understood about differences that may exist at the individual level.

We contribute to the mobility-related life course research by employing a data-driven approach to derive archetypal life course cohorts (Figure I.3.1.4) and examining the effects of different life events on mode use situated within different life trajectory contexts defined by these cohorts. We do this by applying a machine-learning approach called joint social sequence clustering (Pollock 2007) to patterns and timing of events in both family and career dimensions. We apply this method to data from the life history calendar portion of the Whole Traveler Transportation Behavior study survey conducted in the San Francisco Bay Area in 2018. We then estimate the marginal effects on the probability of different travel modes (driving, public transportation,

and walking or biking) associated with the following life event eras: attending school, being employed, living with a partner, and having a child. We investigate how these impacts differ across the life history context cohorts defined using the sequence clustering analysis, and we further disaggregate these impacts by gender and generation to understand how the prevalence of different life course trajectories changes based on these factors as well as how mode use is impacted by these differences.



Figure I.3.1.4 Life course patterns of family, career status, and mode use in five life course cohorts

Our results expand the understanding of the dynamics of travel choices to a longitudinal perspective defined by people's life courses, which cannot be captured with the cross-sectional data that are more traditionally used in life cycle stage analyses. We use the life course itself as a contextual system, enabling mobility decisions and their gender and generational differences to be evaluated for life events situated within a continuum of individuals' past and future experiences and decisions. Beyond the aggregated mode use patterns and changes associated with important life events, this paper contributes to understanding heterogeneity at the individual level by deriving five cohorts with distinctive life-trajectory patterns based on family and career socio-demographic dimensions.

Our aggregate results—averaged across our entire sample of Bay Area survey respondents—are largely consistent with results from the literature regarding the associations between regular mode use and select family and career events. However, the results from our life-trajectory cohort analysis suggest that such aggregate associations cannot fully capture subpopulation heterogeneity, and they enable us to offer novel insights based on a life course perspective.

Events that occur relatively early in life are more strongly associated with changes in mode use behavior compared with events that occur later. This is demonstrated by comparing the association of driving with life events for the Singles, Couples, and 'Have-it-all's' cohorts, which share important life-event similarities and thus enable specific associations to be isolated (Figure I.3.1.4). The literature suggests that, in aggregate, regular driving behavior changes owing to attending school (less driving) and working, partnering, and having children (more driving). However, for these three cohorts, only life events that are prevalent early (before age 35) are associated with changes in driving. All three cohorts have school as their earliest life event, and in all cases, school is associated with decreased driving. All three also have a similar pattern of early employment

associated with increased driving. Yet only two—Couples and ‘Have-it-alls’—are characterized by early partnering, and for only these two is partnering associated with increased driving. Finally, only ‘Have-it-alls’ are characterized by having children early, and only for this cohort is having children associated with increased driving.

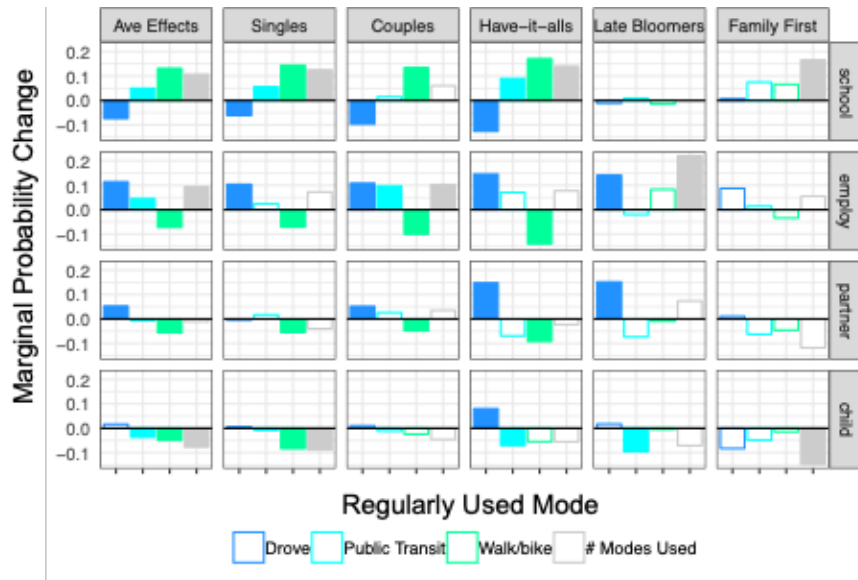


Figure I.3.1.5 Marginal effects of life events (indicated by row facet) on mode use by cohorts (indicated by column facet). Solid bars indicate values are statistically different from zero at the 10% level.

Beyond the timing of events, mode use can also be affected by the relative order of events. For example, Couples and Singles have children relatively late: when they first have children, members of both cohorts would largely be described as “middle-aged, married, and with children.” However, from a life course perspective, the Couples have lived with a partner for a much longer period than the Singles have when they have children, and having children has minimal impact on their travel modes. However, for Singles, having children reduces walking/biking and multimodality. In another example, Singles, Couples, and ‘Have-it-alls’ are employed relatively early in life (before their 30s), but public transit use only increases with employment for Couples, who typically live with a partner but have no children before 30.

The timing and order of life events can have lasting effects on mode use aggregated over entire life cycles. For example, ‘Have-it-alls’ are the only cohort whose driving habits are affected by all the life events considered here. This cohort generally follows a life trajectory of attending school → becoming employed → getting married → having children, all before turning age 35. Their car use increases at each life stage after finishing school, and they reach the highest level of car use earlier than all other cohorts. They also move to locations where public transit is less available when having children, which further increases their dependence on cars. Conversely, Singles only increase their car use when becoming employed, and their car use is minimally affected by family formation later in life. As a result, the Singles have relatively low car dependence over their life cycle. Late Bloomers are the overall least dependent on driving, probably because they have the highest life cycle unemployment rate, which may reduce their need and/or resources to drive.

Our gender analysis suggests that women drive more when having children only when their family formation and career formation are intertwined early in life (i.e., only in the ‘Have-it-alls’ cohort). In contrast to findings from existing literature, our results suggest that having children does not produce differential changes in regular mode use for women relative to men in cohorts characterized by children arriving later in life.

Lastly, we find generational differences in the choice of regularly used modes at the aggregate level are associated with heterogeneous life-event effects across cohorts (Figure I.3.1.5). In general, younger generations rely more on car use than older generations do during familial events when they have a late start to their careers. In contrast, in cohorts with careers starting before people's 30s, no significant generational difference in car use is estimated during these familial events.

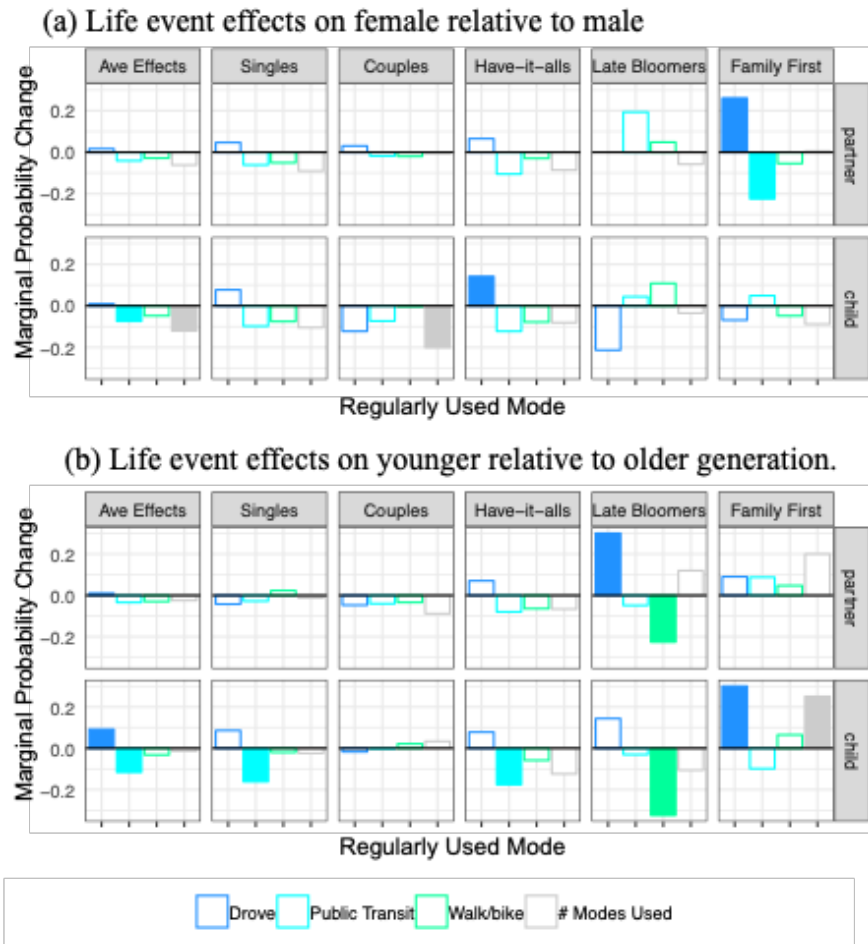


Figure I.3.1.6 Difference in the marginal effects of life events (indicated by row facets) on (a) women relative to men, and (b) on GenX (born in and after 1965) relative to older generation (born before 1965). Solid bars indicate values statistically different from zero at 10% level.

Our results highlight the potential effect of dynamically changing constraints and opportunities within individual travelers' life contexts on the choice of regularly used travel modes, including variation across genders and generations. Understanding these differences can help planners and policymakers better understand the tendencies and constraints faced by different individuals. This understanding might inform better predictions of mode use, and it might aid in designing or promoting policies related to commuting, public transit, or other travel behaviors.

Risk, Personality, Cost, or Household Tasks? Hypothesis Testing of Gender Differences in Plug-in Electric Vehicle Interest

Gender differences in plug-in electric vehicle (PEV) interest and adoption have been observed across several studies, covering a variety of regions and countries. In the context of the U.S., Carley et al. (2013) found an 11.5% gender gap in early interest in PEV for residents of major cities, with men substantially more likely to express interest. Findings from the 2012 California Plug-in Electric Vehicle Owner Survey indicated an even

wider gender difference in actual purchase behavior, with 71% of PEV owners being male (Center for Sustainable Energy, 2012). Similar differences have been observed outside the U.S.; Axsen et al. (2016) found 82% of early Canadian PEV adopters to be male, and surveying PEV users in Denmark and Sweden, Haustein and Jensen (2018) found 92% to be male.

Our analysis makes use of data collected through the 2018 Whole Traveler (WT) study, a survey of transportation preferences, choices, and behaviors of approximately 900 respondents in California's San Francisco Bay Area (Spurlock et al., 2019). Specifically, the WT survey asked about respondents' past, present, and potential future usage or interest in emerging transportation technologies and services, PEV, vehicle automation, and ride-hailing services. Additionally, survey questions covered a wide range of factors with the potential to influence interest in or adoption of particular modes of transportation, such as respondent's demographics, personalities, preferences respecting aspects of vehicle or transportation mode features.

Looking at all respondents in the WT dataset, we observe only a very low share of the population (i.e., less than 5%) had adopted PEV at the time of the WT survey; however, from the familiarity questions we also know who responded "interested in" owning or using PEV in the future. Therefore, we refer to respondent "interest in" rather than ownership of PEV throughout the analysis. There is a statistically significant difference in PEV interest between genders ($p < 0.01$); 63.5% of men and 48.8% of women express interest in owning a PEV in the future. Working with the same dataset, Spurlock et al. (2019) found significant gender differences in interest in PEV after accounting for such factors as income, age, and location.

The focus of our present analysis is to examine the factors underlying the lower rate of interest in plug-in electric vehicles, either hybrid or fully electric, observed among female respondents to WT survey, as well as in previous research. We describe four hypotheses for gendered drivers of vehicle technology interest and adoption, summarized as: 1) risk and safety preferences, 2) personality factors, 3) willingness-to-pay differences, 4) differences in transportation-related tasks and requirements. To test the relevance of these hypotheses to the observed patterns interest in PEV within the WT dataset, we perform means comparisons and logit regression on an extensive set of key variables.

With respect to gender, the WT survey provided a third option as "Other" in addition to the binary classification of female and male, as well as the option not to report a gender. However, as less than 1% of respondents selected an option other than "male" or "female," in this paper we use a binary description of gender (i.e., female or male) due to analytical expediency. For nuanced discussion of the spectrum of gender, see, e.g., Kurani et al. (2018), for its treatment within the context of transportation research.

HYPOTHESES

In generating testable hypotheses, we built on several strands of transportation literature, including research on the interface between psychology and environmental behaviors, economics, gender studies, etc. We ultimately investigated four hypotheses regarding factors that could plausibly impact PEV interest and explain the difference in PEV interest between genders. These specific hypotheses—detailed below—can be summarized as: (H1) women are less interested in PEV because they are more risk averse ("Risk and Safety"); (H2) women are less interested in PEV because of differences in key personality traits ("Personality Factors"); (H3) women are less interested in PEV because of a lower willingness to pay for such technology ("Willingness to Pay"); and (H4) women are less interested in PEV because of gendered preferences or requirements in vehicle and mode features ("Transportation Preferences"). We note that each of our hypotheses includes two parts: 1) that there is a gendered difference in key variables (e.g., expressed importance of safety in transportation mode choice, in reference to H1), and 2) that the key variables are predictive of interest in PEV. This formulation in some respects follows the conceptualization of Luchs and Mooradian (2012).

RESULTS

Means Comparisons Between Men and Women

To test the first segment of the hypotheses (i.e., that there are gendered differences in the key variables), we perform t-tests comparing male and female sample means for the set of variables described above. Decision-Making: Table I.3.1.1 summarizes our findings for the variables related to H1 and H4, for which we additionally discuss any impact of children in the respondent's household. Table I.3.1.2 summarizes our findings for H2 and H3. Except for several of the variables included for H3, we find significant gender differences in most key variables, supporting the second linkage of the hypotheses.

Table I.3.1.2 Means Comparisons: Hypotheses 1 and 4

	Key Variables	Means difference (Female, Male, T-stat, discussion)	
		Means, T	Interpretation
H1: Risk and Safety	Risk averse (monetary)	F: 0.594, M: 0.468, t: 3.87***	A larger proportion of women than men are (monetarily) risk averse. This finding is mitigated by the presence of children in the household, with a smaller difference in sample average rate between women and men with children than those without.
	Safety importance index	F: 4.38, M: 4.22, t: 2.47**	Women score significantly higher on the index of safety importance, indicating an aversion to risks to physical safety. This finding is mitigated by the presence of children in the household, with a smaller difference in index score between women and men with children than those without.
	Vehicle safety rating	F: 3.81, M: 3.53, t: 2.20**	Primary vehicles driven by women have significantly higher safety ratings than those of men. This finding is mitigated by the presence of children in the household, with a smaller difference between women and men with children than those without.
H4: Transport Preferences	Child(ren) in household	F: 0.18, M: 0.13, t: 1.84*	A significantly higher proportion of women than men have a child in their household.
	Child transport importance index	F: 3.04, M: 2.56, t: 2.84***	Women place significantly higher value on the capability to safely transport a young child. Women with children more strongly value child transport than men with children, but not significantly so.
	Multiple stops importance index	F: 3.41, M: 2.99, t: 4.47***	Women place significantly higher value on the ability to make multiple stops while traveling. Women with children more strongly value the ability to make multiple stops than men with children, but not significantly so.
	Short travel time importance index	F: 4.42, M: 4.31, t: 1.89*	Women place significantly higher value than men on having a short commute duration. Women with children more strongly value a short commute than men with children, but not significantly so.
	Number of vehicle seats	F: 5.24, M: 5.10, t: 2.03**	Women's vehicles have a significantly higher number of seats than those of men. This finding is exacerbated by the presence of children in the household; women with children have a significantly higher number of seats than men with or without children.
	Vehicle cargo capacity	F: 37.75, M: 30.99, t: 2.66***	Women's vehicles have significantly higher cargo capacity than those of men. This finding is exacerbated by the presence of children in the household; women with children have the highest cargo capacity of any group, significantly so.
	Primary commute distance	F: 12.01, M: 14.49, t: 2.00**	Women have significantly shorter primary commute distances compared to men. This finding is exacerbated by the presence of children in the household; the difference between women's and men's commute distances is greater for respondents with young children.

Table I.3.1.3 Means Comparisons: Hypotheses 2 and 3

	Key Variables	Means difference (Female, Male, T-stat, discussion)	
		Means, T	Interpretation
H2: Personality Factors	Openness	F: 3.69, M: 3.55, t: 2.53**	Women score significantly higher on the Openness index.
	Neuroticism	F: 2.83, M: 2.49, t: 5.62***	Women score significantly higher on the Neuroticism index.
	Extraversion	F: 3.20, M: 3.01, t: 2.89***	Women score significantly higher on the Extraversion index.
	Agreeableness	F: 3.82, M: 3.67, t: 3.19***	Women score significantly higher on the Agreeableness index.
	Conscientiousness	F: 4.11, M: 3.86, t: 4.78***	Women score significantly higher on the Conscientiousness index.
H3: Willingness to Pay	Income bin	F: 7.48, M: 8.17, t: -4.33***	Women have significantly lower household income than men.
	Discount factor (monetary)	F: 0.79, M: 0.79, t: -0.12	There is no significant difference in discount factor between men and women.
	Low cost importance index	F: 3.90, M: 3.80, t: 1.37	Women place higher value on low cost, but not significantly so.
	Predictable cost importance index	F: 3.80, M: 3.71, t: 1.09	Women place higher value on predictable cost, but not significantly so.
	Used vehicle	F: 0.41, M: 0.37, t: 1.17	Women are more likely to drive a vehicle purchased used, but not significantly so.

Table I.3.1.3 presents the results of our logit analyses, in terms of odds ratios, such that a value greater than 1 represents a positive relationship between interest in PEV and the variable, while a value less than 1 indicates a negative relationship. For variables included in both models, we report the odds ratios and significance levels from Model 1 in Table I.3.1.3 reported are for all variables that were included in both models due to the substantially larger sample size of the model ($n = 759$ vs. $n = 456$); odds ratios and significance are for these variables are were found to be similar between the two models. We note that the odds ratio is a transformation of the logit regression coefficient, which does not impact the level of significance. It is important to note that the relationships between outcome and explanatory variables are not necessarily linear and may differ when computed for upper and lower limits of the sample distribution. Of interest are any variables for which one of the following conditions holds: significant trend in variable marginal effects in logit combined with significant mean difference by gender. We elaborate on these instances in the discussion to follow.

Table I.3.1.4 Logit Results (odd ratios) by Hypothesis

Hypothesis	Variables Selected	Odds Ratio
H1: Risk and safety	Risk averse (monetary)	1.129
	Safety importance index	0.908
	Vehicle safety rating	0.939
H2: Personality factors	BFI Openness score	1.119
	BFI Neuroticism score	1.024
	BFI Extraversion score	1.026
	BFI Agreeableness score	1.312**
H3: Willingness to pay	BFI Conscientiousness score	0.785**
	Income level	1.164***
	Discount factor	1.052
	Low cost importance index	0.908
	Predictable cost importance index	0.818**
H4: Transport preferences	Used vehicle	1.007
	Multiple stops importance index	0.874**
	Presence of child(ren) in household	1.171
	Short travel time importance index	1.200*
	Child transport importance index	0.896*
	Number of vehicle seats	0.794
	Vehicle cargo capacity	0.997
Primary commute distance	0.999	

Notes: Age and location control variables are not reported. *** $p < 0.01$, ** $p < 0.05$, * $p < 0.1$.

DISCUSSION

We now review our analysis results for interest in PEV, evaluating the evidence for each of our four hypotheses. We do not find evidence supporting H1; none of the key variables for this hypothesis are significant and odds ratios are all quite close to 1. For H2, we find two significant variables, one with the expected relationship, but one that runs counter to expectations. However, we find several significant variables among the sets representing H3 and H4.

Hypothesis 1 – Risk and Safety: While we demonstrated significant relationships between gender and the three variables representing this hypothesis (with females averaging higher values than males), none of them meet traditional levels of significance for predicting PEV interest within our logit models. Two of the variables (safety importance index and vehicle safety rating), have odds ratios less than one, which if significant, would have helped to explain the gender gap in PEV interest.

Hypothesis 2 – Personality Factors: We previously demonstrated significant relationships between gender and all five personality factors, with women averaging higher values than men in all cases. Two personality factors are statistically significant in our logit predictions of PEV interest. The odds ratio over 1 for agreeableness agrees with findings from literature we reviewed, but suggests that scoring highly in this aspect of personality in fact increases women's interest in PEV. We find an odds ratio below 1 for conscientiousness, which was not anticipated based on review of literature, but does contribute to explaining a portion of the gender gap in PEV interest.

Hypothesis 3 – Willingness to Pay: We find two significant variables from the group we use to represent this hypothesis: income level and importance of predictable cost. The odds ratio for income is greater than 1, meaning that men's tendency to have significantly greater income levels contribute to the gender gap. While we did not anticipate the odds ratio under 1 that we found, in combination with our previous finding of higher values of the predictable cost variable for women, this finding is also suggestive of supposition that lower female willingness or ability to pay contribute to gendered differences in PEV interest.

Hypothesis 4 – Transport Preferences: We previously identified significant relationships between gender and all variables related to transport preferences and vehicle features, with women on average scoring importance variables higher than men, driving larger vehicles than men, and commuting shorter distances than men. Of these variables, three are significant within our regressions. The odds ratio greater than 1 on the preference for short travel time suggests that scoring highly in this preference is associated with increased interest in PEV. The other two variables, the importance of making multiple stops and the importance of safely transporting a child, are negatively associated with PEV interest while positively associated with female gender, providing support for the idea that a misalignment between women’s household-related tasks and perceptions of PEV’s suitability may contribute to the PEV interest gender gap.

Conclusions

These findings reveal multiple nuanced relationships among transportation choices and their costs and benefits at the individual and system levels. One example is that of e-commerce, where timesaving and convenience benefits of ordering with delivery rather than taking a shopping trip have, in part, helped to spur significant expansion of this type of commerce in the U.S. in recent years. However, while it’s true that on balance we find e-commerce replaces more trips than it adds in delivery activity, there is significant variation across the population in this behavior. Higher-income households and households with children were relatively more likely to choose delivery. However, on the other hand, the time-saving motivation for these categories of households did not translate through to these deliveries being relatively more likely to substitute for shopping trips. Indeed, prepared meal purchase behavior is an interesting case. Households with children (by 15 percentage points) and higher-income households (by 12 percentage points) are significantly more likely to have prepared meal delivery supplement trips relative to their counterparts. This speaks to the fact that increased convenience and time-saving aspects of emerging transportation innovations like e-commerce (and ride-hailing in the example above) can in some cases remove the need for personal vehicle trips and thus increase efficiency and sustainability in the transportation system, but at other times can induce demand for further transportation or delivery vehicle use. In the case of meal delivery, getting a meal delivered may actually be a substitute for cooking at home, rather than a substitute for a trip to a restaurant. Indeed, higher income households are more likely to order prepared meal delivery relative to lower income households, but actually significantly less likely (by 16 percentage points) to substitute the delivery for a vehicle trip relative to lower income households. These results suggest that the marginal activities for those that are either more time constrained or have a higher opportunity cost of time isn’t necessarily the time it takes to make a shopping trip, but appears more so to be the time involved in other activities, such as preparing meals.

The relationships associated with ride-hailing is another prominent example. The benefits of ride-hailing to passengers and drivers have spurred rapid growth in this service. Yet the interaction of ride-hailing with other transportation modes is complicated. Ride-hailing may link with and increase the use of mass transit, thereby reducing overall car use and system-wide energy consumption. However, the tendency of ride-hailing to complement or substitute for mass transit may depend on the relative costs of transportation modes, the individual benefits of ride-hailing for accessing mass transit, and the value individual travelers place on their travel time.

Some projections about the future of transportation paint a picture of relatively extreme transformation. For example, Arbib and Seba (2017) suggest that 95% of all person-miles-traveled will be via transportation-as-a-service (i.e., ride-hailing or similar), and Walker and Johnson (2016) suggest that the United States will hit peak car ownership rates in 2020 and that by 2035 the rate of car ownership will be more than cut in half. If these projections are accurate, then the implications of the above-described benefits and costs of ride-hailing in the system are likely to be enormous. However, there are potential barriers faced by large portions of the population that might limit the extent to which the system can transform.

The detailed demographic analyses enabled by the Whole Traveler study uncover multifaceted interactions between human characteristics and transportation choices. A few interesting associations between demographic groups and the adoption of or interest in various options were found. In particular it was found

that women were significantly less likely to be interested in adopting PEV and automated vehicle technologies (Spurlock et al. 2019). Women play a major role in vehicle purchase decisions, making the currently observed gender gap in interest and adoption of PEV of relevance to all those involved with the evolving landscape of the U.S. transportation sector. A variety of factors play a role in the gender gap in PEV interest. Some of these factors, such as personality attributes, are connected to the innate natures of prospective vehicle purchasers, and therefore may not be likely to change as significantly as some might expect as technology and policies evolve. However, many of the factors we examine can be impacted by manufacturer or policymaker actions (e.g., cost-related factors, vehicle size).

Particularly novel results which speak to barriers to a full-scale transition to the levels of ride-hailing use and reduced reliance on personal vehicles that were suggested by Arbib and Seba (2017) and Walker and Johnson (2016) emerge from the analysis of how lifecycle and life-event impact transportation choices. Transportation behaviors change in response to life events, and can change over time. For example, a child in the home is associated with a household owning more cars overall and making less use of mass transit and walking or biking. These findings reflect a fundamental set of underlying needs and constraints which may inhibit households from being able to transition to very high levels of transportation-as-a-service without vehicle ownership.

Further insights were gained regarding how life-cycle context interplays with the impact children have on transportation choices. Events occurring early in life are most strongly associated with changes in mode-use behavior and mode use can be affected by the order of events. This timing-and-order effect can have lasting repercussions on mode use, and resulting energy consumption, aggregated over an entire life. For example, “Have-it-all” (close to 20% of the sample) who finish their education, start working, partner up, and have children early in life, increase their car use at each step after finishing school, and have the highest rate of car use occurring the earliest of all the cohorts analyzed. This set of findings suggests that fundamental lifestyle and family choices are likely to have lasting impacts on transportation patterns, which may have significant on whether we will adopt a transportation regime defined by extremely low vehicle ownership and high reliance on transportation services.

Key Publications

Submitted for publication and under review

1. Taylor, Margaret, K. Sydney Fujita, Annika Todd, Yulei Shelley He, Victor Walker, Andrew Duvall, Gabrielle Wong-Parodi, Ling Jin, James Sears, Ted Kwasnik and C. Anna Spurlock. “The Whole Traveler Transportation Behavior Survey: Decision-Making Data related to Transportation Energy Use in the San Francisco Bay Area.” (Under review at Transportation)
2. Spurlock, C. Anna, Annika Todd, Gabrielle Wong-Parodi, Victor Walker. “Children, Income, and the Impact of Home-Delivery on Household Shopping Trips.” (Under review at Transportation Research Record)
3. Jin, Ling, Alina Lazar, James Sears, Annika Todd, Alexander Sim, Kesheng Wu, C. Anna Spurlock. “Life Course as a Contextual System to Investigate the Effects of Life Events, Gender, and Generation on Travel Mode Use.” (Under review at Transportation Research Record)

Published

1. Spurlock, C. Anna, James Sears, Gabrielle Wong-Parodi, Victor Walker, Ling Jin, Margaret R. Taylor, Andrew Duvall, Anand Gopal, Annika Todd. 2019. “Describing the users: Understanding adoption of and interest in shared, electrified, and automated transportation in the San Francisco Bay Area.” Transportation Research Part D (In Press) DOI: <https://doi.org/10.1016/j.trd.2019.01.014>

2. Lazar, Alina, Ling Jin, C. Anna Spurlock, Annika Todd, Kesheng Wu and Alex Sim. 2019. "Evaluating the Effects of Missing Values and Mixed Data Types on Social Sequence Clustering Using t-SNE Visualization." *Journal of Data and Information Quality (JDIQ)* 11(2): 7. DOI: <https://doi.org/10.1145/3301294>
3. Lazar, Alina, Ling Jin, C. Anna Spurlock, Annika Todd, Kesheng Wu, Alex Sim. 2017. "Data Quality Challenges with Missing Values and Mixed Types in Joint Sequence Analysis." 2017 IEEE International Conference on Big Data. DOI: <https://doi.org/10.1109/BigData.2017.8258222>

References

1. Arbib, James, and Tony Seba. "Rethinking Transportation 2020-2030." *RethinkX, May* (2017).
2. Axsen, Jonn, Suzanne Goldberg, and Joseph Bailey. "How might potential future plug-in electric vehicle buyers differ from current "Pioneer" owners?" *Transportation Research Part D: Transport and Environment* 47 (2016): 357-370.
3. Beige, Sigrun, and Kay W. Axhausen. "Interdependencies between turning points in life and long-term mobility decisions." *Transportation* 39, no. 4 (2012): 857-872.
4. Beige, Sigrun, and Kay W. Axhausen. "The dynamics of commuting over the life course: Swiss experiences." *Transportation Research Part A: Policy and Practice* 104 (2017): 179-194.
5. Brown, Alan, and Angus Deaton. "Surveys in applied economics: models of consumer behaviour." *The Economic Journal* 82, no. 328 (1972): 1145-1236.
6. Cao, Xinyu, Frank Douma, and Fay Cleaveland. "Influence of e-shopping on shopping travel: evidence from Minnesota's Twin Cities." *Transportation Research Record* 2157, no. 1 (2010): 147-154.
7. Carley, Sanya, Rachel M. Krause, Bradley W. Lane, and John D. Graham. "Intent to purchase a plug-in electric vehicle: A survey of early impressions in large US cities." *Transportation Research Part D: Transport and Environment* 18 (2013): 39-45.
8. Center for Sustainable Energy. "California Plug-in Electric Vehicle Owner Survey." (2012). Retrieved from <https://energycenter.org/sites/default/files/docs/nav/policy/research-and-reports/California Plug-in Electric Vehicle Owner Survey Report-July 2012.pdf>
9. Cervero, Robert. "Built environments and mode choice: toward a normative framework." *Transportation Research Part D: Transport and Environment* 7, no. 4 (2002): 265-284.
10. Chintagunta, Pradeep K., Junhong Chu, and Javier Cebollada. "Quantifying transaction costs in online/off-line grocery channel choice." *Marketing Science* 31, no. 1 (2012): 96-114.
11. Chu, Junhong, Pradeep Chintagunta, and Javier Cebollada. "Research note—a comparison of within-household price sensitivity across online and offline channels." *Marketing Science* 27, no. 2 (2008): 283-299.
12. Clark, Ben, Kiron Chatterjee, and Steve Melia. "Changes to commute mode: The role of life events, spatial context and environmental attitude." *Transportation Research Part A: Policy and Practice* 89 (2016): 89-105.
13. Consumer Reports. *Consumer Reports: Cars* (2019). Retrieved from <https://www.consumerreports.org/cars->

14. Darian, Jean C. "In-home shopping: are there consumer segments?" *Journal of retailing* (1987).
15. Ding, Yu, and Huapu Lu. "The interactions between online shopping and personal activity travel behavior: an analysis with a GPS-based activity travel diary." *Transportation* 44, no. 2 (2017): 311-324.
16. Erhardt, Gregory D., Sneha Roy, Drew Cooper, Bhargava Sana, Mei Chen, and Joe Castiglione. "Do transportation network companies decrease or increase congestion?." *Science advances* 5, no. 5 (2019): eaau2670.
17. Ferrell, Christopher E. "Home-based teleshopping and shopping travel: Where do people find the time?" *Transportation Research Record* 1926, no. 1 (2005): 212-223.
18. Harris, Patricia, Francesca Dall'Olmo Riley, Debra Riley, and Chris Hand. "Online and store patronage: a typology of grocery shoppers." *International Journal of Retail & Distribution Management* 45, no. 4 (2017): 419-445.
19. Haustein, Sonja, and Anders Fjendbo Jensen. "Factors of electric vehicle adoption: A comparison of conventional and electric car users based on an extended theory of planned behavior." *International Journal of Sustainable Transportation* 12, no. 7 (2018): 484-496.
20. Jin, Scarlett T., Hui Kong, Rachel Wu, and Daniel Z. Sui. "Ridesourcing, the sharing economy, and the future of cities." *Cities* 76 (2018): 96-104.
21. Kehily, Mary Jane, Lydia Martens, Kate Burningham, Susan Venn, Ian Christie, Tim Jackson, and Birgitta Gatersleben. "New motherhood: a moment of change in everyday shopping practices?" *Young Consumers* (2014).
22. Kelley Blue Book. Kelley Blue Book: Car Reviews. (2019). Retrieved September 20, 2007, from <https://www.kbb.com/car-reviews/>
23. Kitamura, Ryuichi, Toshio Yoshii, and Toshiyuki Yamamoto, eds. *Expanding Sphere of Travel Behaviour Research: Selected Papers from the 11th International Conference on Travel Behaviour Research*. Emerald Group Publishing, 2009.
24. Kurani, Kenneth S., Nicolette Caperello, and Jennifer TyreeHageman. "Are We Hardwiring Gender Differences into the Plug-in Electric Vehicle Market?" (2018). Retrieved from https://ncst.ucdavis.edu/wp-content/uploads/2016/10/NCST-Report-Kurani_Gender-Differences-in-PEV-Market_Final-Report_MAR-2018-2.pdf
25. Kwan, Mei-Po. "Gender differences in space-time constraints." *Area* 32, no. 2 (2000): 145-156.
26. Lansing, John B., and James N. Morgan. "Consumer finances over the life cycle." *Consumer behavior* 2, no. 4 (1955): 36-50.
27. Lee, Richard J., Ipek N. Sener, Patricia L. Mokhtarian, and Susan L. Handy. "Relationships between the online and in-store shopping frequency of Davis, California residents." *Transportation Research Part A: Policy and Practice* 100 (2017): 40-52.
28. Luchs, Michael G., and Todd A. Mooradian. "Sex, personality, and sustainable consumer behaviour: Elucidating the gender effect." *Journal of Consumer Policy* 35, no. 1 (2012): 127-144.
29. McGuckin, N., and A. Fucci. *Summary of Travel Trends: 2017 National Household Travel Survey*. Publication FHWA-PL-18-019. FHWA, U.S. Department of Transportation (2018).

30. Oakil, Abu Toasin Md, Dick Ettema, Theo Arentze, and Harry Timmermans. "Changing household car ownership level and life cycle events: an action in anticipation or an action on occurrence." *Transportation* 41, no. 4 (2014): 889-904.
31. Oakil, Abu Toasin Md, Dorien Manting, and Hans Nijland. "Dynamics in car ownership: the role of entry into parenthood." *European Journal of Transport and Infrastructure Research* 16, no. 4 (2016).
32. Pollock, Gary. "Holistic trajectories: a study of combined employment, housing and family careers by using multiple-sequence analysis." *Journal of the Royal Statistical Society: Series A (Statistics in Society)* 170, no. 1 (2007): 167-183.
33. Rapier, Graham. *Your Uber Ride Could Get 80% Cheaper over the next Decade*. Business Insider. May, 2019. Retrieved from: www.businessinsider.com/uber-lyft-fare-prices-could-fall-by-80-ubs-estimate-2019-5. Accessed on June 26th, 2019.
34. Rau, Henrike, and Richard Manton. "Life events and mobility milestones: Advances in mobility biography theory and research." *Journal of Transport Geography* 52 (2016): 51-60.
35. Sabatini, Fabio. *Can a click buy a little happiness? The impact of business-to-consumer e-commerce on subjective well-being*. Publication No. 12/2011. Economics and Econometrics Research Institute, 2011.
36. Salomon, Ilan. "Telecommunications and travel relationships: a review." *Transportation Research Part A: General* 20, no. 3 (1986): 223-238.
37. Salomon, Ilan. "Telecommunications and travel: substitution or modified mobility?" *Journal of transport economics and policy* (1985): 219-235.
38. Sim, Loo Lee, and Sze Miang Koi. "Singapore's Internet shoppers and their impact on traditional shopping patterns." *Journal of retailing and consumer services* 9, no. 2 (2002): 115-124.
39. Spurlock, C. Anna, James Sears, Gabrielle Wong-Parodi, Victor Walker, Ling Jin, Margaret Taylor, Andrew Duvall, Anand Gopal, and Annika Todd. "Describing the users: Understanding adoption of and interest in shared, electrified, and automated transportation in the San Francisco Bay Area." *Transportation Research Part D: Transport and Environment* 71 (2019): 283-301.
40. Statista. *Number of Amazon Prime members in the United States as of December 2018 (in millions)*. April, 2019. <https://www.statista.com/statistics/546894/number-of-amazon-prime-paying-members/>. Accessed on June 21, 2019.
41. Suel, Esra, and John W. Polak. "Development of joint models for channel, store, and travel mode choice: Grocery shopping in London." *Transportation Research Part A: Policy and Practice* 99 (2017): 147-162.
42. Susilo, Yusak O., Chengxi Liu, and Maria Börjesson. "The changes of activity-travel participation across gender, life-cycle, and generations in Sweden over 30 years." *Transportation* 46, no. 3 (2019): 793-818.
43. Tonn, Bruce E., and Angela Hemrick. "Impacts of the use of e-mail and the Internet on personal trip-making behavior." *Social Science Computer Review* 22, no. 2 (2004): 270-280.
44. U.S. Census Bureau. *U.S. Census Bureau News: Quarterly Retail E-Commerce Sales 4th Quarter 2012*. Publication CB13-24. U.S. Census Bureau, U.S. Department of Commerce, 2013.

45. U.S. Census Bureau. *U.S. Census Bureau News: Quarterly Retail E-Commerce Sales 4th Quarter 2017*. Publication CB18-21. U.S. Census Bureau, U.S. Department of Commerce, 2018.
46. Verplanken, Bas, Ian Walker, Adrian Davis, and Michaela Jurasek. "Context change and travel mode choice: Combining the habit discontinuity and self-activation hypotheses." *Journal of Environmental Psychology* 28, no. 2 (2008): 121-127.
47. Wagner, Janet, and Sherman Hanna. "The effectiveness of family life cycle variables in consumer expenditure research." *Journal of Consumer Research* 10, no. 3 (1983): 281-291.
48. Walker, Jonathan, and Charlie Johnson. "Peak car ownership: the market opportunity of electric automated mobility services." *Rocky Mountain Institute* (2016). Retrieved from: http://www.rmi.org/peak_car_ownership
49. Weltevreden, Jesse WJ, and Ton van Rietbergen. "E-Shopping versus City Centre Shopping: The Role of Perceived City Centre Attractiveness." *Tijdschrift voor economische en sociale geografie* 98, no. 1 (2007): 68-85.
50. Weltevreden, Jesse WJ, and Ton van Rietbergen. "The implications of e-shopping for in-store shopping at various shopping locations in the Netherlands." *Environment and Planning B: Planning and Design* 36, no. 2 (2009): 279-299.
51. Zhang, Junyi, and Veronique Van Acker. "Life-oriented travel behavior research: An overview." *Transportation Research Part A: Policy and Practice* 104, (2017): 167-178.
52. Zhang, Junyi, Biying Yu, and Makoto Chikaraishi. "Interdependences between household residential and car ownership behavior: a life history analysis." *Journal of Transport Geography* 34 (2014): 165-174.
53. Zhou, Yiwei, and Xiaokun Cara Wang. "Explore the relationship between online shopping and shopping trips: an analysis with the 2009 NHTS data." *Transportation Research Part A: Policy and Practice* 70 (2014): 1-9.

I.3.2 Analyze the Spatial Distribution and Impacts of One-way Car-Sharing Programs on Transit Ridership and Energy Use (LBNL)

Tom Wenzel, Principal Investigator

Lawrence Berkeley National Lab
1 Cyclotron Road
Berkeley, CA 94720
E-mail: tpwenzel@lbl.gov

Susan Shaheen, Principal Investigator

Lawrence Berkeley National Lab
1 Cyclotron Road
Berkeley, CA 94720
E-mail: sshaheen@berkeley.edu

Prasad Gupte, DOE Technology Manager

U.S. Department of Energy
E-mail: prasad.gupte@ee.doe.gov

Start Date: October 1, 2018

End Date: September 30, 2019

Project Funding (FY19): \$50,000

DOE share: \$50,000

Non-DOE share: \$0

Project Introduction

This project aimed to shed light on the spatial distribution of shared mobility impacts as measured with one-way carsharing. In support of this task, researchers previously conducted a survey of car2go members, which contains information on how members changed their behavior as a result of car2go. The survey was conducted in five North American cities, including Washington DC, San Diego, Seattle, Vancouver, and Calgary. The survey data included information on mode shift, household vehicle shedding, household vehicle suppression (not acquiring a vehicle), and changes in driving. The survey also collected information on home and work location, which has been geocoded to intersections and also to census tracts. Researchers also have information on individual trip data in the five cities. This includes data on the distribution of a year's worth of vehicle activity, consisting of origins, destinations, trip time, and vehicle miles traveled.

Researchers have also made an effort to assemble data describing land use and transit infrastructure attributes. This includes data describing transit routes, density of access points (e.g., bus stops), headways (i.e., frequency of service) and land use patterns (e.g., density of road networks, population and employment density) within the cities where the survey was conducted. When combined with survey derived impact data, researchers have sought to understand the member and urban environmental attributes that predict key impacts, and better understand where such systems may substitute and compliment conventional public transit systems. This began with an examination of the spatial distribution of users and individual trips to evaluate how the participation in car2go impacts changes in walking, bicycling, vehicle ownership, and VMT, and further, how those impacts are associated with existing public transit infrastructure, demographics, and land use patterns.

Objectives

The objective of the project is to produce a richer understanding of the spatial distribution of impacts from shared mobility systems. While recent research has produced a stronger understanding of the general magnitude and direction of one-way carsharing impacts, the spatial distribution of such impacts within an urban region are less well understood. Furthermore, the attributes that influence those impacts are also poorly understood. This is partially a function of the fact that the data needed to bring together these insights are difficult to assemble. Such analysis requires a unique data set that characterizes the impacts with a high degree of spatial resolution. It also requires the assembly of land-use and transit system attributes with a similar

degree of spatial resolution that can be correlated with these impacts. The confluence of these datasets is challenging, but can yield enhanced understanding of where one-way carsharing is most impactful, and the types of environments in which one-way carsharing may play a more supportive role in enabling beneficial impacts.

Approach

The approach of this project was to geocode data from surveys collected on car2go members. We geocoded home locations collected in the form of city and intersections. The survey data documented impacts of car2go on rail and bus use, walking, and vehicle ownership. These geocoded impacts were joined with census tracts and mapped on interactive application. The application permitted the creation of maps that could be used for the examination of the spatial distribution of impacts by car2go users. This application enabled researchers to visualize the regions of the city where specific impacts were likely to occur. It further informed researchers of patterns that could be further verified via modeling.

The survey observations were joined with external data sources that described the characteristics of the census tract in which the survey respondent resided. These included land-use and population attributes as well transit system attributes such as the presence of rail stations and the density of bus stops. These attributes, along with the attributes of the individual respondent, were aligned in a logistic model and used to estimate the probability of the impacts observed in the survey. The objective of this model was to produce a model of reasonable re-prediction accuracy that could then be applied to other regions without one-way carsharing to predict impacts on car ownership and mode shift within the metropolitan region.

Results

The spatial analysis of survey data found that impacts were distributed differently within the evaluated cities. For example, the results showed that vehicle shedding was generally concentrated in the core of the city, while personal vehicle suppression (the avoidance of purchasing a car) was more commonly distributed through the periphery of metropolitan regions. Figure I.3.2.1 shows the distribution of impacts for shedding across the five cities evaluated, which included Washington DC, Seattle, Vancouver, San Diego, and Calgary. Shedding activity was limited within the sample, but in several cities, certain tracts had a notably higher concentration of respondents reporting shedding due to car2go. One prominent example was Washington DC, but higher concentrations of vehicle shedding were also seen in Vancouver, Calgary, and San Diego. Shedding impacts were more evenly dispersed in Seattle.

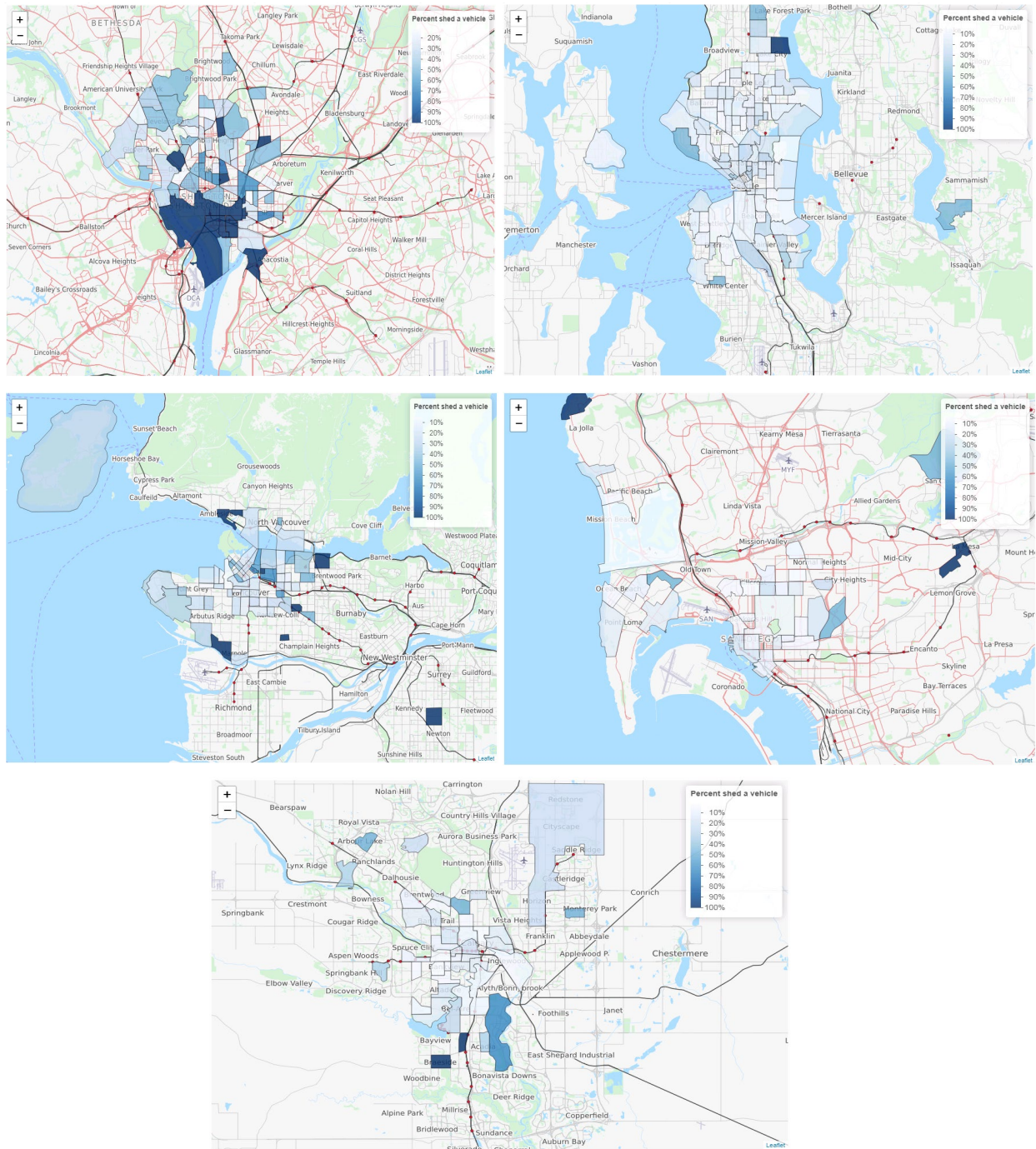


Figure I.3.2.1 Spatial Distribution of Vehicle Shedding

Figure I.3.2.2 shows a spatial distribution of personal vehicle suppression for the five evaluated cities. The spatial patterns of personal vehicle suppression are more prominently on the periphery of each of the urban regions. While suppression was noted throughout each city, concentrations were found more on the edge than the urban core. This finding was generally consistent for all cities in the study, though more prominent in the Canadian versus American cities.

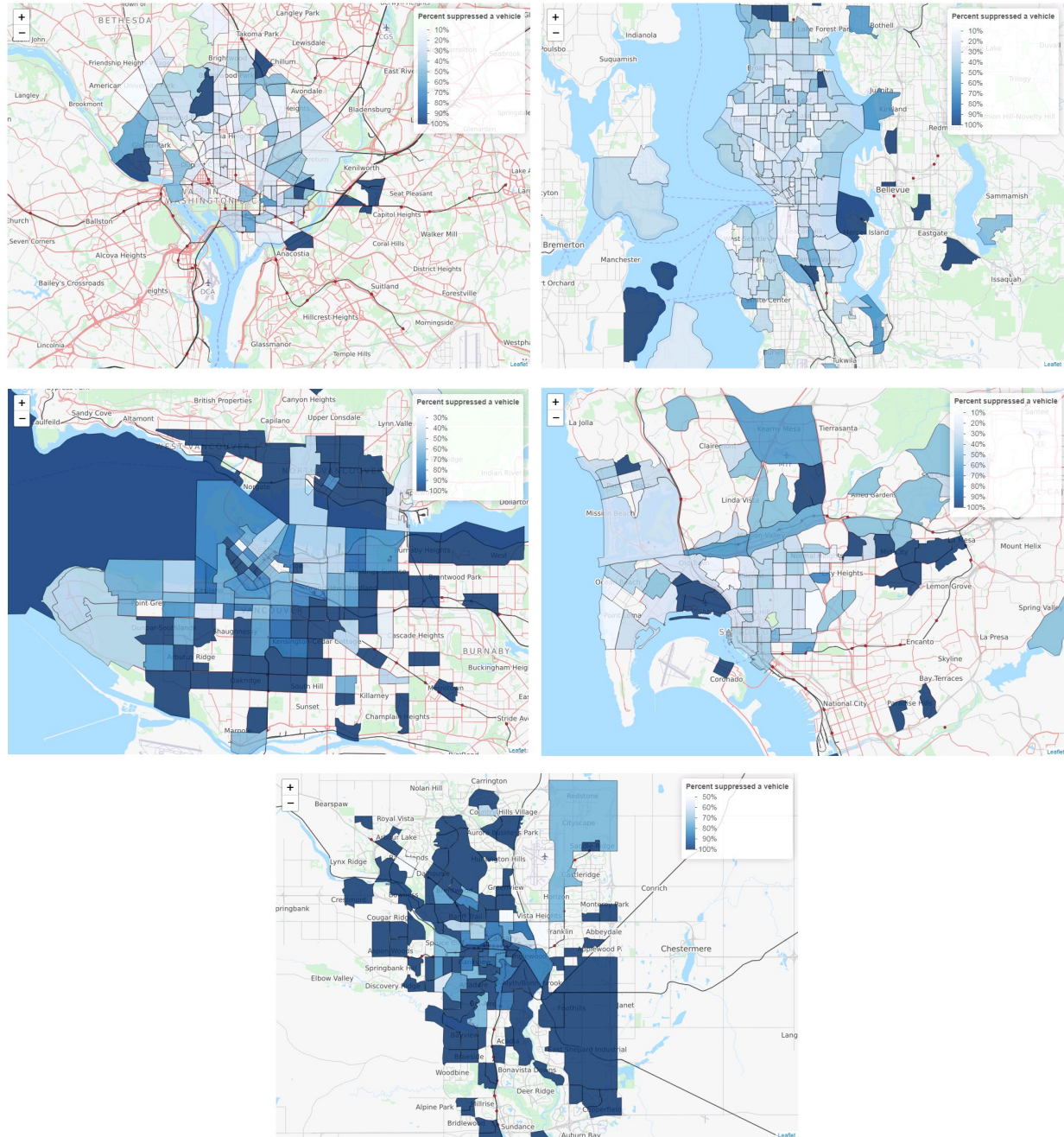


Figure I.3.2.2 Spatial Distribution of Personal Vehicle Suppression

Mode shift impacts can occur in either direction, either an increase or decrease. Figure I.3.2.3 illustrates the spatial distribution of the net change in rail within the five cities. There is a notable diversity in the impact observed across the illustrated regions. One distinguished pattern that emerges is the dominance of shifts away from rail in the core of the urban regions, while some increases in rail use occur at the periphery. The Seattle region is the one exception, where increases in rail use are more modestly observed throughout the city.

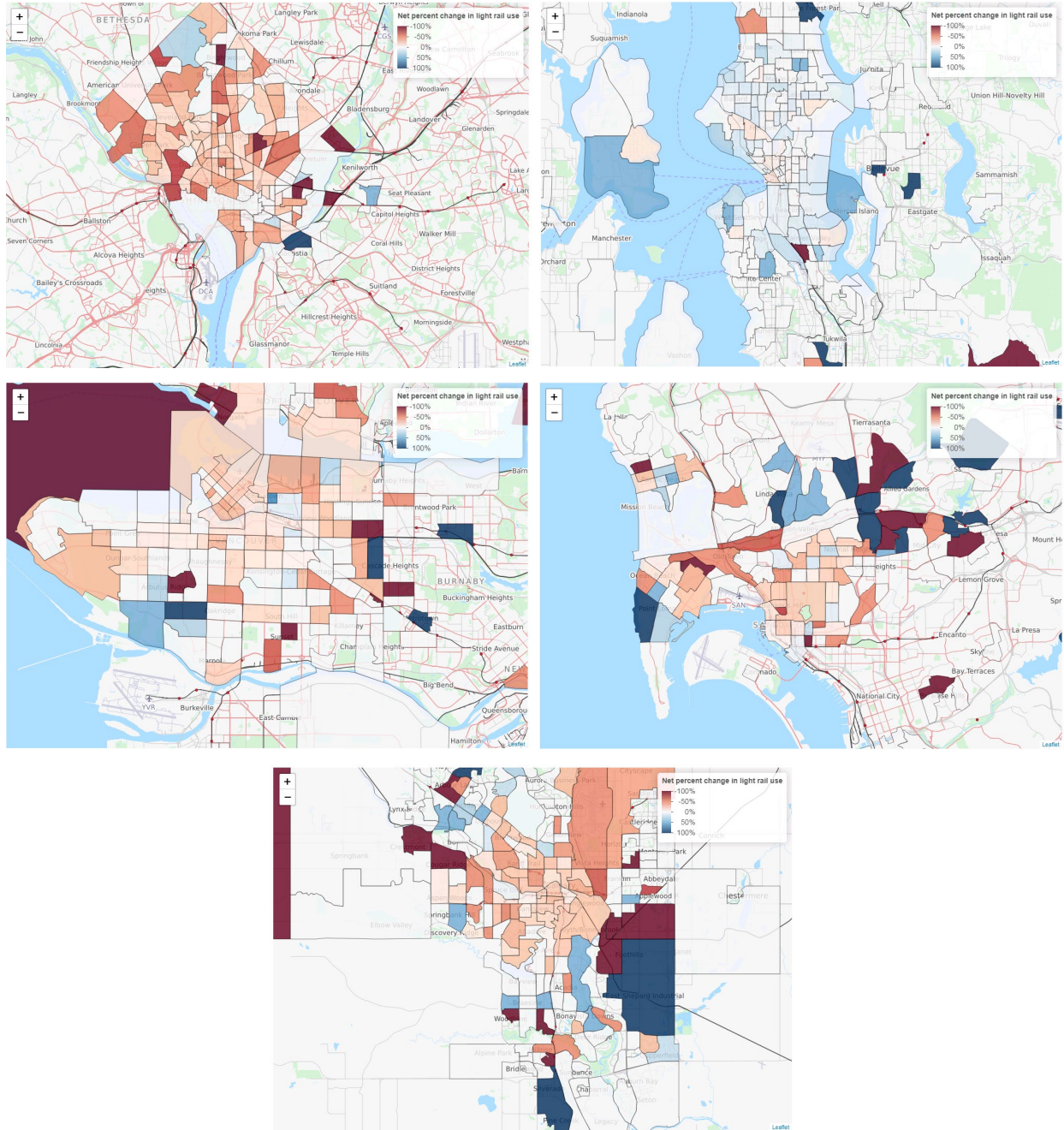


Figure I.3.2.3 Spatial Distribution of Impact on Rail Use

While these distributions are themselves informative, researchers have linked this information with additional data to provide a deeper understanding as to the underlying factors helping to manifest them. The analysis provided a data structure necessary to build a model that identifies the key attributes that are predictive of the behavioral impacts that influence energy use. This model has been used to estimate the coefficients of collected attributes, characterizing the degree and magnitude of their influence on these impacts. The model’s purpose is to estimate the impacts that one-way carsharing could have on cities that does not have an operational system. Several modeling methods were explored, including an aggregated census tract-level model and an individual model. We decided on modeling the individual, so as to take advantage of the respondent attributes as part of the modeling. A

An example of one such estimated model, for vehicle suppression, is shown below.

β_0	β_1	β_2	β_3	β_4	β_5	β_6	β_7	β_8	β_9	β_{10}
-0.6307	0.0997	0.0331	0.2637	0.3507	0.1691	0.0334	0.1704	0.5286	0.1979	-0.0872
β_{11}	β_{12}	β_{13}	β_{14}	β_{15}	β_{16}	β_{17}	β_{18}	β_{19}	β_{20}	β_{21}
-0.0852	0.0339	0.0605	0.1721	0.7311	0.0053	0.4166	0.0782	0.1924	0.0100	-0.2225
β_{22}	β_{23}	β_{24}	β_{25}	β_{26}	β_{27}	β_{28}	β_{29}	β_{30}	β_{31}	β_{32}
0.3650	0.1406	0.1406	0.1643	1.02×10^{-5}	0.0008	0.0002	0.0001	0.0003	1.13×10^{-5}	1.41×10^{-7}
β_{33}										
5.09×10^{-6}										

Where,

- β_0 is the y-intercept
- β_1 is the number of vehicles prior to joining carsharing (from survey)
- β_2 is the number of commute days prior to joining carsharing (from survey)
- β_3 is the dummy variable representing the education status of “Currently in high school” (from survey)
- β_4 is the dummy variable representing the education status of “High school/GED” (from survey)
- β_5 is the dummy variable representing the education status of “2-year college degree” (from survey)
- β_6 is the dummy variable representing the education status of “Post-graduate degree (MA, MS, PhD, MD, JD, etc.)” (from survey)
- β_7 is the dummy variable representing the education status of “Prefer not to answer” (from survey)
- β_8 is the dummy variable representing the ethnicity of “African American” (from survey)
- β_9 is the dummy variable representing the ethnicity of “Asian” (from survey)
- β_{10} is the dummy variable representing the ethnicity of “Caucasian/White” (from survey)
- β_{11} is the dummy variable representing the income bracket of “\$100,000 to \$149,999” (from survey)
- β_{12} is the dummy variable representing the income bracket of “\$150,000 to \$199,999” (from survey)
- β_{13} is the dummy variable representing the income bracket of “Prefer not to answer” (from survey)
- β_{14} is the percentage of tract with a 2-person household (from Census)
- β_{15} is the percentage of tract with a 6-person household (from Census)
- β_{16} is the percentage of tract that leaves during the 9AM hour to get to work (from Census)

- β_{17} is the percentage of tract that bikes to get to work (from Census)
- β_{18} is the percentage of tract that works at home (from Census)
- β_{19} is the percentage of tract that is Asian (from Census)
- β_{20} is the percentage of tract that is Native Hawaiian or Pacific Islander (from Census)
- β_{21} is the percentage of tract that is some other ethnicity (from Census)
- β_{22} is the percentage of tract that has a mixed ethnicity (from Census)
- β_{23} is the percentage of tract that travels less than 15 minutes to get to work (from Census)
- β_{24} is the percentage of tract that travels between 45 to 59 minutes to get to work (from Census)
- β_{25} is the percentage of tract that is between the ages of 45 and 54 (from Census)
- β_{26} is “total land area in acres” (from EPA)
- β_{27} is “gross population density (people/acre) on unprotected land” (from EPA)
- β_{28} is “household workers per job, by CBG” (from EPA)
- β_{29} is “street intersection density (weighted, auto-oriented intersections eliminated)” (from EPA)
- β_{30} is “intersection density in terms of multi-modal intersections having three legs per square mile” (from EPA)
- β_{31} is “intersection density in terms of multi-modal intersections having four or more legs per square mile” (from EPA)
- β_{32} is “jobs within 45 minutes auto travel time, time-decay (network travel time) weighted” (from EPA)
- β_{33} is “jobs within 45-minute transit commute, distance decay (walk network travel time, GTFS schedules), weighted” (from EPA).

This model, and those of other impacts, is being used to predict the relative impacts of one-way carsharing in other urban regions that do not have one-way carsharing. The data and modeling is being applied to two American cities, Pittsburgh and Kansas City, by simulating a population and evaluating the output. The model output may be useful for identifying locations or urban environments that may benefit from one-way carsharing.

Conclusions

This project has advanced our understanding of the spatial impacts of shared mobility in the form of one-way carsharing. The research has allowed us to build an interactive platform for mapping impacts as derived from any system. We find that the spatial impacts of the one-way carsharing are not evenly distributed by space or by type. Impacts such as vehicle shedding appear to have a greater concentration within higher density environments, while vehicle suppression shows greater strength in the periphery. The mode shift analysis shows some similar patterns in most urban environments. The modeling approaches tested suggested that there are advantages to the individual model over modeling at the land-use level from an accuracy and practical perspective. The results can serve to inform evaluations and forecasts of energy impacts from shared mobility systems.

Key Publications

A draft journal article is in development.

References

1. Martin, Elliot W., and Susan A. Shaheen. 2014. "Evaluating Public Transit Modal Shift Dynamics in Response to Bikesharing: A Tale of Two U.S. Cities." *Journal of Transport Geography* 41 (December): 315–24. doi:10.1016/j.jtrangeo.2014.06.026.
2. Martin, Elliot W., and Susan A. Shaheen. 2016. "Impacts of car2go on vehicle ownership, modal shift, vehicle miles traveled, and greenhouse gas emissions: An analysis of five North American cities" Working Paper.

I.3.3 Mobility Behavior Responses to TNC Services (LBNL, NREL)

Tom Wenzel, Principal Investigator

Lawrence Berkeley National Lab
1 Cyclotron Road
Berkeley, CA 94720
E-mail: tpwenzel@lbl.gov

Alejandro Henao, Principal Investigator

National Renewable Energy Lab
1617 Cole Boulevard
Lakewood, CO 80401
E-mail: alejandro.henao@nrel.gov

Prasad Gupte, DOE Technology Manager

U.S. Department of Energy
E-mail: prasad.gupte@ee.doe.gov

Start Date: October 1, 2018

End Date: September 30, 2019

Project Funding (FY19): \$190,000

DOE share: \$190,000

Non-DOE share: \$0

Project Introduction

Transportation Network Companies (TNC) that provide ridesourcing/ridehailing services such as Uber and Lyft are becoming a popular alternative to conventional modes of personal transportation. However, there are scarce data and little research conducted to understand travelers' choice of this transportation mode and impacts on travel behavior and energy consumption. This task analyzes the relationship between the supply of TNCs in a region and impacts on mobility and travel behavior (e.g., vehicle ownership, deadheading, vehicle miles of travel or VMT) and energy use. The results are useful as inputs for travel activity models used in other pillars (e.g., BEAM and POLARIS) to test the sensitivity of the availability of these services to travel and energy use.

Objectives

The main objective of this task is to estimate the effect of TNC services on specific measurements related to energy use including vehicle ownership, percent electric vehicle (EV) registrations, transit ridership, and vehicle miles of travel. This will help the SMART consortium to estimate both the short- and long-run system energy impacts of large-scale TNC deployment using travel activity models developed under other SMART tasks. There were several activities under this task in 2019:

- Finalize journal article on travel and energy implications of TNC services using a database of individual rides provided by a TNC in Austin, Texas.
- Examine the relationship between the entrance of TNC services across U.S. cities (first at the urban area level, and subsequently at the zip code level) and total and new vehicle registrations, percent EV registrations, average rated fuel economy, and transit ridership.
- Examine the relationship between TNC entry on vehicle ownership and VMT in Texas, using dataset of individual vehicle odometer readings.
- Examine publicly available datasets of TNC service in U.S. cities, and report on data gaps and research needs to assess energy mobility and energy consequences of widespread use of TNC services.

Approach

For the analysis on travel and energy implications of a TNC service in Austin, TX, we used a dataset of around 1.5 million individual rides provided by RideAustin, a non-profit TNC established in Austin Texas when Uber and Lyft left that market in May 2016. The data are from May 2016 to April 2017. The RideAustin dataset identifies each driver and passenger, so activity by individual drivers or passengers can be tracked over time. The database includes the location coordinates of each vehicle at several points along a particular ride, as well as the measured distance of the route taken while transporting a passenger. The database also includes the year, make, and model of all vehicles being used by RideAustin drivers.

For the national analysis of the relationship between date of entry of TNC service and vehicle registrations, percent EV registrations, rated fuel economy, and transit ridership, we used the difference-in-difference econometric statistical regression model with the following datasets:

- Dependent variables: Total and new vehicle registrations and electric vehicle registrations at the zip code level (2010-2017) using a national database of individual vehicle registrations provided by IHS Automotive (previously R.L. Polk & Company), aggregated to urban areas; average rated fuel economy from EPA's fuel economy guide; percent of registrations that are electric vehicles transit ridership from the National Transit Database.
- Independent variable: UberX and Lyft entry dates in each urban area (Month/Year).
- Control variables: Population, population density, economic variables such as income and unemployment, from US Census American Community Survey 5-year estimates.

We applied a similar difference-in-difference regression methodology on a database of annual odometer readings from vehicle emissions and safety inspections for individual vehicles in Texas. The data were obtained from the Texas Commission of Environmental Quality (emission inspections in 17 counties around Austin, Dallas/Fort Worth, El Paso, and Houston) and the Texas Department of Safety (safety inspections in the rest of the state). We conducted the analysis at the individual vehicle level, and accounted for time of entry in 24 urban areas in Texas, including control variables for calendar year and vehicle model year, vehicle type, and average fuel price.

We examined publicly available databases of TNC service in Austin and Chicago to understand its use to answer critical research question. We also coordinated with other SMART pillars (e.g., Urban Science, Task 2.1.4) to identify major aspects of TNC services that will affect energy use, both positively and negatively. For example, reducing energy use by increasing vehicle occupancy with pooling services such as UberPool or LyftLine, decrease vehicle ownership moving from an habitual driver to a multimodal traveler, or concentrating VMT in fewer, high-mileage or electric vehicles. At the same time, TNCs can increase VMT and energy use with induced travel, drivers commuting long distances into urban centers, deadheading, or travel mode replacement shifting from more energy efficient modes (transit, bike or walk) to TNCs. We are also actively participating in an inter-lab task force to coordinate a forthcoming request for TNC data. Finally, we identify data gaps and research needs to assess energy mobility and energy consequences of widespread use of TNC services

Results

In FY19 we published one journal article, and drafted three articles for publication. Results from each of these articles are as follows:

1. *Travel and Energy Implications of a ridesourcing service in Austin, TX*

Using detailed data on approximately 1.5 million individual rides provided in the RideAustin ridesourcing program in Austin Texas, we quantified the additional miles TNC drivers drive before beginning and after ending their shifts, to reach a passenger once a ride has been requested, and between consecutive rides (all of which is referred to as deadheading); and the relative fuel efficiency of the vehicles that RideAustin drivers use

compared to the average vehicle registered in Austin (based on registration records from the Texas Department of Motor Vehicles). We conservatively estimate that TNC driver commutes to and from their service areas account for 19% of total ridesourcing VMT; in addition, we estimate TNC drivers drove 55% more miles between ride requests within 60 minutes of each other, accounting for 25% of total ridesourcing VMT. Vehicles used for ridesourcing are on average 3.2 miles per gallon more fuel efficient than comparable light-duty vehicles registered in Austin, with twice as many hybrid-electric vehicles. New generation battery electric vehicle with 200 miles of range would be able to fulfill 90% of full-time drivers' shifts on a single charge. The RideAustin data also indicate that a substantial percentage of all rides start or end at downtown entertainment and airport land uses. We estimate that the net effect of ride sourcing on energy use is a 41% to 90% increase compared to baseline pre-TNC personal travel. Figure I.3.3.1 summarizes the net effect of five factors discussed above on the energy use from ridesourcing operation.

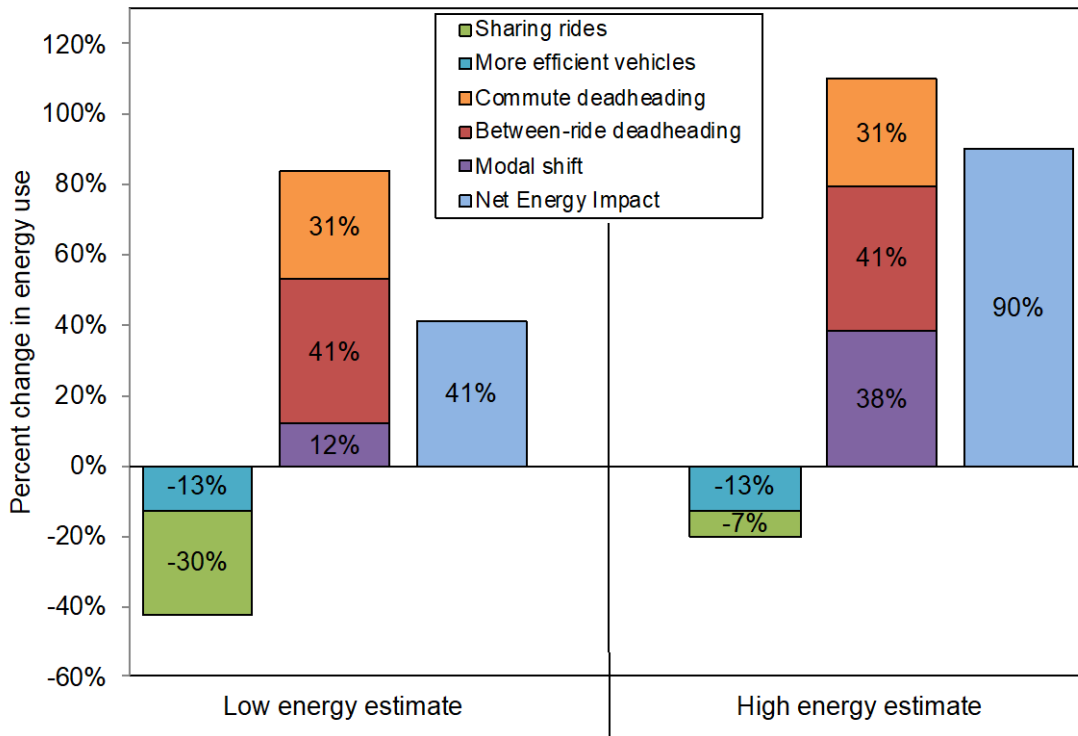


Figure I.3.3.1 Low and high energy estimates of net energy impact of ridesourcing service in Austin

2. Impacts of Ridesourcing on Vehicle Ownership and Other Variables in U.S. Cities

Our analysis suggests that TNC entry increased per-capita vehicle registrations by a statistically significant 0.7% on average across all urban areas of the country, as compared with areas before TNC entry or which have not yet received TNC service. This result contrasts with our previous research at the state level, which found that TNC entry decreased vehicle registrations; a likely explanation of the earlier result is that differing effects at the urban level are “washed out” by averaging heterogeneous effects in different cities in the same state. Figure I.3.3.2 shows the range in the estimated change in vehicle registrations per capita, using a heterogeneous treatment effect analysis, with the estimate ranging from a 12% decrease in registrations to a nearly 15% increase in registrations. 38 cities have an estimated decrease (from a 12% decrease in Redding CA), while 59 have a significant increase (to a nearly 15% increase in Gainesville FL), in per capita registrations after TNC entry (note that the city labels on the horizontal axis only include every third city). We plan on analyzing the effect of TNC entry on clusters of cities with similar characteristics, to understand what characteristics of cities influence the effect of TNC service on changes in vehicle registrations.

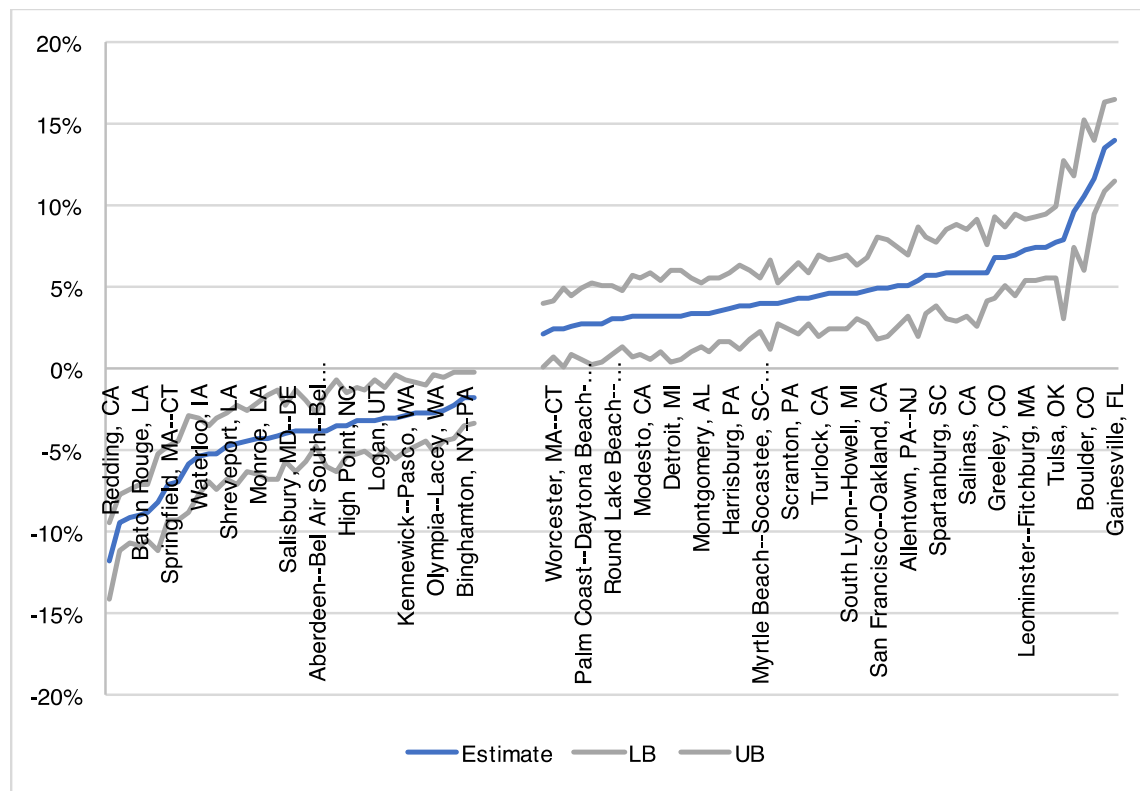


Figure I.3.3.2 Range in estimated change in per capita vehicle registrations after TNC entry, by city (only cities with statistically significant effects shown)

Regarding the other dependent variables, we find that TNC entry is associated with very small and statistically insignificant reductions in the percent of light vehicles that have electric drive trains (0.01%) and per-capita transit trips (0.1%), and a 0.17% increase in the average rated city/highway fuel economy of registered vehicles. Extensive robustness checks and sensitivity analyses support our initial findings for all four dependent variables.

3. Impacts of Ridesourcing on Vehicle Ownership and Use in Texas Cities

As part of the analysis of the effect of TNC entry on vehicle registrations and VMT in Texas cities, we compared vehicle registration counts for Texas from IHS Markit/Polk (henceforth referred to as Polk) with Texas DMV registration records. Figure I.3.3.3 compares total registrations by year, from four sources: state-level registrations from US DOT and Ward's Automotive, and aggregate individual registrations from Polk and the Texas DMV. The dashed orange line shows aggregate Polk vehicle registrations adjusted by LBNL by excluding vehicle makes that clearly are not light-duty vehicles (e.g., Freightliner, Nissan diesel, Peterbilt). US DOT and Ward's report essentially the same state-level registrations for 2005 through 2007; however, starting in 2008, Ward's registrations are consistently lower than US DOT. Aggregate LDV individual registrations from Polk and TX DMV are very similar for 2010 through 2012; however, starting in 2013 Polk registrations are about 3% to 6% higher than TX DMV registrations. This is likely because starting in 2012 Polk began reporting registrations as of December, as opposed to as of the previous July.

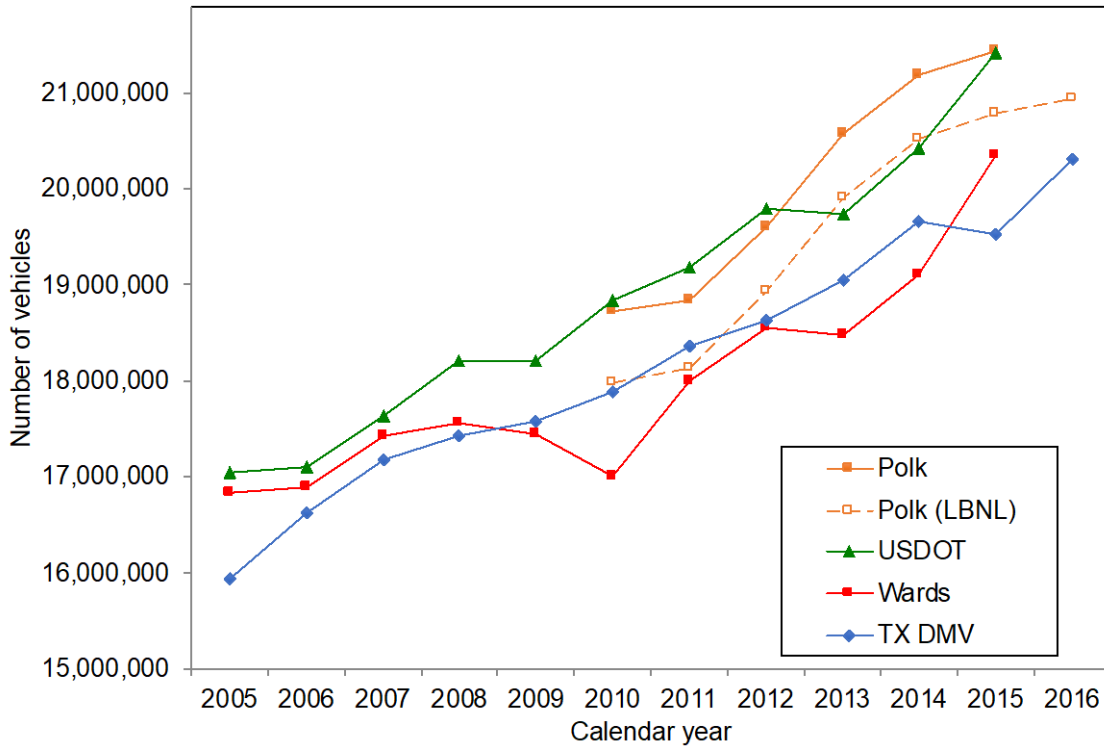


Figure I.3.3.3 Comparison of Texas DMV light-duty vehicle registrations with Polk, US DOT, and Ward’s registrations, by year

A comparison of Texas DMV and Polk registrations for the 47 most popular light-duty vehicle models, which represent just over half of all vehicle models registered, indicates that registrations for most models are within 10% from the two sources. However there are substantial differences for certain vehicle models. Figure I.3.3.4 indicates that Polk (solid symbols and lines) and DMV (open symbols and dashed lines) registrations for Equinox (red) and Fusion (green) are nearly identical in years 2012 through 2016, but Polk registrations are substantially lower than DMV registrations for these two models in 2010 and 2011. The figure also indicates that Polk registrations are consistently substantially higher than DMV registrations for F350 (orange) and Econolines (blue), while the opposite is true for Yukons (purple).

The most likely explanation for discrepancies of registrations for individual vehicle models is different processes used by Polk and LBNL to decode the vehicle identification number (VIN) of individual vehicles into year, make, model, etc. The analyses above accounted for simple differences in how vehicle models are named, but other differences in VIN decoding and naming may remain. However, the substantial difference in registrations for Equinox and Fusion models in 2010 and 2011 are unlikely due to VIN decoding or model naming differences; if many of these two models were sold late in the model year, this difference could be a result of the change in the date of the Polk snapshot of vehicle registrations from July to December starting in 2012.

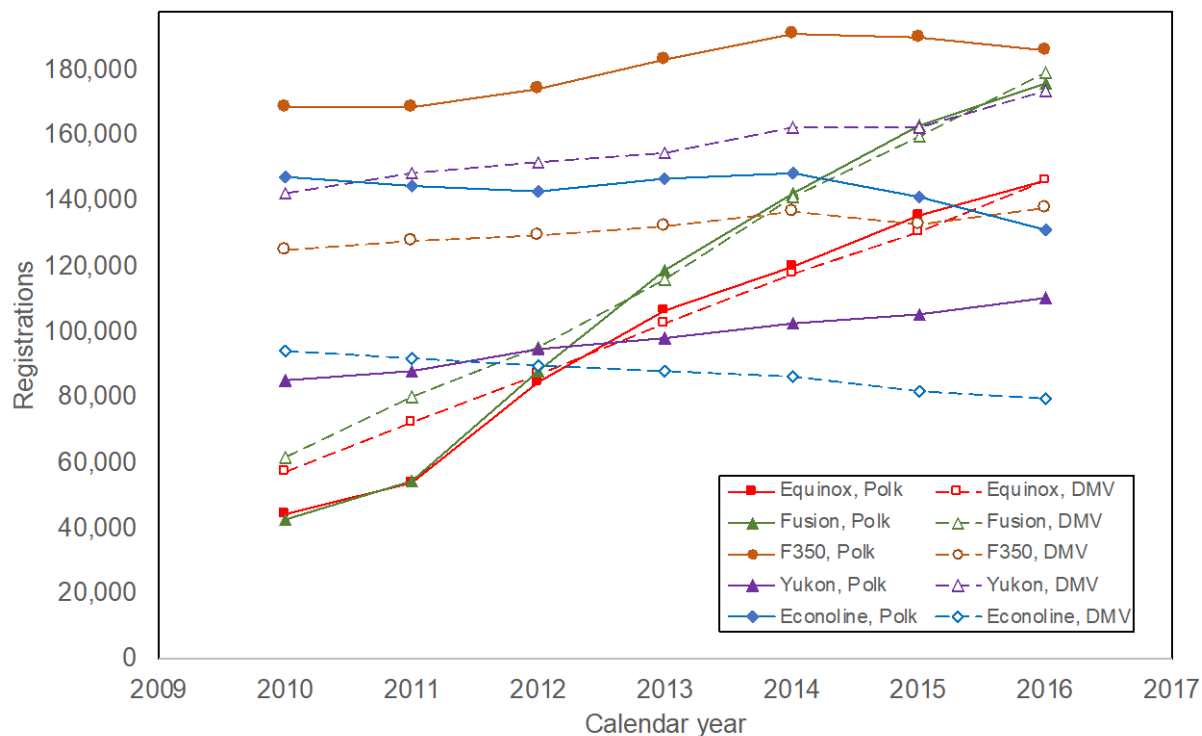


Figure I.3.3.4 Texas DMV and Polk light-duty vehicle registrations for 5 popular models, by year

We next looked at differences in vehicle registrations between TX DMV and Polk for the 50 most populated ZIP codes in Texas, which represent about 13% of all vehicles registered. The difference in vehicle registrations between the two sources was within 10% for most ZIP codes; however, for seven ZIP codes there was a greater than 10% difference. Figure I.3.3.5 indicates that Polk (solid symbols and lines) and DMV (open symbols and dashed lines) registrations were comparable for initial years but diverged for later years in ZIP code 78745 (and two others not shown), and diverged for initial years but were comparable for later years for ZIP code 78572 (and one other not shown); Polk registrations were much larger than DMV registrations in ZIP code 76244 (and one other not shown) across all years.

A plausible explanation for discrepancies in registrations in individual zip codes could be that the DMV data are based on the ZIP code of the vehicle owner, and not the title address, for vehicles that are owned by national companies. While only 2% to 3% of all registered vehicles in any given year are registered to an out-of-state owner, who likely leases them to Texas residents, this fraction is much higher for newer vehicles (e.g., from 11% to 15% of three year old and newer vehicles). The Polk data may include the Texas address where the leased vehicle is garaged. This may account for the ZIP codes where registrations are higher in the Polk data than in the DMV data; but likely would not account for the large discrepancies, or the higher registrations in DMV vs. Polk, in certain ZIP codes, unless companies that lease large numbers of vehicles are located in the ZIP codes shown in Figure I.3.3.5, and large numbers of households that lease vehicles are concentrated in the five other ZIP codes.

We attempted to correct for this difference by replacing the (usually out of state) owner address with the Texas address on the vehicle title, which is likely the local branch of the national company or the address of the vehicle lessee, where such information was provided. This adjustment results in substantially more registered vehicles in the DMV data than in the Polk data for ZIP code 78745 shown in Figure I.3.3.5, but has little effect on the other two ZIP codes.

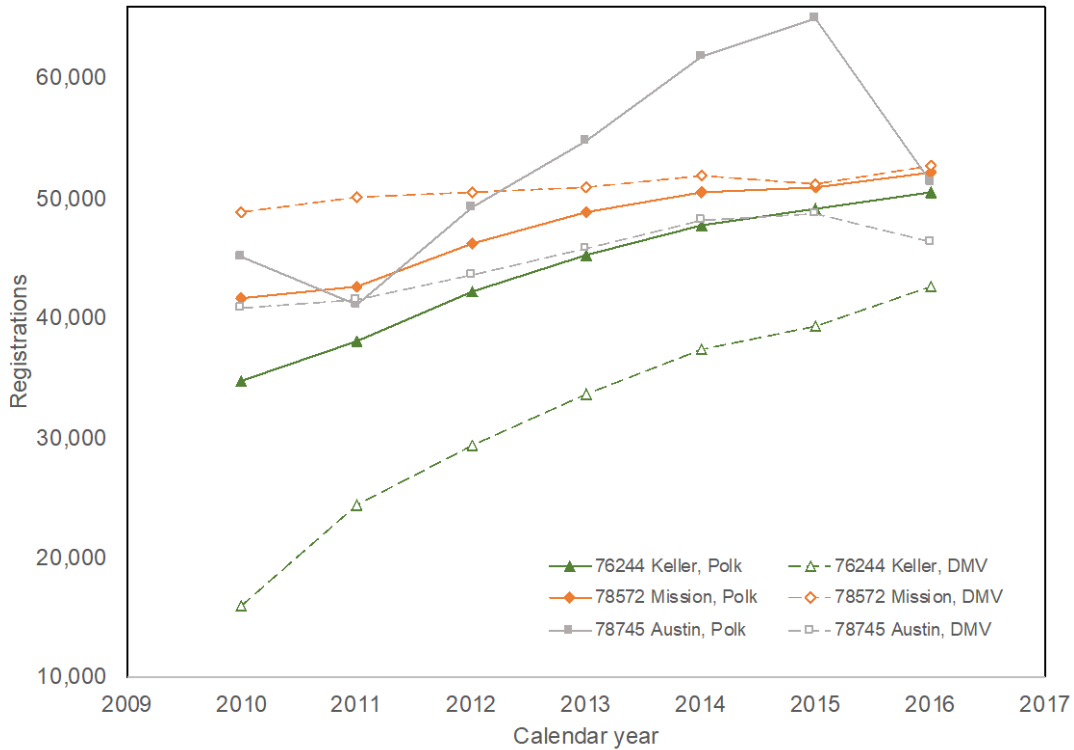


Figure I.3.3.5 Texas DMV and Polk light-duty vehicle registrations in 3 zip codes, by year

We merged three sets of data from three sources to estimate the effect of TNC entry on vehicle registrations and total, average, and 99th percentile VMT in Texas service areas: DMV registration records as of January of 2006 through 2016; annual emission inspection records from March 2002 through August 2019 for vehicles inspected in the 17 counties surrounding Austin, Dallas/Fort Worth, El Paso, and Houston; and annual vehicle safety inspection records from July 2010 through April 2019 for vehicles inspected in the rest of Texas. TNC services became available in 24 urban areas in Texas, from Dallas/Fort Worth in September 2013 to College Station in April 2018.

We first used the inspection data between June 2011 and April 2019 to estimate the effect of TNC entry on annual VMT on the individual vehicle level; we include control variables for vehicle age, light trucks (as opposed to cars), and hybrid vehicles, five variables from the ACS, and fixed effects by urban area and calendar year. We find that TNC entry is associated with a 0.6% decrease in annual VMT per vehicle after the first year after entry, consistently increasing to a 4.5% decrease after the fifth year after entry. Because of the large number of measurements used (over 96 million), these estimates are all statistically significant. We find similar trends after accounting for changes in the price of gasoline, using different time periods after entry (every 6 months and every month after entry), and excluding urban areas that haven't yet received TNC service.

We then aggregated individual vehicle records by urban area to obtain total registered vehicle counts and total VMT per area by year. We calculated these quantities twice for each urban area, based on the month of the year in which TNC service first entered. For example, since TNC service entered Dallas/Fort Worth in September 2013, we sum total registrations and VMT in Dallas Fort/Worth between January and August, and between September and December, for each year; this minimizes any seasonal variation in vehicle sales, registrations, or VMT biasing the estimated effect of TNC entry. As in the vehicle level analysis, we include the five ACS variables and fixed effects for urban area and calendar year. In contrast to the analysis of registrations in U.S. cities, we find that TNC entry in Texas cities is associated with a consistent and increasing

decrease in vehicle registrations over time, with a similar decrease in total VMT, slight changes in average VMT, and increases in 99th percentile VMT. However, when we limit the U.S. city analysis using Polk registration data to only Texas cities, we do find a slight decrease in registrations after TNC entry. We plan to explore these differences in more detail, and conduct additional robustness and sensitivity tests of the analyses at the individual vehicle and UA levels.

4. Datasets, Data Gaps and Research Needs to Quantify the Impacts of TNCs on Transportation and Energy

TNC services have a notable impact across multiple domains such as vehicle miles traveled, parking, safety, and energy use. These services not only affect the traveler and network, but there are also significant impacts in terms of the built environment, future infrastructure (e.g., parking, curb utilization), fleet management, regulations, and key social, economic, and energy implications. Although TNCs have gained rapid popularity, data and research that can inform mobility and energy impacts remains scarce. There is a critical knowledge gap in analyzing the conditions that can drive various emerging mobility services towards societal goals. This task aims to address this gap by reviewing the literature (including datasets) and explore the energy impacts of ride-hailing that span key research questions, hypotheses, data needs, and preliminary analysis. Key findings are summarized below:

Datasets and Data Gaps

For several years New York City was the only major U.S. city that made TNC data publicly available under the Taxi & Limousine Commission (TLC, 2019), providing origins and destinations of individual trips. In April 2019 Chicago publicly released data from three major TNC providers: Uber, Lyft, and Via (City of Chicago, 2019). The Chicago Transportation Network Providers (TNP) data are comprised of three separate datasets of TNC trips, drivers, and vehicles, which help answer important research questions about the type and fuel efficiency of vehicles used in TNC services, passengers' willingness to share rides, and pooling request and match rates. While the Chicago TNP data are the most complete datasets released by a large U.S. city to date, they do not provide information on deadheading distances and times, safety rates, or driver economics necessary to estimate impacts of TNC services across these dimensions.

TNC Energy Impacts Framework

Understanding the full spectrum of TNC impacts on energy use requires data and research needs from different sources, including service providers (e.g., Uber, Lyft, and their drivers), consumers (e.g., TNC users), and regulators (cities).

From the providers' side, four main impacts are identified:

- **Vehicle Fleet:** Metrics are needed on the extent to which vehicles (including electric vehicles or EVs) currently used by ride-hailing drivers are more fuel efficient than the vehicles used by the general population, thereby providing a positive energy benefit.
- **Operations & Style:** Standard metrics are needed for how drivers consume energy with their driving behaviors (e.g., telematics). More information is needed to better understand the effect of allocation and relocation of vehicles, and the timing of their refueling, on energy use by centrally managed fleets of ride-hailing AVs.
- **Supply & Demand:** TNCs try to balance the supply (i.e., number of drivers available) and demand (i.e., number of passenger requests) using surge pricing and other incentives to drivers. If the supply of drivers is higher than demand, vehicles spend more time idling and/or circulating; if the supply of drivers is lower than demand, drivers have to travel longer distances from the point of dispatch to passenger pick-up. Both of these situations have negative implications for overall energy use.

- **Deadheading & Idling:** One of the biggest issues with taxis, TNCs, and future AVs is the congestion and energy use generated by deadheading (i.e., travel without a passenger, zero occupancy vehicles, ZOV). This is clearly a negative effect on transportation and energy use.

The following five topics are related to consumers and their mobility behavior changes:

- **Mode replacement and modality style changes:** More information is needed on the relative efficiency of the travel modes replaced by ride-hailing (especially more efficient modes such as public transportation, biking, and walking). Patterns of modal shift likely vary in specific contexts (such as out of town travel, airport trips, recreational), and where other factors influence decision making (such as avoiding driving after drinking, and the availability or cost of parking).
- **Vehicle ownership and use:** More research is needed on whether TNCs reduce or increase overall vehicle ownership. Our research indicates that in many cases vehicle ownership is increasing. A possible cause is that driving for a TNC may provide access to vehicle ownership while earning money. While TNCs may reduce ownership of personal vehicles, the more important issue is their effect on vehicle use and miles of travel. TNCs may increase energy use if passengers are simply shifting from solo driving to being driven solo.
- **Pooling (i.e., true ridesharing):** While most TNC trips currently are solo passengers, pooling offers a potential benefit. Research is needed on what factors influence people's willingness to pool. More data are needed to quantify the extent to which pooled rides are requested, and to which requested pooled rides are matched. The Chicago TNP data indicated that 26% of TNC riders requested a pooled ride, and of those requested 72% were matched with another party (Yi et al., 2019).

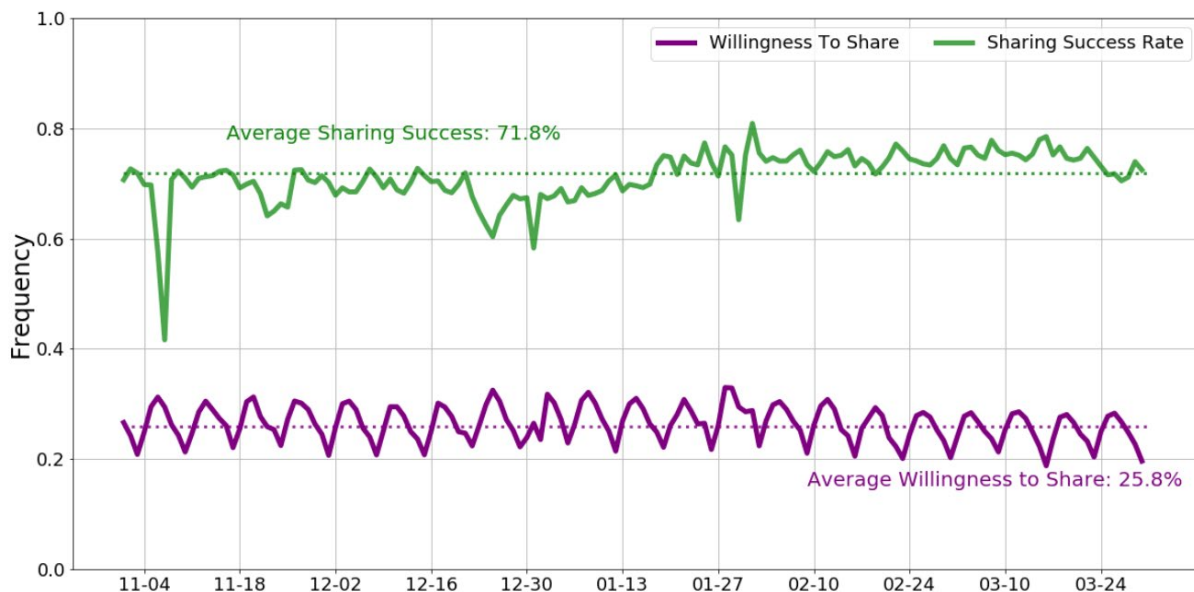


Figure I.3.3.6 Willingness to share and the sharing success rate of authorized trips over time

- **Induced travel:** While induced travel (i.e., trips that would not have happened in the absence of TNCs) increases mobility, it also increases energy use; more research is needed on a metric, such as the Mobility Energy Productivity metric (MEP), that accounts for the change in mobility per unit of energy use. Mode shift surveys document TNC services does induce additional travel.
- **Relocation: residence, travel:** Research is needed to estimate the effect of TNC service on parking requirements and car rentals; airports provide a good case study of these trends (Henao et al., 2018,

Henao et al., 2020). Reduced demand for parking can free up valuable real estate in urban centers for more dense development, which may increase demand for transit and other more efficient modes. Shifting the cost of travel from a fixed to a variable cost may reduce discretionary travel and its associated energy use.

The third actor in the framework is institutions such as cities, airports and other government agencies that regulate TNC operation:

- **Infrastructure, Standards & Regulations:** When unintended consequences occur because of changes at the system level (such as introduction of TNCs), institutions can play a major role in setting guideline. While it is the responsibility of the institutions (such as city planning bodies and metropolitan planning organizations) to make decisions that lead to positive outcomes (such as reduced energy use and an increase in efficient mobility), access to data and research is essential to make well informed decisions. To place policy ahead of the curve, cities should invest in technologies and mechanisms to collect data necessary to guide decision making, while making sure privacy concerns are met. For example, cities should focus on monitoring congestion, vehicle occupancy, parking, density, and mode share in a continuous and efficient manner to guide policy, while setting up policy and mechanisms to incentivize equity, safety, mobility and energy efficiencies.

Conclusions

We have used a variety of sources to examine several aspects of TNCs that provide ridesourcing/ridehailing service, and their implications for overall energy use. We developed a research framework that lays out specific aspects of TNC service that affect energy use, identifies the types of data necessary to estimate each, and lists remaining gaps in our understanding of these services. We then applied much of this framework to a TNC service in Austin, Texas, and estimate that it results in a 41% to 90% increase in net energy use. We have used two different sources of vehicle registration data to estimate what effect staggered entry of TNC services in different cities has on a range of parameters: total and new vehicle registrations; total, average, and 99th percentile VMT; rated fuel economy; percent of registered vehicles that are EVs or hybrids; and transit ridership. We find that TNC services are associated with a small increase in overall vehicle registrations in U.S. cities, although the effect varies considerably by city; for example, for all Texas cities combined entry is associated with a slight decrease in registrations. We also find slight increases in average rated fuel economy of registered vehicles, but slight decreases in the fraction of vehicles that have electric drive trains and per-capita transit trips. Analysis of odometer readings of millions of individual vehicles registered in Texas indicates that TNC service is associated with decreases in registrations, both at the vehicle and city level, and that TNC entry is associated with decreases in new registrations, total VMT, and average VMT, and increases in 99th percentile VMT and rated fuel economy, at the city level.

Key Publications

1. Wenzel, T., Rames, C., Kontou, E., & Henao, A. (2019). Travel and energy implications of ridesourcing service in Austin, Texas. *Transportation Research Part D: Transport and Environment*, 70, 18-34. <https://doi.org/10.1016/j.trd.2019.03.005>
2. Henao, A., Wenzel, T., & Ward, J. (2019). Ride-hailing on Transportation and Energy: Data & Research Needs to Analyze Impacts. (Draft)
3. Ward, J., Henao, A., & Wenzel, T. (2019). Effect of TNC entry on vehicle registrations, fuel economy, and transit ridership in U.S. cities. (Draft)
4. Wenzel, T., Ward, J., & Henao, A. (2019). Effect of TNC entry on vehicle ownership and use in Texas cities (Draft).
5. Wenzel, T., Ward, J., & Henao, A. (2019). Comparison of vehicle registration data from several sources. (Draft).

References

1. City of Chicago. Mayor Emanuel Opens the Books on Transportation Network Provider Data. https://www.chicago.gov/city/en/depts/mayor/press_room/press_releases/2019/april/TransportationNetworkProviderData.html. Accessed July 2019.
2. Henao, A., Sperling, J., Garikapati, V., Hou Y. & Young, S. (2018). Airport Analyses Informing New Mobility Shifts: Opportunities to Adapt Energy-Efficient Mobility Services and Infrastructure. National Renewable Energy Laboratory. NREL/CP-5400-71036. <https://www.nrel.gov/docs/fy18osti/71036.pdf>
3. Henao, A., Sperling, J., & Young S. (2020). Ground Transportation at Airports: Ride-hailing Uptake and Travel Shifts to Test Mode Choice Modeling Assumptions. 99th Annual Meeting of the Transportation Research Board, Washington, D.C.
4. Taxi and Limousine Commission (TLC). NYC Open Data. FHV Base Aggregate Report. <https://data.cityofnewyork.us/Transportation/FHV-Base-Aggregate-Report/2v9c-2k7f>. Accessed July 2019

I.3.4 Travel Time Use and Value with Mobility Services (ANL)

Joshua Auld, Principal Investigator

Argonne National Laboratory
9700 S Cass Avenue, Building 362
Lemont, IL 60439
E-mail: jauld@anl.gov

Paul Leiby, Principal Investigator

Oak Ridge National Laboratory
1 Bethel Valley Road
Oak Ridge, TN 37830
E-mail: leibypn@ornl.gov

Prasad Gupte, DOE Technology Manager

U.S. Department of Energy
E-mail: prasad.gupte@ee.doe.gov

Start Date: October 1, 2018

End Date: September 30, 2019

Project Funding (FY19): \$225,000

DOE Share: \$225,000

Non-DOE Share: \$0

Project Introduction

The perceived value of travel time (VOTT) or value of travel time savings (VOTTS) on the part of travelers is a fundamental concept in travel analysis. This value represents the amount a traveler would theoretically be willing to pay to reduce travel time, usually expressed in dollars per hour, and relates to the perceived burden or disutility of traveling. This value can vary by individual, travel situation, travel mode, and a variety of other factors. Even time spent on different portions of the same trip (e.g., walking to a train versus waiting for a train versus riding on the train) can have different associated values. VOTT, therefore, has an impact not only on the choice of mode when traveling, but also on the choice of route, location, departure time, and many other mobility-related behaviors. Understanding how new mobility services alter time use and perceived time value is central to understanding how they may fundamentally alter travel behaviors and their corresponding impacts. For example, automated vehicles (AVs) may enable travelers to perform various activities while on the road.

Objectives

The project objectives are as follows:

- To estimate VOTT using different types of survey data—time use diaries and travel diaries;
- To explore the variation in VOTT across different population segments and travel conditions;
- To design and conduct surveys addressing the gaps in existing surveys in order to produce VOTT estimates for new mobility services;
- To evaluate the implications of (non)productive time use during travel on VOTT estimates using novel survey data;
- To evaluate the impact of VOTT on key travel indicators, such as vehicle miles traveled (VMT) and vehicle hours traveled (VHT); and
- To evaluate the impact of VOTT on energy consumption by the transportation system.

Approach

A multistage approach was adopted to attain project objectives. First was the indirect estimation of VOTT by time use analysis of widely available survey data. Second was the direct estimation of VOTT by using available survey data. Third was analysis of a survey that was designed and fielded by the University of New South Wales (UNSW) to capture the effect of travel-based activity engagement on VOTT estimates for current and emerging new modes, such as AVs and connected automated vehicles (CAVs).

Indirect Estimation of VOTT

To explore time use, data from different types of surveys, such as the American Time Use Survey (ATUS), National Household Travel Survey (NHTS), and Consumer Expenditure Survey (CES), were examined. The first two surveys provide time allocation information based on different in- and out-of-home activities, while the CES provides expenditure information based on performing different activities. Multiple discrete continuous (MDC) models were applied to analyze time/money allocation across different in- and out-of-home activity categories. In general, the three datasets show substantial variation in time/money allocation behavior across different demographic groups (e.g., age, gender, ethnicity, education, employment status, and marital status, among others). However, the datasets were limiting in the sense that none of the surveys provide complete information on time and cost allocation for activity participation, therefore restricting direct estimation of VOTT. In addition, all three surveys provide information only on primary activity participation; that is, information on secondary activity participation or multitasking was missing.

Direct Estimation of VOTT

The second approach used the travel tracker survey (TTS) conducted by the Chicago Metropolitan Agency for Planning to develop mode choice models for the direct estimation of VOTT. This approach applied six different model specifications to different exogenous population segments. The population was divided into 138 subclasses based on trip-related attributes (e.g., day of week, arrival/departure hour, trip purpose, location of the trip) and socioeconomic attributes (e.g., gender, age, ethnicity, education, income, employment status, household, and vehicle ownership among others). Again, the analysis showed wide variation in estimated VOTTs based on trip-related and socioeconomic attributes.

Survey to Capture Effect of Multitasking on VOTT

A discrete choice experiment (DCE) previously conducted by UNSW among residents of the Chicago Metropolitan Area to explore VOTT for emerging mobility services such as AVs was analyzed to explore the impact of multitasking on VOTT. The DCE presented six modal options to participants—privately owned AV, taxi, bus, train/tram, shared AV, and privately owned car (excluding AV). Twelve attributes were used to describe the modal options. Travel attributes could be grouped into three broad categories: trip-specific (e.g., travel type, wait time, access time, travel time, travel cost, parking cost), environment-related (e.g., traffic condition, crowding inside vehicle, market penetration of the new mobility technology), and activity-engagement-related (e.g., type of and reason for activity engagement while traveling). Figure I.3.4.1 is a screen shot of a typical DCE presented to participants. About 1,000 residents participated in the survey, and each participant was presented with eight DCEs.

Scenario 2 of 8
 You have mentioned earlier that you make the following regular trips each week:
 • Mandatory trips alone

On the basis of similar travelling arrangements to those above, we want you to imagine you are going to travel on the same type of trip in the scenarios below. Please evaluate the options available to you and select the option you would most likely choose.

Travel mode	Privately owned AV	Taxi	Bus	Train/tram	Rideshare / TNC (i.e. Uber, Lyft)	Privately owned car (excluding AV)
Travel type			Mandatory			
Wait time		10 mins	15 mins	15 mins	15 mins	
Access time			5 mins	15 mins	10 mins	
Travel time	10 mins	20 mins	10 mins	20 mins	20 mins	20 mins
Traffic conditions	Light traffic	Light traffic	Light traffic		Light traffic	Light traffic
Crowding			No seats free and a few others standing	Plenty of seats free and do not need to sit next to anyone	A few seats free but need to sit next to someone	
Activities you engage in while travelling will help you earn money	✓	✗	✗	✓	✗	✗
Activities you engage in while travelling will help you reduce daily work load	✓	✗	✗	✗	✓	✗
Activities you engage in while travelling will help you engage in other activities after work	✓	✗	✓	✗	✗	✗
Parking cost (\$ per hour)	\$5.50					\$5.50
Market penetration	40 out of 100 people are currently using this mode				30 out of 100 people are currently using this mode	
Travel cost (excluding any parking costs)	\$12	\$15	\$2	\$2	\$10	\$5
I will choose this option	<input type="radio"/>	<input type="radio"/>	<input type="radio"/>	<input type="radio"/>	<input type="radio"/>	<input type="radio"/>
	<input type="checkbox"/> I will choose to walk or cycle for this trip					

Figure I.3.4.1 A typical example of discrete choice experiment task presented to the respondents

The data collected in the survey were used to develop multinomial logit models of mode choice. The estimated parameters of travel time and travel cost were used to calculate the VOTT for different modes. The VOTT was calculated for the full sample and for the exogenous samples based on gender, age, and income categories. Similar to results from previous studies, VOTT was found to vary across different exogenous population segments. In addition, engaging in activities produced positive utility only for certain ranges of travel duration.

Results

Direct estimation of VOTT showed substantial differences across demographic groups, travel hours, and trip purposes. The average VOTT of transit users (\$7.6/hour, varying from \$0.3 to \$35.3/hour) is much lower than the average VOTT of car users (\$28.5/hour, varying from \$2.1 to \$82.3/hour). VOTT also varies by arrival and departure time, showing higher magnitude in the peak hours and lower magnitude in the off-peak hours for auto and transit users. However, for trips to the central business districts, the model results seem to be counterintuitive: VOTT is higher for work-oriented car trips than for less important purposes like changing transportation type, but the opposite appeared to be true for transit users.

The VOTT for privately owned AVs seems to be similar to that for privately owned cars for mandatory trips but higher for non-mandatory trips. The VOTT for shared AVs seems to be much higher for both mandatory and non-mandatory trips compared to the VOTT for privately owned AVs, but much lower compared to the VOTT for taxis. Females seem to have higher VOTT than males for privately owned AVs and non-AV cars. Low-income households exhibit the highest VOTT for non-mandatory trips for both cars and private AVs, while people from middle- to high-income households have the highest VOTT for mandatory trips for both cars and private AVs. In general, the VOTT for non-mandatory trips seems to be lower than that for mandatory trips for wait time and access time.

Figure I.3.4.2 shows the effect of engaging in activities while traveling on overall mode utility based on travel duration. According to Figure I.3.4.2A, only travel durations less than 60 minutes create positive utility for engaging in activities while traveling in private AVs. According to Figure I.3.4.2B, the relationship between activity engagement and travel utility seems to be convex—travel durations of less than 30 minutes and more than 75 minutes seem to be conducive for engaging in activities while traveling on the bus. For shared AVs, however, only travel times more than 75 minutes seem to be conducive for producing positive travel utility (Figure I.3.4.2C). For taxi travel the opposite seems to be true—shorter travel times seem to be conducive for engaging in activities (Figure I.3.4.2D).

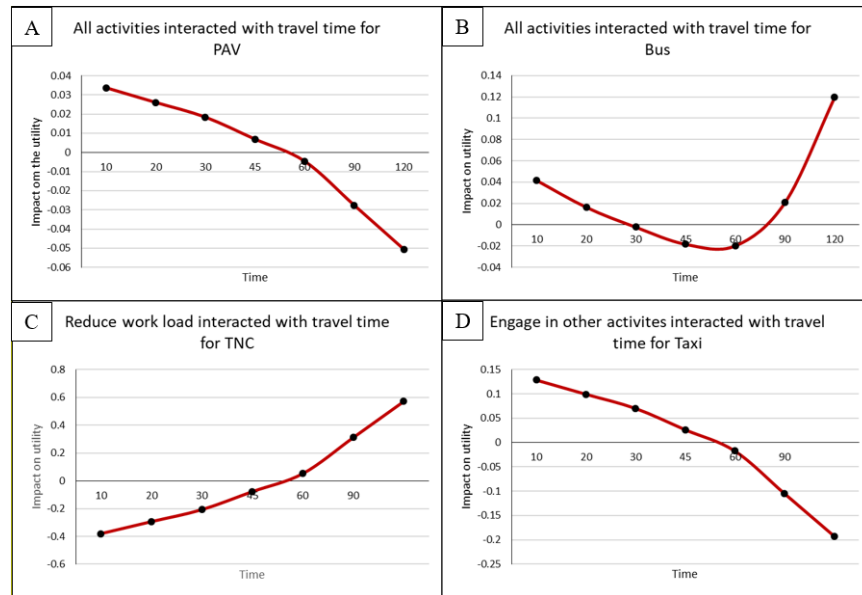


Figure I.3.4.2 The impact of activity engagement on travel utility

Impact of VOTT on System-wide VMT and VHT

A system-level analysis was conducted to quantify the impact of VOTT on mobility and energy metrics using the transportation system simulation tool POLARIS. Figure I.3.4.3 illustrates the relative contribution of VOTT to VMT for Bloomington, Illinois. Compared to other key behavioral parameters, VOTT was found to be the most significant parameter in the mode, destination, and time-of-day choice models. VMT is sensitive to the travel time parameter in the mode and destination choice models, with an elasticity of approximately -0.25 (there is a 2.5% reduction in miles traveled for every 10% increase in the travel time parameters).

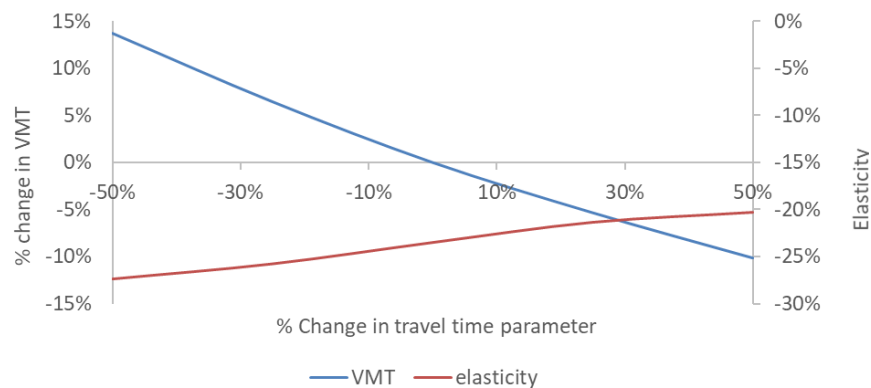


Figure I.3.4.3 Elasticity of VMT with respect to travel time

A parametric study was performed on 10 additional bundles to identify key behavioral parameters for VMT and VHT. Figure I.3.4.4 shows the results of the VMT analysis. The figure demonstrates the sensitivity of regional mobility to travel time by travel mode and travel time. Other parameters that were tested were found to have limited behavioral impacts, likely because of the limited study area. Bloomington is a relatively small city, with poor transit service and a homogenous land-use mix. These factors limit behavior responses, and a large-scale analysis could help identify sensitivities to additional behavioral parameters.



Figure I.3.4.4 Statistically significant VMT and VHT sensitivity to changes in key behavioral parameters

Impact of AV on VMT and VHT

The POLARIS tool was applied to the Chicago Metropolitan Area to test the impact of VOTT on system-level VMT and VHT. The study found that reducing perceived VOTT for travelers (i.e., reducing the cost of traveling) in privately owned AVs would increase VMT and VHT (Table I.3.4.1). This could result in as much as a 46% increase in VHT, a 45% increase in VMT, a 42% increase in fuel consumption, and increased congestion in the high-AV-penetration scenario in which the cost of travel time is assumed to be reduced by 50%. Holding the AV penetration constant and varying the VOTT shows a fairly uniform increase in energy and travel across the region, with the exception of the high-density employment and activity areas. Individuals living downtown and in other urban core areas are already near optimal activity spaces and do not tend to engage in substantial extra travel regardless of VOTT changes.

Table I.3.4.1 Impact on Mobility and Energy as VOTT Changes

AV Penetration	VOTT Reduction	VMT (millions)	VHT (millions)	Avg. Travel Time (min)	Avg. Trip length (mi)	Fuel Use (MM gallons)
0	0%	268.0	8.17	23.4	11.79	4.85
10.1%	30%	306.5	8.37	23.7	13.38	5.62
10.1%	50%	319.2	8.74	24.7	13.99	5.85
36.1%	0%	291.2	7.86	22.2	12.50	5.34
36.1%	30%	324.6	9.04	25.5	14.21	5.94
36.1%	50%	357.8	10.45	29.9	15.77	6.55
75.5%	0%	292.0	7.96	22.5	12.73	5.32
75.5%	30%	337.7	9.64	27.3	14.82	6.14
75.5%	50%	387.4	11.92	34.5	17.40	7.05

Conclusions

The analysis showed that VOTT varies substantially across demographic segments as well as across travel modes and characteristics of the travel environment. With the advent of AVs, additional factors such as multitasking while traveling might be influential for quantification of VOTT. This preliminary study shows that there is ample room for further research on the appropriate quantification of VOTT. A dearth of appropriate data was identified as one of the predicaments of conducting extensive research on VOTT quantification in the age of AVs and CAVs. However, a simulation study conducted for Bloomington and Chicago using the transportation system simulation tool POLARIS identified VOTT as one of the most important behavioral factors affecting VMT, VHT, and fuel consumption.

Key Publications

1. Krueger, R., T. H. Rashidi, and J. Auld, 2019, “Preferences for travel-based multitasking: Evidence from a survey among public transit users in the Chicago metropolitan area,” *Transportation Research Part F: Traffic Psychology and Behaviour* 65: 334–343.
2. Ardesheri, A., T. H. Rashidi, and J. Auld, “The Impact of Autonomous Vehicles and Multitasking on Value of Travel Time for Different Demographic Characteristics,” in review.

I.3.5 Travel Behavior Simulation Modeling in POLARIS :Enhance Existing Models to Estimate Impact of Modal Shifts Intra-City Passenger Travel - Transit Focused (ANL)

Joshua Auld, Principal Investigator

Argonne National Laboratory
9700 S Cass Avenue
Lemont, IL 60439
E-mail: jauld@anl.gov

Prasad Gupte, DOE Technology Manager

U.S. Department of Energy
E-mail: prasad.gupte@ee.doe.gov

Start Date: October 1, 2018

End Date: September 30, 2019

Project Funding (FY19): \$675,000

DOE Share: \$675,000

Non-DOE Share: \$0

Project Introduction

Based on the literature on transportation research, it is evident that potential changes in travel demand are key drivers of uncertainty in regard to the overall impacts of future mobility on energy use. In this task, we seek to extend the transportation system simulation tool POLARIS to better characterize mobility decisions made under new mobility technologies and modes. The core behavioral modeling components, as well as the supply modeling components, of the POLARIS simulator will be enhanced to capture changes in short-term, mid-term, and long-term decision-making brought about by new technologies. The updated POLARIS transportation simulation model will be used to evaluate the mobility, energy, and productivity (MEP) outcomes of these new mobility technologies in the context of the Chicago Metropolitan Area.

Objectives

The project objectives are as follows:

- To develop POLARIS models to better characterize individual traveler and mobility decisions;
- To model traveler behavior in POLARIS in terms of vehicle choice, activity planning, mode choice, multimodal route choice, and other choices sensitive to factors related to future mobility scenarios;
- To understand technological, behavioral, and other factors affecting shifts in MEP;
- To quantify the resulting MEP outcomes of connected autonomous vehicles (CAVs) and other new mobility technologies using the newly developed decision models; and
- To evaluate the energy and emissions outcomes of future mobility technologies in the Chicago Metropolitan Area.

Approach

The approach to achieving project objectives involves implementing various behavioral and supply models developed as part of this research and other mobility decision science (MDS) tasks or drawn from the literature. Models of key traveler behaviors are incorporated into the POLARIS agent-based modeling framework in order to evaluate sensitivities of the various behaviors to potential changes under various MDS scenarios. Figure I.3.5.1 presents an overview of the improvements to the core POLARIS simulation. The primary tasks of the travel-behavior simulation project over the last fiscal year involved the following:

1. Incorporation of a detailed parking structure into POLARIS, which includes parking locations, rates, and type (garage, lot, metered, permitted, and so on) for the Chicago Metropolitan Area;

2. Enhancement of the activity generation model for POLARIS to reflect level of service (LOS) information, for example, accessibility, and value of travel time (VOTT) changes due to multitasking opportunities provided by new mobility services;
3. Simulation of transit buses in mixed traffic;
4. Development of Household e-commerce participation model; and
5. Incorporation of a vehicle disposal model component to quantify households' propensity to relinquish vehicles with the increase in shared automated vehicle (SAV) fleets.

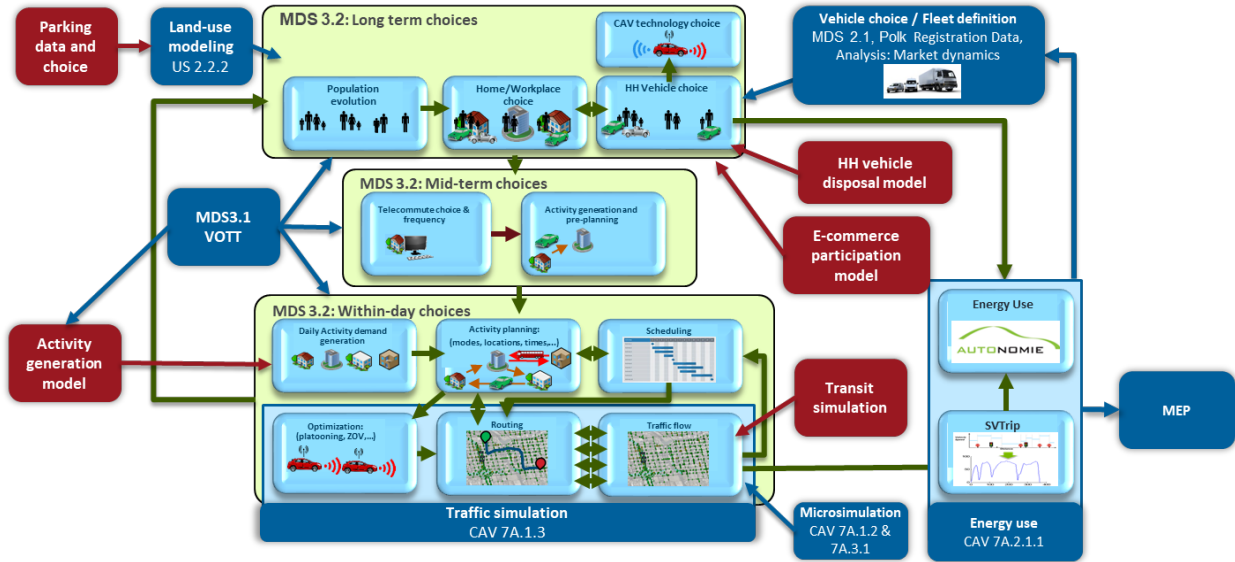


Figure I.3.5.1 Improvements to POLARIS behavioral models under MDS

Addition of Parking Information and Parking Choice Model

Parking is a critical element of individual travel by privately owned automobile, and parking costs have some of the highest impacts on VOTT for trips to heavily congested, high-cost areas, as shown in previous estimates of mode choice models for POLARIS (1). In order to ensure that accurate information is included in the mode choice estimation and application, a database of parking characteristics by location was created for Chicago and incorporated into the POLARIS network supply structure. Parking information on four types of parking—commercial lots, paid garages/lots, metered parking, and on-street parking—from a variety of data sources was combined. Commercial lot information, along with number of spaces in each, was drawn from the CMAP land-use coverage file, which was estimated from satellite imagery. Paid lots and garages were identified through API calls to multiple parking applications in the city, and information included hourly/daily rates and number of spaces. Metered parking spaces were identified through the Chicago Data Portal, and information included hourly meter rates and number of spaces per meter box. Finally, on-street parking was estimated through the Illinois Highway Performance Monitoring System, using lane widths, shoulder widths, shoulder composition, and other factors to determine the existence of parking lanes on each roadway in the system. Nearest parking availability of each type to each activity location was then identified and saved as a property of that location for use in destination choice modeling, and routing when combined with a parking-type choice model.

Enhanced Activity Generation Model

Travel behavior modeling suffers from a lack of longitudinal data because of the high cost of procurement and the difficulty of ensuring data quality. In recent years, ubiquitous data—intercepted from social media, cell detail records, GPS traces—are increasingly being explored to analyze human mobility. However, these data

lack key demographic information, limiting their use for developing causal models of traveler behavior. In this analysis, we use vehicle trajectory data from Ann Arbor along with multiple other data sources for developing a hazard-based activity generation model. The different categories of data used in the analysis are (1) vehicle trajectory data (VTD), (2) American Census Survey (ACS) data, (3) land use data, (4) household travel survey (HTS) data, and (5) smart location data from the U.S. Environmental Protection Agency (EPA). Home and work are identified as the two most frequently visited locations from the VTD and are validated against land use categories of the region. Next a random utility-based model is developed using HTS data to identify other activity purposes as a function of the polynomials of distance from home, activity duration, and departure time. The model developed is then applied to identify the non-home activity purposes in the VTD. Demographic and accessibility information is appended to the VTD from ACS and smart location databases, respectively. The final database is then used to develop a hazard-based activity generation model, similar to the one by Auld et al. (2), based on 2008 Chicago data.

Simulation of Transit Buses in Mixed Traffic

The POLARIS transit layer is built using the General Transit Feed Specification (GTFS) data available online. For the Chicago Metropolitan Area, four sources are used:

- GTFS for Chicago Transit Authority (CTA) (urban bus and urban rail [metro]);
- GTFS for PACE (suburban bus);
- GTFS for Metra (suburban [commuter] rail); and
- GTFS for South Shore (SS) by the Northern Indiana Commuter Transportation District (NICTD) (suburban [commuter] rail).

The GTFS database includes information on agency fare structure, stops, routes, trips, and trip schedules. Any consecutive stop pair served by a trip becomes a transit link in the POLARIS network, while transit stops/stations are modeled as transit nodes. Transit vehicles (bus or rail) move along transit links making stops at the transit nodes. Cars and other road vehicles move along the roadway links, crossing the black nodes or stopping at those. Travelers either walk along walk links, drive/ride on a road vehicle link, or ride in a transit vehicle on a transit link. The walk link connects either two road nodes or a transit node and a road node. In earlier versions of POLARIS, transit buses and trains moved along the transit links only according to the exact schedules published in the GTFS database, while in the updated POLARIS transit movements are impeded by roadway traffic. Using map-matching algorithms developed at Argonne, we have mapped the transit links onto the road links. This map-matching is now part of the POLARIS input database. For every bus trip, POLARIS software reads in the transit links sequence and the road link sequence. Moreover, it reads the fraction(s) of a road link at which the bus stops are located. For every bus trip, two bus agents are generated. One goes through the road network; it creates additional traffic and is affected by traffic. The other is a “phantom” bus moving along the transit links. However, instead of following the GTFS schedule exactly, it “listens” to the bus in traffic. Whenever the bus in traffic arrives at the location that corresponds to stop along the transit link, the “phantom” bus appears on the transit node.

Household E-commerce Participation Model

A behavioral model was developed to jointly quantify households’ decision to participate in e-commerce and the ratio of delivery to retail shopping for the households participating in e-commerce. The model was formulated as a simultaneous binary-ordered probit model in which the binary probit model is used to evaluate the participation decision and the ordered probit model is used to evaluate the delivery-to-retail-shopping ratio. The model was developed using phase 1 data from the WholeTraveler survey. In general, the model produces intuitive results; Table I.3.5.1 presents the parameter estimates of the household e-commerce demand model. Households with a large number of adults were found to be less inclined to participate in e-commerce than households with a small number of adults. Households with high incomes were more likely to participate in e-

commerce than households with low incomes. Also, households not served well by transits were more likely to participate in e-commerce than households well served by transit.

Among the households participating in e-commerce, number of adults, vehicles, household income, and walk accessibility seem to be important determinants of the delivery-to-retail-shopping ratio. High income tends to increase the delivery-to-retail-shopping ratio, while a high number of adults and vehicles tends to decrease the ratio. Households with good walk accessibility seem to have lower delivery-to-retail-shopping ratios.

Table I.3.5.1 Household E-Commerce Demand Model: Parameter Estimates

Variable	Estimate	t-statistic
Binary probit model: households' decision to participate in e-commerce		
Constant	-0.007	-0.07
Number of adults in household	-.047	-1.17
Household income less than \$20k indicator	-0.456	-2.33
Household income between \$25k and \$50k indicator	-0.533	-3.33
Household income between \$50k and \$100k indicator	-0.151	-1.4
Household income greater than \$200k indicator	0.398	3.74
Walking distance to nearest transit stop	0.076	1.16
Ordered probit model: Delivery-to-retail-shop ratio		
Constant	2.703	11.41
Number of adults in household	-0.184	-3.12
Household income greater than \$200k indicator	0.389	3.48
Household walk accessibility	-0.047	-2.45
Number of vehicles in household	-0.145	-2.27

Household Vehicle Disposal Model

It is expected that, with the emergence of AVs and CAVs, households will own fewer vehicles than now because of the increased availability of transportation network companies (TNCs) and other shared modes. However, the number of household vehicles is unlikely to be reduced uniformly; residents in urban areas and near high-quality transit are much more likely to dispose of vehicles than households with lower accessibility (e.g., rural areas, transit poor areas, and the like). To address this issue, the household vehicle disposal model developed by Menon et al. (3) was adapted to suit POLARIS requirements and implemented in the simulation code. The vehicle disposal model quantifies the willingness of households to dispose of vehicles. In addition, a separate distribution is used to quantify the number of vehicles to be disposed of for multivehicle households willing to reduce their vehicle fleet size. This model was applied through POLARIS in all runs of the workflow scenarios.

Results

The improvements made to the POLARIS behavioral simulator were applied to an analysis of the impact of the 13 scenarios developed as a part of the SMART Mobility Workflow. These scenarios included seven baseline cases and three future year cases, including a near-term high-sharing scenario (scenario A), a long-term high-automation, high-sharing scenario (scenario B), and a long-term high-automation but low-sharing scenario (scenario C). The impacts of individual behavior and mobility decisions can be seen in the outcomes of each scenario. First, for scenario C, Figure I.3.5.2 shows that the expectations of increased travel in CAVs because

of lower VOTT were observed in the modeling results. Personal miles traveled increased almost 57%, and hours traveled increased almost 43%. The per-capita person hours traveled for households with a full AV increases to almost 2 hours per day, which is a substantial increase over the average of 1.4 hours for non-AV owners. This, again, is driven by the assumed VOTT increase in the full AV, which represents the ability of travelers to multitask and engage in other activities during AV travel.



Figure I.3.5.2 Changes in (a) PMT and VMT and (b) PHT and VHT per capita by AV ownership for scenario C

Another key driver of the scenario results is household vehicle disposal, assumed to be driven by the increased availability of TNCs and other shared modes. The household vehicle disposal rate was set as a scenario parameter, with values of 45% for scenarios A-low and A-high, 68% and 75% for scenarios B-low and B-high, and 15% and 20% for scenarios C-low and C-high, respectively. However, household vehicles are unlikely to be disposed of uniformly, with residents in urban areas and near high-quality transit much more likely to dispose of vehicles than households with lower accessibility (e.g., rural areas, transit-poor areas, and the like). To address this issue, the household vehicle disposal model developed by Menon et al. (3) was adapted to suit POLARIS requirements and implemented in the simulation code. The proportions of households disposing of vehicles by zone for scenarios A, B, and C high-tech (VTO success) cases are shown in Figure I.3.5.3.

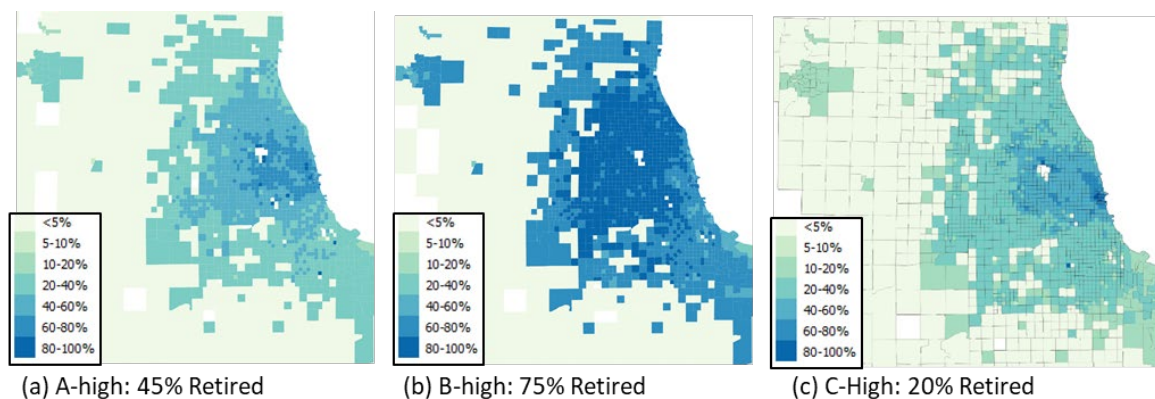


Figure I.3.5.3 Household vehicle retirement rates by traffic analysis zone for (a) A-high, (b) B-high, and (c) C-high scenarios

More detailed results for the individual scenarios are presented in Figure I.3.5.4, showing that the reduction in private vehicle ownership and the high penetration of AV technology in scenario B resulted in increases in transit and TNC travel. It is interesting that the increases in transit and TNC ridership complemented each other, with the ridership growing in the city center and suburbs for transit and TNC, respectively. This finding indicates that the transit and TNC operators can potentially maximize their ridership by coordinating their service areas. This outcome is largely driven by the reduction in vehicle ownership accompanying the high-

sharing automated scenario, with an assumed vehicle replacement rate of 10 household vehicles per new SAV, consistent with many of the previous simulation studies. SAV share also varies substantially across scenarios. In scenario C with a high proportion of private automation, the SAV share nearly matches the base SAV share, whereas the TNC share increases by only 2 to 3 percentage points.

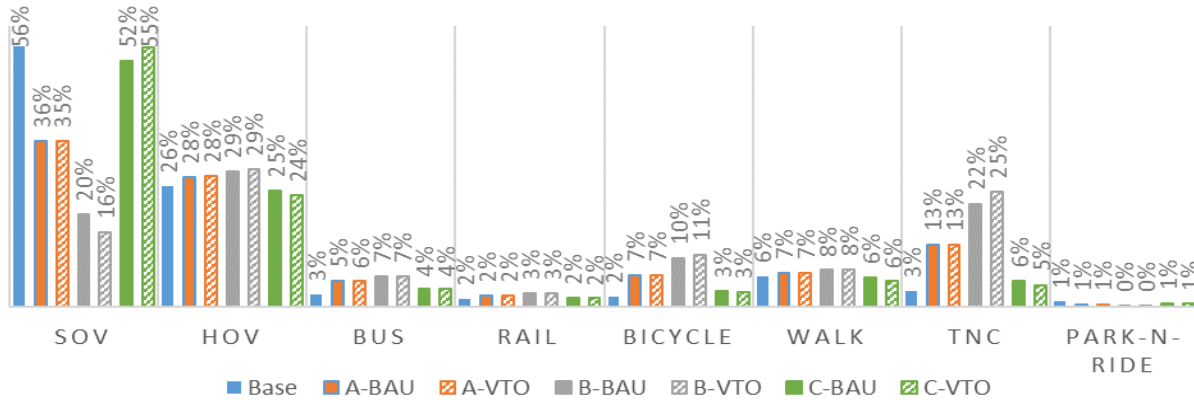


Figure I.3.5.4 Mode share by scenario

Conclusions

Travel behavior is a key driver of the differing results observed across the various scenarios run using the workflow. From the choice of mode, destination, start time, and the like to the response of trip rerouting and re-planning in response to changing congestion patterns, travel behavior forms the core of the POLARIS simulation model and the workflow. Many of the behaviors observed are driven by key scenario assumptions, primarily the assumed change in VOTT in AVs and the household vehicle disposal response to growing TNC availability. Both factors have an outsized influence on the results with the VOTT changes by automation level altering the mode, destination, start time, and route choices. Research conducted on the sensitivity of POLARIS to VOTT changes has shown strong elasticity at -0.25 , that is, about a 2.5% reduction in travel for a 10% increase in the travel time parameters for an individual, although this response is highly contextual and geographically dependent. Given the range of VOTT changes specified as scenario inputs with AV VOTT reduction ranging from 30% to 65% for full AV, we expected substantial increased travel for households with AVs.

Key Publications

1. Rashidi, T.H., J. A. Auld, and N. Saxena, “Studying the Tastes Effecting Mode Choice Behavior of Travelers under Transit Service Disruptions,” *Travel Behaviour and Society*, in review.
2. Shamshiripour, A., R. Shabanpour, N. Golshani, J. Auld, and A. Mohammadian, 2019, “A flexible activity scheduling conflict resolution framework.” Paper presented at the Transportation Research Board 98th Annual Meeting, Washington, DC, Jan. 13–17.
3. M. Javanmardi, J. Auld, and K. Gurumurthy, 2019, “Intra-household fully automated vehicles assignment problem model development and case study.” Paper presented at the Transportation Research Board 98th Annual Meeting, Washington, DC, Jan. 13–17.
4. O. Verbas, J. Auld, and M. Stinson, 2019, “Individualized gap-based convergence in an agent-based dynamic traffic assignment model using an information mixing approach for time-dependent travel times.” Paper presented at the Transportation Research Board 98th Annual Meeting, Washington, DC, Jan. 13–17.

References

1. Auld, J., O. Verbas, and M. Javanmardi, 2019, “Mode Choice Estimation and Simulation Using a New Intermodal Routing Algorithm and Transportation Big Data Sources.” Presented at the 15th International Conference on Travel Behavior Research, Santa Barbara, CA, July 15–19.
2. Auld, J., T. Rashidi, M. Javanmardi, and A. Mohammadian, 2011, “Dynamic Activity Generation Model Using a Competing Hazard Formulation,” *Transportation Research Record: Journal of the Transportation Research Board*, 2254: 28–35.
3. Menon, N., N. Barbour, Y. Zhang, A. R. Pinjari, and F. Mannering, 2019, “Shared autonomous vehicles and their potential impacts on household vehicle ownership: An exploratory empirical assessment,” *International Journal of Sustainable Transportation* 13(2): 111–122.

I.4 Multi-Modal Freight

I.4.1 Multi-Modal Energy Analysis for Inter-City Freight Movement (NREL, ANL)

Alicia Birky, Principal Investigator

National Renewable Energy Laboratory
901 D Street S.W. Suite 930
Washington, DC 20024
E-mail: alicia.birky@nrel.gov

Kyungsoo Jeong, Principal Investigator

National Renewable Energy Laboratory
15013 Denver West Parkway
Golden, CO 80401
E-mail: kyungsoo.jeong@nrel.gov

Joann Zhou, Principal Investigator

Argonne National Laboratory
9700 S Cass Avenue
Lemont, IL 60439
E-mail: yzhou@anl.gov

Prasad Gupte, DOE Technology Manager

U.S. Department of Energy
E-mail: prasad.gupte@ee.doe.gov

Start Date: October 1, 2018

End Date: September 30, 2019

Project Funding (FY19): \$384,000

DOE share: \$384,000

Non-DOE share: \$0

Project Introduction

U.S. transportation of freight consumed the equivalent of 7.4 quadrillion Btu (quads) in 2018 and accounted for 26% of total U.S. transportation energy. According to the 2019 Annual Energy Outlook (AEO), freight energy is projected to grow to 7.8 quads and 30% of transportation energy by 2050 as economic productivity and efficiency in passenger travel increases [1]. Per ton-mile, trucking is the second most energy intensive mode for freight transportation behind aviation. Freight energy use may be reduced through application of emerging technologies and optimization of freight movement. However, new technologies and trends also present possible challenges to improving freight efficiency. Further, measuring the impact of these developments is complicated by the complex, multi-agent, multi-modal, and multi-dimensional nature of freight movement. While many freight performance metrics exist, several must be considered simultaneously to provide a holistic measure of freight energy mobility that can be compared across regions, time, or future scenarios.

Objectives

The primary objective of this research project is to evaluate and understand the potential impacts of emerging technologies on inter-city freight movement and opportunities for reductions in energy consumption. This project addresses the following research questions: “how is mobility energy productivity defined for freight (F-MEP),” and “what is the impact of disruptive technologies and trends on inter-city freight flow, energy, cost, and shipping time?” The specific research goals are to:

- Develop a geographically based, generalizable framework for quantifying F-MEP that is:

- Able to integrate with existing freight modeling tools and publicly available data sources
- Capable of being tailored to a region or commodity
- Capable of measuring performance across various modes (and a combination of modes), both existing and future
- Capable of evaluating the impacts of emerging freight trends and technologies
- Conduct “stand-alone” bounding analyses of the potential impact of the following technologies on inter-city freight energy demand:
 - Automation – truck platooning
 - Truck electrification – hybrid electric (HEV), plug-in hybrid electric (PHEV), and battery electric (BEV) powertrains
 - Connectivity – truck and inter-modal load-pooling.

Approach

Freight Mobility Metric: F-MEP

This research develops a new freight system performance metric, consistent with DOE goals, to quantify freight system energy-productivity. Two methodologies are developed for F-MEP, one each for intra- and inter-city freight movement, both founded on a location-based accessibility theory and using a shipper perspective. An isochrone approach is adapted from the passenger MEP [2] for the intra-city F-MEP and an initial implementation is provided for the city of Columbus, Ohio. A new, gravity-based approach is developed for the inter-city F-MEP and is implemented using the Freight Analysis Framework (FAF) zone structure and commodity flow data [3].

Automation: Platooning

The potential national impact of platooning is analyzed by considering the spatio-temporal distribution of truck movements using FAF 2025 freight flows as the baseline for implementing platooning on the national highway network. Tonnage by origin-destination (OD) is decomposed to a finer geographic resolution than the FAF zone structure, converted to truck movements, and assigned to the highway network. These annual flows are then resolved to daily average peak and off-peak movements to determine geographic and temporal proximity. Vehicle OD demand matrices are developed as inputs to the platooning algorithm: platoonable FAF trucks, non-platoonable FAF trucks, non-FAF trucks, and passenger cars. A baseline scenario provides an estimate of potential fuel savings and a sensitivity analysis is used to explore the impact of fundamental assumptions.

Truck Electrification

An electrification scenario is defined using vehicle simulation results and cost assumptions from the VTO benefits analysis, which considers the impact of U.S. DOE research program goals. This study includes HEVs, PHEVs, and BEVs, in class 7 and 8 (gross vehicle weight rating >26,000 lbs) sleeper and day cab tractors and single unit (SU) trucks. PHEV and BEV all-electric range for sleeper cabs is roughly 250 and 500 miles respectively, and for day cab tractors is around 140 and 250 miles respectively. This study assumes that, due to continued R&D, there is no reduction in payload capacity due to BEV battery size. To obtain an upper bound on energy impacts, optimistic assumptions are used to estimate technology adoption, based on vehicle mileage distributions within trip distance bins from the Vehicle Inventory and Use Survey [4]. Sigmoid diffusion curves are fit between 2025 and 2050 market adoption rates and applied to projected truck sales from the 2019 *Annual Energy Outlook* [1] to estimate future in-use stock energy and petroleum savings.

Connectivity: Load Pooling

A new multi-modal inter-city freight energy model is developed as a bi-level optimization problem based on Zhang, et al. [5]. The lower level estimates inter-city freight movements for each mode and route in the context of system optimal freight assignment on the multi-modal network including truck, rail, water, and intermodal (truck + rail), considering mode- and commodity-specific shipping cost and mode-specific shipping time. Time, cost, and capacity for mode transfer links are included. In the upper level, total energy consumption is calculated given the optimal mode-route freight flows, and the best network design is selected from available alternatives (i.e., combinations of emerging technologies) to minimize the energy consumption. The model is calibrated and validated with 2020 and 2045 FAF estimates respectively. Exploratory scenarios are developed for truck and multi-modal load-pooling enabled by connectivity and collaborative online-markets.

Results

Intra-City F-MEP

The intra-city F-MEP is adapted from the passenger MEP and is a function of the total delivery opportunities o_{ikt} that can be reached by mode k from the i^{th} cell block (location) within a given travel time t (the isochrone), and a mode specific utility function U_{ikt} that depends on energy, travel time and cost:

$$FMEP_i = \sum_k \sum_t (o_{ikt} - o_{ik(t-\Delta t)}) \cdot e^{U_{ikt}}$$

The total opportunity metric for each location, mode, and isochrone is a weighted sum of the individual delivery opportunities by type (o_{ijkt}). The weighting factors are based on the total number of benchmark opportunities across multiple cities (N^*), the total number of opportunities of type j within the subject region (N_j), and the typical frequency of deliveries for opportunity type j (f_j):

$$O_{ikt} = \sum_j o_{ijkt} \cdot \frac{N^*}{N_j} \cdot \frac{f_j}{\sum_j f_j}$$

The intra-city F-MEP is implemented for Columbus, OH using a 1-km by 1-km square grid. Ten preliminary opportunity types associated freight activities are identified based on available establishment data and population (representing residential deliveries). For the purposes of demonstration, delivery frequencies are assumed to be one visit per day to business establishments and six per day to residential locations. The number of post office opportunities is used for the opportunity benchmark factor and average travel times between two locations are obtained from the network. Two modes are assumed: class 6 and class 8 trucks with energy intensity of 8 miles per gallon and 5.8 miles per gallon, respectively. Figure I.4.1.1 presents the overall F-MEP scores, scaled from 0 to 100 and shaded from red to green, for all pixels in the study area. Locations along the highway and close to the center of city have high F-MEP scores, reflecting that shippers in those locations can easily access potential customers in other locations.

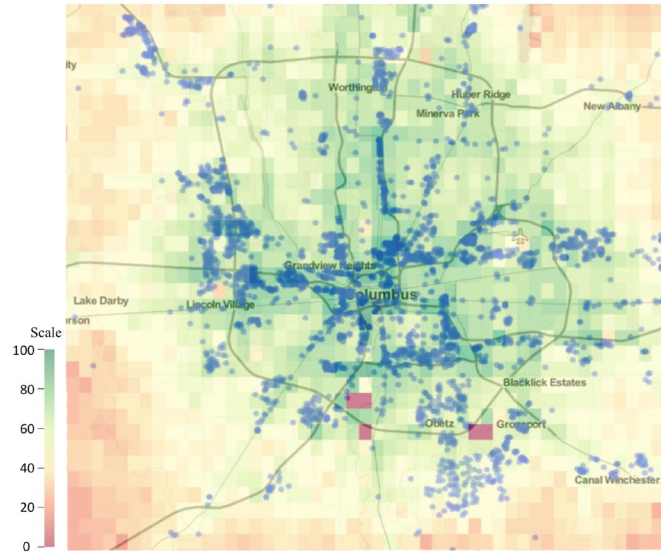


Figure I.4.1.1 Total F-MEP score, illustrative implementation in Columbus, OH

Inter-City F-MEP

The inter-city $F-MEP_i$ for location i is the product of two factors: mobility benefit and impedance. Mobility benefit, B_{cj} , of commodity or business type c delivered to location j , is a function of freight delivery opportunities, \mathbf{X} . Impedance, $f_{c,ij}$ is specified for each mode k and is a function various cost variables, \mathbf{Y} :

$$FMEP_i = \sum_k \sum_c \sum_{j \neq i} B_{cj}(\mathbf{X}) \cdot f_{c,ij}^k(\mathbf{Y})$$

An exponential formulation is selected for the impedance function $f_{c,ij}^k$, including mode-specific measures of energy intensity (E_k), unit logistics costs (p_k), shipping time, and ease of shipping from location i (s_{ik}). The exponential form captures increasing response as costs increase and allows for mode- and commodity-specific parameters in this decay function. Given the correlation within each mode between distance and time, impedance caused by time is captured through the fraction r of commodity c moved by mode k within range l containing the distance between i and j .

$$f_{c,ij}^k = \exp(\alpha E_k + \beta p_k) \cdot r_{ck}^{l_{ij}} \cdot s_{ik}$$

To demonstrate this formulation, the methodology is implemented for the mainland U.S. using the FAF data and zonal structure. For zone i , the benefit B_{cj} of shipping commodity c to zone j is assumed to be captured by the total commodity tonnage shipped from i to j . The impedance function parameter values should reflect the user's (e.g., shipper or planner) perceptions of the relative importance of cost and energy, but to provide an initial illustration, the coefficients for both energy and cost are set to -0.5. The FAF is used to determine commodity fractions (r). Ease of shipping is set to 1 for trucks and calculated as the ratio of the number of modal facilities in zone i divided by the maximum number of facilities in any zone. Energy intensity and logistics cost by mode are estimated from the literature.

Figure I.4.1.2 presents the overall F-MEP scores for each originating zone, aggregated over truck, rail, water, and air modes. The map is coded in a red gradient scale with dark red indicating high scores from that zone. Overall, zones in the Midwest and Mid-Atlantic score higher. These findings are consistent with expectations based on the following: 1) many zones with high F-MEP are in the central U.S. and have relatively short distances to all other zones; 2) zones with high F-MEP have good accessibility to all transportation modes,

including ports; 3) zones with high F-MEP are close to large freight demand markets in the Northeast; and 4) many zones with high F-MEP are located near manufacturing centers that realize high shipping benefits.

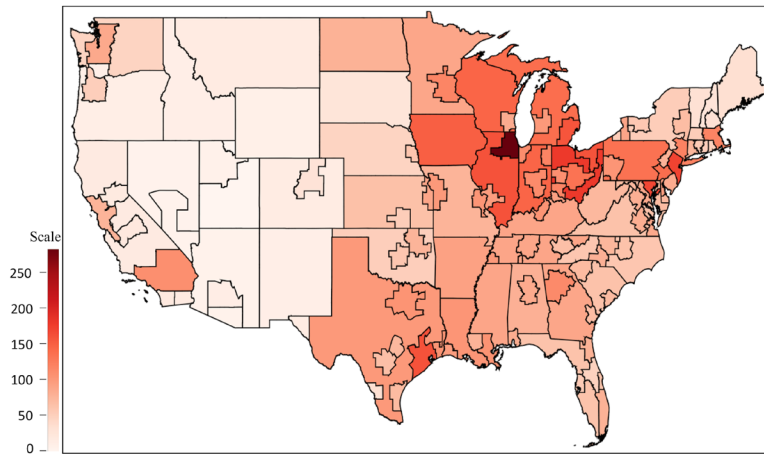


Figure I.4.1.2 National scale inter-city F-MEP map using FAF zonal structure

The F-MEP can be used to examine heterogeneity in opportunities (commodities) and modes and can be disaggregated to a single mode, a single commodity, or a single mode-commodity combination as illustrated in Figure I.4.1.3. This disaggregation capability is an extremely useful feature that enables customized analysis to understand the relative magnitude and geographic distribution of impacts on freight mobility productivity for different technologies, trends, or infrastructure investments.

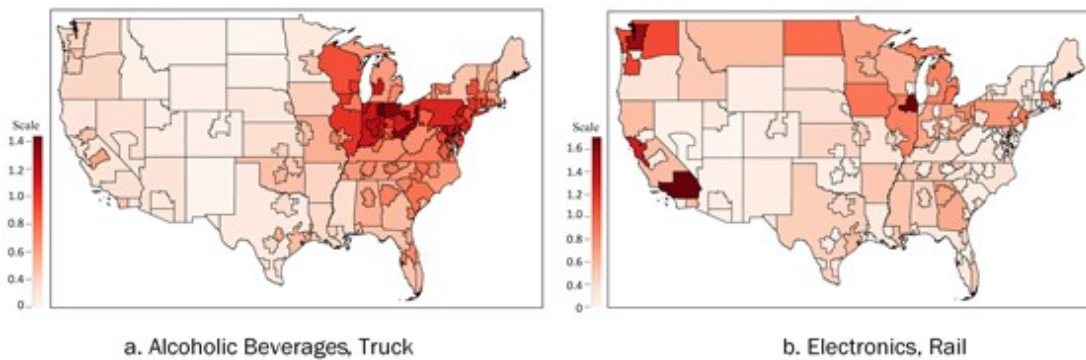


Figure I.4.1.3 Illustration of commodity-mode-specific inter-city F-MEP

The F-MEP can be used to evaluate the impacts of emerging technologies on freight performance at the system level. To demonstrate the responsiveness of F-MEP metric to freight technologies, a hypothetical scenario analysis is presented, where BEVs are deployed in shipments under 500 miles ($l_{ij} \leq 500$) and are assumed to reduce the energy intensity from \$0.0734/ton-mile to \$0.0245/ton-mile. Figure I.4.1.4 illustrates the improvement in F-MEP relative to the baseline case. Zones that have the largest freight movement within 500 miles show the greatest improvement as a result of vehicle electrification.

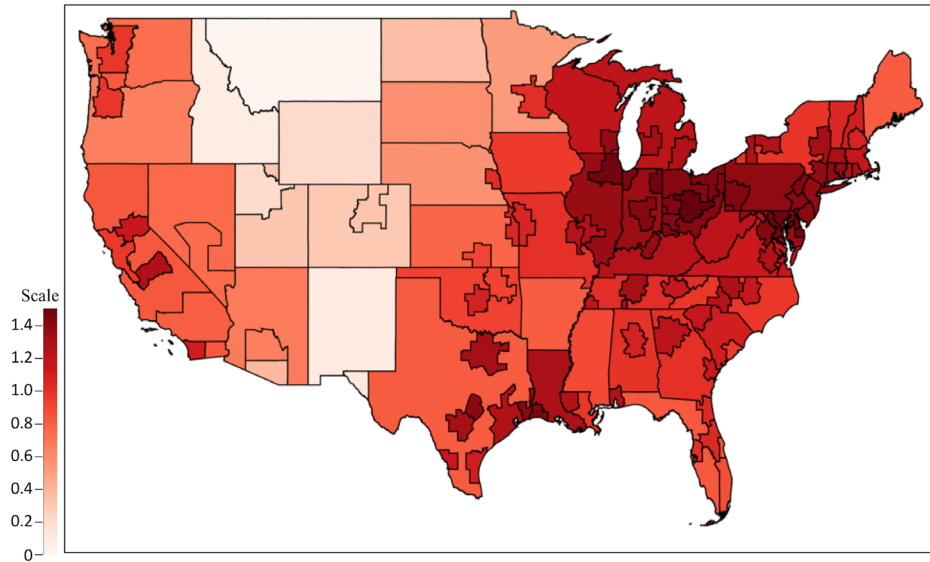


Figure I.4.1.4 Change (%) in total F-MEP for hypothetical truck electrification scenario

Platooning

Analysis of FAF data shows that 67% of commodity and truck flows are intra-zonal, which precludes assigning these flows to the road network and determining truck geographic proximity. Using a clustering methodology, a new zoning system is developed with a higher geographic resolution than FAF but not as fine as county-level, which would result in high computational cost. This methodology results 1,603 sub-FAF zones with intra-zonal freight accounting for only 16% of total flows.

Freight flows (tons) are then converted to number of trucks between sub-FAF zones by applying the methodology developed for Oak Ridge National Laboratory [6]. A total of 45 truck unique truck types (five configurations and nine body types) are identified. Tonnages are assigned to each truck configuration by distance range then converted to number of trucks by type using commodity specific truck equivalency factors. A truck empty factor specific to the truck type is then applied to account for empty movements.

Truck trips between sub-FAF zone pairs are assigned to the national highway network using the User Equilibrium (UE) principle which allows vehicles to interact and together determine the level of congestion. Estimated average annual daily truck traffic is allocated to equivalent average hourly traffic and is validated by comparing the resulting assigned truck trips for 2012 with actual truck network flows from Highway Performance Management System data. A peak-hour factor is then applied to determine peak and off-peak flows as shown in Figure I.4.1.5. Background non-FAF truck and passenger traffic flows are then added.

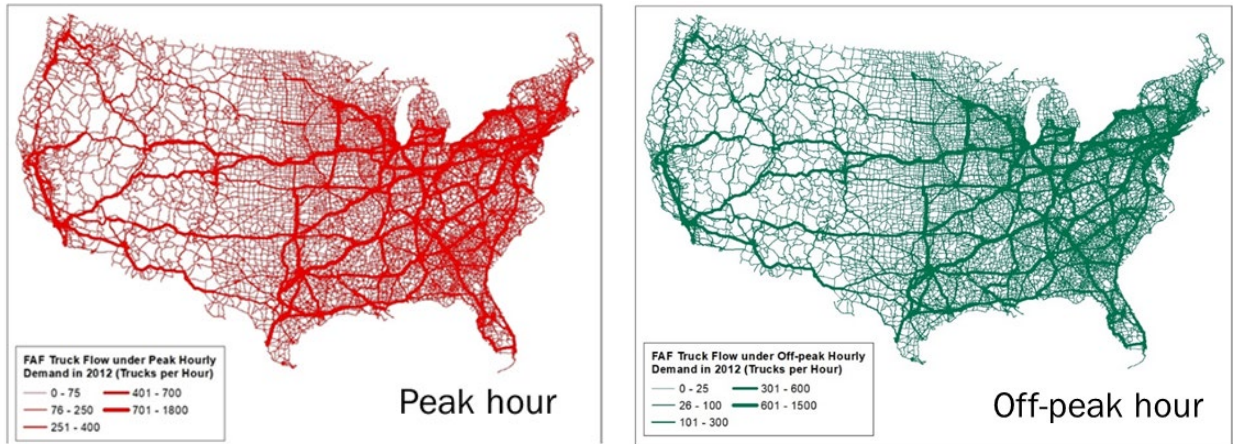


Figure I.4.1.5 Results of truck network assignment and temporal disaggregation

To assess the platooning potential, it is assumed that tractors with double and triple trailer configurations would not participate in platoons while single unit trucks (SU), truck plus trailer (TT), and tractor plus semitrailer combination (CS) are platoonaable. Among the nine truck body types, dry van, platform (flatbed), reefer, livestock, and automobile are considered platoonaable for a total of 15 out of 45 combinations of truck configurations. This accounts for 49% and 52% of 2012 and 2045 truck trips respectively.

In the baseline, 100% of platoonaable trucks are allowed to form a platoon if a road link is eligible for platooning. A road link is considered eligible if it satisfies three criteria as shown in Table I.4.1.1. In the baseline scenario, 60% (35,346 miles) of rural interstate highways are eligible. The baseline scenario assumes three trucks per platoon and an inter-truck gap of 0.4 seconds, which indicates a 9.5% truck-level fuel saving.

Table I.4.1.1 Criteria for Road Link Platooning Eligibility

Criterion	Baseline Value
Road type allowed for platooning	Rural interstate roads only
Road length meets or exceeds minimum threshold	5 miles
Time ratio (exogenous parameter)	0.2

The methodology assumes spontaneous platooning, with the decision to form a platoon based on generalized travel cost. It does not force trucks moving on low-volume routes with low proximity to reroute to form a platoon. The baseline platooning scenario results indicate a system-level fuel saving of 7.9% for all platoonaable FAF trucks across the network. This is 1.6 percentage points smaller than the truck-level fuel saving because not all miles occur in platoons. Platooning increases the total capacity of rural interstate highways by 1.5%. Because of the proximity approach, no changes occur in the total platoonaable truck VMT.

Sensitivity analyses are used to investigate the impact of platoon size and inter-truck gap assumptions on fuel cost savings and system capacity. As shown in Figure I.4.1.6 and Figure I.4.1.7, reducing the platoon size to two trucks significantly reduces system fuel cost savings to 5.6% and capacity improvement to 1.2%, while increasing to four trucks increases fuel cost savings and capacity improvement to 8.3% and 1.7%. Further increasing the platoon to five trucks has a smaller impact on fuel cost savings of only 0.2 percentage points. Figure I.4.1.8 illustrates the impact of the inter-truck gap assumption. Decreasing the gap to 0.2 seconds increases fuel cost savings to 9.5%, while increasing the gap to 0.6 seconds decreases savings to 6.9%.

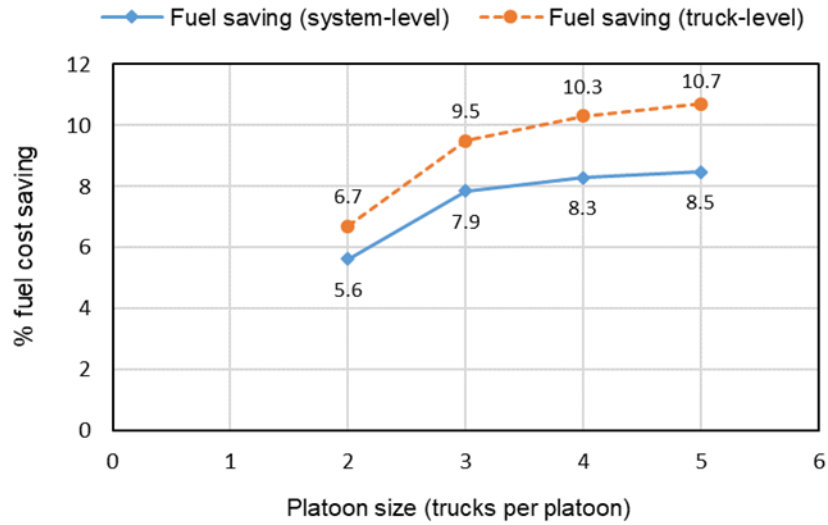


Figure I.4.1.6 Impact of platoon size on fuel cost savings

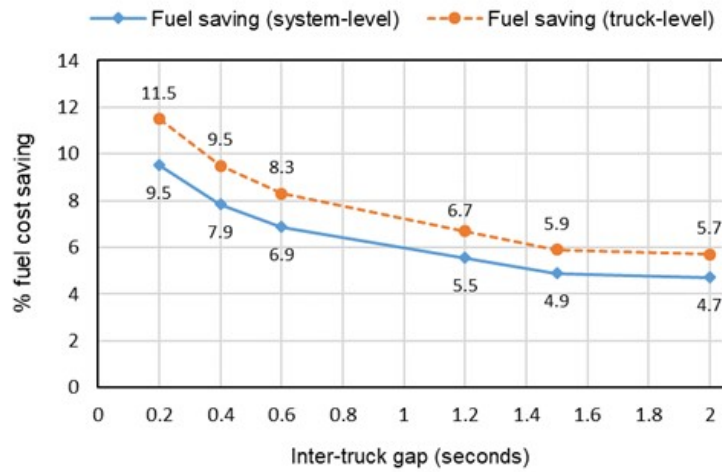


Figure I.4.1.7 Impact of inter-truck gap on fuel cost savings

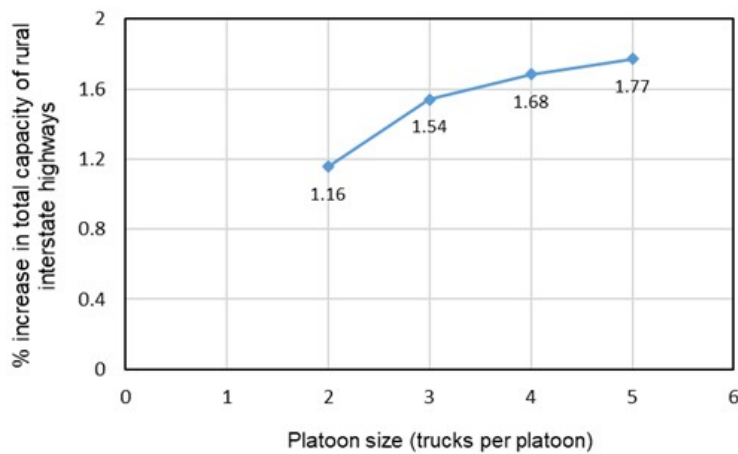


Figure I.4.1.8 Impact of platoon size on rural interstate highway capacity

Truck Electrification

Class 7&8 vehicle input assumptions from VTO benefits analysis are applied in 2025 and 2050 [7]. The following optimistic assumptions are used to estimate technology adoption, based on vehicle mileage:

- Maximum daily range and annual mileage are determined assuming 24-hour operation and average speed calculated from EPA regulator cycles as well as fast charging
- Charge power of 600 kW in 2025 and 800-1000 kW (PHEV and BEV) in 2050
- 100% willingness to adopt a technology if break-even is achieved within 4 years, considering only vehicle and fuel costs on a net present value (NPV) basis with a 7% discount rate
- If multiple technologies break even within 4 years, the one with the lowest lifetime cost is adopted.

Figure I.4.1.9 shows that the tractor market share for electrified class 7&8 tractors could optimistically reach 83% of tractors and 30% of single unit trucks. PHEVs are adopted over BEVs due to their smaller and cheaper batteries coupled with optimistic assumptions about full charging availability and 24-hour operation which maximizes utilization of all-electric mode. Some amount of electrification is adopted in all freight movement, regardless of shipment distance, though no segment is fully electrified (i.e., BEV). As shown in Figure I.4.1.10, class 7&8 petroleum consumption could be reduced by 37% relative to the AEO reference case or 1.4 quads in 2050, while total class 7&8 energy demand could be reduced by 23% or 0.9 quads.

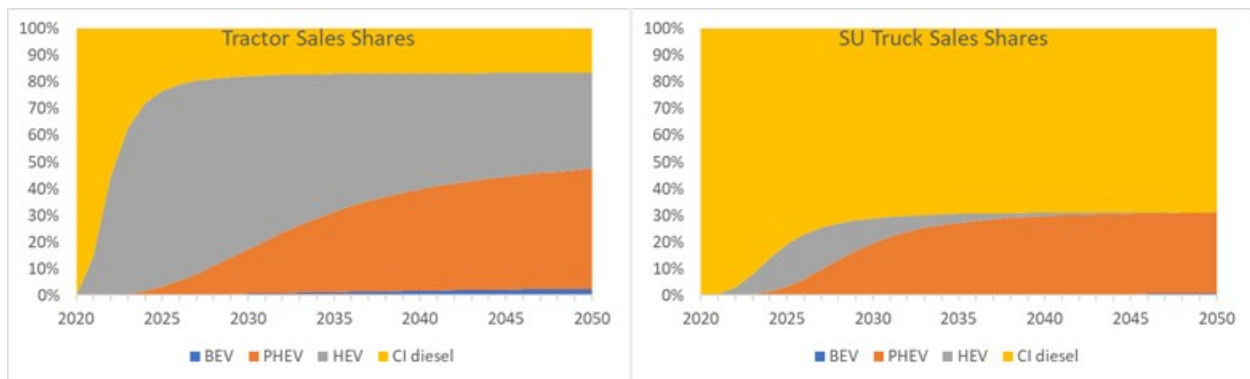


Figure I.4.1.9 Electrified powertrain sales share projection

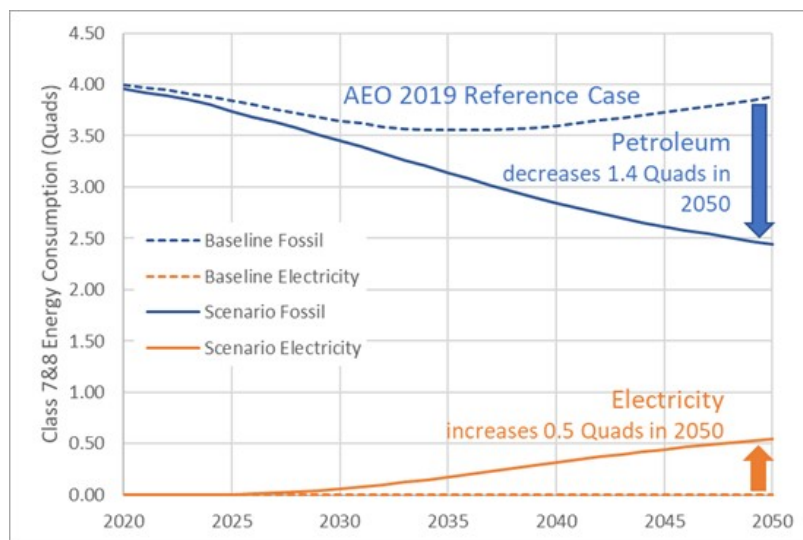


Figure I.4.1.10 Projected petroleum savings potential due to class 7&8 truck electrification

Figure I.4.1.11 the powertrain adoption within primary trip distance bins. Based on payback period and lifetime NPV, PHEVs are the only technology adopted in trips under 200 miles. It should be noted that only 500-mile range BEVs are included in sleeper tractors and it is possible that a lower range BEV would have provided lower cost than the PHEVs in some of these trip bins. BEVs are only adopted in the 201-500-mile trip bin and are the only technology solution for SU trucks in this bin, while tractors in this range also adopt PHEVs. While HEVs are attractive in 2025, they lose share to other powertrains in 2050. HEVs do remain viable in the 500+ mile range where it is assumed that plug-in vehicles must be capable of competing a trip without recharging, precluding BEV deployment and reducing the PHEV all-electric mile fraction. In general, total electrified powertrain adoption is lowest for trucks whose primary trip distance is under 50 miles where low annual mileage results in longer payback time.

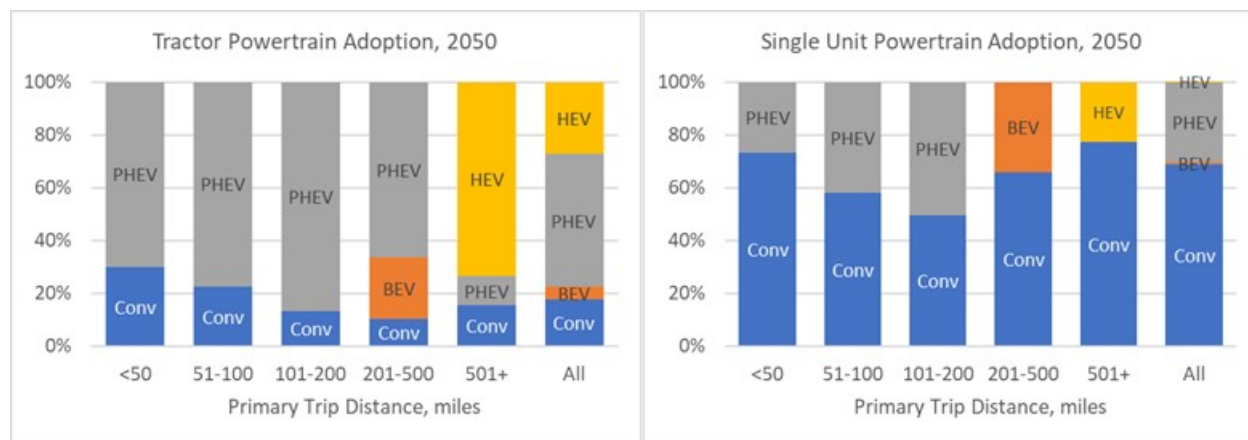


Figure I.4.1.11 Powertrain Adoption within Trip Distance Bins, 2050

Electrification reduces the lifetime cost of the new vehicle fleet, calculated as the NPV of vehicle purchase price and lifetime fuel expenditures. As shown in Table I.4.1.2, cost reductions relative to a 2050 all-diesel fleet range from \$0.030 to \$0.101/mile, with a sales fleet average of \$0.062/mile for tractors and \$0.059/mile for SU trucks. Reductions are highest in the 101-200 mile trip bin where PHEV adoption is highest and electric range is sufficient to cover daily miles. Though technology adoption is small in SU trucks, their absolute costs are higher than tractors due to lower annual usage, resulting in cost reductions of similar magnitude in many cases.

Table I.4.1.2 2050 Sales Fleet Lifetime Cost (\$/mile)

TRIP_PRIMARY	Tractors			Single Unit Trucks		
	Base Diesel	Scenario	Reduction	Base Diesel	Scenario	Reduction
<50 miles	\$0.584	\$0.488	\$0.096	\$0.818	\$0.768	\$0.050
51-100 miles	\$0.553	\$0.452	\$0.101	\$0.707	\$0.631	\$0.076
101-200 miles	\$0.519	\$0.426	\$0.093	\$0.635	\$0.545	\$0.090
201-500 miles	\$0.491	\$0.417	\$0.074	\$0.649	\$0.585	\$0.064
501+ miles	\$0.487	\$0.454	\$0.033	\$0.606	\$0.576	\$0.030
All	\$0.508	\$0.446	\$0.062	\$0.772	\$0.713	\$0.059

Connectivity: Load Pooling

The multi-modal inter-city freight energy model is applied to all freight shipments originating from or destined for the Chicago region. An inverse modelling approach is used to infer model parameters by assuming that FAF tonnage flows between ODs are optimal in the freight assignment problem. The model is calibrated with the 2020 FAF estimates and validated with 2040 FAF estimates. The model is then applied to explore load-pooling scenarios and assess energy consumption for optimized inter-city freight movement.

Load-pooling scenarios are specified based on observed logistics costs in 2016 and truck load and empty factors from FAF. It is assumed that these values remain constant in a baseline projection to 2045 but change according to the scenarios. In truck load-pooling, collaborative logistics through on-line freight markets increases truck payloads (trucks are more fully loaded on average), reduces movement of empty trucks, and decreases logistical costs relative to conventional operations. Six exploratory scenarios are defined by varying market participation from 5% to 30% of the base year truck volume in increments of 5%. In each scenario, truck operational costs are assumed to be reduced by 5%, truck payloads are assumed to increase 10%, and the empty truck factor is assumed to decrease 10%, compared to the baseline values. As shown in Figure I.4.1.12 , the reduction in trucking costs shifts freight from other modes to trucks, with the impact increasing with higher participation rates. Because trucks are more energy intensive on a Btu/ton-mile basis than rail and water, the mode shift increases total freight energy, despite the trucking logistical efficiency gains (Figure I.4.1.13). This finding implies that truck load-pooling without improvement in energy use of truck could result in an increase in energy consumption, depending on the impact on truck utilization.

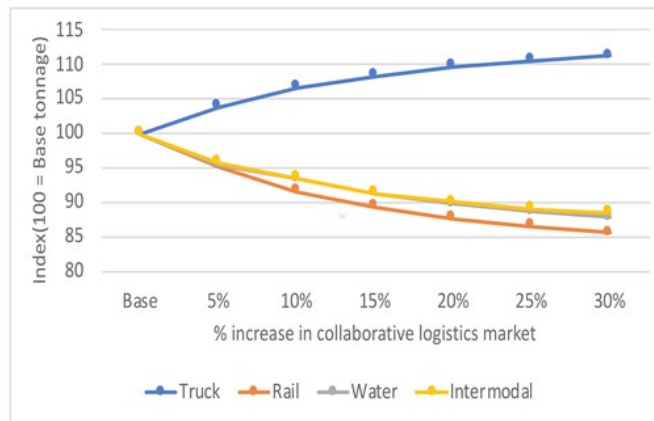


Figure I.4.1.12 Change in 2045 freight flow due to cost reductions from truck load-pooling

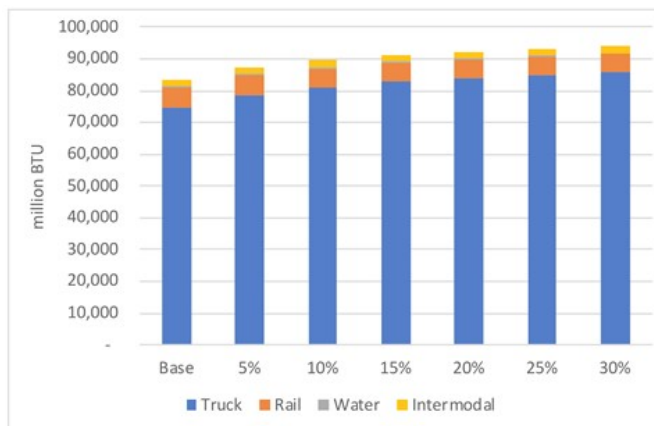


Figure I.4.1.13 Total 2045 freight energy consumption for truck load-pooling scenarios

This finding is further explored for a 30% market participation by varying the payload and empty truck impacts over seven scenarios defined in Table I.4.1.3. Figure I.4.1.14 shows the associated decrease in truck energy consumption as truck utilization improves. The impact is marginal relative to the total increase in freight energy consumption from the modal shift, and energy in the most aggressive scenario, S7, is still higher than the baseline (89.0 versus 83.6 billion Btu). Energy consumption appears to be more sensitive to changes in payload than empty truck factor. These results indicate that more energy efficient powertrain technologies may be required to offset energy increases associated with modal shifts arising from truck load-pooling.

Table I.4.1.3 Scenarios Exploring the Impact of Truck Payload and Empty Truck Factor

	S1	S2	S3	S4	S5	S6	S7
Payload Change	10%	10%	10%	10%	20%	30%	40%
Empty Truck Factor Change	-10%	-20%	-30%	-40%	-10%	-10%	-10%

Note: market participation is 30% and cost reduction is 5% in all scenarios

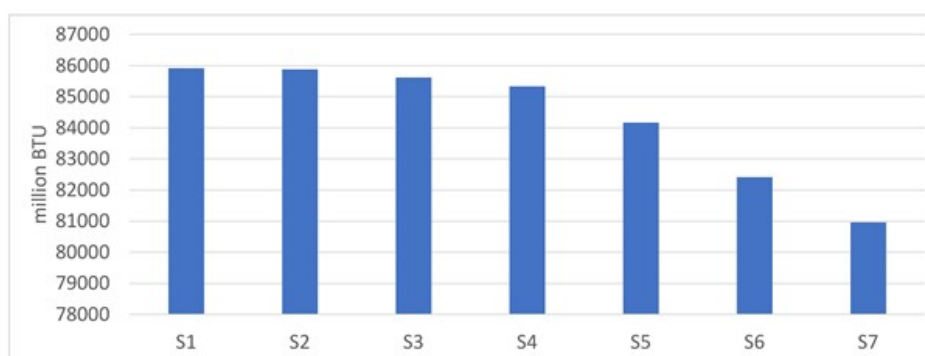


Figure I.4.1.14 Truck energy consumption for payload and empty truck factor scenarios

Note: market participation is 30% and cost reduction is 5% in all scenarios

Multimodal load-pooling is similarly enabled by connectivity and on-line markets, but participation is restricted by current intermodal terminal capacity. Again, six exploratory scenarios are defined by increasing the capacity on intermodal transfer links by 5% to 30% of the inferred baseline capacity. Inter-city freight at the strategic level achieves a system optimum with route and mode assignment determined by minimizing total cost. Since intermodal shipping (truck + rail in this study) provides cost savings compared to truck only, intermodal capacity expansion results in a shift from single-mode truck. Meanwhile, changes in single-mode water and rail tonnage flows are marginal as shown in Figure I.4.1.15. As freight moved by intermodal increases, Figure I.4.1.16 shows that multimodal load-pooling reduces system wide energy consumption.

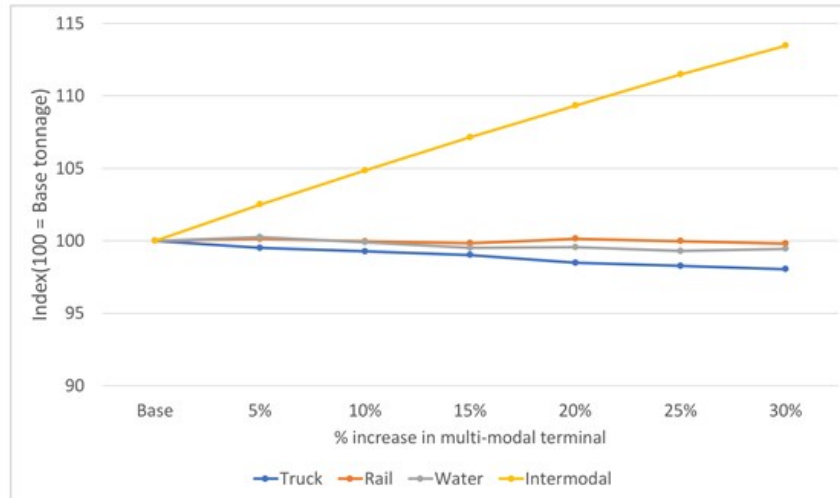


Figure I.4.1.15 Change in freight flows for multimodal load-pooling scenarios in 2045

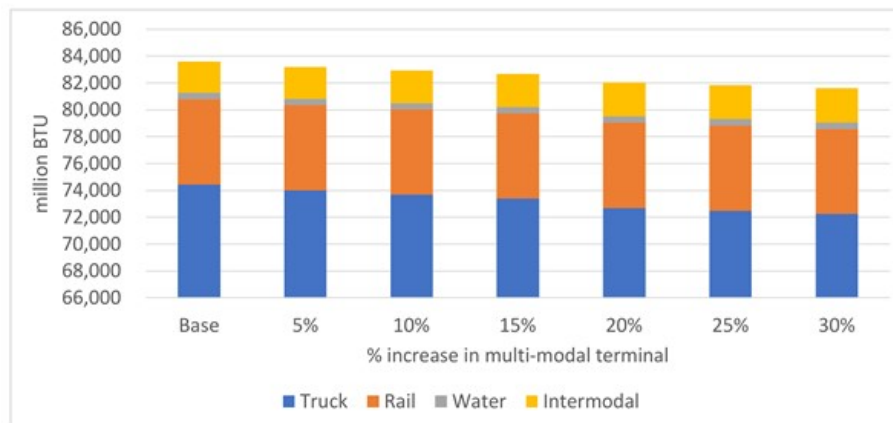


Figure I.4.1.16 Energy consumption in 2045 for multimodal load-pooling scenarios

Conclusions

This research presents two new geographically based metrics to quantify intra- and inter-city freight energy-productivity in a holistic way. Preliminary implementations demonstrate that these metrics can capture the impact of emerging technologies and can be used to compare current and future system productivity across regions, modes, commodities, time, and scenarios.

This project estimates energy impacts of stand-alone emerging automation, electrification, and connectivity technologies. Platooning could lead to a freight truck system-level fuel saving of around 7.9% for all platoenable trucks across the national highway network and could increase the total capacity of rural interstate highways by 1.5%. These savings are sensitive to number of trucks in the platoon and inter-truck gap. Meanwhile, electrification could potentially reduce the petroleum and energy consumption of class 7&8 trucks by 37% and 23% respectively by 2050. Electrification reduces lifetime truck costs per mile on average by 8% and 12% for the SU and tractor sales fleet but by as much as 18% in the 51-200 mileage bins for tractors.

This project provides a new multimodal freight energy model that is used to explore truck and multimodal load-pooling enabled by connectivity. Cost reductions realized through truck-only load-pooling are shown to induce a shift of freight from water and rail to trucks. Depending on the magnitude of associated truck utilization improvements, this modal shift could result in a net increase in freight energy consumption.

Meanwhile, multimodal (truck + rail) load-pooling shifts freight from truck to intermodal and reduces net energy demand. These results highlight the need to understand both the cost and efficiency impacts of freight technologies and consider them within a multimodal framework.

Key Publications

1. Jeong, K., V. Garikapati, Y. Hou, A. Birky, and K. Walkowicz. "A Comprehensive Approach to Measure the Efficiency of Freight Transport: Freight Mobility Energy Productivity Metric." *Accepted for presentation at the 99th Transportation Research Board Annual Meeting and for further publication assessment by the Transportation Research Record.*
2. Y. Zhou and M. Rood, "National Energy Impacts of Heavy Electric Truck Adoption For Freight." Presented at 32nd Electric Vehicle Symposium (EVS32), Lyon, France, May 2019.

References

1. U.S. Energy Information Administration. *Annual Energy Outlook 2019*. Washington, DC: U.S. Department of Energy, 2019. <https://www.eia.gov/outlooks/aeo/pdf/aeo2019.pdf> (accessed October 17, 2019).
2. Hou, Yi, Venu Garikapati, Ambarish Nag, Stanley E. Young, and Tom Grushka. "Novel and Practical Method to Quantify the Quality of Mobility: Mobility Energy Productivity Metric." *Transportation Research Record* (2019): 0361198119848705
3. U.S. DOT. *Freight Analysis Framework*. V4.4.1. June 6, 2018. <https://faf.ornl.gov/fafweb/>
4. U.S. Census Bureau. *2002 Economic Census, Vehicle Inventory and Use Survey*. EC02TV-US. Washington, DC: U.S. Department of Commerce, 2004.
5. Zhang, M., M. Janic, and L. A. Tavasszy. "A freight transport optimization model for integrated network, service, and policy design." *Transportation Research Part E: Logistics and Transportation Review*, 77 (May 2015): 61-76.
6. Maks Inc. *FAF⁴ Freight Traffic Assignment, Final Draft Report*. Submitted to Oak Ridge National Laboratory, August 2016.
7. Stephens, T.S., R. Vijayagopal, M. Dwyer, A. Birky, and A. Rousseau. *Vehicle Technologies and Fuel Cell Technologies Office Research and Development Programs: FY 2020 Prospective Benefits Assessment for Medium- and Heavy-duty Vehicles*. Argonne National Laboratory Report, forthcoming.

Acknowledgements

This work is supported by the U.S. Department of Energy, Office of Energy Efficiency and Renewable Energy (EERE), Vehicle Technologies Office (VTO). We thank David Anderson, Program Manager of Energy Efficient Mobility Systems, for his generous support. We also thank David Smith, the pillar lead of Multi-Modal for his support and guidance on this task. The authors would like to thank Yi Hou and Venu Garikapati of NREL for their contributions to development of the F-MEP, and Bo Zou and Hossein Noruzoliaee of University of Illinois at Chicago for their efforts on development of the platooning model.

I.4.2 Optimization of Intra-City Freight Movement with New Delivery Methods (ORNL, INL) [Task 3.1]

Amy Moore, Principal Investigator

Oak Ridge National Laboratory
2360 Cherahala Boulevard
Knoxville, TN 37932
E-mail: mooream@ornl.gov

Victor Walker, Principal Investigator

Idaho National Laboratory
2525 Fremont Avenue
Idaho Falls, ID 83415
E-mail: victor.walker@inl.gov

Prasad Gupte, DOE Technology Manager

U.S. Department of Energy
E-mail: prasad.gupte@ee.doe.gov

Start Date: October 1, 2018
Project Funding: \$745,000

End Date: September 30, 2019
DOE share: \$745,000 Non-DOE share: \$0

Project Introduction

There has been an increase in the movement of freight delivery vehicles due to a relatively recent shift in consumer preferences to purchase goods online rather than in physical stores. This shift in behavior and business activity has the potential to impact transportation systems, and the entire transportation network, but especially in the last-mile portion of intra-city deliveries.

This research primarily focuses on energy-reduction strategies for moving freight within an urban context. Intra-city freight, or freight moving throughout a metropolitan region, usually confined to the city limits or perimeter highway of a large urban area, has many interactions that long-haul freight does not: besides congestion and lack of available parking and curb space, intra-city freight routes are typically more convoluted, even circuitous, and in large residential areas, involve many more stops. This occurrence presents an opportunity for improving efficiency, especially in terms of energy usage, which is the primary focus of this work.

Due to the myriad ways of addressing the problems associated with a growing population and changing consumer demands, this research was necessary to contribute to further examination of the big picture, by considering the many interactions taking place within transportation systems. The findings from this research not only benefit the private sector from a cost-savings standpoint, but it also benefits public entities responsible for making decisions related to zoning, growth and development of business and residential areas, transportation and infrastructure planning, and linking all of the systems together in a way that both maximizes the utility for residents and respects the environment.

Objectives

The objective of this research was to better understand the future of freight by evaluating the energy impacts of changes in freight delivery in urban environments due to changes in consumer behavior and new delivery technologies and methods. Research in this area is crucial because, as the population continues to grow, especially in urbanized areas, and as e-commerce sales continue to make up a larger percentage of overall consumer purchases, understanding these effects becomes vital to managing the Nation's congestion, infrastructure, and energy usage.

This research aimed at focusing on the micro-level of freight movement; focusing efforts in two metropolitan areas: Columbus, Ohio (Fiscal Years 2017 and 2018) and Chicago, Illinois (Fiscal Year 2019). Although this research focused on localized, intra-city freight, the findings from this research were integrated into two other SMART Mobility efforts, which focused on inter-city freight movement and large-scale metropolitan-wide effects on the overall transportation network introduced by an influx of delivery vehicles mingling with existing passenger vehicles. This research sought to evaluate the potential energy and mobility impacts to intra-city freight movement by the introduction of new delivery modes and through the incorporation of innovative multi-modal last-mile configurations to meet increasing freight demand.

Approach

In order to evaluate the potential energy and mobility impacts to intra-city freight movement by the introduction of new delivery modes, it was necessary to investigate the detailed energy use of different modes and methods of introducing these modes. This included investigation of energy profiles of drones through testing, which was performed in the field and in a laboratory environment. The results from the testing were combined with delivery demand estimates created by obtaining a sample of UPS fleet data from UPS Columbus (Fiscal Year 2018). Consideration of applicability of new delivery technologies was necessary and involved coordination with industry to investigate how to approach the problem by assessing the baseline methods of delivery and potential needs. This was primarily done through coordination with UPS Columbus and Atlanta (Fiscal Year 2018) to obtain data.

A model was developed to estimate a synthetic fleet population and service area for UPS and FedEx Chicago to evaluate baseline energy usage and potential energy savings using new modes. The energy usage estimates of the baseline and new technologies were then used during micro-simulations to better understand small-scale impacts. This was done by evaluating different scenarios using new modes to better understand impacts in different intra-city contexts, which considered development density (urban versus suburban landscapes) and street network connectivity. In the final phase of this research, system-level impacts were investigated by estimating overall parcel delivery demand for Chicago and understanding existing and projected fleet ownership size at major parcel distribution hubs to evaluate energy and mobility impacts by incorporating the scenarios tested in the micro-scale simulations.

Results

Drone Energy Profile

In order to better understand the impacts and methods of implementing new technology, INL performed focused experiments on the use of drone technology and the energy impacts of freight delivery with drones, as this had not been frequently studied in the past. In previous years (Fiscal Years 2017 and 2018), INL had performed controlled experiments using weighted delivery and a hexacopter drone. This continued in 2019 with further characterization tests and experiments in Florida to compare the impacts of lower altitude and increased temperature. Experiments were also performed with external instrumentation to compare against the internal sensor and log-based energy estimates from previous experiments. As a comparison, initial tests were performed using a small quadcopter that could deliver only very small packages (less than one pound) using only battery reduction techniques.

Figure I.4.2.1 shows the results of energy estimates for the delivery of packages in a one-mile route based on the internal sensors and logs. The experiments indicated approximately 10-15% increase in energy with the higher temperature and lower altitude, and approximately 20% increase in energy with every five-pound increase in weight. Figure I.4.2.1 also includes estimates for energy from a light electric vehicle in similar circumstances, which can be used as a comparison.



Figure I.4.2.1 Energy Estimates from one-mile delivery tests (INL)

Through an experiment comparing the results of external monitoring to the internal logs used by the experiments, it was found that the external instruments indicated a lower overall energy use than the logs, and that the total energy could be as much as 40% less than the initial estimates. Figure I.4.2.2 shows the comparison for total energy for the hover test results when comparing the internal log sensors versus the external instrumentation.

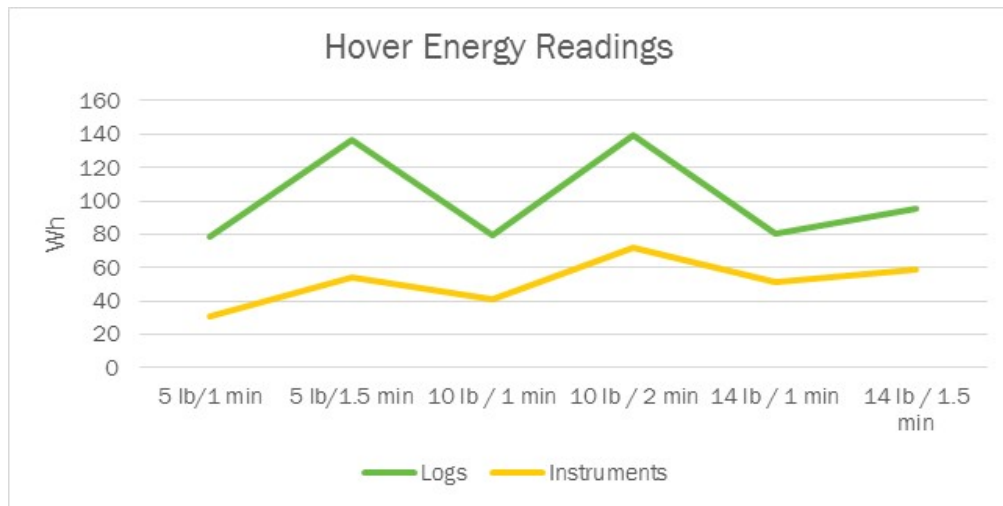


Figure I.4.2.2 Energy estimates from internal logs versus external instruments (INL)

Further experimentation is needed to fully understand the different impacts and exact energy use of drone delivery for freight. The experimental results show that drones have the potential to use significantly less energy than traditional vehicles. In the final analysis, an average estimate based on 5-10 pounds at a slower speed was used as a conservative estimate in the final energy estimates with some expectation of higher energy use based on inefficiencies.

Chicago, Illinois Baseline and Alternative Scenario Modeling Results

The initial modeling work performed in Chicago involved the selection of three case study areas involving simulated delivery routes (tours), which were developed using UPS delivery estimates for the Chicago

Metropolitan Area. As previously done in Columbus, the three tours were chosen to represent varying development densities and levels of road network connectivity (an urban tour, suburban tour, and a tour near the central business district). In the final model, baseline and estimated energy usage for the entire synthetic UPS and FedEx Chicago fleets were developed.

Figure I.4.2.3 shows the results from the final model for Chicago, which provides fleet-level average daily energy estimates for both UPS and FedEx. These estimates represent e-commerce delivery demand based on the current population for Chicago. Five-day average total shopping estimates per traffic analysis zone (TAZ) were obtained from POLARIS (ANL), and these estimates were then altered to only include the current percentage of shopping through e-commerce in order to capture parcel delivery. Current market shares for UPS and FedEx were obtained and applied to the estimates. Using these estimates, delivery locations were estimated, and fleet-level energy usage was estimated for the baseline and the 17 alternatives.

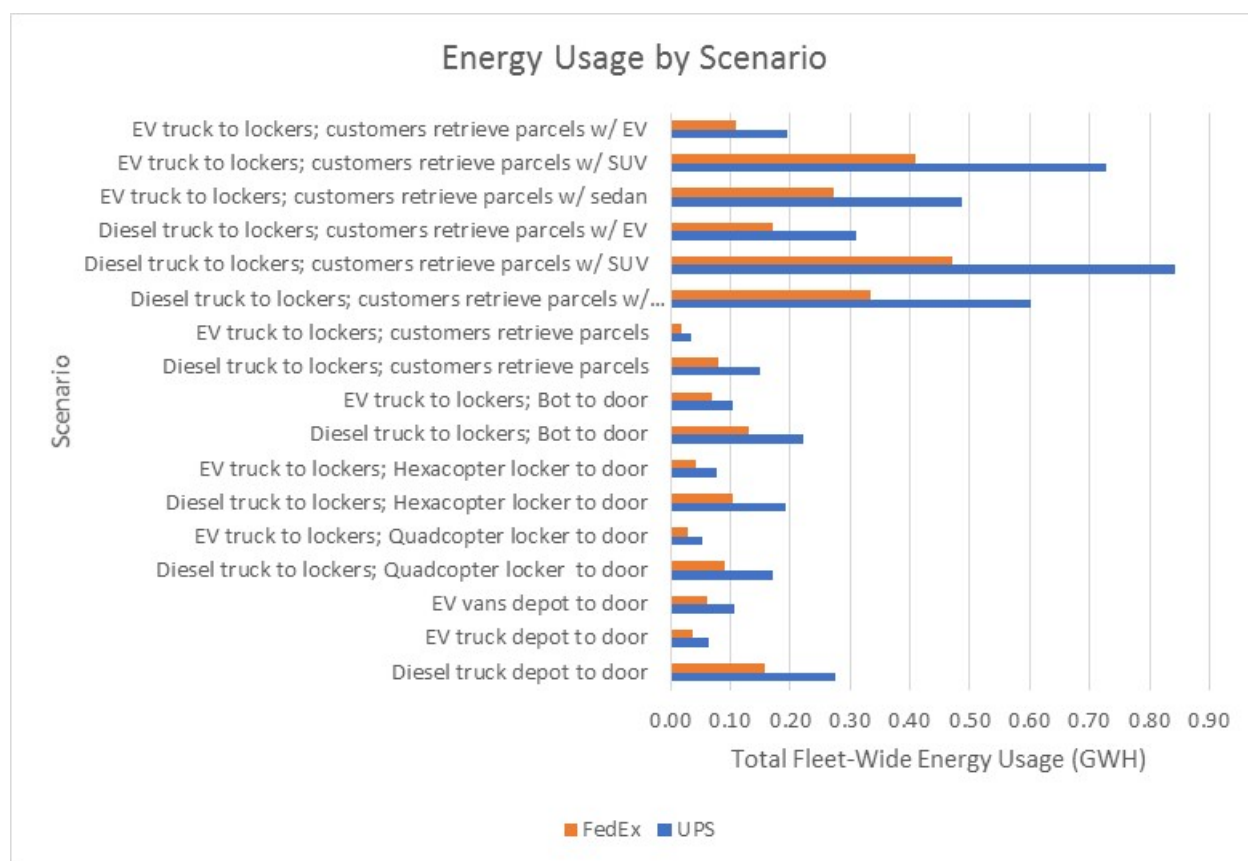


Figure I.4.2.3 Total average daily energy usage by scenario for UPS and FedEx Chicago Fleets

Based on the results from the final Chicago model, it was found that the scenario involving the use of EV trucks and lockers resulted in the greatest reduction in energy usage from the baseline. However, this doesn't include modes to lockers and is only considering energy used by the business, which was the justification for including multiple passenger vehicle types in six of the alternative scenarios. The scenario using EV trucks and quadcopter drones resulted in the second greatest reduction. However, this scenario relied on an average parcel weight of five pounds or less, which only represents approximately half of the parcels in a given truckload. Lastly, the scenarios involving passenger vehicles retrieving parcels from lockers (especially the SUV) resulted in the highest overall energy usage estimates, excluding the scenario involving the EV truck and EV passenger vehicles, because of overall increased VMT (even when considering the optimistic assumption that customers may retrieve the parcel to another destination, which resembles en-route or TNC-style delivery systems).

Figure I.4.2.4 shows the effect of alternative technologies on the fleet-wide average daily energy usage for Chicago from a fleet operator’s perspective. Here, the impact of electrification of the existing Class 6 fleet is substantial as shown by a 77% reduction in energy used. The result is in line with what was found in the previous Columbus study. The effect of land use (parcel lockers, in this case) in Chicago is also similar to the preliminary Columbus analysis.

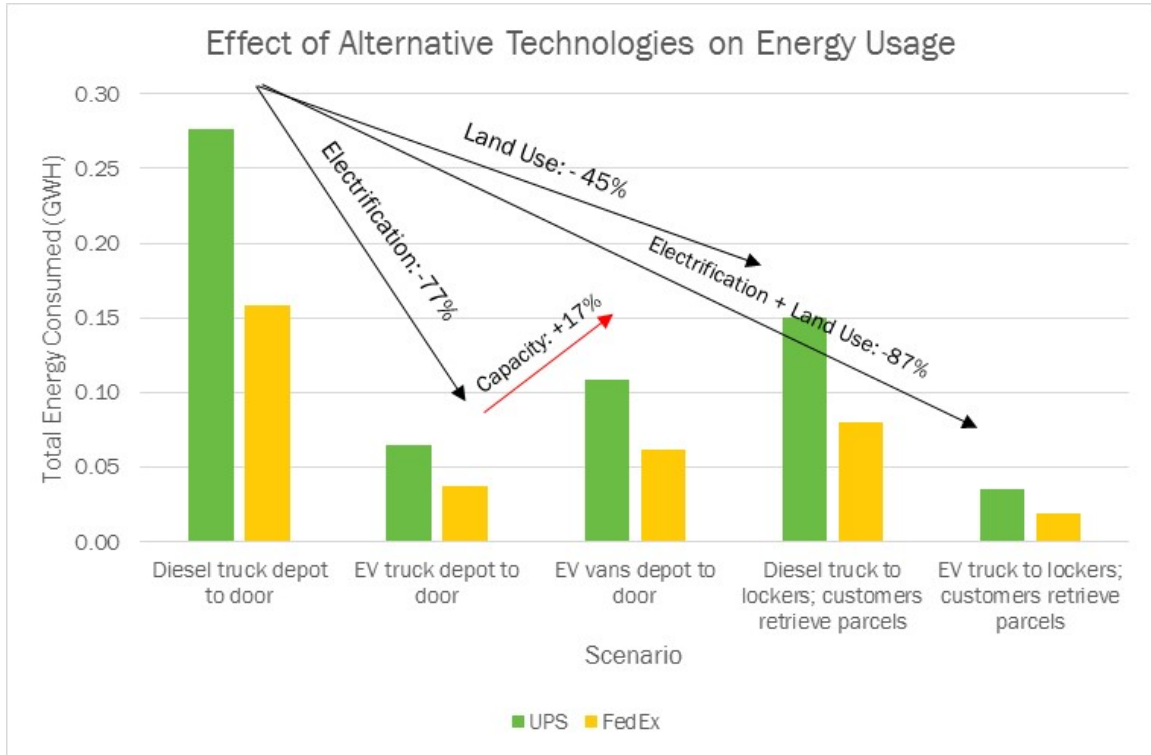


Figure I.4.2.4 Effect of alternative technologies on fleet-wide average daily energy usage for Chicago

Figure I.4.2.5 is a graphical summary of the total energy usage for a full tour when considering delivery to parcel lockers and customer pick up from the parcel locker back to their homes. The alternative scenarios considered are meant to be an extreme case and do not take into consideration combined trips (trip-chaining), although they did include a conservative average distance traveled. In addition, the study breaks out various modes for passenger movement and does not consider an integrated fleet composition of sedans, sport utility vehicles (SUVs), and battery electric vehicles (BEVs). Based on these findings, it appears that parcel lockers have the potential to substantially reduce energy usage for the delivery fleet, while conventional means of personal transportation (gasoline sedans and SUVs) have the potential to significantly raise the total energy usage per tour. Although each scenario in the figure assumes a 100% penetration of the passenger movement mode, a more representative mix would also likely lead to a significant increase in energy usage over the baseline.

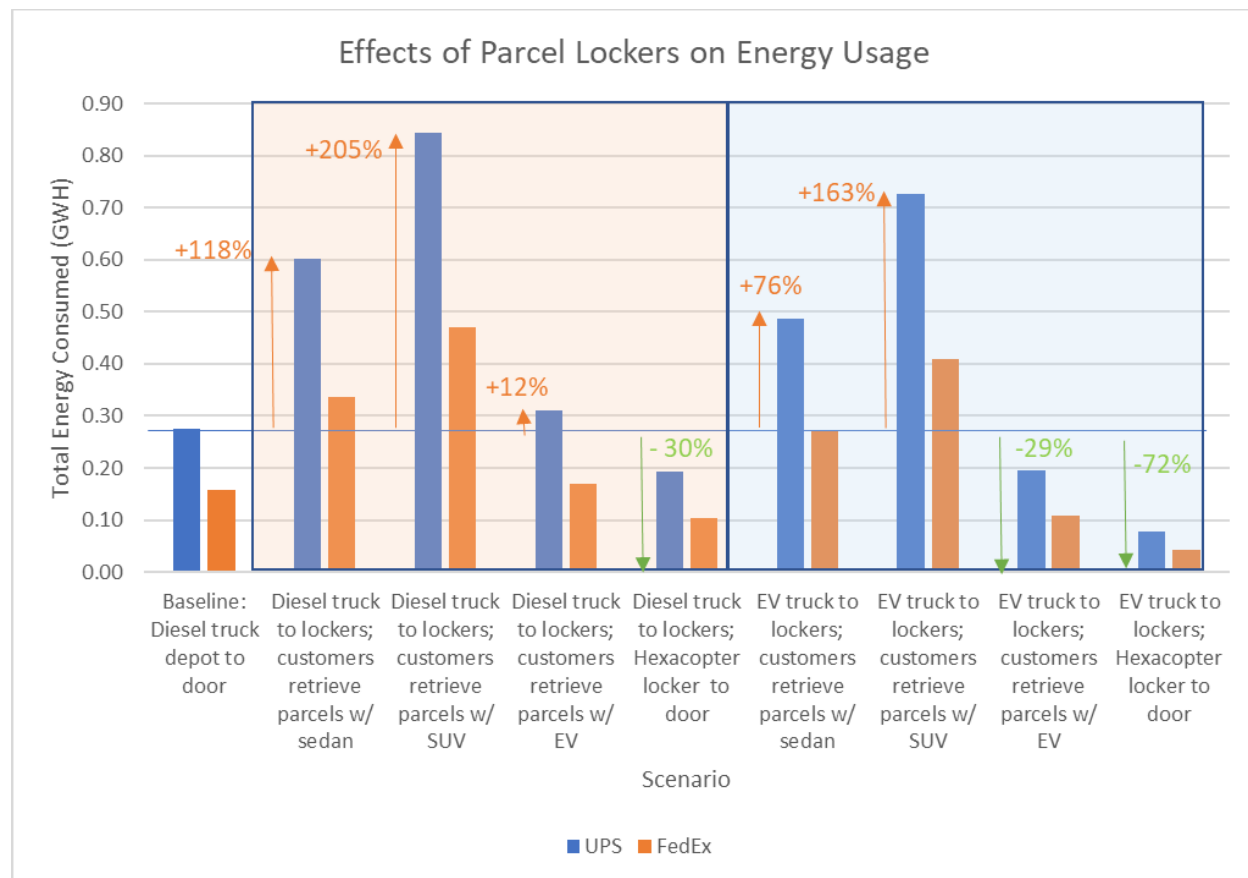


Figure I.4.2.5 Effect of parcel lockers on total energy usage: Chicago

It was also found that delivery of goods from the parcel lockers to a customer's home by drone can have a profound impact on energy reduction by as much as 80% (quadcopters). This is quite a different finding from the Columbus case studies. This finding is likely attributable to the denser development in Chicago, which results in shorter average distances from locker to customer/destination. It may also be due to the synthetic fleets developed for Chicago being more representative of the overall population than the smaller sample (approximately 20 vehicles) used in the Columbus case studies. However, a more realistic mix of delivery vehicle and drone usage should be investigated, but the potential is evident under the right conditions.

Finally, an important finding is that, while delivery vehicle electrification reduces the operating costs for a fleet operator, the net result is not as dramatic when considering parcel lockers and delivery vehicle electrification for a full tour which considers the customer retrieving the parcel. This is due to the substantial reduction in energy usage for the delivery vehicle (electrified or not) when moving to the parcel locker approach. Here, the delivery to the parcel locker represents a very small percentage of the overall energy consumed for the entire tour and is dwarfed by the energy required by the customer to retrieve the parcel.

Conclusions

Based on the findings from this research, retaining the conventional fleet of UPS and FedEx diesel trucks and moving to a more aggregated delivery system results in substantial energy reductions. Although it was found that an increase in passenger vehicles used to retrieve parcels in-lieu of delivery vehicles resulted in significantly higher VMT and energy usage (excluding the scenario involving EV trucks and EV passenger vehicles), further analysis should be undertaken to understand the necessary passenger fleet composition and/or minimum market penetration of BEVs required to realize any potential improvement to overall energy consumption per tour. Based on the initial findings from the passenger car scenarios, and the massive increase

in energy consumed in the scenarios involving SUVs, a reasonable assumption is that the increase in actual SUV sales and the proclivity of automakers to produce more SUVs and fewer sedans will likely exacerbate these potential effects.

The full economics of electrification and implications for infrastructure and land use planning was not considered in this research. For electrification, further work must be undertaken to fully understand the impact of fleet vehicle electrification (conversion of outright purchase), and the associated charging infrastructure requirements for the fleet. At the same time, the siting, permitting, and construction of parcel lockers need a deeper study to understand the true business case to develop a better comparison to the electrification case. However, it is evident that electrification and land use decisions can substantially reduce the overall energy usage for the fleet operator. In terms of electrification of the fleet, capacity and payload play an important role in minimizing VMT. It is significant to note that, in the scenario using smaller electrified vehicles (vans) in place of the Class 6 vehicles, while overall net energy usage is reduced from the baseline, there is a 16% increase in energy consumed from the Class 6 EV case. Even though the energy consumption rate is much less for the EV vans, more vehicles are required to meet the delivery demands of the Chicago area. Therefore, capacity acts as a detriment in this case. Thus, vehicle energy consumption rates must not be solely considered when determining fleet composition and mission.

Key Publications

Amy M. Moore, Innovative scenarios for modeling intra-city freight delivery, Transportation Research Interdisciplinary Perspectives, 2019, 100024, ISSN 2590-1982, <https://doi.org/10.1016/j.trip.2019.100024>.

I.4.3 Energy and Mobility Impact of Inter/Intracity Freight Movement Using Data-Driven Agent-Based System Simulation (ANL)

Monique Stinson, Principal Investigator

Argonne National Laboratory
9700 S Cass Avenue
Lemont, IL 60439
E-mail: mstinson@anl.gov

Prasad Gupte, DOE Technology Manager

U.S. Department of Energy
E-mail: Prasad.Gupte@ee.doe.gov

Start Date: October 1, 2018

End Date: September 30, 2019

Project Funding (FY19): \$75,000

DOE share: \$75,000

Non-DOE share: \$0

Project Introduction

Freight transportation has significant impacts on energy consumption, mobility, and emissions. In the United States, medium-duty trucks (MDTs) and heavy-duty trucks (HDTs) constitute about 10% of traffic, yet consume roughly 30% of transportation energy. Because freight has such major impacts, it is important to consider how freight transportation could change in the advent of new vehicle technologies, shifts in consumer or business behavior, and other factors. Analytical tools that are capable of evaluating both freight transportation and passenger transportation can deliver this type of assessment.

In this project, we develop a powerful, agent-based freight forecasting model. The model uses a behavioral framework, treating business establishments and truck drivers as agents that make decisions. The framework is fully integrated in the Argonne National Laboratory (Argonne) agent-based model platform, POLARIS.

The model is applied to study the impacts of freight transportation on regional mobility, which is measured using vehicle-miles traveled (VMT), and energy use across three types of scenarios. The first type of scenario examines the energy and mobility impacts of commodity flow growth that is projected to occur in the future. The second evaluates the energy impacts of potential future adoption rates of advanced technologies such as electrified powertrains. The third examines the impacts of e-commerce, using “what-if” cases to quantify the potential net effects on mobility and energy as households order increasing numbers of deliveries. These scenario analyses were part of the Smart Mobility Workflow analysis.

The geographic coverage of the model is as follows. Business establishments, supply chains, and shipment trades are modeled at the global, nationwide, and regional levels. The dynamic traffic assignment (DTA) and subsequent energy and mobility analysis focuses on the portions of trips that are in the Chicago metropolitan region.

Objectives

The objective of this project is to estimate the energy and mobility impacts of freight by modeling commercial activity, the movement of goods at the intraregional and intercity levels, and interdependencies between commercial and household activity. The project includes both model development and model application to various case studies. The goal of model development is to produce freight forecasting models that can analyze the impacts of various scenarios on freight transportation and energy consumption within a computational environment. The goal of model application is to evaluate select scenarios of interest. In this study, the model is applied to estimate the baseline impacts of freight on transportation mobility and energy consumption. After the baseline is established and calibrated, the impacts of commodity flow growth, increased use of powertrain technologies, and varying e-commerce demand rates are evaluated.

Approach

The project utilizes two stages to accomplish its objectives. A different freight model is developed in each stage. Both models use freight establishments and truck drivers as agents, but differ in the approach used for generating and allocating shipments to establishments. The initial model accomplishes this using a “top-down” approach, while the second model uses a “ground-up” approach. Since the top-down model could be developed more quickly, it was used to evaluate the Smart Mobility Workflow scenarios. The latter is intended for longer-term use because it is more versatile and powerful than the initial model. Each model is discussed in turn below, along with features that are common to both models.

The top-down model generates shipments between establishments by apportioning inter-regional commodity flows from the Freight Analysis Framework (FAF) [1] to individual pairs of establishments. Establishments are paired to form links in the supply chain based on trip estimates and land use data from the Chicago Metropolitan Agency for Planning (CMAP) [2] and data on buildings from the City of Chicago [3]. An algorithm was developed to transform the inputs into a truck trip table.

The ground-up model, in contrast, begins by synthesizing a population of business establishments around the world. The model agents form trade partnerships with each other, set trade volumes, select shipment sizes and frequencies, and choose mode and logistics-related options. The model is multimodal and currently includes truck, rail, and air shipping options. Logistics options include whether to use a transload or distribution facility.

Both the top-down and ground-up processes result in a table of truck trips. A customized algorithm is then employed to assign these trips to a specific time of day either between 9 AM and 6 PM (for e-commerce deliveries) or in accordance with commercial traffic more generally [4]. Each shipment is then assigned to a vehicle and vehicle technologies are determined based on Workflow parameters. Movement of the resulting trucks is simulated with passenger vehicles in the POLARIS DTA.

Following model development, the ground-up model was applied to evaluate future scenarios. Inputs on vehicle technology market penetration for MDTs and HDTs were provided by the Workflow team. In the base case, hybrid electric vehicle (HEV) powertrains are used in 2.5% of trucks. In the low-tech and high-tech scenarios, this increases to 5% and 13%, respectively, in the short term and 20% and 22% in the long term. Plug-in HEVs are assumed to have no usage among trucks except in the long-term, high-tech scenario (4% market penetration). Battery electric powertrains have: 0% usage in the base case short and long terms and in the baseline low-tech scenario; 2% usage among trucks in the high-tech, short-term scenario; and 11% and 15% usage in the low- and high-tech scenarios, respectively, in the long term.

E-commerce related inputs were developed as follows. First, Argonne staff developed a household-level model of e-commerce demand using data from the Lawrence Berkeley National Laboratory WholeTraveler survey. This model was implemented in POLARIS to predict demand for e-commerce goods for each household in the Chicago region. Second, Oak Ridge National Laboratory estimated parcel delivery tours for major parcel carriers to be commensurate with the household-level demand estimates. These supply and demand elements were integrated in POLARIS and used to estimate the net effect of e-commerce on mobility and energy.

Future commodity flows were estimated as follows. A moderate 1% compound annual growth rate commodity flow growth from FAF was used to adjust the baseline CMAP trip tables. Changes in inter-regional (long-haul) and intraregional flows were developed and applied in this way.

For each scenario, the resulting truck trips were simulated using the network DTA. The scenarios were bundled together, along with numerous other passenger scenario parameters. More information on the entire Workflow analysis can be found in the Workflow Capstone Report.

Results

This section presents results from both the model development and model application aspects of the project. The results for the scenario analyses are then discussed.

Results from Model Development

The objective of developing a top-down model was achieved. The left panel of Figure I.4.3.1 shows the process for implementing the top-down, commodity-flow-based model and applying it to analyze Workflow scenarios. The right panel illustrates how the model is applied to study VMT and energy consumption for one MDT that is delivering e-commerce goods.

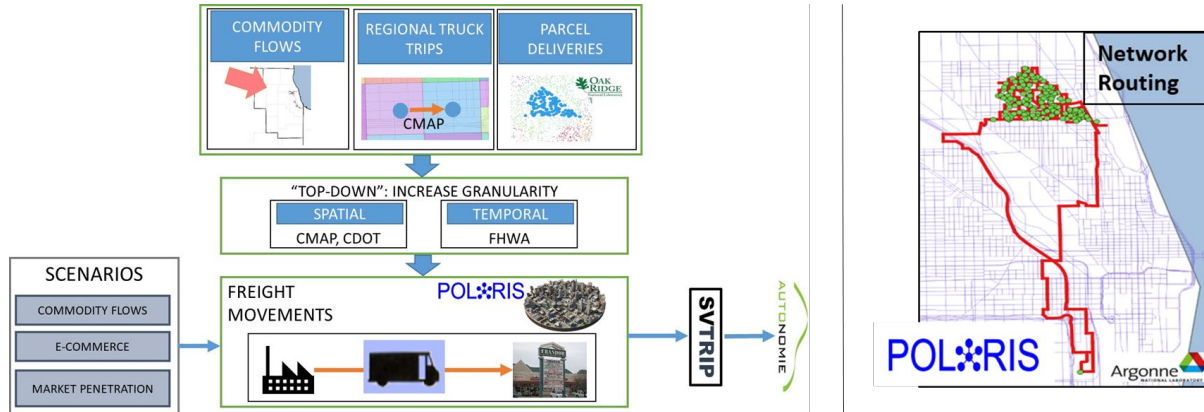


Figure I.4.3.1 Left: Top-Down Model Implementation and Process for Workflow Scenario Analysis; Right: Routing for E-commerce Analysis

The fully agent-based model likewise was successfully developed. Figure I.4.3.2 illustrates one model process in which trade partnerships are generated to form supply chain links.

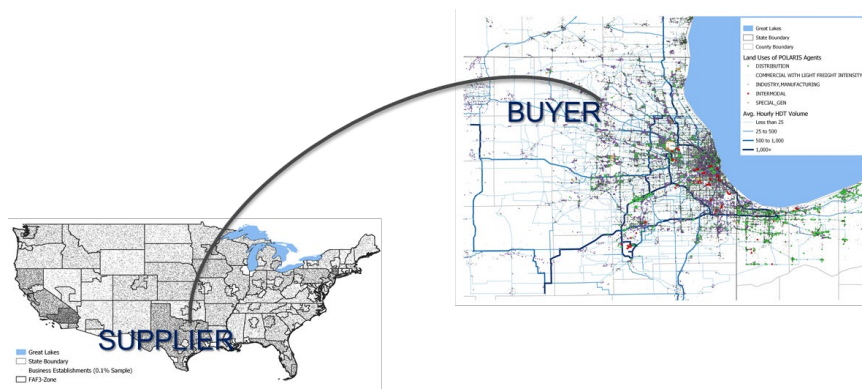


Figure I.4.3.2 Supply Chain Formation in Ground-Up (Fully Agent-Based) Model

Results from Model Application

Table I.4.3.1 shows the model results for MDT and HDT freight across the Workflow scenarios. VMT, fuel, and energy results are combined for MDTs and HDTs. VMT and fuel are also shown for MDTs and HDTs separately. Insights that are gained from these findings and the e-commerce findings are discussed in detail below.

Table I.4.3.1 Results: MDT and HDT Impacts across Workflow Scenarios

MET- RIC ¹	REFERENCE SCENARIOS			FUTURE BASELINE				FUTURE SCENARIOS					
				Short Term		Long Term		Short Term		Long Term		Long Term	
	Current	Short Term	Long Term	Low	High	Low	High	Low	High	Low	High	Low	High
	Base0	Base1	Base4	Base2	Base3	Base5	Base6	A2	A3	B5	B6	C5	C6
VMT ²	23	23	28	23	23	29	29	23	23	30	30	30	31
HDT	20	21	25	20	20	26	26	20	20	26	26	26	26
MDT	2.6	2.9	3.2	2.9	2.9	3.2	3.2	3.3	3.3	4.0	4.0	4.0	4.1
Fuel	4.5	4.6	5.6	3.6	3.2	4.3	3.5	3.6	3.1	4.2	3.5	4.5	3.8
HDT	4.2	4.3	5.3	3.4	3.0	4.1	3.3	3.3	2.9	3.9	3.3	4.2	3.5
MDT	0.3	0.3	0.3	0.3	0.2	0.2	0.2	0.3	0.2	0.3	0.2	0.3	0.2
Energy	166	171	208	135	120	159	130	133	115	157	129	166	141

¹ Units: millions of miles (vehicle-miles traveled); millions of gallons (fuel); billions of Watt-hours, or GWhr (energy).

² VMT: vehicle-miles traveled.

Baseline freight transportation generates about 7–8% of regional VMT (23 of the 300 total million miles; POLARIS) but consumes about 30% of total fuel (4.5 out of 14 million gallons total; POLARIS), which is due in part to the low miles per gallon that MDTs/HDTs currently achieve relative to light-duty vehicles. This comparison is consistent with other studies, which indicate that freight traffic has a disproportionately high impact on energy consumption [5]. Potential improvements in MDT/HDT energy efficiency therefore could have dramatic impacts on transportation energy consumption.

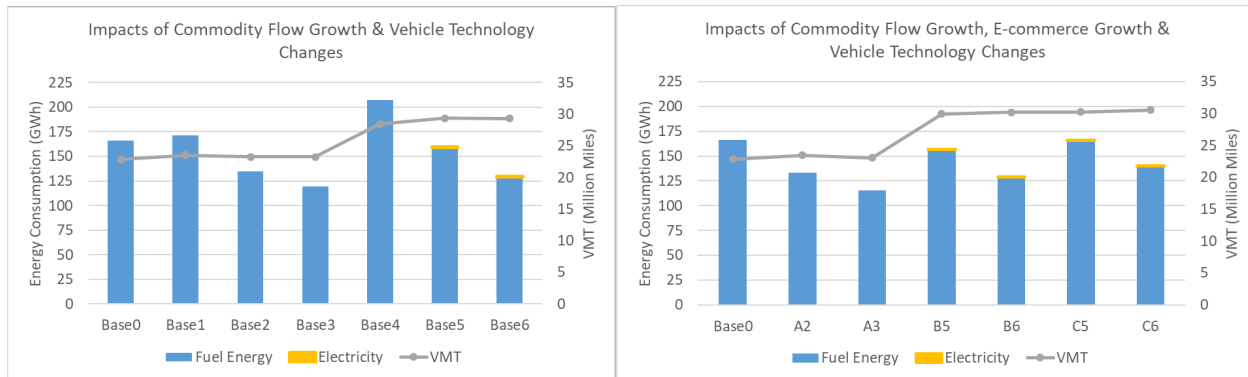


Figure I.4.3.3 Base and Projected MDT/HDT VMT and Energy Consumption across Scenarios

At a moderate rate of commodity flow growth, total freight VMT in the Chicago region would increase slightly from the base year (Base0) to the short term (Base1-Base3), with energy consumption increasing by 5 GWh with no technology improvements (Base0 to Base1) and decreasing by 32 and 47 GWh with technology improvements (Base0 vs. Base2 and Base3). As the left pane of Figure I.4.3.3 shows, a similar trend is forecast for the long term, with VMT growth of 24% (Base0 to Base4). Fuel consumption likewise increases by 25% unless energy-efficient technologies are adopted more widely: Base5 and Base6 have 4% and 22% less fuel use than Base0. Electrification improves energy efficiency modestly in Base5 and Base6.

The right pane of Figure I.4.3.3 shows total truck VMT and energy use including the combined impacts of commodity flow growth, powertrain technology adoption, and e-commerce demand. Total truck VMT is highest in the B and C scenarios, which have both long-term growth in commodity flows and the highest e-commerce rates. Improved technology would help offset increased energy use (e.g., A3 has lower energy use than A2 despite similar VMT levels). The VMT and energy totals are very close for scenarios in the same time period (such as for short-term scenarios Base2, A2 and A3) despite the increase in e-commerce MDT trips which occurs in the A/B/C scenarios but not in the Base scenarios, meaning that the large increase in e-commerce deliveries does not increase total truck impacts by very much. This is due to the nature of efficient e-commerce delivery tours, which optimize drop-offs such that each additional stop only adds a small amount of VMT and energy consumption to a given tour. In comparison, average trip length is 35 miles for other types of truck trips.

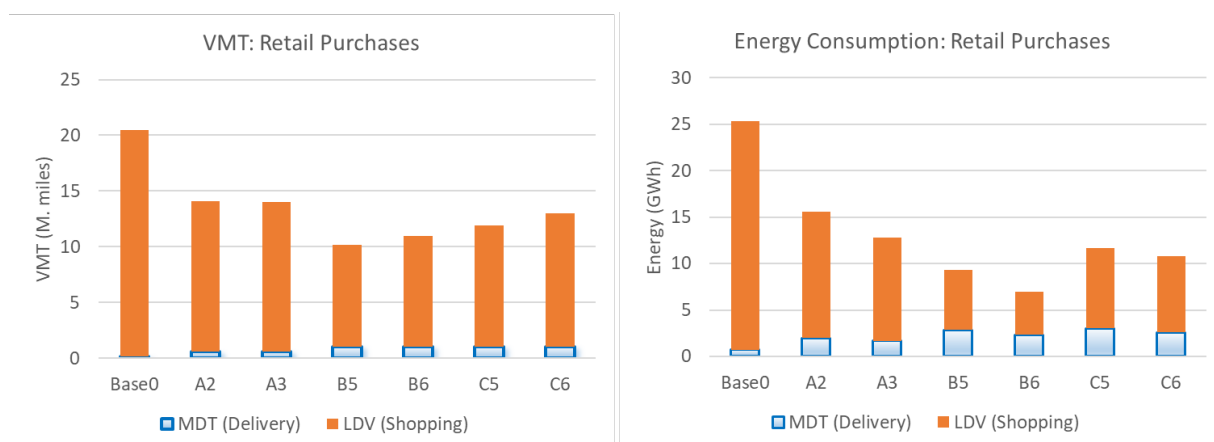


Figure I.4.3.4 VMT and Energy Use with Retail Purchasing and Powertrain Efficiency Improvements

Although e-commerce causes an increase in last-mile delivery, an overall net reduction in retail-related VMT and energy use is forecast to occur due to reductions in shopping trips. Figure I.4.3.4 shows the VMT and energy results attributed to retail purchasing via shopping LDV and MDT delivery trips as the e-commerce delivery rate increases from one delivery per household per week (Base0) to three (A2, A3) to five (B5, B6, C5, C6). The average shopping trip is about 7 to 8 miles long [6], so replacing shopping trips with additional stops on an efficient delivery tour can create sizeable VMT and energy reductions. Compared to Base0, tripling e-commerce demand in the short term reduces total retail-related VMT and energy use by 35% and 42–52%, respectively. In the long term, if household e-commerce rates were to grow to five days per week, retail-based declines of 44–56% in VMT and 59–76% in energy are forecast to occur compared to Base0. Because energy savings due to powertrain improvements account for 34–46% of this total, the net long-term retail-based energy savings due to efficiencies in last-mile e-commerce is between 16% and 33%. The B scenarios have lower VMT and energy use than the C scenarios due to widespread use of an efficient, shared automated vehicle (AV) system (in B) versus the less efficient use of privately owned AVs (in C), which affects shopping LDV totals. Congestion creates additional variations in results.

Conclusions

Two freight models were developed in this study to evaluate the impacts of freight transportation on VMT and energy consumption. The first (top-down) model generates freight flows between individual establishments by using commodity flows. The second (ground-up) model generates flows by first synthesizing a population of agents and their characteristics, then modeling their trading partnerships and subsequent shipment decisions. Both models then conduct vehicle routing in a DTA environment, using route information to estimate VMT and energy use of freight trips. The ground-up model will be applied for future analysis.

The top-down model is applied to evaluate freight transportation impacts across 13 Workflow scenarios. The results establish the baseline energy and VMT impacts of freight, demonstrating that freight vehicles have a disproportionately high energy impact (30% of fuel) relative to their VMT (10% of VMT). With projected increases of 24% in truck traffic in the next two decades, improved powertrain efficiency is needed to mitigate energy consumption. Increased market penetration of efficient powertrain technologies can have sizeable impacts on freight energy consumption, reducing long-term energy use by up to 23–37% compared to the base year in spite of increased freight demand.

E-commerce delivery vehicles create additional truck VMT. However, e-commerce is shown to reduce overall retail VMT by up to 56% because each delivery adds just a small amount of additional distance to an efficient delivery tour, creating net savings by replacing relatively long-distance shopping trips. E-commerce is also estimated to reduce net retail energy use between 16% and 33% in the long term, enhancing the benefits of improved powertrain technologies (which alone account for 34–46% of long-term energy reduction).

Key Publications

1. Stinson, M., A. Enam, A. Moore, and J. Auld. 2019. “Citywide Impacts of E-Commerce: Does Parcel Delivery Travel Outweigh Household Shopping Travel Reductions?” In Proceedings of ACM SCC 2019 Conference (SCC’19). ACM, New York, NY, USA. <https://doi.org/10.1145/357492.3358633>.
2. Stinson, M., J. Auld, and A. (Kouros) Mohammadian. 2019. “Light Duty Vehicle Choice Models Examining Alternative Fuel Technology Preferences among Commercial Fleet Owners.” Presented at the Eleventh International Conference on City Logistics, Dubrovnik, Croatia, June 12–14, 2019.
3. Stinson, M., J. Auld, and A. (Kouros) Mohammadian. 2018. “An Agent-based Model of Freight Transportation with Emerging Trends in POLARIS.” Presented at the 3rd VREF Conference on Urban Freight, Gothenburg, Sweden, October 17–19, 2018.
4. Stinson, M., B. Pandey, A. Enam, A. Rousseau, and J. Auld. 2019. “Spatiotemporal Analysis of the Freight Analysis Framework Data.” Presented at Innovations in Freight Data Workshop, Irvine, CA, April 9–10, 2019.

References

1. Center for Transportation Analysis. 2015. “Freight Analysis Framework Version 4.” Oak Ridge National Laboratory. Accessed February 1, 2019. <https://faf.ornl.gov/fafweb/>.
2. CMAP Data Hub. 2019. “Data.” Chicago Metropolitan Agency for Planning. Accessed February 1, 2019. <https://datahub.cmap.illinois.gov/organization/data>.
3. Chicago Data Portal. 2018. “Building Footprints (Current).” City of Chicago. Accessed February 1, 2019. <https://data.cityofchicago.org>.
4. Federal Highway Administration. 2018. *Traffic Data Computation Method: Pocket Guide*. Publication No. FHWA-PL-18-027. U.S. Department of Transportation. Accessed March 15, 2019. https://www.fhwa.dot.gov/policyinformation/pubs/pl18027_traffic_data_pocket_guide.pdf.
5. U.S. Department of Transportation. 2017. “Beyond Traffic 2045.” Accessed March 1, 2019. https://www.transportation.gov/sites/dot.gov/files/docs/BeyondTraffic_tagged_508_final.pdf.
6. Federal Highway Administration. 2017. “National Household Travel Survey.” Accessed March 1, 2019. <https://nhts.ornl.gov/>.

Acknowledgements

Annesha Enam of Argonne and Amy Moore of ORNL provided inputs to the e-commerce analysis. Vincent Freyermouth of Argonne helped estimate energy consumption. Felipe De Souza, Omer Verbas, and Joshua Auld of Argonne assisted with various aspects of POLARIS. David Anderson, U.S. DOE/EERE/VTO EEMS Program Manager, and Aymeric Rousseau of Argonne provided guidance to this effort.

I.5 Urban Science

I.5.1 Data and Models Informing Smart Cities (NREL) [Task 2.1.1]

Josh Sperling, Principal Investigator
National Renewable Energy Laboratory
15013 Denver West Parkway
Golden, CO 80401
E-mail: Joshua.Sperling@nrel.gov

Prasad Gupte, DOE Technology Development Manager
U.S. Department of Energy
Phone: (202) 287-5688
E-mail: Prasad.Gupte@ee.doe.gov

Start Date: October 1, 2017	End Date: September 30, 2019	
Project Funding (FY18): \$220,000	DOE share: \$220,000	Non-DOE share: \$0

Project Introduction

This task supports the Urban Science pillar of the Department of Energy’s SMART Mobility effort through research focused on assessing the landscape of data and models in emerging smart cities. focuses on understanding the energy implications and opportunities of advanced mobility technologies and services, specifically within diverse urban contexts. More specifically, this includes exploring the linkages between transportation networks, emerging technologies and the built environment, as well as identifying the potential to enhance access to economic opportunity. These emerging mobility technologies, often referred to as automated, connected, efficient (or electrified), and shared (*this is including both vehicle and ride-sharing as the enhanced asset utilization, often in the form of app-based mobility-on demand or mobility as a service choices) (ACES), have the potential to greatly improve mobility and related quality of life in urban areas. The Urban Science team has strived to collect and integrate datasets, model, analyze, and gain unique insights from the perspective of human settlements (the ‘city’) as a living organism. Typically, the urban mobility system includes significant investments in, planning for, and adapting to potential future changes for public transit, private mobility services (such as taxis and transportation network companies, or TNCs), parking and curb management practices, emerging on-demand micromobility services for people and goods movement, e-bikes and scooters, all of which makes the urban space a dynamic ‘observatory’ for exploring data, and modeling, to informing energy efficient mobility systems implications of changing mobility technologies and systems.

Foundational efforts to date, have included 1) providing a data and modeling resources report to help further integrate between transportation research and practice and with the growing reality that advanced transportation, mobility services, and infrastructure modernization are of increasing interest to cities, 2) examine data and modeling solutions within multiple cities, and 3) down-select on city case studies to work together on testing and scaling of urban science using available data and new primary data collected with inputs/validation from local city and regional partners. A focus is on factors that influence mobility options (e.g., travel time, costs, access to opportunities, and emerging mobility energy productivity metric/s) and associated energy-related impacts (e.g., fuel spent, vehicle miles traveled, costs to households) specific to new urban automated, connected, electric and shared mobility strategies developed and evaluated with partner cities. These cities comprise case examples where knowledge generated and coupled mobility-energy assessments can advance efforts across all 498 U.S. urban areas. These efforts have placed emphasis in exploring advances in urban transportation data and modeling to develop, for analysis purposes, a robust, sophisticated and practical framework supporting the ultimate goal of providing an efficient, safe and sustainable mobility system for passenger and goods movement.

Objectives

This project aims to:

- Provide objective and quantifiable data that fills key knowledge gaps, which can be used in modeling/analysis efforts that address questions on how SMART technologies (ACES) impacts urban infrastructure, travelers, and energy.
 - A focus on the effects of Mobility as a Service (MaaS) at airports, which are unique trip generation sites
- Address key research question/s, including:
 - How will ACES impact diverse urban travelers, systems, & services?
 - Long-term energy/travel impacts from changing urban environments?

Mobility options such as shared-use, electric vehicles, micro-transit, connected and automated vehicles and dynamic (real-time) information are already or expected to be part of the daily activities in the near-future, but their effect on the overall transportation system is not yet evident. For example, the use of electric vehicles is expected to reduce energy intensity, but the increase of connected vehicles may or not reduce congestion unless there is a dedicated lane. Similarly, automated vehicles could provide first and last mile accessibility to transit services negating the need for park-n-ride facilities or completely change mode choices with user preferences shifting to Shared Automated Vehicles (SAV) from traditional fixed-route transit services. In addition to the technological advances on the supply side, the opportunity facing us today is making demand management more robust by leveraging technology, behavioral insights, new urban system integration goals, and institutional readiness to overcome barriers inhibiting discovering and selecting a new and efficient mode not used before. As such, cities around the US are fully engaged in developing surveys, reports and plans that may provide a blueprint to prioritize investments via exploring behavioral impacts and system performance.

Approach

The approach for this project includes:

- TNC /MaaS data collection & analysis at major mobility hubs, such as airports and other key destinations, to characterize mobility/energy impacts using novel collection methods that will circumvent relying directly on TNC companies for data informing critical analysis insights.
- Obtaining direct access to city, regional, state databases to characterize mobility/ energy/behavioral impacts from EVs, AVs, other advanced tech & MaaS adoption – overcoming data gaps and obtaining highest possible detail & resolution for analyses to help inform a typology to national impact analysis
- Direct stakeholder engagement, interviews and data collection with the seven USDOT Smart City Finalists; with data obtained directly through interviews, from reviews of city-specific Smart City literature, and/or data sets directly obtained from cities through their partners. Review of information collected and synthesis/comparison across all seven Smart Cities and their stakeholders.

An alignment across urban science tasks enables the research team to bring new data and modeling methods related to Mobility as a Service (TNCs, Car-Sharing, Ride-Sharing and others), automated vehicles and other emerging mobility choices that will extend existing travel demand models and be transferrable to additional cities and regions. This has also included considerations for development of the Mobility-Energy-Productivity (MEP) metric and implementation approaches for airport- behavioral models, to employer provided mobility optimization, & district-scale on-demand services modeling.

Results

The interdisciplinary research in this area sought to identify the key issues, research and development (R&D) knowledge gaps, and data-driven opportunities related to emerging mobility systems in the urban space. The effort was anchored by stakeholder engagement on the key challenges and opportunities, defined within the

context of the emerging data and modeling environments with the seven smart city finalists from the USDOT Smart Cities competition in 2017. Interviews, focus group meetings, and workshops conducted with Columbus, Ohio (Smart City grant awardee – with a ‘smart city’ defined within the guidelines of the U.S. DOT Smart City Challenge (U.S. DOT, 2017)), Portland, OR, Denver, CO, Kansas City, MO, Austin, TX, San Francisco, CA, and Pittsburgh, PA, emphasizing the models, tools, data, and analytics that enable a Smart City, exposed common challenges, gaps, and research opportunities that informed the Urban Science portfolio. Indeed, it was these initial multidisciplinary urban science methods for advancing data collection and applied engineering models, that directly led to several of the research activities, and their insights that are shared in this report. The *Curation of Smart City Models and Data*, as the initiative was initially termed (and later reframed as ‘Data and Models Informing Smart Cities’), interviewed the actors and institutions within the urban area involved in Smart City initiatives, specifically querying on the data infrastructure, metrics, and modeling capacity. The results, summarized in a laboratory report, outlined several commonalities, gaps, and opportunities for the EEMS lab initiative—the most significant of which are bulleted below.

- A robust, modern, flexible data sharing and exchange platform was a priority of all seven cities. However, resources to accomplish this goal are lacking, and as a result, most cities are locked-in to outdated and siloed data architectures that make seamless data sharing and integration—focused on energy implications and opportunities—challenging at best.
- Urban sensing and other related data collection technologies are maturing at a rapid pace, reflecting the reality that models, responses, and research are lagging behind what is happening in the marketplace. An adaptive and evolving approach is therefore needed for many public urban data platforms emphasizing the need for complementary with rapidly evolving industry-available data collection. Nowhere is this more evident than in the area of mobility services, in which vehicle and humans routinely report location and speed, providing rich transportation data that is enabling new observability and potential leapfrogs over existing sensor and historically manual transport data collection systems.
- Mobility models within urban areas, typically managed by the Metropolitan Planning Organization (except in larger metros), are primarily road-vehicle based for the purposes of capital improvement programming, and have little value in their current state for enabling comprehensive multi-modal baseline data and a robust evidence base for measuring effectiveness of changes, to therefore inform plausible modeling scenarios of emerging modes and their impacts. New urban mobility technologies are being implemented with little to no proactive planning or coordination—mainly reacting to market entries with limited data and observability into key changes and trends emerging.
- Understanding the impacts of TNCs such as Uber and Lyft is of significant need to the cities with respect to identifying near to long term impacts and sustainability. As a corollary, the airport has emerged as the “front door” to any medium to large-sized city, being a primary transportation hub and with wider adoption and utilization of new mobility services for connecting travelers in the city to the world—as such, and due to new agile responses by airports to TNCs via a pickup and drop off fee, the impacts of many emerging mobility technologies and practices are now observable at the airport, offering early data-driven understanding of the implications of new mobility services.
- Appropriate metrics for smart city mobility analysis and effectiveness are lacking.

These key findings through engaging with the seven smart city finalists were validated through reviewing proceedings of two workshops—one on modeling and one on data, each with 50+ mobility-energy experts.

New mobility options, most prominently led by TNCs, have descended on urban areas within the last decade, creating a new norm for smartphone app-based mobility that many competitors, even public transit, are attempting to replicate. However, the extent of use of TNCs and their impact on urban mobility (both for the positive and negative) are slowly transitioning from significant data gaps for cities, to some limited data now becoming available from these companies and analyzed by our urban science team (yet mostly in larger cities – e.g., Chicago – see new TRB publications to New York).

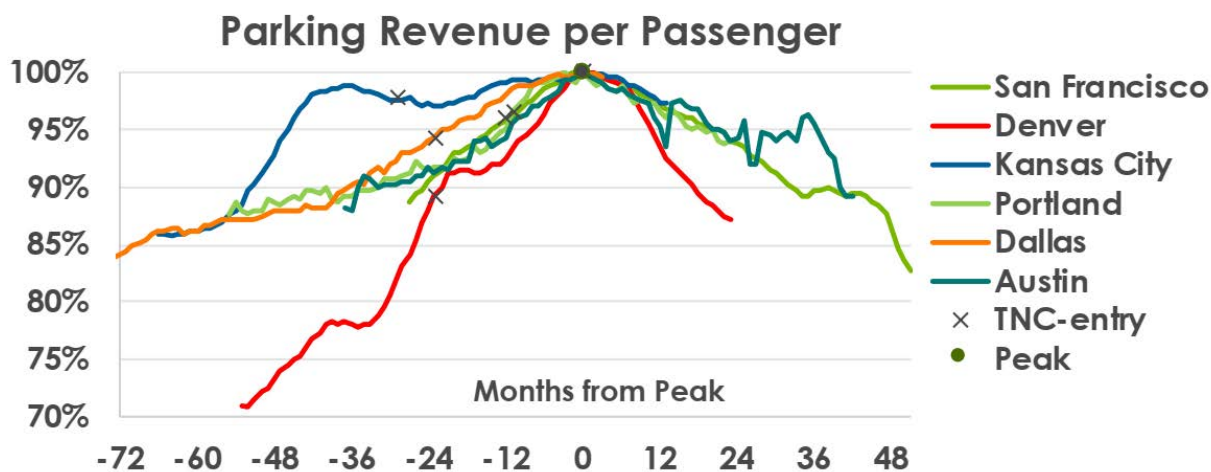


Figure I.5.1.1 Parking Revenue per Passenger

One area in which TNC use is observable is at airports via data obtained through open records requests. Findings in looking at TNC use data from airports are that rapid shifts away from other forms of transportation toward TNC use occur once TNC

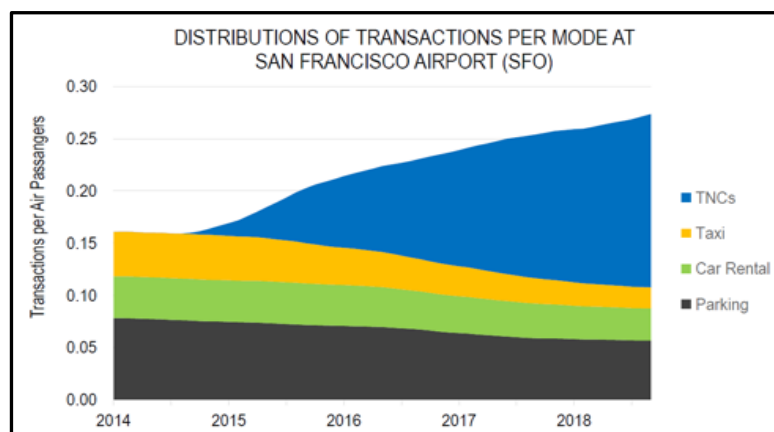


Figure I.5.1.2 Distributions of Transactions per Mode at SFO

services become available. **Data from multiple airports revealed that within 24 months of the introduction of TNC service at an airport, parking revenue on a per passenger basis peaked, and then began to decline.** Revenue records indicated a similar pattern of reduced demand for car rentals. Although no open data sources for parking at a city scale are available to test the hypothesis in the central business district, anecdotal information supports that a similar trend is occurring in downtowns, though at a lesser magnitude. Data obtained from the San Francisco airport, who has had TNC service at the airport longer than any US

city, clearly shows the uptake in TNC use, at a growth rate that has grabbed the attention of airport finance as well as airport curbside management.

The extent to which emerging technologies impact different cities, or different parts of a city, is a primary research question. The US Pillar undertook a city typology effort that sought to establish linkages between impacts and adoption of new mobility technology with measurable urban characteristics such as socio-demographic, governance, education, income, and mobility infrastructure. Initial methodological approaches were applied to the state of New York, specifically testing electric vehicle adoption patterns. The statistical clustering procedures identified four distinct regions, which the researchers labeled *Suburban*, *Urban*, *Rural*, and *Core Urban*, due to their visual correlation with these geographic areas. Note that these labels are not a result of pre-defined geographic groupings, but are simply labels for the four typologies identified by the algorithm. The correlations between these four typologies and the various mobility traits such as propensity for alternative commuting behavior, vehicles per household, average vehicle fuel economy, and the number of registered electric vehicles were assessed (Figure I.5.1.3). ***The typology revealed that the leading adopters of EVs were core urban and suburban residents – and not urban residents, suggesting that EV adoption is more closely correlated to income than geographical traits.*** EV adoption rate for urban dwellers was even less than the rural typology.

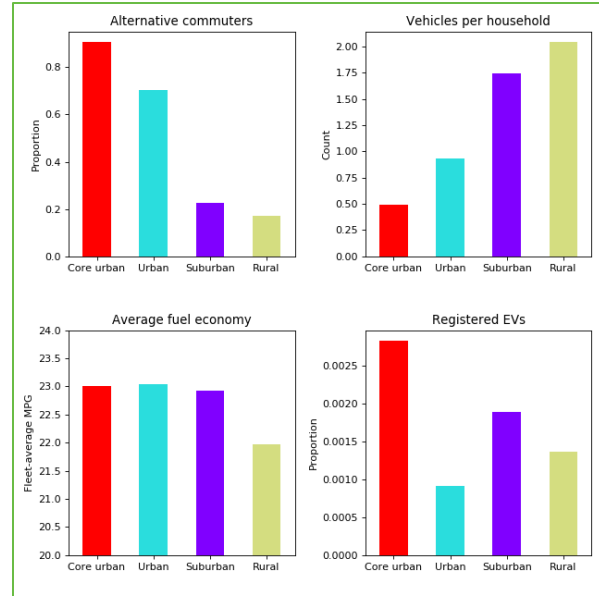


Figure I.5.1.3

Employer Provided Mobility (EPM) refers to increased involvement of the employer to provide sustainable, efficient and timely alternative commute solutions. Transportation Demand Management (TDM) at an urban planning scale has long stressed commuting and transit as a means to reduce congestion and conserve fuel. However, the sprawling urban landscape, and evolution from blue-collar shift work to white-collar knowledge economy has resulted in continuous declines in both car-pooling and transit. EPM, however, has emerged not as a TDM practice, but rather as a requisite benefit in order for employers to compete in the current labor market (Figure I.5.1.4). Based on initial data reviewed, a hypothesis being explored with city data is that of more young people delaying acquisition of a driver’s license and/or purchase of an automobile. This would be

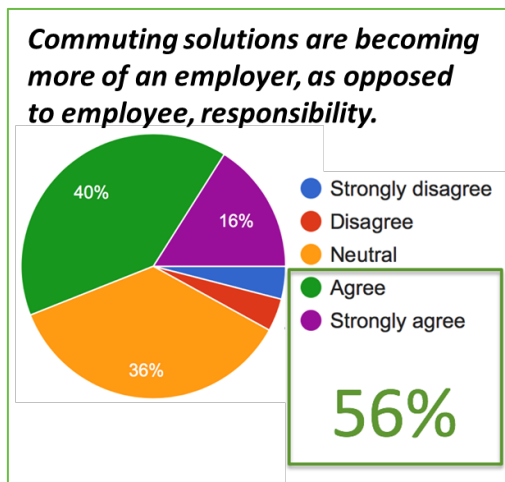


Figure I.5.1.4 Survey Question response statistics

a trend motivating the employer to provide alternatives to attract a growing, and desirable, source of labor. Combined with the fiscal incentive to avoid the sunk cost of parking infrastructure, particularly in urban areas, which could be avoided with fewer single occupancy vehicle (SOV) commuters, employer transportation demand management efforts are a new area of inquiry for data and modeling, focused on the commuting dynamics and efficient mobility opportunities in metro areas. At a workshop co-hosted by NREL and the Denver Chamber of Commerce, under a Mobility Choice Blueprint Initiative (see <http://www.mobilitychoiceblueprintstudy.com>), the participants were surveyed by the Urban Science team with respect to the changing atmosphere, with 56% of the attendees either strongly agreeing or agreeing that commuting solutions are becoming more of an employer, as opposed to employee, responsibility. The US Pillar found, through the workshop survey of providers, that EPM is both a white-collar and blue-collar phenomenon,

encouraged by socio-demographic shifts, fueled by the desire to avoid costs associated with parking infrastructure, and incentivized by a growing number of municipalities as a requirement before business' building or expansion plans are approved. As witnessed by the active involvement of the business community in cities such as in Columbus, Denver, and Seattle, with respect to aspiring Smart Cities mobility plans, employers see the current urban mobility issues as threatening economic productivity, as efficient access to various classes of labor is critical.

A case study of four employment centers in Metro Denver, assuming a modest 2% uptake of EPM (as observed in case studies from other cities), yielded an annual savings of 1.9 million gallons of gasoline (Zimny-Schmitt et al., 2019). EPM is significant in that commuting nationwide represents about a quarter of total vehicle trips, and 15 to 30% of vehicle-miles traveled (BTS, 2017), and directly impacting the most congested periods of the day. In addition, this area of urban mobility science research addresses the trip purpose (getting to work) that is a most significant need for vehicle ownership, thus opening up additional opportunities for car-free or car-light lifestyles.

Development of the Mobility-Energy Productivity Metric

The Smart City data and model curation activity reinforced the view that there was a gap with respect to having holistic metrics in the urban mobility space to measure progress to a maximum-mobility, minimum-energy future. The Urban Science team created a new metric of the effectiveness of the mobility system within an urban area. This metric, termed the Mobility-Energy Productivity (MEP) metric, is, at its heart, a location-based accessibility metric that scores access to employment, goods, and service with respect to travel time, affordability, and energy.

Mobility, with respect to the MEP, is defined as the ability of a transportation system to connect citizens to a wide variety of goods, services, and employment that define a high quality of life.

DOE's Energy Efficient Mobility System will identify and support technologies and innovations that encourage **Maximum-Mobility, Minimum-Energy Future.**

Figure I.5.1.5 EEMS Program Mission Statement

Mobility : The effectiveness of a network or system to connect people to goods, services and employment that define a high quality of life.

Figure I.5.1.6 Definition of Mobility

any mode, encompasses a spectrum of trip purposes informed by established literature, and establishes a quantitative measure of the potential mobility at a location. The MEP metric enables the measurement of the potential of emerging mobility systems to more efficiently connect people to opportunities (with respect to travel time, affordability, and energy) such as employment, health care, groceries, retail, entertainment, education, and recreation. ***In essence, the MEP aims to enable the measurement of mobility per gallon, in addition to miles per gallon and offers wider availability of a new integrated approach to urban mobility systems performance metrics*** (Figure I.5.1.7).

The MEP addresses the lack of open and practical metrics to quantify energy productivity of mobility by creating a new tool and core capability to determine the value and productivity derived from new mobility technologies. The MEP is a scalable, open-source metric that accounts for the infrastructure and land use options when quantifying and comparing the energy productivity of mobility options provided by existing and emerging transportation options. This metric serves as a unifying lens through which research under the SMART Mobility Laboratory Consortium’s portfolio of modeling results is assessed both in a quantitative as well as in a visual sense.

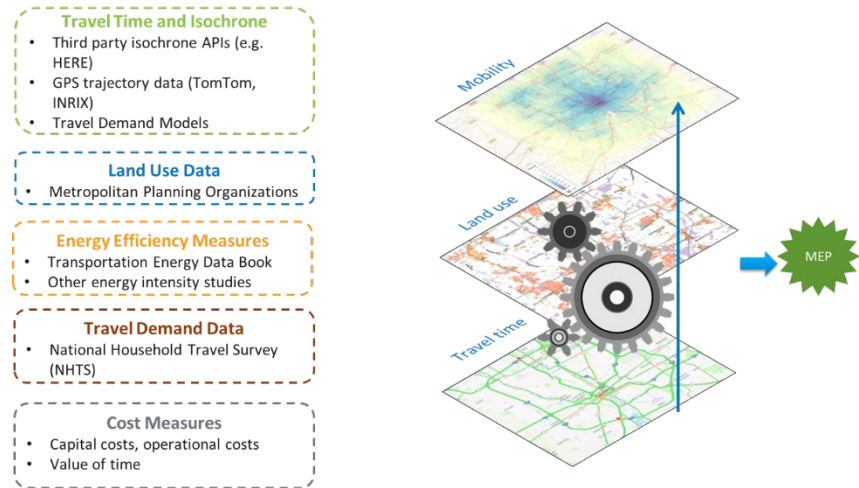


Figure I.5.1.7 Factors that affect the MEP Metric

The generalized MEP formulation weights access to a spectrum of employment, goods, and service opportunities with respect to travel time, affordability, and energy. MEP expands upon familiar and popular metrics such as walk, bike, and transit score [2] which are proprietary and mode specific, creating an open framework and standard to assess the efficiency of the mobility provided by any mode of transport. Specifically, the MEP counts the number of destination accessibility opportunities, including employment, health-care facilities, grocery stores, restaurants, parks, and entertainment destinations within 10, 20, 30, and 40 minutes of a location using different modes. Each count is appropriately weighted based on the mode energy efficiency and affordability. The resulting numeric score provides a robust assessment of the quality of mobility provided to a traveler at any given location, and with access to any mode of travel – both existing and emerging modes. The MEP metric measures how well each mode—as well as a combination of modes—connects the traveler to a variety of opportunities in an open source and easily adaptable framework that can be integrated into the transportation planning process of any urban area. A conceptual formulation of the MEP uses travel time, land-use data, modal energy efficiency, and affordability data, and travel demand data, to assess the ability of the transportation system to connect citizens at any point in the city to a spectrum of opportunities that define quality of life.

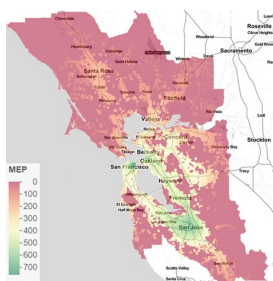


Figure I.5.1.8 MEP Score overlay of SAN Francisco Area

A toolkit has been developed to efficiently implement the MEP metric at the city level. The toolkit is now being applied to baseline MEP calculations for 60+ U.S. cities. Through a partnership with the American Society of Civil Engineers (ASCE), the MEP is being advanced as the foundational metric for the ASCE Transportation and Development Institute (T&DI) ES-X series of standards for Smart Cities. The MEP is also being integrated into a number of regional and statewide models. For example, MEP was chosen by the Colorado Department of Transportation (CDOT) as a key strategic initiative to integrate with the Colorado statewide transportation model to help evaluate major transportation initiatives.

The MEP metric, integrated into the SMART Modeling Workflow process, has served as the top level assessment of changes in mobility of scenarios, allowing for visuals of future scenarios, quickly comparing before and after for future adoption scenarios of automated, connected, electrified, and shared mobility systems and services, as well as their policy, land use, and infrastructure ramifications, all within the lens of the effectiveness of connecting citizens to a spectrum of opportunities - that are increasingly affordable, efficient, and enhance quality of life.

Conclusions

This task advances understanding of the current state of urban data and mobility models along with city goals and priorities in the smart cities-energy-mobility space. City data infrastructure and mobility modeling are enabling analysis and ongoing evolutions in exploring emerging mobility technology services to travel behaviors related to vehicle automation, connectivity, electrification, and sharing. Overall key takeaways from data collection, analyses, and smart city analyses include an increased need to:

- Provide a typology across cities to inventory, integrate, visualize, and map city data and model environments as they transition and transform, in response to disruptive changes in mobility and cyber-physical infrastructure
- Harmonize approaches, both in data and modeling, by developing common methods to observe transitions in impacts resulting from emerging ACES mobility technology, and influences in Mobility Energy Productivity.
- Address specific knowledge and data gaps as critical early-stage research; of particular need is to explore impacts and inform cities and national level understanding at the intersection of mobility and energy.

Key Publications

1. Sperling, J., Young, S., Beck, J., & V. Garikapati. 2019. *Mobility Data and Models Informing Smart Cities*. NREL/TP-5400-70734. <https://www.nrel.gov/docs/fy20osti/70734.pdf>
2. Henao, A., Sperling, J., Garikapati, V., Hou, Y. & S. Young. 2018. “Airport Analyses Informing New Mobility Shifts: Opportunities to Adapt Energy-Efficient Mobility Services and Infrastructure.” Golden, CO: National Renewable Energy Laboratory. NREL/CP-5400-71036. www.nrel.gov/docs/fy18osti/71036.pdf.
3. Butrina, P., Le Vine, S., Henao, A., Sperling, J., Young, S. Municipal Adaptation to Changing Curbside Demands: Findings from Semi-Structured Interviews with Ten U.S. Cities. Accepted for the 2020 TRB Annual Meeting.
4. Romero Lankao, Patricia, Alāna M. Wilson, Joshua Sperling, Clark Miller, Daniel Zimny-Schmitt, Luís Bettencourt, Eric Wood, Stanley Young, Matteo Muratori, Douglas Arent, Mark O’Malley. 2019. Urban Electrification: Knowledge Pathway Toward an Integrated Research and Development Agenda. *SSRN/Elsevier*, Posted 22 August 2019. (https://papers.ssrn.com/sol3/papers.cfm?abstract_id=3440283)
5. Henao, A, Sperling, J, and S. Young. 2019. Ground Transportation at Airports: Ride-hailing Uptake and Travel Shifts to Test Mode Choice Modeling Assumptions. Manuscript accepted for the 2020 TRB Annual Meeting.
6. Wilson, Alāna M., Clement Rames, Daniel Zimny-Schmitt, Carolina Nero, Joshua Sperling, Patricia Romero-Lankao. 2019. Mobility, Energy, and Electric Vehicle Typology for New York State. Manuscript accepted for the 2020 Transportation Review Board Annual Meeting.
7. Zimny-Schmitt, D., Wilson, A., Sperling, J., Duvall, A., and S. Young. Assessing the Energy Savings Potential of Employer Provided Mobility: A Case Study Approach. Manuscript accepted for the 2020 TRB Annual Meeting.
8. Hou, Y, Garikapati, V, Weigl, D, Henao, A, Moniot, M and J Sperling. Factors Influencing Willingness to share (or ‘pool’) ride-hailing trips. Manuscript submitted for the 2020 TRB Annual Meeting (accepted).
9. Wilson, A., Rames, C., Zimny-Schmitt, Neri, C, Sperling, J, P Romero-Lankao. 2019. Data-Driven Mobility-Energy Typology Framework for New York. *Environment & Planning B: Urban Analytics & City Science* (Submitted)

10. Holden, J., Nanayakkara, S., Sperling, J. and P Romero-Lankao. 2019. Exploring Synergies of Sustainable Infrastructure, Air, and Electrification Transitions: An Initial Rural-to-Urban Continuum Analysis. AGU 2019: Interdisciplinary Sustainable Solutions for Urban Areas. (accepted)

References

1. U.S. Department of Transportation. 2017. “Round Two: Seven Finalists Create Plans to Implement Their Visions.” <https://www.transportation.gov/smartcity/7-finalists-cities>
2. WalkScore. Accessed Nov 2019: <https://www.walkscore.com>
3. Clewlow, Regina R. and Gouri Shankar Mishra (2017) *Disruptive Transportation: The Adoption, Utilization, and Impacts of Ride-Hailing in the United States*. Institute of Transportation Studies, University of California, Davis, Research Report UCD-ITS-RR-17-07
4. Schaller, Bruce. *The New Automobility: Lyft, Uber and the Future of American Cities*. 2018. <http://www.schallerconsult.com/rideservices/index.html>
5. BTS. 2001/2017. National Household Travel Survey: Accessed: www.bts.gov/archive/publications/highlights_of_the_2001_national_household_travel_survey/section_02
https://nhts.ornl.gov/assets/2017_nhts_summary_travel_trends.pdf

Acknowledgements

We acknowledge the contribution from all Urban Science team members, cities,. We also acknowledge the contributions from the U.S. DOE/EERE/VTO EEMS Program Manager, and EEMS Technology Managers.

I.5.2 Mobility Energy Productivity Metric (NREL) [task 2.1.2]

Venu Garikapati, Principal Investigator

National Renewable Energy Laboratory
15013 Denver West Parkway
Golden, CO 80401
E-mail: venu.garikapati@nrel.gov

Prasad Gupte, DOE Technology Development Manager

U.S. Department of Energy
E-mail: Prasad.Gupte@ee.doe.gov

Start Date: October 1, 2017

End Date: September 30, 2019

Project Funding (FY19): \$300,000

DOE share: \$300,000

Non-DOE share: \$0

Project Introduction

Inspired by the Energy Efficient Mobility Systems (EEMS) mantra of creating a ‘maximum mobility minimum energy future’, and informed by the Smart City data model curation activity (pertaining to lack of appropriate holistic metrics in the urban mobility space), the Urban Science team created a new paradigm for evaluating mobility options within an urban area. This metric termed the Mobility-Energy Productivity (MEP) metric is, at its heart, an accessibility metric appropriately weighted with respect to travel time, affordability, and energy. Mobility is assessed with respect to a transportation system’s efficiency to connect citizens to a wide variety of goods, services, and employment that define a high quality of life. The metric, built upon established literature, is assessed for any mode, encompasses a spectrum of trip purposes, and creates a mobility potential field with which to monitor fundamental advances in the urban mobility systems with respect to efficiently connecting people to opportunities which encompass employment, health care, groceries, retail, entertainment, education, and recreation.

Objectives

- Develop and test a comprehensive metric that reflects energy productivity, affordability and accessibility of current and future mobility services
- Develop a MEP calculation module that can be integrated into travel demand models in order to accurately capture the primary as well as secondary impacts of various scenarios on mobility of a region.

Approach

At the heart of the MEP metric are accessibility measures that build on established accessibility theory and methodologies, assessing the number of jobs, goods, and service opportunities available within prescribed travel times from a location. This approach is fundamentally a geospatial analysis, providing both a visual map for comparative analysis and a numeric score to baseline performance metrics. Data to support travel-time calculations and land use (i.e., available goods, services, and employment opportunities) are readily available using third-party travel data or outputs from regional travel demand models along with land-use data from cities, metropolitan planning organizations, or commercial entities. Isochrones—that is, lines on a map of a region showing what can be accessed within a given timeframe using a selected mode of travel—are constructed for each mode. For example, isochrones are constructed to reflect how far an individual can travel within 10, 20, 30, and 40 minutes from a location by walking, biking, driving, or using public transit. Figure I.5.2.1 is an example of 30 minute isochrone showing reachable opportunities (color coded by land use) by bicycle from a location in Columbus Ohio (roughly corresponding to the campus of Ohio State University).

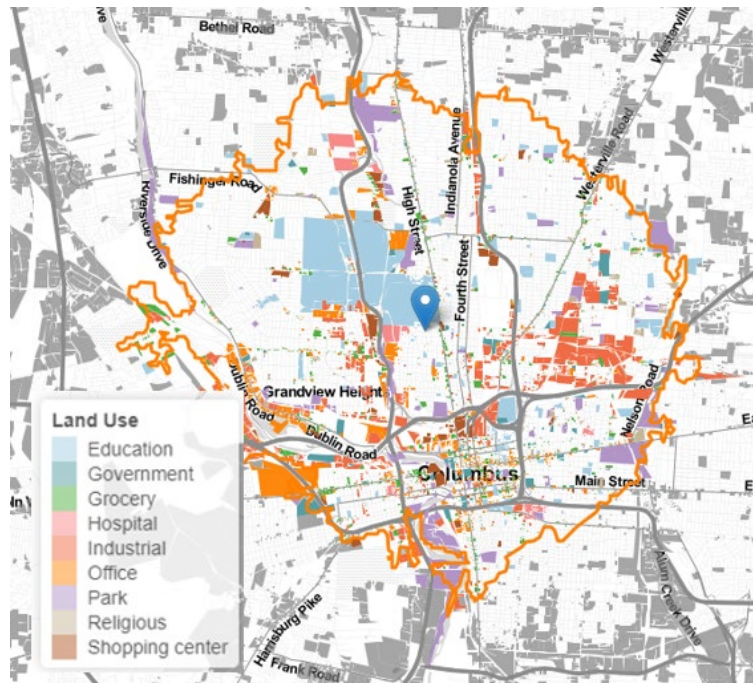


Figure I.5.2.1 Thirty minute isochrone for biking

The MEP formulation from a visual-graphical sense is to create a 10, 20, 30, and 40 minute isochrone for each mode, for each place. For each isochrone area, the job opportunities, grocery stores, restaurants, recreation facilities, medical service providers, and more are counted. These counts are appropriately weighted based on travel time, affordability, and energy use of each mode. Each opportunity count (be it job, grocery stores, medical services, etc.) are also appropriately weighted based on the frequency with which people make those sort of trips as revealed by travel surveys. Land use is indexed to purpose (e.g., education, shopping-retail, health) as well as to job-opportunity potential (number of employees or jobs).

Results

MEP Calculation Based on Third Party Data Sources

The MEP calculation procedure has been coded using statistical programming language R. The MEP package takes external inputs associated with travel time, land use, activity engagement characteristics, and modal energy and cost factors, and computes a MEP score for any given region. The MEP calculation culminates with a MEP metric for a location, which can be aggregated to any desired geographical resolution by weighting with appropriate population-density measures. The example shown below evaluates MEP at the resolution of a square kilometer land area, referred to as a pixel. The one square kilometer pixels were chosen to balance the granularity needed for analysis against the data complexity and computational burden, as well as the underlying homogeneity and variation of mobility from place to place. The resolution of MEP calculation can be at a greater aggregation (which may be appropriate for rural based MEP calculations) or more granular (which may be appropriate for highly dense central urban cores). Figure I.5.2.2 (Panels A–C) shows the MEP metric (for all activities) in the Denver metropolitan region for different modal combinations.

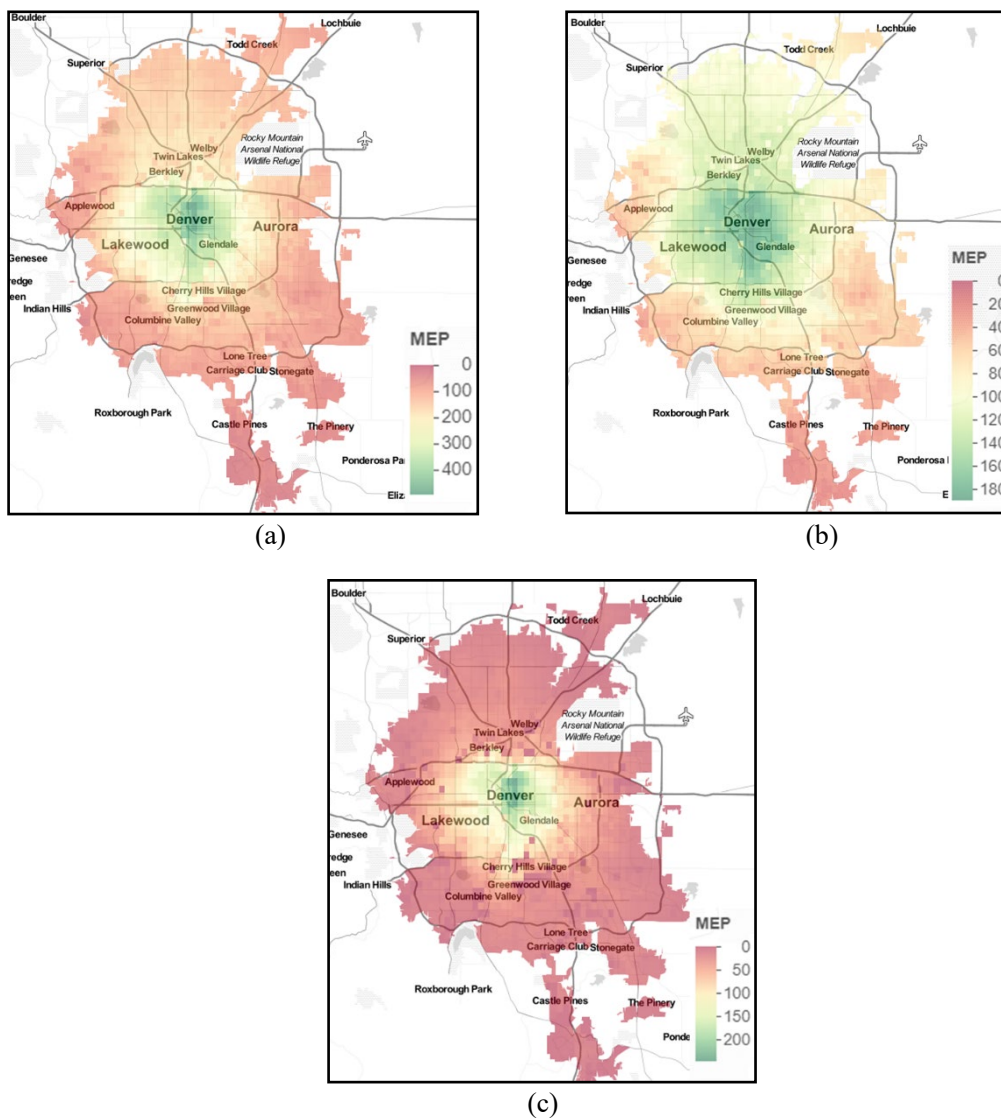


Figure I.5.2.2 MEP maps by mode for Denver, CO: A) All modes; B) Car; C) Transit, walk, and bike combined

Note not only the visual contrast, but also the difference in scale between the modes in Panels B and C, reflecting that the spectrum of opportunity accessible to a person is severely compromised if relying only on transit, walking and biking as compared to vehicle access. The MEP calculation procedure has been applied to compute MEP scores for fifty cities across the United States (most populous city in each state).

While the base MEP calculations provide a great way to benchmark the existing MEP scores for a city, the method is limited by data in capturing MEP scores resulting from forecasts of future travel in a city. Such forecasts are often carried out using travel demand models that are able to capture the changes in travel trends resulting from introduction of new transportation technologies (such as automated vehicles, and electric vehicles), and improvements in infrastructure (such as a new lane of freeway or investment in transit).

Integration with Agent Based Models POLARIS and BEAM

Acknowledging the importance of capturing secondary impacts of emerging transportation technologies (and infrastructural changes) while calculating transportation system efficiencies, NREL researchers, in collaboration with researchers at ANL, and LBNL have linked the MEP calculation procedure to sophisticated travel demand

models, POLARIS and BEAM so that the results of any scenario analysis can be used to generate MEP metrics. The MEP code was customized to use data provided by various model components (including POLARIS and BEAM) within the SMART workflow implementation. Table I.5.2.1 shows the data inputs to MEP from various components of the workflow.

Table I.5.2.1 MEP Inputs from Various Models across the Workflow

Model	Data Generated
BEAM/POLARIS	Study Area Boundary
	Travel Times by Mode
	TNC Wait Times
	Activity Engagement Frequencies
	Operational cost (per passenger mile) by mode
UrbanSim	Land use
	Population
	Employment
Autonomie/Route E	Energy Consumption (per passenger mile) by mode
Default	Coefficients for time/cost/energy parameters

The MEP calculation procedure was run for various scenario outputs from POLARIS and BEAM. Figure I.5.2.3 shows MEP map comparisons of baseline versus scenario A, based on the outputs from POLARIS SMART workflow runs. Scenario A in the workflow runs is defined by the following characteristics:

- New technology (e.g., integrated apps) enables people to significantly increase use of transit, car sharing, and multi-modal travel.
- Low vehicle automation (e.g., CACC) is being introduced mainly on the highway system.

Panel A in the figure above shows the baseline MEP visualization while Panel B depicts the MEP map for Scenario A. To further highlight the difference between baseline and scenario A, Panel C shows the difference in MEP scores (for each pixel) between baseline and Scenario A. It can be observed from the figure that MEP scores in scenario A see a proportional increase, in and around central Chicago. As this scenario deals with a high degree of shared trips (and transit trips), it makes intuitive sense to see MEP score increase in areas with a high trip density. It should also be noted here that from baseline to scenario A, the overall MEP scores see an increase of 31%, meaning that all else remaining the same, improvements in technology leading to increase in shared trips, will create relatively modest increases in MEP scores. Other scenarios associated with power train improvements see 60-160% increase in city-level MEP values, underscoring the importance of vehicle level enhancements in increase energy productivity of mobility.

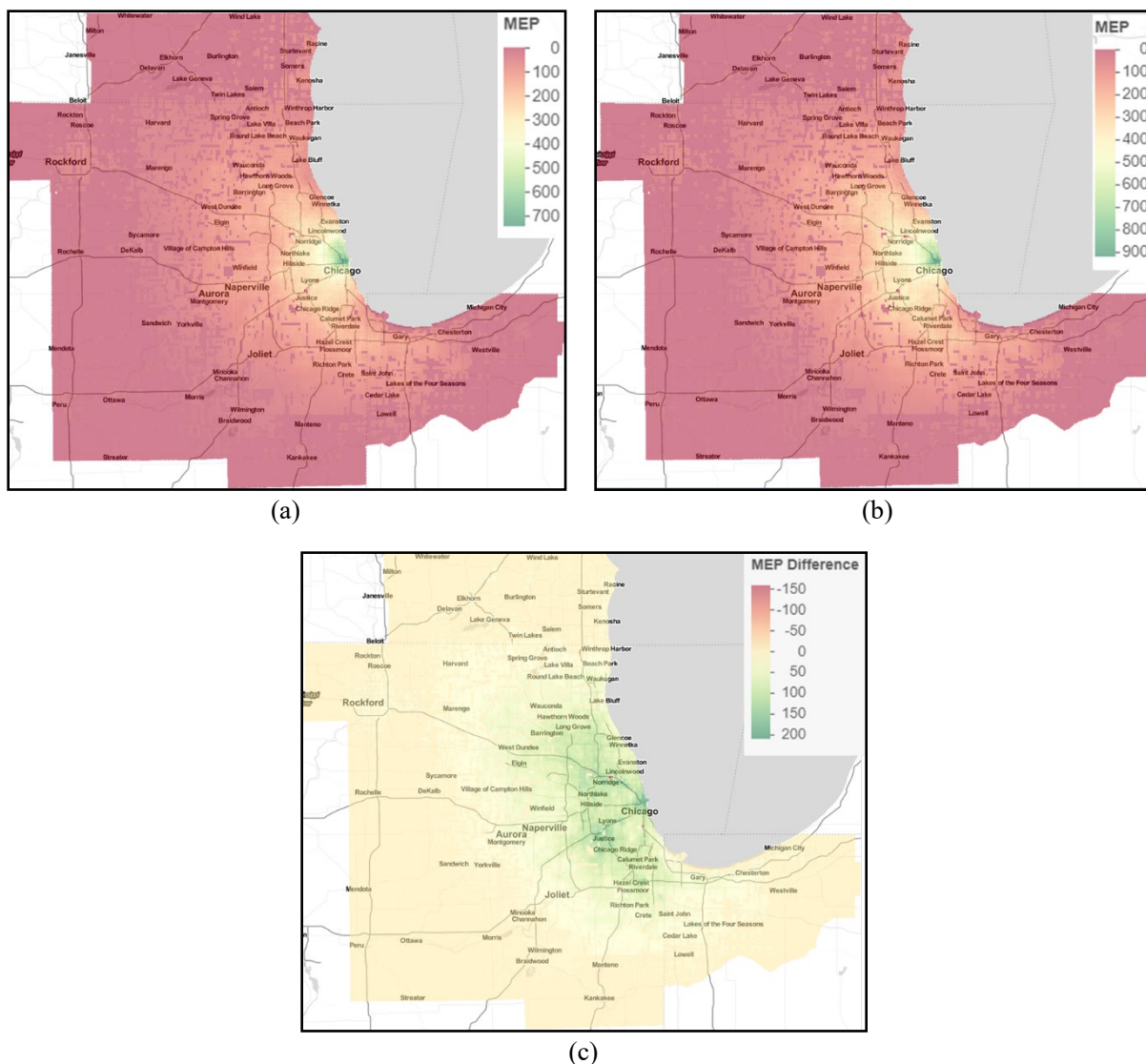


Figure I.5.2.3 MEP Scenario Analysis Results for Chicago, IL.

Conclusions

New mobility choices will have critical impacts on the functioning of metropolitan areas and decision making for transportation, energy use, and infrastructure. Communities of the future will need to measure the quality of a multitude of modal options, infrastructure investments, and policy adoptions available to enhance mobility of their citizens, and do this in light of sustainability concerns. A methodology for the comprehensive Mobility Energy Productivity (MEP) metric quantifies the effectiveness of a city's transportation system to connect citizens with a variety of goods, services and employment, weighted by time, energy, and affordability. The MEP metric allows communities to disaggregate the score to isolate the impacts of certain mobility options at specific locations and track progress over time, as well as aggregate upward to reflect an overall dashboard of fundamental impacts citywide. Recognizing the potential for the MEP metric, American Society of Civil Engineers (ASCE) is partnering with NREL to create standardized formulation of the MEP for use in smart cities. Although several refinements and extensions of the MEP continue, the basic framework and theory of operation, that of assessing the overall effectiveness of a transportation system to connect citizens with goods, services, and employment relative to travel time, affordability, and energy, fill a fundamental gap identified through Smart City stakeholder interaction, as well as provide a central lens for the DOE EEMS work.

Key Publications

1. Hou, Yi, Venu Garikapati, Ambarish Nag, Stanley E. Young, and Tom Grushka. "Novel and Practical Method to Quantify the Quality of Mobility: Mobility Energy Productivity Metric." *Transportation Research Record* (2019): 0361198119848705.
2. Garikapati, Venu, Stan Young, and Yi Hou. Measuring Fundamental Improvements in Sustainable Urban Mobility: The Mobility-Energy Productivity Metric. In proceedings of the *2019 ASCE International Conference on Transportation and Development* (2019).

Acknowledgements

From the PI:

- The PI would like to acknowledge the wonderful project team (Yi Hou, Rob Fitzgerald, Ambarish Nag, Jinghui Wang, and Tom Grushka) for all their diligent efforts in the development of this metric.

From the project team:

- Sincere thanks go to Dr. Stan Young (SMART Consortium Urban Science Pillar Lead) for his guidance on the development of this metric.
- The project team would like to extend their sincere thanks to the DOE leadership (David Anderson; Michael Berube; Stephen Chalk), EEMS Technology Managers (Prasad Gupte; Heather Croteau; and Erin Boyd) for their regular feedback on the development of this metric.
- The team would also like to acknowledge their gratitude to Joshua Auld (Argonne National Lab), and Colin Sheppard (Lawrence Berkeley National Lab) for their constant feedback on the metric development and guidance in integrating the MEP metric with POLARIS and BEAM models.

I.5.3 SMART Urban Typology (NREL, LBNL) [Task 2.1.5]

Patricia Romero-Lankao, Principal Investigator

Center for Integrated Mobility Sciences
National Renewable Energy Laboratory
Golden, CO 80401
E-mail: Paty.RomeroLankao@nrel.gov

Tom Wenzel, Principal Investigator

Lawrence Berkeley National Laboratory
1 Cyclotron Road
Berkeley, CA 94720
E-mail: tpwenzel@lbl.gov

Prasad Gupte, DOE Technology Manager

U.S. Department of Energy
E-mail: prasad.gupte@ee.doe.gov

Start Date: October 1, 2018	End Date: September 30, 2019	
Project Funding (FY19): \$1,100,000	DOE share: \$300,000	Non-DOE share: \$800,000

Project Introduction

Mobility patterns, technology adoption, and associated energy outcomes vary across settlement types, as acknowledged by the DOE in that ‘the ways connected, automated and shared vehicles are integrated in rural areas may differ substantially with how they are integrated into urban areas’. The range of projects conducted within the SMART Mobility initiative is broad, while the in-depth application of the Modeling Workflow process is, at present, limited to two metropolitan areas, Chicago and San Francisco. A key goal of our research will be to determine how findings from one location may be translated for implementation to another location. This will increase the value of the SMART Consortium research and modeling and enable research outcomes to become more meaningful to informing mobility strategies in other SMART locations. However, identifying how implementing or modeling of emerging mobility technologies in one city may play out in another is not simple; context with respect to multiple variables that define the settlement type is important

Objectives

The urban typology effort undertaken by the US Pillar seeks to examine how various geographic factors that span social, economic, techno-infrastructure, and environmental contexts impact variations in adoption, use, and associated outcomes of new mobility technology.

Approach

Methodology:

Typology approach is to cluster locations by key social, economic, techno-infrastructure, and other mobility relevant attributes.

Data:

Census block group level data for about 15 indicators across independent and outcome variables. The thirteen initial independent variables used in this analysis are: population density, intersection density, employment access, age (% over 65), gender (% female), race (% white), education (% with bachelor’s degree or higher), household income, home tenure (% homeowners), combined housing and transportation costs as a percentage of income (H+T Index), PM2.5 levels, cancer risk from air toxics and respiratory hazard index from air toxics.

The four dependent variables included commute mode, vehicles per household, vehicle fuel economy, and prevalence of electric vehicles (EVs, measured as the number of EVs per 1,000 vehicle registrations)

Analytical Methods:

Scaling techniques to normalize the data: The panel data used encompasses very diverse data sources with large variance within and between variables. For factor and cluster analyses, and in order to make results easier to interpret and visualize, all variables were scaled on a 0 to 100 range, using scikitlearn's pre-processing MinMaxScaler method in Python

Factor analysis to reduce dimensionality: In order to cluster these variables effectively, it is necessary to reduce the dimensionality of this dataset. Factor analysis was conducted using the FactorAnalyzer package in Python and resulted in three factors being used as input to the clustering.

Hierarchical clustering to group similar block groups and build distinct multidimensional socio-spatial typologies. Agglomerative (i.e., bottom up) hierarchical clustering was selected as the approach to identify census block groups with maximum similarities across the three previously derived factors, per the methods of Oke et al. (2019).

Results

NREL's initial demonstrative results from New York state:

The methodology produced four distinct typologies (see Figure I.5.3.1). The four typologies were interpreted (and labeled) as core urban (11% of total population), urban (37%), suburban (37%), and rural (15%) as demonstrated in Figure I.5.3.2. It is important to note that these four identified settlement typologies are the result of the clustering of key social, economic, techno-infrastructure, and other mobility relevant attributes, and not any particular independent variable or pre-existing spatial classification such as from the census, as the cluster labels may suggest. Upstate New York is dominated geographically by the rural typology, while suburban and urban typologies are found in or near every major city in New York, as well as many smaller cities. There are small pockets of core urban typologies in cities including Buffalo, Rochester, and Albany, while the majority is concentrated in New York City itself, though New York City has elements of all four typologies.

The spider plots highlight the different indicators across which each of the typologies vary (Figure I.5.3.3). Urban and Core Urban typologies unsurprisingly rank high on density and job access measures. They also see higher air pollution (PM2.5 concentrations, cancer and air toxics risk) than Suburban and Rural areas. Homeowners comprise the vast majority of the population in Suburban and Rural typologies but are largely absent in Urban and Core Urban areas. Household income disparities between the typologies highlight the socioeconomic segregation of the state, with affluent urban cores and suburbs standing in stark contrast with working class inner cities and rural areas. However, the H+T affordability index offers some nuance. Rural and suburban populations spend 59% and 56% of their income respectively on housing and transportation combined. Somewhat counter-intuitively, poor and wealthy urban dwellers, spend 39% and 44% respectively.

The typology categories were tested against dependent variables such as EV adoption rates, vehicle per household, average fuel economy, and alternative commuting modes (anything other than single occupancy vehicle travel), with the results illustrated in Figure I.5.3.4. This typology demonstrated insight into various mobility behaviors. For example, for EV adoption, the core urban population, which is wealthy and highly educated, in contrast to other typologies, adopt EVs at three times the rate per capita than the urban typology. Preponderance of alternative commuting modes was found to be closely linked with population and employment density, with more than 90% of core urbanites and 70% of the urban typology using transit or other alternative modes, compared with only 22% of suburbanites and 17% of rural residents. Household vehicle ownership also varies, with vehicles per household in rural areas the highest, followed by suburban, urban and core urban.

LBNL has an ongoing contract with the Office of Transportation Policy Studies in the Department of Transportation's Federal Highway Administration (FHWA) to cluster areas of the country into a number of geotypologies or geotypes. LBNL is also developing a modeling tool to assess the impacts of reallocation of the street and transit system rights of way to different modes of travel (conventional public transit; transportation network companies such as Lyft and Uber; carsharing services; micromobility services such as shared bikes, e-bikes and e-scooters; and walking) on systemwide mobility, accessibility, and safety within each geotype. LBNL will compare the sensitivity of clustering under the FHWA project with that conducted by NREL under the SMART project, for the states in which there is overlap.

There are several key differences in the objectives and methods of the FHWA and SMART clustering projects. Current travel patterns, and public transit infrastructure, are explicitly excluded in the development of geotypes under the FHWA project. The rationale is that regions with similar characteristics that may support certain travel patterns and modes will be grouped together based on their potential, regardless of whether a specific mode (i.e., public transit) is currently being provided. Although current travel is excluded in the development of the FHWA geotypes, LBNL plans to use measures of travel trends to validate the clustering in the geotypes. In addition, the FHWA geotypes will be developed, and system outcomes modeled under different scenarios, with an eye on improving mobility and accessibility, while at a minimum maintaining safety, rather than on reducing energy consumption per se. However, the energy implications of scenarios modeled in each geotype under the FHWA project can be readily calculated from the modeled changes in mobility.

The geotypes for the FHWA project will be constructed based on the primary geospatial and socioeconomic drivers of travel demand, characteristics of the street and off-street (but not transit) networks, and the climate and topographical features of each area (items shown in red in the figure below). We plan to use a two-stage approach, where detailed characteristics of 'micro-types' at the census block group level are aggregated into the larger geotypes, most likely at an existing jurisdictional level (e.g., county level). Demographic variables will not be directly included in the definition of the geotypes, but will be used in the modeling phase of the project to estimate mode choice and to understand whether the outcomes under different scenarios are equitably distributed. The focus will be on passenger travel in the early stages of the project, but will eventually be expanded to include freight transport and goods delivery.

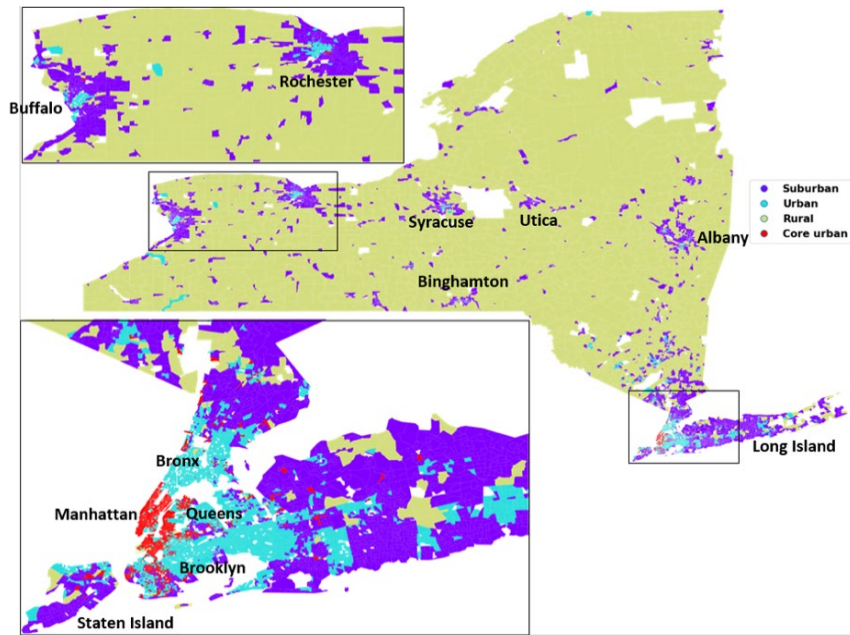


Figure I.5.3.1 Map of New York state clustering results

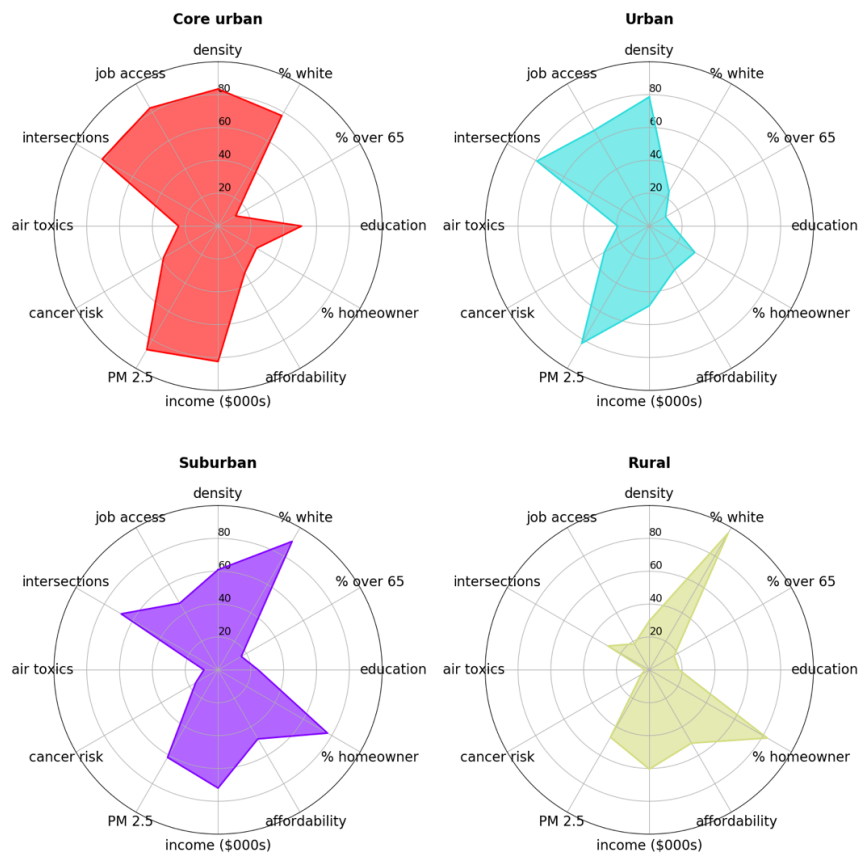


Figure I.5.3.2 Spider plots showing indicators of independent variables, in scaled relation to each other, for each of the four cluster settlement types

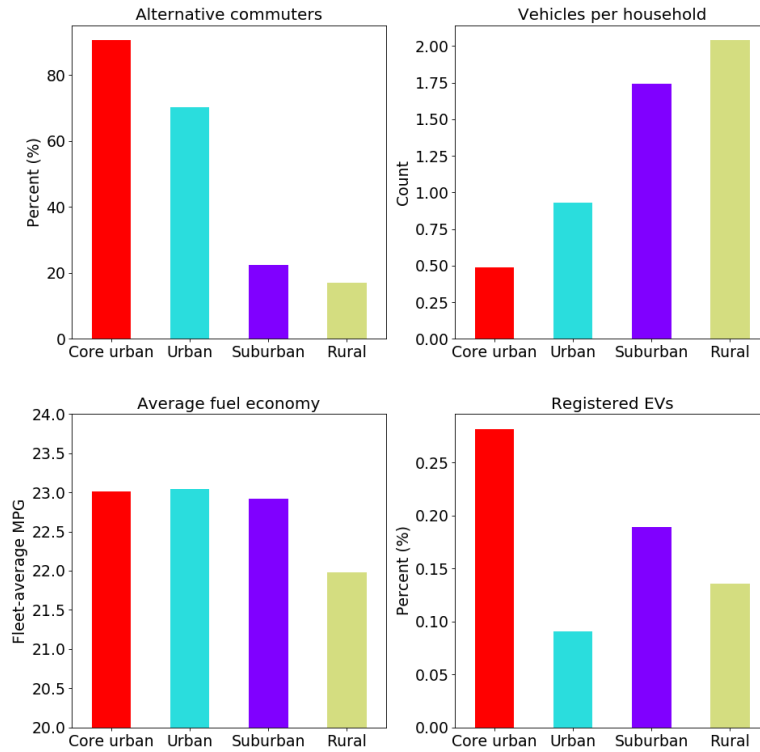


Figure I.5.3.3 Mobility and energy outcomes by typology

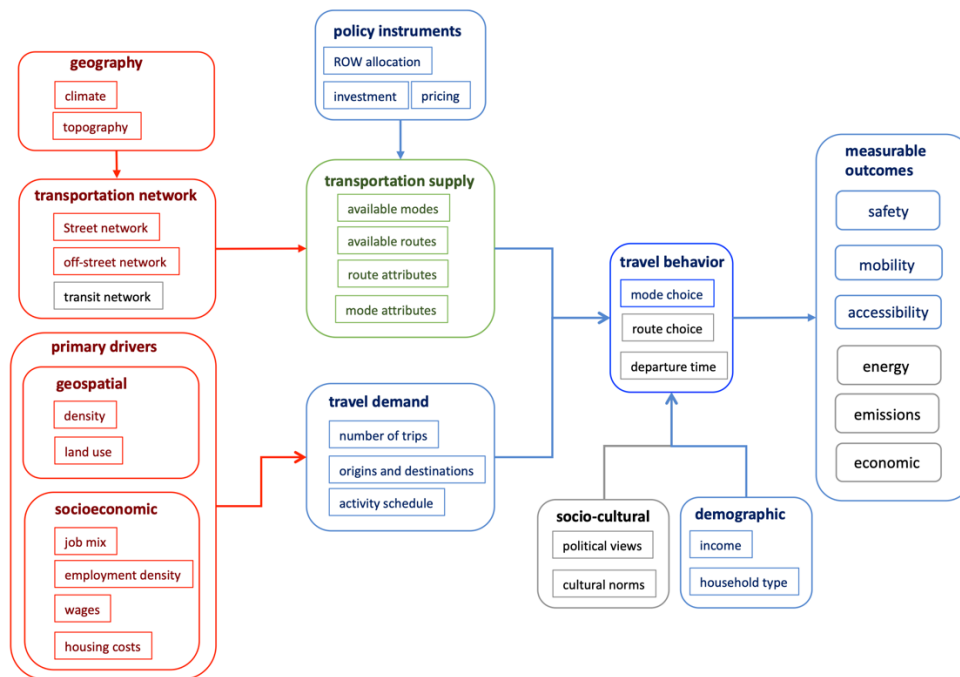


Figure I.5.3.4 Overview of Interactions in Transportation Systems

Conclusions

From New York State Study

Currently, EV adoption is geographically concentrated in Core Urban settlements inhabited by highly educated and wealthy early adopters—3 out of every 1000 of their vehicles were electric in 2017—and similar associations have been shown in the UK (Morton, Lovelace, and Anable 2017). In contrast, people in Rural typology areas drive longer daily distances and lack access to charging infrastructure, which may explain the lower rate of adoption. Lower EV adoption among Urban populations may be due to lack of capacity to afford the higher upfront cost of EVs, which points to the relevance of both spatial and socioeconomic factors. Interestingly, fuel economy remains constant at 23 mpg across all typologies, except the Rural typology, with a 22 mpg average. This is likely a combination of older and larger vehicles in rural areas, as has been shown in Australia as well (Li, Dodson, and Sipe 2015).

This typology differs from other typologies largely due to the more detailed geographic resolution of its analysis. While other recent typology projects have used the city as their unit of comparison (Oke et al. 2019; Creutzig et al. 2015; McIntosh et al. 2014), this typology's use of census block groups as a level of analysis allows for comparisons of sub-city level dynamics that are not possible with city-level typologies. Incentive programs from local government entities and other targeted initiatives may find this higher resolution data more useful for their purposes. For example, services aimed at reducing the need for individual car ownership, such as car-pooling, might be prioritized in Rural areas. Likewise, the availability of second hand electric vehicles may be key to EV adoption in modest Urban households.

Building on current typology work, future analyses could expand to a 10 state test bed, with the eventual goal of a nationwide typology aimed at identifying and characterizing mobility typologies that are consistent across the U.S., in order to gain insight on similarities of adoption patterns of new mobility technology, and thus anticipated benefits, and energy consumption consequences. This in turn could be used to extend the result of current SMART Consortium research (Chicago and San Francisco for example) to other cities in the U.S. through use of the geo-spatial typology breakdown and transferability.

Key Publications

1. Alāna M. Wilson, Clement Rames, Daniel Zimny-Schmitt, Carolina Neri, Joshua Sperling, Patricia Romero-Lankao (2019) "Mobility, Energy, and Electric Vehicle Typology for New York State", accepted for presentation at the 2020 TRB Annual Meeting
2. Clement Rames, Alāna M. Wilson, Daniel Zimny-Schmitt, Carolina Neri, Joshua Sperling, Patricia Romero-Lankao (2019) "A Data-Driven Mobility-Energy Typology Framework for New York State", under review at Environment and Planning B: Urban Analytics and City Science

References

1. Creutzig, Felix, Giovanni Baiocchi, Robert Bierkandt, Peter-Paul Pichler, and Karen C. Seto. 2015. "Global Typology of Urban Energy Use and Potentials for an Urbanization Mitigation Wedge." *Proceedings of the National Academy of Sciences* 112 (20): 6283–88. <https://doi.org/10.1073/pnas.1315545112>.
2. Li, Tiebei, Jago Dodson, and Neil Sipe. 2015. "Exploring Social and Spatial Patterns in Private Vehicle Fuel Efficiency: A Case Study of Brisbane and Sydney, Australia." *Australian Geographer*, April. <https://www.tandfonline.com/doi/pdf/10.1080/00049182.2015.1020994?needAccess=true&>.
3. Morton, Craig, Robin Lovelace, and Jillian Anable. 2017. "Exploring the Effect of Local Transport Policies on the Adoption of Low Emission Vehicles: Evidence from the London Congestion Charge and Hybrid Electric Vehicles." *Transport Policy* 60 (November): 34–46. <https://doi.org/10.1016/j.tranpol.2017.08.007>.
4. Oke, Olufolajimi, Youssef Medhat Aboutaleb, Arun Prakash Akkinapally, Carlos Lima Azevedo, Yafei Han, P. Christopher Zegras, Joseph Ferreira, and Moshe Ben-Akiva. 2019. "A Novel Global

Urban Typology Framework for Sustainable Mobility Futures.” *Environmental Research Letters*.
<https://doi.org/10.1088/1748-9326/ab22c7>.

Acknowledgements

The following people at NREL contributed to the Urban typology: Alāna M. Wilson, Clement Rames, Daniel Zimny-Schmitt, Carolina Neri, and Joshua Sperling.

I.5.4 Long-Term Land Use and Infrastructure: Coupling Land Use Models and Network Flow Models (LBNL) [Task 2.2.2]

Paul Waddell, Principal Investigator

Lawrence Berkeley National Lab
1 Cyclotron Road
Berkeley, CA 94720
E-mail: waddell@berkeley.edu

Prasad Gupte, DOE Technology Manager

U.S. Department of Energy
E-mail: prasad.gupte@ee.doe.gov

Start Date: October 1, 2018	End Date: September 30, 2019	
Project Funding (FY19): \$430,000	DOE share: \$430,000	Non-DOE share: \$0

Project Introduction

Conceptually the purpose of this project is to provide travel demand and traffic modelers – both within the SMART Mobility Consortium as well as in the transportation technology research community at large – with a more defensible point of departure for studying scenarios of future mobility. Most of the vehicle technologies studied by the Consortium are years if not decades away from fruition, and it is not realistic to expect the rest of society to sit idly by in the meantime. Any credible attempt to model the impact of future mobility technology must take into account the changes in land use, demographics, and real estate markets that are sure to have significantly altered our urban landscapes by the time the first fully electrified fleet of CAVs hits the road.

Integrated urban models of transportation and land use have long been the gold standard of regional planning, yet models that live-up to model integration requirements for closed loop feedback systems are rare. Many planning agencies who claim to have an integrated model are simply handing off the results of 30-year land use forecasts to their travel modelers and calling it good enough. The trouble with this approach is that interdependencies between transportation and land use exist in both directions, and yet play out on vastly different time scales. The goal of Task 2.2.2 is therefore to extend current state-of-the-art land use models to allow for tight coupling with travel models and properly account for closed-loop feedback effects.

Objectives

Couple land use and transportation models to quantify the impact of urban growth on mobility patterns and consequent energy use—and the impact of SMART technologies on long-term urban growth patterns:

Approach

- Extend UrbanSim with a travel model to allow for closed-loop feedback in simulation of land-use/urban infrastructure.
- Build fast models for key variables such as vehicle ownership, workplace choice, time of day, and mode for mandatory activities (work and school), etc.
- Complete a tight integration of UrbanSim with BEAM
- Develop 30-year scenarios for Bay Area
- Run cloud scaled network flow model at metropolitan scale integrated with a long-term urban simulation model.

Results

In FY19 Q1 we completed the first phase of development of ActivitySynth, a standalone suite of statistical models designed for ingesting population data and generating a day's worth of activity plans for each person. The code base we used has been published and made available online at <https://github.com/ual/activitysynth>. The initial implementation of ActivitySynth supports only the generation and scheduling of mandatory trips, i.e., home-to-work and work-to-home. As such, the current sub-models that comprise ActivitySynth are workplace location choice, departure time assignment, auto ownership, and preferred commute mode. ActivitySynth is currently configured with an output specification that maps directly to the inputs required for running BEAM. Support for POLARIS will be implemented next. The next phase of development will focus on implementing a school location choice model to support mandatory trips for non-workers, and then generation of discretionary trips as well.

In FY19 Q2 we completed the first integrated scenario runs of UrbanSim, ActivitySynth, and BEAM. We ran 4 scenarios out to the year 2040, along with a baseline, with explicit integration between the land use and transportation models occurring at years 2010, 2025, and 2040 (Figure I.5.4.1).

We “containerized” the UrbanSim and ActivitySynth platforms so that can be run as simple Docker executables without any data or software dependencies (apart from Docker). These containerized versions have been tested and executed by BEAM developers. This kind of high level work flow will enable us to fully automate the integration in the next phase of development. Additionally, we developed a shared, cloud-hosted data store to facilitate the handoff of model inputs/outputs. Both the land use and transport models are now reading/writing to this repository.

We re-estimated the suite of UrbanSim models to use skim-based generalized costs to compute the accessibility measures upon which all our parameter estimates depend. In general, a skim matrix provides travel time, distance, costs, or a combination thereof (called Generalized Costs) for each origin-destination pair.

As expected, we found the transport model (BEAM) to be the slowest component in the integrated workflow. To ingest BEAM outputs, run the land use models, and generate BEAM inputs typically takes ~2-3 hours, while the BEAM components take ~1-2 days to complete. Within the land use models, however, the departure time assignment in ActivitySynth is the slowest individual sub-component by a factor of ~3x. A more efficient implementation is currently being tested that promises to cut the run time of this model in half.

In terms of predictive accuracy, the primary mode choice model performs the worst, with a current predictive accuracy of ~67%. By this metric, the model would perform better if we simply assigned all trips to “drive alone”, since “drive alone” accounts for roughly 78% of the trips observed in our sample data. In addition to refining the model specification itself, we are investigating the use alternative scoring metrics for evaluating model performance since measures like predictive accuracy are technically “improper” scoring metrics for the case of logistic regression.

In FY19 Q3 we developed PILATES: a Platform for Integrated Landuse And Transportation Experiments and Simulation. PILATES provides the high-level software infrastructure for orchestrating and executing integrated runs of land use and travel model simulation scenarios such as we've documented in previous quarterly reports of US 2.2.2., and allows the entire workflow to be executed with a single command. The software relies on UrbanSim and ActivitySynth for simulating future land use data and generating agent-based activity plans for a synthetic population, but is modular enough to accommodate the use of any user-specified travel modeling software for updating the network-based accessibility measures that get fed back into the land use models each iteration, provided these updated metrics are reported by the travel model in the form of travel time and cost “skims”. Most of the testing and development thus far, however, has relied on BEAM as the principal travel model. PILATES allows the user to specify: 1) the simulation duration, i.e., how far into the

future we are forecasting; 2) the degree of integration, i.e., the interval or frequency (in simulation years) with which the land use and travel models exchange information; and 3) a scenario name for keeping track of simulation inputs and outputs.

In addition to PILATES development, we completed additional integrated scenario runs of UrbanSim, ActivitySynth, and BEAM, as well as integrated runs using POLARIS in the workflow as the travel model in place of BEAM. The results of these runs matched our experimental hypotheses, primarily insofar as we found a positive feedback loop between increasing traffic congestion and decreasing commute distances. In other words, in simulations for travel scenarios associated with the highest degree of increased network congestion, we also observe the highest degree of decrease in commute distances, which indicates our synthetic agents are responding to the integration of travel scenario data in a way that matches our intuition about how this process plays out in real life.

In Q4, we continued to fine tune the UrbanSim and ActivitySynth models to increase their sensitivity to the skim-based accessibility metrics, thereby increasing the degree of interdependence between the land use and transport models. This was accomplished primarily by re-estimating individual models (e.g., workplace location choice) using skim-based accessibility parameters in place of distance-based parameters.

Analysis of Scenario Simulation Results. Results from simulating multiple scenarios of vehicle automation and sharing provide insights into their implications for urban development patterns. First, we note the general results of these scenarios on travel conditions and patterns (Figure I.5.4.1). The base scenario has the highest generalized time and generalized costs of all scenarios, followed by the All About Me (C) scenarios. The All About Me scenarios also are highest in actual travel times and miles traveled. These differences seem plausible based on prior expectations and do indicate that the differences in value of time among the scenarios play a significant role in distinguishing them.

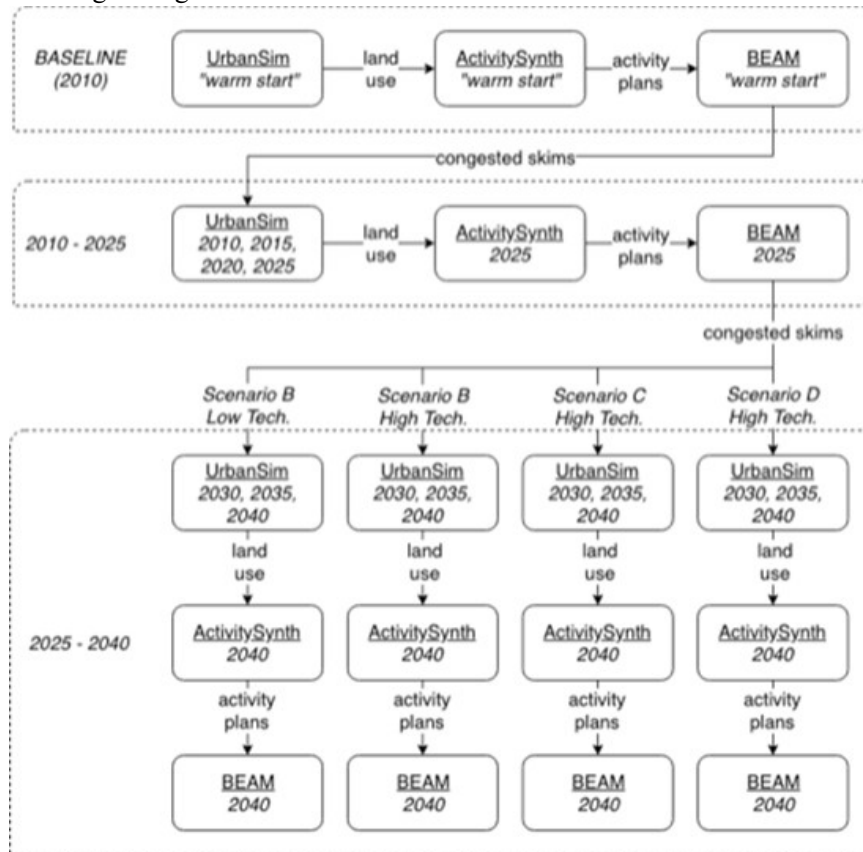


Figure I.5.4.1 Diagram of integrated workflow for Scenarios B and C.

The differences between vehicle adoption of BAU and VTO rates of adoption tend to be muted compared to the other differences among scenarios.

In urban economics it is well understood that as cities have evolved over many decades in response to changes in transportation technology that has rapidly reduced the cost of travel (or increased speeds), this trend has resulted in a decline of the land rent gradient and density gradient of cities. To explain this phenomenon and how rent and density are related, consider that households trade off accessibility and housing prices. When transportation costs decline due to advances in transportation technology or investment in infrastructure, it changes the relative attractiveness of locations that are farther away from the urban core, since land is less expensive in less accessible locations. But as transportation costs decline, outlying places that were previously inaccessible see significant increases in their accessibility, and the demand for those locations increases. This leads to increases in land costs as competition for those locations goes up. And along the gradient from the urban core to the periphery, land costs follow a gradient of decline.

These land price patterns then translate into changes in the building stock. Those locations with low land prices tend to use more land as a factor of production, relative to capital. Those locations that are more expensive do the opposite: they substitute towards capital and away from land. In other words, developers build taller buildings in places that have higher land costs, and lower density in places that have lower land costs. Simple production economics produces this result.

Now returning to the SMART scenarios, we can anticipate that we should see a flattening of the rent gradient in the scenarios that show the biggest declines in **perceived** travel times. It is important to consider that the perceived and actual travel times are quite different, as is evident in the charts above. Notice that the baseline is the highest in perceived travel time, but is in the middle of the pack in terms of actual travel time. The All About Me scenarios are highest in actual travel time, but lower than the baseline in perceived travel time.

We have specified UrbanSim models to use generalized travel time in order to account for the way people are expected to change their value of time. Being transported in a CAV may feel much less stressful than having to spend the same amount of time actually driving a vehicle. Models including residential location choice, workplace choice and employment (firm) location choice all were specified to be sensitive to generalized times. As a result, we expect the rent and density gradients to change in ways that could be predicted using urban economic theory.

Looking at the simulated results from interfacing UrbanSim and BEAM to the year 2040, we see some of these expectations realized in the results. Rents per square foot in residential buildings (Figure I.5.4.2), for example, have the steepest gradient from high to low job access locations, compared to the remaining scenarios. And the tech takeover scenarios show the greatest flattening of the rent gradient. These results are fully consistent with expectations.

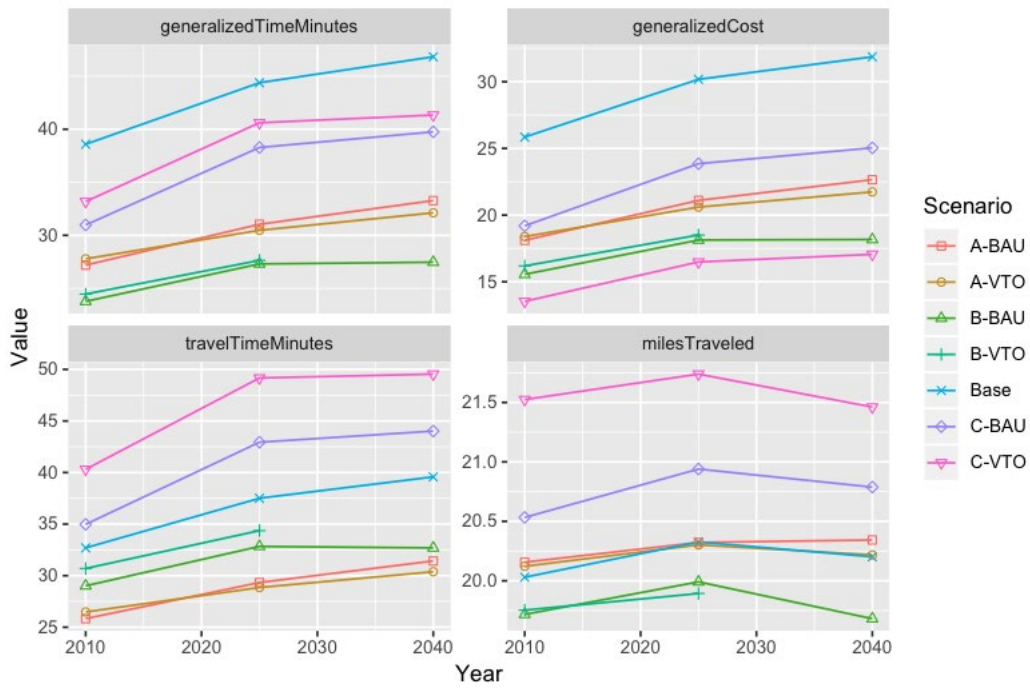


Figure I.5.4.2 A: Sharing is Caring, B: Tech Takeover, C: All About Me, BAU: Business as Usual (vehicle tech.), VTO: VTO Goals Achieved (vehicle tech.)

The next set of results we examine are the density gradients for employment (Figure I.5.4.3). Here we also see that the steepest gradient is for the baseline scenario, and the tech takeover scenario has the flattest gradient in 2040. So, rents and jobs both conform to expectations.

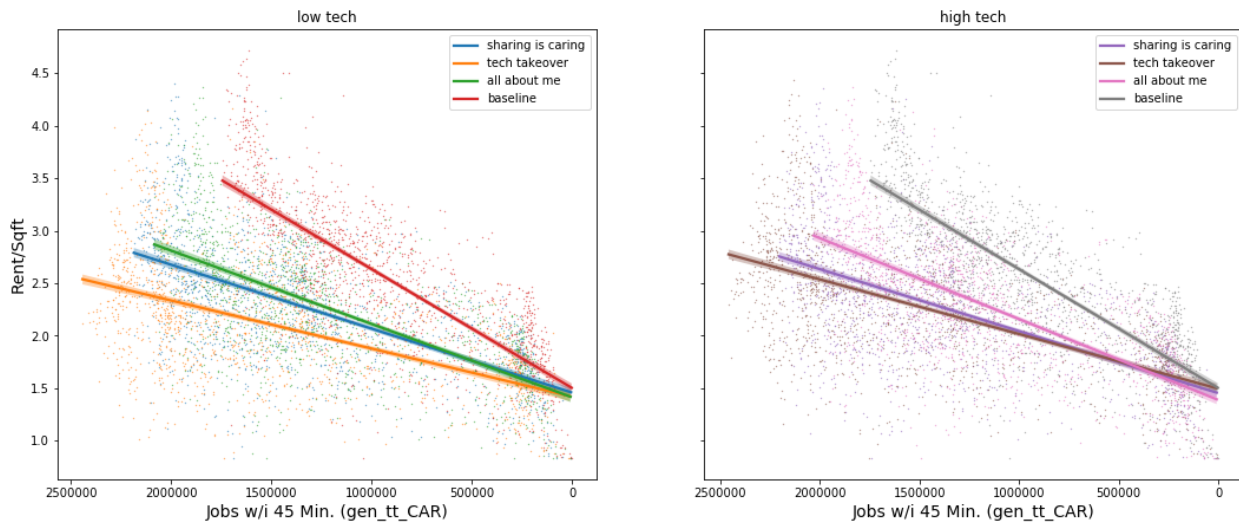


Figure I.5.4.3 Rent vs. Jobs Nearby

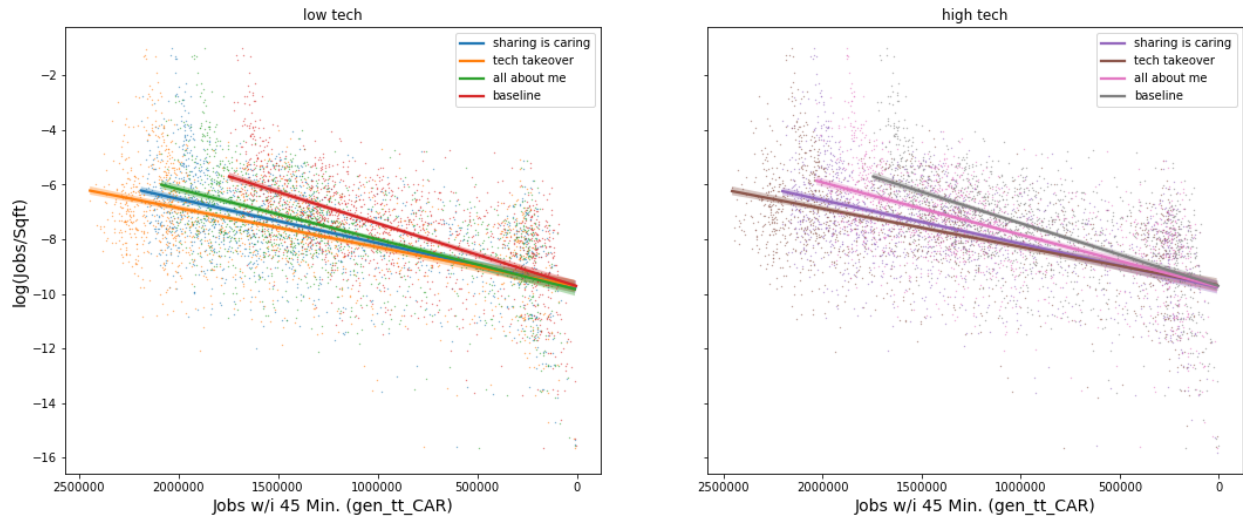


Figure I.5.4.4 Job Density vs Jobs Nearby

We would expect households to also follow this pattern across scenarios. The results do not at this point completely align with these expectations, however. Figure I.5.4.4 suggests there is relatively little difference in the population density gradients, and second the small deviations among alternatives seem to be in the wrong direction. We think there are a couple of explanations for these counter-intuitive results. One is that residential

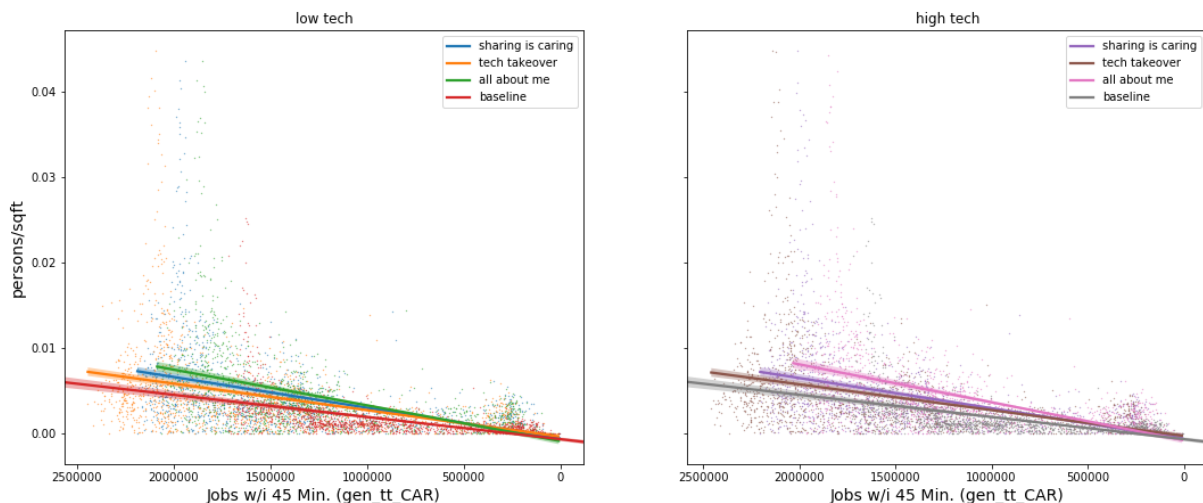


Figure I.5.4.5 Population Density vs. Jobs Nearby

location model (household location choice model) was built by the Metropolitan Transportation Commission and has not been completely re-specified by our research team. Its specification was less sensitive to generalized times than the employment location or workplace choice models. Second, since there was a clear response in the rent predictions, those locations that had higher accessibility differences had higher prices, and households choosing among alternative locations traded off higher prices against a muted difference in accessibility since the accessibility signal was not as strong due to the model specification. We anticipate that a deeper re-specification of the residential location choice model would address this.

Finally, we examine impacts on commute distances. The results, owing to the mixed results of the residential location choice model, produces a similarly mixed result, shown in Figure I.5.4.6. Commute distances decline

for all scenarios, and about the same amount for both the baseline scenario and the tech takeover scenario. Shorter commutes are expected for the more congested base case, but it is somewhat surprising to see the tech takeover scenario show a comparable decline in commute distance, though the differences in commute distances among all the scenarios is narrowly bounded between 13.85 and 13.95 miles. The baseline scenario reduces commutes due to the influence of jobs choosing more centralized locations and workers choosing jobs closer to their residential location. The tech takeover result arises in a different way, with jobs decentralizing in this scenario, moving them closer to workers, and enabling shorter commutes.

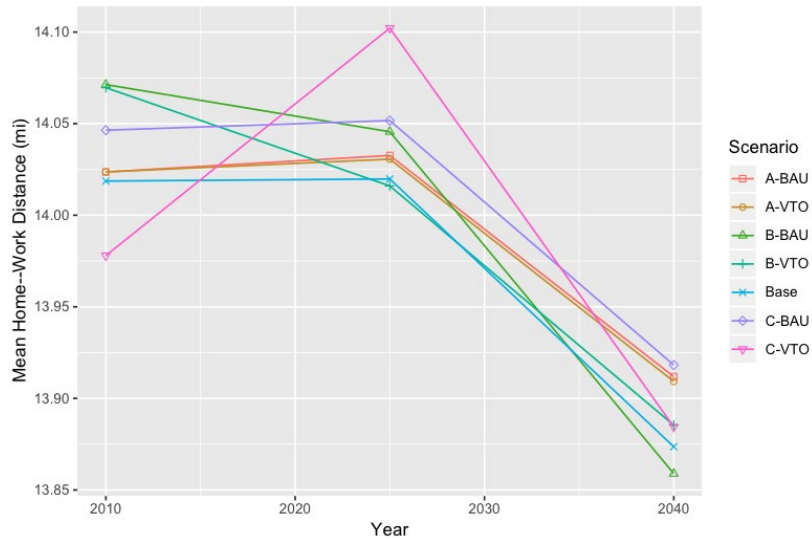


Figure I.5.4.6 A: Sharing is Caring, B: Tech Takeover, C: All About Me, BAU: Business as Usual (vehicle tech.), VTO: VTO Goals Achieved (vehicle tech.)

Conclusions

The Key conclusions from work performed in FY19 are:

- The project team coupled land use and transportation models to produce preliminary quantified impacts of urban growth on mobility patterns and consequent energy use. The integrated models also generated preliminary quantified impacts of SMART technologies on long-term urban growth patterns
- The analysis during FY19 addressed several scenarios where the differences in value of time among the scenarios play a significant role in distinguishing them.
- The integrated model produced estimates of SMART transportation impacts in terms of long term trends in Urban characteristics such as rental costs per square foot, density gradients for employment, and commute times. The preliminary results suggest that the continued development and validation of this model is warranted and will produce useful insights in the future.

Acknowledgements

We would like to thank Colin Sheppard, Rashid Waraich, and the entire BEAM development team for their assistance in making this integration possible.

I.5.5 Long SMART Cities Topology – Curbs and Parking (NREL) [Task 2.2.5]

Alejandro Henao, Principal Investigator

National Renewable Energy Laboratory
 1617 Cole Boulevard
 Lakewood, CO 80401
 E-mail: alejandro.henao@nrel.gov

Stanley Young, Principal Investigator

National Renewable Energy Laboratory
 E-mail: Stanley.young@nrel.gov

Prasad Gupte, DOE Technology Manager

U.S. Department of Energy
 E-mail: prasad.gupte@ee.doe.gov

Start Date: March 1, 2019	End Date: September 30, 2019	
Project Funding (FY19): \$300,000	DOE share: \$300,000	Non-DOE share: \$0

Project Introduction

Besides traditional vehicles and freight; transportation network companies or TNCs (e.g., Uber, Lyft) and other emerging technology services (e-scooters, automated vehicles) impose a unique mix of new demands on the curb, road network and wider transportation system that didn't exist a few years ago.

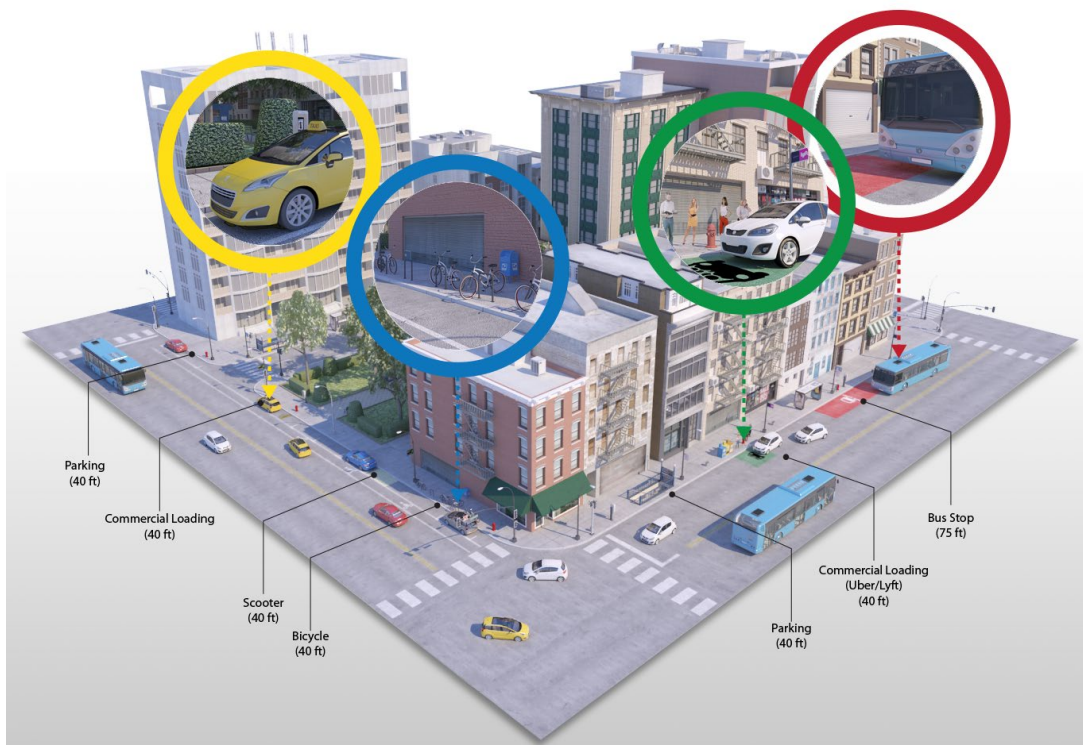


Figure I.5.5.1 Diagram of schematic curbside allocation in a dense urban area

Given competing demands for curb space, research is needed to better understand impacts and to prioritize space allocation to optimize mobility operations and energy use. Besides traditional on-street parking and bus stops, curb space needs to be allocated for pick-up and drop-off (PUDOs) zones, freight, and additional emerging mobility technologies.

Objectives

The main objectives of this task are as follows:

- Establish how cities are currently handling the changing pressures on their curbside space.
- Provide generic methodological approaches that can be employed by transportation network managers to support rational re-allocation of curbside space, capable of optimizing outcomes such as economic welfare or energy consumption.

Approach

The research team focuses on three main themes to accomplish the objectives established:

- Literature Review of studies on how academics and practitioners are modeling curb activity (including TNCs), as well as impacts on land use and urban infrastructure.
- Interview experts (within cities, metropolitan regions, airports, providers) with parking, curbside, land use, and emerging modes responsibility. The intent is to understand the key requirements and priorities for quantitative methods.
- Optimization Framework and Microsimulation: Develop mathematical models to optimally allocate/manage curbside space. The models will then be implemented using SUMO open source traffic microsimulation software, to expose the properties of the proposed models.

Results

During the six months of FY19, the research team developed two main publishable journal articles, one focusing on identification of current practices and municipal needs, and the other one focusing on the optimization framework. The team also initiated microsimulation scenarios for a basic intersection to be representative of the optimization framework. Results from each of the two articles are as follows:

Identification of Current Practices and Municipal Needs

The first task of the Topology research was a semi-structured interviewing approach to learn how municipalities are adapting to these new pressures on their curbside, and to identify the specific research needs as perceived by municipalities. Interviews were conducted with senior staff responsible for the curbside policy of ten large U.S. municipalities, with populations ranging from ~250,000 to ~5,000,000 (and the majority of which are the central city of their metropolitan region). Interviews were also conducted with two airport operators and two Metropolitan Planning Organizations (MPOs).

The interviews identified several new findings about how curbside management is changing (see summary in Table I.5.5.1 below). First, an organizational shift has occurred in most (eight of ten) of the municipalities with respect to restructuring and increasing staff to respond to these curbside pressures. Second, flows of data between ride-hailing operators and municipalities were found to be highly diverse, with some cities receiving data on pick-up and drop-off activity while other cities reported not being provided. Third, cities reported that operational failures at the curbside spill over into travel lanes of their arterial network, with impacts on public safety that are particularly acute in situations such as at closing times of bars in nightlife districts. Allocating curbside space is seen as a complex trade-off of municipal revenue, serving land uses efficiently, congestion management, and safety of the public. Finally, cities reported seeking more real-time data on curb activity in the future, as well as the ability to manage the curbside dynamically.

Table I.5.5.1: Summary of Selected Findings, Organized by City ID

(“√” for Yes; “-” for No; “?” for Unknown). *Note that numbered themes for which commonalities were not identified are discussed in the text but not included in this table.*

	A	B	C	D	E	F	G	H	I	J
Theme #1: Organization Structure										
Increased staffing during past five years	√	√	√	√	√	√	-	√	-	√
Municipality has staff that regulates TNCs	-	-	√	-	-	?	-	-	-	-
Theme #2: Current Curbside Activity										
Rapid growth in TNC usage	√	√	√	√	√	√	√	√	√	√
TNCs are regulated on the state level	√	√	?	?	-	√	√	√	√	√
Theme #3: Curb Management Pilot Projects										
Curb management pilot project	√	-	√	√	√	√	√	√	√	-
TNC curb management pilot project	√	-	√	√	√	-	√	√	√	-
Freight curb management pilot project	-	-	√	√	√	-	-	?	-	-
Micromobility curb pilot project	√	-	√	?	?	-	-	?	-	?
Monetary charges for using curb space	-	-	-	-	-	-	-	-	-	-
Theme #4: Research Needs and Envisioned Future of the Curb										
Additional curb-related data	√	√	√	√	√	√	√	√	√	√
Data aggregation and visualization tools	√	√	-	-	√	-	√	-	-	-
Digital curb inventory	√	-	√	-	√	√	√	√	-	√
Capability to manage the curb dynamically	√	√	√	√	-	√	√	√	-	√
Asset free curb and flexible payment technology expected in future	-	√	√	-	-	√	-	√	-	√
Autonomous vehicles expected to have future impacts	-	-	-	√	√	√	-	-	√	√

Optimization Framework

The second task of this project was to develop a new framework to support road network operators to make optimal curbside-management decisions. This is a novel research question, as transportation modeling has typically focused on road segments and intersections, neglecting curbside activity and hence providing no decision support to guide policy actions targeted at the curbside. The Optimization Framework simulates various types of activities competing for curbside space, with each linear portion of curbside space being allocated to the use that is optimal for that portion. The Framework builds on the Bid-Rent theory of urban land use, with extensions to account for the unique curbside context. Using a small-scale schematic layout (see Figure I.5.5.2 below), the proposed framework was implemented to model how a network manager would optimally re-allocate curbside space between traffic flow, on-street parking, bus stop, and ride-hailing pick-up/drop-off (PUDO) zones. The optimization process is flexible, so can incorporate outcomes such as economic welfare (as in this example), energy efficiency, or travel time minimization.

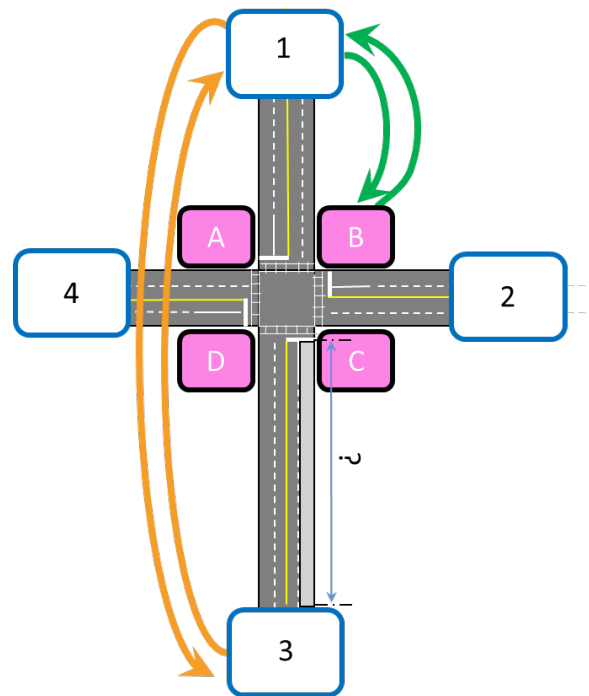


Figure I.5.5.2 Schematic spatial layout of case study.

Note: Central business district (CBD) zones are lettered, and outlying zones are numbered. Green arrows conceptually show one set of travel demands between outlying zones and CBD, and orange arrows show similar demands between two outlying zones that pass through the CBD. In the numerical case study, the decision is how to allocate the curbside shown with a question mark.

Table I.5.5.2 shows results from a variety of sensitivity analyses using the Optimization Framework, demonstrating intuitive and reasonable sensitivity to a range of stimuli. For instance, decreasing the demand for pick-up/drop-off activities leads to the optimal solution being to allocate less space to this activity, and more to parking for private automobiles (see Scenario #2 in Table I.5.5.2). To take another example, reducing the demand for travel through the intersection leads to a decision to reduce the distance from the stopbar where no stopping is allowed and only moving traffic is accommodated.

Table I.5.5.2: Results from case study sensitivity analyses

Scenario #	Description	Optimal number of 25' increments allocated (starting at stopbar) to Curbside Lane for Through Travel	Optimal number of 50' increments allocated to PUDO Zone (after Through Travel increments, before On-Street Parking)	Optimal number of 25' increments allocated to On-Street Parking (after PUDO zone)
Baseline	--	6	4	26
2	Decreased PUDO demand	6	3	28
3	Increased PUDO service rate	6	3	28
4	Increased VoT	6	4	26
5	Increased On-Street Parking demand	5	3	29
6	Decreased Through Travel demand	3	4	29
7	Increased On-Street Parking dwell time	5	3	29

Conclusions

The primary takeaways of the topology work include:

- Municipalities have been making ad-hoc, rule-of-thumb curb-management decisions for many decades. With the rise of on-demand mobility and e-commerce, and new uses of the curbspace seeking access to the same physical space that has historically been allocated mainly to parking, ad-hoc decision-making is becoming untenable.
- Early in Topology, outreach to municipalities at the forefront of the rise of on-demand mobility identified a wide variety of current practices, but a similar set of research and data needs.
- Topology proposed a new framework to allow municipalities to optimize curbspace allocation decisions, built on longstanding theory of urban real estate markets. Next steps will enrich the framework's applicability to larger-scale real-world sites.
- Data gaps for curb optimization were identified as key inputs for the model, including movement of people and good per vehicle and length of time, vehicle size, and spatial-temporal elements.

Key Publications

1. Butrina, P., Le Vine, S., Henao, A., Sperling, J., Young, S. Municipal Adaptation to Changing Curbside Demands: Findings from Semi-Structured Interviews with Ten U.S. Cities. Paper accepted for presentation at *99th Annual Meeting of the Transportation Research Board, Washington, D.C. in 2020*.
2. Kong, Y., Le Vine, S., Henao, A., Young, S. A framework for optimal allocation of curbside space. Paper accepted for presentation at *99th Annual Meeting of the Transportation Research Board, Washington, D.C. in 2020*.
3. Butrina, P., Le Vine, S., Henao, A., Sperling, J., Young, S. Municipal Adaptation to Changing Curbside Demands: Findings from Semi-Structured Interviews with Ten U.S. Cities. Paper submitted to *Transport Policy Journal* (Nov 2019)
4. Kong, Y., Le Vine, S., Henao, A., Young, S. A framework for optimal allocation of curbside space. Paper to be submitted for publication to *Transportation Research Part A*. (Draft)

References

1. Alonso, W. (1960) A Model of the Urban Land Market: Location and Densities of Dwellings and Businesses. University of Pennsylvania. Doctoral Dissertation, Economics Department.

I.5.6 Assessing Urban Impact: Automated Mobility Districts (NREL) [Task 2.4.1]

Venu Garikapati, Principal Investigator

Organization: National Renewable Energy Laboratory
 15013 Denver West Parkway
 Golden, CO 80401
 Phone: (303) 275-4784
 E-mail: venu.garikapati@nrel.gov

Prasad Gupte, DOE Technology Manager

U.S. Department of Energy
 E-mail: prasad.gupte@ee.doe.gov

Start Date: October 1, 2016	End Date: September 30, 2019	
Project Funding (FY19): \$250,000	DOE share: \$250,000	Non-DOE share: \$0

Project Introduction

Major disruptive technologies are set to re-define the way in which people view travel, particularly in dense urban areas. Shared – automated – public mobility resulting from the cross-hybridization of AVs with on-demand mobility service will bring economic and system efficiencies. Along these lines, a concept called the Automated Mobility Districts (AMDs) has emerged which describes a campus-sized implementation of automated/connected vehicle technology to realize the full benefits of an automated-vehicle (AV) shared-mobility service within a confined geographic region or district. In an AMD, autonomous fleets of shuttles (electric or gasoline) are expected to serve a majority of mobility needs of the people in the district, thereby dissuading the use of personal vehicles.

AMDs as are now certainly within the near to medium term planning horizon for dense urban settings. However, the availability of practical and efficient planning tools appropriate for analyzing the complexities of the AV fleet operations within AMDs is a significant issue. The breadth of options for operational planning of AMDs span from aggregate calculations, to advanced agent-based models. While aggregate back of the envelope calculations are an inexpensive solution, the estimates produced by such calculations would be too coarse for planning optimal deployment of fleets of AES vehicles. On the other hand, while agent-based travel models (ABMs) can produce precise results that can help plan the best possible deployment, developing and maintaining an ABM just for planning an AMD (which would be the order of a few square miles) would be too time-, and cost-consuming. This project aims to address this gap by developing a modeling and simulation toolkit that can be used for operational planning of shuttle services in an AMD. The AMD modeling and simulation toolkit is being developed with a view to be integrated as a special generator sub-model within existing travel models.

Objectives

The primary objective of this task is to develop a modeling architecture to quantify the mobility and energy benefits of AMDs. Specifically, FY19 efforts were dedicated to

- Development of a module for fleet and route optimization for AMD deployment
- Development of a mode choice module that is endogenous to the AMD toolkit
- Enrich the modeling components of the AMD toolkit with data from real-world AMD deployments.

Approach

Figure I.5.6.1 depicts the workflow of the AMD toolkit.

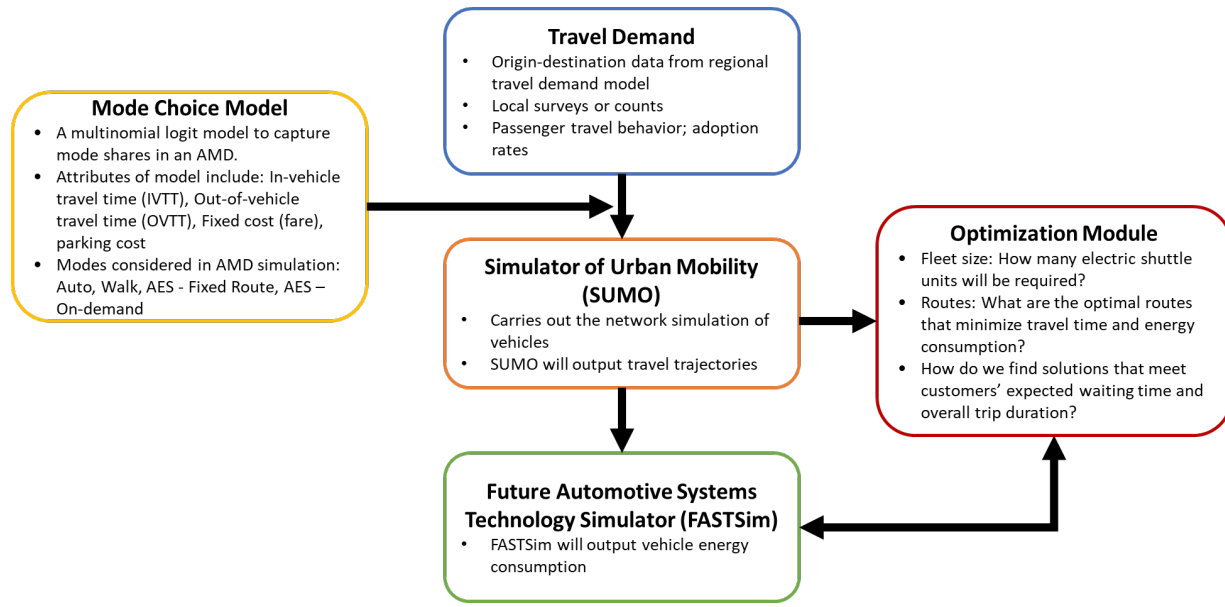


Figure I.5.6.1 Workflow of the AMD Modeling and Simulation Toolkit

The modeling and simulation process in the toolkit starts with an external input (existing travel demand) for the region in which the AMD deployment is planned. This can be obtained from existing travel demand models in a region. Where available, it is prudent to get as much information from the travel demand model as possible (origin-destination (OD) matrices, local surveys, adoption rates etc.). However, all of this information may not be readily available in cities or regions thinking of AMD deployments. Therefore, the toolkit is developed to work with as much (or as less) information, as available externally. The only critical input that the toolkit needs is existing trip exchanges (or OD matrices) between various traffic analysis zones in an AMD. Once this information is obtained, the toolkit applies a generic mode choice model (which can be adjusted as necessary) to obtain the market share of various modes being considered in an AMD. OD matrices by mode are sent as an input to the SUMO microsimulation model. SUMO (Krajzewicz et al. 2012) is an open-source, microscopic and multimodal traffic simulation suite, which can be customized with specialty modules to control the network simulation of vehicles. In the context of the AMD toolkit, the SUMO model has been enhanced with capabilities to simulate AES vehicles, both in a fixed-route as well as an on-demand mode of operation.

FASTSim is an open-source advanced vehicle powertrain system analysis model (Brooker et al., 2015). FASTSim inputs include operational details at drive cycle level (at 1Hz frequency) as well as vehicle design parameters such as aerodynamic drag, frontal area, mass, and rolling resistance. The second-by-second vehicle traces generated by SUMO (for car, and AES modes) are sent as an input to the FASTSim module for energy analysis. FASTSim computes the total energy expended for each trip, based on stock vehicle categories (say a 2018 Toyota Camry) for car mode, and based on a low-speed automated shuttle design parameters for the AES mode. Outputs from SUMO help in understating the mobility benefits of AMDs (such as passenger wait times, vehicle occupancy etc.), while outputs from FASTSim help quantify the energy benefits of mode shift from car mode to AES vehicles. If an AMD deployment is already aware of the operational specification (meaning the number of shuttles, routes, and frequencies), the AMD toolkit can be invoked to quantify the mobility and energy impacts of deploying AES vehicles in a geofenced region. However, if a deployment is in planning stages and is seeking for answers related to operational configuration, the SUMO module itself falls short in answering these questions. For scenarios such as this, an optimization module is developed and integrated into the AMD toolkit (Aziz et al, 2019). The module will help early stage AMD deployments with decisions-support related to:

- Optimal fleet size and route guidance

- Sensitivity of optimal fleet size and routes to: Range constraints for electric shuttles, Customer waiting time, Demand level.
- On-demand request handling without prior information on the future demand.

The current state of the AMD toolkit allows the user to model the functionality of the AMD by simulating travel patterns within an AMD (intra-zonal movements). Efforts are underway to make the toolkit available as an open source software for early stage AMD deployments. Future research efforts will focus on integrating the AMD toolkit into a regional TDM as a special generator, and also on modeling travel between an AMD and the rest of the region and on travel between multiple AMDs (and other special generators such as the airport) in a region to evoke to the inter-regional impacts.

Results

Findings from Greenville, SC test network

To demonstrate the applicability of the optimization model and developed solution technique, we analyzed deployment scenarios for a proposed AMD in Greenville, South Carolina (SC) network. The Greenville A-Taxi (or AMD) deployment, as described in the FHWA grant proposal (FHWA, 2017), consists of two phases as depicted in Figure I.5.6.2. Greenville County provided the detailed road network, and travel demand data for the region.



Figure I.5.6.2 Satellite Photo and Simulation Route Configuration. The modeling and simul -Taxi Test Field Phase 0 (CU-ICAR) and Phase 1 (Verdae District) at Greenville, SC: (a) satellite image (b) AMD Simulation Network And Fixed-Route Configuration

The Greenville AMD simulation includes four modes: 1) regular car (CAR); 2) pedestrian (WAK); 3) on-demand door-to-door ridesharing (DTD); 4) on-demand fixed-route ridesharing (FXR). DTD fleet comprised of four shared automated vehicles (SAV) which can operate anywhere in Phase 0 and Phase 1. FXR mode comprises of a fleet of six SAVs, two of which operate on a fixed route in Phase 0 and the remaining four SAVs operate on the fixed route in Phase 1 (see Figure I.5.6.2 (b)). Each SAV has a seating capacity of four passengers. The blue lines in Figure I.5.6.2 (b) represent the two fixed routes, and SAV stops are indicated with yellow-colored text.

Optimization Module

Origin-destination level trip distribution and network configuration for Greenville, SC were obtained from the regional travel demand model in the Greenville-Pickens Area Transportation Study (GPATS). The trip demand

and network pertaining to AMD deployment locations were extracted and imported to the SUMO platform to estimate travel time at link level. While the GPATS metro area spans across six hundred and eighty-five Traffic Analysis Zones (TAZs), the AMD deployment test network consists of eight TAZs. The travel demand data provided by GPATS include four origin-destination (OD) tables pertaining to (i) AM Peak (06:01 - 09:00 am), 2) Mid-Day (09:01 am - 4:00 pm), 3) PM Peak (4:01 - 07:00 pm), 4) Nighttime (07:01 pm - 06:00 am). The AM Peak travel demand data consisting of a total of 378 trips was used for the purposes of the simulation. For the scenario analyses, AES vehicles are expected to be deployed in two forms. On-demand fixed route AES vehicles are expected to serve passengers on a fixed route, but operate as an on-demand mode. Such vehicles will pick-up and drop off passengers only at designated drop-off and pick-up locations. On-demand door-to-door AES vehicles can pick-up and drop-off passengers anywhere in the network (similar to Uber or Lyft vehicles). In addition to the base line scenario (described next, in the mode share sub-section), two additional scenarios namely low demand (where demand for AES vehicles is 25% less than baseline), and high demand (where demand for AES vehicles is 10% more than baseline) are considered in this simulation experiment.

The solutions from Tabu-search routine are compared with a strategy commonly used in practice by the Transportation Network Companies and a few automated fleet management entities around the world. The strategy titled ‘Real-time Solution with Rolling Horizon (RSRH)’ routing uses limited information about future requests from the customers in solving the optimization problem for minimizing travel cost over the entire network. The technique can adopt a flexible rolling-horizon depending upon the data availability and prediction model in effect.

Comparison of Travel Cost

Figure I.5.6.3 shows the system-wide travel cost metrics as obtained from the Tabu-search based optimization at different demand levels and charging ranges. The capacity of the shuttle and maximum passenger wait time are assumed as 8 passengers and 120 seconds respectively.

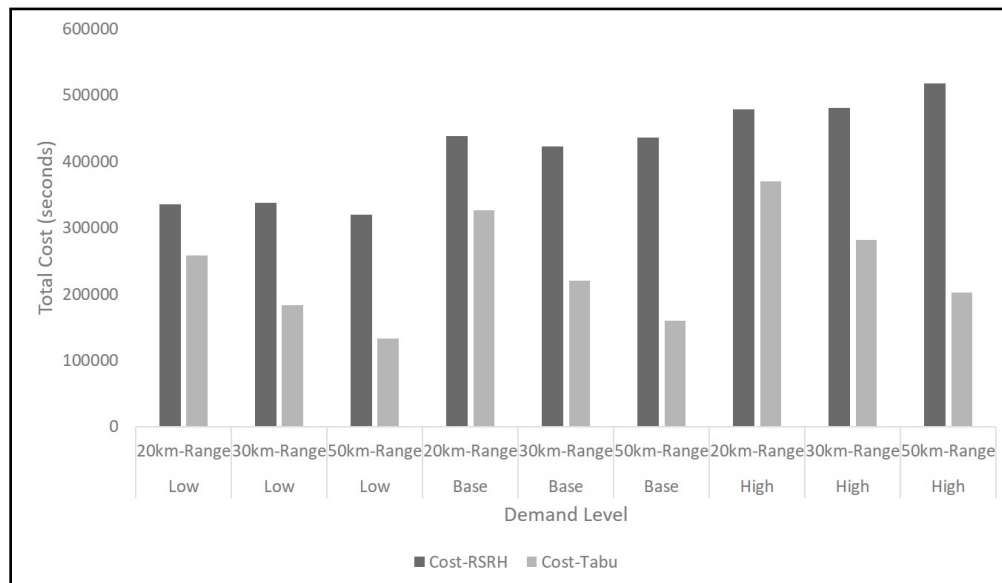


Figure I.5.6.3 Travel costs with Tabu-search based optimization and RSRH

Two trends are worth noting in Figure I.5.6.3. First, observing any given range (say 20 km) across low, base, and high demand, the system-wide travel cost increases with increasing demand which is to be expected. Second, for any given demand (say low demand), the travel cost decreases with increasing battery range for the shuttles. The key finding that would help an AMD deployment here is: For a given demand how much

travel cost (or travel time) saving is possible with increasing shuttle range? This information will prove critical in making benefit-to-cost ratio tradeoffs in vehicle purchase decisions.

Mode Choice Module

It is safe to say that robust data for modeling individual's preferences for SAV modes are practically non-existent, as the world is yet to experience such modes in reality. Some studies have shed light on the application of empirical unit cost of travel time and distance information to model preferences for SAV mode (Liu et al, 2017). Adopting the multinomial logit (MNL) mode choice model from Liu et al. (2017), a mode choice model considering SAV modes together with car and walk modes is incorporated in the AMD modeling toolkit. The utility function of each mode in the model is composed of the following components: constant cost or fare, distance, in-vehicle travel time, and two out-of-vehicle travel times (waiting time for SAV, and walking time to departure SAV stops).

Mode Choice - Simulation Results

Mode choice simulation was carried out with CAR, WAK, Door-to-Door Rideshare (DTD), and Fixed Route Ride Share (FXR) modes, respectively. DTD mode is able to conduct pick-ups and drop-offs anywhere in network, while FXR mode SAV runs on designated routes with fixed SAV stops. OD data for mode choice simulation was obtained in the same way as explained in the optimization section. Table I.5.6.1 presents the simulation performance metrics of CAR, DTD, and FXR modes. The service performance metrics for the two ridesharing modes and car mode consist of:

- Vehicle miles traveled (VMT) in miles for DTD, FXR, CAR modes
- Vehicle travel time (VTT) in seconds for DTD, FXR, and CAR modes
- Vehicle deadheading distance (VDH) in miles for DTD and FXR modes
- Vehicle loading rate (VLR) for DTD and FXR mode. VLR defines number of passengers onboard weighted by the vehicle distance traveled for all SAVs. VLR is an indicator of vehicle's efficiency in transporting more people per mile of travel.
- Vehicle detour factor (VDF) for DTD and FXR modes. VDF is calculated as trip distance of ridesharing modes divided by trip distance of regular car mode of Time Dependent Shortest Path (TDSP). An efficient rideshare mode is expected to have a lower VDF.
- Passenger waiting time (PWT) in seconds for DTD and FXR modes
- Passenger walking time (WKT) in seconds for FXR mode.

Walk mode is excluded from this table as it has no direct impact on traffic in the simulation experiment. It should be noted that, although FXR mode has a total of six SAVs available, only four SAVs (the ones in phase 1) were used in the simulation depending on the trip requests, because the number of trip requests in phase 0 was very low. Comparing the shared modes, DTD has a higher VDH/VMT ratio which is very close to the VDH/VMT ratio for TNC vehicles such as Uber and Lyft (Henao and Marshall, 2018). This consistent with expectation, since DTD mode can pick up and drop off passengers anywhere in the network, leading to detours with empty vehicles. FXR mode, however, travels on a fixed route and is not allowed any detours. The average vehicle passenger loading (AVG. VLR) is higher for FXR mode since travelers may need to cluster at SAV stops, which could increase vehicle occupancy. The overall VMT and VTT values are higher for car mode than other modes, because there is a higher number of cars in the network compared to SAVs.

Table I.5.6.1 Performance Metrics of Mode Choice Results

<i>METRICS</i>	DTD	FXR	CAR
OVERALL MOBILITY PERFORMANCE			
<i># OF VEHICLES</i>	4	4	94
<i>TOTAL VMT (MILE)</i>	110	87	223
<i>TOTAL VDH (MILE)</i>	60	43	0
<i>VDH/ VMT</i>	0.55	0.49	0
<i>TOTAL VTT (SEC.)</i>	20022	15297	30013
<i>AVG. VLR</i>	0.49	0.72	1.00
TRIP AVERAGE PERFORMANCE			
<i># OF TRIPS</i>	31	18	94
<i>AVG. VMT (MILE)</i>	3.55	4.83	2.37
<i>AVG. VTT (SEC.)</i>	646	850	319
<i>AVG. VDF</i>	1.21	1.55	1.00
<i>AVG. PWT (SEC.)</i>	324	294	0
<i>AVG. WKT (SEC.)</i>	0	990	0

At trip level, DTD mode has lower average VMT, VTT, and VDF than FXR mode, which may be attributed to the routing flexibility of DTD mode. CAR mode beats both shared modes in average VMT, VTT, and VDF as private cars don't need to detour for ridesharing. As for the level of service, the average passenger waiting time (AVG. PWT) for both SAV modes were close to 300 seconds. However, FXR mode has an extra 990 seconds of walk time per trip, making it slightly unattractive compared to DTD mode.

Simulation results demonstrate the benefits from the use of the SAV mode. A total of 49 trips are served by 8 SAVs; meaning, each SAV can replace 6 regular cars to serve trip requests. This benefit however comes with a cost in that passengers have to wait longer (as evidenced by PWT, WKT factors), and vehicles have to travel longer (as evidenced by VDF factor) in the network, meaning a higher amount of energy consumed. While electrification of SAV fleets can mitigate some of these adverse effects, sophisticated fleet dispatching strategies along with an increased demand for these services will provide a better solution for this problem.

Conclusions

This year's efforts on the project have focused primarily on the Optimization and Mode Choice Modules of the AMD modeling and simulation toolkit.

From the simulation results of the optimization module, it is observed that there both travel cost and energy consumption increase with number of shuttle requests. While travel costs (within a given demand scenario) decrease with increasing shuttle battery range, it was interesting to find that energy consumption is higher when vehicles with longer range are deployed. The additional energy consumption can be attributed to higher number of start/stops of the longer-range shuttle buses. The effect of waiting-time threshold shows a mixed pattern—following different trends for low and high number of on-demand requests.

From the mode choice simulation results, it is seen that the performance metrics for various modes obtained from the simulation are found to be in alignment with mode shares observed for respective modes. The framework was further put to test by starting the simulation with drastically different mode shares under the same simulation setting. It turned out that no matter what initial mode share values were given to the simulation, the iterative mode choice updating procedure always converged to the same result. Results also reveal that relaxing waiting time constraints increases the share of SAV trips, and that mode share of SAV drops with decreasing fleet size and seat capacity.

Future endeavors for the AMD modeling and simulation toolkit will also focus on:

1. Extending the capabilities of the toolkit to incorporate new modes such as e-scooter, dock-less bikes etc.
2. Incorporating additional constraints in the optimization routine such as enroute vehicle charging, and stochastic demand generation.
3. Integrating AMD toolkit with a regional model to assess inter-regional impacts of shared automated vehicles.

Key Publications FY19

1. Aziz, Husain, Venu Garikapati, Tony Rodriguez, Lei Zhu, Bingrong Sun, Stanley Young, and Yuche Chen. Route And Fleet Optimization To Serve On-Demand Mobility With Automated Electric Shuttles. Submitted to *International Journal of Sustainable Transportation*, 2020.
2. Huang, Yantao, Kara Kockelman, Venu Garikapati, Lei Zhu, and Stanley Young. An Integrated Model of Mode Choice and Micro-simulation for Informing Early-stage Deployments of On-demand Shared Automated Mobility. Selected for presentation at the 99th Annual Meeting of the Transportation Research Board, January 12–16, 2020, Washington, DC, and in review for Publication in *Transportation Research Record*, 2019.
3. Zhu, Lei, Jinghui Wang, Venu Garikapati, and Stanley Young. A Decision Support Tool for Planning Neighborhood-Scale Deployment of Low-Speed Shared Automated Shuttles. Selected for presentation at the 99th Annual Meeting of the Transportation Research Board, January 12–16, 2020, Washington, DC, and in review for Publication in *Transportation Research Record*, 2019.
4. Zhu, L., Wang, J., Garikapati, V. M., Young, S. E. (2019). An Integrated Model of Mode Choice and Micro-simulation for Informing Early-stage Deployments of On-demand Shared Automated Mobility. Submitted to *Transportation Research Part C: Emerging Technologies*, 2019.

References

1. Brooker, Aaron, Jeffrey Gonder, Lijuan Wang, Eric Wood, Sean Lopp, and Laurie Ramroth. *FASTSim: A model to estimate vehicle efficiency, cost and performance*. No. 2015-01-0973. SAE Technical Paper, 2015.
2. Henaó, Alejandro, and Wesley E. Marshall. "The impact of ride-hailing on vehicle miles traveled." *Transportation* (2018): 1-22.
3. Krajzewicz, Daniel, Jakob Erdmann, Michael Behrisch, and Laura Bieker. "Recent development and applications of SUMO-Simulation of Urban Mobility." *International Journal On Advances in Systems and Measurements* 5, no. 3&4 (2012).
4. Liu, Jun, Kara M. Kockelman, Patrick M. Boesch, and Francesco Ciari. "Tracking a system of shared autonomous vehicles across the Austin, Texas network using agent-based simulation." *Transportation* 44, no. 6 (2017): 1261-1278.

Acknowledgements

- The PI would like to acknowledge the efforts of NREL team (Lei Zhu, and Bingrong Sun), ORNL team (Husain Aziz, and Tony Rodriguez), and Yuche Chen on the project.
- Sincere thanks go to Dr. Stan Young (SMART Consortium Urban Science Pillar Lead) for his vision and guidance on the project.
- The project team would like to acknowledge the support from Greenville City Council member Mr. Fred Payne, who continues to help with collaboration efforts in Greenville, SC.

I.5.7 UrbanSim to ABM Workflow Integration (LBNL) [Task 2.5]

Paul Waddell, Principal Investigator

Lawrence Berkeley National Lab
1 Cyclotron Road
Berkeley, CA 94720
E-mail: waddell@berkeley.edu

Joshua Auld, Principal Investigator

Argonne National Lab
E-mail: jauld@anl.gov

Erin Boyd, DOE Technology Manager

U.S. Department of Energy
E-mail: erin.boyd@ee.doe.gov

Start Date: October 1, 2018

End Date: September 30, 2019

Project Funding (FY19): \$225,000

DOE share: \$225,000

Non-DOE share: \$0

Project Introduction

Substantial interactions and feedback mechanisms exist between urban form and transportation which are likely to shift as mobility options change. These interactions and mechanisms need to be accounted for as a part of the Smart Mobility Workflow.

Objectives

Connect the UrbanSim land use simulation model to the POLARIS travel demand models in order to explore the impacts of future mobility technologies and travel demand on urban form and regional mobility energy productivity.

Approach

Our project approach is as follows:

1. **Develop I/O specification and process:** The team will document the inputs and outputs from each model relating to land use and network performance, detail all input and output file requirements, identify data mismatches or opportunities for greater alignment, and make changes to I/O processes as needed to ensure required data flows between each model system.
2. **Assemble input data and implement UrbanSim for Chicago metropolitan region:** Generate demographic and land use projections for Chicago to align with the inputs required by POLARIS
3. **Incorporate UrbanSim land use projections in POLARIS simulations:** Incorporate UrbanSim land use projections from the Baseline (tract-level) Chicago model into the scenario analysis made using the POLARIS Chicago model in place of the fixed land use projections currently provided by the local MPO. Evaluate the impact of various land use forecasts on mobility characteristics.
4. **Provide POLARIS network assignment results to UrbanSim team:** The POLARIS model will be used to generate network level of service and other performance characteristics, and modal travel time and cost skims, which will be provided to the UrbanSim team for evaluation and incorporation into land use projections.
5. **Repeat steps 3 and 4 as needed:** steps 3 and 4 represent the structural feedback loop between the land use and transport models. See Figure I.5.7.1 for the workflow.

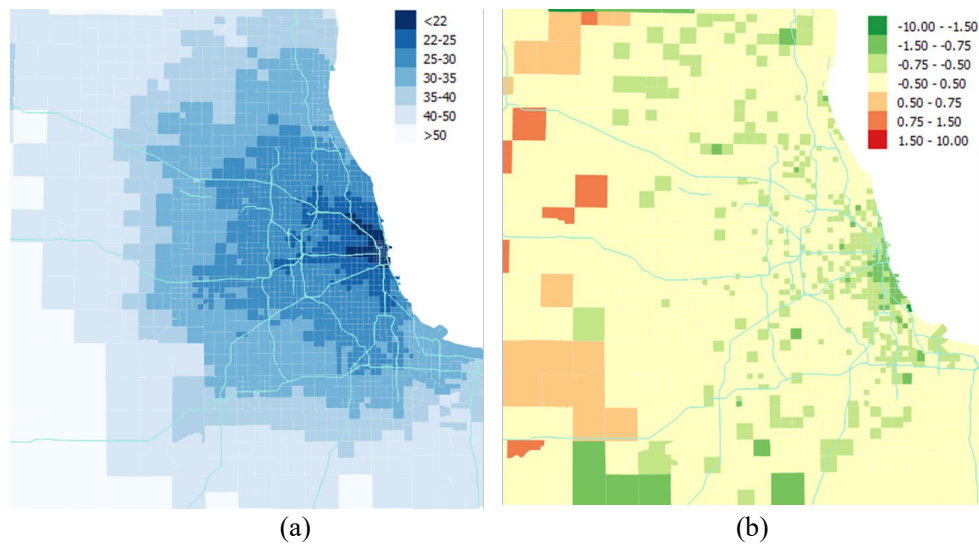


Figure I.5.7.2 POLARIS accessibility measures for (a) base2015 and (b) difference between base2025 and base2015

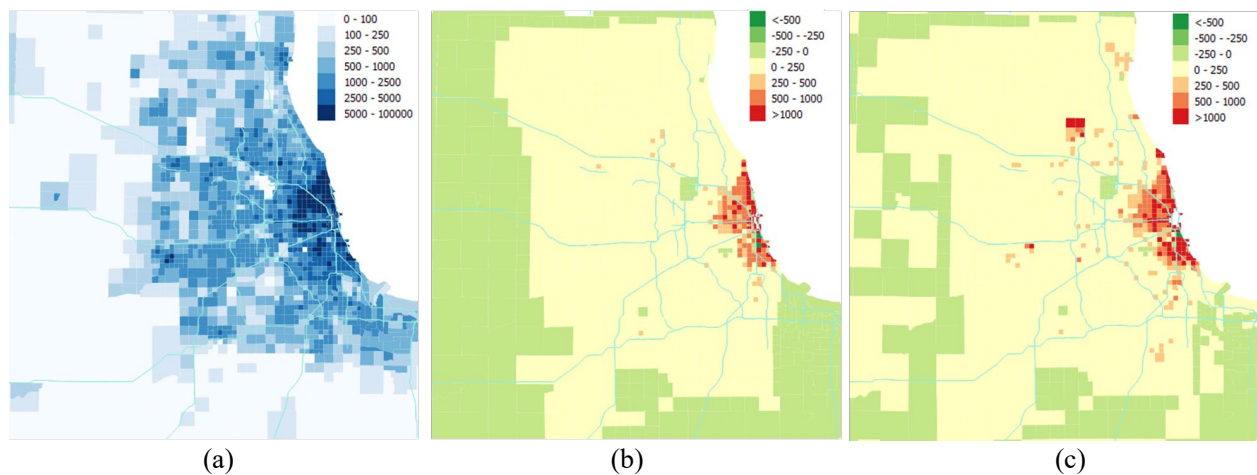


Figure I.5.7.3 Population density from UrbanSim runs for (a) base 2015, (b) base 2025 and (c) base 2040

The I/O specifications for the integration are well-defined and documented. The data flow in either direction is established using post-processing scripts developed by ANL and LBNL. Preliminary results demonstrate good compatibility between the two platforms. However, some land use characteristics, e.g., population and employment density, appear to have lower responsiveness than expected to changes in travel demand that arise from the various scenarios that were modeled

Conclusions

Further diagnostics are needed to better understand the sensitivity of UrbanSim's core models (e.g., household location choice, firm location choice, etc.) to changes in congested travel times and costs. One contributing factor to the apparent unresponsiveness of certain land use indicators to network changes is the fact that under the current integration configuration, POLARIS is responsible for assigning agents to workplace locations, rather than UrbanSim. However, because the only POLARIS outputs used by UrbanSim are network travel times, UrbanSim's household location choice model, for example, never knows about updated workplace locations, and thus cannot account for updated commute times.

Furthermore, the travel models are run at a much lower frequency than the land use models owing to their much longer run times. Thus, when we allow the travel models to perform workplace assignment, the work locations may be updated as few times as once per 30-year simulation. The fewer times these models are run, the fewer opportunities the agents have to respond to changes to simulation environment, which may help explain the low sensitivities of the population and employment to network travel times. We found we were able to compensate for this dynamic by running the UrbanSim models at a higher frequency (e.g., every year vs. every fifth year), which yielded much higher sensitivities of the land use model to changes in travel demand.

Lastly, it is likely that UrbanSim's core land use models simply need to be re-estimated in order to make them more responsive to changes in travel time. UrbanSim's current Chicago model was adapted from an off-the-shelf implementation and could greatly benefit from further refinement. In sum, the results presented herein represents a successful proof of concept, demonstrating a fundamental compatibility between UrbanSim and POLARIS that warrants a continuation of these efforts to develop a tightly coupled modeling platform.

I.5.8 The Signal Control Network as the Urban Mobility Nerve Center (NREL, ORNL, KSU) [Task 4.1]

Stanley Young, Principal Investigator

National Renewable Energy Laboratory
15013 Denver West Parkway
Golden, CO 80401
E-mail: Stanley.Young@nrel.gov

Hong Wang, Principal Investigator

Oak Ridge National Laboratory
P.O. Box 2008
Oak Ridge, TN 37831
E-mail: wangh6@ornl.gov

Husain. M. Abdul Aziz, Principal Investigator

Kansas State University
Civil Engineering Department
Manhattan, KS 66506
E-mail: azizhusain@k-state.edu

Christopher Day, Principal Investigator

Iowa State University
352 Town Engineering
813 Bissell Road
Ames, IA 50011
E-mail: cmday@iastate.edu

Stephen Remias, Principal Investigator

Wayne State University
5050 Anthony Wayne Drive
Detroit, MI 48202
E-mail: sremias@wayne.edu

Lei Zhu, Principal Investigator

National Renewable Energy Laboratory
15013 Denver West Parkway
Golden, CO 80401
E-mail: Lei.Zhu@nrel.gov

Prasad Gupte, DOE Technology Manager

U.S. Department of Energy
E-mail: prasad.gupte@ee.doe.gov

Start Date: October 1, 2018

End Date: September 30, 2019

Project Funding (FY19): \$375,000

DOE share: \$375,000

Non-DOE share: \$0

Project Introduction

Whereas the freeway system is characterized by interstate and inter-regional continuous flow, even at the junction of major highways, the urban context consisting of major and minor collectors and some minor arterials is characterized by a network of signalized intersections whose performance is governed primarily by the performance of the intersection control algorithms to limit delay and minimize energy. Whereas low volume intersections can be regulated with stop and yield signage, or more recently roundabouts, once volumes exceed defined thresholds, signalization is warranted to de-conflict traffic movement safely, and promote efficient progression.

Signal control originated with pre-timed sequences implemented with electro-mechanical controllers, a few of which are still in operation today. However, most control has been turned over to software control within signal cabinets sometimes operating with simple pre-timed sequences for particular time of day and day of week, and sometimes in demand responsive mode, altering timing in real-time in response to feedback from infrastructure sensors, primarily inductive loops (and technologies developed to directly replace inductive loops, while emulating their signals). Even modern adaptive control systems are fundamentally limited by the information provided to them from sensors, which typically are inductive loops or one of its many technology emulators. With more traditional fixed-timing approaches for corridors, sometimes sensors placed on side streets limit green time to when a vehicle is detected. Sometimes sensors are placed on the dominant through-street movement approximately 400 feet in advance of the signal, extending green times when more vehicles are sensed, or shortening green times when sensors detect the queue has been expended and no other vehicles are approaching the intersection. In any of these scenarios, the control algorithm is limited by the information that sensors (inductive loops and equivalent technologies) provide to the controller. Such information is at best incomplete and provides only partial observability. Even video sensors which are becoming more and more prevalent over the past decade, are engineered to mimic the equivalent information that an inductive loop typically provides a controller.

Under this research theme, the US Pillar investigated the **potential reduction in delay and energy as well as increase in safety that can result from the heightened observability** that is possible with connected vehicles (CV) and with enhanced infrastructure sensing. Connected vehicles (CV) provide a full description of the vehicle and its path along a corridor through a communications link to the signal controller, such as DSRC, or possibly 5G. The controller can effectively see all CV equipped vehicles as they approach the intersection. If the percentage of vehicles equipped with CV technology is sufficient, the controller can infer detailed traffic characteristics with which to further optimize signal timing. Infrastructure sensing (either LiDAR or video image processing) is similar to traditional sensors, in that it detects and reports on 100% of the vehicles that are within its detection range but differs from traditional sensors in that it provides full trajectory information for each vehicle. Limits of infrastructure sensing is primarily its zone or range and its reliability of detection.

Objectives

The group of signal control projects in the Urban Science portfolio is building toward the need for continuous observable, fail-safe, fault-tolerant frameworks to ensure efficient and safe passage of vehicles, pedestrians, and emerging modes of AVs and micro-transit as our society moves to more CV and AV controlled vehicles. Already automated shuttle companies augment their vehicle sensing suite with infrastructure sensing at critical intersections, to insure safe passage. Research results point toward the need for a full, fault tolerant sensing framework design that utilizes all available data (CV, infrastructure, and trajectory data from fleets) for optimization across delay, energy, and, most critically, safety.

Approach

The research and insights in this section cover **five** primary research initiatives. In the first area, signal optimization routines are developed using modern reinforcement learning (RL) techniques to examine the trade-off between optimizing signal control to minimize delay versus minimization of energy. These results, first tabulated assuming 100% CV penetration, are then explored to understand the relationship with CV penetration rate, assessing the critical penetration threshold needed to begin to gain optimization benefits.

In the second area of research, modern stochastic control theory is applied to a grid of signal controllers (whereas the first areas explored RL based optimization) to examine the envelope of benefits of stochastic control under the assumption of full observability as provided by connected vehicles. The algorithm attempts to balance traffic and minimize delay across the grid network of controllers that determines north-south and east-west flow quality. Lastly, this effort began to examine robust methods to detect and compensate for CV faults, that is errors or omissions of data from the CV system.

The third area of research characterizes the traffic control benefits of spatial sensing that perceives, classifies and tracks object. The benefits in efficiency (either delay or energy) resulting from applying richer information to the controller are characterizes as the range of sensing necessary to provide the equivalent benefit of a 100% CV penetration scenario.

All intersection control is first and chiefly governed by safety, allowing for safe progression of conflicting traffic movements by sequencing through and servicing all legs of the intersection. Approximately 50% of all crashes occur at intersections. Quality signal timing has been shown not only to decrease delay, but also to increase safety through the reduction of crashes (Stevanovic et al. 2011; Retting et al. 2002; Sunkari 2004). Whereas most energy benefits are derived from more efficient vehicle flow, this fourth effort takes a holistic analysis at the energy consequences of improved safety. This includes energy consequences from avoiding fatal, injury, and property-damage-only (PDO) incidents. Such benefits result not only from avoidance of traffic congestion, but also more prominently from avoidance of loss of human capital and its associated economic productivity from either fatal or debilitating injuries, suggesting that energy consequences from enhanced signal control may be understated when only observing enhance flow or avoidance of stops.

In the fifth research initiative in support of the Smart Columbus initiative industry trip trajectory data sets were demonstrated as a scalable method to assess traffic signal performance and optimize pre-timed signal control on ten major corridors in Columbus. The research initiative leveraged this probe vehicle trajectory data to demonstrate scalable signal performance assessment and optimization at a scale that is not available otherwise without major investments in sensor and controller upgrades. This research demonstrates scalability of new data and methods to keep existing signal control (though pre-timed) in continuous and optimum maintenance.

Results

The major findings from those five research tasks are summarized below.

Task 1: Energy and Delay Minimization with Reinforcement Learning and Connected Vehicles

The RL algorithm was implemented under the assumption of 100% CV penetration with three different strategies or goals: (1) minimize only delay, (2) minimize only energy/fuel, and (3) minimize energy/fuel simultaneously with a penalty for number of stops at the signalized intersections.

Under control strategy one, delay could be minimized, reducing queue delay by 16.7%, but at the expense of 10.5% increase in energy. With control strategy two, it was possible to reduce energy consumption by 47% compared with the base case which were the existing signal settings in the Lankershim Boulevard corridor of Los Angeles, CA over which the NG-SIM data set was collected. However, the average travel time increases by 256% when only energy was minimized. To address the trade-off, a third strategy was implemented which ran an energy optimization but also introduced penalty values for stopping vehicles. Scenario number three was iterated over varying penalties for stopped vehicle, and the results show it is possible to have an 8.48% reduction in average travel time and 8.49% reduction in energy consumption compared with the base case.

Task 2: Stochastic and Distributed Signal Control with Connected and Automated Vehicles

In this research, stochastic distribution control theory was applied to a network of traffic signals to minimize traffic delays under the assumption of full observability as would be provided by 100% penetration of connected & automated vehicles (CAVs). CAVs increases the observability of the traffic flow conditions yet it does not change the random nature of traffic flow dynamics (i.e., a number and pattern of vehicles approaching

an intersection during any time interval remains random.) Automation allows the control system to provide communication to the vehicles on the optimal path and speed through the grid.

This research consisted of the following three aspects:

- a) Modeling for networked intersections in terms of signal timing and traffic state (such as the queue length of approaching vehicles and travel delays, etc.);
- b) Development of implementable real-time feedback signal control strategies to achieve smooth traffic flow at intersections;
- c) Fault tolerant intersectional control for 100% CAVs penetration;

In terms of modelling, a first order dynamic model was built for a typical single intersection, which shows the basic relationship between traffic state (travel delays or approaching queue length) and signal timing. This model provided stochastic distribution control model for the concerned networked intersections. Using these novel modelling tools together with step response testing, a multi-input and multi-output (MIMO) model was established that reflects the dynamics of networked intersections for the city of Bellevue, in Washington State as shown in the following Figure I.5.8.1. The project team also performed sensitivity analysis with the model where random disturbances for vehicle demand were applied to the model, i.e., random disturbance in the number of vehicles approaching the area.



Figure I.5.8.1 Vissim simulation model for the studied comparisons traffic network

Using a MIMO model, a simple feedback H-matrix control and stochastic linear optimal control (LQR) strategy was designed capable of achieving global control over the roadway grid network shown in Figure I.5.8.1, with individual signal control at each intersection. The purpose is to control the signal timing of these 35 intersections so that the travel delays at each intersection are minimized. The simulation results using Vissim are shown in Figure I.5.8.2 and Figure I.5.8.3. Figure I.5.8.2 plots the response of average vehicle delay (averaged across 70 delay measurements for each time interval) along with the progression of through the simulation time, with initial green time = 60s. The LQR control method (solid line) had better performance than that of the pretimed and simple linear controls. Figure I.5.8.3 presents the distribution of approach delays over the simulation period. For each control method, we flattened the 55×70 delay matrix and plotted a normalized histogram. As can be seen, the LQR control had fewer larger delays than pretimed and linear control. The obtained collaborative real-time feedback controls for signal timing of networked intersections in this example were shown to reduce the average travel delays by up to 40% compared to the existing pretimed controls.

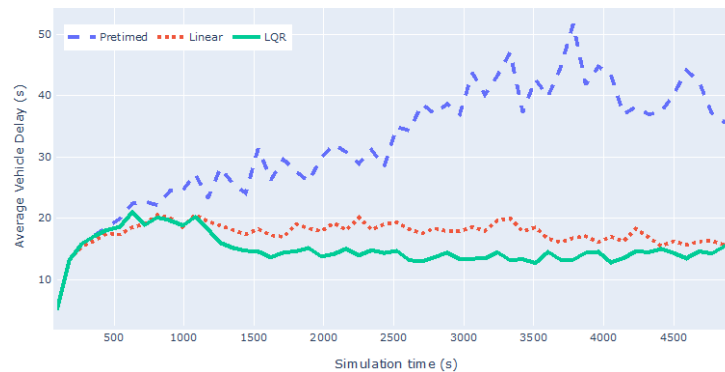


Figure I.5.8.2 Comparison of average vehicle delay during the simulation test period for three types of control: pre-time (base case), linear control and linear optimal control. Initial green = 60s,

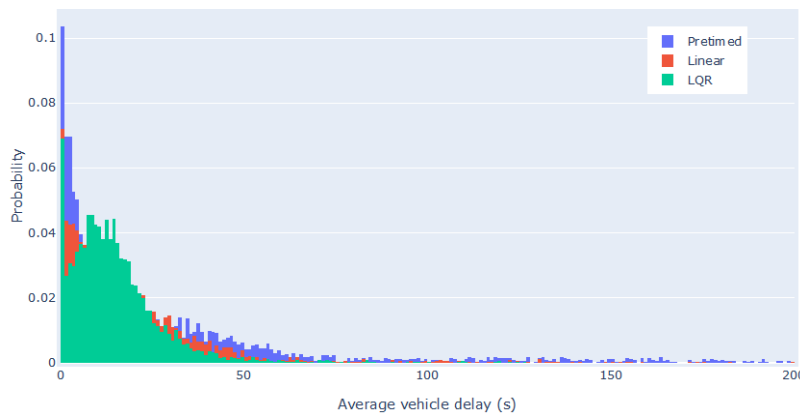


Figure I.5.8.3 Distribution of the delays over the simulation test period for pre-timed (base case), linear control and linear optimal control. Initial green = 60s,

Task 3: Infrastructure Spatial Sensing at Intersections

Algorithms for advanced signal control based on CV data are selected as the basis for research implementation. The assumption is made that 100% of traffic can be detected by the sensor, but only within a defined sensing range. Once within this range, the position and speed of any vehicle, pedestrian or other moving object are available for signal optimization. The goal of the research is to identify the impact of this sensing range on the control performance.

Work began with a literature review to identify potential algorithms for testing revealed that numerous algorithms to optimize signals based on CV data have been published. Two of these algorithms were selected for implementation in a simulation environment with infrastructure spatial sensing (ISS), representing two different approaches to signal control. The first of these is a method proposed by a research team at University of Arizona, based on the RHODES adaptive control system, but augmented for CV data. Similar to many adaptive signal control methods, this algorithm identifies a schedule for green times to be provided within a rolling horizon, using an objective of minimizing delay. The second algorithm takes a fundamentally different approach, which incorporates vehicle position data into a secondary, or virtual, sensor actuation decision scheme in a more traditional corridor progression signal timing framework. The data is incorporated into a continuous decision of whether or not to extend the major street green time. This research replaced its table of predicted arrivals (based on virtual detection derived from CV data) with real-time arrivals from ISS.

The follow-on component of both approaches was to vary the sensing range from which the traffic information is made available in the algorithms and determine the impact on the performance. Results obtained from single-intersection test network, are presented in Figure I.5.8.4. Figure I.5.8.4(a) shows results for Algorithm 1 (rolling-horizon) and Figure I.5.8.4(b) shows results for Algorithm 2 (continuous-decision). Each chart shows a series of travel times for movements along the major through corridor (not from side streets), for different simulation runs where the sensing range was adjusted. These preliminary charts show a decrease in travel time as the sensing range is increases, as anticipated. The impact of sensor range is more pronounced in the case of Algorithm 2. The results from both algorithms converge beyond a sensing range of 20 seconds from the intersection. Note that in these initial studies, sensing range was depicted as a time horizon from arrival at the intersection due to expediency of constructing the simulation with time based data. A corollary of these results is that CV performance can be achieved with infrastructure-based sensing if the sensors can detect vehicles 20 seconds or greater from the signal (in this case, 20 seconds corresponds to a distance of approximately 250 m). Algorithm 1 exhibits only a slight difference in performance across the range of values considered.

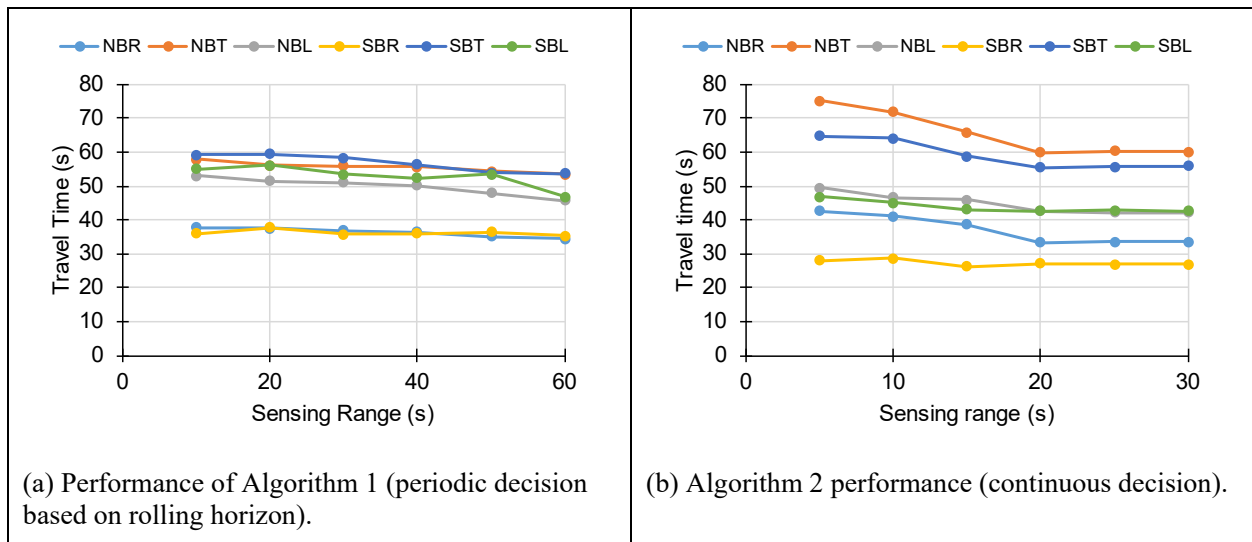


Figure I.5.8.4 Algorithm performance as a function of sensing range.

Task 4: Energy Equivalence of Safety – Intersection applications

The US Pillar extended the concept of exploring the potential mobility and energy benefits of ISS at intersections to improve traffic flow to also consider the mobility and energy benefits of reduced crashes. The safety criticality of intersections to deconflict turning movements, safely allowing for vehicles (and pedestrians, bicycles, and scooters) to traverse the intersection is paramount. The energy equivalence of safety suggests, and underscores, that avoidance of crashes is vital in intersection control. This research showed that increasing safety on roadways can fundamentally decreased energy consumption equivalent to 5.6% of the total U.S. energy consumption, and systems that could reduce the crash frequency could have an order of magnitude (or more) impact on energy productivity than energy efficiency related to reduced stops or smoother traffic flow.

Table I.5.8.1 Energy Equivalence of Safety at All Roads and Intersections**All Roads (year 2010)**

	Fatal	Injury	PDO
Number of crashes on all roads*	30,296	2,969,963	10,565,514
Direct Energy Cost (GGE) per crash	10,987	1,710	382
HC Energy Cost (GGE) per crash	76,475	694	6
WTP Energy Cost (GGE) per crash	484,357	6,536	N/A
Total Energy Cost (GGE) per crash	571,819	8,939	388
Intersections (year 2010)			
# of person-vehicle crashes*	8,682	4,829,008	10,127,014
# of crashes equivalence	7,971	1,686,345	5,780,930
% of crashes at intersections	26%	57%	55%

*: data directly read from “The Economic and societal impact of motor vehicle crashes, 2010” (Blincoe et al. 2015)

The research effort proposed a framework for estimating the GDP-weighted energy equivalence of safety at intersections based on previous extensive studies of the economic value of crash impacts. Based on this holistic analysis, the energy consequences of crashes are estimated to be equivalent to roughly 5.6% of the total U.S. energy consumption. Although a first order estimate, this research suggests that the energy savings from improved safety in terms of human productivity and human capital at a minimum rival that obtained from improved traffic flow and may be an order of magnitude greater. For example, the congestion cost accounts for 12 percent of total economic crash costs (Blincoe et al. 2015). In terms of energy consumption of equivalence, it accounts for 0.06% of total GGE of a fatal crash.

Task 5: Harnessing Vehicle Trajectory Data for Pre-timed Signal Optimization

This research leveraged a probe vehicle trajectory data set to demonstrate pre-timed signal performance assessment and optimization at a scale that is not available without major investments in traditional roadway sensors and controller upgrades. The dominant majority of signal control throughout the United States remains pre-timed. Even most actuated control is contingent on a high-quality fixed timing plan that is adjusted to account for perturbances in expected traffic flow. This research demonstrates the use of big data, in the form of trajectory data sets (measured in the 100’s of GB to terabyte scale) combined with machine learning to assess the quality of existing signal control on ten major corridors in Columbus, Ohio, using a method which can scale to a state or national scale.

Recognizing the tie between safety and signal timing quality, researchers assessed quality of signal timing (measured in percent arrivals on green) with respect to safety (measured in number of accidents). It has long been acknowledged that good signal timing enhanced safety at intersections, but the ability to correlate safety (as in the number of crashes) with the quality of signal timing has been limited due primarily due to the inefficiency of assessing signal timing performance with any level of significant detail. In an initial attempt to correlate the two, data from the Columbus analysis was correlated to recorded traffic crashes during 2018, indexing the number of crashes to the arrival on green (AOG) statistic. The higher the AOG, the better timed an intersection or corridor is. This initial chart from intersections studies in Columbus is shown in Figure I.5.8.5. Although this chart has not been normalized and calibrated, the overwhelming evidence as depicted by

a negative slope with respect to AOG provides quantitative support of the link between quality signal timing and safety. This combined with previous work, directly linking safety (with respect to number and type of crashes) with energy, begins to bring a holistic analysis research and development framework to the topic of traffic signal control.

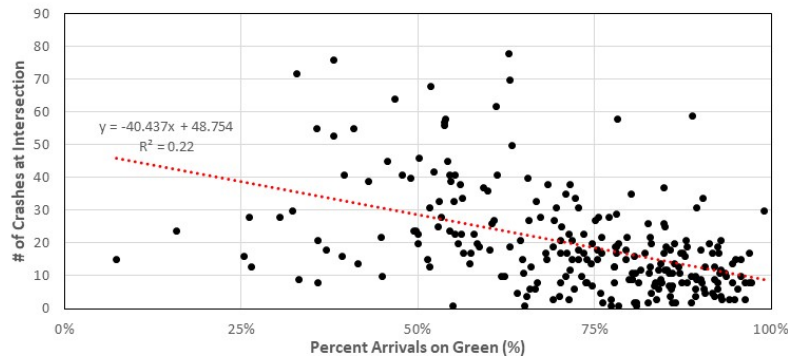


Figure I.5.8.5 Safety comparison between signal performance and crashes at an intersection

Conclusions

The group of signal control projects in the Urban Science portfolio demonstrated potential performance enhancement through use of more detailed spatial data of vehicles enabled initially through connected vehicle technology (CV), and then through use of infrastructure sensing. Full knowledge of each vehicle's location and trajectory communicated to the traffic controller allows for increased optimization of both delay, stops and energy, either on an arterial corridor or a grid based street system. Follow on work demonstrated that such benefits could also be achieved with spatial sensors, that is placement of sensors such as LIDAR, radar, and AI enabled video processing such that the location and trajectory of each vehicle is known to the controller, similar to a CV scenario. Work conducted in conjunction with advanced trajectory data available within Columbus, Ohio demonstrated that high-fidelity traffic signal performance measures could be extracted from currently available industry data, such that performance could be continuously assessed, leading to better maintenance, and less fuel consumption. Furthermore, the accident history was correlated to arrival on green (AOG) showing a consistent relationship between improved AOG and improved safety. Lastly, the tie between energy productivity and crashes, using a framework derived from economic impacts of crashes, revealed that the energy consequences associated from the loss of human capital and productivity are significant and may dwarf those related to simply more efficient signal operation. In total, the combined work points to the need for a full, fault tolerant sensing framework design that utilizes all available data (CV, infrastructure, and trajectory data from fleets) for optimization across delay, energy, and, most critically, safety.

Key Publications

1. Zhu, Lei, Young, Stanley E, and Day, Christopher M. Exploring First-Order Approximation of Energy Equivalence of Safety at Intersections: Preprint. United States: N. p., 2019. Web.

References

1. Stevanovic, Aleksandar, Jelka Stevanovic, and Cameron Kergaye. "Optimizing signal timings to improve safety of signalized arterials," In 3rd International Conference on Road Safety and Simulation, Indianapolis, USA, vol. 14. 2011.
2. Sunkari, Srinivasa, "The benefits of retiming traffic signals," ITE journal, 2004, 26-29.
3. Retting, R. A., Chapline, J. F., & Williams, A. F. (2002). "Changes in crash risk following re-timing of traffic signal change intervals," Accident Analysis & Prevention, 34(2), 215-220.

4. Blincoe, L. J., Miller, T. R., Zaloshnja, E., & Lawrence, B. A. (2015, May). The economic and societal impact of motor vehicle crashes, 2010. (Revised) (Report No. DOT HS 812 013). Washington, DC: National Highway Traffic Safety Administration.

I.6 Workflow

I.6.1 General Microsimulation to Meso-simulation (LBNL, ANL)

Xiao-Yun Lu, Principal Investigator

Building 190
Lawrence Berkeley National Laboratory (LBNL)
1 Cyclotron Road, Berkeley, CA
E-mail: xiaoyunlu@lbl.gov

Joshua Auld, Principal Investigator

Argonne National Laboratory
9700 S Cass Avenue
Lemont, IL 60439
Email: jauld@anl.gov

Felipe Augusto de Souza, Principal Investigator

Argonne National Laboratory
Email: fdesouza@anl.gov

Erin Boyd, DOE Technology Manager

U.S. Department of Energy
E-mail: erin.boyd@ee.doe.gov

Start Date: October 1, 2018	End Date: September 30, 2019	
Project Funding (FY19): \$400,000	DOE share: \$400,000	Non-DOE share: \$0

Project Introduction

This project contains two parts of work: (1) Micro-to-Meso: to build the link between micro-simulation and meso-simulation of mixed traffic with manually driven and CAVs (Connected Automated Vehicles); (2) TNC Simulation: to preliminarily develop microscopic traffic simulation with TNC vehicles and evaluate their impact on other traffic in pick-up and drop-off. In each section of this report, those two topics will be reported separately.

Micro-to-Meso

Meso and macroscopic traffic simulation are usually used for planning purposes for a regional or metropolitan area. Such tools could provide some reasonable references in the past because the transportation modes did not have significant changes. For example, almost all are manually driven vehicles in road networks including freeway and arterials. Although those road vehicles could have different powertrain and drivetrain, their performance is still dominated by the driver behavior which is the main deterministic factor for meso and macroscopic traffic pattern. Therefore, the model for meso-macro simulation was to capture the aggregated traffic characteristics dominated by the demands and driver behaviors in those levels. Those simulation models can be calibrated with field collected traffic data to match the Fundamental Diagram(FD) of the two, which describes the traffic pattern in flow-density or speed-density relationships.

In the mesoscopic simulation, vehicles are collected/aggregated into traffic cells and streams and their movements are based upon known capacities and speed-density functions which can be defined by a dynamical model such as Cell-Transmission-Model (CTM) or the second order MEATNET Model, or Newell's simplified kinematic wave model. A meso and macroscopic simulation model is usually calibrated with Fundamental Diagram at different locations where field traffic detector data are available. Examples of meso and macroscopic traffic simulation include POLARIS (ANL), Aurora (Berkeley), and several others.

Directly using meso or macroscopic simulation to mimic mixed traffic with manually driven and automatic vehicles is impossible since there is no field test data that could produce sensible Fundamental Diagram for different market penetration levels of Connected Automated Vehicles (CAVs). However, it is possible to generate reasonable microscopic simulation with appropriate dynamic relationship between manually driven and CAVs with field test data which can be collected with CAVs driving with public traffic in small scales. Therefore, a reasonable way to calibrate meso-macro simulation with mixed traffic is to use FD generated from such calibrated microscopic simulation models.

For microscopic simulation, the traffic pattern is determined by underneath car-following models. For most commercially available traffic simulation packages, Newell and Gipps models are usually used, which determine the driver behaviors. Once the demand is determined, the traffic pattern can be calibrated using field collected meso or macroscopic network traffic data.

However, to simulate mixed traffic of manually driven vehicles and CAVs, such calibration is not possible since there is no such traffic data with adequate CAVs which can have persistent and noticeable traffic impact. For this reason, one possible way for modeling the mixed traffic with CAVs is to start from the microscopic level by modeling the dynamic intersection between CAV and manually driven vehicles (i.e., mixed car-following models) based on some limited field experimental data. Those dynamical interactions are essential for developing a reasonable microscopic network traffic with both manually and automatically driven vehicle. Then the output can be used to generate FDs which models the traffic pattern in an aggregated level. Those FDs can then be applied to the meso-simulation for modeling and model calibration.

The network traffic pattern is not only affected by static/dynamic demands and driver behavior anymore. With the progress of Active Traffic Management (ATM), the overall traffic pattern is also significantly affected by ATM measures. Those measures include:

- For freeway: Ramp Metering (RM), Coordinated RM (CRM), Lane Management (LM), Coordinated or semi-coordinated merge, routing, etc.;
- For arterial/surface street: Active Traffic Signal Control (ATSC), such as Traffic Responsive Signal Control, Coordinated Traffic Signal Control for arterial corridors
- For network including both freeway and arterials: ATM for freeway, ATSC for arterials, and the coordination of the two control systems.

The key methodology for understanding the impact of a wide variety of technologies on traffic flow at a system-wide perspective is through the generalization of microscopic traffic simulation to mesoscopic-simulation studies on network performance; such generalization not only include the network scope expansion, but also include multi-modes inter-operability and a variety of detailed scenarios.

TNC Simulation

With rapidly increasing shared transportation system (e.g., Uber, Lyft), the performance of the road network may change. Traffic flow may easily be disrupted by vehicles of transportation network company (TNC), as they perform pick-ups and drop-offs of passengers in the middle of roadway corridors. Some arterial roads may contain some pockets or temporary parking spaces for these actions. TNC drivers usually maneuver into the parking slots moving backward from downstream or moving forward from upstream by changing the lane. However, this parking maneuver makes the TNC vehicles occupy the mainline that leads to blockage of traffic stream until the completion of parking. They may also interrupt the traffic stream by changing lane to the mainline from the parking slots. Therefore, a study to investigate the effect of TNC vehicles' parking maneuvers in arterial corridors on traffic is necessary. In this research, the parking maneuver algorithm of TNC vehicles is developed and implemented using Aimsun.

Objectives

Micro-to-Meso

The objective is to develop Parameterized Fundamental Diagram (PFD) calibrated from simulation data of traffic with proper vehicle following behaviors in mixed traffic (with both manually driven vehicles and CAVs). The vehicle following behavior should capture the dynamic interaction between manually driven vehicles and CAVs in traffic. We intend to model the PFD at different locations of a freeway corridor with respect to the market penetration of Cooperative Adaptive Cruise Control (CACC) Vehicles. The CACC vehicle car-following models are calibrated with field test data in public traffic. We tried our best to model the dynamic interaction of CACC vehicles and manually driven vehicles.

TNC Simulation

The first objective of this research is to develop the driving model to depict the parking maneuvers of TNC vehicles on arterial roads. This model targets to illustrate the microscopic behavior of forward and parallel (i.e., backward) parking maneuvers. Regarding the parking maneuvers, there have been initiative research investigations on trajectory planning of automatic moving objects and vehicles under a predefined parking condition, where the parking spaces are orientated parallel, vertical, or diagonal with respect to the driving direction [1]-[8].

The second objective of this research is to implement the proposed model to simulate the traffic flow with TNC vehicles' pick-ups and drop-offs. This experiment attempts to analyze the traffic performance in terms of flow, speed, density, total delay, and total travel time, for a real network of San Pablo in California with increasing market penetration of TNCs from 0% to 5%.

Approach

Micro-to-Meso

We have tried several FD models and finally decided to use the Underwood model to add new parameters with respect to the CACC market penetration parameters. The model represents the functional relationship between distance mean speed and density.

We intended to model the PFD at some representative locations of a freeway corridor in Aimsun. The traffic network in SR-99 NB from Elk Grove to interchange with SR 50, which is about 15 miles long with 16 onramp and 11 off-ramps. The baseline traffic calibrated was for in AM peak hours. The baseline traffic (without CACC vehicles) data was collected from PeMS (Performance Measurement System). This corridor is currently operating Coordinated Ramp Metering since 2017. After the baseline traffic model calibration, we have added the CACC models.

We have calibrated the PFD as several representative locations including: major bottleneck such as on-ramp merging section, weaving section (freeway split), off-ramp, etc. Obviously, those locations cannot exhaust all traffic characteristics of a freeway corridor. We do not claim that the calibrated PFD will be able to transfer to other freeway corridors, which is yet to be verified.

The traffic flow simulation model was adapted in POLARIS by the ANL team in order to replicate the generated curves. Since the traffic flow model in POLARIS assumes a triangular fundamental diagram (density-flow relationship), the model and parameter were implemented in POLARIS with a triangular fundamental diagram. The relative impacts of the penetration rate of CACC on capacity remained the same.

TNC Simulation

In this section, the methodology to simulate the impact of TNC vehicles on the arterial road network is presented. First, the parking maneuver model is proposed. Second, the programming limitation with Aimsun functionalities in implementing the proposed model is explained and their solutions are described. Third, the model is validated for the two-mile long real-network of San Pablo Avenue, California. The detailed description of the methodology is given as below.

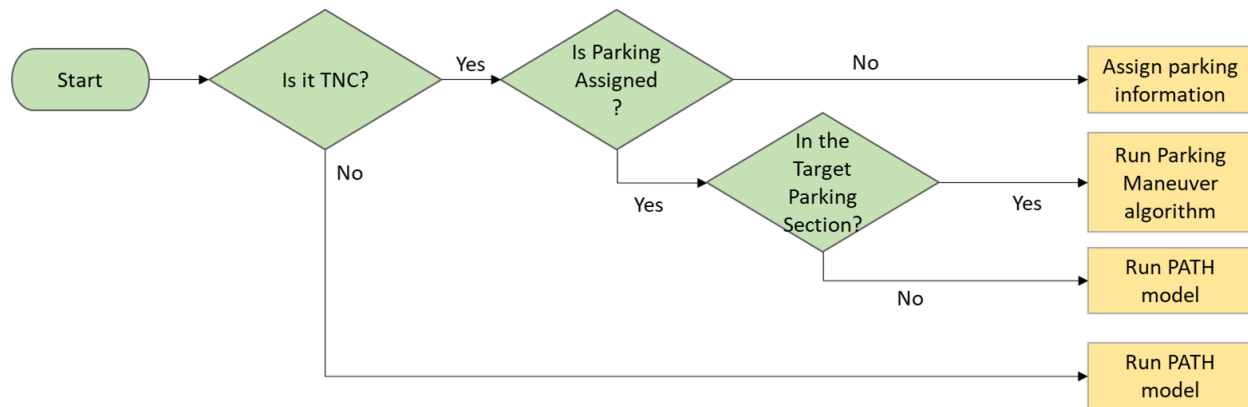


Figure I.6.1.1 The Framework for the Model of TNC Parking Maneuver with PATH Model

First, the parking maneuver model of TNC vehicles is proposed as follows. Refer to Figure I.6.1.1. Using the PATH model as the baseline driving model, the proposed model describes the additional parking maneuver of the TNC vehicles. The algorithm flow shown in the figure is run for every vehicle and every time step of the simulation. The framework first checks if the subject vehicle's type for the TNC vehicle or non-TNC vehicle. If it is not a TNC vehicle, that the PATH model is run. If it is a TNC vehicle, the framework checks if there is a parking objective for this subject vehicle. The parking assignment determines the parking information, such as parking location, parking duration, and parking method (parallel or forward parking). If the TNC vehicle with parking information is in the target parking section, i.e., the road section of pick-ups and drop-offs, the parking maneuver algorithm is executed. The parking maneuver algorithm is explained in the following paragraph.

The parking maneuver algorithm has an upper layer that describes the stages of parking execution, and a lower layer that describes the detailed car-following model for the parking stages. Refer to Figure I.6.1.2. If a TNC vehicle has not completed its parking, the vehicle approaches to its target parking location. While approaching, the vehicle evaluates if it needs to change lane to be at the right-most lane. Also, it observes if a target parking slot is occupied or not. If the vehicle needs to change lane to be in the right-most lane, it follows the lane change model similar to the PATH model. It prepares to find an acceptable gap in the target lane in Before-Lane-Change Car Following (BCF) mode. With an acceptable gap, it changes lane (LC). Once the TNC vehicle has arrived around the target parking location, it follows into the execution stage. If the parking slot is occupied, the vehicle waits in the Waiting Car Following (WCF) mode. If it not occupied, the TNC vehicle executes its parking, either in Forward-Parking Car Following (FPCF) mode or in Parallel-Parking Car Following (PPCF) mode.

During the parking duration, where the TNC vehicle presumably lets the passengers in and out, the vehicle is simulated to be stopped at a location. This mode is not described in the figure. If the vehicle checks that its parking is complete, the vehicle leaves the parking location to join the traffic stream. This allows vehicle to be in the exit stage, where it may or may not execute a lane change to continue driving on the road.

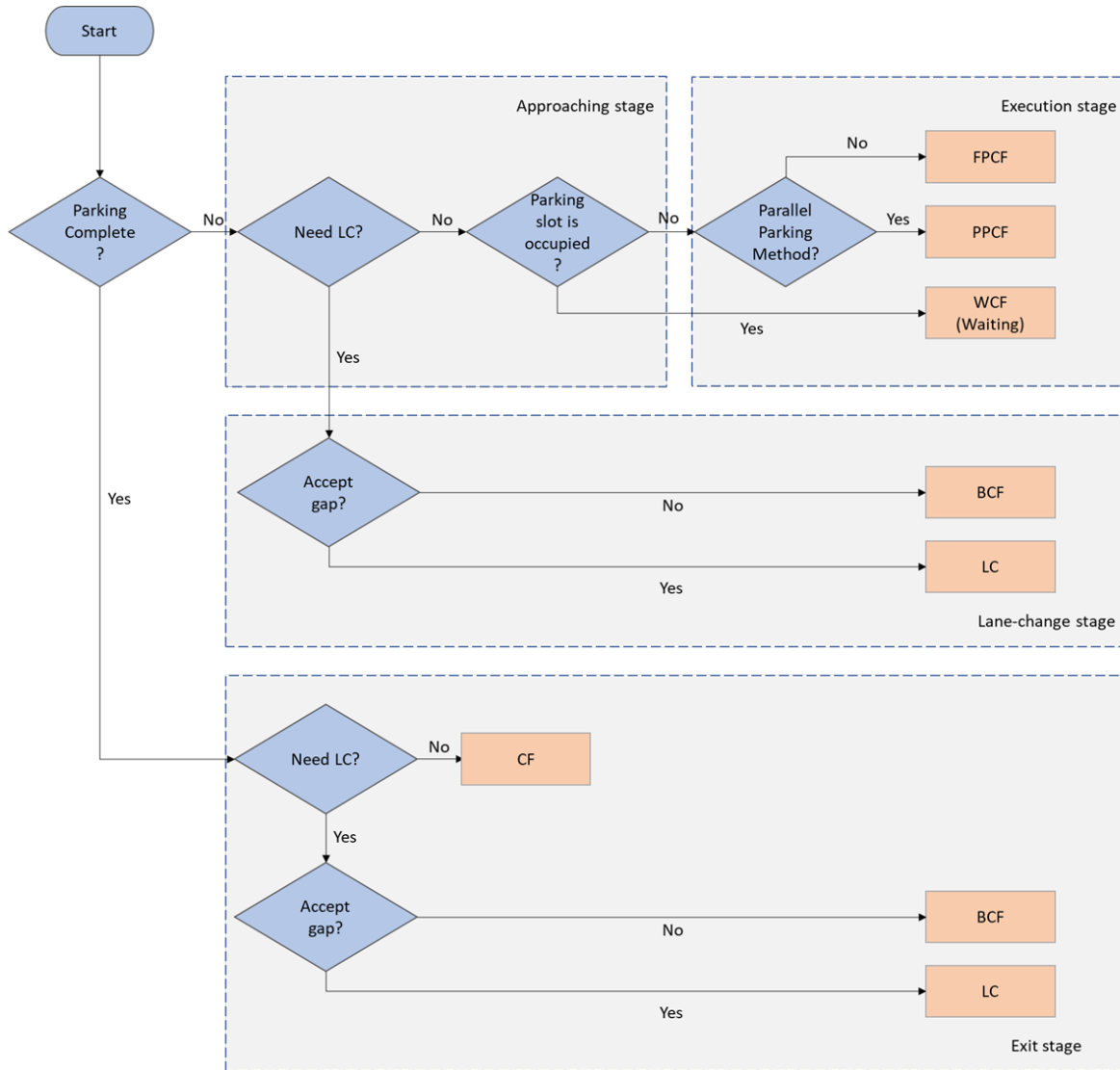


Figure I.6.1.2 Parking Maneuver Algorithm

Second, the parking maneuver model is implemented using the microscopic traffic simulation program, Aimsun. The implementation is complemented by MicroSDK, which is an external library developed to describe detailed individual driving behavior. Note that there were some software restrictions of the Aimsun program. For instance, Aimsun does not support lateral movements within a lane, which is required to model and illustrate the vehicle’s position in the gradual parking maneuver into another lane. Also, Aimsun does not allow backward movement within the program. Therefore, the coordinates of parking vehicles in the backward moving stage were forcefully re-located every simulation time step, as well as the lane assignment into the parking space. After successfully moving to the target parking slot, the vehicle stops moving for a duration of time to complete the pick-up and drop-off operation. Finally, they join to the mainline flow by another lane change.

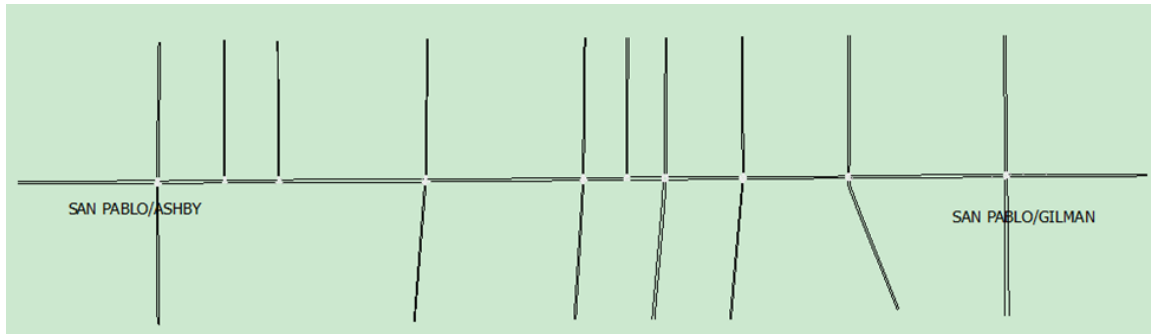


Figure I.6.1.3 San Pablo Avenue Network for simulation

Third, the model is applied to experiment the traffic performance with a two-mile long stretch of San Pablo Avenue in California, from Ashby Avenue to Gilman Street as shown in Figure I.6.1.3. This study uses the real traffic demand of the San Pablo network that was collected by the City of Berkeley during May 2015. The turning movement was collected as hourly flow at each intersection, as well as the signal timing plan at each intersection. The traffic demand describes a typical weekday during the evening peak time with traffic congestion. The simulation experiments addressed various scenarios, such as market penetration of TNC vehicles from 0% to 5% in increments of 1% and parking duration of TNC vehicles from 30 to 120 seconds. The traffic performance is evaluated in terms of the total time spent, harmonic mean speed for sections of pickups and drop-offs, and number of stops

Results

Micro-to-Meso

Parameterized FD Modeling

1.1 Original Underwood Model

Underwood model is a function relationship between distance mean density and speed. The following model was originally proposed by Underwood [3]:

$$v(\rho) = \exp(w_1 + w_3\rho) \quad (1)$$

Where

ρ – density: number of vehicles per mile

v – distance mean speed in miles per hour

(w_1, w_3) – are unit-less parameters to be determined/calibrated by data

1.2 Parameterized Underwood Model

To model the market penetration levels of CAVs with the Underwood model above, a market penetration parameter is introduced as follows in the speed density relationship:

2. Generalized Underwood Model (Model 1):

$$v(\rho) = \exp(w_1 + w_2\kappa + (w_3 + w_4\kappa)\rho) \quad (2)$$

(w_1, w_2, w_3, w_4) – parameters to be determined/calibrated by data

$0 \leq \kappa \leq 1$ – given market penetration parameter

The calibrated coefficients of (2) are listed in Table I.6.1.1 and Table I.6.1.2 with different demands.

2.1 Parameterized Flow-Density Relationship Based on Underwood Model

Model 2:

One-limb flow-density relationship is obtained from (2) with the flow-density-speed relationship $q = \rho v$

$$q(\rho) = \rho \exp(w_1 + w_3 \kappa + (w_2 + w_4 \kappa) \rho)$$

q – number of vehicles per-lane per hour

Model 3:

Considering that, if the density is lower than the critical density, the traffic will generally be in free-flow. In this case, the flow is linearly proportional to the density with constant free-flow speed V_f which is usually close to the roadside posted speed limit in practice.

The two-limb flow-density relationship based on the generalized Underwood model can be expressed as:

$$1. \quad q(\rho) = \begin{cases} V_f \rho, & \rho(\kappa) \leq \rho_c(\kappa) \\ \rho \exp(w_1 + w_3 \kappa + (w_2 + w_4 \kappa) \rho), & \rho(\kappa) > \rho_c(\kappa) \end{cases} \quad (3)$$

q – number of vehicles per-lane per hour

$0 \leq \kappa \leq 1$ – given CACC market penetration parameter in percentage

$\rho_c(\kappa)$ – critical density

V_f – Free-flow speed (depending on freeway speed limit, but independent from κ)

(w_1, w_2, w_3, w_4) – parameters to be determined/calibrated by data

It is noted that both $\rho(\kappa), \rho_c(\kappa)$ are market penetration dependent. For a given market penetration level κ , $\rho_c(\kappa)$ is determined in the following way:

From aggregated (2.5 [min]) simulation data, we can determine the maximum flow $q_{\max}(\kappa)$. The density corresponding to the $q_{\max}(\kappa)$ is the critical density

The calibrated coefficients for the right limb are listed in Table I.6.1.3. Note that there is no unknown parameter in the left limb in equation (3).

2.2 Parameterized Flow-Density Relationship Based on 3rd Order Polynomial Model

Model 4: 1-limb polynomial model

$$q(\rho) = w_1 + \kappa w_2 + (w_3 + \kappa w_4) \rho + (w_5 + \kappa w_6) \rho^2 + (w_7 + \kappa w_8) \rho^3$$

where $(w_1, w_2, w_3, w_4, w_5, w_6, w_7, w_8)$ – are parameters to be determined/calibrated by simulation data for mixed traffic.

Similarly, we can have 2-limb flow-density relationship (PFD) as argued above:

Downtown Sacramento



Figure I.6.1.4 Microscopic traffic simulation in Aimsun. Left: the scope of the freeway corridor with location of detector stations from PeMS; Right: the Aimsun network model

Model 5: 2-limb polynomial model

$$q(\rho) = \begin{cases} V_f \rho, & \rho(\kappa) \leq \rho_c(\kappa) \\ w_1 + \kappa w_2 + (w_3 + \kappa w_4) \rho + (w_5 + \kappa w_6) \rho^2 + (w_7 + \kappa w_8) \rho^3, & \rho(\kappa) > \rho_c(\kappa) \end{cases}$$

where $(w_1, w_2, w_3, w_4, w_5, w_6, w_7, w_8)$ – are parameters to be determined/calibrated by simulation data for mixed traffic.

3. Model Calibration

This section discusses how the model parameters for those PFDs are determined with simulated data of mixed traffic with manually driven vehicles and CAVs.

3.1 Traffic Network Model

The microscopic traffic simulation in Aimsun is a well-calibrated freeway corridor SR-99 NB from Elk Grove to interchange with SR-50 as shown in the map with detector locations from PeMS.

- 13-mile urban corridor coded in Aimsun
- 15 onramps and 11 off-ramps
- 8-hour traffic demand from PeMS dataset
- High traffic volume in AM Peak hours

- Coordinated Ramp Metering in operation [1]

The basic car following models used were from [4] implemented with MicroSDK in Aimsun, which were initially calibrated with NGSIM data. The model has been made some revision and refinement and calibrated against field collected data [1]. The CAV models were established with field test of Cooperative Adaptive Cruise Control vehicles in public traffic [2] to capture the dynamic interactions between manually driven vehicles and the ACC and CACC vehicles. The microscopic simulation model was then further calibrated and revised as reported in [2]. It is noted that the platoon forming is assumed to be randomly. Therefore, a CACC capable vehicle could be driven in ACC (Adaptive Cruise Control) mode. The leader vehicle in a CACC string is also assumed to drive in ACC mode. The lane change behavior was still the same as the baseline traffic as modeled and calibrated in [1]. With several rounds of model calibration and revision, it is believed that the model could reasonably simulate the mixed traffic.

3.2 Traffic Demand Used in Simulation

The initial model calibration mentioned before for baseline traffic used the field collected data only. To conduct the sensitivity analysis of the mixed traffic with CAVs, different demands (from all on-ramps and the most upstream mainline) with increment of 5%, were used for simulation of mixed traffic with respect to different market penetration levels as follows:

- 5% ~20% more demands: CACC market penetration levels range: 0~100%
- 25% ~30% more demands: CACC market penetration levels range: 60~100%
- 35% ~40% more demands: CACC market penetration levels range: 80~100%.

It is noted that the valid density range is: 0 ~ 140 vehicle per-lane-per-mile

The reason for adopting the demand increase strategy is that higher demand increases over the baseline traffic could only be handled by higher market penetration levels of CAVs.

3.3 Simulation Data for Model Calibration/Fitting

The default simulation time step was set to 0.1 [s]. The data saving time interval is 30 [s] with internal Aimsun aggregation. The data has been further aggregated to 2.5 [minutes] for model calibration/fitting. It is clear that the polynomial model is linear in unknown coefficients with given CACC market penetration level. Although, the 1-limb and 2-limb PFD models based on Underwood model are nonlinear in unknown parameters, applying $\ln(\cdot)$ function on both sides, they will become linear. Therefore, linear Least Square Methods in *Matlab* was used for the determining the unknown parameters in the models, which is straightforward.

The following approach was used for the critical density selection for the 2-limb generalized Underwood model and the polynomial model:

- Fixed at 28 vehicles per mile
- Changing from 28 to 35 vehicle per mile as CAV market penetration level increases.

It seems that the second approach could bring better data fitting, but it is not significant. It is believed that this may need further investigation later.

3.4 Traffic Data Location Selections

It is well known that freeway traffic pattern depends many factors including: demand, road geometry (number of lanes, on-ramp, off-ramp locations, lane drop etc.), and driver behavior etc. For the initial modeling, the above flow-density models were calibrated at nine selected locations which has different characteristics

including: on-ramp, off-ramp, lane drop, freeway split, bottleneck, weaving section etc. which have been listed in the coefficient tables to be presented.

4. Calibration Results

The following Table I.6.1.1 – Table I.6.1.3 shows the coefficients of the PFDs at nine locations of the freeway corridor for 20% demand over the baseline traffic. The demand was from field observed baseline traffic data. The critical density is fixed as $\rho_c(\kappa) = 28$.

Table I.6.1.1 $v - \rho$ PFD Coefficients Determined with Baseline Traffic Demand for All Market Penetration Levels

Section ID	w1	w2	w3	w4	Feature	Onramp, offramp name & ID
16573	4.295862	0.042278	-0.016384	0.001539	mainline upstream	up Florin WB;
16711	4.295051	0.027397	-0.016998	0.002928	47th St, Weaving section & lane reduction	EB onramp ID 16785 & offramp ID 16565
16823	4.285251	0.002087	-0.016557	0.002026	offramp	12th Ave; 16833
16873	4.286035	0.024981	-0.016824	0.002469	freeway split	SR99 and SR50 offramp split
17266	4.286425	0.024113	-0.016896	0.002661	upstream of Calvin	bottleneck
26655	4.280416	0.019984	-0.016727	0.002583	mainline section at onramp	Calvin Onramp
26664	4.293887	0.04412	-0.016536	0.001996	47th St, WB onramp	WB onramp ID 16731
26684	4.285251	0.002087	-0.016557	0.002026	Node	Florin Onramp WB; 16571
26744	4.275638	-0.101094	-0.016639	0.00347	onramp	12th Ave; 16833

The following Table I.6.1.2 shows the coefficients of the PFDs at nine locations of the freeway corridor, the same as those in Table I.6.1.1. The demand is 20% higher than field observed baseline traffic demand.

Table I.6.1.2 $v - \rho$ PFD Coefficients Calibrated with Simulation Data with 20% Higher Demand over the Baseline T

Section ID	w1	w2	w3	w4	Feature	Onramp, offramp name & ID
16573	4.33599	-0.014158	-0.017496	0.004289	mainline upstream	up Florin WB;
16711	4.329973	0.004325	-0.01799	0.00499	47th St, Weaving section & lane reduction	EB onramp ID 16785 & offramp ID 16565
16823	4.3172	-0.07221	-0.017376	0.004634	offramp	12th Ave; 16833
16873	4.325519	-0.02296	-0.017911	0.005108	freeway split	SR99 and SR50 offramp split
17266	4.269999	0.056901	-0.016484	0.003113	upstream of Calvin	
26655	4.282642	0.023259	-0.016814	0.003752	mainline section at onramp	Calvin Onramp
26664	4.331372	0.010379	-0.017567	0.004296	47th St, WB onramp	WB onramp ID 16731
26684	4.3172	-0.07221	-0.017376	0.004634	Node	Florin Onramp WB; 16571
26744	4.294444	-0.176749	-0.016954	0.005375	onramp	12th Ave; 16833



Table I.6.1.3 $q - \rho$ PFD Coefficients for the Right Limb Calibrated with Simulation Data with 20% Higher Demand over the Baseline Traffic

Section ID	w1	w2	w3	w4	Feature	Onramp, offramp name & ID
16573	4.180355	0.016506	-0.012999	0.00164	mainline upstream	up Florin WB;
16711	4.171758	0.021918	-0.013853	0.002453	47th St, Weaving section & lane reduction	EB onramp ID 16785 & offramp ID 16565
16823	4.220269	-0.10614	-0.01334	0.003026	offramp	12th Ave; 16833
16873	4.244488	-0.052227	-0.014654	0.003312	freeway split	SR99 and SR50 offramp split
17266	4.337745	-0.154052	-0.016517	0.005369	upstream of Calvin	
26655	4.312119"	-0.128239	-0.01599	0.004864	mainline section at onramp	Calvin Onramp
26664	4.168044	0.018276	-0.013431	0.002135	47th St, WB onramp	WB onramp ID 16731
26684	4.220269	-0.10614	-0.01334	0.003026	Node	Florin Onramp WB; 16571
26744	4.227543	-0.135376	-0.013314	0.003328	onramp	12 th Ave; 16833

To assess the impacts of CACC on the regional level, we tested two cases for the Chicago Metropolitan Area with results based on the Workflow Scenarios. Figure I.6.1.5 depicts the network loading curve (number of vehicles in the network) for scenarios with 0% and 100% penetration rates (PR). Observe the two curves almost overlap for most of the day besides the morning peaks. This is expected as the freeway operates under capacity. In the peaks, the scenario with 100% penetration rate outperforms the baseline case. As in POLARIS vehicles are responding to prevailing travel times, a higher portion of the traffic is moved to the freeway offsetting part of the difference in capacity. Throughout the whole day, the difference in total time spent was 4.5%.

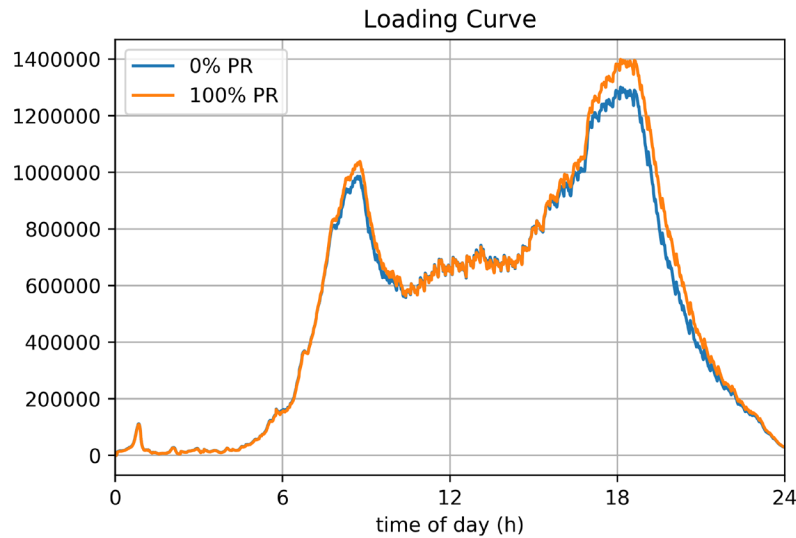


Figure I.6.1.5 Time-dependent network density

The speed profile for these two scenarios are depicted in Figure I.6.1.6 which the pattern repeats. Throughout most of the time, the average speed in the network almost overlaps, except at the peaks. The higher penetration

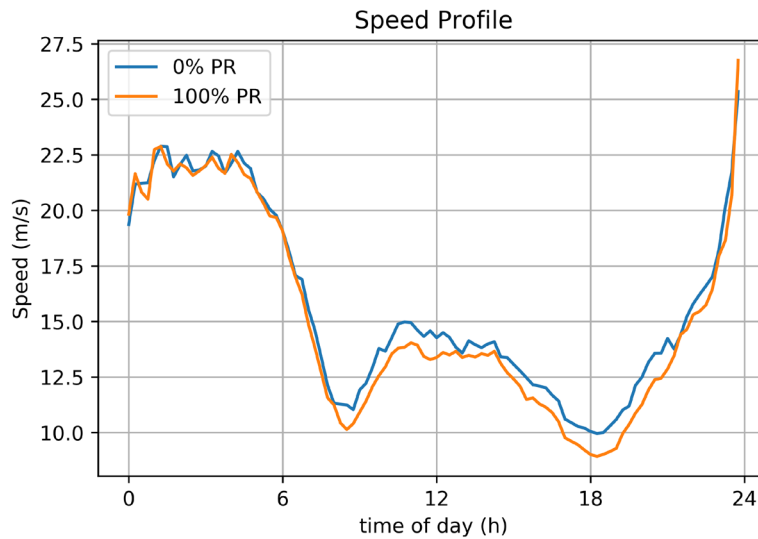


Figure I.6.1.6 Average speed in the network

rate of CACC lead to higher average speed on the peaks. Observe that it has lingering effects and the average speed limit remains higher until 8PM.

5. TNC Simulation

Since the demand data for TNC vehicles is not available to us for the time period of the available traffic demand data, the traffic was simulated by varying the market share of TNC vehicles from 0% to 5% of total traffic demand of San Pablo Avenue network. The traffic performance is evaluated in terms of total time spent, harmonic mean speed, and number of stops.

Table I.6.1.4 Simulation Results Varying the Market Share of TNC Vehicles

Market Penetration of TNC Vehicles	0%	1%	2%	3%	4%	5%
Total time spent (hr)	647.11 (-)	653.24 (+0.95%)	661.17 (+2.17%)	670.53 (+3.62%)	681.72 (+5.35%)	693.47 (+7.16%)
Harmonic mean speed (km/h)	27.21	26.93 (-1.02%)	26.88 (-1.21%)	26.85 (-1.32%)	26.64 (-2.09%)	26.4 (-2.98%)
Number of stops (#/veh/km)	0.03	0.03	0.04	0.04	0.04	0.05

Refer to the Table I.6.1.4. As the market penetration of TNC vehicle increases, the total time spent and the number of stops per vehicle gradually increase. As the TNC market penetration increases from 0 to 5%, traffic performance deteriorates. Also, as the market penetration increases, the harmonic speed decreases for the road section, where parking slots are located. For the given traffic demand, the market penetration of TNC vehicles and its parking maneuver seem to negatively influence the traffic performance.

In addition, the traffic was simulated to evaluate the impact of the parking duration of TNC vehicles for performing the pick-ups and drop-offs of passengers. Time period of 30 seconds, 1 minute, and 2 minutes are tested. However, the result showed no significant change with respect to the parking duration to the traffic performance. The TNC vehicles seem to affect the traffic flow only during the parking maneuvers to move to the parking slot and during the maneuvers to join back to the traffic stream after parking, i.e., only during the parking execution stages shown in Figure I.6.1.2. While parked, the TNC vehicles seem to have no effect on the traffic.

Conclusions

Micro-to-Meso

Fundamental Diagram (FD) is the flow-density or speed density function relationships in mesoscopic traffic modeling. The intention of this project is to develop Parameterized Fundamental Diagram (PFD) with an additional parameter of market penetration level of CAVs in mixed traffic. Simulation data from a properly calibrated 13-miles long freeway corridor SR-99 NB with different levels of market penetration of CAVs are used for the modeling. The demand is increased by 20% over the field observed. The coefficients of four models have been determined at nine representative locations have been preliminarily determined using Least Squares Methods. Fitting errors are also compared for those methods. The remaining work in this project will consider higher levels of demands up to 30% over the observed baseline traffic demand in the field. During the next phase of this project will apply the PFD to the calibration of mesoscopic simulation of mixed traffic with CAVs.

The CACC models have been applied by ANL team in all 13 Workflow Scenarios in the Chicago Metropolitan Area. The scenarios with presence of Automated Vehicles has higher demands due to the increased convenience of travel. The CACC model was responsible to partially mitigate the increased demand on these scenarios.

TNC Simulation

To evaluate the impact of transportation network company vehicles on the traffic flow, this research aims to develop a model for parking maneuvers. The model, which integrates to the PATH driving model, is implemented on a microscopic traffic simulation program Aimsun with MicroSDK. The parallel parking and forward parking maneuvers are modeled by dividing the maneuvers into different parking stages. The parking maneuver algorithm overcomes the functional limitations of Aimsun simulator, such as prohibition of backward movement, and successfully simulates natural parking movements. The parking maneuver algorithm is implemented, integrated with the PATH model.

A real traffic network and traffic demand are used to simulate the impact of TNC vehicles on the traffic, using a 2-mile long segment of San Pablo avenue in California. The traffic performance is evaluated at market penetration of TNC vehicles from 0% to 5% in 1% increments. The results show that with an increasing market penetration of TNC vehicles, the traffic performance deteriorates with an increase of total time spent and a decrease of harmonic mean speed for road segments of parking. Different parking duration of TNC vehicles, however, seems to have no significant impact on the traffic performance.

This study has limitations that should be considered for further work. First, the parking method—parallel or forward, is randomly selected for this study. However, the TNC driver should decide a preferred or appropriate parking method based on the length of available parking slot. The parking algorithm will be more realistic with a decision algorithm for parking method. Second, the algorithm does not reflect the real-world problem of double park, i.e., TNC vehicles stops in the main lane when there is no parking space available or does not want to take a burden of parking. This is problematic, since the TNC vehicle disrupts the traffic flow like a temporary lane reduction. The parking algorithm can also improve by modeling this maneuver.

Key Publications

Micro-to-Meso

1. X. Y. Lu, H. Liu, and S. Shladover, Parameterized Fundamental Diagram Modeling for Mixed Traffic with Connected Automated Vehicles (CAVs), submitted to 99th Annual TRB Meeting Washington, D.C., Jan. 2020
2. X. Y. Lu, H. Liu, and S. E. Shladover, CAV Traffic Impact Modeling and Simulation: Parameterized Fundamental Diagram, AVS 2019, July 15-18, Orlando, USA

References

Micro-to-Meso

1. [lu2017] X. Y. Lu, D. Kan, S. Shladover, D. Wei, and R. Ferlis, An Enhanced Microscopic Traffic Simulation Model For Application To Connected Automated Vehicles, 96th Transportation Research Board Annual Meeting, Washington D. C. Jan 8—12, 2017
2. [milan2014] V. Milanés, S. E. Shladover, J. Spring, C. Nowakowski, H. Kawazoe, H., and M. Nakamura, Cooperative Adaptive Cruise Control in Real Traffic Situations. *IEEE Transactions on Intelligent Transportation Systems*, 15(1), pp. 296-305, 2014.
3. [under1961] R. T. Underwood, (1961). Speed, volume and density relationships, *Quality and Theory of Traffic Flow*, Yale Bureau of Highway Traffic, p141-88
4. [yeo2008] H. Yeo, et al. Oversaturated Freeway Flow Algorithm for Use in Next Generation 1 Simulation. *Transportation Research Record: Journal of the Transportation Research 2 Board #2088*, TRB, Washington, D.C., 2008, pp. 68-79.

TNC Simulation

1. Müller, B., Deutscher, J., Grodde, S., Giesen, F., & Roppenecker, G. (2007). Universal Trajectory Planning for Automatic Parking. *ATZ worldwide*, 109(1), 25-28.
2. Liu, W., Li, Z., Li, L., & Wang, F. Y. (2017). Parking like a human: A direct trajectory planning solution. *IEEE Transactions on Intelligent Transportation Systems*, 18(12), 3388-3397.
3. Zips, P., Böck, M., & Kugi, A. (2016). Optimisation based path planning for car parking in narrow environments. *Robotics and Autonomous Systems*, 79, 1-11.
4. Li, B., & Shao, Z. (2015). A unified motion planning method for parking an autonomous vehicle in the presence of irregularly placed obstacles. *Knowledge-Based Systems*, 86, 11-20.
5. Xu, J., Chen, G., & Xie, M. (2000, October). Vision-guided automatic parking for smart car. In *Proceedings of the IEEE Intelligent Vehicles Symposium 2000* (Cat. No. 00TH8511) (pp. 725-730). IEEE.
6. Döge, K. P., & Krimmling, J. (2012). Video-based parking space analysis for traffic management. *IFAC Proceedings Volumes*, 45(24), 43-47.
7. Vorobieva, H., Glaser, S., Minoiu-Enache, N., & Mammari, S. (2012). Geometric path planning for automatic parallel parking in tiny spots. *IFAC Proceedings Volumes*, 45(24), 36-42.
8. GRUL, HALIL ERTU. (2013). An FPGA Implementation of two-step Trajectory Planning for Automatic Parking. PhD Thesis. Middle East Technical University.

I.6.2 SMART Mobility Tools and Process Development (ANL)

Aymeric Rousseau, Principal Investigator

Argonne National Laboratory
9700 S Cass Avenue
Lemont, IL 60439
E-mail: arousseau@anl.gov

Erin Boyd, DOE Technology Manager

U.S. Department of Energy
E-mail: Erin.Boyd@ee.doe.gov

Start Date: October 1, 2018	End Date: September 30, 2019	
Project Funding (FY19): \$1,020,000	DOE share: \$1,000,000	Non-DOE share: \$20,000

Project Introduction

The objective of the Smart Mobility Modeling Workflow is to evaluate new transportation technologies such as connectivity, automation, sharing and electrification through multi-level system analysis to consider the interactions between technologies. An integrated approach that considers multiple levels of fidelity is required to understand the impacts of new mobility technologies and services at scale:

- At the individual vehicle level, detailed models are required to represent powertrain component technologies and control algorithms across powertrain and vehicle classes.
- To quantify the impact of connectivity (vehicle to infrastructure(V2I), vehicle to vehicle(V2V), infrastructure to vehicle(I2V)), a multi-vehicle analysis is required to develop connected and automated vehicles(CAVs)-enabled vehicle and powertrain control algorithms and quantify their energy impacts.
- Micro-simulation models that represent tens of thousands of vehicles can then be used to quantify the impact of those new controls on traffic flow based on specific demands.
- Mesoscopic transportation system models are used to model travel behavior and assess the impact of hundreds of thousands or millions of travelers on mobility.

A dedicated workflow integrating multiple models across different levels of fidelity was developed to understand and quantify the impact of new mobility technologies at the system level. In order to support the SMART Mobility workflow, different system simulation tools need to be developed and deployed on high performance computing (HPC) platforms.

Objectives

The objectives of the projects include:

- Develop and deploy a LINUX version of POLARIS on a HPC platform
- Enhance RoadRunner framework to support large number of simulations
 - Develop and deploy new workflow to the entire user community using AMBER including
 - RoadRunner (new user interface will to setup and run studies with multiple vehicles within their environment),
 - POLARIS (facilitate parametric studies and large scale simulations to assess the impact of new technologies on mobility, energy, GHG and MEP) and

- Linkage to micro-simulation tools (support for ORNL and PATH tasks).

Approach

Best software practices were followed for the development of the different simulation tools, including

- Defining requirements,
- Following Agile project management and
- Employing test driven development.

JIRA, Jenkins and other tooling were used to produce high quality code meeting the requirements.

Results

POLARIS

POLARIS Linux-and BEBOP Compatible Version

Based on transportation research literature, potential changes in travel demand are key drivers of uncertainty in regard to the overall impacts of future mobility on energy use. As POLARIS, Argonne's transportation system simulation tool, is extended to better characterize mobility decisions made under new mobility technologies and modes, the core behavioral modeling components, as well as the supply modeling components were enhanced to capture changes in short-term, mid-term, and long-term decision-making brought about by new technologies. With these enhancements, the updated POLARIS transportation simulation model was used to evaluate the mobility, energy, and productivity (MEP) outcomes of these new mobility technologies in the context of the different metropolitan areas under the SMART Mobility Consortium.

Running POLARIS for a large metropolitan area at full capacity requires significant computing resources. The more computing power, the higher the fidelity of the simulations and thus the deeper the insights which can be obtained. This project leveraged BEBOP, one of many Argonne super computer resources, which includes 1024 public nodes that fall into two architecture categories: Intel Broadwell and Intel Knights Landing. The Broadwell nodes have 36 cores per node and the Knights landing nodes have 64 cores per node.



Figure I.6.2.1 BEBOP Super Computer Resource at Argonne

To manage such a large pool of computing resources, a Slurm job manager runs on top of a Linux operating system. To run on a Linux OS, the POLARIS code, written in C++, was ported over and compiled for the architecture. Although C++ is portable, many of the OS dependent tasks such as file system interfacing, multithreading and memory allocation have to be ported over and tested on the Linux OS. The dynamically linked libraries, which the code is compiled against, have to be swapped out for their Linux equivalents and

even the compiler changed from targeting Windows to targeting Linux. This includes refactoring the template class system to work on Linux-compatible compilers. Every class within the project needs to be modified to fit the new standard. The code can then be moved from using the Microsoft Visual Studio Compiler to the GNU Compiler Collection (gcc).

Integration with EMEWS

The Linux-and Bebop compatible version uses EMEWS (Extreme-scale Model Exploration with Swift) to allow multi-language model exploration. This allows scaling dynamic computational experiments to very large numbers (millions) of models on all major HPC platforms. EMEWS has been successfully implemented with the new POLARIS-LINUX version.

External Optimization Support

POLARIS allows external calculations on HPC clusters. The current implementation targets highly parallelizable calculations using standard MPI techniques. Parsl (parsl-project.org) allows POLARIS to utilize a workflow where input data is transferred to a cluster (Bebop) and submit jobs on many nodes. POLARIS then waits until the calculations are completed and the resulting data imported into the model before continuing. This allows millions of calculations in a short period. The Windows version of POLARIS currently implements this by submitting jobs on Bebop. The new approach was used to optimize personally owned shared vehicles in one of the SMART Mobility scenarios.

POLARIS OPT

High-dimensionality is becoming increasingly encountered in a large number of disciplines, which heavily rely on modeling and optimization tools to address real-world problems. While parallelization and efficient exploration methods provide a strong aid, dimensionality reduction is a unique tool that tackles this exponential difficulty directly. Any method seeking to employ reduction must be capable of encoding and decoding data into the lower dimensional structure and this has led to primarily linear methods to proliferate.

The computational speed of several calculations of the activity based modeling within POLARIS was improved by replacing them with nonlinear models fit using Bayesian Optimization. Using surrogate models for facilitating optimization and uncertainty analysis of computationally expensive simulators, Bayesian Optimization (BO) seeks to quickly learn an unknown response surface through the iterative construction of a cheaper, stochastic emulator. The resulting probabilistic representation can then be leveraged to reason about unobserved portions of the domain a measured degree of certainty. The main features of these high dimensionality aspects of the POLARIS model can be successfully encoded in lower dimensional non-linear methods, for example, within lower dimensional neural networks.

We have demonstrated that the translation obstacle encountered by non-linear methods, more specifically neural networks, are not burdensome enough to eliminate their use in the field and should be considered when incorporating reduction methods with other statistical tools strained by high-dimensionality. For example of successful implementations, the authors point to [Snoek et al., 2015, Schultz and Sokolov, 2018, Lawrence, 2004, Ma et al., 2018].

RoadRunner

RoadRunner development was initiated to support research on energy-focused CAV controls. RoadRunner is a framework that can simulate multiple vehicles with full powertrain models and the interactions between vehicles and their environment. RoadRunner uses powertrain models from Autonomie, Argonne's established vehicle energy-consumption simulator, but adds new capabilities such as multi-vehicle simulation, models of the road, causal models of human driving, V2X communications, and sensors. Figure I.6.2.2 illustrates the steps in a typical RoadRunner use case. The user first defines a scenario: the route, the number of vehicles, the type of vehicles, and the type of CAV technology for each vehicle. RoadRunner then automatically builds the Simulink diagram, runs the simulation, and post-processes the results for the user to analyze.

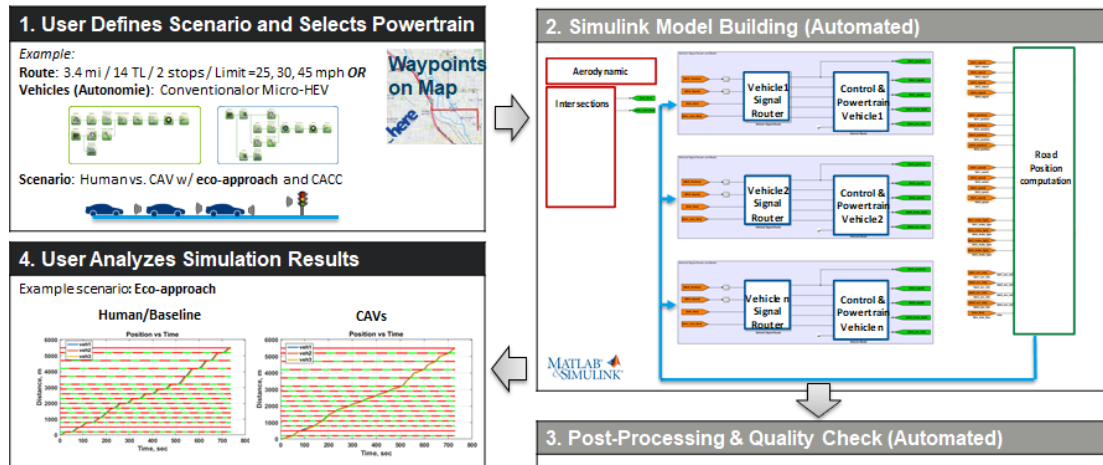


Figure I.6.2.2 RoadRunner workflow to simulate a CAV scenario

Migration towards AMBER API

When the user initiates a RoadRunner simulation, an automated building combines and connects all of the subsystems. Each vehicle includes a powertrain model, adapted from Autonomie, and which is also built automatically. We converted that vehicle building process from Autonomie R16 to the new AMBER building algorithms. This new feature allows the use of the most recent Autonomie vehicle models, and will ensure proper integration with AMBER.

Autonomie component control override

The controllers developed in RoadRunner may control the corresponding Autonomie powertrain through different interfaces:

- Accelerator pedal position
- Wheel torque demand
- Component commands (e.g., engine torque, gear)
- A combination of those.

The type of interface depends on the use case, the objective of the controls and the type of vehicle. Moving away from one predefined interface, we modified the building process in both RoadRunner and Autonomie to allow any signal from RoadRunner control model to override any control variable in Autonomie, for example gear demand. This process previously required manual manipulation of the Simulink diagram, and is now automatic.

Simulation process improvements

The simulation process was improved to run a large number of scenarios with post-processing capabilities for energy impact evaluation. We introduced the concept of a run file (`.run`), common in Autonomie, which is an XML file that lists all the simulation parameters (e.g., number of vehicles, route, Autonomie vehicle and control) and that is then used by the building process to build and initialize the Simulink diagram, and then run and analyze the simulation. We also developed a process to run large-case studies, as illustrated in Figure I.6.2.3. It was used extensively to evaluate the energy impacts of advanced eco-driving algorithms.

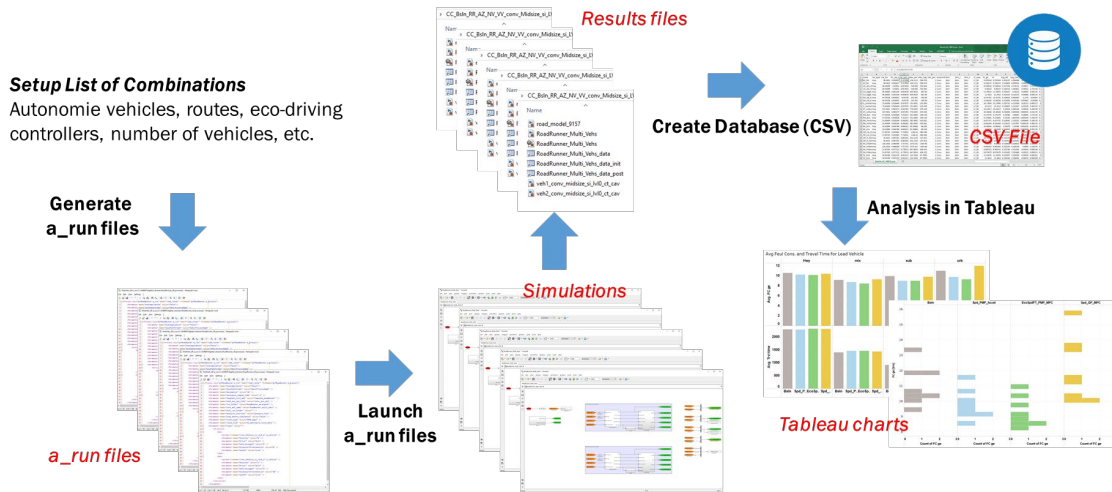


Figure I.6.2.3 Large-scale RoadRunner simulation workflow

Linkages with 3rd party tools

The complexity of the environment model (road, other vehicles) in RoadRunner is tailored support CAV control development with a focus on energy by simulating long routes extracted from a digital maps, such as HERE maps. However, more realistic and complex environment are also necessary to consider different scenarios. As a result, we initiated linkages with multiple tools (Figure I.6.2.4), including:

- CARLA (Car Learning to Act) is an open-source simulator for autonomous driving research that comes with a rich library of 3D digital assets (urban layouts, buildings, vehicles) to model a broad range of scenarios. Using CARLA, engineers can experiment various sensor suites, driving strategies and various types of artificial intelligence. CAV controls developed in RoadRunner can now be simulated in CARLA, which provides more realistic driving conditions.
- CarMaker is a commercial tool developed by IPG (Germany) focused on virtual testing of vehicle dynamics and the safety of Advanced Driver Assistance Systems (ADAS). Testing scenarios include vehicles as well entire surrounding environment, such as other vehicles, roads, drivers and traffic. We demonstrated the integration of CAV controls developed in RoadRunner with CarMaker, a tool commonly used by OEMs.

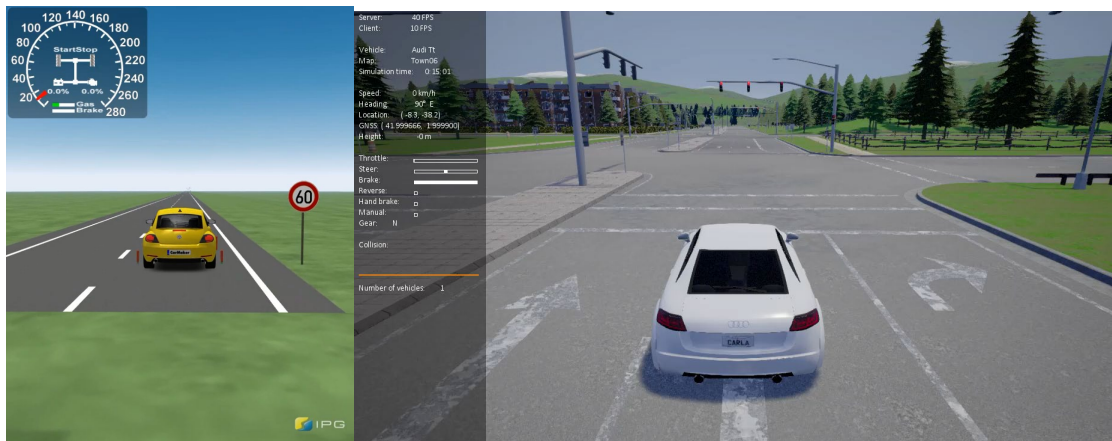


Figure I.6.2.4 RoadRunner vehicles can now be run in IPG CarMaker (left) and CARLA (right)

AMBER**RoadRunner User Interface Prototype**

Figure I.6.2.5 shows a new user interface (UI) for RoadRunner developed based on RoadRunner current requirements. The new UI is currently used internally to gather additional requirements and will be deployed in future AMBER releases. The example below allows the construction of a vehicle platoon with vehicle type, spacing and driver all configurable.

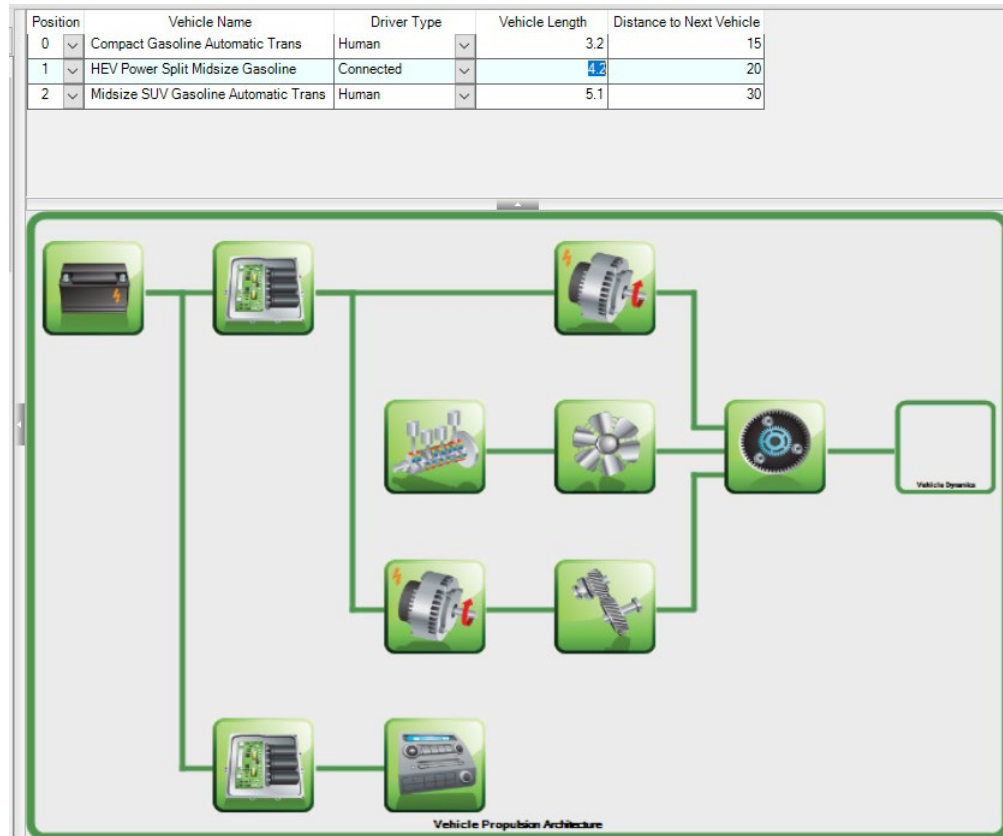


Figure I.6.2.5 RoadRunner user interface based on AMBER framework

SVTrip User Interface Prototype

A new UI (Figure I.6.2.6) was developed to allow users to generate vehicle speed traces from large number of routes using SVTrip. The user can select different file types from which to generate their trips. For instance, the output of POLARIS can be selected and used to generate trips, which are compatible with Autonomie vehicles. The trips generated from SVTrip can be used with any vehicle model built in Simulink or even exported to a csv format that can be imported and used with many other vehicle modeling tools. This application is independent of Autonomie and comes in its own deployable package, which is distributed on top of the AMBER framework.

SVTRip x

1) Trip Selection 2) SVTRip Parameters 3) Launch SVTRip 4) Results

Select Trip File Type POLARIS Trips Select Input Type trip_tbl_convert CSV File: C:

Drag a column header here to group by that column.

trip	vehicle	veh_type	link_number	link_id	link_dir
1001	115280	9	1	85775	1
1001	115280	9	2	12626	0
1001	115280	9	3	12619	1
1001	115280	9	4	12618	0
1001	115280	9	5	12621	0
1001	115280	9	6	12610	1
1001	115280	9	7	12609	0
1001	115280	9	8	82302	0
1001	115280	9	9	12604	1
1001	115280	9	10	12603	0
1001	115280	9	11	12596	1
1001	115280	9	12	85286	1
1001	115280	9	13	12577	1
1001	115280	9	14	12576	0
1001	115280	9	15	12562	1
1001	115280	9	16	12538	1
1001	115280	9	17	12537	0
1001	115280	9	18	12510	1

Figure I.6.2.6 SVTRip user interface based on AMBER framework

Conclusions

As part of the project, existing system simulation tools were successfully enhanced to support current and future US DOE Vehicle Technologies Office studies. The new capabilities were already successfully implemented in several Smart Mobility Consortium projects. Several new Graphical User Interfaces were developed in AMBER to deploy the new tools and features to the users community.

References:

1. Jasper Snoek, Oren Rippel, Kevin Swersky, Ryan Kiros, Nadathur Satish, Narayanan Sundaram, Md. Mostofa Ali Patwary, Prabhat, and Ryan P. Adams. Scalable Bayesian Optimization Using Deep Neural Networks. arXiv e-prints, page arXiv:1502.05700, February 2015.
2. Laura Schultz and Vadim Sokolov. Bayesian Optimization for Transportation Simulators. Procedia Computer Science, 130:973–978, 2018.
3. Neil D. Lawrence. Gaussian process latent variable models for visualization of high dimensional data. In Advances in neural information processing systems, pages 329–336, 2004.

I.6.3 Workflow to simulate connected and automated vehicle control under realistic traffic conditions (ANL, LBNL)

Dominik Karbowski, Principal Investigator

Argonne National Laboratory
9700 S Cass Avenue, Building 362
Lemont, IL 60439
E-mail: dkarbowski@anl.gov

Erin Boyd, DOE Technology Manager

U.S. Department of Energy
E-mail: Erin.Boyd@ee.doe.gov

Start Date: October 1, 2018

End Date: September 30, 2019

Project Funding (FY19): \$375,000

DOE Share: \$375,000

Non-DOE Share: \$0

Project Introduction

The SMART Mobility Consortium has developed an integrated workflow to enable multilevel analysis of new transportation technologies. It facilitates linkages between simulation tools and establishes common scenarios. Within this workflow, RoadRunner (Kim et al. 2018) is a software framework developed at Argonne National Laboratory to simulate multiple vehicles with full powertrain models and the interactions between vehicles and their environment. Researchers use RoadRunner to develop energy-focused connected and automated vehicle (CAV) controls. RoadRunner can simulate multiple vehicles but is not designed to model traffic flow dynamics, which involves a much larger number of vehicles or external data sources. As a result, the objective of this project is to establish a workflow for the simulation of vehicle-centric eco-driving control algorithms developed in RoadRunner within realistic traffic conditions. This is done through the linkage between RoadRunner and the Stochastic Vehicle TRIP Prediction tool (SVTRIP) or microsimulation tools. With this workflow, researchers will be able to design more robust eco-driving controllers, as well as analyze the traffic flow impact of CAV controls developed at the vehicle level in RoadRunner.

Objectives

The objectives of this project are as follows:

- To enable the simulation of controls developed in RoadRunner within realistic traffic conditions.
- To link RoadRunner with SVTRIP, a lightweight generator of naturalistic speed profiles, so that traffic conditions can be simulated within RoadRunner and for any type of road.
- To link Roadrunner with the PATH microsimulation model in order to
 - Enable the simulation of RoadRunner vehicles within complex road and traffic situations; and
 - Enable the assessment of the impact of controls developed in RoadRunner on traffic flow.

Approach

The approach in this project is to add the capability of simulating traffic conditions within RoadRunner through two distinct methods, as illustrated in Figure I.6.3.1. The first method relies on SVTRIP, enabling the lightweight simulation of traffic conditions within RoadRunner for any type of road. The second method consists of linking the tool with the PATH model, developed in Aimsun, a commercial microsimulation tool for more detailed traffic simulations on predefined road network models.

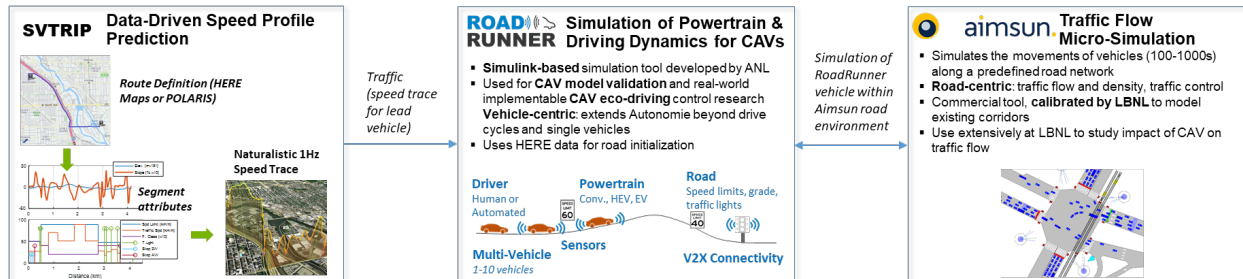


Figure I.6.3.1 Adding realistic traffic to RoadRunner simulations through linkages with SVTRIP and Aimsun

Linkage of RoadRunner with SVTRIP

The first method of introducing traffic into RoadRunner relies on SVTRIP, a software tool developed at Argonne (Karbowksi et al. 2014) that “predicts” the drive cycle—the second-by-second vehicle speed—based on the attributes of each segment of the trip. SVTRIP relies on digital maps for trip-specific data and generates the speed signal through a constrained Markov chain algorithm trained on thousands of hours of real world driving data. SVTRIP can be used as a lightweight proxy model for exogenous traffic in RoadRunner.

The linkage is made through a lead dummy vehicle that behaves as if it was operating within real traffic situations by following a speed schedule computed by SVTRIP, while the following vehicles are regular RoadRunner vehicle models. However, the speed schedule of the lead vehicle cannot be predefined and fixed for the entire simulation and must be updated periodically. One reason is related to traffic lights: since RoadRunner has its own model instance for each traffic light along the route and since the vehicle speed is also dynamically calculated, it cannot be predicted exactly when a vehicle will arrive at the intersection. It is therefore not possible to predict whether it will have to stop at a red light, cruise through at a green light, or any situation in-between. In SVTRIP, however, the decision to stop or not is decided before the speed trace is generated. It also is desirable to periodically reconsider the relative gap between the two vehicles, to model the fact that in the real world, preceding vehicles “appear” and “disappear” by slowing down or speeding up, changing lanes, or entering/exiting the roadway.

As a result, we integrated SVTRIP directly into the RoadRunner/Simulink diagram, as shown in Figure I.6.3.2. Unlike the traditional RoadRunner vehicles, the lead vehicle does not include a powertrain model, nor a vehicle dynamics model. Its speed is the synthetic speed profile generated by SVTRIP function calls at the start of the current segment, unless the vehicle needs to stop at a traffic light, in which case it reverts to the baseline braking logic. Both RoadRunner and SVTRIP are linked to HERE Location Services API (HERE.com 2019), and as result, the same route topography and speed limits can be used in both tools, and SVTRIP uses average speed in traffic to compute the speed profile.

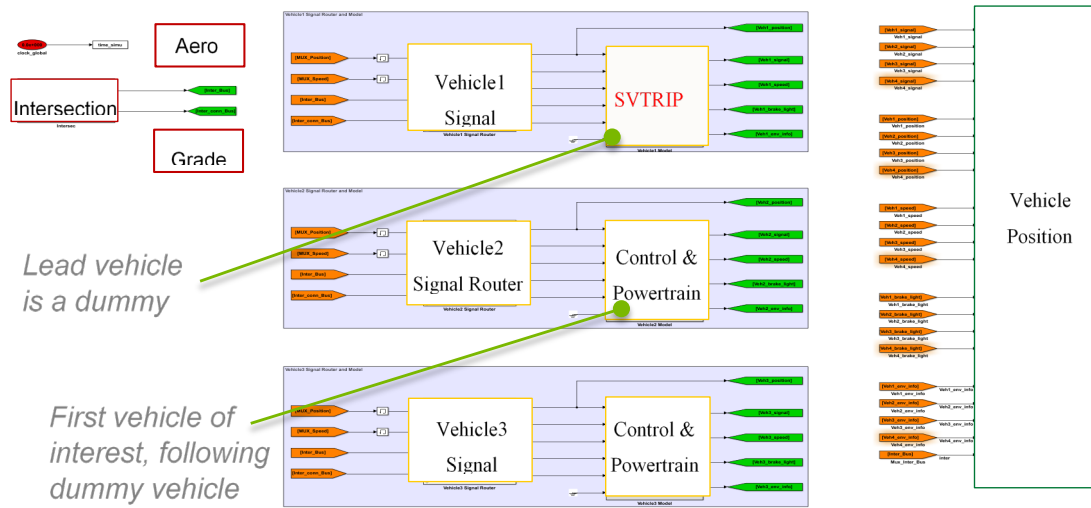
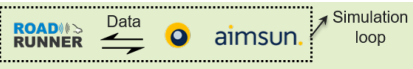


Figure I.6.3.2 Simulink diagram of a RoadRunner scenario with dummy lead SVTRIP vehicle

Linkage of RoadRunner with Microsimulation

Researchers use traffic flow microsimulation to study traffic flow dynamics, especially in the context of greater adoption of CAVs. A microsimulation tool simulates hundreds or thousands of vehicles traveling through a defined road network, such as a highway or an urban corridor. Researchers at Lawrence Berkeley National Laboratory(LBNL) and PATH (Lu et al. 2017) have developed a framework based on Aimsun (2019), a commercial microsimulation tool, and have validated several network models with real-world data measurements. Linking RoadRunner with Aimsun not only enables simulation of vehicles developed in RoadRunner in the context of realistic traffic conditions, but also provides a way to evaluate their impact on traffic, if adopted at scale. There are two ways to link RoadRunner to Aimsun: RoadRunner vehicles can be used with Aimsun in cosimulation or as compiled dynamic library link (DLL) files inside of Aimsun, as summarized in Table I.6.3.1. In both cases, RoadRunner vehicles use information, such as the current state of the vehicle itself and surrounding vehicles to compute their state taking into account complex powertrain dynamics. Their state is applied to the corresponding vehicle entered in the network, and its resulting driving behavior is visualized in Aimsun. This procedure is repeated at every simulation step.

Table I.6.3.1 Summary of Two Possible Ways to Link RoadRunner to Aimsun

	Aimsun microAPI	Aimsun microSDK
Schematic Diagram		
Method	Aimsun and RoadRunner cosimulation TCP/IP communication	Aimsun simulation only Explicit linking with DLLs
Merits	Easy modification, early verification, and validation	Reduced simulation time, a large-scale study
Objective	To develop and improve controllers	To analyze traffic impacts of controllers

Aimsun microAPI

Aimsun microAPI (Micro Advanced Programming Interface), either C++ or Python based, aims to communicate with external applications that can get access to the prescribed objects of Aimsun during simulation. This module follows three steps in controlling the prescribed vehicles:

Step 1. Once the prescribed vehicles enter the Aimsun network, they must be set as tracked, and their static parameters must be modified to emulate controlled vehicles.

Step 2 The prescribed vehicles can retrieve the required information.

Step 3 The prescribed vehicles can be controlled in a way of modifying the speed, not using the speed computed by the default Aimsun model.

To establish a connection through the Transmission Control Protocol/Internet Protocol (TCP/IP) port between Aimsun and RoadRunner, we used the MATLAB instrument control toolbox that provides specific blocks for communicating with Aimsun in Simulink. In conjunction with RoadRunner vehicle models, these blocks allow data to be sent to Aimsun and data to be received from Aimsun quickly; Aimsun serves as a server, whereas RoadRunner serves as a client, as shown in Figure I.6.3.3.

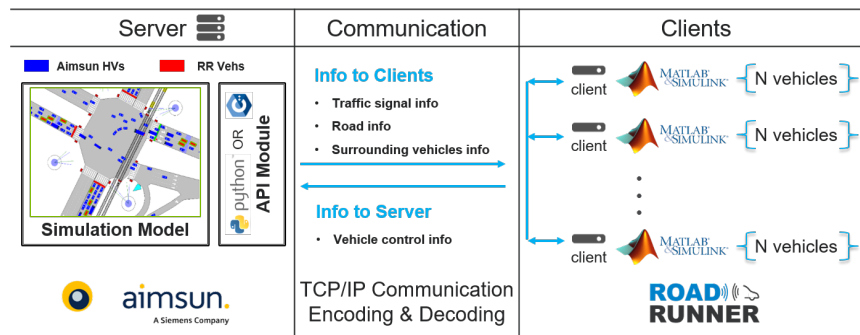


Figure I.6.3.3 Structure using Aimsun microAPI to link RoadRunner to Aimsun

Aimsun microSDK

The C++ based Aimsun microSDK (Micro Software Development Kit) aims to implement new behavioral models (e.g., car-following, lane-changing) for the prescribed vehicles and overwrite default Aimsun models, directly within Aimsun. Figure I.6.3.4 shows the structure using microSDK, in which the RoadRunner vehicle model is compiled as a DLL file, and as the new behavioral model, this DLL is called at every simulation step through the explicit linking with microSDK. The explicit linking allows us to swap or add new DLL files easily without any modification. Because this DLL can be used for all vehicles entering the network or for a subset of vehicles, we can generate various scenarios with different penetration rates of RoadRunner vehicles.

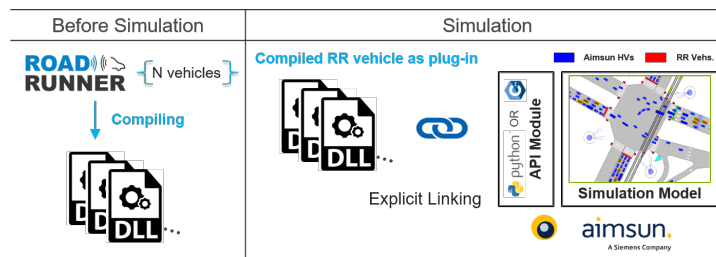


Figure I.6.3.4 Structure using Aimsun microSDK to link RoadRunner to Aimsun

To compile the RoadRunner vehicle models, we reconfigured and redefined inputs and outputs, and used the MATLAB embedded coder toolbox that automatically generates C source code and builds a DLL file.

At each step in the traffic simulation interval, the PATH model in Aimsun first evaluates each vehicle’s lane changing behavior. The PATH model then calls different car-following models to calculate the longitudinal behaviors for manually driven vehicles and CAVs. With the new integration of RoadRunner into the PATH

Aimsun platform, it will be possible to use control models developed in RoadRunner to update vehicles' longitudinal movements (i.e., position, speed, and acceleration) for a user-defined share of vehicles.

Results

Linkage of RoadRunner with SVTRIP

We experimented the RoadRunner–SVTRIP linkage for a two-km road with two traffic lights with a 22 m/s (50 mph) speed limit and an average speed in traffic of 15 m/s (34 mph). Two non-connected vehicles were simulated. Figure I.6.3.5 shows the speed of the dummy vehicle preceding these two vehicles. SVTRIP is called at the beginning of each segment (green dot in the figure), that is, when passing an intersection (scenario 2) or when the state of a close-by incoming traffic light goes from red to green (scenarios 1 and 4). However, the dummy vehicle switches to the baseline braking logic if the incoming light is red (red square), as in scenario 3.

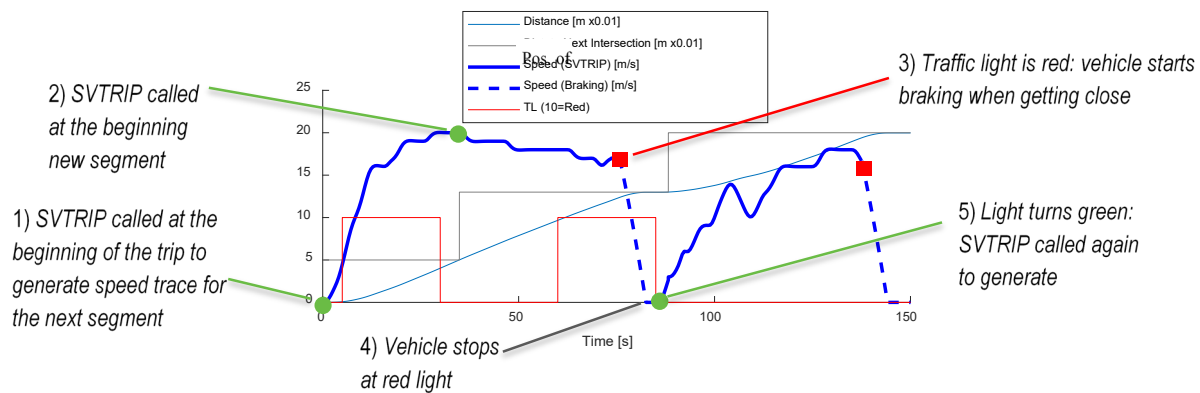
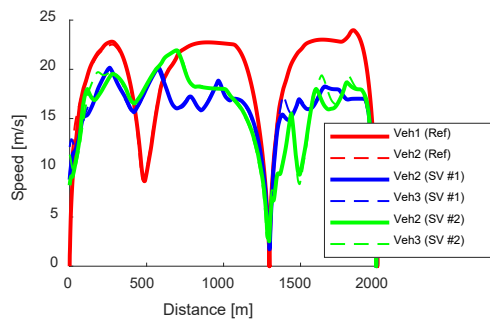


Figure I.6.3.5 Speed of dummy SVTRIP vehicle called within RoadRunner

We compared the results of the RoadRunner+SVTRIP runs with the reference, in which the lead vehicle is not preceded by any vehicle, as if it were driven on an empty road. Figure I.6.3.6 (left) shows the speeds of the first two vehicles of interest (solid = first; dash = second) for the reference scenario (red) and for two different RoadRunner-SVTRIP runs (blue and green); each run with SVTRIP produces different results because it is stochastic by nature. The table on the right shows the resulting fuel consumed for the first vehicle of interest, that is, the lead vehicle without the preceding vehicle in the reference scenario, and the first vehicle following the dummy vehicle in the SVTRIP scenario (it includes an additional third SVTRIP run) compared to the figure. In this example, the vehicle in traffic consumes less fuel than the reference without traffic. This is partly due to the particular phase and timing of the lights in the road scenario: the vehicle in the reference scenario reaches the speed limit in each segment, but has to brake or come to a full stop more often than the vehicle in “traffic” (SVTRIP case), leading to a greater waste of kinetic energy.



Simulation	Fuel
Reference	167 g
SVTRIP #1	117 g
SVTRIP #2	123 g
SVTRIP #3	131 g

Figure I.6.3.6 Vehicle speed for 2 vehicles with or without traffic (left), and fuel consumed by the first vehicle (right)

Linkage to RoadRunner with Microsimulation

To demonstrate the linkage between RoadRunner and Aimsun, using the Aimsun microAPI, we considered a simple scenario in which five RoadRunner vehicles, which are either human-driven vehicles or eco-driving CAVs, enter the network with two signalized intersections. Figure I.6.3.7 shows that all the human-driven vehicles (Aimsun and RoadRunner vehicles) stop at the red light and idle until the signal switches to green (A), whereas eco-driving CAVs get informed in advance and use the SPaT information to optimally slow down so that they can avoid stops at two intersections (B). Avoiding unnecessary stops saves energy. Note that frequent cut-ins of the surrounding Aimsun vehicles cause RoadRunner vehicles to suddenly brake, a situation not encountered in RoadRunner-only simulations.

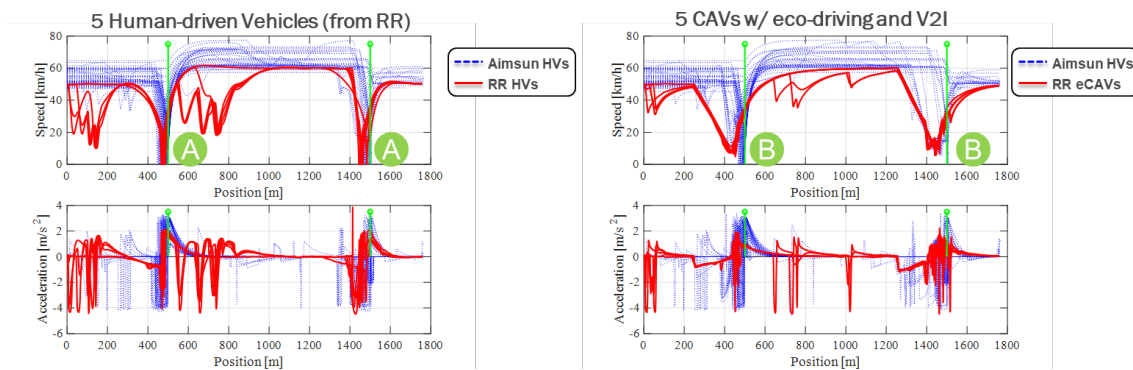


Figure I.6.3.7 Speed and acceleration trajectory of five RoadRunner vehicles [solid red lines], which are either human-driven vehicles [left] or eco-driving CAVs [right], and default Aimsun human-driven vehicles [dotted blue lines]

Conclusions

We have developed and demonstrated two methods for introducing traffic dynamics into RoadRunner and the CAV energy-focused research it enables. The first method is based on SVTRIP and allows us to simulate traffic using a data-driven model through a proxy lead vehicle, for any kind of road scenario and with limited computation overhead. In the second method, RoadRunner vehicles can be directly simulated in the PATH microsimulation model developed in Aimsun and can interact with a high-fidelity model of the road and of the traffic, including surrounding vehicles, lane changes, and the like.

This project links multiple tools in the SMART Mobility workflow and will enable new multilevel CAV research. In particular, adding traffic conditions will make CAV eco-driving controls developed with RoadRunner more robust and will lead to more representative analysis results. We will also be able to evaluate the impact on traffic of these algorithms if adopted at scale. Future developments will include automation of the linkages and further testing.

References

1. Aimsun, 2019, home page. Available at www.aimsun.com. Accessed Oct. 2019.
2. HERE.com, 2019, “Location-based services and mapping.” Available at www.here.com/products/location-based-services. Accessed Oct. 2019.
3. Lu, X.-Y., D. Kan, S. E. Shladover, D. Wei, and R. A. Ferlis, 2017, “An enhanced microscopic traffic simulation model for application to connected automated vehicles.” Paper presented at the 96th Annual Meeting of the Transportation Research Board, Washington, DC, Jan. 8–12.
4. Karbowski, D., A. Rousseau, V. Smis-Michel, and V. Vermeulen, 2014, “Trip Prediction Using GIS for Vehicle Energy Efficiency.” 21st ITS World Congress Proceedings, Detroit, MI, Sept. 7–11. Available at <https://is.gd/svtrip2014>.

5. Kim, N., D. Karbowski, and A. Rousseau, 2018, “A Modeling Framework for Connectivity and Automation Co-Simulation,” SAE Technical Paper 2018-01-0607. Available at doi.org/10.4271/2018-01-0607.

Acknowledgements

We acknowledge the contributions of Jihun Han (ANL), Xiao-Yun Lu, (LBNL), and Hao Liu, (Partners for Advanced Transportation Technology (PATH), UC Berkeley)

I.6.4 Demonstrate MEP Benefit of Intelligent EV Infrastructure Design Using ABMs (NREL, LBNL, ANL)

Eric Wood, Principal Investigator

National Renewable Energy Laboratory
15013 Denver West Parkway
Golden, CO 80401
E-mail: eric.wood@nrel.gov

Colin Sheppard, Principal Investigator,

Lawrence Berkeley National Laboratory
1 Cyclotron Road
Berkeley, CA 94720
E-mail: colin.sheppard@lbl.gov

Omer Verbas, Principal Investigator

Argonne National Laboratory
9700 S Cass Avenue
Lemont, IL 60439
E-mail: omer@anl.gov

Erin Boyd, DOE Technology Manager

U.S. Department of Energy
E-mail: erin.boyd@ee.doe.gov

Start Date: January 1, 2019

End Date: September 30, 2019

Project Funding (FY19): \$500,000

DOE share: \$500,000

Non-DOE share: \$0

Project Introduction

Emerging urban mobility options are poised to fundamentally transform modern transportation systems in ways that cannot be understood without complex modeling approaches. Supply - and demand of various mobility options are effectively represented using agent-based models (ABMs) at ANL (POLARIS) and LBNL (BEAM). Parallel with new mobility options, electricity is predicted to become a significant source of transportation fuel in existing vehicle-based modes. NREL's Electric Vehicle Infrastructure Projection Tool (EVI-Pro) projects consumer demand for various types of charging infrastructure. Quantification of impacts from simultaneous introduction of new travel modes and electrification of existing ones presents a challenge to weigh the inherent tradeoffs between mobility, energy, and productivity. NREL's Mobility Energy Productivity (MEP) framework provides the necessary structured analytical approach to weight said costs and benefits. This project leverages all these tools in a demonstration of the value of the SMART Modeling Workflow focused on MEP benefits of intelligent electric vehicle (EV) charging infrastructure design.

Objectives

In this project, we seek to understand the impact of EV charging availability and charging behavior on regional travel demand, as well as the reciprocal impact of travel demand on the deployment of additional EV chargers, through simulation analysis. The focus on computational efficiency and extensibility in the development of the POLARIS and BEAM agent-based simulation engines allow for the efficient extension to Electric-Vehicle Supply Equipment (EVSE) and grid interaction simulation. Simulation systems for analyzing interactions between vehicle charging and travel demand have previously been implemented, but generally involve simplified representations of traveler behavior, vehicle energy consumption or both.

By leveraging EVI-Pro to develop infrastructure solutions for vehicle electrification scenarios in VTO ABMs of San Francisco and Chicago, this project will:

- Establish integration pathways between VTO ABMs, infrastructure models, and MEP calculations.
- Provide ABMs with a set of infrastructure solutions aligning with high electrification future scenarios.
- Improve VTO infrastructure analysis tools by contrasting simulation approaches for charging behavior.

Approach

EVI-Pro is a planning model used for estimating consumer demand for electric vehicle residential, workplace, and public charging infrastructure. EVI-Pro has been developed by NREL in collaboration with the California Energy Commission and with additional support from the US Department of Energy's Vehicle Technologies Office.

EVI-Pro uses detailed data on personal vehicle travel patterns, electric vehicle attributes, and charging station characteristics in bottom-up simulations to estimate the quantity and type of charging infrastructure necessary to support regional adoption of electric vehicles. EVI-Pro has been used for detailed studies in Massachusetts [1], Columbus [2], California [3], Maryland [4], and for a National Analysis of U.S. communities and corridors [5]. A simplified version of EVI-Pro is publicly accessible via the US Department of Energy Alternative Fuels Data Center (EVI-Pro Lite).

This project implements functionally equivalent EVI-Pro integration pathways for POLARIS and BEAM, including:

- Identifying high electrification scenarios of interest to VTO, including personal LDVs and TNCs.
- Invoking unconstrained charging infrastructure simulations in both ABMs.
- Providing unconstrained EV charging demand to EVI-Pro for spatial/temporal aggregation.
- Sending realistic charging network designs back to ABMs in an iterative process.
- Quantifying MEP benefits of modeled EV charging infrastructure scenarios.

POLARIS & EVI-Pro Integration

A workflow between POLARIS and EVI-Pro has been developed to support residential and public charging network designs. An iterative multi-step process has been adopted:

1. Every POLARIS run starts with population synthesis where around 10 million individuals living in around 3 million households within the metropolitan region of Chicago are generated. Among various socio-demographic characteristics of these households, vehicle ownership is also determined.
2. This information is provided to EVI-Pro to estimate availability of residential charging for each household based on residence type, tenure, household density, income, and residential parking availability.
3. The household-level residential charging availability information is then provided back to POLARIS and simulated assuming an unconstrained network of public chargers.
4. The public charging demand placed on the unconstrained network is used by EVI-Pro to design a public network of Level 2 and direct current fast charging stations to meet driver demand in a realistic manner.

5. A final round of POLARIS simulations is conducted using the constrained public charging network and a detailed charging decision algorithm.

In order to estimate residential charging availability across Chicago, present-day data from the US Census Public Use Microdata Sample (PUMS) database is utilized, providing distributions of residence type, tenure, light-duty vehicle ownership, and income. These distributions are coupled with present-day survey data from the University of California Davis [6] describing availability of residential charging with respect to residence type.

Using EVI-Pro's residential charging network, POLARIS is then used to simulate public charging demand in Chicago assuming an unconstrained network of chargers with vehicles utilizing charging stations on an as-necessary basis. Simulated demand from the unconstrained network is then spatially aggregated using a hierarchical clustering algorithm in EVI-Pro to generate a set of discrete charging locations each with a limited number of plugs and charging capacity. A map of POLARIS-simulated PEV public charging demand and EVI-Pro synthesized charging station locations from downtown Chicago can be seen in the below figure.

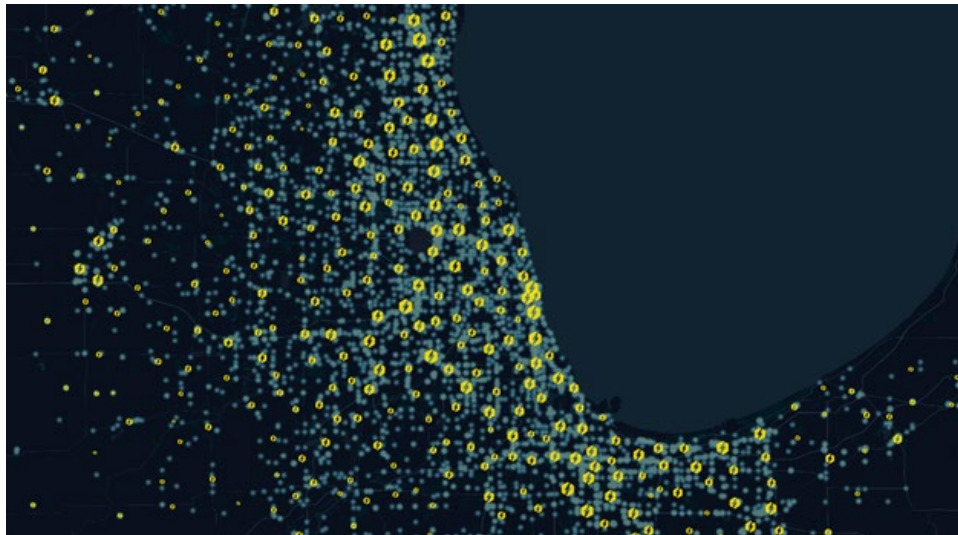


Figure I.6.4.1 POLARIS-simulated PEV public charging demand from unconstrained network (background) and EVI-Pro synthesized charging station locations (foreground).

BEAM & EVI-Pro Integration

Residential and public charging network designs for BEAM workflow simulations are provided using EVI-Pro. As shown in the below schematic, an iterative multi-step process has been adopted. For each simulation scenario, BEAM determines which households across San Francisco to be simulated as owning a battery electric vehicle (BEV) based on vehicle adoption distributions from the ADOPT model. These distributions are conditioned on the household income of each residence. For each household owning a BEV, housing stock characteristics from UrbanSim (tenure, residency type) are used to make “on-the-fly” estimates of residential charging availability based on EVI-Pro residential charging assumptions. Household-level residential charging availability estimates are used within BEAM to simulate utilization of an unconstrained public charging network.

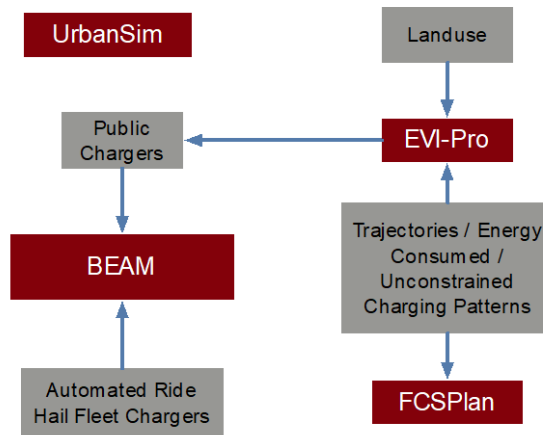


Figure I.6.4.2 Modeling workflow between BEAM, EVI-Pro, and FCSPan (Fast Charging Station Plan) to site charging infrastructure for BEAM simulations.

Public charging demand placed on the unconstrained network is used by EVI-Pro to design a public network of Level 2 and direct current fast charging stations to meet driver demand in a realistic manner. A final round of BEAM simulations is conducted using the constrained public charging network. A similar approach is taken by LBNL's Fast Charging Station Plan (FCSPan – a joint fleet size and PEV charging station planning model) in designing a dedicated network of charging stations for the automated, electric ride hail fleet in BEAM. A map of BEAM-simulated PEV public charging demand and EVI-Pro synthesized charging station locations from the San Francisco Bay area can be seen in the below figure.



Figure I.6.4.3 BEAM-simulated PEV public charging demand from unconstrained network (background) and EVI-Pro synthesized charging station locations (foreground).

Results

Chicago Area Simulation Results

Simulation of approximately 450,000 personal BEVs in Chicago suggests that 6,880 fast charging plugs could be necessary to meet consumer demand (a 35x increase over existing infrastructure). The below figure shows maps of POLARIS-simulated charging demand overlaid with public charging networks from EVI-Pro. As the total BEV population increases across each scenario, as expected, the count of public charging events also increases. However, the increase is not proportional as increased levels of BEV adoption result in better network utilization (events per plug increases with fleet size). As real-world travel data at this scale is either non-existent or cost prohibitive to acquire, POLARIS provides an efficient approach to exploring infrastructure requirements for high-penetration electrification scenarios.

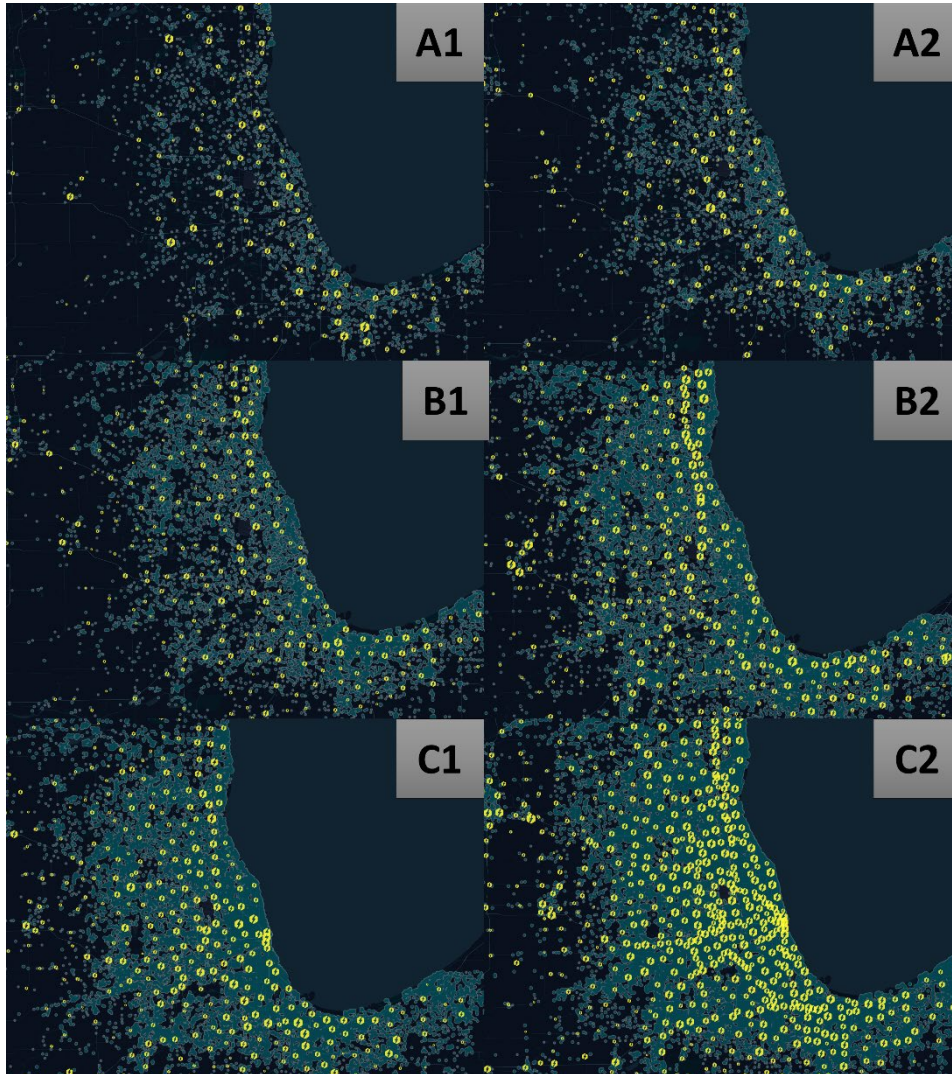


Figure I.6.4.4 Simulated charging demand across Chicago in the six workflow scenarios.

San Francisco Bay Area Simulation Results

Simulation of approximately 420,000 personal and ride-hailing PEVs in San Francisco suggests that 7,770 fast charging plugs could be necessary to meet consumer demand (a 9x increase over existing infrastructure). The below table provides quantitative simulation results for each workflow scenario. The PEV fleet in BEAM is comprised of two powertrain types (PHEVs and BEVs) and three use cases (personal ownership, human driven

ride-hailing, and CAV ride-hailing). Personal and ride-hailing PEVs are assumed to have access to a network of workplace and public charging stations (PHEVs are assumed only capable of L2 charging). CAV ride-hailing vehicles are assumed to utilize a separate network of private fast charging stations (as designed by FCSPlan).

Despite BEAM simulating significantly more public charging events than workplace charging events in all scenarios, the size of the workplace and public charging networks (number of stations and plugs) is similar. This speaks to the fact that much of the activity at public charging stations consists of fast charging (typically shorter charging times and higher vehicle throughput) and that vehicle arrival patterns at workplace stations tends to limit the ability for drivers to share charging infrastructure (drivers are assumed to plug-in and begin charging immediately upon arrival at a destination). These results demonstrate that design of future charging networks can benefit from advanced simulation that quantify complex relationships between PEV fleet size, driving patterns, and infrastructure utilization.

Table I.6.4.1 Summary of EVI-Pro public charging networks simulated for BEAM workflow.

Scenario	A1	A2	B1	B2	C1	C2
<i>Personal PHEVs</i>	69,860	115,270	26,250	23,950	51,660	54,440
<i>Personal BEVs</i>	93,380	162,560	150,570	159,520	280,110	357,540
<i>Human Ride-Hail PHEVs</i>	1,170	1,390	3,280	340	600	1,020
<i>Human Ride-Hail BEVs</i>	1,940	1,990	13,890	3,420	3,320	5,780
<i>Workplace Charge Events</i>	8,210	13,300	9,500	9,930	21,690	27,990
<i>Workplace Stations</i>	880	1,190	980	1,110	1,800	2,200
<i>Public Charge Events</i>	36,920	63,480	39,810	37,670	70,750	79,380
<i>Public Stations</i>	1,520	2,090	1,690	1,580	2,160	2,320
Workplace L2 EVSE						
<i>Plug Count</i>	6,660	9,530	8,020	8,550	18,520	23,920
<i>Avg Events/Plug</i>	1.2	1.4	1.2	1.2	1.2	1.2
<i>Avg Plugs/Station</i>	7.6	8.0	8.2	7.7	10.3	10.9
<i>Avg Plugs/1000 PEVs</i>	40	34	41	46	55	57
Public L2 EVSE						
<i>Plug Count</i>	4,840	8,300	5,330	5,770	10,310	11,540
<i>Avg Events/Plug</i>	1.5	1.5	1.3	1.2	1.3	1.4
<i>Avg Plugs/Station</i>	3.2	4.0	3.2	3.7	4.8	5.0
<i>Avg Plugs/1000 PEVs</i>	29	30	27	31	31	28
Public DCFC						
<i>Plug Count</i>	4,110	5,860	5,080	4,380	7,620	7,770
<i>Avg Events/Plug</i>	7.2	8.7	6.5	7.0	7.5	8.2
<i>Avg Plugs/Station</i>	2.7	2.8	3.0	2.8	3.5	3.3
<i>Avg Plugs/1000 PEVs</i>	25	21	26	23	23	19

Conclusions

Significant investments are currently being made in PEV charging infrastructure. These investments are occurring in parallel with the evolution of urban mobility. EVI-Pro has been integrated with POLARIS and BEAM to estimate infrastructure requirements supporting transportation electrification. This integration has included:

- POLARIS undergoing significant capability enhancements to accurately represent EV energy consumption using machine learning and represent EV charging (residential and public).
- BEAM/EVI-Pro charging behavior logic compared with a high degree of similarity.
- Implementation of human and CAV electric ride-hailing fleets within BEAM.
- Data exchanges between POLARIS, BEAM, and EVI-Pro to generate a hypothetical charging networks for the SMART Mobility Workflow Scenarios.

References

1. Wood, E., Raghavan, S., Rames, C., Eichman, J., and Melaina, M. “Regional Charging Infrastructure for Plug-In Electric Vehicles: A Case Study of Massachusetts” NREL/TP-5400-67436, January 2017, <https://www.nrel.gov/docs/fy17osti/67436.pdf>
2. Wood, E., C. Rames, M. Muratori, S. Raghavan, S. Young, 2018. *Charging Electric Vehicles in Smart Cities: An EVI-Pro Analysis of Columbus, Ohio*, NREL Technical Report NREL/TP-5400-70367, Available at: <https://www.nrel.gov/docs/fy18osti/70367.pdf>
3. Bedir, A., N. Crisostomo, J. Allen, E. Wood, C. Rames, 2018. *California Plug-In Electric Vehicle Infrastructure Projections: 2017-2025*, CEC Staff Report CEC-600-2018-001, Available at: <https://www.nrel.gov/docs/fy18osti/70893.pdf>
4. Moniot, M., Rames, C., and Wood, E., 2019 “Meeting 2025 Zero Emission Vehicle Goals: An Assessment of Electric Vehicle Charging Infrastructure in Maryland” NREL Technical Report NREL/TP-5400-71198, Available at: <https://www.nrel.gov/docs/fy19osti/71198.pdf>
5. Wood, E., Rames, C., Muratori, M., Raghavan, S., Melaina, M. “National Plug-In Electric Vehicle Infrastructure Analysis” Report from the US DOE Office of Energy Efficiency and Renewable Energy, September 2017, <https://www.nrel.gov/docs/fy17osti/69031.pdf>
6. Tal, G., Lee, J.H., Nicholas, M.A. “Observed Charging Rates in California” University of California Davis Research Report – UCD-ITS-WP-18-02, September 2018, <https://escholarship.org/uc/item/2038613r>

I.6.5 Transportation System Control for Taxi/TNC Simulations (ANL, LBNL)

Joshua Auld, Principal Investigator

Argonne National Laboratory
9700 South Cass Avenue, Building 362
Argonne, IL 60439
E-mail: jauld@anl.gov

Colin Sheppard, Principal Investigator

Lawrence Berkeley National Laboratory
1 Cyclotron Road, Building 90
Berkeley, CA 94720
Email: colin.sheppard@lbl.gov

Prasad Gupte, DOE Technology Manager

U.S. Department of Energy
Phone: (202) 287-5688
E-mail: prasad.gupte@ee.doe.gov

Start Date: October 1, 2018

End Date: September 30, 2019

Project Funding (FY19): \$900,000

DOE share: \$900,000

Non-DOE share: \$0

Project Introduction

Mobility services mediated by cell-phone applications became a convenient and affordable transportation mode in recent years. Uber and Lyft are two common examples of Transportation Network Companies (TNC) that offers point to point transportation on demand. With the emergence of fully automated vehicles, TNC may play an important role and can become the primary transportation mode for households (supplanting personally owned vehicles). This project aims to integrate TNC's agents into the POLARIS and BEAM agent-based framework packages in order to evaluate the impacts of on-demand mobility services in a variety of scenarios including fleet size, matching algorithms, and the possibility of ride-sharing. The developed models can then be used to evaluate the impacts of such services on mobility, congestion, and energy consumption. Also, the complete simulation model can also be used to evaluate management strategies related to TNC services such traveler-vehicle matching strategy, repositioning algorithms, and pooling incentives.

Objectives

The TNC Simulation environment developed on this project has the following goals:

- Evaluate the energy impacts of current and future TNC's under different management strategies and scenarios.
- Assess the potential shortcomings of TNC's. In particular, such services has the potential to induce more demand due to empty or unproductive trips associated with the pick-up trips of these services.
- Evaluate the impacts of different algorithms in terms of operational metrics including traveler waiting time, empty vehicles-miles-traveled (VMT) under different matching algorithm and policy (with and without pooling) and fleet sizes.
- Develop algorithms for matching that achieves satisfactory performance and computationally fast so that it can be used in large-scale metropolitan area simulations.

Approach

POLARIS Framework:

The approach adopted is extending the POLARIS framework to handle TNC operation. This is achieved by implementing two modules on POLARIS framework, one for handling the vehicle operation and another for the TNC fleet operation. Figure I.6.5.1 depicts the schematic of the modules associated to TNC operation. The

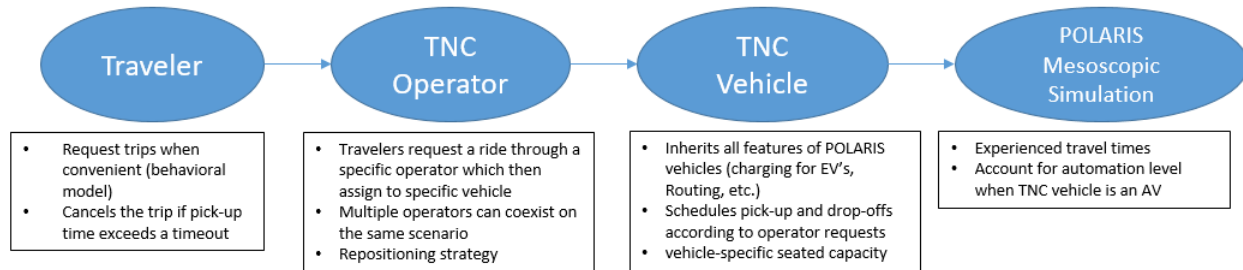


Figure I.6.5.1 Modules associated with TNC Operation in POLARIS

traveler and the POLARIS Mesoscopic Simulation are modules that had already been featured in POLARIS. The TNC operator is responsible to handle incoming requests to an available vehicle in the network. Additionally, especially for operation with autonomous vehicles, the operator is also responsible to balance demand (number of requests on a specific area) and supply (number of vehicles able to serve requests in that area). This is done by requesting repositioning trips for vehicles in low demand areas into high demand areas so that reducing the waiting time of forthcoming requests. POLARIS allows for multiple operators to coexist on the same simulation. The TNC vehicle is the component responsible to perform the pickup and dropoff trips on the requested order assigned by the TNC operator. The TNC vehicle also embeds the appropriate driving behavior according to the scenario specification. For example, some scenarios may allow repositioning trips by drivers from low to high demand areas and cancellation of pick-up trips that had just started that was reassigned to another vehicle. In addition, the TNC vehicle inherits all the features embedded in POLARIS related to electric vehicles and traffic flow impact of AV, e.g., Cooperative Adaptive Cruise Control (CACC).

BEAM Framework:

BEAM simulates the operation of TNC fleets in detail, allowing the model to determine an equilibrium between TNC supply and demand that is sensitive to variations in traveler value of time, ride hail fleet automation and charging requirements, road network speeds, and the spatial distribution of travel demand. Human TNC vehicle drivers are assumed to follow shifts that average about four hours in duration and roughly coincide with the temporal distribution of travel demand, while automated TNC vehicles are assumed to be available all day except when they are charging. TNC ride pricing is modeled as having a fixed component, a distance component, and a time component, with parameters estimated from TNC operations data published by the City of Chicago. Driverless TNC vehicles are assumed to be priced without a time component, lowering prices perceived by travelers due to lower labor costs for operators. Idle TNC vehicles are matched with trip requests using an adaptation of the Alonso-Mora pooling algorithm, which prioritizes maximizing vehicle occupancy while constraining the added waiting and travel time associated with forming pooled itineraries. Idle ride hail vehicles are modeled as probabilistically deciding to relocate to areas with higher demand, with the likelihood of rebalancing calibrated to bring the proportion of empty TNC vehicle miles traveled in Baseline in line with observed values.

BEAM also simulates the impacts of the different levels of vehicle automation between the different vehicle technologies cases. In the TNC fleet, fully automated vehicles are assumed to operate all day rather than in shifts, increasing the effective size of the TNC fleet but sometimes leading to oversupply in off-peak periods. Privately owned fully automated vehicles are assumed to be shared among family members, with each CAV's schedule optimized to maximize its utilization throughout the day. Vehicle automation also impacts traffic

flow, with partially and fully automated vehicles simulated as participating in Cooperative Adaptive Cruise Control (CACC), increasing road capacity as the portion of CACC-equipped vehicles increases.

Results

We present here two different studies in which the TNC module was used. In the first part we present the specific TNC results as part of the set of scenarios part of the Workflow in the Chicago Metropolitan Area. In the following subsection we present results of a sensitivity analysis of TNC operation with respect to both demand and supply aspects.

POLARIS Workflow Results:

In the context of the Workflow of the SMART program, a set of exploratory scenarios were designed to assess future impacts of emerging technologies on urban mobility. Along with the baseline scenario, six different scenarios of Chicago Metropolitan Area were simulated using the POLARIS framework. Figure I.6.5.2 depicts key TNC metrics. All scenarios yield more TNC trips compared to baseline. Scenarios A and C having twice as much as the baseline while scenarios B low and high have around 5 times more TNC trips compared to the baseline scenario. All other key metrics scale roughly at the same proportion as the number of trips.

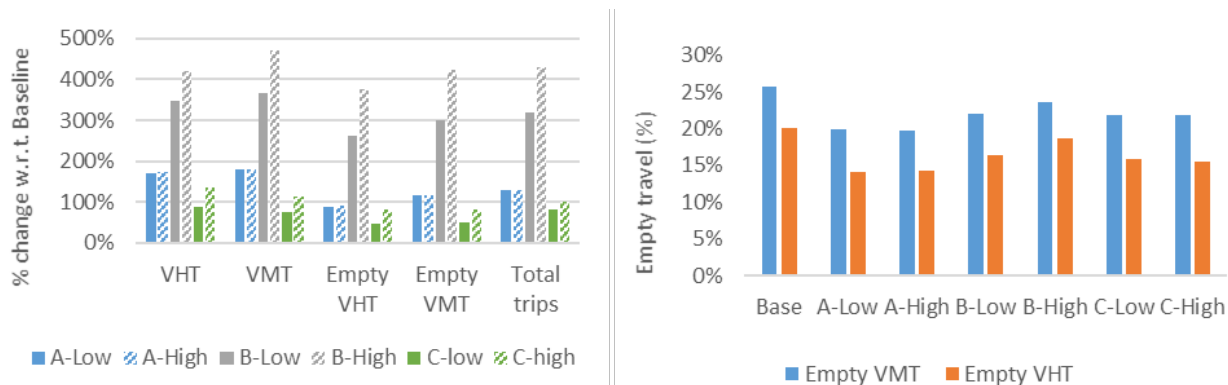


Figure I.6.5.2 TNC Results (a) Change in key TNC metrics from baseline (b) share of empty miles and travel hours

A particular concern of TNC operation is distance traveled without carrying any passenger or miles traveled that would not exist with travelers driving their own vehicles. With TNC, the pickup trips are the source of these unproductive miles. Figure I.6.6.2 Figure I.6.5.2 depicts the shares of VMT and VHT on pickup trips across all the scenarios. In all scenarios, the share of empty VMT remained between 20% and 25% while the VHT share stays between 15% and 20%. As the key finding of these scenarios, the simulations are consistent with previous research that had found that one Autonomous Vehicle of shared use can replace around 10 household vehicles.

POLARIS Large-scale Demand and Supply Sensitivity Analysis:

In this study, the POLARIS framework is used to analyze concurrently the effects of both demand and supply for TNC. On the demand side, a vehicle ownership model is used at the household level to distribute vehicles based on household characteristics. A vehicle fleet distribution model determines the percentage of human-driven vehicles and AVs in the simulation. On the supply side, trip travel times and congestion effects are an outcome of the mesoscopic traffic assignment model, which also takes care of transit schedules and TNC vehicles for an integrated operations simulation. Fleet sizes of one TNC vehicle for every 25, 35, 50, and 100 residents, were tested for present-day conditions, and two levels of future reduction in vehicle ownership informed by the implemented model. The scenarios tested here are named A1-A4 for smaller change in vehicle ownership in the region, with 1-4 denoting increasing fleet size, or decreasing fleet availability. Similarly, B1-B4 denote the larger change in vehicle ownership that will considerably increase the demand for TNCs. Table

I.6.5.1 reports the average wait time, percent TNC trip requests served, percent of empty VMT (eVMT) and repositioning (rVMT), and average trips made by each TNC vehicle.

Table I.6.5.1 – TNC Fleet Impacts by Size and Demand

Sc.	TNC Availability (1 for X residents)	#TNC Trips per 100 Residents	%eVMT	% rVMT	Avg. Wait Time (min)	% Served Trips
Base	35	10	49.0	36.0	7.9	97.1
A1	100	38	43.0	10.0	13.4	70.5
A2	50		41.4	19.3	9.8	89.6
A3	35		42.3	24.6	8.5	93.7
A4	25		44.6	29.1	8.1	95.6
B1	100	65	44.2	8.1	13.2	50.1
B2	50		40.6	11.0	11.9	79.4
B3	35		39.8	17.2	9.3	90.0
B4	25		40.9	21.7	8.4	93.1

In all scenarios there were unserved trips including the scenarios with low demand and high fleet sizes. Most of the unserved trips occurs at morning peak on the suburban area. Across both future scenarios of change in vehicle ownership, the TNC availability and percent rVMT was seen to be an influential factor in large percent eVMT values. Larger the TNC demand, the more imperative that regions regulate TNC fleet sizes. Small fleets are able to be more efficient with high average trips made per vehicle per day when there is higher demand, serving trips with similar average wait times. This becomes clear in Figure I.6.5.3, which shows the share of vehicles either performing different operations or idling. Figure I.6.5.3a shows the shares for cases A1 and A4, while Figure I.6.5.3b shows the same for scenarios B1 and B4. For the smaller fleets (dashed lines, cases A1 and B1), most of the vehicles are either performing pickup or dropoff trips and the share of idle vehicles are small throughout the day. As the fleet increases, there are more idle vehicles and some of these vehicles are able to perform repositioning trips to other areas of the network.

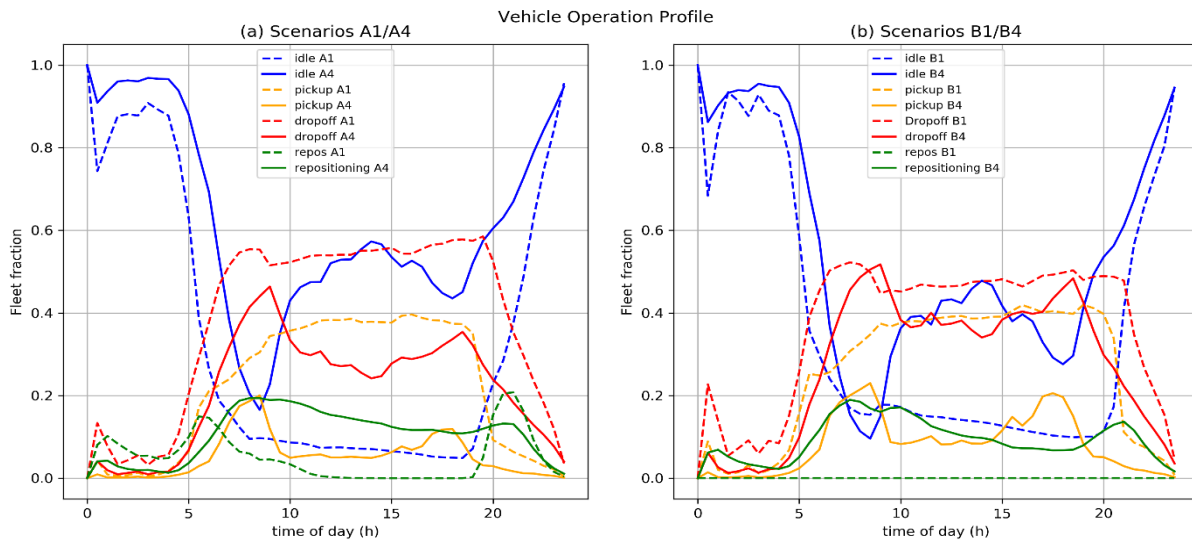


Figure I.6.5.3 Share of vehicles performing pickup, dropoff, repositioning trips or idle by time of day for scenarios (a) A1 and A4, (b) B1 and B4

BEAM Workflow Results:

An overarching finding across scenarios is that increasing ride hail occupancy while maintaining high enough quality service to attract travelers is a fundamentally difficult problem. Scenarios B2 & B3, with large fleets of ridehail vehicles and widespread willingness to share rides, have the highest portion of both empty (no-passenger) vehicle miles and the highest portion of shared miles (Figure I.6.5.4). Scenario B3 has the highest portion of autonomous TNC vehicles, accounting for the majority of the fleet. These vehicles remain on line all day and charge riders a lower price, leading to a greater TNC mode share but a substantial number of empty miles traveled. In calibration, it was found that decreases to the TNC fleet size do reduce the portion of empty miles traveled but also increase wait times, decreasing the attractiveness of choosing the TNC mode and degrading service quality. We expect that ongoing developments to the algorithm that pools TNC riders into shared vehicles and the algorithm that moves TNC drivers to areas of higher demand are likely to increase the number of both shared and empty miles. However, these results suggest that fundamental constraints associated with demand patterns and the willingness of travelers to accept delays will make increasing TNC occupancy from less than one to a value significantly greater than one unlikely. Therefore, improved TNC matching and rebalancing algorithms are unlikely to reduce total energy use by a substantial margin.

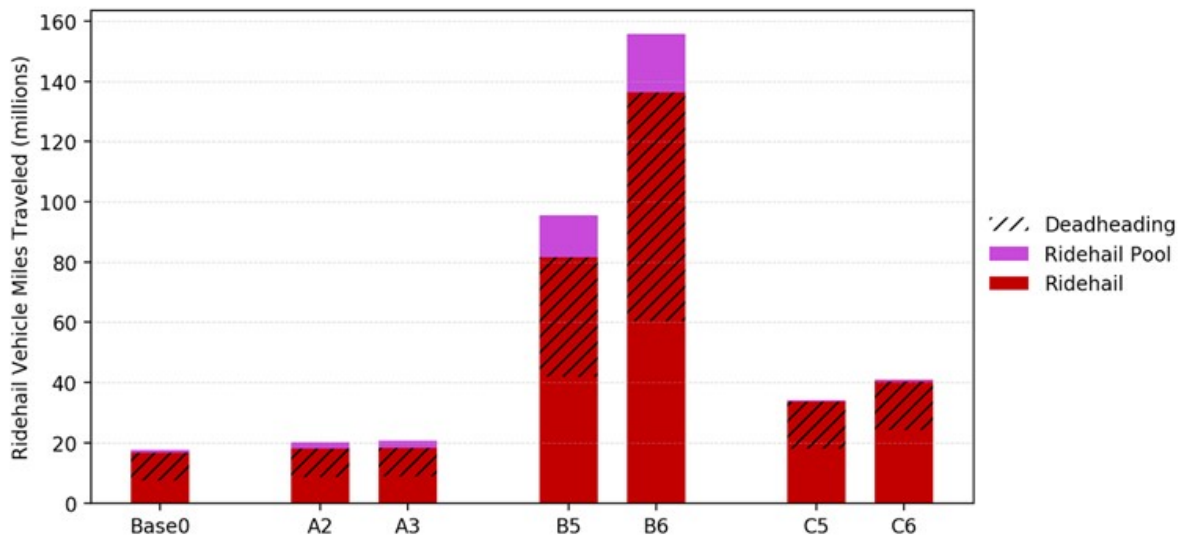


Figure I.6.5.4 Vehicle miles traveled by TNC's for the San Francisco Bay Area across the workflow scenarios, differentiating between miles without a passenger (hatched) and miles with multiple passengers (blue).

The appropriate TNC fleet size is determined by trade-offs between wait times and fleet utilization that differ between scenarios. Differences in TNC fleet performance are also driven by variations in valuation of travel time across scenarios. For a given fleet composition and size, the number of ride hail trips served exists in an equilibrium with wait times that is tuned by pricing and generalized time. Varying an input that serves to increase demand for ride hail trips will increase the utilization of the TNC fleet, decreasing the number of idle vehicles that can be matched with new requests and therefore increasing average wait times. This increase in wait times makes ride hail less attractive and serves to partially but not fully counteract the initial increase in TNC use. In Scenario A, lower costs and increased acceptance of shared rides means that travelers are more willing to put up with longer wait times and still take TNC trips (Figure I.6.5.5). In Scenario B, the proliferation of automated TNC vehicles allows for higher availability and utilization of the TNC fleet, an effect that serves to drive down wait times. In Scenario C, travelers prefer not to share rides, and so this increase in perceived cost of ride hail trips means that utilization needs to be less and wait times need to be lower in order for ride hail trips to be competitive.

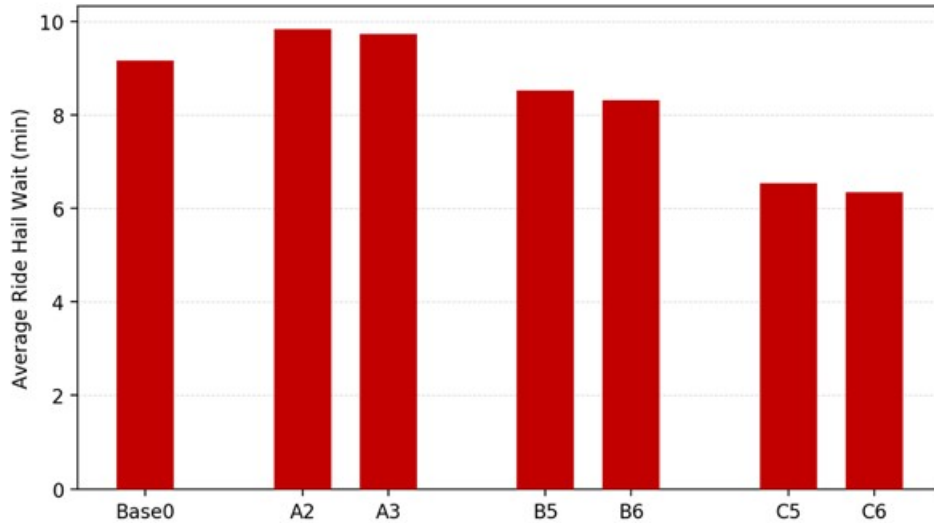


Figure I.6.5.5 Average wait times for TNC trips across the workflow scenarios.

Conclusions

A module for simulating TNC operation was developed on top of the POLARIS agent-based framework. The module is flexible so it can be employed to analyze current day TNC operation with human-driven vehicles as well as fleets of shared autonomous vehicles (SAV's). The key distinction to other tools for TNC simulation is combining explicit models of demand and supply in the framework. Therefore, we are able to simulate the interaction between the TNC supply (fleet size), demand (TNC cost, availability of other modes, etc.) and network congestion in the same platform. Results of three different studies were presented. In the context of Workflow scenarios, it was found that the share of empty VMT and VHT stays around 20%. Also, in all future scenarios with reduced vehicle ownership, one TNC vehicle can replace around 10 household vehicles. The geofencing experiment results shows that constraining TNC operation into the suburban core can lead to operation benefits with more trips being served with lower waiting time for travelers. Finally, in the sensitivity analysis with varying demand and supply, we found that even at scenarios with low demand and high TNC availability presents a small share of unserved trips. The unserved trips mostly occur on the low-density suburbs. In ongoing research, we are integrating different assignment and repositioning algorithms into the framework and dynamic ride sharing.

BEAM simulates the operation of TNC fleets in detail, allowing the travel demand model to determine an equilibrium between TNC supply and demand that is sensitive to variations in traveler value of time, ride hail fleet automation and charging requirements, road network speeds, and the spatial distribution of travel demand. We find that there is a fundamental tension between increasing vehicle occupancy of ride hail fleets and decreasing overall VMT. As more customers seek pooled rides, the wait times and overall travel delays increase which limit uptake by other customers. In addition, empty vehicle miles traveled also increase which counteract the benefits of pooling. More analysis is necessary to explore these dynamics across a wider range of scenarios and with more strategies to optimize fleet operations.

Key Publications

Gurumurthy, K.M., de Souza, Felipe, Enam, Annesha, Auld, Joshua. A Large-Scale Simulation of Shared Autonomous Vehicles: Integrating the Supply and Demand Perspectives. Accepted for Transportation Research Board Annual Meeting, 2020.

{Publications published as a result of this project/funding.}

I.6.6 BEAM (LBNL)

Colin Sheppard, Principal Investigator

Lawrence Berkeley National Lab
1 Cyclotron Road
Berkeley, CA 94720
E-mail: colin.sheppard@lbl.gov

Prasad Gupte, DOE Technology Manager

U.S. Department of Energy
E-mail: prasad.gupte@ee.doe.gov

Start Date: October 1, 2018

End Date: September 30, 2019

Project Funding (FY19): \$500,000

DOE share: \$500,000

Non-DOE share: \$0

Project Introduction

The objective of the Smart Mobility Modeling Workflow is to evaluate new transportation technologies such as connectivity, automation, sharing, and electrification through multi-level system analysis to consider the interactions between technologies. An integrated approach that considers multiple levels of fidelity is required to understand the impacts of new mobility technologies and services at scale:

- At the individual vehicle level, detailed models are required to represent powertrain component technologies and control algorithms across powertrain and vehicle classes.
- Micro-simulation models that represent tens of thousands of vehicles can then be used to quantify the impact of those new controls on traffic flow based on specific demands.
- Mesoscopic transportation system models are used to model travel behavior and assess the impact of hundreds of thousands or millions of travelers' individual decisions on systemwide outcomes.

A dedicated workflow integrating multiple models across different levels of fidelity was developed to understand and quantify the impact of new mobility technologies at the system level. This report describes the Behavior, Energy, Autonomy, and Mobility (BEAM) model and how it was used within the context of the SMART mobility workflow to analyze the complex feedbacks between transportation supply and demand.

Objectives

By simulating the choices of travelers and performance of the transportation system in these scenarios, the BEAM model approximates an equilibrium outcome that captures many of the complex interaction that determine regional travel patterns. BEAM incorporates complicated constraints on mobility associated with personal schedules, vehicle technology, the transport network, and operational realities of different modes. This allows the evaluation of the feasibility of different potential futures and better understand of the directionality and relative magnitude of the relationship between different technology and policy developments and system wide outcomes.

Approach

CAVs / CACC Integration into BEAM

BEAM simulates the impacts of the different levels of vehicle automation between the different vehicle technologies cases. In the TNC fleet, fully automated vehicles are assumed to operate all day rather than in shifts, increasing the effective size of the TNC fleet but sometimes leading to oversupply in off-peak periods. Privately owned fully automated vehicles are assumed to be shared among family members, with each CAV's schedule optimized to maximize its utilization throughout the day. Vehicle automation also impacts traffic

flow, with partially and fully automated vehicles simulated as participating in Cooperative Adaptive Cruise Control (CACC), increasing road capacity as the portion of CACC-equipped vehicles increases .

Land Use and UrbanSim Coupling

BEAM is coupled with the land use model UrbanSim to generate activity patterns for travelers and model how changes in transportation network performance interact with changes in development patterns. Starting with current demographic data, the UrbanSim submodel ActivitySynth produces a set of work activity locations and start and end times for the synthetic population of the San Francisco Bay Area. This population and its plans are used as inputs into BEAM, which simulates travel behavior and transport network performance until the system converges. As part of its mesoscopic simulation, BEAM produces a set of transportation network skims that measure the generalized time and cost associated with trips between different origins and destinations on the network. UrbanSim uses these skims to estimate the accessibility and desirability of different locations for housing and firm development and location.

Mobility Energy Productivity (MEP) Integration

New technologies influence many metrics across a metropolitan area, including energy, productivity, mobility, affordability. The MEP metric was developed by NREL to evaluate mobility options in a given area with respect to time, cost, and energy. The metric measures accessibility and appropriately weights it with travel time, cost, and energy of modes that provide access to opportunities in any given location. The MEP code was customized to use data provided by BEAM and UrbanSim in order to produce results for the San Francisco Bay Area.

Vehicle Energy Consumption

BEAM incorporates vehicle technology in multiple ways, allowing for a thorough picture of the impact of changes in vehicle technology on a transportation system. BEAM simulates trip-dependent vehicle energy consumption using the Route-E model, capturing how the impact of trip characteristics on energy use can vary by powertrain type. Calculating vehicle energy consumption on the fly during simulation using RouteE also allows us to model electric vehicle charging requirements, an issue that is especially important for electric TNC vehicles, where the number of refueling stops depends on the battery capacities determined by ADOPT that vary by technology scenario.

Scenarios

Transportation systems are currently influenced by major trends including connectivity, automation, sharing and electrification. Within each trend, a large number of technologies (e.g., partial vs full automation) and market penetrations are possible. In addition, each trend influences the entire system (e.g., full electrification of shared fleets would lead to different vehicle usage, charging requirements, etc.). While the overall objective of the SMART Mobility Consortium is to quantify the impact of each individual technology and their combination at the system level, a limited number of scenarios were selected to highlight some of the key parameters influencing traffic flow, travel behavior and system control.

As shown in Figure I.6.6.1, in addition to the baseline, three main scenarios were selected:

- Scenario A: This scenario models potential near future timeframe characterized by high-sharing (i.e., TNC) and penetration of partially automated vehicle technologies (e.g., advanced driver assistance systems). Scenarios A2 and A3 represent business as usual vehicle technology development and VTO target success, respectively.
- Scenario B: This scenario represents a long-term future timeframe where fully automated vehicles (i.e., driverless) are owned by shared fleet operators. It is a high-sharing case with high penetration of full AV (i.e., auto-taxis). Scenarios B5 and B6 represent business as usual vehicle technology development and VTO target success, respectively.

- Scenario C: Similar to Scenario B, this scenario represents a long-term future timeframe with fully automated vehicles. In this case, however, those are owned by individuals and shared within the household. It is a low sharing case with high full AV penetration (i.e., privately owned AV). Scenarios C5 and C6 represent business as usual vehicle technology development and VTO target success, respectively.

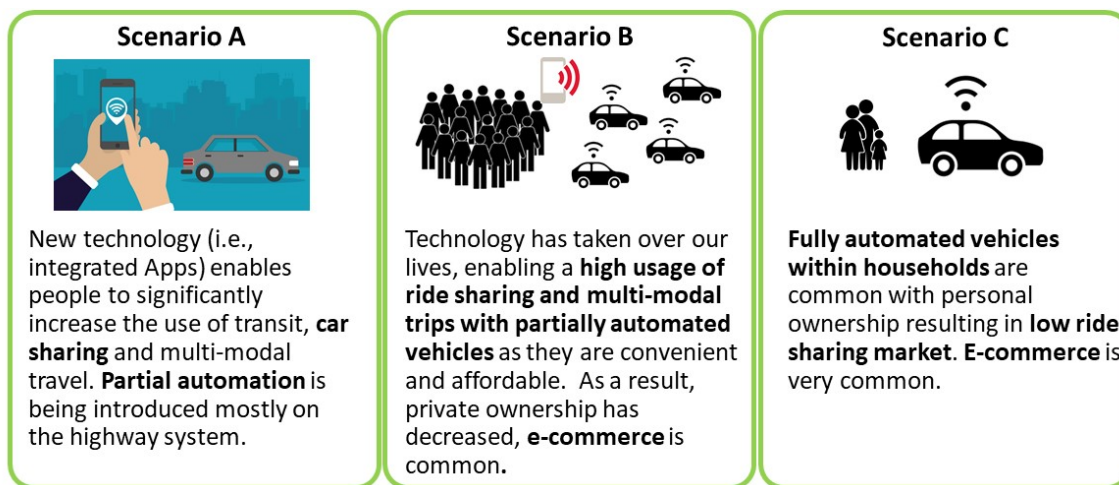


Figure I.6.6.1 High Level Scenario Description

Results

Simulations of the San Francisco Bay Area for the scenarios start from different assumptions related to travel preferences and levels of technology advancement, leading to different outcomes in terms of overall mobility patterns, aggregate energy consumption, and MEP. The results highlighted in the workflow consider passenger travel but do not include freight. The key metrics related to mobility (Vehicle Miles Traveled (VMT) & Passenger Miles Traveled (PMT)) and energy use for passenger travel for each scenario are shown in Table I.6.6.1.

Table I.6.6.1 Differences in various aggregate metrics from baseline across the Workflow Scenarios.

Metric	Base0	A2 / Base0	A3 / Base0	B5 / Base0	B6 / Base0	C5 / Base0	C6 / Base0
Population (millions)	6.83	14%	14%	19%	19%	19%	19%
VMT (million miles)	324	5%	5%	12%	17%	25%	25%
VMT/capita (miles)	47	-8%	-8%	-6%	-2%	5%	5%
PMT (million miles)	332	10%	10%	17%	22%	25%	25%
PMT/capita (miles)	49	-3%	-3%	-2%	2%	5%	5%
Average Speed (mi/h)	43	-4%	-5%	-8%	-5%	-11%	-10%
Energy (MJ/Cap)	139	-20%	-35%	-32%	-44%	-28%	-49%
Vehicle Energy (TJ)	949	-8%	-26%	-19%	-33%	-14%	-39%
MEP	15804	35%	39%	83%	87%	140%	220%
Personal Car Ownership	100%	-45%	-45%	-68%	-75%	-15%	-20%
Avg. VOTT Factor	1.19	-33%	-33%	-6%	-3%	-20%	-28%

Valuations of travel time (Figure I.6.6.2) and household vehicle ownership (Table I.6.6.1) assumptions are the main drivers of variation in mode share (Figure I.6.6.3) across scenarios. The Base0 scenario represents current travel patterns in the San Francisco region, with over 70% of trips taken by car. In the Scenarios A2 and A3, travelers rely on non-motorized modes for almost three times as many trips, and more than twice the proportion of ride hail trips are requested as pooled. Despite these differences, the majority of trips are still taken in personally owned cars due to their continued dominance in cost and travel time—which stays low due to mode shift to non-motorized modes—showing how the region’s built environment and transit infrastructure constrains potential changes in travel behavior. In Scenarios B5 and B6, changes to modal split are more dramatic. Lower personal vehicle ownership and a larger ride hail fleet drive many travelers to replace trips in personally owned vehicles with trips in ride hail vehicles. The greater availability of automated CAVs and associated cheaper fares in B5 further increases ride hail mode share, also providing increase first- and last-mile connections to transit trips. In the scenarios C5 and C6, human-driven car trips from the Base0 scenario are replaced by a combination of household-owned CAV trips and ride hail trips. Of the ride hail trips, fewer are pooled.

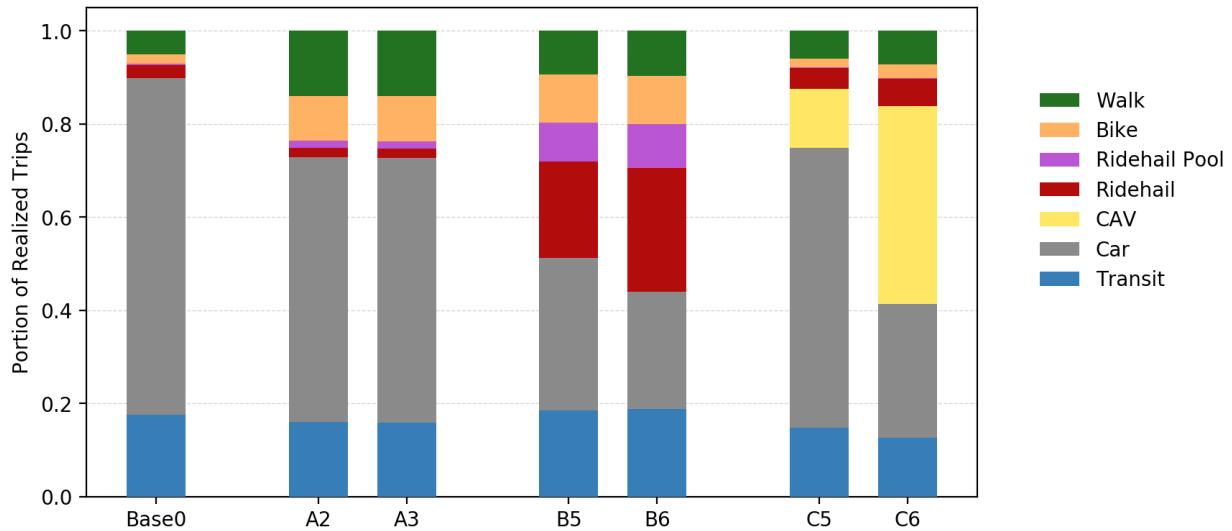


Figure I.6.6.2 Modal Market Shares for the San Francisco Bay Area across Scenarios.

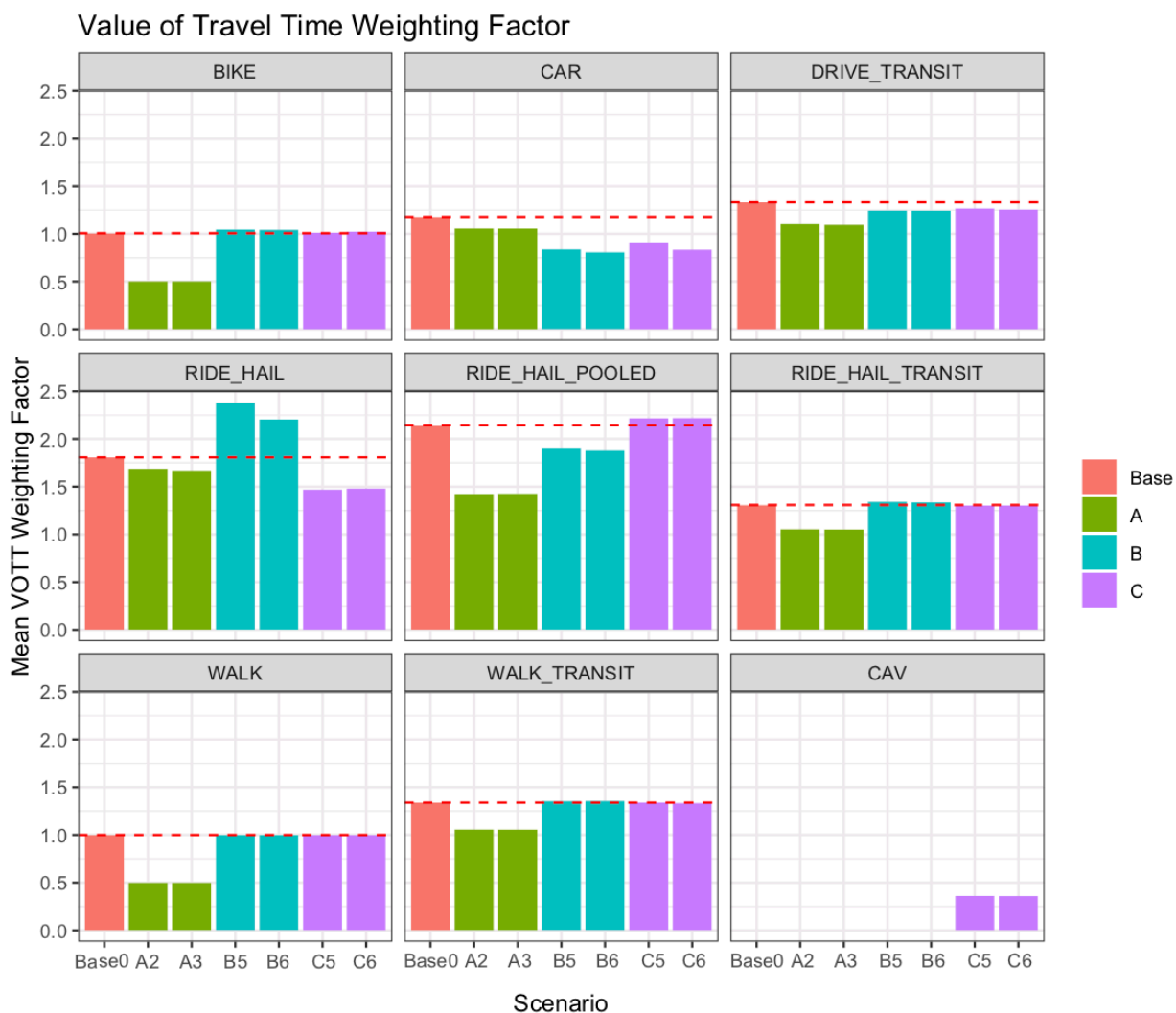


Figure I.6.6.3 Context-specific value of travel time (VOTT) weighting factors averaged over all trips for each mode, across the workflow scenarios. Because travel time is undesirable, lower VOTT factors make a mode more attractive, leading to higher modal shares as well as higher MEP which is based on generalized travel time

MEP scores are strongly tied to road network congestion and value of travel time (VOTT) assumptions. Passengers in personal CAVs in C are willing to put up with slow trips on heavily-utilized roads, increasing congestion and reducing aggregated accessibility and MEP in highway-dependent areas.

Across all of these scenarios with different land use, travel behavior, and vehicle technology assumptions, MEP provides a quantitative method for weighing different costs and benefits associated with different travel patterns. An increase in MEP over the baseline was observed for all of the workflow scenarios simulated (Figure I.6.6.3), ranging from a 35% increase for A2 to a 220% increase for Scenario C6. Increases in MEP are the most substantial in the Scenario C5 and C6, assuming both BAU and VTO technology. This is due in large part to increases in accessibility associated with much lower VOTT for travelers using private owned CAVs (Figure I.6.6.4). This suggests that increased willingness to endure congested highway trips by some owners of partially or fully automated vehicles in C6 could be having disproportionately positive impacts of aggregate accessibility on the transport network. Within the other workflow scenarios, meeting VTO goals is found to increase MEP in every case, due in large part to higher energy efficiency of the light duty fleet and an increase in automation throughout the system.

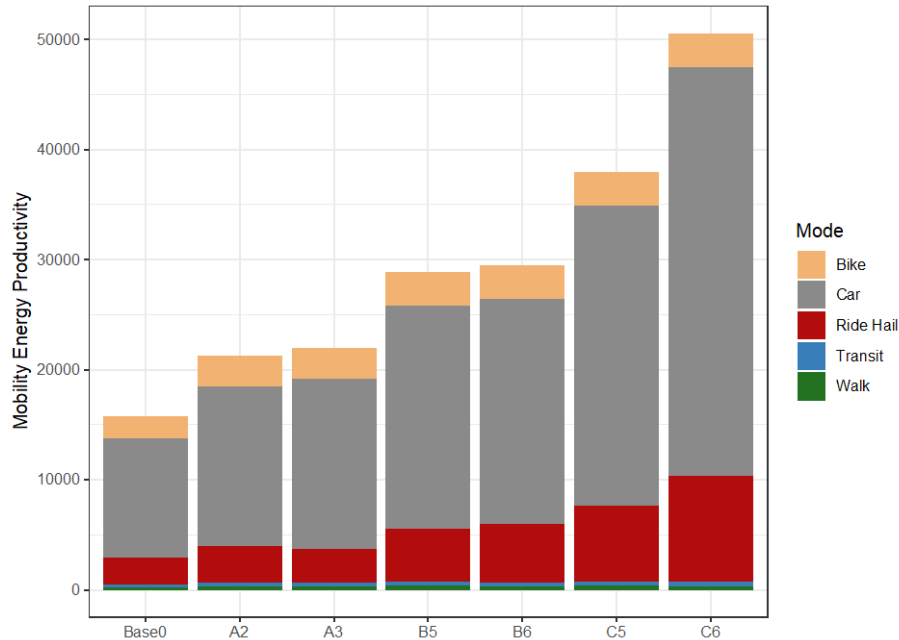


Figure I.6.6.4 Aggregate MEP values for the workflow scenarios disaggregated by mode

Conclusions

Through the addition of new features and a direct integration with the Urbansim land use model, BEAM is able to capture many of the factors that influence regional travel patterns. This workflow models processes happening at vastly different time scales, from land use and development, workplace and household location, and household vehicle ownership decisions, to the charging requirements of an electric TNC fleet, parking constraints in downtown areas, the impact of CACC on traffic flow, and traveler decisions between many potentially multi-modal travel options. Coupling all of these features together and then simulating a broad and comprehensive set of scenarios brings value in several ways. These simulations allow us to assign numerical estimates to expected outcomes, such as finding that achieving the VTO technology goals can be expected to reduce energy consumption by approximately 20-50%. They allow us to make directional predictions, for example that achieving VTO goals will lead to a larger decrease in energy consumption in a future with less emphasis on shared modes and more private vehicle ownership.

Acknowledgements

The following individuals and teams contributed to the results presented in this report: DOE Vehicle Technologies Office: Energy Efficient Mobility Systems Program including David Anderson, Erin Boyd, Prasad Gupte, and Heather Croteau. The BEAM Development and Research Team: Colin Sheppard, Rashid Waraich, Zachary Needel, Haitam Laarabi, Sid Feygin, Michael Zilske, Cong Zhang, Robert Fitzgerald, Johannes Hiry, Andrew Campbell, Zeeshan Bilal, Muhammad Asif, Art Balayan, Justin Pihony, Rajnikant Sharma, Bhavya Latha Bandaru, Kirill Mitin, Carlos Caldas, David Arias, Denis Serdyuk, Salman Abdul Waheed. LBNL collaborators: Tom Wenzel, Anna Spurlock, Annika Todd, Tom Kirchstetter, Mike Mills. UC Berkeley: Paul Waddell, Max Gardner, Tim Lipman, Xiao-Yun Lu, Alex Bayen, Joan Walker, Hongcai Zhang, Teng Zheng, Gordon Bauer. SMART Mobility: NREL (Jeff Gonder, Aaron Brooker, Jake Holden, Eric Wood, Stan Young, Venu Garikapati, Chris Gearhart), INL (John Smart, Zonggen Yi), ANL (Aymeric Rousseau, Josh Auld)

II High Performance Computing and Big Data

II.1.1 HPC-Enabled Deep-Learning and Simulation for AV Development (ORNL, NREL)

Robert Patton, Principal Investigator

Oak Ridge National Laboratory
PO Box 2008
Oak Ridge, TN 37831
E-mail: pattonrm@ornl.gov

Peter Graf, Principal Investigator

National Renewable Energy Laboratory
15013 Denver West Parkway
Golden, CO 80401
E-mail: peter.graf@nrel.gov

Erin Boyd, DOE Technology Manager

U.S. Department of Energy
E-mail: erin.boyd@ee.doe.gov

Start Date: October 1, 2018

End Date: September 30, 2019

Project Funding (FY19): \$1,984,000

DOE share: \$1,984,000

Non-DOE share: \$0

Project Introduction

DOE's most powerful and innovative High Performance Computing (HPC) resources will be applied to the challenge of developing efficient and safe perception and control algorithms for autonomous vehicle operation in a greatly expedited process. The core approach will be first to conduct deep-learning analysis of vehicle sensor data sets with new methods such as ORNL's MENNDL, using high performance computing, to accelerate the discovery of efficient analysis and control algorithms. A second phase will develop a virtual environment to test the algorithms for millions of scenarios and miles in faster than real time simulations. This virtual environment will be developed with support of human- and hardware-in-the-loop systems. Additional benefits will be derived from adapting the analytics methods to prognostics of truck and car electronic systems (whether autonomous or not) for vehicle "self-awareness" regarding fuel efficiency and cyber security.

Objectives

This project seeks to achieve the following objectives: 1) increase affordability, convenience, safety, and energy productivity of mobility, 2) reduce transportation fuel use/GHG emissions, 3) validate safety of automated vehicles through accelerated simulation environments, and 4) explore and validate innovative vehicle control strategies at the system level.

To demonstrate the achievement of these objectives, this project will:

- Demonstrate HPC-based ability to analyze large data sets from prototype self-driving vehicles and discover higher performance and resilient operating algorithms in an expedited cadence.
- Develop and demonstrate new machine learning based algorithms for vehicle operating controls that are capable of scaling to "Level 5" autonomous vehicle capabilities.
- Develop a virtual test environment capable of safely evaluating autonomous vehicle operating controls over millions of miles and scenarios/environments expected to be encountered. There is expected

applicability to advanced conventional vehicles by examining electronic controls for powertrain functions.

Questions to be addressed:

1. How do we leverage machine learning for perception and control of a single autonomous vehicle given the constraints / objectives of safety, destination arrival, and energy efficiency? (FY19)
2. How do we leverage machine learning for perception and control of multiple autonomous vehicles given the constraints / objectives of safety, destination arrival, and energy efficiency? (FY20)
3. How do we leverage machine learning for perception and control of multiple autonomous vehicles in a connected environment given the constraints / objectives of safety, destination arrival, and energy efficiency? (FY21)

Approach

The work described here uses the CARLA simulator. CARLA is an open source urban driving simulator that uses the Unreal Engine 4 for rendering and simulation dynamics. CARLA provides RESTful type application programming interfaces (APIs) that enable researchers and developers to create autonomous driving systems and evaluate their behavior. These APIs allow for controlling a vehicle's steering, braking, and acceleration as well as defining the environment in which to drive. This enables the machine learning community to focus on the development of the automated system. Further, multiple towns are available for use wherein each town provides a different network of roads with a range of differences such as the lane width, lane markings, curvature of turns, etc. In addition to multiple towns, the APIs allow for changing other scenario variables such as the weather conditions, time of day, traffic and pedestrian volume, etc. Thus, the number of scenario combinations on which to train and test an automated system is extremely large although many of those combinations would not provide sufficient variation for training purposes if used in the same training set (e.g., keeping all scenario variables the same except changing the time of day by one minute). This range of scenario combinations helps to evaluate how well a particular machine learning technique can generalize its driving behavior to scenarios on which it has not been trained.

The work described here draws inspiration from many of the prior works and combine them into a coherent framework. Further, this work attempts to address shortcomings of many prior works such as inadequately describing data sets. For example, prior works simply say that their work uses X hours of driving data from a human expert. However, there is no further description of the data, the expertise of the human, nor is the data set available for others.

This work provides the following contributions: 1) for IL, we demonstrate the use of non-expert, non-human data derived from another machine for IL training, 2) a description of how to collect and augment the IL training data, 3) a description of a virtual driver's test for evaluating neural network driving behavior, 4) the development of an OpenAI Gym environment for CARLA that supports the use of a single server using multi-scenarios for parallel reinforcement learning (RL) training, and 5) quantitative evidence (not previously provided by prior works) to show that IL-accelerated RL provides a significant increase in the convergence speed of a neural network.

Our work leverages a heterogeneous machine learning approach by using imitation learning (IL) to accelerate RL performance. However, our work incorporates inspiration from prior works by leveraging non-expert, non-human data that is derived from the roaming agent within the CARLA driving simulator. Further, our IL training data incorporates lessons learned from prior works by including noise and recovery data within our training set. The goal of our IL approach is to create a trained neural network that works as well as possible under most general driving conditions, and then allow the RL process to fine tune under more specific scenarios, which incorporates lessons learned from prior works. Each of the learning processes can then be iterative via changes to the training data or scenarios to further enhance the neural network driving behavior.

Finally, the respective training processes can be computationally expensive given the search space size of algorithm hyper-parameters and driving scenarios. Consequently, our work has begun to leverage the use of the Department of Energy’s high-performance computing platforms: Oak Ridge National Laboratory’s Summit and National Renewable Energy Laboratory’s Eagle systems. These systems enable the parallel exploration of hyperparameter values as well as the number of driving scenarios to evaluate autonomous driving behavior.

Results

ORNL enhanced the MENNDL system in order to more effectively develop neural network structures for CAV perception. Notably:

- MENNDL can now create more complex network structures to support object detection
- MENNDL can now provide multi-objective optimizations beyond just accuracy to include network size, power, hardware constraints
- MENNDL can now perform layer specific evolution (speciation) in addition to the existing full network evolution capability

ORNL developed an initial synthetic data set to support imitation learning. This data set has the following characteristics:

- 60 hours’ worth of driving data from CARLA driving simulator containing 23.8 million images using 1.7 TB of disk space
- Three camera types (RGB, Semantic Segmentation, Depth), three positions each (Right, Center, Left); Example images shown in Figure II.1.1.1 – Figure II.1.1.3. There are nine images per timestamp, each image is 200 x 90 pixels; brake, steering, throttle values with each timestamped set of images

ORNL developed Conditional Imitation Learning framework:

- Designed system combining convolutional neural network for image processing and vector inputs for additional control.
- Augmented training data with “bad driving and recovery” examples.
- Trained network using supervised learning.
- Verified trained network can drive in simple settings.
- Provided this trained network to NREL for further (RL) training.

NREL developed a Reinforcement Learning (RL) framework to support training for CAV control:

- Constructed AI-gym environment for CARLA; defined and coded state, observation, action, and reward spaces, as well as simple scenarios for training.
- Integrated it with several state-of-the-art reinforcement learning frameworks (RL-lib, spinning-up).
- Implemented, installed, and tested on HPC systems (Figure II.1.1.4).
- Integrating ORNL conditional imitation learning model as pre-trained policy (Figure II.1.1.5).

NREL developed a 2D vehicle simulator and tools to integrate it with both CARLA and microscopic traffic simulator SUMO:

- RL can be inefficient and potentially infeasible when using only high fidelity (i.e., CARLA, 3D) simulators; lower fidelity simulations allow for algorithmic training at orders of magnitude higher throughput; a modular approach to CAVs control increases relevance of 2D model.
- Created K-Road, a 2D AI-gym (Figure II.1.1.6); exercised 2D gym on several standard navigation and obstacle avoidance tasks.
- Integrated 2D AI-gym into microscopic traffic simulator “Simulator of Urban Mobility”, SUMO (Figure II.1.1.7).
- Implemented mechanism to export CARLA town to its 2D equivalent, hybridizing 3D CARLA and 2D K-Road simulators, allowing for expedited combined learning (Figure II.1.1.8).
- Tools that span and allow for RL at a variety of fidelities and directly connect existing simulators (e.g., CARLA, K-Road, and SUMO) provide a rich set of modalities to explore machine learning for CAVs control.

Overall, ORNL / NREL achieved their Go/No Go decision point by developing a rudimentary proof of concept for machine learning framework that is capable of learning to drive a car using the CARLA driving simulator running on a small, multi-GPU machine. ORNL has successfully run their code using a Nvidia DGX2 machine while NREL has successfully run their code on a few nodes of their Eagle supercomputer.



Figure II.1.1.1 Example RGB Image from CARLA
(https://carla.readthedocs.io/en/latest/cameras_and_sensors/)

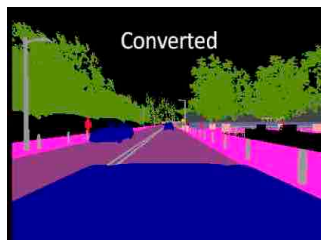


Figure II.1.1.2 Example Semantic Segmented Image from CARLA
(https://carla.readthedocs.io/en/latest/cameras_and_sensors/)

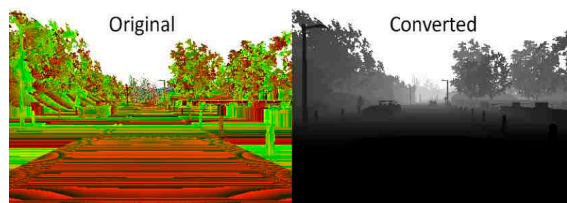


Figure II.1.1.3 Example Depth Images from CARLA
(https://carla.readthedocs.io/en/latest/cameras_and_sensors/)

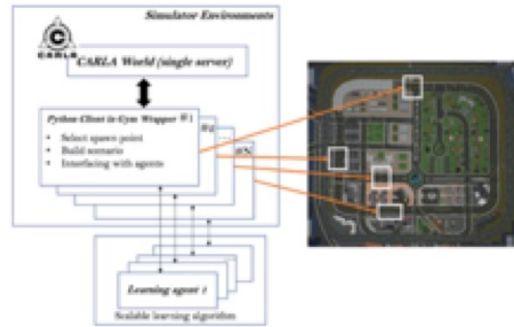


Figure II.1.1.4 Scalable learning architecture for multi-client learning. AI-gym RL framework for CARLA capable of running on large GPU-based HPC systems.

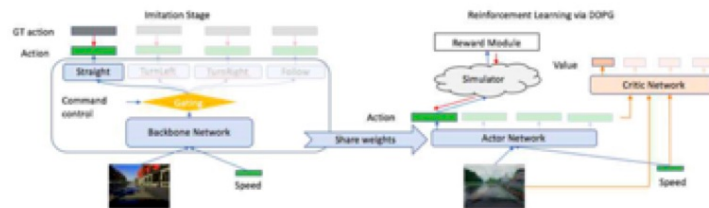


Figure II.1.1.5 Combining imitation learning and reinforcement learning to accelerate vehicle controller training (from [1])

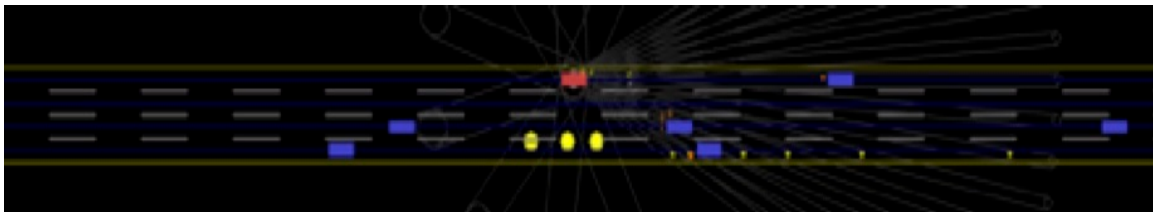


Figure II.1.1.6 2D AI-gym driving simulator. Learning to drive in 2D (with “distance to obstacles” and/or “location of obstacles” as observation) is much faster than learning directly in CARLA

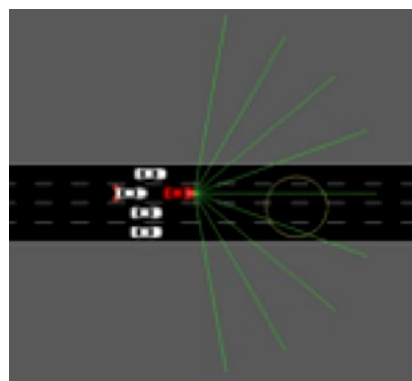


Figure II.1.1.7 SUMO gym environment allows for RL using realistic driving (continuous control) within existing microscopic traffic simulator.

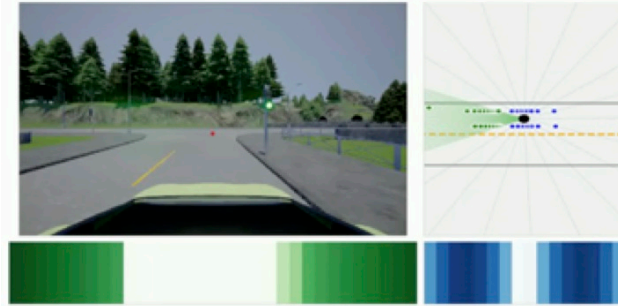


Figure II.1.1.8 Combining simulated driving in 2D and 3D. (top left) Camera view in CARLA, (top right) corresponding view in 2D simulator showing pseudo-LIDAR beams, (bottom) the “observation” in 2D providing distance-to-lane-boundary as a function of angle (green=forward “view”, blue=side and back “view”)

Conclusions

Our approach utilizes a combination of conditional imitation learning with a static dataset, reinforcement learning with a simulation environment, and high-performance computing to train a neural network. As a result, this reduces the “time to solution” compared to the existing human-based approach and provides an extensible framework to address the challenge of generalizing driving behavior to a wider range of scenarios.

The work described here, however, highlights a number of existing key challenges that must be addressed in future work so that machine learning techniques advance the state of the art for autonomous vehicles. First, a standardized approach to evaluating driving behavior is needed. In another words, a virtual driver’s test that eliminates variability as much as possible and enables different machine learning techniques to be quantitatively and objectively evaluated. The work described here is a first effort towards that goal but needs continued improvement. Secondly, there is a critical need for a standardized training data set. Currently, many data sets are not available, or do not contain a broad set of driving scenarios, or need to be further augmented to become useful, or organized in a manner such that the training process can be effective and efficient. This further complicates the ability to effectively compare and quantify the driving behavior of different machine learning techniques. Finally, there remains a significant need for the machine learning community in cooperation with the automotive community to develop scalable training processes for machine learning algorithms to incorporate the extremely large combinatorial search space of driving scenarios. Scalable training processes could then better leverage existing high-performance computing resources.

References

1. Liang, Xiaodan, Tairui Wang, Luona Yang and Eric P. Xing. “CIRL: Controllable Imitative Reinforcement Learning for Vision-Based Self-driving.” ECCV (2018)

II.1.2 Real-Time Data and Simulation for Optimizing Regional Mobility in the United States

Jibonananda Sanyal, Principal Investigator

Oak Ridge National Laboratory
1 Bethel Valley Road
Oak Ridge, TN 37831
E-mail: sanyalj@ornl.gov

Wesley Jones, Principal Investigator

15013 Denver West Parkway
Golden, CO 80401
E-mail: Wesley.Jones@nrel.gov

Prasad Gupte, DOE Technology Manager

U.S. Department of Energy
E-mail: prasad.gupte@ee.doe.gov

Start Date: October 1, 2018	End Date: September 30, 2020	
Project Funding (FY19): \$2,000,000	DOE share: \$2,000,000	Non-DOE share: \$0

Project Introduction

Highway congestion wastes over 3 billion gallons of fuel each year and causes 7 billion hours of lost productivity. Highway congestion costs freight movers ~\$63 billion dollars per year, ranging from \$5600-30,000 per truck (and is increasing). Research has shown the ability to introduce near-real time traffic monitoring and adaptive signal control (including small numbers of connected vehicles) can yield up to 30% reduction in congestion. Deploying this approach at a regional scale, that has high-volume and transient traffic, extreme data volumes, and potentially 100,000 vehicles, sensors, and control devices requires High Performance Computing (HPC). We created a ‘Digital Twin’ of the Chattanooga region with simultaneous pairing of both the virtual and physical world providing real-time situational awareness. This Digital Twin will be the basis of a cyber physical control system with high-speed bidirectional communication and control of the highway infrastructure and connected vehicles in the ecosystem to achieve a 20% energy savings in a region. If successful, the results of this project could be replicated region-by-region to commercialize the approach across the entire U.S., so that over the next 10 years, this project accelerates a reliable intelligent mobility system implementation to reduce overall mobility-related energy consumption by 20% and recover \$100 Billion of lost productivity in congestion.

The availability of real-time data from vehicles and the deployment of supporting infrastructure such as high-speed fiber networks has opened up an unprecedented opportunity to bring together high-performance computing, advanced mobility simulations, and existing transportation expertise to create a platform that could have a decadal impact in transforming regional mobility in the United States. We propose to optimize the movement of both people and freight in and around Chattanooga, TN, a representative urban/suburban region, by leveraging high performance computing, data analytics, and machine learning. Near real-time insights provided by the integration of data from emerging mobility technologies and services can inform all phases of strategic planning, design, operation, modernization, and decommissioning of ageing/legacy systems. Lessons learned and capabilities developed and deployed for regional mobility can be applied to optimize mobility nationally deploying region-by-region.

Objectives

The project will drive energy-efficient mobility science and technologies from early stage HPC-based R&D through demonstration to commercialize the optimization of mobility, energy efficiency, and productivity in a regional traffic domain. Although there is emphasis in this proposal on real-time traffic management, the

models and data will be immensely beneficial for planning transportation infrastructure. With the proper approach, preparedness for future population of connected and autonomous vehicles (CAVs) will be achieved, yet benefits will come in the nearer-term from accelerated intelligent infrastructure impact on the operation and movement of conventional vehicles. The project will develop and deploy approaches and capabilities that are scalable to larger and more densely populated regions, ultimately to national scale.

A key goal is to demonstrate the ability to deliver a 20% decrease in energy consumption through the Realtime Digital Twin and Cyber Physical Control of regional highway system.

Approach

The functional capability of the “Digital Twin” is being built in several phases:

Digital Twin Phase One—Phase one establishes observability. It will ingest and reflect the point-in-time state-of-the-system on both the signalized arterials as well as the regional highway and principal arterial system. This takes in data from signals, sensors, safety, as well as integrates a modern probe data traffic feed from either INRIX, HERE, or TomTom. Showing real-time speeds is particularly essential. Visualization of the data feeds to reflect the volume and velocity without abstracting away details allows us to meet and potentially go beyond existing analytics packages like RITIS and Iteris IPEMS. The majority of this work is expected in year 1. Year 2 will be about refining, adjusting, and tweaking

Digital Twin Phase Two: a. Simulation and Modeling—Phase two will integrate modeling—specifically an arterial model (Lee Highway is identified at this time) for within Chattanooga, TN, and freeway model for the freight and congestion issues on the freeway. The real-time data will feed the models, and the models will provide operational insight (not control). — that is next part b). All metrics will be reported in near real-time. The arterial model will be able to inform the state-of-operation and possibly suggest changes. This work will start in year 1 and go into year 2.

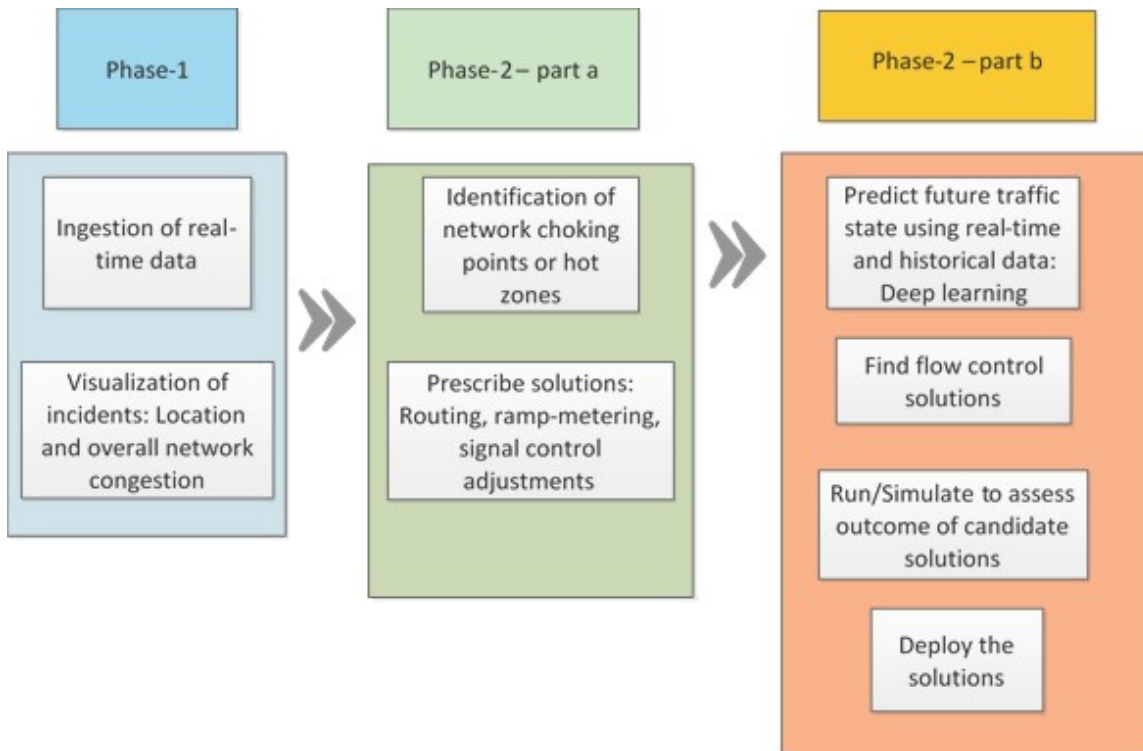


Figure II.1.2.1

Digital Twin Phase Two: b. Cyber-physical control—Building on phase two part a)—the feedback loop will be completed allowing for some level of automated response to perturbations in the network, such as changing signal timing. Also, the modeling can look forward to known events and simulate ahead of the fact to inform/insight into operations in the coming hours—perhaps in response to incidents, etc. Most of this work will be done during the latter part of year 2. The specifics of what is doable will become clearer as we make progress with the simulation and modeling.

One example application could be the digital twin will observe the traffic state in real-time and will allow changing the traffic signal settings accordingly. For instance, if we observe an incident on I-75 near the City of Chattanooga. The digital twin provides the resulting drop in capacity and congestion propagation. Further, a regional-level simulation with prediction model using historical and real-time data will provide future traffic flow propagation to answer questions like “when will the congestion hit inside the City of Chattanooga?”, e.g., the intersection on Brainard Rd. will have an oversaturated condition. Communication will occur between the digital twin and the TMC at Chattanooga informing the need to adjust signal settings to absorb the predicted shock due to the incident. Similar examples can be provided for ramp-metering, such as providing route guidance through dynamic message signs and controlling access of freight for entry-exit points of the freeway.

Further, historical incident data can be used to inform the daily traffic profiles so that expectations of flow disruptions can be modeled by incident type, location, and duration. These results will then provide a baseline for modeling future disruption behaviors in the faster-than-real-time simulation environment. The incident-informed daily traffic profiles will provide a baseline measure of Travel Time Reliability (TTR) against which the optimization methods developed may be assessed in simulation and situ. Improvements in TTR are associated with lowered rates of traffic congestion which would factor into lowered energy consumption.

Results

Milestone Outcome Summaries: Financial Year 19 had four milestones that were met. The milestone outcomes are summarized below:

Milestone 1, FY19Q1:

Complete data exchange plan between TDOT, City of Chattanooga, and National Labs

Summary: The objective of this milestone was to establish all the necessary arrangements with project partners to catalog the data available and determine the mechanisms to access the data. To that effect, the team worked with the primary project partners City of Chattanooga and the Tennessee Department of Transportation to determine the data available, how to get the data, and establish the paperwork needed to enable access.

Milestone 2, FY19Q2:

Complete the development of metrics and approach for calculating a baseline.

Summary: The objective of this milestone is to identify current baseline system performance measures covering aspects of mobility, safety, energy and productivity for Chattanooga. The metrics are part of the existing regional transportation system. By quantifying these metrics, we can understand and evaluate the effectiveness of various control strategies required to optimize mobility and achieve 20% energy efficiency for the region.

Milestone 3, FY19Q3:

Complete the development of the Situational Awareness (SA) tool working prototype for Chattanooga.

Summary: The objective of this milestone is to design, develop and demonstrate a working prototype of the digital twin in the form of SA tool for the City of Chattanooga. This tool serves as a virtual representation of the study region, wherein the reference data provides various spatial and temporal attributes of the infrastructure that are both static and dynamic. The intended outcome of this milestone is to demonstrate the capability of ingesting various data and provide analytical insights into the transportation system performance. The SA tool aims to serve as a decision support system to various stakeholders and policy makers in optimizing regional mobility that alleviates congestion and energy consumption.

Milestone 4, FY19Q4:

Complete design of the transportation modeling approach for traffic optimization.

Summary: The team continued extending the simulation modeling work started in the first quarter by acquiring additional data sources for simulation validation, setting up a pipeline for simulation calibration, calibrating existing microscopic simulations, building mesoscopic simulations for modeling the Chattanooga-Hamilton regional traffic, and identifying potential traffic management and control methods for energy-efficient mobility. The goal was to construct pipelines for modeling Chattanooga's local and regional transportation systems in simulation and evaluating the simulations' usability for traffic control and optimization strategies. Additionally, the team focused on extending and improving the simulation modeling effort started in the first quarter and accessed the simulations' capacity to support the optimization of the movement of people and freight in Chattanooga, Tennessee, region. The goal was to set up a modeling framework to inform and evaluate traffic control decisions and optimization techniques that increase mobility energy-efficiency.

Key activities in FY19:

ORNL and NREL held multiple conference calls with Tennessee Department of Transportation (TDOT) and Chattanooga Department of Transportation (CDOT) to define the available data and further develop the data access plan. A face-to-face project kick-off and planning meeting with project stakeholders in Chattanooga was held on October 2, 2018. Representatives included TDOT, City of Chattanooga, Chattanooga Traffic Engineers, and TDOT Region 2 Transportation Management Center operational staff.

Establishing data access was the primary focus during this Phase 1-FY19 Quarter 1. Several follow on meetings were held with key project stakeholders to further define and clarify specific data that is needed for the successful creation of a digital twin.

On November 5, 2018, ORNL representatives met with CDOT in Chattanooga, TN. During this meeting, ORNL discussed, in depth, the plans for this development and the potential benefit for the city. CDOT also requested and reviewed a Non-Disclosure Agreement (NDA) drafted by ORNL. The NDA was subsequently finalized on December 5, 2018.

CDOT's information technology division gave one of the ORNL team members access credentials for a VPNs setup into their infrastructure. ORNL has since then been able to get into CDOT systems. Setting up of software to access traffic data proved cumbersome; however, a pathway to get data from signal controllers has been identified.

On December 7, 2018, ORNL representatives met with TDOT in Nashville, TN. During this meeting, ORNL discussed in depth the plans for this development and the benefit potential for future applications within the state. TDOT reviewed a Non-Disclosure Agreement (NDA) drafted by ORNL; however, TDOT did not require to establish one as they considered the data being shared as public.

TDOT system administrators have setup a daily file upload of the data collected by their Radar Detector Stations to ORNL. Mechanisms for delivery of other identified data was discussed.

On December 13, 2018, the DOE Vehicle Technologies Office Technology Manager, Prasad Gupte met with ORNL and NREL along with key project stakeholders TDOT and CDOT to review the project's progress and kick-off planned development. Representatives included TDOT, City of Chattanooga, Chattanooga Traffic Engineers, and TDOT Region 2 Transportation Management Center operational staff. TDOT gave all attendees a tour of the TDOT Traffic Management Center (TMC).

Following discussions with TDOT and CDOT, ORNL has reached out to several other agencies to coordinate data access. These include the Hamilton County TPO, the Metropolitan Planning Organization, the Department of Public Safety, and the Georgia Department of Transportation.

Digital Twin Phase 1 development activities continued during FY19 Quarter 2. ORNL and NREL teams focused on understanding the baseline energy usage and developing the metrics from which the project can quantify real-world impact on energy consumption, congestion, safety and the combination of mobility, energy and productivity encapsulated in the MEP. Furthermore, the project team also focused on setting-up a pipeline for traffic simulation data acquired to-date.

A whitepaper was written which defines metrics for energy consumption, congestion, safety and MEP. This document guides how this project can measure the success of future intervening traffic control.

Connections with industry partners such as TomTom, ATRI, HERE, INRIX, and NPMRDS were made during Q2. Data acquisition is being considered to fill the gaps in freight data.

NREL explored partnership with TomTom to bring both historical and real-time volume estimates for use in this project. Donation of three months of trip data from INRIX was confirmed and received in Q3 and has been received and being hosted at NREL. The data is of value for arterial and freeway performance metrics, OD data for modeling, and freight modeling and simulation. Data use agreements with NREL prevented the open sharing of the data.

Initial setup and demonstration of traffic simulation with available data using Simulation of Urban Mobility (SUMO) tool was started in Q2. The simulation is very critical in evaluating the strategies including control needed to achieve goals in optimizing mobility and reducing energy consumption by 20%.

A revised AOP was developed for submission to DOE.

A TACTICS meeting with CDOT was held in Chattanooga, TN on March 7th and 8th. This meeting focused on gaining access to TACTICS and SPaT Data for historical and real-time feeds.

Digital Twin Phase 1 development activities continued during FY19 Quarter 3. ORNL and NREL teams primarily focused on development of the SA tool prototype along with data ingestion and processing for analytical insights into the transportation system for the study region. These data feeds are from various sources that were available and ready-to-use for this effort. Some data feeds are not yet available in real-time from partner agencies. The primary focus of the standing up of the application prototype is to demonstrate the SA tool in-terms of real-time and non real-time data feeds, implement conceptualized elements of the software system, illustrate analytical capabilities for static and dynamic infrastructure features, and use the tool to gain feedback from stakeholders and tune next efforts.

Development of the SA web-based prototype application tool that represents the Chattanooga region was done. Development of web interfaces was done to represent data feeds when available in real-time, as well as non real-time feeds with the design objective of easy adaptability when real-time becomes

available. For non real-time feeds, focus on the dates of December 3–9, 2018 for developing representative visualizations. Note that data from other time ranges are available. These dates were chosen sometime in Q2 as a representative sample of the data feeds.

Developed prototype algorithms were done that will get incorporated into the SA tool for performance metrics related to mobility, safety and energy from multiple data sources.

NREL is proceeding with volume estimates in partnership with TomTom to bring both historical and real-time volumes for use in this project. Initial (historic) 24-hour volume estimates for a typical weekday have been delivered.

ORNL has been working with ATRI to get access to the commercial truck movements for 8-week timeframe to better inform modeling and simulation efforts. This data was delivered in Q4.

The team also gained access to the CDOT TACTICS database environment based at the meeting held in Q3. This database provides the signal timing and plans; however, a lot of issues were discovered including how often the database is updated is questionable. It proved inadequate to obtain real-time information.

Incident data in the study area from the Hamilton County 911 records along with daily incident data was received and was data warehoused for near real-time access.

Continued efforts on demonstration of traffic simulation with Simulation of Urban Mobility (SUMO) platform. Primarily, the Q3 efforts were related to setting up the simulation for extracted area focusing on Shallowford Corridor from Lee Highway to Gun Barrel Road. Efforts included in testing various hypothetical scenarios actuated and coordinates signal control settings along with corridor for testing energy and mobility impacts.

Computing infrastructure, housed at ORNL, was setup for the project.

Assessment and calibration of simulation modeling tools for the region was performed in Q4. Extending and calibrating existing microscopic simulation for Shallowford Road corridor, building the mesoscopic simulation representing regional traffic in the Chattanooga-Hamilton metropolitan area, traffic control strategy and optimization for efficient mobility, signal timings and optimization, responsive and adaptive traffic signal control, speed harmonization, real-time information-sharing for traffic coordination, ramp metering and junction controls, part-time shoulder use, and other operational strategies were identified as key congestion mitigation approaches and a subset of these will be evaluated for the region in FY20.

Exercising pipelines to generate energy estimates was initiated: Energy estimates with RouteE and FastSim, as well as generating baseline MEP calculation using third party data sources.

The Situational Awareness tool was enhanced to better integrate additional data streams and make it available for feedback from stakeholders and user engagement.

Preparing for phase 2 of the project by identifying milestones and tasks was also done in Q4.

Detailed Report on subset of key activities

1. Assessment and calibration of simulation modeling tools for the region

We used the Simulation of Urban Mobility (SUMO) simulator, an open-source traffic simulator that handles large-scale simulations and that is widely used and supported (Krajzewicz et al., 2012). The project team and the CDOT identified Shallowford Road as a candidate arterial where to explore real-time signal control algorithms for improved mobility. We started by building a simulation for this area using the SUMO

microscopic model. The small-scale simulation enabled us to quickly and easily develop pipelines for constructing simulation and exercising SUMO capabilities. We then extended the existing workflows for building a regional-level simulation using the SUMO mesoscopic model.

Prior to running the simulations, we fused the node and network files that were provided by Hamilton County Transportation Planning Organization (TPO) with elevation data from USGS to create a network with elevation as fuel use strongly depends on grade changes. Next, we generated demand for morning, peak, afternoon peak, and off-peak hours using SUMO's OD2TRIPS module and aggregated volume counts from TDOT's Radar Detector Systems (RDS). Finally, we calibrated the simulated volume estimates by using volume estimates created with a machine-learning model that fuses 24-hour short-term count traffic volume data from TDOT, TomTom network, speed, and probe count, and weather data to generate network-level calibrated volume estimates.

Microscopic SUMO Simulation Results

We evaluated the fuel consumption for all the vehicles in the Shallowford Rd. region (including highways and streets around Shallowford Rd.). Figure II.1.2.2 shows the average fuel consumptions in every five minutes of the simulation under the original signal timing and our improved signal timing. The improved timing resulted in less fuel consumptions compared to the original timing.

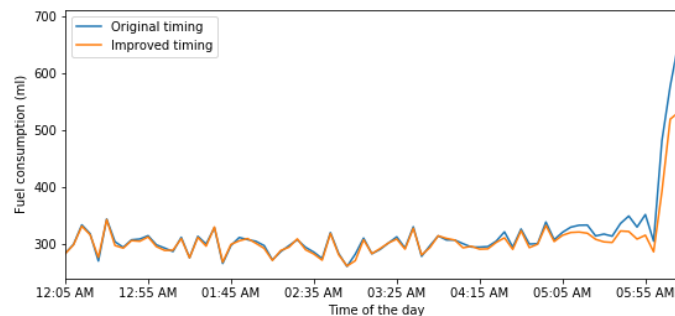


Figure II.1.2.2 Fuel consumption for Shallowford Rd. Region for the original signal timing and for an improved signal timing plan.

Mesoscopic SUMO Simulation Results

We simulated the Chattanooga-Hamilton region for an average day's afternoon peak period from 2:30 pm to 5:30 pm. We first analyzed the impact of road elevation on traffic movement including delay and speed. To this end, we compared the regional simulation with a flat network to a simulation with a network that had elevation data. Looking at Figure II.1.2.3, we can observe that for freight traffic, elevation incurs more penalty

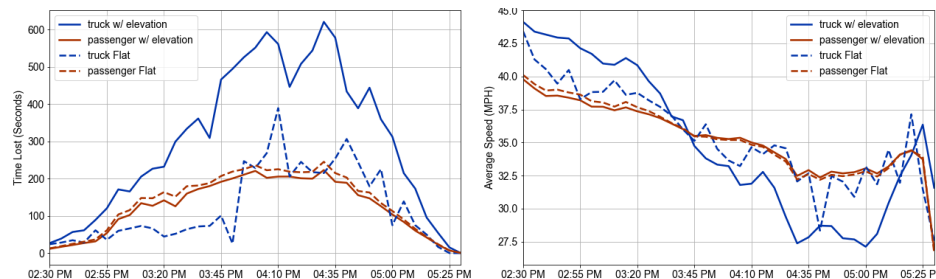


Figure II.1.2.3 Time lost (left) and average speeds (right) for passenger (orange) and truck (blue) traffic. Solid lines denote results with elevation data whereas dashed lines are without elevation.

for time loss than that of the flat network, along with lower average speeds for the elevation network. We did not see significant elevation impact in time loss or average speed for passenger vehicles.

2. *Traffic control strategy and optimization for efficient mobility*

While traffic congestion tends to continuously increase, growth in transportation infrastructure is limited by financial and land availability constraints, especially in urban areas. This has led to the use of Intelligent Transportation Systems (ITS) to manage existing transportation systems efficiently, including Active Traffic Management (ATM) strategies, which manage the transportation system by responding to prevailing road, traffic, and weather conditions in real-time, to increase mobility and safety. Traffic management strategies can be broadly categorized into planning and operational, where planning-level strategies target congestion management in the long-run, whereas operational strategies are meant for real-time and short-term needs. From this viewpoint, there are several traffic control strategies that can be evaluated in Hamilton County to further understand the effectiveness of these in reducing congestion and energy consumption while also improving traffic safety. In the context of ATM strategies, following are some of the most common controls implemented in congestion reduction.

Signal timings and optimization: Operational strategies confined to arterial and local roads involve the usage of advanced signal systems (e.g., actuated and coordinated) along with signal retiming that allow for efficient traffic flow and lower queue lengths. Specifically, the strategies such as signal prioritization for freight further enrich traffic mobility, with targeted approaches that can be investigated along a corridor for specific time periods.

Responsive and adaptive traffic signal control: Although people's daily trips have certain observable pattern, the traffic demand can easily be affected by certain random factors (e.g., special events, weather, stochasticity in human behavior, etc.). High resolution traffic sensors that can provide near-real-time traffic states make responsive and adaptive traffic signal control possible. Most traffic controllers in use have traffic responsive control functions. Adaptive traffic signal control does not depend on a library of pre-selected scenarios and requires less maintenance from engineers than traffic responsive control. The optimization is done in real time with the knowledge of the current or near future traffic states.

Speed Harmonization: Speed harmonization is a method to reduce traffic congestion and improve system performance. This method is applied to at points where lanes merge and form bottlenecks, which is a major cause of congestion nationwide. The strategy involves gradually lowering traffic speeds before heavily congested area in order to reduce stop-and-go traffic thereby potentially reducing fuel consumption and improving safety.

Real-time Information-Sharing for Traffic Coordination: Systems that share real-time traffic condition data with drivers can enable modifying drivers' behavior and routes to reduce network-level congestion. Proactive guidance systems are example of such systems that integrate real-time data collection at a system perspective and seek to reduce the network-level congestion, while minimizing the travel inconvenience experienced by drivers (Angelelli, E., et al., 2016; Pan, Juan, et al., 2012).

Ramp Metering & Junction Controls: Ramp metering is the use of traffic signals at freeway on-ramps to control the rate of vehicles entering the freeway. The metering rate is set to optimize freeway flow and minimize congestion. The fundamental premise of ramp metering is to improve freeway flow by regulating merging traffic from on-ramps, typically in the form of automated traffic signal controls, by requiring all merging vehicles to stop for several seconds.

Part-time Shoulder Use: According to FHWA, 40% of the congestion in the U.S. is a result of insufficient capacity. Part-time shoulder usage (or hard shoulder running) is a temporary operation of hard shoulders as running lanes for normal traffic. It provides a quick access to additional capacity without any infrastructure expansion requirements.

Other Operational Strategies: Further operational strategies that can be employed for traffic mobility and energy reduction are also diverse with some of the following that we anticipate on evaluating in a simulation environment.

Freight focused improvements such as truck only lanes, flow restrictions during peak periods along with parking restrictions shall further enable freight traffic in the region. The availability of truck GPS routes along with key freight hubs in the region is important for these strategies.

Passenger focused improvements such as parking restrictions and dynamic pricing strategies during peak-periods further help in demand management.

3. Exercising Pipelines for Generating Energy Estimates

In this task, we constructed and exercised pipelines to generate preliminary energy estimates with RouteE, FASTSim and MEP tools. The energy estimates from these tools will enable us to evaluate an energy consumption baseline for mobility in the Chattanooga-Hamilton region and evaluate the effectiveness of proposed traffic control strategies in improving mobility energy-efficiency.

Energy Estimates with RouteE

The RouteE package has been used to calculate the link-wise energy consumption for the Chattanooga road network. It contains six pre-trained generalized vehicle models that are appropriate for the Chattanooga region. The inputs (features) required by these pre-trained models to predict the energy consumption for a trip are: the average speed in mile/hour for the trip, the percentage change in grade between the origin and the destination, the length of the trip in miles and the average number of lanes for the trip. The estimation of link-level energy estimation requires link-level speed and grade data. A close examination of the maps for the percentage change in grade across each link indicates that highest values for the percentage change are localized to some regions. This pattern is consistent with alternating ridges/mountains and narrow valleys in the Chattanooga region.

Figure II.1.2.4 shows the energy consumption for a conventional gasoline vehicle. Equivalent results were also created for PZEVs and battery-operated vehicles.

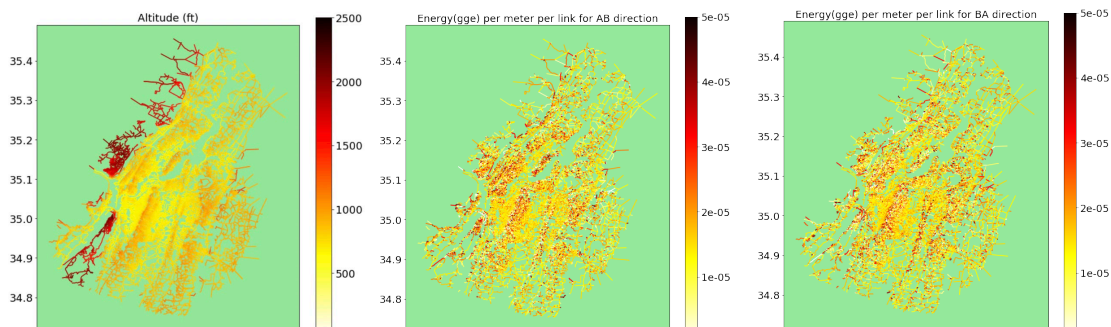


Figure II.1.2.4 Chattanooga-Hamilton road network color coded according to maximum altitude in feet of each link in the network (left), and normalized energy consumption (gge per meter) for each link in the AB (middle) and BA (right) directions, predicted by a generalized model for a conventional vehicle running on gasoline.

Energy Estimates with FastSim

FASTSim is an open-source vehicle powertrain analysis model that provides a rapid and efficient capability to compare powertrains and estimate the impact of different technologies and cost improvements for light- and heavy-duty vehicles. Results from FASTSim include vehicle energy efficiency (energy consumption per second) and performance (0-60 mph acceleration in seconds, etc.), cost, and battery life (if it is an electric vehicle). Inputs include operational details at the drivetrain component level (i.e., driving cycles), as well as vehicle design parameters such as aerodynamic drag, frontal area, mass reduction, and rolling resistance.

The energy estimates for a 3-hour SUMO simulation scenario in Chattanooga, TN, are illustrated in the diagram below. The fuel consumption of three types of powertrain, including passenger, trailer, and truck is denoted as gallon gas of equivalence (GGE). The total distance traveled by three vehicle types also showed in the blue line. As expected, Figure II.1.2.5 indicates that passenger cars have better fuel economy than trailers and trucks.

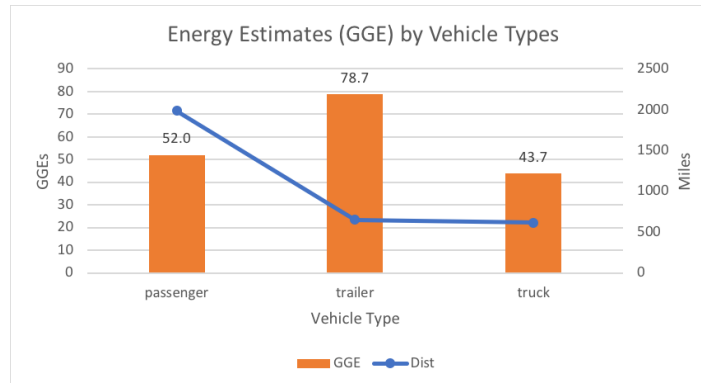


Figure II.1.2.5 The estimated energy consumption of vehicles running in the SUMO. Passenger cars consumed less energy despite having traveled the longest distance (about 2000 miles). Trailers consumed the most significant amount of fuel. Trailers and trucks only traveled about one-third of the distance of passenger cars.

Generating baseline MEP calculation using third party data sources

A baseline Mobility Energy Production (MEP) metric (Hou et al, 2019) is calculated for Chattanooga, TN using TomTom network, costar land use data, and population and employment data from US census. MEP is constructed based on accessibility theory and take consideration of mode availability, affordability, sustainability, and efficiency. The MEP calculation starts with the computation of a cumulative opportunity measure by counting the number of land use objects and jobs that can be reached within a certain travel time threshold (10, 20, 30, and 40 minutes) by different transportation mode (driving, walking, biking, and transit). More weight should be assigned to opportunities that can be accessed with more available, sustainable, and affordable modes in less travel time, and vice versa. Along this line of thought, the concept of a modal weighting factor is introduced. A comprehensive metric to quantify the quality of mobility is then calculated by weighting the cumulative opportunities using a negative exponential function applied on the weighting factor. A higher MEP score means the easier access to more services, goods, and jobs with lower cost, less energy, and more mode choices. Figure 6 (bottom right) illustrates the results for Chattanooga: as expected, the downtown area has higher MEP score than the outskirt areas, since there are more opportunities and better transit systems in downtown.

4. Refine and improve the Situational Awareness Tool

Situational Awareness Tool: The situational awareness platform serves a virtual representation for the City of Chattanooga by providing real-time data feeds, where available, from the deployed sensors. Ultimately, the SA tool is a component of the Digital Twin which envisions predicting future anticipated events in the real-world, along with ability to evaluate the impact of control decisions, faster than real-time. The SA tool uses spatial reference data that provides information on location and infrastructure characteristics for the region.

Platform Development: Development of the SA tool to this point has been comprised of several facets contributing to the current instance of the tool prototype, mainly infrastructure, network operations, development operations, data engineering, and application development. Infrastructure for this project has been provisioned within ORNL-managed cloud infrastructure. The cloud infrastructure managed on premises will allow portability of applications and services and provide high availability of service of the application among other benefits.

Application development has revolved around a microservice approach to software development where a separation of components is achieved by creating services from the smallest logical unit of work using a containerized abstraction. Using Docker in conjunction with container orchestration platforms such as Kubernetes and Rancher, forms the basis of an approach allowing increased flexibility in deployment and portability and collaboration among a diverse team. Architecture of the web application revolves around a classic client-server archetype where a presentation layer is driven by data retrieved from a data backend via a data-access and business logic layer. The presentation layer is built around the Angular framework, which provides a highly customizable and flexible platform for creating a rich user experience. Several specialized TypeScript libraries are included to augment Angular's capabilities, such as OpenLayers for the mapping client and HighChart for adding dynamic charting capabilities.

User Interface The user interface consists of a Home page, a map-based Region page, a Corridors page, an Incidents page, and a Metrics page. The following screenshots illustrate the prototype.

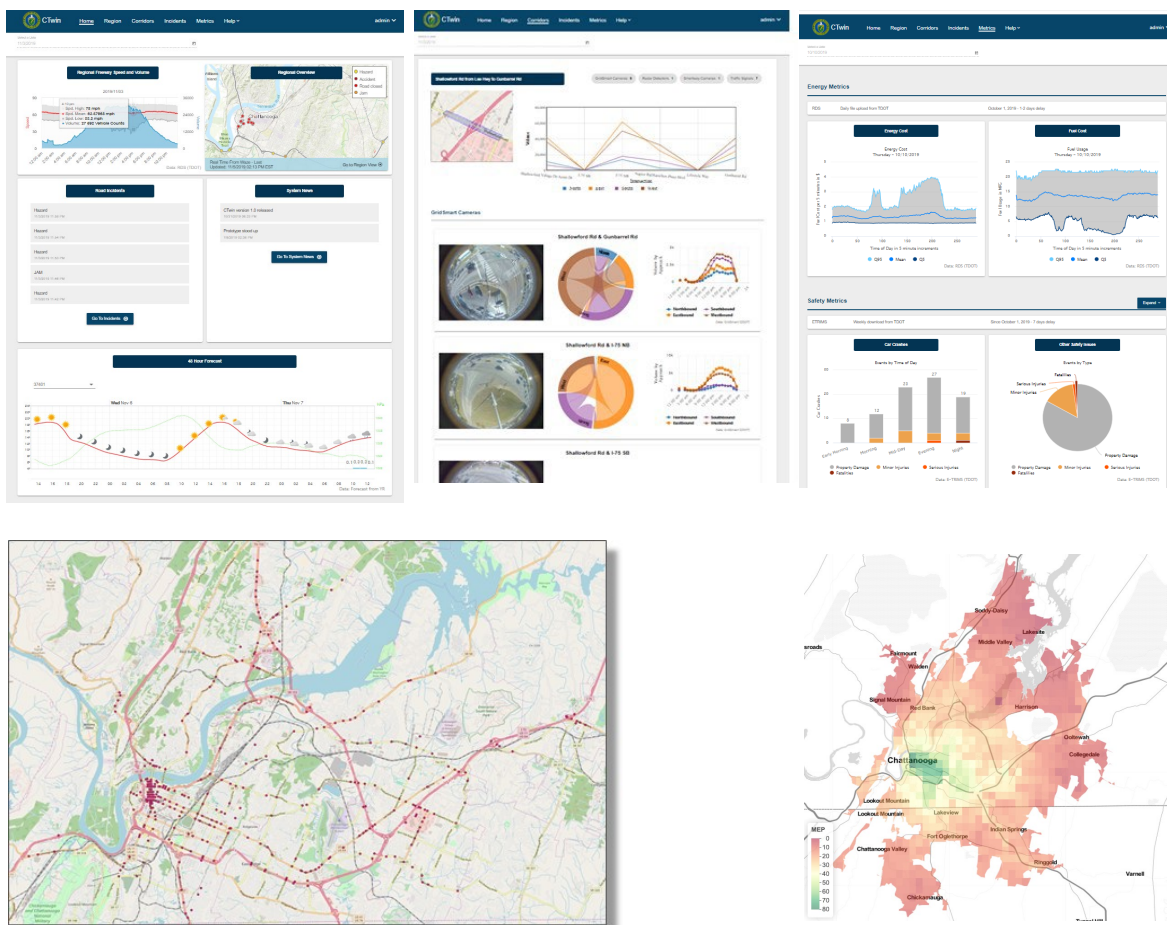


Figure II.1.2.6 Screenshots of different parts of the situational awareness tool. Top: Landing page (left), corridors page (middle), and metrics page (right). Bottom: Region view with some of the sensors (left) and MEP (right).

Data and Analytical Insights

Primarily, we focus on regional and corridor level insights in tracking transportation system performance measures. System performance metrics span across various aspects of regional mobility that include—congestion (e.g., average speed, travel delay, and reliability), safety (rate of traffic accidents), energy consumption (e.g., miles per gallon, vehicle miles traveled) and mobility-energy-productivity (MEP) that provides an estimate of the quality of mobility per unit time, cost, and energy.

Priority data necessary to create the regional Digital Twin are identified as: Radar Detection Systems (RDS), GridSmart intersection cameras, the geometry of the transportation network, incident data from the county and state, TACTICS, and the Signal Phase and Timing (SPaT) Infrastructure locations. CDOT has shared the locations of all their signals with the project team. While the team has access to the Chattanooga VPN, getting access to the data itself has proven challenging.

We make use of the RDS data to quantify the system performance along the freeways in the region as measured by congestion - average speed and traffic demand at 5-minutes aggregates. At the regional level the system wide congestion can be measured by aggregating data from all sensors for a given day, as seen in the top left graph on the landing page (Figure II.1.2.6): the dip in traffic speed (as low as 25mph) and the spike in traffic volume during the morning and evening hours indicate the rush-hour traffic patterns in the region. We also use RDS data to derive energy metrics related to fuel usage and fuel cost based on the observed speed recorded from the sensors, as seen in the top two charts on the metrics page (Figure II.1.2.6). The fuel usage metrics are derived based on the non-linear relationship between vehicle speed and fuel usage as documented by Transportation Energy Handbook, which is further converted into fuel cost based on the assumption that fuel costs \$3 per gallon.

Data from grid-smart cameras contain various attributes related to traffic flow such as intersection-level turning movements, vehicle speed profiles and green light wait time among many others. This data is represented in the corridors page of the SA tool (Figure II.1.2.6). We characterize traffic flow along a corridor by the volume change between intersections. To reflect this, the visualization places the intersections’ values on the x-axis, with distances proportional to that between the individual intersections. Each traffic flow direction is represented by a different color. Furthermore, we provide turn movement visualization using a Chord diagram: the four cardinal directions are represented as arcs of a circle. Traffic flow between each pair of cardinal directions is represented by a band spanning between the pair of corresponding arcs. The size of arcs and bands is proportional to the corresponding traffic volume. Each traffic flow direction is represented by a different color.

The traffic incident data comprises of two primary sources. Traffic crashes are extracted from the TITAN database, which provides information on traffic accidents along with attributes on crash severity such number of fatal crashes, serious injuries and property damage only accidents, which are presented in the safety tab (left). Additionally, the Hamilton County 911 registry provides information on a wider range of incident types, but with less detailed information, which are available in the incidents tab (middle/right).



Figure II.1.2.7 Traffic crashes from the TITAN database for December 3–9, 2018 (left), and Hamilton County 911 vehicle and non-vehicle incidents by time of day (middle) and day of the week (right).

Engagement with Stakeholders

A major development in Q4 was related to engaging and outreach to the stakeholders—CDOT and TDOT for feedback and improvements needed for a successful digital twin. It is anticipated that a stakeholder facing web-tool will be made available early in FY20Q1. On 24 September, ORNL hosted Tommy Trotter and Cindy Shell from CDOT. They provided an overview and an in-depth discussion of the setup of signals and control in the city. A Siemens M60 controller was left with ORNL to start the investigation of how to establish a link into the hardware for future programmatic cyber-physical control.



Figure II.1.2.8 A Siemens M60 controller used for traffic signal control in the city of Chattanooga

Conclusions

The above sections summarize all activities in the project in FY19. The first year of the project has educated the team about the challenges and opportunities in the scope of what we are trying to accomplish. Having understood the data, simulation approaches, and real-world needs, the second year will be focused on delivering impact on several fronts. A key activity will be the prototype cyber-physical control in the city. Metrics will be tracked and the effect of the employed strategies will be measured.

Key Publications

1. Anne Berres, Srinath Ravulaparth, Jibonananda Sanyal: Transportation Systems Analysis and Visualization: A Multiscale and Multivariate Approach to Shopping Districts. 9th International Visualization in Transportation Symposium: A Better View (Presented 11/2019)
2. Haowen Xu, Anne Berres, Srinath Ravulaparth, Jibonananda Sanyal: A Client-side Web Application for Visualizing Massive Regional Mobility Data Collected from Real-Time Traffic Sensors. Submitted AGU Fall Meeting. 2019
3. Srinath Ravulaparth, Steven Peterson, Anne Berres, Austin Todd, Ambarish Nag, Jibonananda Sanyal: Alternative Frameworks for Spatiotemporal Data Imputation Methodologies: Case-Study Analysis for Traffic Volume Forecasting. Submitted to Innovations in Transportation Modeling.
4. Haowen Xu, Jibonananda Sanyal, Anne Berres, Sarah Tennille, Optimization of Network Datasets for Web-based System using Composite Bezier Curves, submitted to AAG Annual Meetings, 2019
5. Juliette Ugirumurera, Wesley Jones, Jibonananda Sanyal, High Performance Computing Traffic Simulations for Real-time Traffic Control of Mobility in Chattanooga Region, Tennessee Sustainable Transportation Forum & Expo, 2019.
6. Juliette Ugirumurera, Real-time answers for traffic jams, <https://sciencenode.org/feature/Real-time%20answers%20for%20traffic%20jams.php>, 2019

II.1.3 Reinforcement Learning-based Traffic Control to Optimize Energy Usage and Throughput (ORNL)

Thomas P Karnowski, Principal Investigator

Oak Ridge National Laboratory
One Bethel Valley Road
Oak Ridge, TN 37831
karnowskitp@ornl.gov

Prasad Gupte, DOE Technology Manager

U.S. Department of Energy
E-mail: Prasad.Gupte@ee.doe.gov

Start Date: October 1, 2018	End Date: July 31, 2019	
Project Funding (FY19): \$187,087	DOE share: \$150,877	Non-DOE share: \$36,210

Project Introduction

The US roadways are critical to meeting the mobility and economic needs of the nation. The United States uses 28% of its energy in moving goods and people, with approximately 60% of that used by cars, light trucks, and motorcycles. Thus, improved transportation efficiency is vital to America's economic progress. The increasing congestion and energy resource requirements of transportation systems for metropolitan areas require research in methods to improve and optimize control methods. Coordinating and optimizing traffic in urban areas might introduce hundreds of thousands of vehicles and traffic management systems, which can require high-performance computing (HPC) resources to model and manage. In this work, we seek to use machine learning, computer vision, and HPC to improve the energy efficiency aspects of traffic control by leveraging GRIDSMART traffic cameras as sensors for adaptive traffic control, with a sensitivity to the fuel consumption characteristics of the traffic in the camera's visual field. Traffic control use cases using reinforcement learning have been published and achieved good results. Surveys from DOE national laboratories estimate that the fuel cost of idling is six billion gallons wasted annually [1]. GRIDSMART cameras—an existing, fielded commercial product—sense the presence of vehicles at intersections and replace more conventional sensors (such as inductive loops) to issue calls to traffic control. These cameras, which have horizon-to-horizon view, offer the potential for an improved view of the traffic environment, which can be used to generate better control algorithms.

Objectives

There are two primary objectives in this project. The first is to develop algorithms that essentially teach GRIDSMART cameras to estimate fuel consumption of vehicles in their visual field. The second is to use this capability to improve energy efficiency by changing timing and phasing of traffic lights, while minimizing penalties to throughput and mobility. HPC can play a role in both objectives by allowing more complete exploration of the machine learning architectures, parameters, and methods that enable the capability to determine vehicle types. HPC-based simulations that model traffic and capture the performance of GRIDSMART cameras in estimating the visual field (extrapolated from real data using developed algorithms and models) serve as training and testing data for reinforcement learning algorithms that learn policies for traffic camera control. The key outcome of this work will be control strategies generated through a novel reinforcement learning framework, with performance measured through simulations and validation data and oriented toward the GRIDSMART sensing capability. Other important outcomes include projections of the required sensing capabilities to achieve these control strategies. This will pave the way for future research to expand the number of studied intersections, investigate the potential of wide-range coordinated control, add naturalistic driving study data for higher resolution and simulation detail, extend sensing capabilities to other technologies such as RFID/cellular and/or connected vehicle technology, and incorporate direct vehicle emissions sensing to minimize cumulative emissions measured.

Approach

As this is the final year of the project, the basic approach is summarized here, with changes in the most recent fiscal year indicated. The GRIDSMART cameras will be trained to estimate fuel consumption by using a ground-based camera system located under a GRIDSMART instrumented intersection at ORNL. The simultaneous capture of the ground-based camera image with the GRIDSMART camera image will allow a view from the “GRIDSMART perspective” along with a view from the ground camera. The latter will then be classified into a vehicle class (i.e., make and model), ideally using a commercial application procured for this purpose. ORNL will leverage an existing, ongoing project that is collecting data on the reservation as part of another project. The data used here will allow the creation of a training set of images—from the unique GRIDSMART view—that will be used to create a machine-learning model to classify vehicle make and model and therefore estimate fuel consumption. The approach is shown in Figure II.1.3.1. We had a few contingencies in the approach and took advantage of these in FY2019. First, we assume, to a first approximation, that the vehicle make / model were the leading indicators of fuel consumption and reserve vehicle dynamics for future applications. We also found that we were not able to get sufficient data to train deep learning models on the estimates of vehicle class, so we used an existing data set which was not from overhead cameras to understand the limitations of this approach [2]. We planned to use the Multi-Node Evolutionary Neural Networks for Deep Learning (MENNDL) HPC software package to evolve convolutional neural network topologies for better estimate of fuel economy from the visual images. Finally, we planned to utilize the data set we were able to collect to perform basic estimates of vehicle class, size, make and model as appropriate given the data we collected.

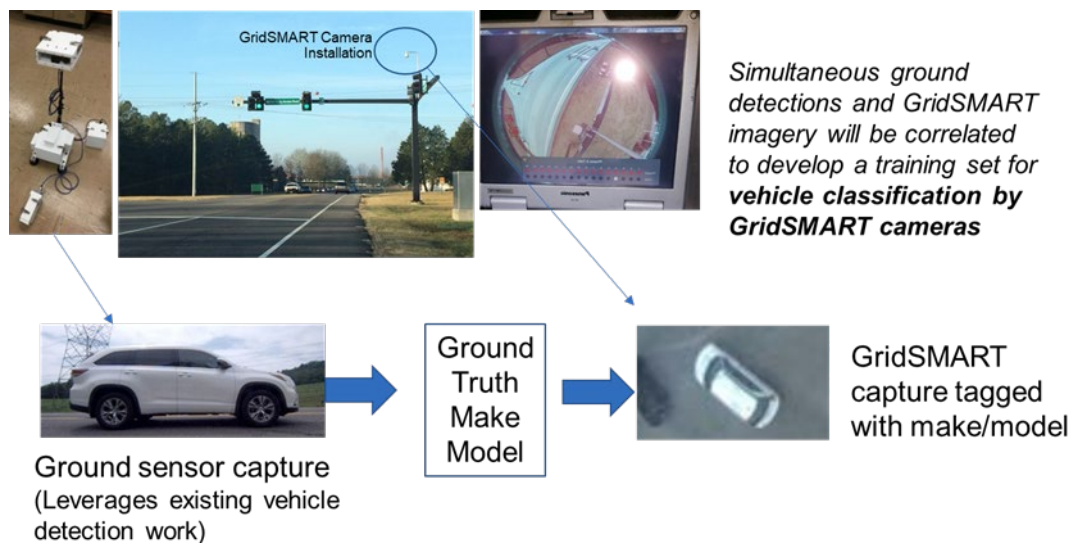


Figure II.1.3.1 Data collection to estimate fuel consumption using GRIDSMART cameras. GRIDSMART installations at ORNL will be used in conjunction with a ground imaging system. The simultaneous captures will be used to produce a library of images suitable for training a machine learning algorithm to estimate fuel consumption.

Our approach for teaching grids of GRIDSMART-instrumented intersections to improve fuel efficiency through adaptive signal control, used reinforcement learning (RL) and simulations performed on an HPC platform. The approach leveraged the visual classification performance characteristics developed in the first objective. The control strategies development began with single intersections and expanded to multiple intersections with studies on scalability and impact. The HPC simulations have a goal of producing control strategies that can be deployed in environments with a small computational footprint such as a distributed network of GRIDSMART cameras. RL finds solutions to problems where an actor or set of actors learn to respond to dynamic environmental conditions to achieve an overall optimized solution such as winning a game or controlling a process. In this collaboration, the actions are the activation of one or more traffic signals in

response to sensed vehicle types (and corresponding fuel economy metrics), and throughput objectives. The optimization goal is a combination of throughput and energy efficiency. The huge input space (combinations of vehicle types, vehicular dynamics, and multiple signal lights) represents a large dimensional problem that will require HPC for simulations and deep RL for solutions. While our initial planned approach was to develop a custom simulation environment for the vehicle simulation, we abandoned this goal and instead used the open source Simulation of Urban Mobility (SUMO) package as it became clear that this approach would have numerous advantages, and could be integrated with a sensor model, a machine learning platform for control, and ported to HPC.

Results

Visual Estimates of Fuel Consumption

Our vehicle data collection effort ended in November 2018 but underwent considerable data hygiene to create a data set useful for our purposes. We recognized that our vehicle collection effort would not achieve the numbers of images required to train deep models from scratch and therefore our traffic simulations used the ground-based data set [2] with the AlexNet topology. As detailed in last year's report, we used a simple image degradation model to estimate how the fuel consumption estimates performed with distance to the camera with the simulation.

However, we were able to use the data set we developed to prove numerous goals for the first objective of "teaching a GRIDSMArt camera how to estimate vehicle fuel consumption". First, we emulated the GRIDSMArt segmentation process (the image processing operation of determining which pixels in an image are a vehicle and which are not) and included this in our data set. Second, we used this model to create oriented bounding boxes on vehicles in a manner emulative of GRIDSMArt. We combined this data with the ground-based sensor imagery, classification, and fuel economy estimate as applicable to create the data set of 6,695 vehicles. A number of larger vehicles that were not identified in the ground-based sensor were manually labeled based on the size of their bounding boxes and the lack of classification from the ground-based sensor. The relevant vehicle categories included "18-wheelers", large multi-axel trucks, motorcycles, bicycles, and busses. In the resultant data set, a total of 6,695 vehicles were identified in 685 different vehicle categories. The vehicle distribution is not evenly spread, as roughly 150 categories have a single vehicle, and some have as many as 238. The median number in each category is only 4.

There are three main locations where the images were taken, which we refer to as "NearLane", "TurnLane", and "FarLane". We took the region around these core areas and analyzed the vehicles within each region. A threshold on the oriented bounding box length was set, and the average fuel economy of all vehicles above the threshold was computed. This analysis showed that we can functionally discriminate between high fuel consumers and lower consumers (i.e., "average" vehicles) simply on the basis of the oriented bounding box length. This finding shows that there is value in the visual estimates made virtually "for free" from vehicle segmentation such as that which GRIDSMArt already produces, in that the bounding box sizes can generally distinguish heavy fuel consumers from lighter fuel consumers.

Another result that uses the bounding box is concerned with discriminating "regular" vehicles from the special vehicle classes of high fuel consumers. To this end, we took the largest 100 "regular" vehicles from each region and assigned them to a single class and then attempted to discriminate between the large classes (18Wheeler, Bus, MultiAxle, DeliveryVan, and Chevrolet Express Bus). As the data set has a limited number of examples of Bus, we elected to combine this class with the 18Wheeler class. Three experiments were conducted, one on each of the NearLane, FarLane, and TurnLane locations. The overall data set was reduced to 60 random examples of each class (18WheelerBus, MultiAxle, DeliveryVan, Chevrolet Express Bus) and 60 random examples from the 100 largest examples of the "regular" vehicle class. A pre-trained convolutional neural network based on the MobilenetV2 [5] topology was utilized, except that the output of the last fully connected layer was used to create a 1000-dimension feature vector. The data set of 300 vectors was split into five folds, each with a training set of 210 vectors evenly divided between the classes and a testing set of 90 vectors. This was then used to train and test a classifier using an error-correcting output code model [6] for

multiple classes with support vector machines. After each set of folds was completed, a new set was generated using a new random set of examples, and the process repeated 10 times. The overall performance for each lane was approximately 86% regardless of the lane of traffic, indicating that there is a high level of discrimination possible between the largest vehicle types as well as with “regular” vehicles with large bounding boxes. An example of the confusion matrix for the near lane of travel is shown in Table II.1.3.1.

Table II.1.3.1 Confusion Matrix for Near Lane

	18Wheeler+Bus (est)	Chevrolet Express Bus (est)	Delivery Van (est)	Multi-Axel (est)	Other Vehicles (est)
18Wheeler+Bus	45.8	0.50	7.2	5.5	1.0
Chevrolet Express Bus	0.30	58.3	1.40	0.0	0.0
Delivery Van	7.9	0.50	45.6	4.6	1.4
Multi-Axel	4.5	1.0	3.9	49.7	0.90
Other	0.30	0.80	0.90	0.900	57.1

As a final note, we also used the MENNDL processing engine [4] on ORNL’s Titan supercomputer to attempt to evolve a better topology for fuel efficiency estimates. The efforts evolved new convolutional neural network(CNN) topologies that were able to distinguish between the gross vehicle classes with results comparable to the Alexnet results used to inform the simulation model. We believe further efforts could improve the classification, but those efforts would require additional computational hours beyond the current effort which ended in July 2019.

Using Visual Information for Adaptive Control and Energy Efficiency

Our vehicle simulations focused on a single intersection with the SUMO platform for proof of principle. We extended the single-intersection work to a grid by simulating sensors at adjacent intersections. We were also able to show that RL policies learned on some distributions of traffic could generalize to other distributions. We compared timed policies, occupancy-based policies, heuristic visual policies, and RL policies and found that the latter outperformed the others consistently. An example result is shown in Figure II.1.3.2, which uses information from adjacent traffic intersections as well as the “current” intersection. Each point represents a vehicle, with fuel usage (mL/s) on the x axis and stopped time on the y-axis. The two main distributions are obvious, with larger fuel consumers on the right and “regular” vehicles on the left. The flattening of the right distribution indicates that the traffic controller has learned to let these larger vehicles pass with minimal stopped time.

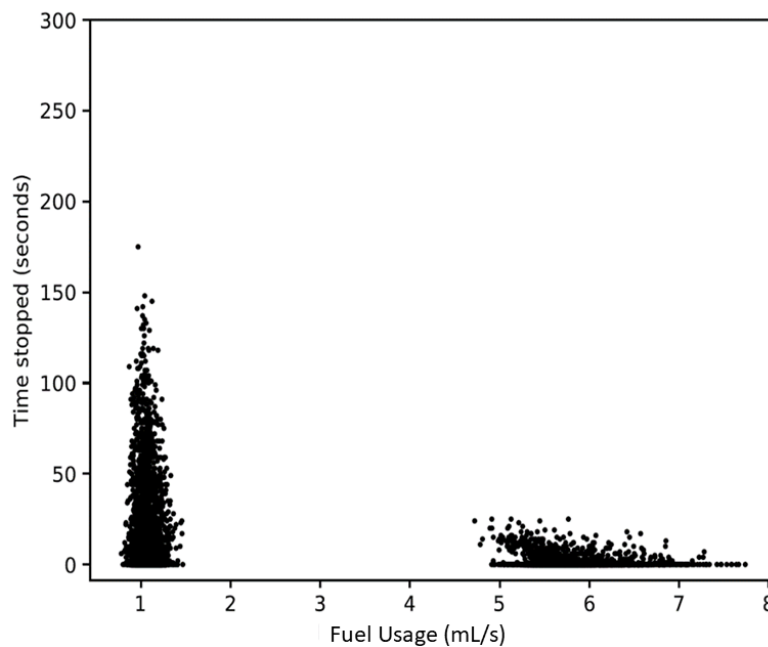


Figure II.1.3.2 SUMO simulation with Deep Q-Learning with visual information from adjacent intersections. “Regular” fuel consumers are on the left and heavy fuel consumers are on the right. These results show a flattening of the right distribution indicating the learned control policy using GRIDSMART-like visual information stops heavy fuel consumers for minimal times.

Conclusions

In this period of performance, we achieved our two major goals of showing GRIDSMART imagery can be used to estimate fuel consumption and this information can be used to improve fuel consumption through adaptive control with reinforcement learning. We completed our data collection at the ORNL campus, performed data hygiene, published a publicly-available data set (the ORNL Overhead Vehicle Dataset or OOVD), and showed its utility for estimating vehicle fuel consumption from GRIDSMART imagery. We used the MENNDL tools to evolve convolutional neural networks in an effort to improve image-based estimates of vehicle fuel consumption. We ported the SUMO package to ORNL HPC Titan. We integrated the tool with machine learning tools Keras and TensorFlow, and performed simulations based on estimates of GRIDSMART vehicle classifications to show that RL policies can out-perform timer policies, heuristic policies, and occupancy policies to improve fuel efficiency. We showed that information from adjacent intersections improves these results to provide a path toward true grid control. Our provisions for contingencies helped the project achieve its goals with the limited budget and resources available. We published a final CRADA report, submitted a paper on the effort, and published a publicly-available dataset of images, segmentations, vehicle classes and fuel consumption characteristics with GRIDSMART and ORNL approval. More information on the overall project can be found in the CRADA report which is publicly available through OSTI.

Key Publications

1. Karnowski, Thomas, Eicholtz, Matthew, Elwasif, Wael, Ferrell, Regina, Naughton III, Thomas, Oesch, T Sean, Patton, Robert, Rose, Derek, Tokola, Ryan, and Young, Steven. "Reinforcement Learning-based Traffic Control to Optimize Energy Usage and Throughput (CRADA report)". United States. doi:10.2172/1560460. <https://www.osti.gov/servlets/purl/1560460>.
2. The ORNL Overhead Vehicle Dataset (OOVD), available at OOVD web site <https://www.ornl.gov/project/ornl-overhead-vehicle-dataset-ovod>

3. Karnowski et al, “Estimating Vehicle Fuel Economy from Overhead Camera Imagery and Application for Traffic Control”, submitted to SPIE Electronic Imaging 2020, Conference on Intelligent Robotics and Industrial Applications using Computer Vision 2020

References

1. <https://www.anl.gov/energy-systems/project/reducing-vehicle-idling>
2. Gebru, Timnit, Jonathan Krause, Yilun Wang, Duyun Chen, Jia Deng, Erez Lieberman Aiden, and Li Fei-Fei. 2017. “Using Deep Learning and Google Street View to Estimate the Demographic Makeup of the US.” arXiv preprint arXiv:1702.06683.
3. Krizhevsky, Alex, Ilya Sutskever, and Geoffrey E. Hinton. 2012. “Imagenet classification with deep convolutional neural networks.” *Advances in neural information processing systems*. pp. 1097–1105.
4. Young, Steven R., Derek C. Rose, Thomas P. Karnowski, Seung-Hwan Lim, and Robert M. Patton. 2015. “Optimizing deep learning hyper-parameters through an evolutionary algorithm.” *In Proceedings of the Workshop on Machine Learning in High-Performance Computing Environments*. p. 4. ACM.
5. Sandler, Mark, Andrew Howard, Menglong Zhu, Andrey Zhmoginov, and Liang-Chieh Chen. “Mobilenetv2: Inverted residuals and linear bottlenecks.” In *Proceedings of the IEEE Conference on Computer Vision and Pattern Recognition*, pp. 4510-4520. 2018.
6. Fürnkranz, Johannes. “Round robin classification.” *Journal of Machine Learning Research* 2, no. Mar (2002): 721-747.

Acknowledgements

We acknowledge the contributions of the ORNL team, including Matt Eicholtz, Russ Henderson, Johnathan Sewell, Eva Freer, Regina Ferrell, Travis Johnston, Sean Oesch, Thomas Naughton, Wael Elwasif, Ryan Tokola, Steven Young, Derek Rose, Hong Wang, Rich Davies, David Smith, and Claus Daniel.

II.1.4 Ubiquitous Traffic Volume Estimation through Machine Learning Procedures (NREL)

Venu Garikapati, Principal Investigator

National Renewable Energy Laboratory
15013 Denver West Parkway
Golden, CO 80401
Phone: (303) 275-4784
E-mail: venu.garikapati@nrel.gov

Erin Boyd, DOE Technology Manager

U.S. Department of Energy
E-mail: erin.boyd@ee.doe.gov

Start Date: October 1, 2018

End Date: September 30, 2019

Project Funding (FY19): \$250,000

DOE share: \$250,000

Non-DOE share: \$0

Project Introduction

High-quality traffic volume data is critical for the purposes of quantifying the following traffic volume estimation parameters:

- user delay,
- congestion impacts,
- delay resulting from signal operations or
- non-recurring congestion events such as those induced by crashes and weather,
- sustainability measures such as energy/fossil fuel use, locating alternative fueling (EV charging) stations, and calculations of transportation-based greenhouse gas emissions.

However, high-confidence volume data currently collected through sensor-based devices, the most prolific of which is continuous count stations (CCS) as part of the Highway Performance Monitoring System, is extremely sparse. This sparseness hampers its use in traffic operations to effectively monitor highway capacity in the event of detours, construction, and evacuation. Most non-freeway monitoring is limited to periodic 48 hour counts as dictated by federal aid reporting, a frequency and sparseness that makes such data incompatible for most operations uses. Traffic counters for any given city or region cover only a small amount of the road network (typically 5–10%), leaving the remaining (90–95%) network with no volume information. Installing traffic counters on all road segments is impractical and prohibitively expensive. The cost of sensor installation, mounting, power, and communications can escalate life cycle costs to several thousand dollars per year per sensor location. Commercial probe traffic data (analogous to the methods used for the traffic data that drives Waze and Google Maps) has already revolutionized travel time and speed reporting both for government agencies as well as the general traveling public. With the escalating ratio of probe vehicles in the traffic stream, now approaching 1 in 10 (but highly variable), the number of observed probes can be combined with other data, and run through machine learning (ML) models to produce estimates of traffic volume with a high degree of statistical confidence. By utilizing information from existing traffic counters and combining it with vehicle probe data, as well as other relevant information (e.g., weather and road geometry), this project aims to bring to market, a product that can provide high-quality estimates of vehicle volumes across the entire road network of a city, state or even the nation at all times (24x7x365) and all locations. An overview of the modeling framework is presented in Figure II.1.4.1.

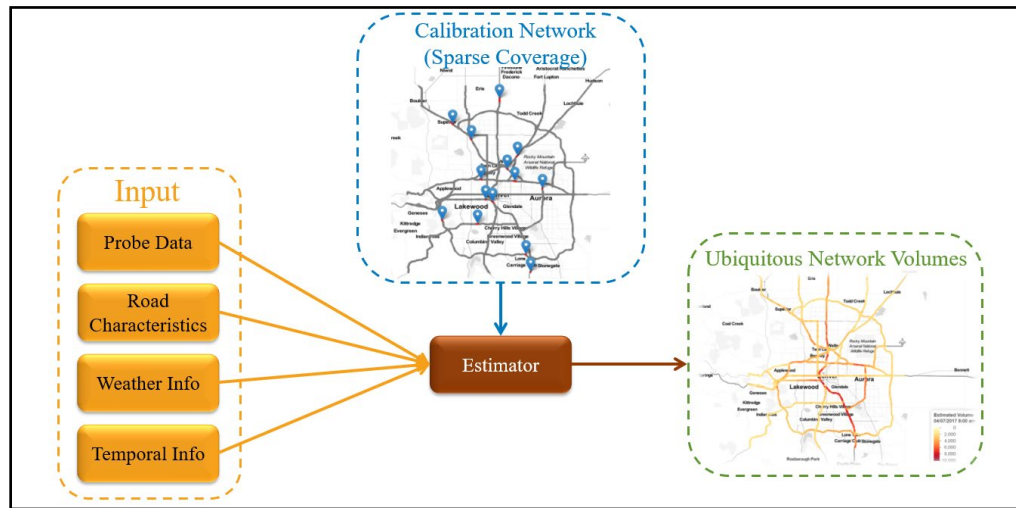


Figure II.1.4.1 Volume estimation modeling framework

Developing a mature commercialized product that reduces the cost, increases observability, and improves the robustness of obtaining traffic volume estimates will benefit the transportation planning and transportation-energy research communities, as well as serve other commercial purposes. The basic method has been demonstrated by the National Renewable Energy Laboratory (NREL) in collaboration with the I95 Corridor Coalition and the University of Maryland (UMD), under a grant from the Federal Highway Administration (FHWA). At full scale deployment, this technology can provide any measure of central tendency of traffic volume, as well as monitor the roadways in real-time for perturbances resulting from unusual events.

Objectives

The primary objective of this project is to increase the observability of traffic volume information in the nation. With increasing proliferation of technology in the form of automated, connected, electrified, efficient, and shared vehicle systems, it is critical now more than ever to have an accurate understanding of how much traffic is on the roads, each hour of the day, and each day of the year everywhere on the network. Such information has enormous utility in transportation as well as energy domains.

- Transportation planners can use this information to check the adequacy of existing transportation infrastructure.
- Traffic operations personnel can make use of this information to effectively re-route the traffic in case of unexpected network congestion events.
- The energy community can benefit from more accurate estimates of travel related energy and emissions.

Approach

NREL researchers have developed volume estimation models using state-of-the-art machine learning techniques to estimate accurate network-wide ubiquitous traffic volumes using data from the Denver metro region. This work, sponsored by the I-95 Corridor Coalition, established the viability of the approach. In the proof-of-concept work, three months of data from 14 CCS within the Denver metropolitan area were used, along with details about roadway geometry, weather, traffic speed, and other publicly-available road attribute data, to train ML algorithms in conjunction with the commercial vehicle probe data (number of probe observations and average observed speed). Then, the well-trained ML algorithms were used to estimate volume for any hour, anywhere on the network. Performance of the methodology was discerned by reserving

data from one of the 14 stations for validation, training the ML algorithm on the remaining 13 stations, and then applying the training algorithm on the reserved station and calculating its accuracy.

A web application prototype that estimates the traffic volume on major corridors and freeways in Denver was also developed at NREL. As displayed in Figure II.1.4.2, given any time of day, any day of month, and any month of the year, the web application displays estimated traffic volumes everywhere on the network.

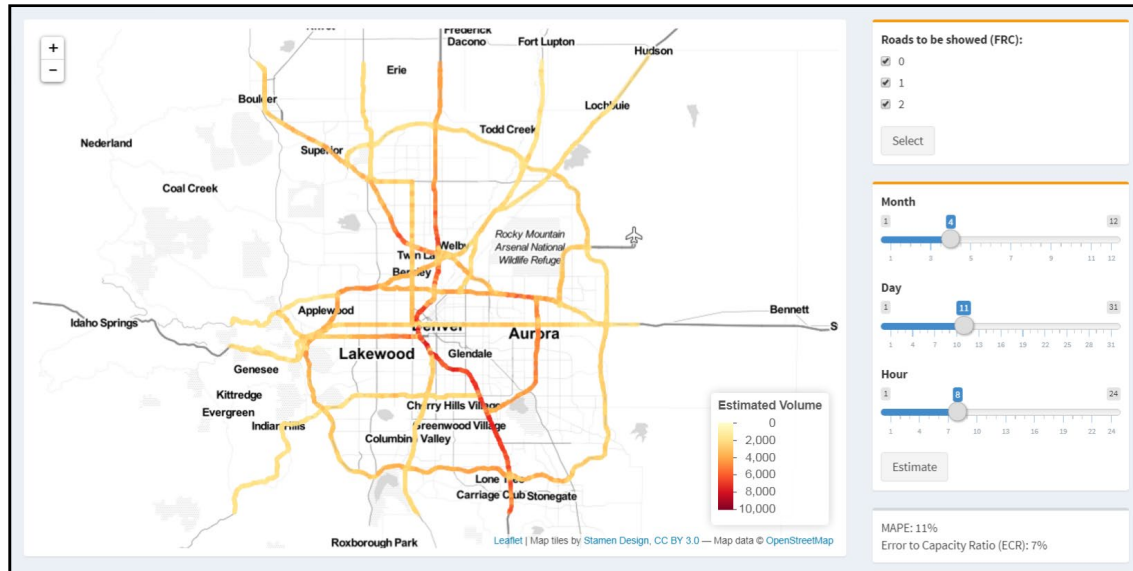


Figure II.1.4.2 A web application prototype for the volume estimation

The initial validation results from the proposed methodology have been shared with several state DOTs (CDOT, Virginia DOT, Kansas DOT, Maryland State Highway Administration and others). Under the TCF project, the volume estimation methodology and the web application prototype will be further validated and refined into a commercial grade product/service that DOTs (federal, state and local) can readily adopt to gain 100% observability of network traffic volumes. The funding from the TCF will take the process out of the lab and exercise it in broad operational settings, vetting the technology and identifying any critical implementation and integration issues.

Results

Preliminary development of the volume estimation algorithm was conducted using data obtained from the roadway network in Denver metropolitan area. The dataset used for estimation was merged from three data sources—TomTom probe vehicle data, Colorado Department of Transportation (CDOT) CCS data, and weather information from Weather Underground. TomTom probe vehicle data collects travel time, speed, and probe vehicle count through their GPS devices, as well as road characteristics such as speed limit and functional road class information on every segment of TomTom road network. CDOT CCS data includes ground truth traffic volume and lane count at locations where CCSs deployed on Colorado highway system. Weather Underground provides daily weather information such as temperature, visibility, wind, and precipitation. All the data was aggregated on an hourly basis. Three months of data from Feb 1, 2017 to April 30, 2017 for all 14 CCS locations in Denver roadway network was retrieved and aggregated by location and time for modeling. Figure II.1.4.3 shows the geospatial distribution of CCSs on Denver roadway network and their matched TomTom segments marked in red. Three machine learning models namely Random Forest (RF),

Gradient Boost (GB) and Extreme Gradient Boost (XGB) were compared to identify the model that provides best predictions, with high computational efficiency.

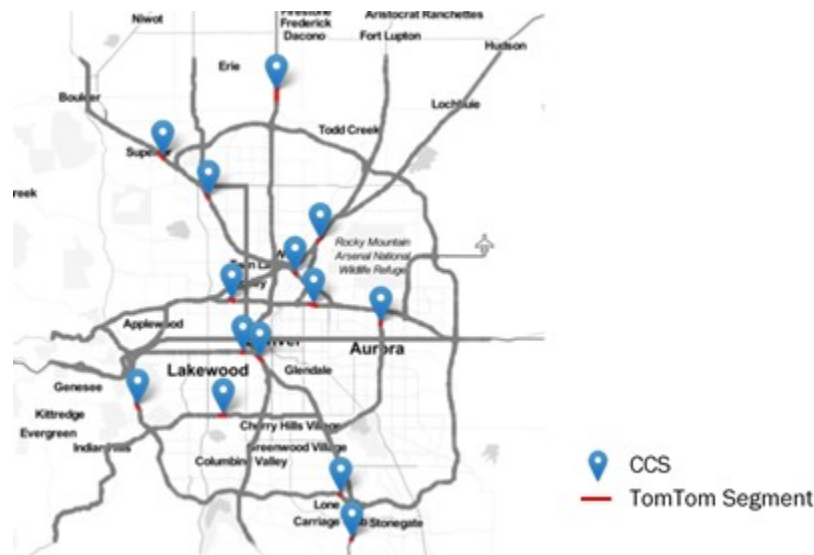


Figure II.1.4.3 Geospatial distribution of CCSs on Denver roadway network

Comparison Between Various Machine Learning Models

The model performance averaged across all 14 CCS locations is presented in Table II.1.4.1. The observed and estimated hourly volumes at a given station are used to compute the Mean Absolute Percentage Error (MAPE), Error to theoretical Capacity (ETCR), and Coefficient of Determination (R^2) values as show in the equations below.

$$\text{MAPE} = \frac{1}{N} \sum_{i=1}^N \frac{|V_i - \hat{V}_i|}{V_i} \quad (1)$$

$$\text{ETCR} = \frac{1}{N} \sum_{i=1}^N \frac{|V_i - \hat{V}_i|}{C_i} \quad (2)$$

$$R^2 = \frac{\sum_{i=1}^N (\hat{V}_i - \bar{V})}{\sum_{i=1}^N (V_i - \bar{V})} \quad (3)$$

Where

V_i is the observed volume

\hat{V}_i is the estimated volume

\bar{V} is the average volume

C_i is the roadway capacity

N is the total number of observations

The error measures presented below are based on the values of these error measures across the 14 iterations of the validation. From Table II.1.4.1, it can be observed that RF, GBM, and XGBoost yield very similar results with an R^2 of 0.92, 0.93, and 0.91, MAPE of 17.8%, 18.3% and 17.7%, and ETCR of 5.2%, 4.8% and 5.3%. The high R^2 of values indicate that the models fit the data very well. For all three models, ETCR is about 5%. Recently, Young et al. (2017) conducted a survey asking representatives from state DOTs what they think is a reasonable level of accuracy for volume estimation to be considered as ‘useful’ for transportation planning and operations purposes. The survey elicited responses of representatives from 14 state DOTs, and an

overwhelming majority responded that the preferred level of accuracy for the model estimation is to be within 10% of roadway capacity. It can be observed from Table II.1.4.1 that accuracy of all the three models exceed the expected accuracy level from the survey results, and hence can be considered useful for transportation planning as well as operations purposes. Though GBM provides the best predictions of all the ML methods tested, XGBoost was chosen for implementation purposes as it provides results almost as good as GBM and requires only a tenth of the time to train compared to GBM. As volume estimation models need to be trained and calibrated on a regular basis, having a computationally efficient algorithm will be beneficial.

In addition to comparisons across various machine learning models, an exercise was undertaken to quantify the impact that probe data has on the effectiveness of the predictive algorithm. To identify this, two algorithms with the exact set of input variables, one with and one without probe data were estimated. From results presented in last row of Table II.1.4.1, it can be seen that probe data helps cut the MAPE and ETCR by about half and improves the R² value greatly.

Table II.1.4.1 Performance Assessment of Various Machine Learning Models to Predict Hourly Traffic Volumes

Model	MAPE	ETCR	R2	Training Time
RF	17.8%	5.2%	0.92	73s
GBM	18.3%	4.8%	0.93	124s
XGBoost (with Probe Data)	17.7%	5.3%	0.91	13s
XGBoost (without Probe Data)	39.4%	12.4%	0.65	--

Colorado Freeway Results

The developed models were tested by estimating the temporal variation of volume for a whole week. The station ID 4 on freeway US-36 eastbound during the one-week period from Feb 21 to Feb 27, 2017 was selected for test. US-36 is the major freeway for commute between Boulder and Denver. The volume estimation results for XGBoost method are shown in Figure II.1.4.4.

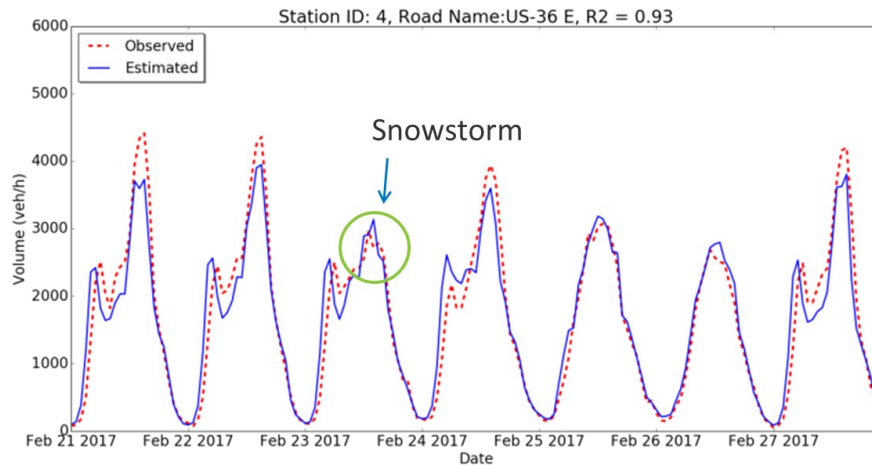


Figure II.1.4.4 Performance of XGBoost Algorithm in Predicting Traffic Volumes

The blue line indicates estimated volume, while the red dashed line represents the actual volume measured by CCS at that location. It can be observed from the figure that the methodology not only provides accurate volume predictions for both peak and off-peak traffic conditions, but also captures the abnormal volume variations during inclement weather (a snowstorm that occurred on Feb. 23, 2018). These initial findings, coupled with observations on importance of probe data presented above, confirmed the potential for probe data derived volume estimates to move further toward full-fledged development of a large-scale product.

Conclusions

An initial research effort tested the use of commercial probe data to estimate traffic volumes in conjunction with other available roadway attributes and weather data. Three tree-based ensemble learning models—RF, GBM and XGBoost were built to estimate traffic volume on the transportation network in the metropolitan area of Denver. All the three machine learning models were demonstrated to be able to capture the temporal variation of traffic volume under both off-peak and peak hour traffic conditions. However, XGBoost was observed to have greater computational efficiency than the other two methods. Consistent with expectations, it was observed that probe vehicle data is critical in accurately estimating traffic volumes. The estimators were calibrated using volume data from 14 CCS locations in the Denver metropolitan region, and then applied to estimate ubiquitous traffic volumes on all freeways and major highways in an around Denver. The accuracy of the volume estimates demonstrates the viability of the approach and affirms that ubiquitous volume data (similar to speed data) is now within reach.

Through the technology commercialization fund, the ML algorithms will be fine-tuned further, and the volume estimation method will be tested in additional states. The ideal end-state of this project is a web-based traffic volume estimation product that provides hourly traffic volumes across all the roads in a state or region, accessed either visually (through thematic maps) or through an API call for a specific roadway and time for machine to machine communication. Mechanisms will be built into the system for periodic self-calibration (every week, every month etc.) based on reference data available at high confidence. The data will be seamlessly integrated into existing transportation and energy applications at DOTs and energy planning offices.

Key Publications

1. Hou, Yi, Stanley E. Young, Anuj Dimri, Venu M. Garikapati, and Nicholas Cohn. “Network Scale Ubiquitous Hourly Volume Estimation Using Tree-Based Ensemble Learning Methods”. *Submitted to Expert Systems With Application*, 2019.

References

1. Young, Stanley E., Yi Hou, Kaveh Sadabadi, Przemysław Sekula, and Denise Markow. Estimating Highway Volumes Using Vehicle Probe Data—Proof of Concept. Presented at 24th ITS World Congress, Montreal, Canada, 2017.

Acknowledgements

- The PI would like to acknowledge the efforts of the NREL team (Yi Hou, Anuj Dimri, Jinghui Wang, and Kevin Kasundra) in the development of the volume estimation models using machine learning techniques.
- The project team offer their thanks to John Auble and his team at TomTom, Inc. for their continued support and encouragement in commercializing the NREL-developed volume estimation algorithm.
- Sincere thanks go to Dr. Stan Young for his guidance and expert assessment in revising model results.
- The project team would like to extend their sincere thanks to DOE Technology Manager Erin Boyd, for her guidance on the project.

II.1.5 Transportation Data Analytics (Big Data Systems for Mobility (BDSM)) (LBNL)

Jane Macfarlane, Principal Investigator

Lawrence Berkeley National Laboratory
1 Cyclotron Road
Berkeley, CA 94720
E-mail: jfmacfarlane@lbl.gov

Eric Rask, Principal Investigator

Argonne National Laboratory
9700 S Cass Avenue
Lemont, IL 60439
E-mail: erask@anl.gov

Robert Rallo, Principal Investigator

Pacific Northwest National Laboratory
902 Battelle Boulevard
Richland, WA 99354
E-mail: robert.rallo@pnnl.gov

Prasad Gupte, DOE Technology Manager

U.S. Department of Energy
E-mail: prasad.gupte@ee.doe.gov

Start Date: October 1, 2018	End Date: September 30, 2019	
Project Funding (FY19): \$2,000,000	DOE share: \$2,000,000	Non-DOE share: \$20,000

Project Introduction

The purpose of this program is to develop the data science and high performance computing (HPC) supported computational framework needed to build next-generation transportation/mobility system models and operational analytics. In order to represent real-world urban systems, the models and analytics must scale both in spatial and temporal complexity. We will build on previous work in transportation systems, electrical grid analytics, and atmospheric modeling that has been developed within the partnered laboratories.

This work will focus on four key objectives that address critical transportation modeling challenges:

- Develop transportation system modeling approaches that permit parallel implementation or are limited by computational complexity and can be implemented on HPC,
- Develop methods for capturing and adjusting for data velocity and veracity across both temporal and geospatial scales,
- Understand the appropriate role of machine learning, agent-based models, and streaming analytics including feedback mechanisms, extensibility, and propagation of data veracity through those systems, and
- Develop mechanisms for semantically tuning lower level learning systems in order to create robust automated solutions.

Objectives

By leveraging high-performance computing and big data analytics we will further our understanding of transportation systems. Specifically, current transportation planners in urban areas do not have adequate tools

for understanding the complex dynamics of their cities. Our objective is to focus on creating an ability to rapidly model urban scale transportation networks using real-world, near real-time data to optimize traffic for mobility, energy and productivity. Specific goals include:

- Learn patterns in the real-world data to inform our modeling with the goal of understanding how to respond to transient events such as accidents, emergency response, and transportation network changes
- Investigate the drivers of those patterns and how we might impact those patterns and optimize on energy versus traditional throughput models
- Develop control ideas for large-scale urban transportation networks through tractable computational simulations that can describe emergent behavior of vehicle dynamics
- Provide urban scale modeling tools that can integrate into urban planning and design processes and tools.

Approach

1. Define Appropriate Role of HPC in Transportation Planning
 - Determining the best use of HPC capabilities in the Transportation Planning field.
2. Automated Collection, Modeling and Validation of Data Using HPC
 - Higher level algorithms that operate on historical data to predict future dynamics.
3. Develop HPC Network Models
 - Modeling of urban scale transportation networks.
4. Couple Data Ingestion into Modeling Platform
 - Define a common platform for the data ingestion and modeling tools. This includes data ingestion and preprocessing methods for raw data cleaning, error detection and correction, and missing data imputation.
 - Real-world data will eventually come from the Connected Corridor program supported by CalTrans in Los Angeles

Results

Task 1: Define Appropriate Role of HPC in Transportation Planning

We have established strong relationships with San Jose and LA Metro. We have also reached out to Boise, Seattle and Portland. The project was designed to focus on the LA region due to the relationship with the UCB Connected Corridor which is designed to do real-time infrastructure sensing. We have also developed a relationship with Portland that can provide access to data that could be useful to test data algorithms and compare with LA data.

Task 2: Automated Collection, Modeling and Validation of Data Using HPC

Traffic Forecasting and Diffusion Convolutional Recurrent Neural Network (DCRNN)

Traffic forecasting approaches are critical to developing adaptive strategies for mobility. Traffic patterns have complex spatial and temporal dependencies that make accurate forecasting on large highway networks a challenging task. Previously, within these and additional efforts, Diffusion Convolutional Recurrent Neural Networks (DCRNNs) have achieved state-of-the-art results in traffic forecasting by capturing the spatiotemporal dynamics of the traffic. Despite the promising results, DCRNNs for large highway networks still remain elusive because of computational and memory bottlenecks. Within this section, this year's work

focused on an approach to apply DCRNN for a very large highway network (much larger than previous examples in the literature). A graph-partitioning approach was used to decompose a large highway network into smaller networks and train them simultaneously on a cluster with Graphics Processing Units (GPU).

Using this approach, we forecast the traffic of the entire California highway network with 11,160 traffic sensor locations simultaneously (a first as far as the project investigators are aware). The very large number of sensors is also key as the techniques will be applied to probe-based data as well. The applied approach can be trained within 3 hours of wall-clock time using 64 GPUs to forecast speed with high accuracy. Further improvements in the accuracy are attained by including overlapping sensor locations from nearby partitions and finding high-performing hyperparameter configurations for the DCRNN using DeepHyper, a hyperparameter tuning package. Work done in this fiscal year also demonstrated that a single DCRNN model can be used to train and forecast the speed and flow simultaneously and the results preserve fundamental traffic flow dynamics. These prediction capabilities support the overall goals of the project allowing for advanced highway traffic monitoring systems, where forecasts can be used to adjust traffic management strategies proactively given anticipated future conditions.

For modeling the California highway network, data from the PeMS system was used. It provides access to real-time and historical performance data from over 39,000 individual sensors. The individual sensors placed on the different highway lanes are aggregated across several lanes and are fed into vehicle detector stations. The official PeMs website shows that 69.59% of the $\approx 18K$ stations are in good working condition. The remaining 30.41% do not capture time series data throughout the year. These are excluded from our dataset. Thus, the final dataset has 11,160 stations for the year 2018 with granularity of 5 minutes. The data includes timestamp, station ID, district, freeway, direction of travel, total flow, and average speed(mph). For the experimental evaluation, ANL's Cooley, a GPU-based cluster at the Argonne Leadership Computing Facility, was used. It has 126 compute nodes, where each node consists of two 2.413 GHz Intel Haswell E5-2620 v3 processors (6 cores per CPU, 12 cores total), one NVIDIA TeslaK80 (two GPUs per node), 384 GB RAM per node, and 24 GB GPU RAM per node (12 GB per GPU). The compute nodes are interconnected via an InfiniBand fabric. The input data for different partitions (time series, and adjacency matrix of the graph) were prepared offline and loaded into the partition-specific DCRNN before the training started.

Impact of number of graph partitions on accuracy and training time

One focus was to experiment with different numbers of graph partitions and show that partitions with larger number of nodes require longer training time and partitions with fewer nodes can reduce the forecasting accuracy. Metis was used to obtain 2, 4, 8, 16, 32, 64, and 128 partitions of the California highway network graph. The average number of nodes in each case is 5,580, 2,790, 1395, 697, 348, 174, and 87, respectively. Figure II.1.5.1 shows the distribution of mean absolute error (MAE) for all nodes obtained using box-and-whisker plots. From the results we can observe that medians, 75% quantiles, and the maximum MAE values show a trend in which an increase in the number of partitions decreases the MAE. From 4 to 64 partitions, the median of MAE decreases from 2.11 to 2.02. The increase in accuracy can be attributed to the effectiveness of the graph partitioning of Metis that separates nodes that were not temporally and spatially correlated. For smaller number of partitions, presence of such nodes increases MAE. For 128 partitions (with only 87 nodes per partition), the observed MAE values are higher than that of 64 partitions. This is because the graph partition results in significant number of spatially correlated nodes ending up in different partitions. This can be assumed as a tipping point for graph partitioning, which relates to the size and spread of the actual network.

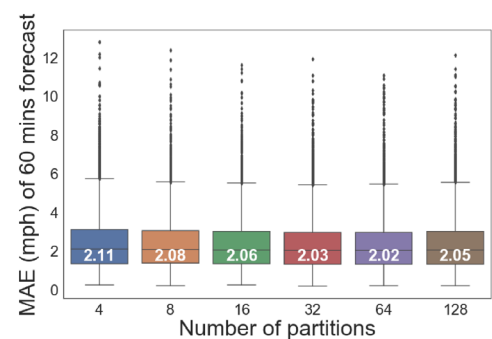


Figure II.1.5.1 Distribution of MAE for different number of partitions.

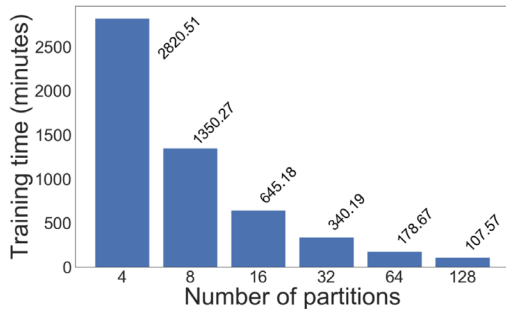


Figure II.1.5.2 Training time for DCRNNs with different number of partitions

Figure II.1.5.2 shows the training time required for different numbers of partitions. One can observe that the training time decreases significantly with an increase in the number of partitions. One can also observe that our approach reduces the training time from 2,820 minutes on 4 partitions (= 4 GPUs) to 178.67 minutes on 64 partitions (= 64 GPUs), resulting in a 15.78x speedup. Until 64 partitions, we observe almost a linear speedup, where doubling the number of partitions (and GPUs) results in $\approx 2X$ speed-up. However, the speedup gains drop significantly with 128 nodes. This can be attributed to the reduction in the work load per GPU, where there is not enough workload for the GPU given that there are only 87 nodes per partition. Since the best forecasting accuracy and speedup were obtained by using 64 partitions, it was used for the remainder of work discussed in this report.

Impact of training data size

From the full 36 weeks of training data, the last 1, 2, 4, 12, and 20 weeks of data were selected for training the DCRNN. The last weeks of data were chosen to minimize the impact of highway and sensor upgrades. The figure below shows the distribution of MAE of all nodes obtained using box-and-whisker plots. From the plots it can be observed that the medians, the 75% quantiles, and the maximum MAE values show that increasing the training data size decreases the MAE. These results show that DCRNN, similar to other state of the art neural networks, can leverage large amounts of data to improve accuracy. Therefore, we use the entire 36 weeks of training data in the rest of the experiments.

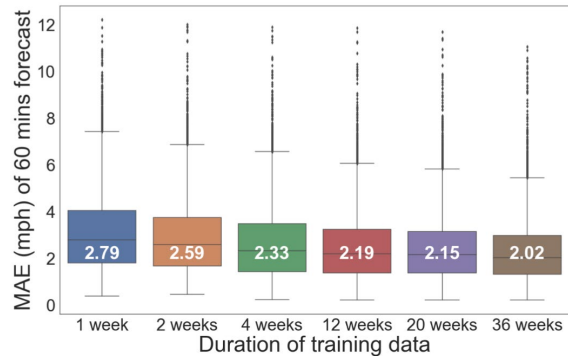


Figure II.1.5.3 Distribution of MAE of all nodes

Multi-output forecasting

This year’s experiments has shown that a single DCRNN model can be used to predict the speed and flow simultaneously and the forecasting results preserve the fundamental properties of traffic flow. Figure II.1.5.3 shows the distribution of MAE of all nodes using box-and-whisker plots. In Figure II.1.5.4, the first and second box plots show the speed forecast from the DCRNN models that are trained to forecast only speed and to forecast speed and flow simultaneously. Similarly, the third and fourth box plots are for flow forecasts. The median of MAE from speed only model (first box plot) is 2.02 mph, which got reduced to 1.98 mph when the multi-output model (second box plot) is used. Similarly, the median of MAE from flow only model (third box plot) is 21.20 veh./hr, which was reduced to 20.64 veh./hr when the multi-output model (fourth box plot) is used.

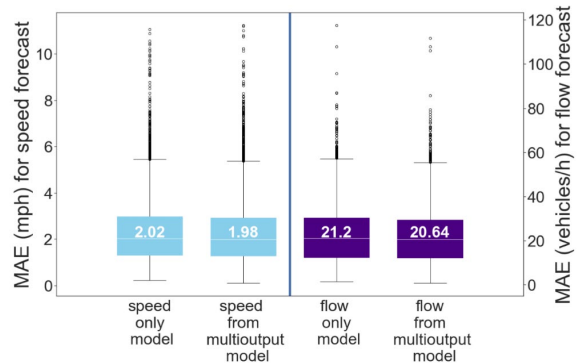


Figure II.1.5.4 Box plot distribution of MAE for speed and flow forecasting. From left to right the box plots show the results of: speed forecasting from speed only model, speed forecasting from multi-output model, flow forecasting from flow only model, and flow forecasting from multi-output model

Figure II.1.5.5 shows the speed and flow forecasting results for a congested node1 (ID: 717322 located on the highway 60-E in Los Angeles area) are shown in a scatter plot. It can be observed that the speed and flow forecast values closely follow the fundamental flow diagram with three distinct phases of congestion, bounded, and free flow. This forecasting pattern of DCRNN shows that the model has learned and preserved the properties of traffic flow.

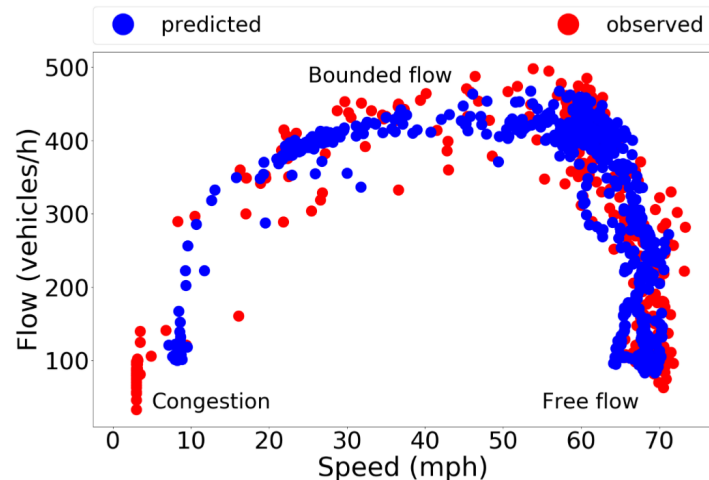


Figure II.1.5.5 Closeness of the predicted flow and speed with observed flow and speed plotted in the form of a fundamental traffic flow diagram.

In the last quarter of FY19, as part of their automated collection of data efforts, we continued working on developing code to validate raw data and to generate relevant metadata information for the LA Metro dataset, integrating additional data points (Caltrans - traffic flow, weather), explored fault-tolerant methodology for the data collection framework, and explored faster data ingestion options using a database engine optimized to store and process time-series data. Figure II.1.5.6 depicts the overall layout of the data ingestion framework being developed. In the context of streaming data analytics, we evaluated several methodologies and techniques for data imputation of near real-time data and explored anomaly detection in streaming data from the perspective data conditioning as well as incident detection.

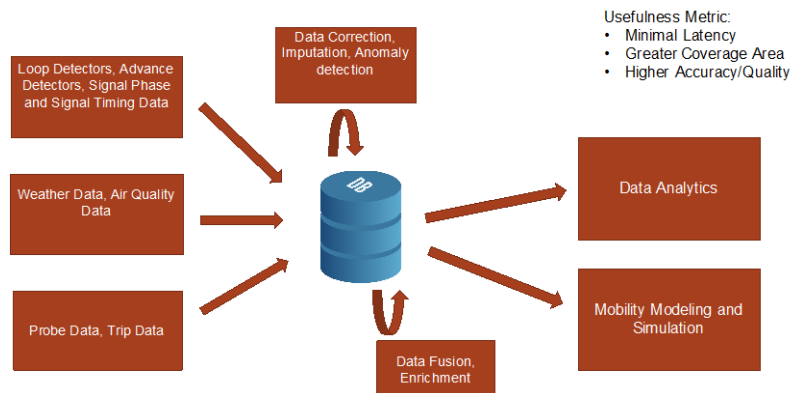


Figure II.1.5.6 Data ingestion framework

Task 3: Develop HPC Network Models

We have continued our development of the Mobiliti distributed-memory, parallel simulation framework to enable new features and demonstrate its capabilities on high-performance computing platforms. Our progress includes the addition of vehicle controllers to evaluate dynamic vehicle rerouting behavior, demonstrating the simulator using improved maps from HERE Technologies for both San Francisco and Los Angeles

metropolitan areas, improving our demand model input using SFCTA's newest CHAMP6 model data and the Los Angeles SCAG demand model data, and maintaining parallel scalability to achieve high performance on distributed, parallel computing platforms.

As described in previous reports, Mobiliti is structured as a distributed parallel discrete event simulation, with actors that pass events between each other. The model includes link actors that are responsible for mediating vehicle congestion (the more vehicles try to use a link at the same time, the slower they traverse the link). Vehicles are modeled with events passed between link actors that represent vehicles traversing from link to link as they move from their origin to their destination.

In order to capture the behavior of vehicles that change their routes in response to unexpected or emergent congestion, we have added vehicle controllers, another class of actors that are responsible for servicing dynamic vehicle re-routing requests. Link actors periodically send updates about their congestion state to the vehicle controllers, which update their knowledge about the current status of the road network. Vehicles with active routing enabled can periodically check with a local vehicle controller to determine if a new route should be taken given this information.

Also, the simulator can now read a scenario input file that modifies the traversal time on the specified links at the specified times to mimic the impact of a traffic incident. Researchers can evaluate new scenarios by supplying their own files that modify the properties of the road network. We further enhanced the instrumentation of the simulator to capture relevant metrics such as vehicle controller behavior (number of reroute check requests, number of route calculations, number of vehicle diversions), vehicle behavior (differences in trip routes, times, distance, and fuel), and link behavior (impact on storage occupancy and utilization ratios).

We demonstrated how researchers might use the simulator to evaluate the impact of varying degrees of dynamic rerouting with an experiment that simulated a hypothetical traffic incident that caused a major slow down on the US-101 freeway in San Francisco. (Figure II.1.5.7 below.)

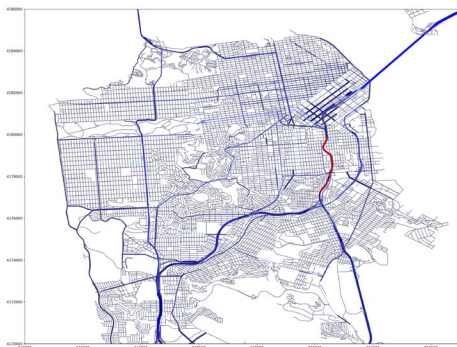


Figure II.1.5.7 Hypothetical incident location in red

We did a parameter sweep for different penetrations of vehicles with dynamic rerouting capability and showed how major alternative arterials were able to absorb the diverted traffic off of the US-101 freeway. Figure II.1.5.8 and Figure II.1.5.9 below show the impact of dynamic rerouting on flow rates for the road network around the traffic incident.

This was a demonstration of the type of experiment mobility researchers can conduct with our simulator. Further details about this experiment will be reported in a paper that we have submitted for publication. We have also improved various other aspects of the link model, including the addition of a link storage capacity constraint that captures upstream spillback as links become congested.

In addition to capturing link dynamics accurately, it is important for the Mobiliti simulator to be able to take advantage of the most realistic road network data and demand data available for accurate results. To this end, we have implemented additional software modules to load and clean map data from HERE Technologies and trip data from both the SFCTA's newest



Figure II.1.5.8 Traffic flow without rerouting



Figure II.1.5.9 Traffic flow with rerouting

CHAMP6 demand model and the LA SCAG data set used by the Connected Corridors project. These improvements have increased the spatial resolution of the simulated trip legs by specifying trips using multi-level traffic analysis zones for origin and destination node selection, as well as the temporal resolution by specifying start times at the granularity of minutes rather than multi-hour time periods. Furthermore, the new model includes metadata to associate multiple trip legs to the same persons and the purpose of each trip leg, which will enable researchers to model electric vehicle charging choices and vary the time spent at each stop.

We have also improved other aspects of the simulator such as the quality of the link actor partitioning, which is important to achieve scalable performance for parallel execution. Even though dynamic rerouting is very computationally expensive due to the large cost of each new routing calculation on large graphs, we have successfully run our simulator for the San Francisco Bay Area (1.1 million nodes and 2.2 million links with 22 million trip legs) with dynamic re-routing enabled in just a few minutes of parallel execution on up to 512 cores of the Cori computer at NERSC. (See Figure II.1.5.10.)

Energy Modeling:

To estimate the energy impacts of a particular drive trace, a data-driven methodology to estimate vehicle energy/fuel usage was developed to provide a fast and reasonably accurate estimate of the energy usage of a particular driving pattern (Speed versus Time), which will ultimately be predicted using a similar process to the DCRNN traffic predictions discussed above. To these ends, representative vehicles were chosen from Argonne’s Dynamometer Database and used as a trial set for a simple, data-driven energy consumption prediction based on vehicle speeds and accelerations for a particular drive cycle. Figure II.1.5.11 below highlights the vehicles used for a preliminary (and BEV/Conv. focused) assessment of the techniques.

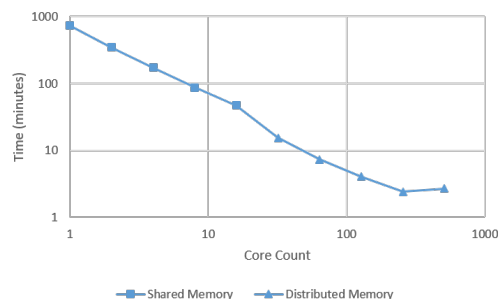


Figure II.1.5.10 Simulation parallel scaling with 100% active vehicle rerouting penetration on Cori

	2015 BMW i3 EV	2018 Mazda CX-9	2012 Ford Focus ST	2018 Chevrolet Bolt EV	2017 Ford F-150	2017 Toyota Highlander
Technology	22 kWh 360 V Li-ion, direct drive EV	Turbocharged I4, 4 valve per cylinder	Turbocharged I4, 4 valve per cylinder, direct injection	60 kWh ~400V, Li-ion, direct drive EV	Twin-turbocharged and intercooled DDHC 24-valve V6, VVT, aluminum block and heads, port & direct fuel injection	DDHC Aluminon cycle, Direct Injection V6, all aluminum, VVT4
Motor/Engine	25 kW (68 bhp)	2.5-liter SkyActive, 89 x 100mm, 2,488 cc, 13.0:1, 188 kW (255 hp) @5500 RPM, 310 lb-ft @ 2,000 rpm (420 N-m)	EcoBoost 2.0L I4, 2000cc, direct injection, 184kW @ 5500rpm, 350Nm from 1750-4000rpm	Permanent magnetic drive motor, 150 kW (200hp)	286 Nm (268 ft-lb)	3.5 liter (3,456 cc), 24-valve DOHC V6 engine, 207 kW (278 HP) at 6000 rpm and 359 N-m (265 lb-ft) at 4600 rpm.
Transmission	1 speed direct drive	6-speed automatic	6-speed automatic/manual	1 speed direct drive	10 speed automatic	8-speed shifttable automatic
Battery	60Ah (18.8 kWh)	-	-	60 kWh 350 V Ultram-ion	-	-
City/Hwy [mpg]	137 MPG-e (25 kW-hrs/100 mi) 111 MPG-e (20 kW-hrs/100 mi)	-	29 City / 32 Hwy	128 City / 110 Hwy	City: 18-19 / Hwy 21-26	20 City / 26 Hwy

Figure II.1.5.11 Preliminary vehicles assessed for data-driven estimation technique

Using the laboratory data and specific information about the vehicle, evaluated speed traces can be turned into a scatter of speed/tractive force points which correspond to the cycles evaluated within previous laboratory testing. This process is summarized below in the left (speed vs. time) and right (tractive load versus speed) subplots in Figure II.1.5.12 below.

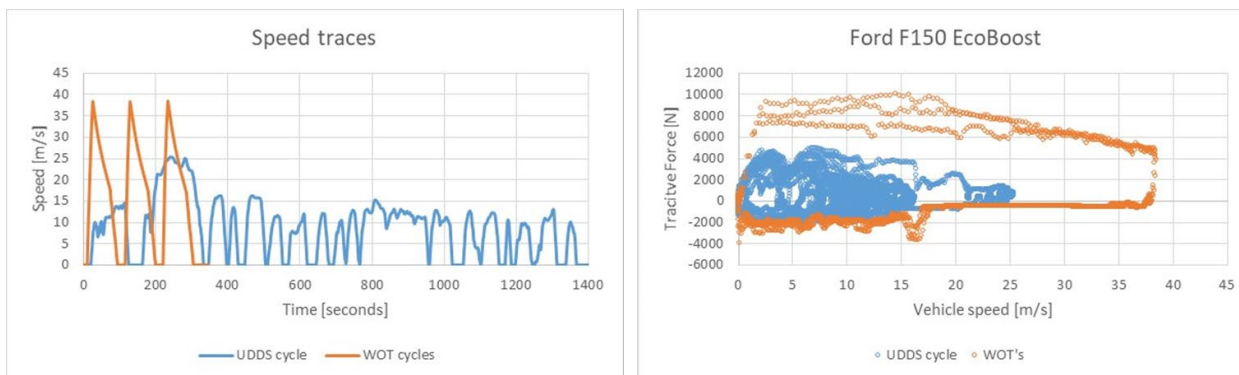


Figure II.1.5.12 Example Speed vs Time and corresponding tractive force versus speed plots for two example drive cycles

If sufficient data is provided from laboratory testing, the entire speed/force chart can be supplemented with an expected instantaneous fuel or battery energy usage, which can then be used to sum energy across various time-steps and calculate overall energy/fuel usage.

A variety of data-driven, machine learning based methods were assessed for this prediction (energy = fcn (speed,force)), but ultimately a boosted decision tree methodology, based on XGBoost, was used for its fast response and accuracy for the candidate datasets used. Future work may refine or modify this methodology, but high accuracy results are still expected for a range of techniques. Training data for the proposed estimation was taken from laboratory testing across the UDDS, Hwy, and US06 drive cycles, supplemented by “Wide-Open-Throttle”, maximum acceleration-based tests to provide the maximum operational envelope for a particular vehicle. While all vehicles evaluated showed very accurate energy estimates across a range of drive cycles, Figure II.1.5.13 below highlights results for a Chevrolet Bolt Electric Vehicle. Even for drive cycles not used in training, the proposed method predicts the energy consumption within less the 1% of actual, well within a reasonable error for integration into the overall methodologies.

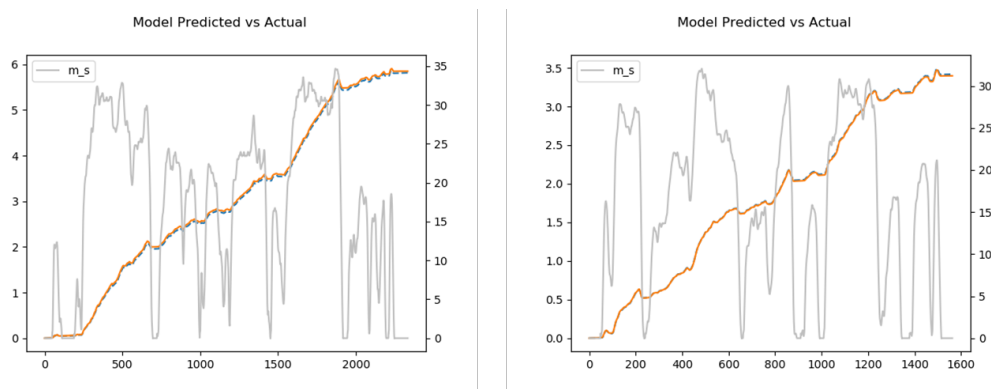


Figure II.1.5.13 Chevrolet Bolt predicted versus actual energy consumption

Ultimately, these data-driven predictions will be integrated into the overall project’s methodologies to better understand the energy implications of a particular link’s driving dynamics as predicted by traffic flow trends employing the DCRNN prediction capabilities discussed above.

In addition to the boosted decision tree methodology (XGBoost), the team also investigated the deep learning approaches based on the recurrent neural networks (long short-term memory) to build even more complex correlations between the instant fuel consumption rate and the historical measurements of features that include fuel consumption estimation itself as a time series. According to dynamometer test datasets, even with similar tractive force and vehicle speed, the fuel rate measurements can be varied significantly due to the fact that hidden factors in the drive cycles are not always captured effectively. For instance, the impact of engine temperature on the fuel consumption and emission rate is significant but it can only be revealed by looking at the historical measurement data. Therefore, we extend the fuel map-based methods with model-free and data-driven approaches to incorporate the hidden feature within the drive cycle patterns. Specifically, dynamometer datasets are processed as time series and then deep recurrent neural networks, i.e., long short-term memory (LSTM), are utilized to capture the complex correlations between instantaneous fuel consumption rate with a number of features in time series that include tractive force, vehicle speed, engine coolant temperature and engine speed for the conventional vehicles. Note that the historical fuel consumption values are also treated as new features. We have achieved up to 0.95 R^2 score over the blind test datasets for conventional vehicles, i.e., Mazda-CX-9.

The real-time fuel and energy prediction results are shown in the following figures. In Figure II.1.5.14, 2013 Nissan Altima is selected for model validation, i.e., 90% drive cycles from the raw measurement data is used for training the LSTM and the remaining 10% randomly selected cycles will be treated as new observed speed

trajectories and the instantaneous estimation is made using the trained LSTM model. Finally, the estimation is compared with the measurement data to validate the model accuracy. LSTM achieves significantly high accuracy for the fuel rate prediction, especially during extreme driving events, e.g., instant accelerations/decelerations. In Figure II.1.5.14 and Figure II.1.5.15, Nissan Leaf is selected to represent the advanced electric powertrain characteristics with additional measurements that are not involved in the conventional vehicle testing, e.g., the voltage and current values for both the AC and DC power supplies.

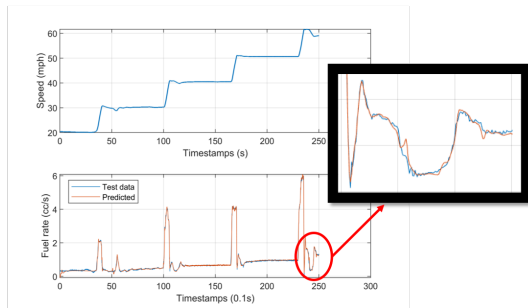


Figure II.1.5.14 Instant fuel consumption prediction for Nissan Altima using LSTM

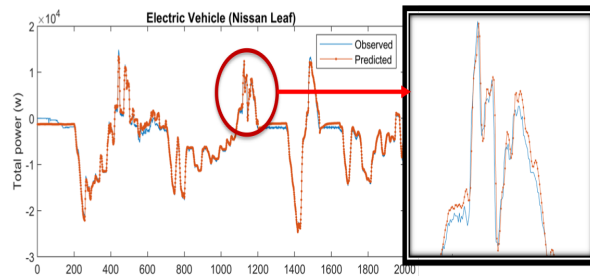


Figure II.1.5.15 Instant energy consumption prediction for Nissan Leaf using LSTM. Note negative values denote discharging energy from the battery, i.e., driving, and the positive values mean the charging energy into the battery, i.e., braking mode.

Furthermore, real-world speed trajectory data, provided by HERE Technologies Inc., is coupled with map-based fuel models to estimate energy performance of the drive cycles located on the I210 highway in Los Angeles. Trajectories with 1 Hz GPS data are processed into time series. We select a time window from Oct. 15th to Oct. 20th and applied different vehicle types (energy models) with the speed trajectories and investigated the energy consumption patterns. The visualization of the time-averaged fuel consumption (Litre/s) is shown in the Figure II.1.5.16 below, where the value of each point refers to the averaged fuel consumption rate per trajectory and periodical patterns can be observed.

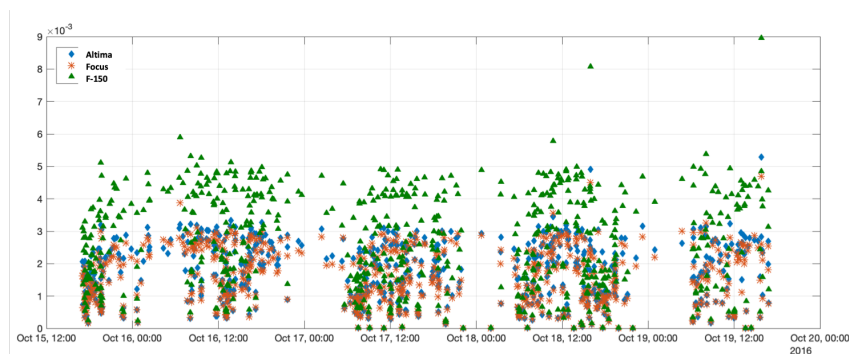


Figure II.1.5.16 Average fuel consumption rate calculations using the GPS probe data for Nissan Altima, Ford Focus and Ford F-150

Task 4: Couple Data Ingestion into Modeling Platform

Streaming Data Analytics

Multiple data sources were used for testing before focusing on the LA region, including the AMS Dallas Testbed data, for which we developed customized data ingestion and preprocessing methods for raw data cleaning, error detection and correction. Basic Safety Messaging data from Wyoming I-80 corridor; from Seattle DOT, WSDOT were also explored. Annual average daily traffic (count), annual average weekday traffic (count) and hourly traffic data (permanent traffic recorders) were calculated.

A summary of the current data sources/streams ingested and collected include:

- *Streaming Data from Caltrans and LA-Metro* We collected data every 60 seconds for the LA-Metro data, and every 30 seconds from Caltrans (raw data), as well as 5 minutes intervals for the Caltrans processed data. Data are ingested in a high-performance time series database, from loop counters for district 5, 7, 8 and 12.
- *Uber data from the City of Los Angeles.* We received quarterly data released by Uber from 2016 till 2018 (~3.5Gb/year). Data analysis tasks performed with this dataset included the exploration of travel times by hour of the day. Recently, we have initiated the processing of the new Uber datasets for average speed information.

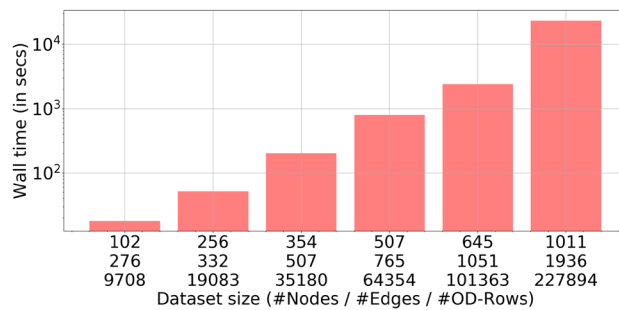


Figure II.1.5.17 Scaling Performance and the need for HPC.

We identified two paths forward for defining performance requirements for ingestion and analysis of near real time data: (i) scalability of graph algorithms, and (ii) real time processing of data. We are continuing the process of exploring the scalability of the published travel time estimation model from the algorithmic point of view. The model has the computational complexity of $O(ET)$, where E is the number of road segment (Edges) and T is the total number of Trips (OD- rows) for the geographic area under consideration. Figure II.1.5.17 shows that the execution time increases exponentially as the number of road segments and

the number of Trips increases and it takes close to an hour to estimate travel time for a reasonably sized road network.

With respect to real time processing, we are assessing data assimilation and data imputation techniques suitable for close to real-time requirements. We also identified that the paths to near real time ingestion and analysis, require a scalable computing platform which is easy to use for a transportation expert with limited HPC knowledge. During the last quarter of FY19, we received and installed Arkouda, a Chapel enabled backend for Python, on a local HPC system. Arkouda is a DoD developed system which enables user to run python scripts transparently on an HPC system. Arkouda has been shown to scale up to 10,000 processors. The Arkouda system will be used to provide scalability to the estimation process. The platform will serve to support efforts related to the validation of transportation models and simulations.

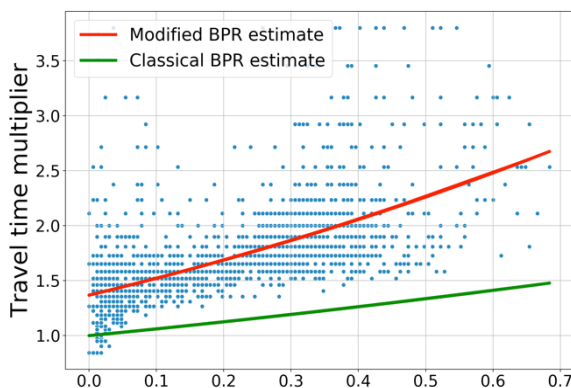


Figure II.1.5.18 Comparing the prediction of the classical BPR function with that of the data-driven counterpart. Classical BPR underestimates the travel time (in other words paints a more optimistic picture)

In the last quarter of 2019, in support of the travel time estimation work, we extended the TAZ-TAZ graph analytics and optimization work to the street level, introduced a scheme for simulating trips between sampled origin and destination vertices within the Origin and Destination TAZs, developed a sampling heuristic for choosing origin-destination (O/D) vertices based on vertex betweenness (i.e., importance), developed a biased trip duration sampling by correlating sampled trip times with free flow travel times for the routes based on shortest path, and developed sparsification routines for problem size reduction, based on edge betweenness and graph connectedness. The team also began exploring HPC strategies for scaling the solution framework; the full

framework has been coded in Python and tested on problem sizes up to 3-mile radius around the LA downtown area. Additionally, support for HERE maps in the code has been completed. As it relates to the Data-driven BPR functions, we developed a parameterized BPR model for prediction of travel times from vehicle flow and link capacity. Figure II.1.5.18 shows the comparison between the predictions of the data driven BPR function relative to the classical BPR formulation. High quality data obtained for the city of Arcadia were used to perform and assess a preliminary reparameterization of the BPR function for two particular links. After adjusting the non-linear model, the form of the data driven BPR function is as follows:

$$t_{tr}(l) = 1.37t_{ff}(l) \left(1 + 0.3 \left(\frac{v(l)}{c(l)} \right) \right)^{3.59}$$

Other notable activities in FY2019 included the development of datasets to support Mobiliti's model validation. We developed a coarse TAZ-TAZ prototype model for travel time estimation from the Uber data for LA, which incorporates graph analytics and optimization procedures (i.e., non-negative least-squares) to identify model parameters. The performance of the model was validated using a subset of the complete UBER data.

Conclusions

We have made significant progress towards our goals in the past year. Our initial work to use machine learning to evaluate and predict the geospatial, temporal device data has shown promising results. Specifically, Temporal Convolution Networks had been applied and appear transferable for our initial traffic estimation problem. Automated hyper-parameter search and tuning has been developed and allow efficiencies that will be foundational to our future work. Initial efforts are underway to consider data veracity issues associated with big data feeds from a variety of mobile devices. Algorithms to detect and correct poor data quality are being developed for both ingestion at real-time and quasi real-time. Our urban simulation work has leveraged an existing code base for grid simulation and has allowed us to build urban-scale simulations of the Bay Area and LA Basin road networks with run times on the order of minutes. We support simulating the SFCTA and LA SCAG demand models that specify 21.7M and 41.6M vehicle trips, respectively. We have demonstrated the capability to simulate and evaluate the impact of active dynamic routing at metropolitan scale. We have also improved our link model to include a storage capacity constraint. This type of behavior is much more reflective of real-world urban dynamics. Energy modeling has been tied to the foundational simulation mechanisms and models fuel consumption using the dynamometer derived data from ANL. In addition to the initial ORNL energy modeling using CART, NREL has provided additional input to this initial model and an on-going improvement to this model is underway.

A cloud-based platform that captures and ingests, in real-time, data provided by multiple traffic sensors in the LA basin area has been developed. The developed algorithm for estimating travel times (informed by real traffic data) provides reasonable estimates for inter TAZ travel times as well as for travel times across arterial links. Current work focuses on adapting the algorithms to leverage HPC resources to scale the calculations to the full metropolitan network. The method will be extended to use the same demand data and routing models used in the Mobiliti simulation to provide realistic scenarios to validate the simulation results. Similarly, high-resolution traffic data for the city of Arcadia is being used to develop data-informed surrogates for the BPR function. The new data-driven link travel time models will be provided to the Mobiliti simulation to allow for more realistic link dynamics.

Key Publications

1. Tanwi Mallick, Prasanna Balaprakash, Eric Rask, Jane Macfarlane. 2019. Graph-Partitioning-Based Diffusion Convolution Recurrent Neural Network for Large-Scale Traffic Forecasting, to be presented at TRB 2020.
2. Arun V. Sathanur, Vinay Amatya, Arif Khan, Robert Rallo, and Kelsey Maass. 2019. Graph Analytics and Optimization Methods for Insights from the Uber Movement Data. In Proceedings of the 2nd

ACM/EIGSCC Symposium on Smart Cities and Communities (SCC '19). ACM, New York, NY, USA,

3. Visweswara Sathanur A., V.C. Amatya, M.H. Khan, R.J. Rallo Moya, K.E. Wolf, and R.D. Deshmukh. 07/10/2019. "Characterizing Arterial Travel from Mobility Data." Presented by K.E. Wolf at Global Cities Team Challenge, Washington, District of Columbia. PNNL-SA-145074
4. Cy Chan, Bin Wang, John Bachman, Jane Macfarlane. 2019. "Simulating the impact of dynamic re-routing on urban-scale road networks" Submitted to special issue GeoInformatica.
5. Kanaad Deodhar, Colin Laurence, Jane Macfarlane. 2019. "Creating "Mode Shift Opportunity" with Metropolitan Scale Simulation, SCC 2019 Conference Portland OR.

References

1. <https://www.influxdata.com/>

III Advanced Technology R&D

III.1.1 Energy Impact of Connected and Automated Vehicle Technologies (University of Michigan, ANL)

Huei Peng, Principal Investigator

University of Michigan
G036 Lay Auto Lab., Ann Arbor, MI 48109
E-mail: hpeng@umich.edu

Jason Conley, DOE Project Manager

U.S. Department of Energy
E-mail: John.Conley@netl.doe.gov

David Anderson, DOE Program Manager

U.S. Department of Energy
Email: David.Anderson@ee.doe.gov

Start Date: October 1, 2015	End Date: December 31, 2018	
Total Project Cost: \$2,970,197	DOE share: \$2,673,096	Non-DOE share: \$297,101

Project Introduction

Modern vehicles can generate tens to hundreds of GB of data every hour. Much of the utility of connected vehicle technologies lies in the potential value of this vast amount of data, including vehicle internal states, geographic road features, traffic flow and density, and individual vehicle movements, some of which are now available in separated repositories. The confluence of connected mobility data and emerging big data analytics presents both a challenge and an opportunity. The available data is then used to better understand driver behavior, energy and carbon emission, and traffic dynamics. For this project, data have been collected to (1) develop behavioral models representing how drivers react to information they are provided, (2) validate the traffic flow simulation model of Ann Arbor developed in POLARIS and (3) develop new driver model for Autonomie (e.g., how do drivers react to traffic signal information projected on a screen).

Another current trend in the industry is the rapid development of automated vehicle technologies. Recent breakthroughs in sensors, perception, and control technologies make vehicle automation much closer to reality. Almost all major OEMs and first tier suppliers have active programs for Connected and Automated Vehicles (CAVs). Many of them have aggressively target dates to bring their concepts to the market. While many research activities have occurred in the US over the past couple of years, the vast majority of those projects have been focused on safety rather than on energy and mobility.

The University of Michigan (UM) researchers have extensive experience equipping vehicles, collecting data, and analyzing the data to gain insight, or build models to understand various aspects of the transportation systems. The UM researchers will lead the experimentation part of this project, equipping 500 vehicles with ODB-port dongles to collect vehicle velocity and fuel consumption information.

The experimental data has been collected and used to develop and calibrate an open-source transportation network models POLARIS, which can be used in coordination with a more detailed energy simulation tool Autonomie to simulate the vehicles driving in the City of Ann Arbor traffic. The calibrated fuel consumption model has been used to develop and implement energy-saving concepts such as eco-routing, and adaptive traffic signal control for congestion reduction and energy saving. The learning experience can be extrapolated to other cities if data can be collected, model re-calibrated, and the control concepts adapted to the new transportation system.

Objectives

The objective of the project is to study the energy impacts of connected and automated vehicle technologies for a wide range of use cases and technology scenarios using both test data and high-fidelity models. The project evaluates the impact of a fast-emerging technology on the energy benefit of current and future vehicle technologies through test data currently not available and by providing guidance for future R&D directions (i.e., component requirements, operating conditions) through the use of simulation tools.

Approach

This project consists of five inter-connected tasks, involving close-collaboration between the University of Michigan, the Argonne National Lab, and the Idaho National Lab. The approach of these five tasks are described below

- Task 1 Instrumentation and data acquisition of energy related information
 - Define candidate vehicle signals to be collected for energy purposes.
 - Outfit 500 vehicles with the ODB-II logger, validation of the system – including the backhaul – and maintaining operations.
 - Provide data to researchers in other Tasks of this project for model/control development
- Task 2 Display energy related information to study its influence on the driver
 - Identify CAV user functions, co-design and prioritize signals.
 - Develop driver information display hardware and communication.
 - Design vehicle information display screen(s) and experimental cases.
 - Review human test results. Review the field performance of the designed user interface.
- Task 3 Travel Behavior Modeling
 - Experiment and survey design for travel behavior model.
 - Model departure-time choice behavior.
 - Model route choice behavior.
 - Model travel activity pattern change.
 - Calibration of POLARIS traveler behavior model.
- Task 4 System Model Development and Validation
 - Develop the Ann Arbor and Ypsilanti region baseline POLARIS model.
 - Determine data needs for further model development.
 - Query, collect, and process data from the connected vehicle fleet.
 - Implement traveler and CAV agent behavior rules.
- Task 5 Adaptive Signal Control
 - Build and calibrate the traffic simulation environment for the adaptive traffic signal control.

- Develop the adaptive signal control algorithm.
- Deploy and conduct field experiment at MCity and the Plymouth Road corridor.

Evaluate the energy saving of adaptive signal control.

Results

The most notable results of this project are summarized below

- Task 1 Instrumentation and data acquisition of energy related information
 - Collected data using the OBD-port dongles from > 500 vehicles
 - The collected data is from > 750k trips, 7.1M miles
 - Data shared within the research team, EPA, and selected UM students for research.
 - ANL researchers analyzed and used the data for their Polaris model development.
- Task 2 Display energy related information to study its influence on the driver
 - Designed human participant experiment
 - Completed all experimental data collection from 32 participants, reduced driving data by using geo-fences and conducted analysis on user acceptance and behavior measures.
 - Analysis results used to develop human driver behavior models under advisory CAV functions.
- Task 3 Travel Behavior Modeling
 - Modeled baseline activity patterns of Ann Arbor using collected vehicle trip information
 - Conducted analysis of the impact of CAVs on traffic and energy consumption
 - Studied the potential of using CAV fleet to serve the mobility of multiple families using the travel behavior information
- Task 4 System Model Development and Validation
 - Using the collected Ann Arbor travel data to calibrate a Polaris model that simulates mesoscopic traffic behavior of the city of Ann Arbor and its surroundings.
 - Embedded Energy Estimation function in POLARIS based on machine learning.
 - Simulated the energy impacts of CAV functions such as Adaptive Cruise Control, Eco-approaching, and Eco-Routing.
- Task 5 Adaptive Signal Control
 - Developed an algorithm to accurately estimate the traffic flow around intersections under low connected vehicle penetration rate
 - Data collection from 6 intersections on Plymouth Rd, Ann Arbor.
 - Developed an adaptive signal control algorithm and confirmed its effectiveness in simulations

- Working with several other cities including Chattanooga, TN to explore collaborative opportunities for field deployment.

Conclusions

At the initiation of this project, there are a few key gaps in understanding the potential impacts of connected and automated vehicles (CAVs) to overall energy consumption, including the lack of real field test data, the lack of a high-fidelity model, and lack of real CAV functions evaluated at a large scale (e.g., for a mid-sized city like Ann Arbor). This success of this project fills several of the data, model and CAV function gaps:

- Collected field data from > 500 vehicles, which provides the basis of vehicle trips (origin-destination, travel speed, time) and energy consumption information. At the conclusion of this project, we estimate the total amount of data available will be more than 8 million miles.
- The field data is used by the Argonne National Lab to develop and calibrate their Polaris model for Ann Arbor. The model has shown to match the travel pattern of the City accurately.
- By collaborating with University of Michigan researchers the travel data has also been used to develop and calibrate a SUMO model (an open-source traffic simulation platform).
- Two representative CAV functions have been analyzed using the Ann Arbor data/model. The Eco-approaching algorithm using real human driver data collected from the Plymouth Corridor of Ann Arbor shows very encouraging (albeit idealized) potential in reducing fuel consumption by >30%. The eco-routing algorithm evaluated in the Ann Arbor-wide traffic simulation for 800 vehicle trips using the SUMO model has demonstrated 6% fuel consumption reduction.

While the work by the team over the last three years has addressed a few key gaps, many more challenges remain to explore the full potential of CAVs.

Key Publications

1. Di, X., Liu, H.X., Ban, X., Yang, H., 2016. Ridesharing User Equilibrium and Its Implications for High-Occupancy Toll Lane Pricing, *Transportation Research Record*, 2667, doi: 10.3141/2667-05.
2. Zheng, J. and Liu, H.X., 2017. Estimating traffic volumes for signalized intersections using connected vehicle data. *Transportation Research Part C: Emerging Technologies*, 79, pp.347-362.
3. Feng, Y., Yu, C., Liu, H.X., Spatial-temporal Intersection Control in a Connected and Automated Vehicle Environment. *Transp. Res. Part C Emerg. Technology*
4. Yu, C., Feng, Y., Liu, H.X., Lane-based integrated optimization of traffic signals and vehicle trajectories at isolated urban intersections. *Transp. Res. Part B Methodological*.
5. Feng, Y., Zheng J., and Liu, H.X., A Real-time Detector-free Adaptive Signal Control with Low Penetration of Connected Vehicles. *Transportation Research Record*.
6. Di, X., Zhao, Y., Zhang, Z., and Liu, H., Data-Driven Similarity Analysis for Activity-based Travel Demand Modeling, Submitted to 2017 TRB Annual Meeting for Presentation.
7. Huang, X. and Peng, H., 2017, May. Speed trajectory planning at signalized intersections using sequential convex optimization. In *American Control Conference (ACC)*, 2017(pp. 2992-2997). IEEE.
8. Di, X., Liu, H.X., Ban, X., Yang, H., 2016. Ridesharing User Equilibrium and Its Implications for High-Occupancy Toll Lane Pricing, *Transportation Research Record*, 2667, doi: 10.3141/2667-05.
9. Huang, X. & Peng, H., 2018. Eco-Routing based on a Data Driven Fuel Consumption Model. To appear in 14th International Symposium on Advanced Vehicle Control, AVEC'18.

10. Huang, X. & Peng, H., 2018. Efficient Mobility-on-Demand System with Ride-Sharing. Submitted to The 21st IEEE International Conference on Intelligent Transportation Systems.
11. Zheng, J. and Liu, H.X., 2017. Estimating traffic volumes for signalized intersections using connected vehicle data. *Transportation Research Part C: Emerging Technologies*, 79, pp.347-362.
12. Feng, Y., Yu, C. and Liu, H.X., 2018. Spatiotemporal Intersection Control in a Connected and Automated Vehicle Environment. *Transportation Research Part C: Emerging Technologies*, 89, pp.364-383.
13. Yu, C., Feng, Y., Liu, H.X., Ma, W. and Yang X., 2018. Integrated optimization of traffic signals and vehicle trajectories at isolated urban intersections. *Transportation Research Part B: Methodological*. (In Press)
14. Feng, Y., Zheng, J. and Liu, H.X., 2018. A Real-time Detector-Free Adaptive Signal Control with
15. Low Penetration of Connected Vehicles. *Transportation Research Record*. (In Press)

Acknowledgements

The project team would like to thank David Anderson for his insightful guidance and suggestions throughout the course of this project.

III.1.2 Boosting Energy Efficiency of Heterogeneous Connected and Automated Vehicle (CAV) Fleets via Anticipative and Cooperative Vehicle Guidance (Clemson University)

Ardalan Vahidi, Principal Investigator

Clemson University
208 Fluor Daniel Building, Clemson University, Clemson, SC 29634
E-mail: avahidi@clemson.edu

Yuni Jia, Co-Principal Investigator

Clemson University International Center for Automotive Research (CU-ICAR)
4 Research Drive, Greenville, SC 29607
E-mail: yunyij@clemson.edu

Beshah Ayalew, Co-Principal Investigator

Clemson University International Center for Automotive Research (CU-ICAR)
4 Research Drive, Greenville, SC 29607
E-mail: besah@clemson.edu

Dominik Karbowski, Co-Principal Investigator

Argonne National Laboratory-ANL
9700 South Cass Avenue, #362, Argonne, IL 60439
Email: dkarbowski@anl.gov

John Tabacchi, DOE Project Manager

U.S. Department of Energy
E-mail: john.tabacchi@netl.doe.gov

Prasad Gupte, DOE Technology Manager

U.S. Department of Energy
E-mail: prasad.gupte@ee.doe.gov

Start Date: September 1, 2018	End Date: January 31, 2020	
Project Funding (FY19): \$647,261	DOE share: \$567,888	Non-DOE share: \$79,373

Project Introduction

This project introduces novel anticipative car following and lane selection schemes for Connected and Automated Vehicles (CAVs). Our control schemes benefit from collaboration and information exchange between CAVs to save energy, reduce braking, and harmonize traffic. The proposed schemes will be implemented in traffic microsimulations at different levels of CAV penetration to analyze energy saving benefits. We will create a Vehicle-in-the-Loop (VIL) testbed to demonstrate the benefits to real CAVs driven on a test-track. Clemson has partnered with Argonne National Laboratory to integrate the vehicle guidance algorithms with Autonomie, Argonne's detailed vehicle energy utilization simulation software. Clemson has partnered with PTV to incorporate the proposed algorithms in their state-of-the-art traffic micro-simulation tool, VISSIM. Clemson also has partnered with International Transportation Innovation Center (ITIC) to conduct experiments for evaluating the proposed technical approach with novel co-simulations of traffic and physical automated vehicles on a test track in Greenville, South Carolina.

Objectives

The three main objectives of the project are:

1. Developing anticipative vehicle guidance algorithms including perception and prediction of motion of surrounding vehicles. Designing the car following and lane selection algorithms to demonstrate >5%

efficiency gain in mixed traffic with 30% CAV penetration. Generating the corresponding custom code for PTV VISSIM Traffic Microsimulation.

2. Detailed energy evaluation using high-fidelity powertrain models of heterogeneous vehicles to demonstrate >5% (10%) average efficiency gain in mixed traffic for CAV penetration >30% (60%).
3. Vehicle instrumentation and experimental testing via Vehicle-in-the-Loop (VIL) platform. Demonstrating stable co-simulation of two experimental vehicles and <10 virtual vehicles and document >5% average energy efficiency gain for the entire fleet. Documenting >5% additional average efficiency gain resulting from collaborative driving.

Approach

Anticipative Car Following Scheme

A combined probability modeling and Model Predictive Control (MPC) system is employed to boost the energy efficiency of CAVs. MPC utilizes a preview of disturbances and optimizes a modeled system over a finite time horizon. In heterogeneous traffic, CAVs using MPC communicate their intentions to other CAVs. When interacting with conventional vehicles, a CAV must predict using current and historic sensed data.

Optimal Lane Changing in Mixed Traffic

The model predictive control (MPC) algorithm for multilane guidance utilizes a preview of surrounding vehicle (SV) motion. In homogeneous connected traffic, other agents can provide this preview wirelessly. In mixed traffic, however, each CAV must predict how conventional vehicles will move and cope with greater uncertainty in this prediction. The prediction module takes a simple kinematic approach with either a constant acceleration or constant speed depending on position along the road. Constant-speed lateral prediction saturates upon reaching a lane center.

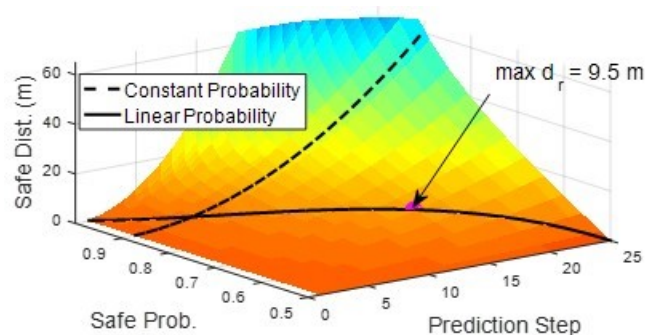


Figure III.1.2.1 Inverse probability density function of position with comparison of constant and linearly decaying probability.

Chance constraints account for uncertainty as described in 3. The cumulative distribution function of SV position is inverted to obtain the safe distance needed to avoid a collision with some probability. To avoid excessive conservatism and take advantage of closed-loop disturbance rejection, the safe probability decays linearly over prediction from 99.999% one step ahead to deterministic at the end of the prediction horizon as in Figure III.1.2.1.

Integrating Long-Term Speed Planning with Lane Change Control

The MPC-only lane changing algorithm described in 4 minimizes the ego vehicle's acceleration and deviation from the target speed, but this generally produces short-sighted results in a drive between two stopping points. Furthermore, it does not enable closed loop targeting of an arrival time. To address these shortcomings, a parabolic reference trajectory from the current state to the final position and time is generated at each control loop and provided to MPC as a target. MPC then approximates this trajectory as closely as possible subject to traffic constraints. The parabolic trajectory minimizes both acceleration and electric vehicle (EV) energy. This and other optimal lane change enhancements are described in 5.

Collaborative Multilane Guidance

Techniques for improving the collective performance of groups of CAVs on multilane roads were developed in a collaboration with IFP Energies nouvelles. The previously described multilane guidance algorithm shares intentions between CAVs that solve sequential optimal control problems (OCPs), with the solution depending

on the computation order. In a new distributed approach, the CAVs share their sensitivity to constraints in order to dynamically select computation orders that reduce collective cost. Centralized optimization where one lead agent solves a unified OCP and dictates other agents' solutions was also prototyped as a high-performing benchmark. Publication 6 describes these algorithms in detail.

Anticipative Lane Selection Scheme (non-linear programming model predictive control method)

The non-linear programming (NLP) model predictive control (MPC) optimal lane selection framework from 1 was expanded to a distributed control framework by taking advantage of connected vehicle technologies permitting the connected and autonomous vehicles (CAVs) to share their future intentions 8. Figure III.1.2.2 presents an overview of the distributed control framework and an in-depth description may be found in 8. The framework was implemented within the traffic simulation software PTV VISSIM and results will be discussed further within the results section of this report. Although the current algorithms for the reference speed assigner and object vehicle prediction blocks are sufficient there is still room for improvement. To this end, ongoing work is focused on improving the motion prediction of unconnected object vehicles and the reference speed assigner in order to realize further improvements in energy consumption.

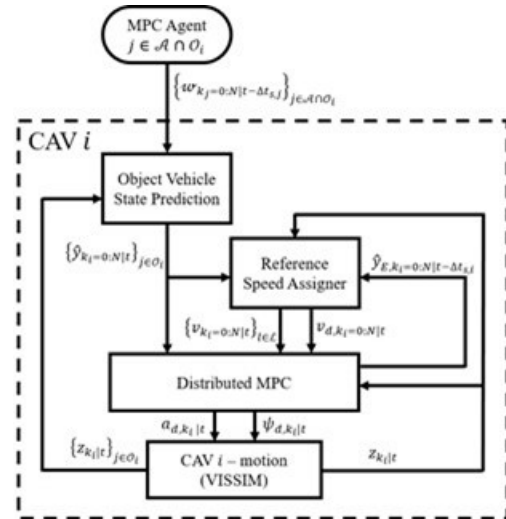


Figure III.1.2.2 Block diagram of the optimal lane selection NLP distributed MPC framework.

Vehicle-in-the-Loop Testbed and On-Road Energy Consumption Estimation

We have constructed a VIL testbed at ITIC test track where our two real CAVs interact with virtual traffic in the VISSIM simulation. However, in order to conduct preliminary VIL verifications, we have our test vehicle run on a chassis dynamometer following a preceding vehicle, simulated using a point mass simulator (Figure III.1.2.3). The energy consumption of experimental CAVs are estimated via On-Board Diagnostics (OBD-II) port accessed by our iOS application 23. As shown in Figure III.1.2.3, we use a flow meter 4 to track the actual fuel usage of Mazda CX7 vehicle. We use the flow meter data to verify and calibrate our OBD-based fuel rate estimations on the chassis dynamometer. Because of safety concerns and limited space in our test vehicle, we can't use this flow meter on the test track.

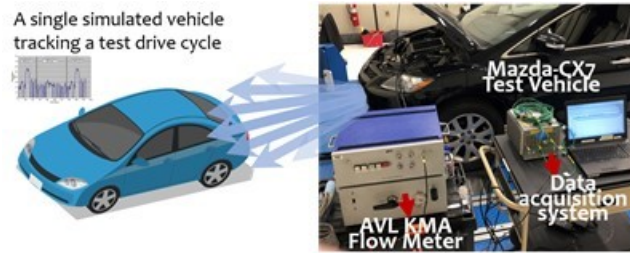


Figure III.1.2.3 The chassis dynamometer VIL setup.

Results

PTV VISSIM Traffic Microsimulation Car-Following Results

Realistic microsimulations were set up by imposing headway distributions sampled from highway traffic data on the Wiedemann (WIE) driver model used in VISSIM. We then show that the introduction of CAVs allows for traffic smoothing effects: the cell density plots in Figure III.1.2.4 show natural shockwaves propagating backwards through the network at 2000 veh/hour, which are subsequently dissipated as CAV penetration increases. This included some secondary effects of improved fuel economy for WIE drivers, particularly at high penetration of CAVs. Furthermore, we observe that CAVs drive with significant fuel benefit over WIE drivers in high volume scenarios: we found between 8% and 33% fuel improvement for the CAVs over WIE drivers (see Figure III.1.2.5). This was the most significant fuel improvement source observed in the network:

the majority of CAVs drive more efficiently than WIE drivers, so average fleet fuel performance increased with greater densities of CAVs. Further details are depicted in 7.

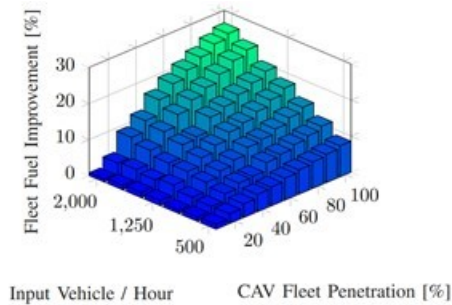


Figure III.1.2.4 Mean fleet fuel efficiency improvements over the 0% CAV case at each input vehicle volume/hour.

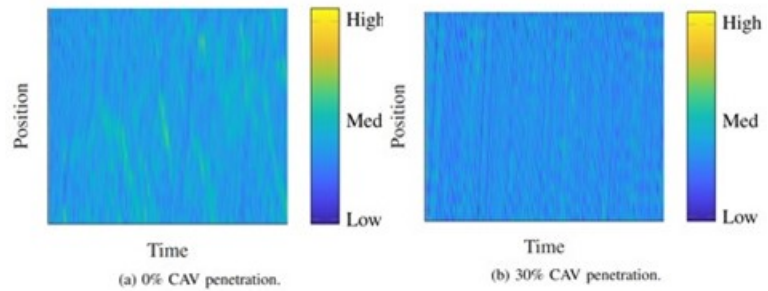


Figure III.1.2.5 Cell density plots showing dense groups of vehicles in the network at 0%, 30% CAV penetration. With the introduction of CAVs, shockwave effects were dissipated.

Optimal Lane Changing Simulation Studies Including Mixed Traffic

Two road links were modeled to evaluate multilane guidance algorithms. The first, based on US-123 in Clemson, SC, features 12 vehicles beginning and ending at rest and targeting individualized lanes. The second was based on Interstate 85 in Greenville, SC with the far-left lane omitted. It involves merging among vehicles introduced at a frequency of either 4 s or 2 s. A baseline controller used the Intelligent Driver Model for longitudinal acceleration and the reactive rule-based algorithm detailed in 3 for lane selection. As given in Table III.1.2.1, The optimal control approach consistently improved energy, travel time, and lane selection performance metrics relative the baseline. Unconnected vehicles were also introduced in the arterial scenario. In these simulations, final time was controlled to isolate the energy impact. Figure III.1.2.6 shows the fleet energy improvement as CAVs were added.

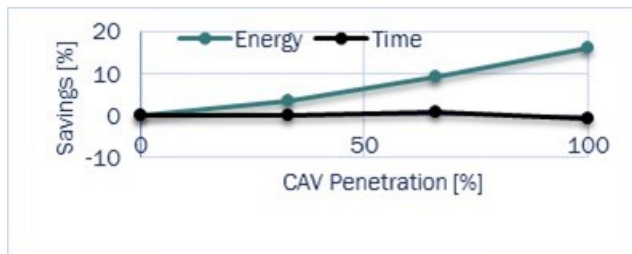


Figure III.1.2.6 Energy improvement relative to the reactive baseline algorithm of 3 at varied CAV market penetration rate.

Table III.1.2.1 Relative performance results in homogeneous CAV traffic.

	Energy	Time	Lane Success Rate
HW 4s	8.9%	5.2%	13.8%
HW 2s	10.0%	9.7%	99.6%
Arterial	13.7%	10.3%	12.1%

Collaborative Multilane Guidance

Three electric CAVs navigating a three-lane-to-one-lane choke point were simulated in MATLAB using either randomly chosen computation order (baseline), centralized control, or the sensitivity-based collaborative approach. Although centralized control yielded the best performance with an 8.6% reduction in energy use compared to the baseline, computation time was infeasible for implementation. The distributed controller reduced energy consumption by 6.7% with similar computation time to the baseline. More detailed results are provided in 6.

Anticipative Lane Selection Scheme (NLP distributed MPC framework)

The optimal lane selection non-linear programming (NLP) distributed model predictive control (MPC) framework was implemented within the traffic simulation software VISSIM using the external driver model interface and the ACADO toolkit NLP solver 5. Simulations were completed on a traffic network consisting of a three-lane highway 5km long as shown in Figure III.1.2.7. The fuel consumption and time results were evaluated over 4km, from 500m to 4500m, within the network. Simulations were run for 12 minutes of simulation time and the data prior to the time at which the network was saturated was ignored.

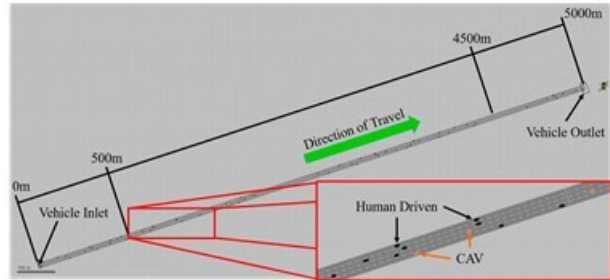


Figure III.1.2.7 VISSIM traffic network.

The results for simulations with flow rates of 1924, 2478, and 3927 vehicles per hour and desired speeds distributed about 80 kph as well as, connected and automated vehicle (CAV) penetration rates of 0%, 25%, 50%, 75% and 100% are presented in Figure III.1.2.8. The baseline scenario was human driven vehicles that were restricted from changing lanes or non-lane changing vehicles (NLC). Human drivers (HDs) are those that are free to change lanes and CAVs are the vehicles running the optimal lane selection NLP distributed MPC. A 0% CAV penetration corresponds to all vehicles in the network being HDs and 100% CAV penetration corresponds to all vehicles being CAVs. The CAVs show the potential for a 20.2% reduction in fuel consumption over NLC vehicles and 13.4% reduction compared to HDs at 100% penetration and 3972 veh/hr. This does come at the minimal cost of an increase in travel time of 0.8% with respect to a fleet of only HD vehicles. Some additional results may be found within 8.

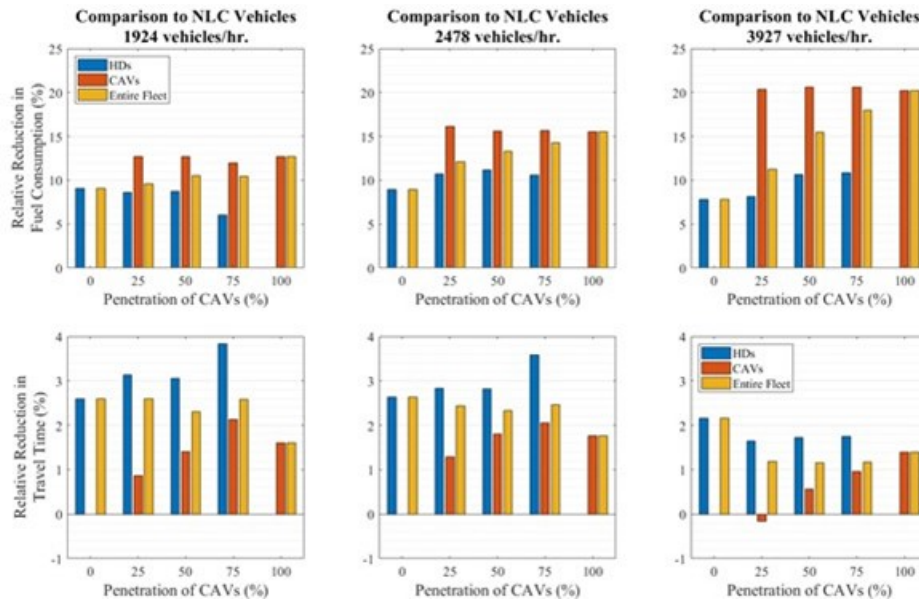


Figure III.1.2.8 Percent reduction in fuel consumption (bottom) and travel time (top) compared to NLC vehicles at 1924 (left), 2478 (center), and 3927 (right) vehicles per hour and desired speeds distributed about 80 kph.

Instrumenting and Automating the experimental CAVs

The instrumentation of our second test vehicle (Mazda CX-7) and the tuning of its robotic control system have been finished. The same calibration process was conducted on dyno to calibrate the throttle and brake response map of the vehicle. To accelerate the test process, reduce test cost and more importantly, obtain results in a controlled environment, a test plan that ran the vehicle on a chassis dynamometer instead of on actual roads was designed. A real-time data acquisition system was adopted to measure and send the wheel speed of the

vehicle to control computer. The wheel speed was used to estimate the vehicle's odometry on the virtual test rack.

The low-level controller was combined with MPC high-level controller to test the second vehicle's speed tracking performance on the chassis dynamometer. The result is shown in Table III.1.2.2. It can be seen that both vehicles manage to achieve good speed tracking accuracy with both high-level controllers. Despite that the average speed tracking error is small enough, at the beginning, it was observed that in very low speed range (below 1.4m/s), the low-level controller could not follow the command from car-following controller very well. The low-level controller could not stop the vehicle effectively and would generate speed ripples. After an investigation, it was found that this issue was because the speed controller used two pedal control calibration maps: the 1st one for decelerating in high speed range using brake pedal, and the 2nd one for decelerating/accelerating in high speed range using throttle pedal. But in very low speed range, vehicle speed is completely controlled by brake pedal, which is not covered by the calibration maps. To solve this control challenge, we have added two more pedal control calibration maps: the 3rd one for low speed range decelerating using brake pedal only, and the 4th one for low speed range accelerating using brake pedal only. The control performance comparison between using two, three and four calibration maps is shown in Figure III.1.2.9. It can be seen that using three calibration maps could reduce continuous speed ripples to several spikes and using four calibration maps could completely eliminate speed ripples and spikes in low speed range. In addition, during the calibration, the first two maps were updated with more precise vehicle parameters. In addition to the chassis dynamometer work, a new look ahead point selection method and speed limitation algorithm were also developed to mitigate the speed and acceleration jerk issue that occurred during vehicle testing on the test track especially at the U-turn sections.

Vehicle-in-the-Loop Simulation

Using our VIL setup shown in Figure III.1.2.3, we were able to conduct verifications on a chassis dynamometer where the preceding vehicle was simulated one time following the Federal Test Procedure (FTP) test cycle 8 and the other time following the US06 test cycle 9. The real vehicle followed the simulated vehicle, at first using the Intelligent Driver Model (IDM) and then using our MPC-based car following model. The vehicle-to-vehicle connectivity was also added between the real and simulated vehicle extending the event horizon of the real vehicle. In this connected case, a 16 second horizon of the preceding vehicle's intentions was communicated to the real vehicle. The battery data of our Nissan Leaf test vehicle and the gasoline engine data of our Mazda CX7 test vehicle were logged by our OBD logger. The results of the tests are not provided here because of software bugs that were later found in our car-following algorithm. We will repeat these tests on the chassis dynamometer reporting the energy consumption reduction potentials before we continue our VIL verification at ITIC test track where our two real CAVs interact with virtual traffic in the VISSIM simulation.

Table III.1.2.2 Dynamic Speed Tracking Performance.

Vehicle	Nissan Leaf		Mazda CX-7	
Controller	MPC	IDM	MPC	IDM
Mean Abs. Error (m/s)	0.038	0.045	0.028	0.0319

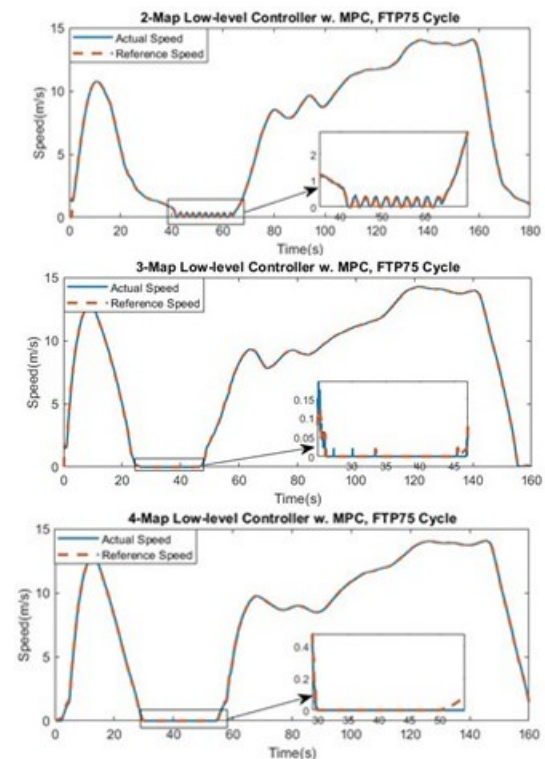


Figure III.1.2.9 Low-level speed controller performance comparison at low speed range

OBD-based Energy Consumption Measurement

Our implemented iOS application connects to commercial WiFi OBDII readers supporting ELM327 chip 6. We adjusted ELM327 settings and improved our iOS OBD logger coding to obtain faster OBD scanning rates. We were able to increase the maximum OBD data sampling frequency of our iOS application from 2Hz to about 4Hz. We installed a flow meter to track the actual fuel consumed by our combustion test vehicle on a chassis dynamometer (Figure III.1.2.3). The main goal was first, to calibrate one of our OBD-based estimation methods, and second, to evaluate our OBD-based fuel rate estimation methods. We started each test with an empty fuel tank before putting certain amount of fuel in the tank. We repeated three times putting 1 gal, 2.5 gal, and 3 gal in an empty tank. We had the vehicle ran on a chassis dynamometer until it ran out of fuel. The results are given in Table III.1.2.3 where the total fuel measured by an AVL KMA flow meter 4 and estimated by our OBD-based methods (basic and calibration methods) are all compared to the total fuel we had put in the empty tank of the vehicle.

Table III.1.2.3 The Errors in Flow Meter Measurements and OBD Estimations Compared to the Initial Fuel in the Tank.

	Test Duration	Flow Meter	OBDII (basic)	OBDII (calibrated)
Test 1 1 gal (3.79 lit)	1h 20min	3.94 liter (+4.0%)	3.60 liter (-5.0%)	3.95 liter (+4.2%)
Test 2 2.5 gal (9.46 liter)	3h 41min	10.22 liter (+8.0%)	8.58 liter (-9.3%)	8.97 liter (-5.2%)
Test 3 3 gal (11.36 liter)	1h 45min	11.51 liter (+1.4%)	10.98 liter (-3.3%)	11.66 liter (+2.6%)

Vehicle-in-the-loop (VIL) Communication Setup

The communication between the physical vehicle and the simulation server has been established using cellular network at ITIC test track and Wi-Fi at chassis dynamometer. In order to apply Dedicated Short Range Communications (DSRC) to our VIL platform, we have successfully configured two iSmartWays On-board Equipment (OBE) 7 and one Road Side Equipment (RSE). We have tested the RSE-OBE communication for tuning the RSE position and measuring the packet reception/dropping rate in 1.2-mile stretch of ITIC test track facility. With 1 Hz broadcast rate and while whole test track is considered, the packet reception rate is 97% and consecutive packet drop probability is 0.1%. For 10 Hz broadcast rate, the packet receptions decline; however, while the test area is limited to the 800 m radius from the RSE, the packet reception probability is around 96% and consecutive packet drop probability is 0%.

Conclusions

The instrumentation of the Nissan Leaf and Mazda CX7 test vehicles are finished and both vehicles are ready for energy efficiency tests. The low-level controllers and speed tracking performances of both vehicles were tuned on the chassis dynamometer eliminating speed ripples and spikes in low speed range. Both vehicles are programmed to have a bidirectional communication with VISSIM simulation server. During our next test at ITIC track, we will evaluate the simultaneous and real-time visualization of our two vehicles in VISSIM virtual network using cellular network and DSRC. Based on our experimental verification, one DSRC RSE can sufficiently cover almost the whole ITIC track (1.2-mile stretch). With 1 Hz broadcast rate and while whole test track was considered, the packet reception rate was 97% and consecutive packet dropped probability was 0.1%.

Multiple tests were conducted on the chassis dynamometer following one single simulated vehicle as a preparation for our final test track VIL simulations. However, few software bugs affected our test results and we plan to repeat the tests. Connectivity is already added between the real and the simulated vehicle. More energy usage improvement is expected by this connectivity because the event horizon of the real vehicle will be extended. This will be verified during our final tests on the chassis dynamometer. Our iOS application is now capable of collecting data from OBD ports of our experimental CAVs at 4Hz (previously 2Hz). We successfully installed a flow meter to track the actual fuel consumed by our combustion test vehicle on the

chassis dynamometer. We used the collected fuel rate data to calibrate one of our OBD-based estimation methods. Based on our experimental tests on the chassis dynamometer, the flow meter did not show an advantage over our OBD-based estimation method; as a result, our OBD logger application will be used during our on-road tests.

The lane decision MPC was extended for speed trajectory planning and uncertainty handling in mixed traffic. Energy improvement in MATLAB simulations relative to the intelligent driver model with rule-based lane selection are on track and implementation in VISSIM is underway. Collaborative algorithms were also prototyped, and MATLAB simulations suggest that such a strategy could yield an additional 7% energy improvement over decentralized optimal control in some collaboration-intensive scenarios. Implementation of our anticipative car following in VISSIM is complete and we have generated results for varied traffic volumes and varied penetration of CAVs. We observe that CAVs drive with significant fuel benefit over native VISSIM human drivers in high volume scenarios: we found between 8% and 33% fuel improvement for the CAVs over human drivers. This was the most significant fuel improvement source observed in the network: the majority of CAVs drive more efficiently than human drivers, so average fleet fuel performance increased with greater densities of CAVs. The non-linear programming (NLP) based model predictive control (MPC) lane decision algorithm was also implemented within VISSIM and fuel consumption results were obtained for CAV penetration and traffic flow rates. Ongoing research is focused on improving the reference speed assigner in order to unify desired speed, as well as, improving the longitudinal and lateral prediction methods for the motion of unconnected vehicles. Our work will continue to finalize the implementation of the lane decision MPC within VISSIM and obtain fuel efficiency results from simulations with different penetrations of CAVs.

Key Publications

1. R. Austin Dollar, and Ardalan Vahidi. "Quantifying the impact of limited information and control robustness on connected automated platoons." IEEE 20th International Conference on Intelligent Transportation Systems (ITSC), 2017, pp. 1-7. IEEE, 2017.
2. R. Austin Dollar, and Ardalan Vahidi. "Efficient and Collision-Free Anticipative Cruise Control in Randomly Mixed Strings." IEEE Transactions on Intelligent Vehicles, vol. 3, no. 4, pp. 439-452 (2018).
3. R. Austin Dollar, and Ardalan Vahidi. "Automated Vehicles in Hazardous Merging Traffic: A Chance-Constrained Approach."* In IFAC-PapersOnLine 52, no. 5 (2019): 218-223.
4. R. Austin Dollar, and Ardalan Vahidi. "Predictively Coordinated Vehicle Acceleration and Lane Selection Using Mixed Integer Programming."** In Proceedings of the ASME DSCC, 2018.
5. R. Austin Dollar, and Ardalan Vahidi. "Automated Driving with Variational Optimal Control and Mixed Integer Programming." In review, IEEE Transactions on Control Systems Technology (2019).
6. R. Austin Dollar, Antonio Sciarretta, and Ardalan Vahidi. "Multi-Agent Control of Lane-Switching Automated Vehicles for Energy Efficiency." In review, American Control Conference, 2020.
7. T. Ard, R. A. Dollar, D. Karbowski, Y. Zhang, and A. Vahidi. "Evaluating the Impact of Automated Vehicles with Optimal Eco-Driving in High Fidelity Traffic Microsimulations." In preparation, Transportation Research Part C (2019).
8. N. Goulet and B. Ayalew (2019) "Coordinated Model Predictive Control on Multi-lane Roads" Proceedings of the ASME 2019 International Design Engineering Technical Conferences & Computers and Information in Engineering Conference, DETC2019-98117, August 18-21, 2019, Anaheim, CA.
9. X. Wang, L. Guo and Y. Jia, "Human Intervention Detection on a Retrofit Steering Actuation System in Autonomous Vehicles," SAE Technical Paper, 2018. (Trevor O. Jones Outstanding Paper Award)

10. X. Wang, L. Guo and Y. Jia, "Online Sensing of Human Steering Intervention Torque for Autonomous Driving Actuation Systems," IEEE Sensors Journal, vol. 18, no. 8, pp. 3444-3453, 2018.
11. G. G. M. Nawaz Ali, Beshah Ayalew, Ardalan Vahidi, and Md. Noor-A-Rahim, "Analysis of Reliabilities Under Different Path Loss Models in Urban/Sub-urban Vehicular Networks", Proceedings of IEEE 90th Vehicular Technology Conference (IEEE VTC-Fall'19), Honolulu, HI, 2019.
12. G. G. M. Nawaz Ali, Beshah Ayalew, Ardalan Vahidi, and Md. Noor-A-Rahim, "Feedbackless Relaying for Enhancing Reliability of Connected Vehicles," in review, IEEE Transactions on Vehicular Technology, 2019.

* Young Author Award

** Automotive and Transportation Systems Best Paper Award

References

1. Q. Wang, B. Ayalew, and T. Weiskircher, "Optimal assigner decisions in a hybrid predictive control of an autonomous vehicle in public traffic," in 2016 American Control Conference (ACC), 2016, vol. 2016–July, pp. 3468–3473.
2. S. A. Fayazi, A. Vahidi, and A. Luckow, "A Vehicle-in-the-loop (VIL) Verification of an all-Autonomous Intersection Control Scheme," Transportation Research Part C: Emerging Technologies, Special Issue on CAV Control, vol. 107, pp. 193-210, Oct. 2019.
3. OBD Log iOS Application introduction, available online: <https://youtu.be/7zWhUk7hEZQ>
4. AVL KMA Mobile fuel consumption measurement system, <https://www.avl.com/-/avl-kma-mobile>
5. R. Quirynen, M. Vukov, M. Zanon, and M. Diehl, "Autogenerating microsecond solvers for nonlinear MPC: A tutorial using ACADO integrators," Optim. Control Appl. Methods, vol. 36, no. 5, pp. 685–704, Sep. 2015.
6. "ELM327, OBD to RS232 interpreter," ELM Electronics, 2012, available online: www.elmelectronics.com/DSheets/ELM327DS.pdf
7. iSmartWays Technology Inc., <http://www.ismartways.com/>
8. The Federal Test Procedure (FTP), <https://www.epa.gov/vehicle-and-fuel-emissions-testing/dynamometer-drive-schedules>
9. The EPA US06 or Supplemental Federal Test Procedures (SFTP), <https://www.epa.gov/emission-standards-reference-guide/epa-us06-or-supplemental-federal-test-procedures-sftp>

Acknowledgements

The Principal Investigators would like to acknowledge the critical work of the other authors of this work: R. Austin Dollar, Tyler Ard, Ali Reza Fayazi, Longxiang Guo, Nathan Goulet, and G. G. Md. Nawaz Ali. The collaborative guidance algorithm discussion in the "Collaborative Multilane Guidance" subsection was developed jointly with IFP Energies nouvelles under the joint supervision of Antonio Sciarretta and Ardalan Vahidi

III.1.3 Evaluating Energy Efficiency Opportunities from Connected and Automated Vehicle Deployments Coupled with Shared Mobility in California (UCR/NREL)

Matthew Barth, Principal Investigator

University of California, Riverside – CE-CERT
1084 Columbia Avenue
Riverside, CA 92507
E-mail: barth@cert.ucr.edu

John Tabacchi, DOE Project Manager

U.S. Department of Energy
E-mail: john.tabacchi@netl.doe.gov

Prasad Gupte, DOE Technology Manager

U.S. Department of Energy
E-mail: prasad.gupte@ee.doe.gov

Start Date: October 1, 2017

End Date: March 31, 2020

Project Funding (FY19): \$1,207,460

DOE share: \$ 1,094,578

Non-DOE share: \$ 122,882

Project Introduction

With the rapid growth of information and communication technologies, Connected and Automated Vehicles (CAVs) are deemed to be disruptive with the potential to significantly improve overall transportation system efficiency, however, may increase vehicle miles traveled (VMT). Further, shared mobility systems are another disruptive force that is reshaping our travel patterns, with the potential to reduce VMT. The goal of this project is to extensively collect data from vehicles and associated infrastructure equipped with CAV technologies from both real-world experiments and simulation studies mainly deployed in California, and develop a comprehensive framework for evaluating energy efficiency opportunities from large-scale (e.g., statewide) introduction of CAVs and wide deployment of shared mobility systems under a variety of scenarios. To quantify the combined impact of CAV and shared mobility on travel behavior, traffic performance and energy efficiency, a mesoscopic simulation-based model is being developed for mobility and energy efficiency evaluation considering the disruptive transportation technologies.

Objectives

As a complement to existing studies on nationwide evaluation of CAVs' energy impacts, this project is focusing on data collection efforts and CAV applications under congested traffic environments that are frequently experienced on a massive scale across the major metropolitan areas in California. Another key component of this project is to consider the interaction between different CAV technologies and shared mobility models, and the compound effect on energy efficiency. The outcomes from this project are expected to help close the knowledge gap on recognizing the potential energy impacts of a broad (regional or statewide) deployment of CAV technologies across a wide range of roadway infrastructure with varying levels of congestion and different penetration rates of shared mobility systems. In addition, the results from this project will support policymakers in steering CAV development and deployment, coupled with shared mobility systems, in an energy favorable direction. To realize these outcomes, the specific objectives of this project are:

- To collect data from both real-world implementations (including experiments, demonstrations, and early deployments) and simulation studies of CAV technologies, potentially coupled with shared mobility, mainly in California. The real-world data will be used to model the energy efficiency from each individual CAV technology with a small fleet of equipped vehicles, while simulation data will facilitate the analysis of aggregated effects on traffic with multiple CAV technologies concurrently deployed.

- To implement models for quantifying the impacts of CAV technologies on energy intensity (e.g., energy consumption per unit distance for different driving conditions) and for quantifying the amount of driving (measured by vehicle miles traveled or VMT) represented by each driving condition. The models will include the consideration of vehicle class, roadway type, level of traffic, penetration rate, and level of vehicle automation.
- To construct a regional or statewide energy inventory under various CAV technology deployment scenarios by incorporating datasets and models for predicting vehicle market share and vehicle usage, which are tightly associated with the penetration of shared mobility systems, including transportation network companies (TNCs), ride-sharing, carsharing, ride sourcing, etc.

Approach

This research project has been divided into three phases:

Phase I – Data Collection and Processing (completed in FY18)

During this phase, real-world data were collected from multiple sources, e.g., on-road test vehicles and testbeds, Dynamometer-in-the-Loop (DIL) testing systems, and published data from existing experiments. The research team has also developed and implemented multiple CAV applications, such as Eco-Approach and Departure, Eco-Cooperative Adaptive Cruise Control, and Eco-Speed Harmonization, in traffic micro-simulation software. Based on the real world and simulation-based data from various CAV applications, we developed a CAV mobility and energy efficiency database (CAVMEED), consisting of processed and archived data that have been used to support model implementation and energy impact evaluation.

Phase II – Model Implementation (completed)

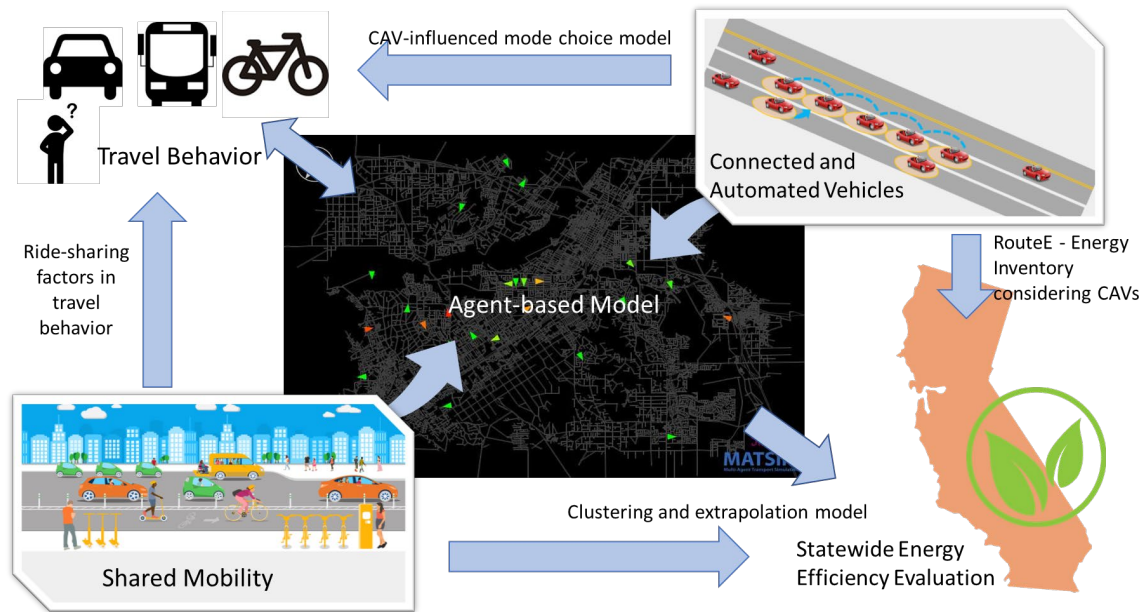


Figure III.1.3.1 Model framework

The research team has developed a comprehensive framework to investigate the impacts on energy intensity due to the deployment of CAV and electrification technologies, and to estimate the changes in modal activity resulting from the introduction of CAVs and shared mobility, as illustrated in Figure III.1.3.1. In this framework, an agent-based model that can simulate and evaluate different CAV and shared mobility scenarios is essential to the energy impact evaluation process. This framework directly links traveler behavior with the transportation system network, allowing us to quantify the impact of new mobility technologies. After

evaluating a number of mesoscopic agent-based traffic simulators (e.g., MATSIM, Polaris), the research team selected BEAM (developed at LBNL) as the main simulation platform due to its support of shared mobility modeling, its ability to deal with large-scale networks, and its synergistic nature with other ongoing work in California. Other key modules were integrated in to the BEAM-based evaluation process, including travel behavior models, CAV characteristics, and shared mobility characteristics. With these tools, we are able to carry-out statewide energy efficiency analysis.

RouteE - Energy Inventory considering CAVs

Taking advantage of nearly 1 million miles of real-world drive cycle data made available by the Transportation Secure Data Center (TSDC) and hundreds of available FASTSim powertrain models, we have developed a modular Python package called *RouteE* that allows users to obtain energy estimates for a variety of vehicle types “out-of-the-box”. In this research, a library of 175 pre-trained *RouteE* vehicle models have been integrated into BEAM to support a number of SMART-Mobility tasks. This integration enables us to calculate energy consumption over many full-BEAM scenarios, where we can disaggregate the energy consumption down to individual vehicles in the simulation as they traverse individual links in the road network. We further enhanced the *RouteE* models to adapt the change of energy consumption and driving behavior of CAVs vehicles. CAVs technologies can have micro-, meso-, and macro- level drive cycle effects that change vehicle energy efficiency when going from human-driving to varying levels of connectivity and automation. At the micro-level, CAVs technologies may smooth small perturbations while maintaining the same average speed that a human-driven vehicle would. Meso-level effects are due to shifting of the operating condition altogether, for example, a given number of manually-driven vehicles may cause congestion to occur on a section of highway, but the same number of partially- or fully-automated vehicles may be able to travel without congestion occurring and hence remain at higher average driving speeds. In another situation, eco-approach and departure (EAD) technology may eliminate stops from a drive cycle and thus enable higher average travel speeds along a section of surface streets. Microsimulation results from CAVs technologies such as Cooperative Adaptive Cruise Control (CACC) and EAD were collected and processed to quantify their impacts on energy consumption and vehicle-miles traveled (VMT) under different penetration rates. In addition to these drive cycle effects, CAVs technologies in many cases contribute to a significantly higher vehicle accessory loads (i.e., to power the additional required sensor hardware and computational resources). The impacts of these additional power demands are simulated by adding the corresponding supplemental accessory loads to each *FASTSim* powertrain model and re-running them over the real-world drive cycles.

Mode choice model considering new transportation services

The introduction of new transportation technologies such as CAV and shared mobility is expected to greatly affect daily travel behaviors and consequently influence the mobility and energy performance of the transportation system. In order to evaluate the impacts of these new transportation services on travelers’ mode choice behaviors, the research team is currently developing a mode choice model which can consider such new transportation services. One of the major difficulties is the lack of observed mode choice data from new transportation services (e.g., CAVs and shared mobility). Instead of using stated preference data which is criticized for not reflecting travelers’ preference in real life, the research team proposed a mode choice model with critical generic variables. The generic variables are a set of variables that travelers consider for mode choice decisions and also can be used to define and describe any transportation mode. Therefore, the model can be estimated with observed data from existing transportation modes and later be applied to investigate travelers’ mode choice behavior in the scenarios with new transportation modes which are defined with generic variables. We proposed the utility function of the proposed model with seven fundamental influencing factors with U_j as the utility of alternative j for a decision maker. The definitions of the variables in the equation are shown in Table III.1.3.1.

$$U_j = \beta_1 Acc_{T_{O,j}} + \beta_2 Acc_{T_{D,j}} + \beta_3 T_{task,j} + \beta_4 T_{shared,j} + \beta_5 T_{productive,j} + \beta_6 Cost_j + \beta_7 L_{physical,j} + \varepsilon_j$$

Existing literature typically assumes that travelers with different sociodemographic characteristics have different travel preference and has shown so with empirical data. Therefore, the research team also adopted this assumption and use the sociodemographic characteristics to group individuals with different mode choice

preferences. Instead of determining the groups exogenously, a latent class model structure was adopted to find the best groupings that can capture the most preference heterogeneity. Instead of determining the groups exogenously, a latent class model structure was adopted to find the best groupings that capture the most preferred heterogeneity. It should be noted that directly introducing sociodemographic characteristics into the mode structure of a typical multinomial logit modeling approach would introduce mode-specific constants, and would contradict the proposed model approach which considers all the modes the same (i.e., the mode specific constants should be zero for all fundamental influencing factors). The structure of the latent class modeling approach does not have this issue, and therefore the latent class modeling structure was adopted for our mode choice model.

Table III.1.3.1 Fundamental Influencing Factors

Variables	Definition	Way to obtain
AccTo _j	Access time at the origin, e.g., walk to bus stop	Data from Google Maps API
AccTD _j	Access time at the destination, e.g., parking lot to office	Data from Google Maps API
T _{Task_j}	Travel time for performing tasks, e.g., driving, bicycling	In-vehicle travel time × P _{Task}
T _{shared_j}	Travel time can be shared with strangers	In-vehicle travel time × P _{Shared}
T _{productive_j}	Travel time can be used to engage productive activities	In-vehicle travel time × P _{Productive}
Cost _j	Cost for service, car purchasing, maintenance, fuel cost, etc.	Statistics from literature
L _{physical_j}	Level of required physical exertion	Statistics from literature

Phase III – Energy Impact Evaluation (ongoing)

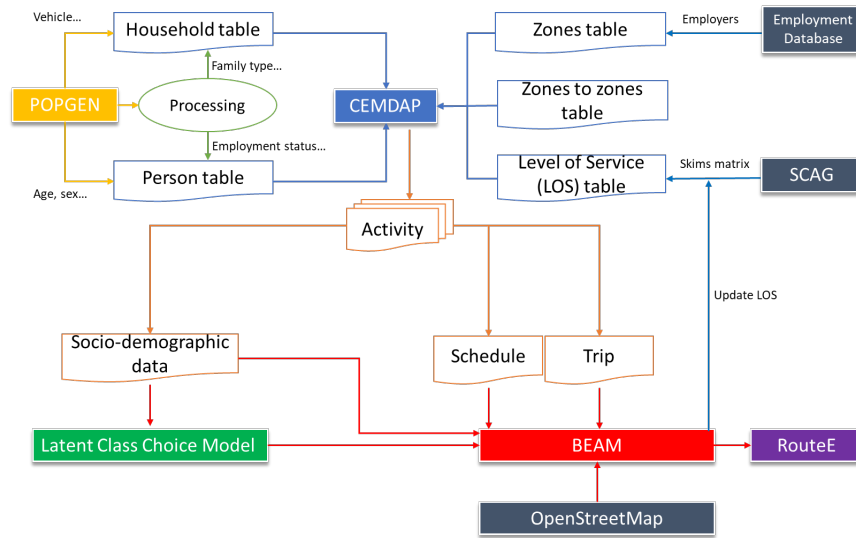


Figure III.1.3.2 System architecture for the activity generation and simulation model

City of Riverside BEAM Model

As part of the energy-impact evaluation, our BEAM-based evaluation system is being applied in Southern California, specifically for the City of Riverside, for a number of different scenarios. The BEAM development team at LBNL is mainly focusing on the Northern California Bay Area network. Complementarily, we have chosen the City of Riverside as an example of Southern California and have developed a well-calibrated BEAM network for the city. The road network is derived from OpenStreetMap database, which includes the geographical information

along with the key attributes of roads, such as road type and capacity. As an agent-based model, BEAM requires the traveler's trip-by-trip activity data for demand generation and traffic simulation. To build a realistic BEAM model for the Riverside area, we refined the Riverside activity-based model using multiple software modules. *Popgen* was applied to generate socio-economic characteristics for each person and for each household in the area. The Southern California Association of Government (SCAG) travel demand model (developed in TransCAD) was used to estimate the transportation system level of services (LOS). The "Comprehensive Econometric Micro-simulator for Daily Activity-travel Patterns" (CEMDAP) loads all the input files and simulates daily activities and travel patterns of all individuals in the region, providing high resolution activity input data for the BEAM model. It is important to note that the travel time and cost results from BEAM can be reversely fed into the CEMDAP model to update the LOS, which can be utilized to represent the potential extra demand induced by CAVs and shared mobility. Figure III.1.3.2 show the system architecture of the City of Riverside BEAM model implementation.

Extrapolation to State-Level

BEAM is a mesoscopic simulator which performs well in representing network level demand-supply dynamics. However, it is difficult, if not impossible, to represent all the details of a mesoscopic model at the state level. Therefore, the research team has developed an approach to extract information from highly detailed regional level model and extrapolate it to the state level. In BEAM, the energy consumption per person was calculated based on the energy consumption estimates and occupancy information provided in the events file. Agent socio-demographic and household attributes are stored in different files in BEAM definition. Some of the network-related attributes are found in the BEAM network definition. The rest of the network attributes such as population density, accessibility to transit, etc. are gathered from publicly available datasets. The BEAM model has a unique identifier for each person agents in the simulation model. Estimated energy consumption for all the different scenarios is linked using the unique identifier. Since the research team is currently defining some of the scenarios regarding CAV deployment and shared mobility, the actual linking will be completed once all the scenarios are defined and executed within BEAM.

Results

Energy Intensity Model based on RouteE

Vehicle energy consumption over each of the vehicle trajectories in the microsimulation results was simulated for a variety of vehicles types using NREL's FASTSim powertrain modeling software. Results are shown in the following figures for a conventional powertrain. The conventional powertrain results in Figure III.1.3.3 show a slight increase in VMT at low speeds (~10 mph) and a steadily improved fuel consumption rate in every speed bin. The most notable improvement is in the 30-40 mph range. This can likely be attributed to vehicle connectivity which effectively improves and smooths the car following behavior in the microsimulation, which reduces the frequency of small decelerations and accelerations, resulting in a lower average fuel consumption rate.

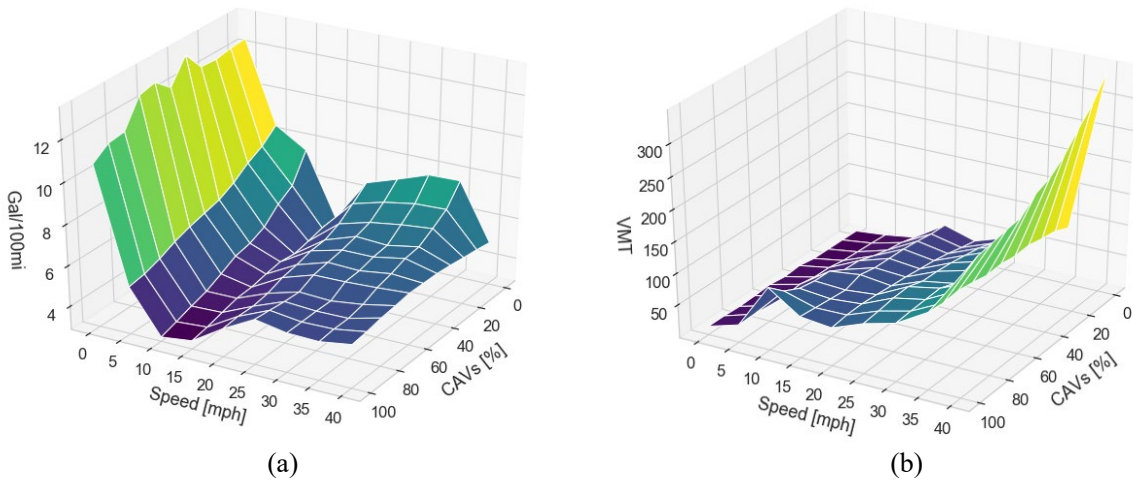


Figure III.1.3.3 RouteE energy inventory (a) fuel consumption rate response surface by speed and CAVs penetration rate for a conventional vehicle and (b) VMT Distribution by speed bin for various CAVs penetration scenarios.

CAV-Influenced Mode Choice Model

Based on the proposed CAV-influenced mode choice model, new modes of automated vehicles (AVs) were added to the existing choice set of the National Household Travel Survey for California, where specific choice probabilities can be calculated. As an example, shows the mode shares before and after introducing AVs. As expected, adding AVs leads to the decrease of existing modes’ shares. Walk and Bike have little further reduction as the price of an AV keeps decreasing, indicating that they are not sensitive to the further price reduction of AVs. This means that Walk and Bike would still be main travel modes of very short trips (<0.5 miles) for respondents in the dataset, even if AVs became available and were operated with the assumed price structure. We then incorporated the new factors to the latent class model. Given an individual with certain sociodemographic characteristics, the membership function can be used to determine which class this individual most likely belongs to. The appropriate class-specific behavior model can be finally applied to predict the individual’s mode choice decisions given certain activity pattern (such as the example in Figure III.1.3.5) and mode-specific time/cost.

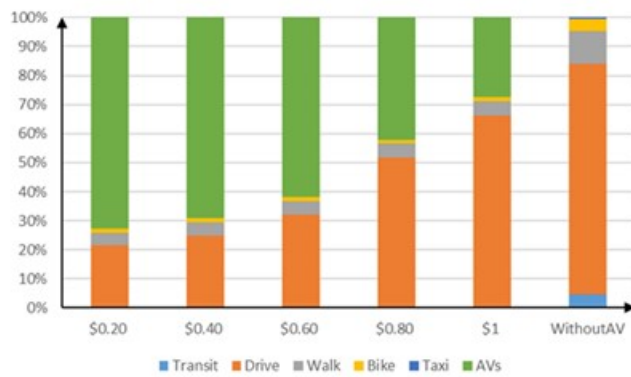


Figure III.1.3.4 Mode shares before and after introducing AVs

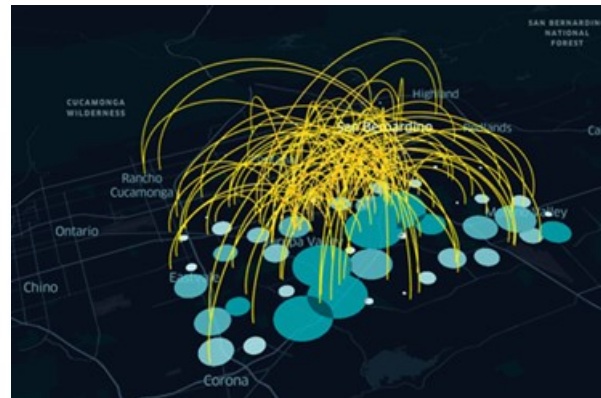


Figure III.1.3.5 Activities in northern City of Riverside area

Simulation Results on the Impact of CAV Penetration Rate

With the BEAM Riverside model, we are investigating the impact of CAV penetration rate on the traffic flow and travel time. Figure III.1.3.6(a) indicates the connection between CAV penetration rate and the traffic throughput for signalized intersections obtained by TOSCo (Traffic Optimization for Signalized Corridors) module, which is

a combination of CACC and EAD. This can be used to estimate the CAV impact in the BEAM simulation by adjusting the road network characteristics, which can be realized by tuning the parameter in the BEAM-integrated Java Discrete Event Queue Simulator (JDEQSim). Figure III.1.3.6(b) shows that the vehicle average travel time will decrease as the CAV penetration increases. This indicates that high penetration rate of CAVs will improve the traffic condition by regulating the vehicle headway and increase the road capacity.

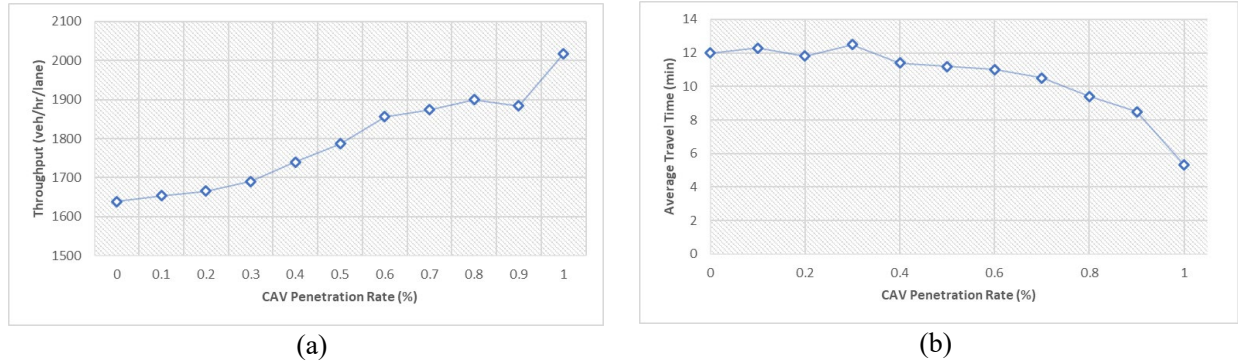


Figure III.1.3.6 The impact of CAV penetration rate on (a) traffic throughput capacity and (b) travel time

Conclusions

In this project, we have created an extensive real-world data set for CAVs and shared mobility systems, and are able to model a variety of energy scenarios, that vary with different vehicle types and fuel/powertrain technologies, combination of CAV applications, various levels of automation, roadway characteristics, and traffic conditions. The outcomes from this project are expected to help close the knowledge gap on recognizing the potential performance and energy impacts of a broad deployment of CAV and shared mobility technologies across a wide range of roadway infrastructure with varying levels of congestion. This will: 1) support policymakers in steering CAV development and deployment in an energy favorable direction; 2) increase the confidence of CAV technology investors both on the infrastructure side (i.e., transportation agencies) and on the vehicle side (i.e., OEMs); and 3) expedite the deployment of promising CAV and shared mobility applications.

Key Publications

1. The paper, “Evaluating the Environmental Impacts of Connected and Automated Vehicles: Potential Shortcomings of a Binned-Based Emissions Model”, is being presented at the 2019 IEEE Intelligent Transportation Systems Conference (ITSC) in Auckland, New Zealand, and will be published in its proceedings. It summarizes the data collection and analysis work in Riverside during this project.

Acknowledgements

This research is supported by Department of Energy Vehicle Technologies Office, under the Energy Efficient Mobility Systems (EEMS) Program. The authors would like to thank Colin Sheppard, Dr. Tom Wenzel and the BEAM development team for their support on BEAM model.

III.1.4 Developing an Eco-Cooperative Automated Control System (Virginia Tech)

Hesham Rakha, Principal Investigator

Virginia Tech Transportation Institute
3500 Transportation Research Plaza (0536)
Blacksburg, VA 24061
E-mail: hrakha@vt.edu

Kyoungho Ahn, Co-Principal Investigator

Virginia Tech Transportation Institute
3500 Transportation Research Plaza (0536)
Blacksburg, VA 24061
E-mail: hrakha@vt.edu

John Tabacchi, DOE Project Manager

U.S. Department of Energy
E-mail: john.tabacchi@netl.doe.gov

Prasad Gupte, DOE Technology Manager

U.S. Department of Energy
E-mail: prasad.gupte@ee.doe.gov

Start Date: October 1, 2017

End Date: June 30, 2020

Project Funding: \$1,675,265

DOE share: \$1,507,197

Non-DOE share: \$168,068

Project Introduction

The transportation sector accounts for 69% of the nation's petroleum consumption and 33% of the nation's CO₂ emissions. Consequently, any reductions in the energy consumed by the transportation sector will have significant environmental benefits. Connected Vehicle (CV) systems comprise sets of applications that connect vehicles to each other and to the roadway infrastructure using vehicle-to-vehicle (V2V) and vehicle-to-infrastructure (V2I) communications, collectively known as V2X. While Automated Vehicles (AVs) offer enhanced operation of individual vehicles, CVs produce cooperative, network-wide benefits through the exchange of information. These new technological advancements have the potential to drastically improve the efficiency and sustainability of our transportation system. Consequently, as part of the proposed research effort we are taking a revolutionary approach to developing a next-generation, vehicle dynamics (VD) Connected Automated Vehicle (CAV) system that builds on existing CAV technologies to reduce the energy/fuel consumption of internal combustion engine vehicles (ICEVs), battery-only electric vehicles (BEVs), plug-in hybrid electric vehicles (PHEVs), and hybrid electric vehicles (HEVs).

Objectives

The main project goal of this effort is to substantially reduce vehicle fuel/energy consumption by integrating vehicle control strategies with CAV applications. Specifically, the team is developing a novel integrated control system that (1) routes vehicles in a fuel/energy-efficient manner and balances the flow of traffic entering congested regions, (2) selects vehicle speeds based on anticipated traffic network evolution to avoid or delay the breakdown of a sub-region, (3) minimizes local fluctuations in vehicle speeds (also known as speed volatility), and (4) enhances the fuel/energy efficiency of ICEVs, BEVs, HEVs, and PHEVs.

Approach

We are taking a revolutionary approach to developing a next-generation CAV system (Figure III.1.4.1) that builds on existing CAV technologies to reduce the energy/fuel consumption of ICEVs, BEVs, HEVs, and

PHEVs. The development of the Eco-Cooperative Automated Control (Eco-CAC) system will involve the following key steps and components:

1. Develop a CV eco-routing controller that can be used for various vehicle types. This unique eco-router will use a dynamic feedback controller, employ key link parameters that capture the entire drive cycle, compute vehicle-specific link energy functions using these link parameters, and compute user-optimum routings.
2. Develop a speed harmonization (SPD-HARM) controller that regulates the flow of traffic approaching network bottlenecks identified using the Fundamental Diagram (FD) and/or the Network Fundamental Diagram (NFD). This controller will be fully integrated with the vehicle router, resulting in a unique strategic controller that can route traffic away from congested areas and regulate the flow of traffic entering congested areas using gating techniques.
3. Develop a multi-modal (ICEV, BEV, PHEV, and HEV) Eco-CACC-I controller that computes and implements optimum vehicle trajectories (ICEVs, BEVs, PHEVs, and HEVs) along multi-intersection roadways within CAVs considering dynamic vehicle queue predictions.
4. Develop an Eco-CACC-U controller that provides local longitudinal energy-optimal control in consideration of homogenous and non-homogeneous vehicle platooning of ICEVs, BEVs, PHEVs, and HEVs.

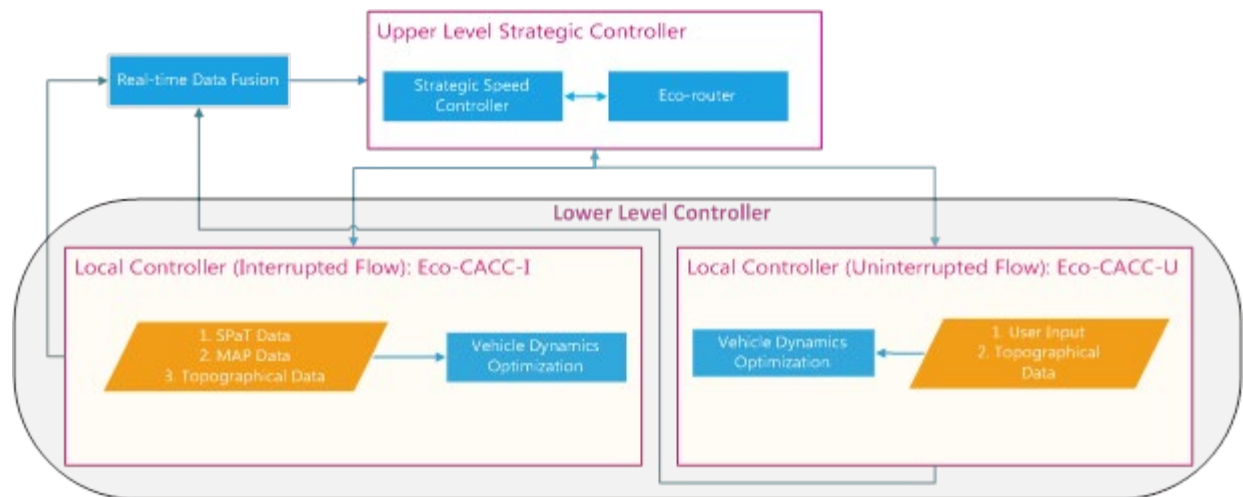


Figure III.1.4.1 Proposed Eco-CAC system

At the upper level, the strategic controller (eco-router and strategic speed controller) will compute the energy/fuel-optimum route and vehicle optimum speeds (upper and lower bounds) required to regulate the flow of traffic approaching downstream sub-networks and/or bottlenecks, thus preventing or delaying the breakdown of traffic flow and mitigating traffic congestion. This strategic controller will extend traditional eco-routing and SPD-HARM systems beyond the currently used isolated control to a fully integrated, network-wide controller that identifies bottlenecks and controls the flows approaching the bottlenecks in real-time. The eco-router within the strategic controller will develop optimum eco-routes using a vehicle-specific feedback controller. Unlike a predictive controller, a feedback controller does not require a link-specific analytical fuel consumption function, which is typically difficult to develop, inaccurate, and not vehicle-specific. Instead, the eco-router controller uses information shared by other CVs to compute the link cost estimates. In addition, a SPD-HARM controller will be developed and integrated with the eco-router to regulate the traffic flow approaching transportation bottlenecks. At the lower level, a VD controller will operate along the routes and within the speeds recommended by the strategic controller to compute energy-efficient vehicle speeds based on

local conditions using two local controllers: an Eco-CACC-I and an Eco-CACC-U controller. The Eco-CACC-I controller will compute energy-optimum vehicle trajectories through signalized intersections (i.e., interrupted flow conditions) using traffic count and signal phase and timing (SPaT) data. The Eco-CACC-U controller will develop fuel/energy efficient platooning strategies along uninterrupted road facilities. The VD lower-level controller will use the planned vehicle routes and trajectories to anticipate the vehicle operational mode and compute the optimum VD strategies. The fully functional Eco-CAC system will be implemented in a traffic simulation environment so that it can be tested at a network level. The proposed CAV applications, testing parameters, and validation methods will be used to quantify the Eco-CAC system's benefits.

Results

The team investigated the impacts of eco-routing on multiple large-scale networks for BEVs, HEVs, and ICEVs using INTEGRATION microscopic traffic simulation software. Table III.1.4.1 demonstrates the effects of eco-routing in the case of the Columbus and Cleveland, OH networks. The results show that eco-routing of ICEVs resulted in reductions in their fuel consumption levels by up to 4.8% and 5.0% for the Cleveland and Columbus networks, respectively, when compared to traditional travel time (TT) routing. The study found that eco-routing 100% of the ICEVs increased their travel time by 3.6% and 5.9%, and their delay by 11.7% and 19.4%, but reduced their trip distance by 5.8% and 5.9% for the Cleveland and the Columbus networks, respectively. In addition, the eco-routing of BEVs reduced their energy use by up to 41.2% and 25.9% for the Cleveland and the Columbus networks, respectively, when compared to the traditional TT-optimum routing.

Table III.1.4.1 System-Wide Impacts of Eco-routing on Large Networks

Vehicle Type	MOE	Cleveland network			Columbus network		
		TT-routing	Eco-routing	Comparison	TT-routing	Eco-routing	Comparison
ICEV	Trip Distance (km)	4.8	4.5	-5.8%	4.8	4.5	-5.8%
	Travel time (s)	314.5	325.9	3.6%	314.5	325.9	3.6%
	Delay (s)	76.1	85.1	11.7%	76.1	85.1	11.7%
	Fuel (l)	0.571	0.543	-4.8%	0.571	0.543	-4.8%
BEV	Trip Distance (km)	4.8	3.5	-25.9%	4.8	3.5	-25.9%
	Travel time (s)	315.4	500.7	58.8%	315.4	500.7	58.8%
	Delay (s)	76.6	252.0	228.9%	76.6	252.0	228.9%
	Fuel (l)	3,198.8	1,880.5	-41.2%	3,198.8	1,880.5	-41.2%
HEV	Trip Distance (km)	4.8	3.6	-24.1%	4.8	3.6	-24.1%
	Travel time (s)	315.0	520.0	65.1%	315.0	520.0	65.1%
	Delay (s)	76.4	265.3	247.3%	76.4	265.3	247.3%
	Fuel (l)	0.247	0.149	-39.7%	0.247	0.149	-39.7%

BEVs were able to achieve larger energy savings due to the many alternative routes that the two large networks provide. The study, however, found that BEVs experienced significant increases in travel time and delay even when using the eco-optimum routes. The simulation study found that for 100% eco-routing, BEVs increased their average travel time from 315.4 s to 500.7 s and from 314.5 s to 531.9 s on both the Cleveland and the Columbus networks, respectively. Further, the eco-routing option increased the average delays by up to 228.9% and 250.4%, respectively. The study found that eco-routing HEVs' average fuel savings on the Cleveland and Columbus networks were 39.7% and 23.1%, respectively, when compared to TT-routing. However, similar to the BEVs' results, eco-routing of HEVs also significantly increased their average travel time by up to 65.1% and 84.0% and the average delay by up to 247.3% and 325.4% on the Cleveland and Columbus networks.

The eco-routing results demonstrate that energy optimum routes may be very different than TT-optimum routes. The simulation results demonstrate that TT-optimum routings produce vehicle travel times that are almost identical, at 314.5 s, 315.4 s, and 315 s for ICEVs, BEVs, and HEVs, respectively. However, eco-routing of BEVs and HEVs significantly increased their average travel times. The most energy efficient ICEV driving condition is a moderate speed highway driving cycle. Thus, eco-routing ICEVs mostly selected high-speed routes and did not significantly increase their travel times. However, eco-routing of BEVs and HEVs resulted in the selection of low-speed routes that reduced their energy/fuel energy consumption and maximized their regenerative energy. The study indicates that further exploration is required to develop a multi-objective eco-routing model that can reduce energy consumption with minimum impacts to BEV and HEV travel times.

The team developed and tested the speed harmonization (SH) logic coupled with the sliding mode controller (SM) on a network. SH was implemented on a downtown LA network as presented in Figure III.1.4.2. The network has 3,556 links, 331 of which are freeways, and includes 457 signalized intersections, 285 stop signs, and 23 yield signs. The simulation was conducted during the morning peak hour (7:00–8:00 a.m.), and the simulation time was set to 10,000 s (2.77 h). The study found that the proposed SH logic saved 12.17% of average travel time, 20.67 % of total delay, 39.58% of stopped delay, 2.6% of fuel consumption, and 3.3% of CO₂ emissions, as summarized in Table III.1.4.2.



Figure III.1.4.2 LA network - speed harmonization logic test network (LA network)

Table III.1.4.2 Network-Wide Benefits of Speed Harmonization Logic

	No SH	SH	Improvement
Average TT (s)	1034.27	908.37	12.17
Total Delay (s)	557.46	442.25	20.67
Stopped Delay (s)	256.77	155.13	39.58
Fuel (l)	1.16	1.13	2.60
CO2 (g)	2482.13	2400.15	3.30

The team also developed multi-intersection ICEV and BEV Eco-CACC-I controllers that calculate energy-optimized speed trajectories. The study found that the ICEV Eco-CACC-I controllers produced fuel savings for all demand levels compared to the basic case without the Eco-CACC-I controller, as illustrated in Figure III.1.4.3. The average fuel savings produced by using the ICEV Eco-CACC-I single intersection (1S) controller were 3.9%, 4.8%, 6.3%, 6.1%, and 5.9% for demand levels of 100, 300, 500, 700, and 900 veh/h/lane, respectively. The Eco-CACC-I multiple intersection (MS) controller further improved the average fuel savings by 10.6%, 11.1%, 11.8%, 11.4%, and 11.1% under the same demand levels. Note that the demand of 500 veh/h/lane resulted in maximum fuel savings of 11.8% for the entire traffic network. The results demonstrate that the ICEV Eco-CACC-I MS controller produced average fuel savings of 11.2%, outperforming the Eco-CACC-I 1S controller, which had 5.4% average fuel savings. The results demonstrate that the BEV Eco-CACC-I controllers produced energy savings for all demand levels compared to the base case without the Eco-CACC-I controller. The average energy savings produced by using the BEV Eco-CACC-I 1S controller were 3.4%, 5.6%, 5.85%, 5.83%, and 5.82% for demand levels of 100, 300, 500, 700, and 900 veh/h/lane, respectively. The Eco-CACC-I MS controller further improved the average energy savings by 9.8%, 10.6%, 11.0%, 10.8%, and 10.6% for the same demand levels. Note that the demand of 500 veh/h/lane resulted in maximum energy savings of 11% for the entire traffic network. The results demonstrate that the BEV Eco-CACC-I MS controller produced average fuel savings of 10.6%, outperforming the Eco-CACC-I 1S controller, which produced 5.3% savings in average energy consumption.

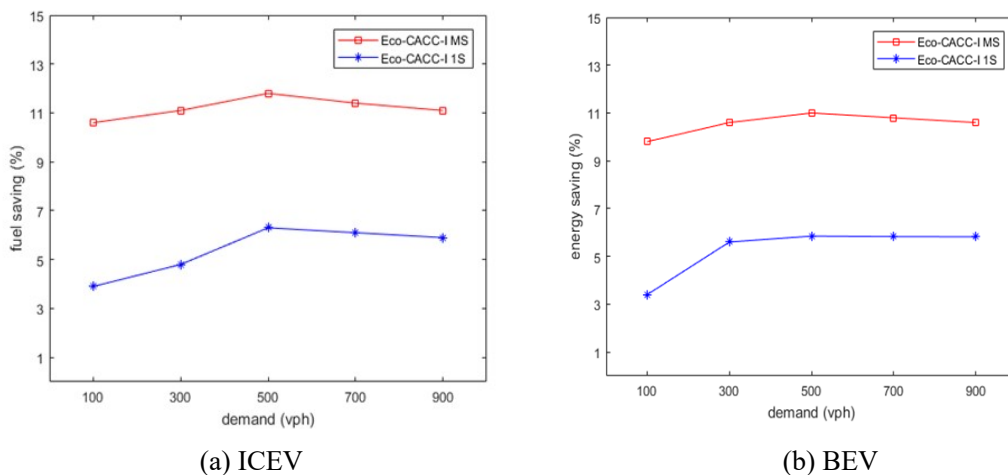


Figure III.1.4.3 Eco-CACC-I controller test results

The team also developed an Eco-CACC-U controller and the new system saved energy consumption by up to 18%, 6.2%, 7.9%, and 11.4% for ICEVs, BEVs, HEVs, and PHEVs, respectively, compared to non-Eco-CACC-U controlled vehicles. The milestone of this task was producing fuel consumption/energy savings of 5% or more compared to non-Eco-CACC-U controlled vehicles. In particular, the team evaluated the performance of the eco-predictive control system on a section of Interstate 81 (I-81). The energy savings produced by the proposed eco-predictive control increased as the speed range widened for both southbound and northbound sections. The proposed system reduced the energy consumption of an ICEV (2011 Toyota Camry), BEV (2013 Nissan Leaf), HEV (2011 Toyota Prius), and PHEV (2013 Chevy Volt) by up to 18%, 6.2%, 7.9%, and 11.4% respectively on the I-81 southbound section. The team also found that all platooning vehicles experienced reduced fuel consumption levels. In a case study, the lead vehicle consumed 0.9645 liters of gasoline and the following vehicles consumed 0.9668, 0.9657, 0.9652, 0.9652, and 0.9651 liters of gasoline, respectively.

Conclusions

This project develops a novel Eco-CAC system that integrates VD control with CAV applications. The research team is currently working on developing the Eco-CAC system and the simulation modeling framework development. The team completed the eco-routing system development, the strategic control algorithm development, the Eco-CACC-I algorithm development, and the Eco-CACC-U algorithm development. The team will refine and integrate the various system components to develop the integrated Eco-CAC system, combining the upper-level strategic controller with the lower-level Eco-CACC-I and Eco-CACC-U controllers. The controllers will operate with the objectives of balancing flow and minimizing queues throughout the network, especially when fast-propagating congestion exists. The team will adopt a horizontal integration of the various components to support communication between the four subsystems: eco-routing, SPD-HARM, Eco-CACC-I, and Eco-CACC-U. This approach will create a modular Eco-CAC system that can easily manage data flows between subsystems and integrate new CAV subsystems as needed.

Key Publications

1. Chen H. and Rakha H.A. (2019), "Developing a Traffic Signal Eco-Cooperative Adaptive Cruise Control System for Battery Electric Vehicles," Transportation Research Board (TRB) 98th Annual Meeting, Washington DC, Jan. 13-17, Paper: 19-00572. [DOE-VT-0008209-C01]
2. Du J. and Rakha H.A. (2019), "Constructing a Network Fundamental Diagram: A Synthetic Origin-Destination Approach," Transportation Research Board (TRB) 98th Annual Meeting, Washington DC, Jan. 13-17, Paper: 19-00044. [DOE-VT-0008209-C02]
3. Bichiou Y., Elouni M. and Rakha H.A. (2019), "A Novel Sliding Mode Network Perimeter Controller," Transportation Research Board (TRB) 98th Annual Meeting, Washington DC, Jan. 13-17, Paper: 19-00476. [DOE-VT-0008209-C03]
4. Elouni M., Rakha H.A., and Bichiou Y. (2019), "Implementation and Investigation of a Weather- and Jam Density-tuned Network Perimeter Controller," Transportation Research Board (TRB) 98th Annual Meeting, Washington DC, Jan. 13-17, Paper: 19-04765. [DOE-VT-0008209-C04]
5. Elbery A. and Rakha H.A. (2019), "City-wide Eco-routing Navigation Considering Vehicular Communication Impacts," Sensors, Volume 19, Issue 2. [DOE-VT-0008209-J01]
6. Wang J., Elbery A., and Rakha H.A. (2019), "A real-time vehicle-specific eco-routing model for onboard navigation applications capturing transient vehicle behavior," Transportation Research Part C: Emerging Technologies, Volume 19, Issue 2, pp. 1-21. [DOE-VT-0008209-J02]
7. Fadhoun K. and Rakha H.A. (2019), "A novel vehicle dynamics and human behavior car-following model: Model development and preliminary testing," International Journal of Transportation Science and Technology, ISSN 2046-0430. [DOE-VT-0008209-J03]

8. Du J. and Rakha H.A. (2019), “Constructing a Network Fundamental Diagram: A Synthetic Origin-Destination Approach,” Transportation Research Record (TRR), DOI: 10.1177/0361198119851445. [DOE-VT-0008209-J04]

IV Core Modeling, Simulation, and Evaluation

IV.1.1 Livewire Data Platform (NREL, INL, PNNL)

Kay Kelly, Principal Investigator

National Renewable Energy Laboratory
15013 Denver West Parkway
Golden, CO 80401
E-mail: kay.kelly@nrel.gov

Chitra Sivaraman, Principal Investigator

Pacific Northwest National Laboratory
902 Batelle Boulevard
Richland, WA 99354
E-mail: chitra.sivaraman@pnnl.gov

John Smart, Principal Investigator

Idaho National Laboratory
2525 Fremont Avenue
Idaho Falls, ID 83402
E-mail: john.smart@inl.gov

Erin Boyd, DOE Technology Manager

U.S. Department of Energy
E-mail: erin.boyd@ee.doe.gov

Start Date: October 1, 2018	End Date: September 30, 2021	
Project Funding (FY19): \$2,200,000	DOE share: \$2,200,000	Non-DOE share: \$0

Project Introduction

To bring about the transformational changes in our transportation system like those being explored by the EEMS program, data sharing must be endemic. The data landscape for transportation and mobility is complex. Current EEMS models require data from vehicles, sensors, and travelers and these data volumes are growing beyond the capabilities of spreadsheets and relational databases. Historically, valuable EEMS datasets have been protected by non-disclosure agreements (NDAs) and licenses or hoarded as a competitive advantage, which makes sharing legally challenging. Even sharing data developed in the public space is limited because of size, quality, or complexity. These obstacles limit data accessibility, which prevents or delays multi-institution research collaboration. For EEMS to succeed, data collaboration is critical, and successful data management must consider factors such as data integrity, privacy, and security.

Objectives

The Livewire Data Platform supports the EEMS Program's strategic goal of sharing research insights and coordinating and collaborating with stakeholders to support energy efficient local and regional transportation systems by providing a common platform for stakeholders to discover and access datasets. The Livewire Data Platform has three specific objectives. First, to provide a platform allowing easy and secure data sharing and discovery making it easy to search and share transportation and mobility-related data. Second, to create a community that builds partnerships and collaboration around data rather than competition. Finally, to create a system that allows shared data to grow in size and complexity as EEMS evolves.

Approach

Leveraging deep transportation data expertise and decades of experience managing and sharing open and proprietary data sources alike, NREL, INL and PNNL are collaborating to develop the Livewire Data Platform. This new platform leverages existing successful software assets and will facilitate easy and secure data sharing and discovery among EEMS researchers giving them the data they need to generate impactful research results.

NREL brings an application programming interface (API) management platform which provides for secure data sharing between researchers. PNNL brings a secure data discovery platform allowing for cataloging and exploration of datasets. Together, these lightweight solutions provide the basis of a flexible and customizable data solution for EEMS and leverage broad funding to support platform maintenance. INL brings a depth of expertise in data quality assurance and supports the project with development of metadata standards and quality assurance strategies.

The project is split into three tasks executed in parallel over a three-year period of performance.

1. Create data management platform and expose datasets
2. Build capabilities for managing complex data leveraging Fleet DNA and the Transportation Secure Data Center (TSDC), along with maintaining and sharing data from these resources
3. Facilitate partnerships, data collection, and resolution of data sharing challenges

Results

Task 1: Create data management platform and expose datasets

Following dozens of interviews with EEMS researchers to understand their data sharing capacities and requirements along with completion of DOE web governance team approval, the Livewire Data Platform (<https://livewire.energy.gov>) launched in year 1 sharing 38 datasets from nine projects. The platform allows for three methods of data sharing: as a datahub which allows files to be uploaded and downloaded directly from the site, by API's allowing computers to share data in a standard machine-readable format, and via links which allow data that is already being shared successfully on other websites to be directly discoverable from the Livewire Data Platform.

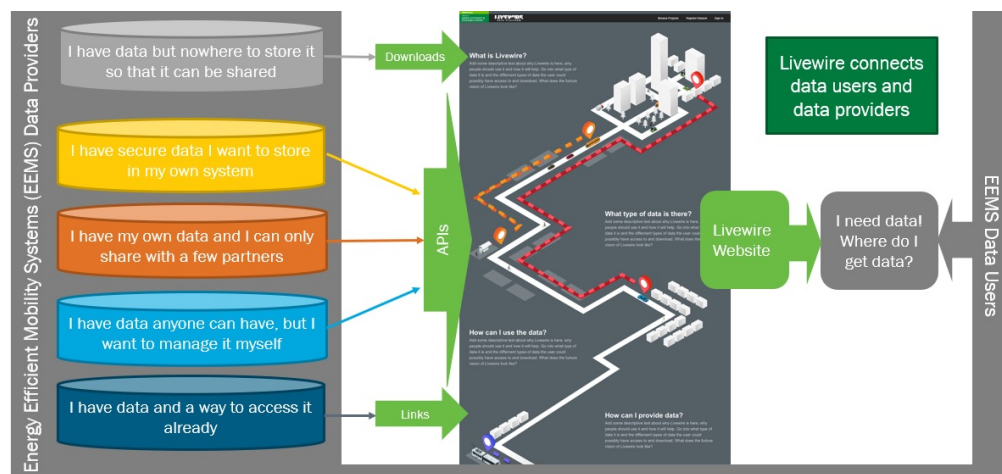


Figure IV.1.1.1 Livewire Data Platform Concept

Building on the successful Atmosphere to Electrons (A2e) platform for the DOE Wind Energy Technologies office, PNNL established the Data Archive and Portal (DAP) for the Livewire Data Platform. This included development of simple front-end user access and authentication services, backend capability to receive and store data, methods to link data to external portals, methods to search and access data stored within the

platform, the capability to collect metrics on users, data orders and data storage and the adoption of metadata schema to drive the content of the dataset landing pages.

NREL’s open source API Umbrella platform allowed existing EEMS partners to expose their data via an API. APIs are industry standard for sharing both small and large datasets. This allowed partners who wanted to continue storing and maintaining their own data to also share it with EEMS partners. This platform handles authentication; role-based data access; rate limiting (ensuring that a single user’s data requests won’t bring down the system); and analytics (understanding who is accessing which dataset how often.)

Knowing that quality and discoverability are important considerations with data-driven research, INL developed a schema for high-level metadata (information about projects, datasets, points of contact, keywords, etc., that drive the Livewire Data Platform user interface) based on the existing Project Open Data (POD) schema used by data.gov. INL and NREL cataloged high-level metadata for each of the initial data-sharing projects in the platform. INL also created a draft schema for low-level metadata (detailed information about the content, structure, and quality of data in each of the datasets) and cataloged low-level metadata for the first dataset.

Task 2: Build capabilities for managing complex data leveraging Fleet DNA and the Transportation Secure Data Center (TSDC), along with maintaining and sharing data from these resources

NREL, INL and PNNL team members spent considerable time surveying the EEMS research community to determine the nature of datasets and priority for data sharing. Results from these interviews identified the typology of data sharing needs and informed the initial data platform development strategy. Two NREL datasets of initial interest for sharing with the EEMS community were the TSDC and Fleet DNA data.

Established in 2009, the TSDC provides centralized access to detailed transportation data from a wide assortment of travel surveys and studies conducted across the nation. The TSDC’s two-level access approach—a public website for downloading cleansed datasets and a secure online portal for approved users to work with detailed spatial data—facilitates data availability for legitimate research while maintaining the anonymity of survey participants. Maintained by NREL in partnership with the U.S. Department of Transportation, the TSDC features millions of data points for all modes of travel, including second-by-second global position system (GPS) readings, vehicle characteristics (if applicable), and demographics. NREL screens the initial data for quality control, translates each data set into a consistent format, and interprets the data for spatial analysis. NREL’s processing routines add information on vehicle fuel economy and road grades and join data points to the road network. In FY19, more than 546,000 household trips and more than 8,600 high resolution GPS trip data were added to the TSDC (see Figure IV.1.1.2 FY19 TSDC Data Additions).



Figure IV.1.1.2 FY19 TSDC Data Additions

NREL's software development team worked with TSDC researchers to expose transportation studies and survey data on the Livewire Data Platform resulting in the availability of 88 data downloads and 21 data links. In the coming year, NREL plans to expand availability of TSDC data through the Livewire Data Platform.

Established in 2012, the Fleet DNA clearinghouse now features over 10 million miles of high-fidelity vehicle and operations data from more than 2,000 medium- and heavy-duty vehicles, including delivery vans and trucks, school buses, transit buses, bucket trucks, service vans, tractor trailers, and refuse trucks. In FY19, over 360 thousand miles were added to Fleet DNA database including shuttle buses at Dallas Fort Worth and Los Angeles International airports; yard tractors at the Port of Long Beach and the Port Authority of New York and New Jersey; National Park Service shuttle buses at Zion, Bryce Canyon, and Yosemite National Parks; UPS line-haul trucks supporting the Super Truck II projects; and regional-haul trucks participating in the North American Council for Freight Efficiency's Run on Less program (see Figure IV.1.1.3 FY19 Fleet DNA Data Additions). Aggregated duty cycle statistics, summaries, and visualizations are available for download via the public website while a secure database stores and protects the raw data. Fleet DNA can be combined with other models, tools, and data resources, and subjected to data fusion, multivariate analysis, and advanced visualization techniques to investigate complex, multi-dimensional transportation issues and solutions. For example, Fleet DNA data can be fused with datasets pertaining to chassis dynamometer results, road networks, road grade, weather, vehicle specifications, and vehicle registrations, and combined with other tools such as FASTSim and the Drive-Cycle Rapid Investigation, Visualization, and Evaluation (DRIVE) analysis tool, which uses GPS and controller area network (CAN) data to characterize vehicle operation and produce statistically representative drive cycles based on real-world activity.

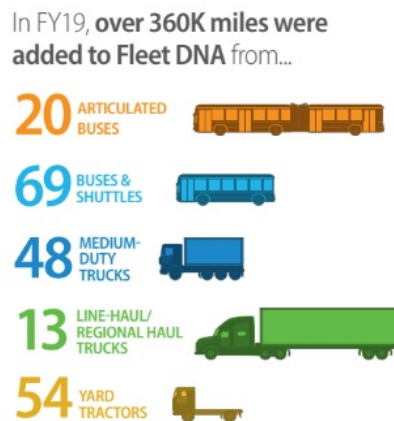


Figure IV.1.1.3 Fleet DNA Data Additions

NREL's software development team worked with Fleet DNA researchers to expose a Fleet DNA summary data API and three cleansed datafiles on the Livewire Data Platform. In the coming year, NREL plans to expand data access, continue to respond to data requests from EEMS labs, provide detailed data dictionaries and descriptive summary information on individual data sets such as the application, number and types of vehicles, geographic location, etc.

Task 3: Facilitate partnerships, data collection, and resolution of data sharing challenges

The team conducted dozens of data interviews with EEMS researchers during the initial year of the project. These conversations provided the data use cases that informed initial development of the data platform and highlighted areas for improved functionality that the software team can focus on in future years. With the platform now available to explore and with new functionality being added to address additional data use cases, the team plans to continue working with EEMS researchers to provide an easy and secure data sharing experience.

Conclusions

The primary objective during year one of the Livewire Data Platform project was to launch an initial version of a data sharing website. The Livewire Data Platform met that goal and launched successfully sharing 38 datasets from nine projects. The platform allows for three methods of data sharing: as a datahub, by API, and direct links. Major efforts during the initial year were to make Fleet DNA and TSDC data discoverable through the Livewire Data Platform, with refinements to big data management strategies coming in future years. Additional future work includes continued development of the data platform, development and incorporation of information about data quality into the platform to help guide selection of datasets of value, the addition of more high value EEMS datasets to the platform including continuing to grow and maintain the Fleet DNA and TSDC data resources, and the formation of a data working group to address human factors and legal agreements that limit data sharing.

Acknowledgements

The Livewire Data Platform team would like to thank the many EEMS researchers who provided input, feedback, and datasets for the initial launch of the platform.

IV.1.2 Virtual and Physical Proving Ground for Development and Validation of Future Mobility Technologies (ORNL)

Dean Deter, Principal Investigator

Oak Ridge National Laboratory
1 Bethel Valley Road
Oak Ridge, TN 37831
Phone: 865-946-1580
E-mail: deterdd@ornl.gov

Erin Boyd, DOE Technology Manager

U.S. Department of Energy
E-mail: erin.boyd@ee.doe.gov

Start Date: October 1, 2018

End Date: September 30, 2021

Project Funding: \$1,150,000

DOE share: \$1,150,000

Non-DOE share: \$0

Project Introduction

Emphasis on pushing the state of the art of advanced transportation technologies, specifically connected and automated vehicles (CAVs), has recently gained significant momentum in both government and industry. The Department of Energy's SMART Mobility program is attacking the "transportation as a system" problem from multiple angles. Therefore, modeling, simulation, and analysis form the backbone for future prediction of the impacts of various technologies on mobility for the nation, in the form of the Mobility Energy Productivity (MEP) metric. A need has been identified to experimentally evaluate these solutions to ascertain the validity of their respective claims, as well as to generate critical data to feed back into SMART Mobility-developed tools for more detailed analyses. An advanced hardware-in-the-loop (HIL) platform capable of bridging the gap between analytical models and real-world hardware provides the intermediary to identify the most promising technologies that should be fully verified at the vehicle system level.

Model-based design has become the industry standard for developing vehicle supervisory and powertrain control systems. However, this approach misses the complexity of the interactions of physical hardware in real-world driving conditions. The novel approach proposed by ORNL advances the state-of-the-art research by exercising actual hardware in real-world traffic situations, in which the vehicle is expected to be operated, to capture the subtle effects of communication timing/latencies, actual powertrain energy consumption, emissions, and other dynamic phenomena. The ability to subject actual hardware to simulated real-world conditions allows diverse scenarios to be simulated for enhancing strategies and algorithms, as well as responding to micro- and macro-level traffic environments that current high-level traffic network models fail to capture. In addition, this framework provides a repeatable, cost effective environment for rapid development and validation of CAV technologies, including their respective vehicle controls and communication protocols. This capability offers the benefit of absolute safety, since the control algorithms are evaluated thoroughly in a controlled HIL laboratory environment before being targeted to an actual test vehicle for on-road or track testing.

Objectives

The objective is to accurately verify the energy benefits and emissions impacts of these advanced technologies with actual powertrain hardware physically installed in the laboratory and subjected to virtual traffic conditions for research. This approach presents the opportunity to research, develop, and evaluate a large matrix of CAV technologies over a greater, customizable design space at a time when vehicle-to-vehicle (V2V) and vehicle-to-infrastructure (V2I) hardware has not even been completely developed or is not available for full-scale testing.

ORNL will investigate early stage “smart” technologies as a system, regardless of the powertrain architecture or actual physical design selected by the researchers. Multiple research facilities within ORNL will be virtually connected to develop a novel and flexible approach to examine multiple hardware components in a variety of powertrain configurations and traffic environments in real-time, high-fidelity, traffic simulations while subjecting actual powertrain(s) to emulated real-world traffic conditions. This approach will allow for the development of control strategies and algorithms specifically targeted at advanced vehicle technologies, as well infrastructure controls.

Approach

Task 1: “Virtual-Physical” Proving Ground

Considering the efforts of the Vehicle Technologies Office (VTO) to tackle difficult questions regarding current and future smart vehicle technologies and their impact on mobility, the EEMS program and SMART Mobility Consortium analyzed many different CAV and SMART Mobility technologies that identified the most promising and efficient methods for future transportation and corresponding infrastructure. This work highlighted a real need for cross-collaboration among different scientific skill sets in order to produce a well-analyzed and validated answer that began in modeling and simulation and ended in validated HIL and vehicle-level laboratory experiments, which in turn provides data to improve the modeling activities. ORNL is addressing this need by bringing together its various skill sets for use in the Virtual-Physical Proving Ground.

Objective: Establish and verify a capability to test and validate the analytical results of current and future SMART Mobility and EEMS modeling, simulation, and analysis, as well as other relevant VTO programs.

Task 1.1: Standardized Virtual Proving Ground Framework

The goal of Task 1.1 is to allow flexibility in creating combinations of modeling, simulation, HIL, and vehicle-level testing. This task focuses on establishing a standardized framework that allows for the integration of multiple HIL -based research capabilities within ORNL, as well as provisions for connectivity with other national laboratory facilities, tools, and capabilities. This will allow for greater flexibility and for ease of integrating required formats, including macro traffic simulations and high-fidelity vehicle environment simulations. This is an important aspect of Task 1.1 because of the many different DOE tools that are currently being developed by DOE laboratories, as well as industry tools already in use both within the DOE laboratory system and by industry partners. One critical aspect of this task is to ensure alignment of this framework with the developing SMART Mobility Workflow. Once the framework is completed, ORNL will begin to integrate various EEMS and SMART Mobility tools and data sets into a verification tool and as a high-fidelity data collection effort for more robust, validated models.

Task 1.2: Virtual Proving Ground Applied to HD Platooning

As part of an ORNL Laboratory Directed Research and Development project, a traffic network is being constructed off Interstate I-40 in the Knoxville area. This task will apply the framework developed in Task 1.1 to better understand the impacts of platooning in real-world traffic conditions on both urban and rural highway systems. Test track data from the SMART Mobility CAV Pillar for platooned HD vehicles will be leveraged to establish the aerodynamic parameters for first, second, and third trucks. Cummins, a long-time partner of ORNL, will assist in getting a current-production X-15 Class 8 engine and aftertreatment package coupled with an Eaton Smart Advantage Ultra-Shift transmission operational in the Vehicle Systems Integration (VSI) Laboratory. This powertrain will be “virtually” installed in the platooned vehicles to fully characterize fuel consumption and emissions impacts of platooning in a host of various traffic conditions and interactive traffic objects.

Task 1.3: Virtual Proving Ground Applied to SMART Mobility Freight

Commercial vehicles have become a focus within VTO at large, particularly in the SMART Mobility Consortium. An array of powertrain technologies and multi-mode approaches are being investigated to improve understanding of the best practices for reducing energy consumption and increasing the MEP metric. Task 1.3 will utilize the Virtual Proving Ground framework with the SMART Freight Taskforce to verify

energy impacts of various last-mile delivery technologies. Building upon Task 1.2, ORNL will introduce various inter-city and intra-city freight operations and routing scenarios into the framework with actual hardware, such as a medium-duty Cummins ISB engine for last-mile delivery. A better understanding of the actual reduction in fuel energy for a large variety of multi-modal approaches can be attained.

Task 2: (V2X) Communication Modeling, Development, and Validation

Currently, V2V, V2I, and other vehicle communications (V2X) are in their infancy. What final V2X infrastructure and capabilities look like is an ever-changing landscape. This situation emphasizes the need for development and testing platforms that are extremely flexible, programmable, and able to go back and forth from the modeling/simulation space to real hardware testing. ORNL's VSI Laboratory, as well as ORNL's Vehicle Research Laboratory and Vehicle Security Laboratory, are extremely well suited for achieving the goals in Task 2. With the current virtual vehicle environment, V2X hardware can be tested while tied to a virtual vehicle in a real-time HIL environment or can be tied to an entire vehicle or powertrain in the test cell. This testing is in an extremely flexible environment that allows for low- to high-fidelity data streams, quick programming changes, and repeatable laboratory results.

Objective: Expand the capabilities of the EEMS program to not only test V2X in virtual environments but also allow for using HIL methodologies to test V2X hardware in real time.

Task 2.1: Integration of V2X Communications Hardware into Virtual Proving Ground Framework

Task 2.1 enhances the Virtual Proving Ground with a communications-focused testing platform consisting of multiple V2X communication hardware units integrated into several ORNL vehicle and HIL-enabled test facilities. This approach enhances the overall Virtual Proving Ground capability with the ability to understand V2X hardware integration, communication, latency, controls delays, reliability, interference issues, and so on.

Task 2.2: Light-Duty Virtual Proving Ground for V2X Evaluation

As a means of proving the capability established in Task 2.1, the team will collaborate with the American Center for Mobility (ACM). The objective of Task 2.2 is to replicate "virtual versions" of each of these respective facilities so that CAV technologies and control strategies can quickly and easily be verified in a safe, secure setting before vehicle deployment. Since actual powertrain components will be exercised through modeling, simulation, and HIL approaches, an understanding of the expected energy impacts can be achieved. The most promising technologies and approaches can be built out to full vehicle levels and verified at ACM. Working closely with ACM, the approach presented a cost-effective method that multiplied the possible design space of new and emerging technologies with a higher degree of accuracy (due to HIL principles) while providing insight into test plan development for full vehicle/system testing.

Task 2.3: Real-Time Cooperative and Automated Vehicle Merging of On-Ramps

As a part of the DOE SMART Mobility initiative, ORNL developed an approach for optimizing CAV control and coordination. This modeling framework can be adapted to different traffic scenarios and can be used in a real-time system, given its analytical, closed-form solution. The approach taken to coordinate vehicles has been used to assess the impact of full penetration of optimally coordinated CAVs across different traffic scenarios. Applying this concept to vehicle HIL will validate the fuel-saving trends that have been found through simulation. To this end, actual V2X communication, between the vehicles located in various ORNL HIL laboratories and a central coordinator, will habilitate a real-time optimal merging coordination algorithm. A chassis dynamometer and HIL components will interact through a traffic simulation with virtual vehicles. All the vehicles will receive control inputs from the centralized coordinator according to the optimal controller computations. The vehicles located in the various HIL dyno laboratories will be operated by both real and virtual drivers that will follow the instructions given by the central coordinator.

Results

Task 1.1: Standardized Virtual Proving Ground Framework

Being the first year of this project, Task 1.1 has made up much of the work because it is the backbone for the rest of the tasks. The team identified three legacy models for comparable use cases to previous work in the IPG Car/Truckmaker virtual vehicle environment. The identified models were: an Autonomie battery electric vehicle (BEV) model; MathWorks Simulink BEV model from the powertrain blockset; and an ORNL HIL validated Class 8 Freightliner heavy-duty (HD) line haul truck model. These three models were selected as baselines because they represent models used by national laboratories, academia, and industry as well as have direct applications to ORNL's currently available test units in the VSI Laboratory.

Once the baseline models were transitioned to IPG's environment, a test scenario was created for the vehicle to drive through an urban area with other vehicles, traffic lights, speed limit recognition, and routing. The team also was able to also integrate the two Lidar model types into the vehicle control structure, a free space sensor and a physics-based lidar model. The free space model used simple 3D geometry intersections for detection in the rendered environment, the physics-based radar model was a raw sensor interface model that utilized NVIDIA's OptiX Ray Tracing Engine for emulating the infrared lasers used in lidar and its reflections. The proof of concept BEV use cases was then tested and validated on in the HIL laboratory as seen in Figure IV.1.2.1, below.

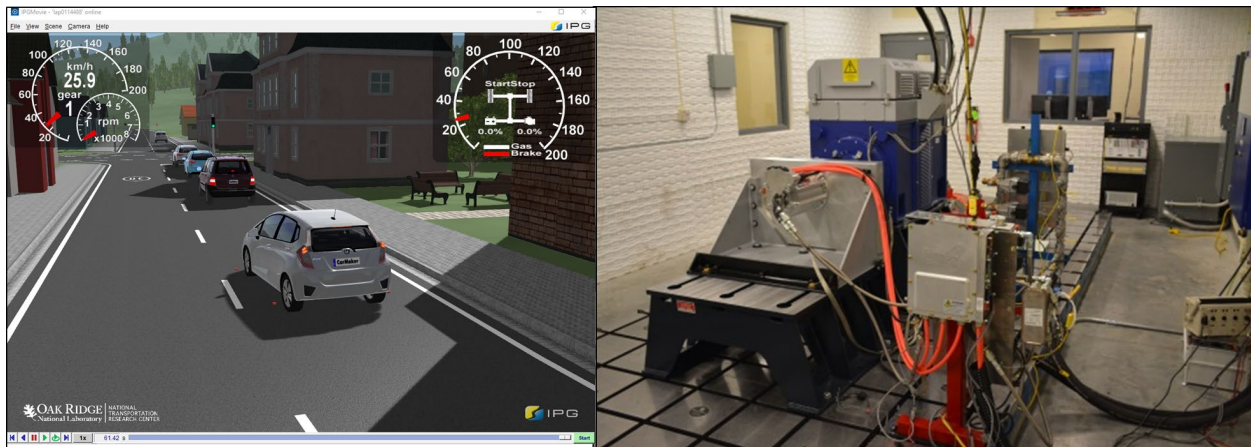


Figure IV.1.2.1 Electric drive in-the-loop installation utilizing IPG Carmaker Real-Time environment.

With baseline cases working in both simulation and with HIL's real-time requirements, the team then focused on getting the micro-traffic simulation tool Vissim and IPG's virtual environment to co-simulate together in a single environment (Figure IV.1.2.2). This was important for a few reasons, but the largest of which was to allow for the ability of full vehicle dynamics models to be integrated into the co-simulation. Agent-based models like those found in Vissim, often have unrealistic vehicle dynamics, but are still used for coordinated controls development. For this, these controls are often idealized and may not be able to run stably in real application.

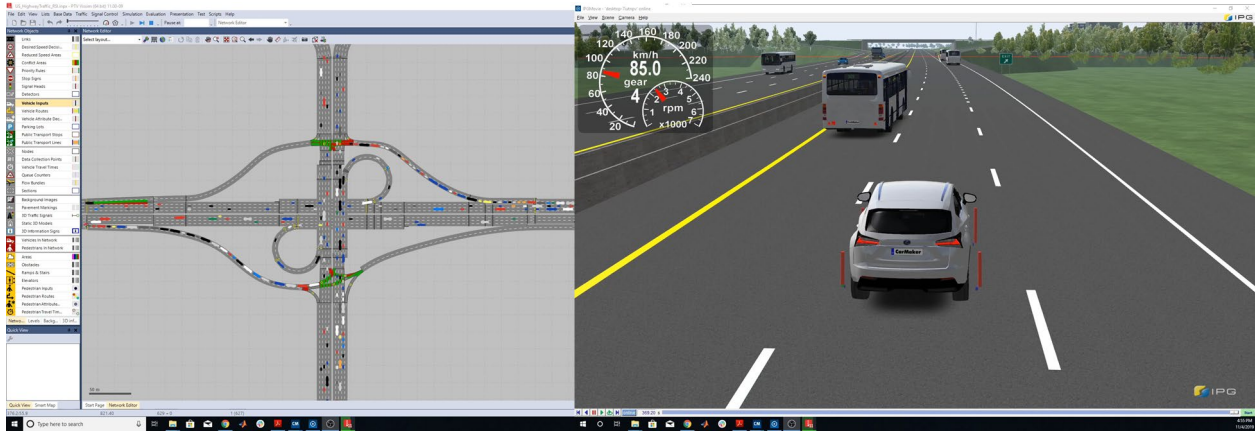


Figure IV.1.2.2 PTV Vissim micro-traffic and IPG Carmaker co-simulating in a single environment.

Task 1.2: Virtual Proving Ground Applied to HD Platooning

Basic controls for starting and establishing a platoon were completed, this included the use of emulated radar sensors for controlling gap distance. Figure IV.1.2.3 shows the lead truck and following truck as well as the radar sensor streams. To have realistic platooning control, the high definition radar model was integrated with the platooning control utilizing V2V communications and the post sensor structure was designed to replicate a Delphi ESR and SSR radar system, which was analogous of off-the-shelf radar solutions used in the past for other ORNL projects. This work included all of the realistic control required to perform pre- and post-processing task and manipulation of larger data streams and target lists.

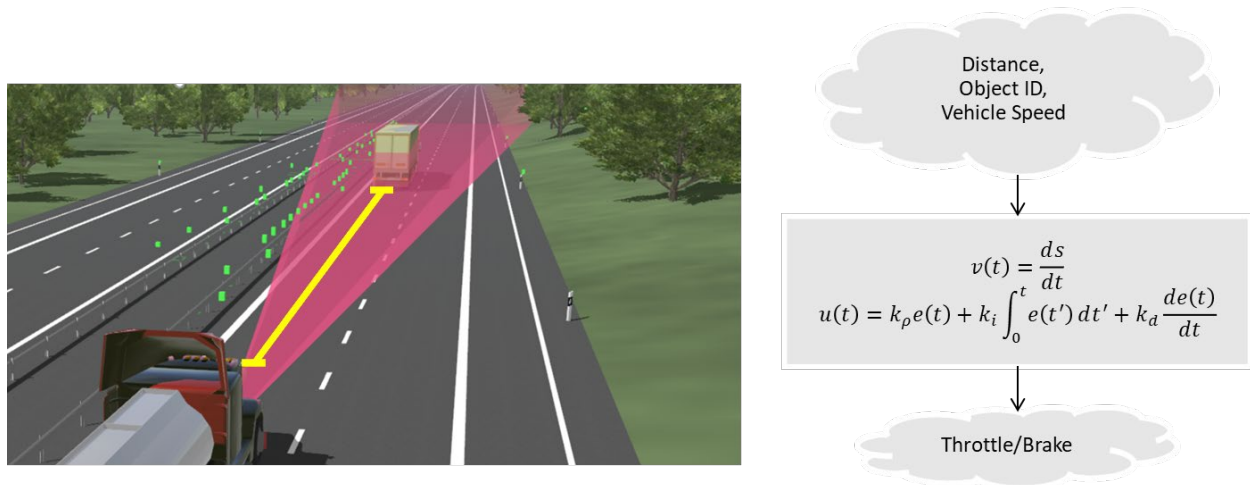


Figure IV.1.2.3 ORNL truck following algorithm in practice utilizing the High Definition phenological radar model.

Task 2.1: Integration of V2X Communications Hardware into Virtual Proving Ground Framework

As shown in Figure IV.1.2.4, the team developed a modular communication stack for leveraging its capabilities of replicating 4G long-term evolution (LTE) and dedicated short-range communications (DSRC) like comms. It was also configured to broadcast using current SAE standards (J2735). The units also include the ability to integrate authentication and encryption and the architecture of multiple communication routes was also possible. This new system allowed for testing of latency, message/packet loss, and signal corruption and its effects on vehicles in a safe virtual environment.

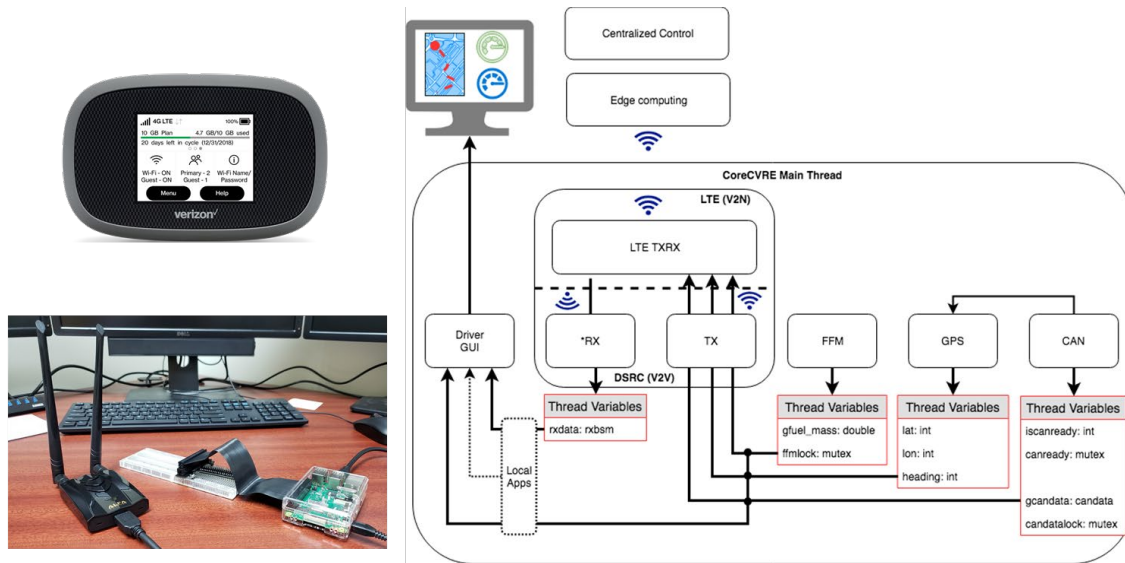


Figure IV.1.2.4 ORNL modular communications stack.

Utilizing this wireless communications system, the team demonstrated the physical communication layer was fully up and running and could be transposed into CAN messages that were connected to virtual vehicles in the environment and demonstrated data being passed V2V using the physical hardware (Fig. I.1.1.5).



Figure IV.1.2.5 HIL testing of the V2V test in the IPG Carmaker environment.

Conclusions

This being the first year of the project, the majority of the work performed was mostly setup for the more application or validation driven work that will occur in years 2 and 3 of the project. However, there was significant accomplishments in the areas of bridging the gap between pure simulation and hardware application utilizing HIL methodologies and techniques. The biggest of these achievements being found in adding real communications devices to HIL testing, thus allowing for testing of interference and package loss testing of V2V and V2I applications. The other important steps forward this year was the ability to co-simulate virtual vehicle environments and micro-traffic simulation in a single environment, giving the flexibility of adding more complex dynamics to the SMART work that was done at ORNL.

Acknowledgements

ORNL would like to thank U.S. DOE/EERE/VTO EEMS Program Manager, David Anderson and EEMS Technology Manager, Erin Boyd for their continued support on this project.

IV.1.3 Core Modeling, Simulation and Evaluation (ANL)

Phillip Sharer, Principal Investigator

Argonne National Laboratory
9700 S Cass Avenue
Lemont, IL 60439

Kevin Stutenberg, Principal Investigator

Argonne National Laboratory
9700 S Cass Avenue
Lemont, IL 60439

Michael Duoba, Principal Investigator

Argonne National Laboratory
9700 S Cass Avenue
Lemont, IL 60439

Aymeric Rousseau, Principal Investigator

Argonne National Laboratory
9700 S Cass Avenue
Lemont, IL 60439
E-mail: arousseau@anl.gov

Thomas Wallner, Principal Investigator

Argonne National Laboratory
9700 S Cass Avenue
Lemont, IL 60439

Erin Boyd, DOE Technology Manager

Office of Vehicle Technologies
U.S. Department of Energy
E-mail: erin.boyd@ee.doe.gov

Start Date: October 1, 2018

End Date: September 30, 2021

Project Funding (FY19): \$2,000,000

DOE share: \$2,000,000

Non-DOE share: \$0

Project Introduction

The U.S. Department of Energy (DOE) Vehicle Technologies Office (VTO), along with national laboratories, performs research to advance vehicle powertrain technologies, including internal combustion engines, batteries, electric machines, light-weighting, fuels and lubricants. The rise of connected and automated vehicles (CAVs) and smart mobility technologies has the ability to change traveler mobility choices as we currently know them, leading to potentially dramatic impacts on both mobility and energy. CAVs also enable higher traffic density at highway speeds with fewer transients, which allows for smaller vehicle-to-vehicle gaps—especially in the case of coordinated driving.

Given the large number of transportation and vehicle technologies, vehicle classes and operating conditions (vehicle trip profile, temperature etc.), tens or hundreds of thousands of combinations must be considered. Since it would not be possible to test and evaluate every possible combination, VTO has been relying on vehicle system modeling and simulation to estimate the potential of each technology at a system level to provide R&D guidance to VTO managers (on, for example, battery power and energy requirements) as well as maximize the potential of each technology.

Assessing the impact of new technologies across a wide range of scenarios requires the development of new systems simulation tools and workflow (e.g., HPC) and processes (e.g., vehicle-in-the-loop) supported by test data (e.g., road load changes with varying gap distances for varying vehicle types).

Objectives

This project focuses on the following main objectives:

- Enhance Autonomie vehicle models to accurately simulate the latest technologies in a computationally efficient manner through HPC.
- Integrate and deploy the new processes and tools through AMBER (Advanced Model Based Engineering Repository) and the new test data through D3 (Downloadable Dynamometer Database).
- Quantify the impact of advanced technologies on energy and cost (excluding smart mobility technologies).
- Develop the experimental process to measure road load changes on multiple vehicle platoons (sensors, control algorithm and hardware, vehicle interface), and validate the method by running the experiments.
- Analyze test data to characterize platooning vehicles' road load changes under various gaps, vehicle sizes, vehicle position offsets and configurations.

Results

Autonomie and AMBER

As shown in Figure IV.1.3.1, quantifying the impact of advanced technologies requires a series of tools that range in focus from an individual vehicle to an entire urban area. AMBER is an extensible framework that allows engineers to create, customize and deploy workflows to answer specific questions. AMBER developments focused on adding new workflows and features both to support current DOE studies and to further original equipment manufacturer (OEM) adoption, including:

- Importing Advanced Mobility Technology Laboratory (AMTL) test data to automatically generate component performance maps and vehicle models.
- Sizing powertrain components to meet vehicle technical specifications (VTS) for multiple combinations of vehicle architecture and performance criteria.
- Editing the controller and performance maps in the user interface (UI), including parametric studies.
- Creating a new UI that simultaneously changes a collection of configurations, models, files, and parameters in a vehicle to transform it from a conventional to an integrated starter generator (ISG) hybrid, or from a hybrid electric vehicle (HEV) to a PHEV, or from a time-based to distance-based driver.
- Creating a new result-differencing workflow to compare vehicles.
- Developing a new quality assurance/quality control (QA/QC) workflow to compare results between studies.



Figure IV.1.3.1 Energy for transportation workflow

Among the various improvements made in Autonomie [1] over the past year, the most important is the implementation of a new gear-shifting algorithm that enables gear skipping. This new algorithm is required to properly model 9- and 10-speed transmissions for passenger cars as well as class 8 sleeper trucks (up to 18 gears). In addition to this, several improvements were implemented, including:

- Addition of new fuel cell and motor efficiency data
- Addition of a compressed natural gas (CNG) engine map based on test data from Argonne’s test bench
- Improved hill hold capability for electric vehicles
- New configurations for large off-road vehicles
- Improved result representation from Pounder optimization runs.

The gear-skipping shifting algorithm was developed based on AMTL test data using Ford F150 test data. The impact of the gear-skipping algorithm on fuel economy using Autonomie is shown in Table IV.1.3.1.

Table IV.1.3.1 Gear-Skipping Impact on Pickup Truck Drive-Cycle Fuel Economy

Drive Cycle	Sequential (mpg)	Skip-Shift (mpg)	Fuel economy gain (%)
UDDS	20.27	20.66	1.9
US06	16.47	17.77	7.9
HWFET	29.08	29.17	0.2

Table IV.1.3.2 Gear-skipping impact on pickup truck acceleration performance

Acceleration	Sequential Shift(s)	Skip-Shift(s)
IVM to 30 mph	3.2	3.3
IVM to 60 mph	8.6	8.6
IVM to 65 mph	9.8	9.7
30–60 mph	5.3	5.2
45–65 mph	3.8	3.7

Table IV.1.3.2 shows that the fuel economy improvement is achieved without sacrificing any performance. In fact, we see slight improvements due to better gear selection. One observation from the test data was that the gears that can be skipped are often restricted by the gearbox design. The generic control algorithm does not consider this limitation; however, it can be calibrated to match the behavior observed in actual test data.

Vehicle Technology Benefits

The sizing algorithms were originally developed for Autonomie, and several steps were required to migrate the code to be compliant with AMBER. The algorithms have now been successfully implemented into AMBER and also support the latest MathWorks versions. While existing powertrain sizing algorithms were focused on light-duty vehicles, they were expanded to support medium- and heavy-duty vehicles as shown in Figure IV.1.3.2. Since the technical specifications are slightly different for different types of vehicles, a new UI will guide users to select the appropriate specifications.

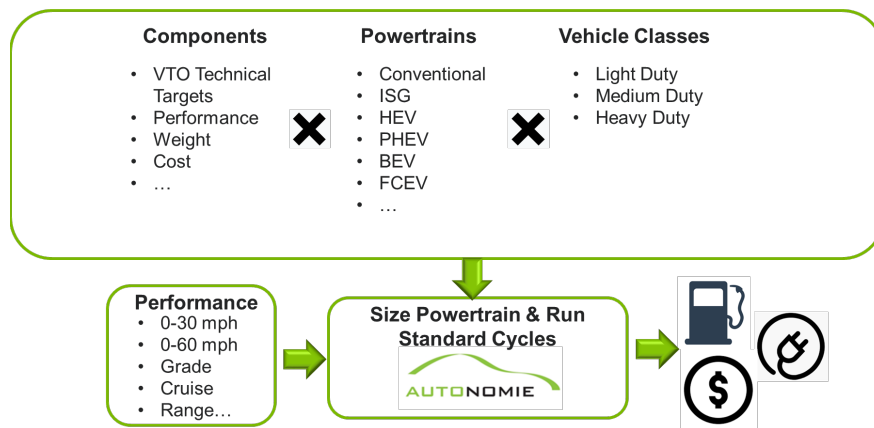


Figure IV.1.3.2 Overview of the sizing and performance evaluation process in AMBER

The powertrain sizing algorithms can be found in the paper published on this topic [1]. The sizing rules for medium- and heavy-duty vehicles are summarized in Table IV.1.3.3 below.

Table IV.1.3.3 Sizing Requirement Summary for Components Used in Heavy Vehicles

Powertrain	Engine	Motor	Battery
Conventional	Acceleration grade and cruise	Size based on starter and alternator	Energy: sustain electric loads for at least one minute
ISG			Power and energy: sustain peak motor output during acceleration, as well as regenerative braking events
HEV		Maximize regen in ARB transient	
PHEV	Grade and cruise	Acceleration grade and cruise	Energy: Electric range determined on EPA65 cycle for trucks. LDVs use UDDS cycle. Power: To support motor & aux. loads
BEV	N/A		

Vehicle-in-the-Loop Capabilities Development

Innovative methods are required to validate the energy impact of connected and automated vehicles. To this end, Argonne has developed a unique system to evaluate vehicle longitudinal control enabled by automation, as well as the transition from the human driver, on a chassis dynamometer. Leveraging the controlled environment of a chassis dynamometer eliminates safety risks, greatly expands available instrumentation, and ensures test repeatability and consistency. The system, called vehicle-in-the-loop (VIL), combines the advantages of model-based system engineering and full scale on-road testing by expanding a chassis

dynamometer environment to include the functionalities needed to interact with the vehicle for testing advanced driver assistance features. The VIL offers several advantages:

- Flexible: Any “linked” vehicle with flexible instrumentation can be evaluated.
- Precise and repeatable: Environment (e.g., temperature) and scenarios are reproducible.
- Safer: A stationary vehicle offers a much safer environment for control model development and validation than a moving vehicle.
- Reduced cost: New scenarios can be quickly implemented.
- Portable to road: Vehicles with validated control require little effort to transfer to track or on-road.

One of the core enabling features in the VIL system is the ability to use simulated data as input to the vehicle’s control, effectively “linking” the vehicle to the test environment. This link was accomplished in two separate ways, depended upon the specific design and architecture of the test vehicle.

- Object emulation: The vehicle perception sensors are bypassed with a single lead object (aka the lead vehicle) operating on a chosen drive cycle. A man-in-the-middle (MiM) is placed between the vehicle’s stock sensing equipment and the controller that commands acceleration. Communication at the point of the MiM, both raw signals and security messages, is decoded to allow for alteration by the testing environment. The number and relative positioning of “objects” can then be varied and injected into the vehicle driver controller. Communication messages that are not modified are directly bypassed to preserve the rest of the vehicle functionalities. Though this first method provides a unique implementation pathway for the test vehicle to the testing environment, an alternative method is required to provide flexibility for alternative longitudinal control models.
- Acceleration emulation: This method bypasses the vehicle’s motion planning and control system, sending direct acceleration and deceleration commands to the vehicle’s powertrain.

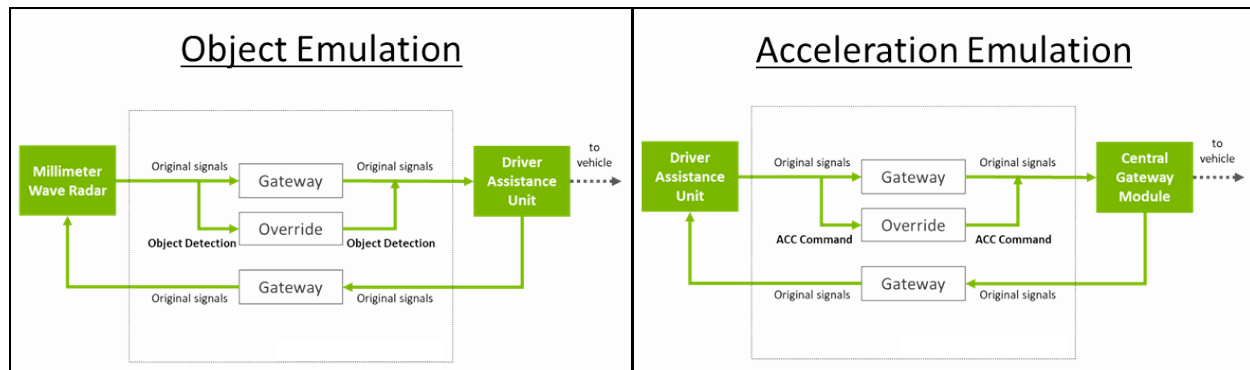


Figure IV.1.3.3 Vehicle-in-the-loop concepts

Following the successful “link” allowing for direct vehicle control, the larger simulation environment is established. The vehicle hardware interface, which translates information from the testing environment to direct vehicle control messages, was developed in Simulink and deployed to a Dspace MicroAutobox. The vehicle hardware interface then translates generic object positioning in the virtual environment into the vehicle-specific signals and states required for operation. The hardware environment also provides further flexibility with direct communication with the chassis dynamometer, allowing the virtual environment to dynamically change vehicle road load, accounting for varying aerodynamic loads (such as closely following a lead vehicle) or grade changes on the virtual drive.

Figure IV.1.3.4 shows the “vehicle-following” behavior of the 2017 Toyota Prius Prime, with the stock longitudinal control model (gap set to close follow) and the collision avoidance model over one US06 cycle. The results show that while the stock longitudinal model has a higher time constant in acceleration compared to the collision avoidance model, it maintains a constant time gap once it has reached the target speed. Meanwhile, the collision avoidance model maintains a constant time gap with the leading vehicle throughout the entire drive cycle. The controlled environment and flexible instrumentation of the chassis dynamometer allow for a repeatable test with focused data collection leading to insight into the different effects on energy consumption and vehicle operation of these two models.

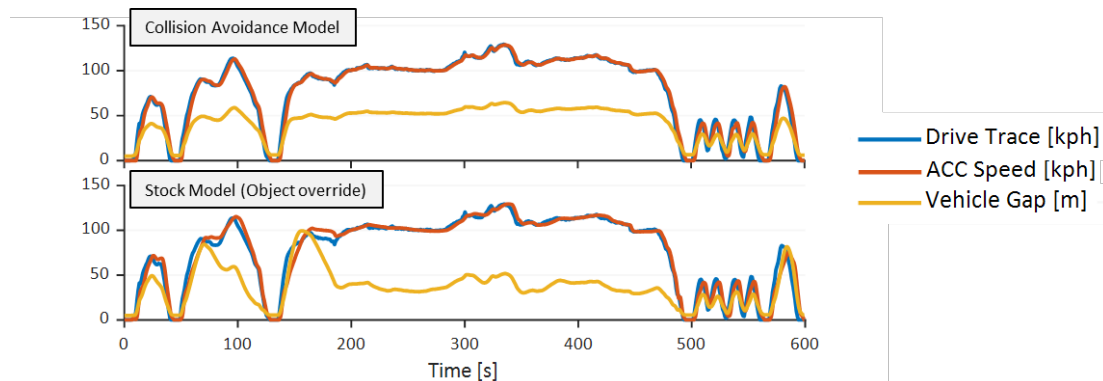


Figure IV.1.3.4 Comparison of test vehicle operation on a US06 cycle with varying longitudinal models

In order to validate new control algorithms developed under the SMART Consortium, the virtual environment was expanded by implementing Argonne’s RoadRunner in the real-time environment. Using RoadRunner allows a closed-loop real time simulation of vehicles and traffic infrastructure surrounding the test vehicle.

Figure IV.1.3.5 provides an overview of the vehicle-in-the-loop environment.

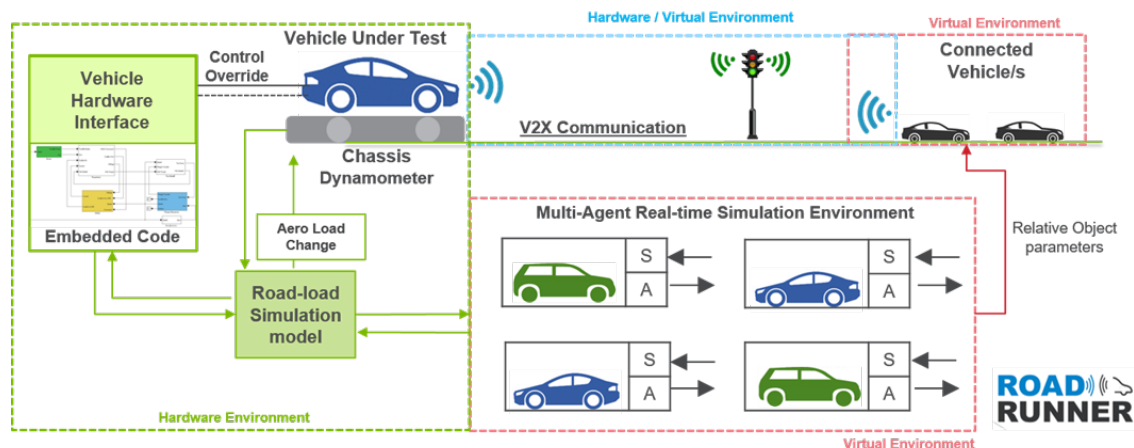


Figure IV.1.3.5 Overview of the vehicle-in-the-loop environment

Direct Aero/Roadload Measurements On-Track for Multi- and Mixed-Vehicle Platoons

A two-vehicle platoon with similar full-sized sedans was tested first, followed by a mixed set of three vehicles of varying sizes and types (SUV, pickup truck, and full-size passenger car). Three-vehicle platooning required new longitudinal control methods, control hardware, sensors, vehicle interface method, and data acquisition.

Cooperative adaptive cruise control (CACC) equations were developed to allow an operator to specify a specific target gap and speed in engineering units. Argonne has capabilities in bypassing cruise control

commands with a “man-in-middle” controller, but because the protocols are quite different from car to car, a more generic approach of sending analog accelerator pedal voltages directly to the vehicle was implemented. Our control equations output acceleration, so each vehicle required a pedal “map” to convert the acceleration rate to the two pedal voltages needed to command a desired torque, based on a response surface model derived from dynamometer testing. Additional circuits were added to enable the driver to override the computer commands by pressing the stock pedal (brakes work normally).

The control equations were ported to an interactive simulation tool for researchers to learn how the various parameters interacted and practice tuning. Safe baseline parameter values were found for initial track testing. Because the goal is steady-state speed control, the acceleration rates were also limited, and parameter tuning at the track focused on steady speed and gap behavior rather than fast response time. Initial two-vehicle testing was conducted at the three-mile oval track at the Navistar proving grounds in nearby Indiana; however, the best track within a reasonable driving distance was found to be the high-speed 7.5-mile oval track at TRC in Ohio.

Two-Vehicle Platoon

The initial two-vehicle test data were analyzed and a paper published to summarize the findings [2]. A phenomenological model for platooning vehicles [3] was successfully fitted to the data in Figure IV.1.3.6. The trend is, of course, greater load reductions at smaller gaps. The most notable finding was the correlation between our data and the literature model’s load reduction reversal when approaching very small gaps. In multiple test outings, we found this reversal phenomenon at small gaps of roughly 5 to 10 meters (at highway speeds). These efforts represent the beginning of our work in finding robust, comprehensive trends and numerical models that will define close-following road loads in large, multi-vehicle simulation studies.

Three-Vehicle Platoon

After substantial development with control algorithms, sensor integration and vehicle interfaces, testing was performed with three-vehicle platoons at a larger test track. While the two-vehicle platoon used similar full-sized sedans, the vehicles chosen for the three-vehicle platoon were purposefully varied to explore realistic vehicle-to-vehicle variations. The three vehicles were: 1) Mazda CX9 SUV, 2) Ford F-150 pickup truck, and 3) Ford Fusion hybrid sedan.

Using a larger track helped us realize many of our objectives, with preliminary analysis showing improved results. The longer track provided enough data to average out transient variations from the controls, transitions from turns to straightaways, and any wind shifts. Numerous “baseline” tests are interspersed throughout the test cases to provide enough control conditions to quantify load reductions accurately, as weather and track conditions change during testing. Results from the three-vehicle platoon at 70 MPH are shown in Figure IV.1.3.7. Considerable road load reductions are seen in both the second and third vehicles, which could amount to a fuel savings on the order of 15-20%, but efficiency improvements were not observed in the first vehicle.

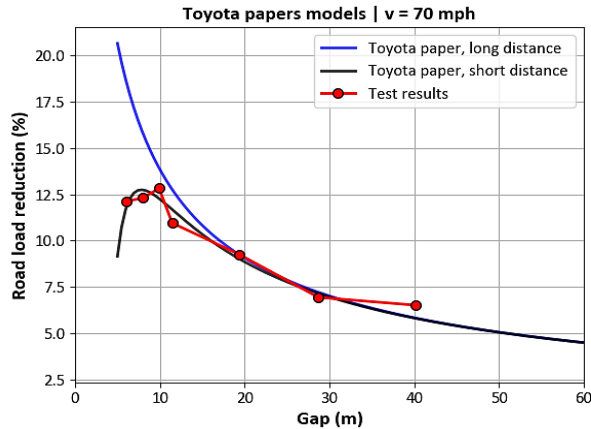


Figure IV.1.3.6 Road load reduction data from second vehicle in two-vehicle platoon at 70 MPH along with a fit of a phenomenological model from the literature

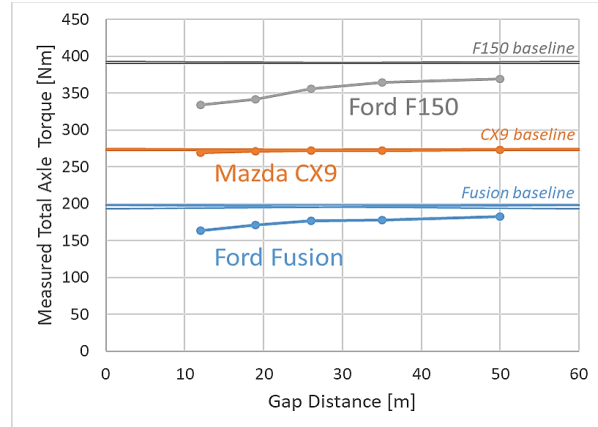


Figure IV.1.3.7 Three-vehicle platoon direct axle torque results for various gaps at 70 MPH

Conclusions

As part of this project, new system simulation capabilities and test data have been successfully developed:

- New features have been added to both AMBER (e.g., new workflows) and Autonomie (e.g., new models, powertrain sizing algorithms) to continue to support U.S. DOE VTO studies. Many new capabilities have already been used to support other VTO projects (e.g., medium- and heavy-duty vehicle energy consumption and cost estimation). New releases of the tools have also been provided to researchers with the more than 250 organizations currently licensing Autonomie and AMBER.
- The newly developed vehicle-in-the-loop platform provides a unique framework leveraging state-of-the-art system simulation tools to quantify the energy impact of advanced longitudinal vehicle control, enabled by connectivity and automation in an emulated environment.
- The ability to measure road load changes with varying gap distances for varying vehicle types has been demonstrated. Baseline results measured over the course of four hours had very little test-to-test variability, giving us confidence in using more rapid sequencing strategies in future tests over longer periods of time than originally conceived. The middle and rear vehicle had similar load reductions, which were significant in magnitude (17% and 20% respectively). All our testing so far confirms there are noticeable driving load reductions even for quite long-distance gaps that can be found in current ACC systems (40–50 meter and 1.5 sec gaps). That being said, the lead vehicle load reduction data demand more investigation (i.e., the lead vehicle from the three-vehicle platoon had virtually no change in load, but earlier two-vehicle data showed some measureable load reductions).

References / Publications

1. R. Vijayagopal et al., “Benefits of electrified powertrains in medium and heavy duty vehicles,” EVS 32, Lyon, France, May 2019.
2. Duoba, M. and Fernandez Canosa, A., “On-Track Measurement of Road Load Changes in Two Close-Following Vehicles: Methods and Results,” SAE Technical Paper 2019-01-0755, doi:10.421/2019-01-0755.

3. Tadakuma, K., Doi, T., Shida, M. and Maeda, K., “Prediction Formula of Aerodynamic Drag Reduction in Multiple-Vehicle Platooning Based on Wake Analysis and On-road Experiments,” SAE Int. J. Passeng. Cars—Mech. Syst. 9(2):645–656, 2016, <https://doi.org/10.4271/2016-01-1596>.

(This page intentionally left blank)

U.S. DEPARTMENT OF
ENERGY

Office of
**ENERGY EFFICIENCY &
RENEWABLE ENERGY**

For more information, visit:
energy.gov/vehicles

DOE/EE-1988 May 2020